The structural history of Tasmania from the Devonian to the Recent

Andrew Stacey B.Sc. (Hons)

Submitted in fulfilment of the requirements
for the degree of Doctor of Philosophy

University of Tasmania

June 2009

DECLARATION OF ORIGINALITY

This thesis contains no material which has been accepted for a degree or diploma by the University or any other institution, except by way of background information and duly acknowledged in the thesis. To the best of my knowledge and belief the thesis contains no material previously published or written by another person except where due acknowledgement is made in the text of the thesis.

Andrew Stacey

Date:

STATEMENT OF AUTHORITY OF ACCESS

This thesis may be made available for loan and limited copying in accordance with the *Copyright Act 1968.*

Andrew Stacey

Date:

ABSTRACT

Onshore Tasmania is a frontier exploration province, where exploration using modern methods has not previously been attempted. Bitumen, oil and gas seeps have been widely reported from onshore Tasmania over the last hundred years. Over 40 exploration wells have been drilled, however none have been successful. Most wells were drilled in the vicinity of alleged seeps with little or no knowledge of stratigraphy or structure. No exploration well has been drilled on a target identified from a seismic reflection survey.

The primary aim of this research is to establish the geometry and age of structures affecting the Permo-Triassic Tasmania Basin, and also the Tertiary basins and Palaeozoic fold-thrust belt. The findings are used to define the distribution and style of potential hydrocarbon traps, and to assess the potential influence the age of trap formation has on hydrocarbon prospectivity.

The Tasmania Basin developed in a back-bulge depozone inboard of the major foreland basin formed behind the Andean-style eastern margin of Gondwana. The eroded remnant of the Tasmania Basin covers an area greater then 30 000 km^2 in central and eastern Tasmania. In the Middle Jurassic, Tasmania was part of the Karoo/Ferrar/Tasmania large igneous field with large volumes of dolerite intruded into the Parmeener Supergroup. From the middle Cretaceous to Tertiary, Tasmania was subject to uplift, erosion and northeast directed extension associated with the break up of Gondwana. Tertiary sediments were deposited in a series of linked half-grabens including the northwest striking Longford Sub-basin.

The geology and structure of the pre-Late Carboniferous basement is known from outcrop around the margins of the Tasmania Basin. To a large extent the basin lies along the boundary between the Western Tasmania Terrane and the Eastern Tasmania Terrane. In north eastern Tasmania the dominant folds were formed during north-eastward transport, while in western Tasmania Devonian structures verge to the south-west. Current models suggest these terranes were brought together during the Tabberabberan Orogeny along a major crustal dislocation, the Tamar Fracture System.

A detailed structural analysis was conducted using regional 2D seismic data and a high resolution digital elevation model. The interpretation is supported by geological mapping, and drill-hole, velocity and gravity data. Six hundred kilometres of regional seismic data (23 lines) were acquired across the Central Highlands and Longford Sub-basin in 2001. The seismic lines are widely spaced and mainly recorded along public roads. Crooked line geometry and inverted near-surface velocity contrast caused by dolerite are major problems affecting the quality of the migrated seismic sections. The seismic dataset forms the core of this analysis, providing information about the geometry and age of folding and faulting.

Four periods of deformation have affected onshore Tasmania since the Devonian. In the basement, a zone of north-east dipping thrusts lies beneath the Launceston Tertiary Basin. These thrusts form the boundary between the Western and Eastern Tasmania Terranes. Southwest of this boundary the basement becomes increasingly fold dominated with kilometre scale folding identified on the westernmost seismic sections. The folds and thrusts seen in the seismic sections are similar to structures mapped in nearby basement outcrop which formed during the Middle Devonian Tabberabberan Orogeny.

The Tasmania Basin was faulted and weakly folded prior to and/or during the intrusion of dolerite in the Middle Jurassic. Structures of this age are common in the Central Highlands but difficult to recognise in the Longford Sub-basin/Northern Midlands regions. Gentle folds and faults with both normal and reverse offset are recognised. Some faults have acted as conduits for dolerite dykes and step ups in sills.

Following the intrusion of dolerite the Tasmania Basin was affected by uplift, erosion and extensional faulting. Folds and faults formed in the Tasmania Basin at this time are more common then earlier structures. While this phase of deformation affected the entire basin, the density of faulting is far greater beneath the Launceston Tertiary Basin then in the Central Highlands. The locus of extension lies above the Tamar Fracture System where reactivation of basement thrusts resulted in the widespread development of half-grabens. The Central Highlands region was little affected, acting as a competent block during this event.

The final event to affect Tasmania was mild northwest compression in the Mio-Pliocene. This event is indicated by inversion structures affecting Tertiary sequences on the seismic sections and from the present topography.

The Digital Elevation Model of Tasmania provides a continuous, unbiased image of geomorphologic responses to environmental conditions and tectonic events from which active geological processes and the nature of the underlying geology may be interpreted. The model applied here is that the contemporary topography of Tasmania is dominated by Tertiary tectonics modified by erosion. Based on this concept, the DEM was used to determine the pattern of Tertiary faulting. The Tertiary Fault Pattern is relatively simple in the north with extension concentrated on the Launceston Tertiary Basin where the strike of the basement faults is near orthogonal to the extension direction. In southern Tasmania the basement structure is more complex and the extensional geometry is dominated by strongly curved faults and soft-linked grabens. The style of Tertiary faulting in Tasmania reflects the basement structure.

Two petroleum systems have been proposed for onshore Tasmania, a Larapintine Petroleum System in the Late Cambrian to Early Devonian Wurawina Supergroup and a Gondwana Petroleum System in the Parmeener Supergroup (Tasmania Basin). Maturation of, and migration from, the Larapintine Petroleum System probably occurred in the Early Devonian, with a possible second phase of generation in the Middle Jurassic to Late Cretaceous when the Gondwana Petroleum System is thought to have matured.

From analysis of the seismic sections, potential hydrocarbon traps were developed in the first three phases of the structural history reported here. During the Tabberabberan Orogeny large folds developed in western and south-western Tasmania, these form part of a possible Larapintine play. Another Larapintine play involves sub-unconformity and palaeokarst traps developed beneath the Tasmania Basin.

Plays in the Gondwana system involve a diversity of structural traps developed by both pre- and post- dolerite tectonic events and stratigraphic traps resulting from pinch outs with dolerite sheets. The best potential traps are formed by rollover anticlines and numerous tilted fault blocks in the Longford Sub-basin. Large fault bounded blocks are the most common style in the Northern Midlands. Gentle anticlines form the most probable trap structures in the Central Highlands.

The major risks to onshore Tasmanian traps is the timing of their development in relation to predicted timing of hydrocarbon generation, and their possible destruction by later tectonic events. It is improbable that Middle Devonian anticlines were charged by hydrocarbons generated in the Early Devonian. However, these structures were available to hydrocarbons generated during the subsequent thermal event, as were palaeokarst and sub-unconformity traps.

In the Tasmania Basin, traps developed before the intrusion of dolerite carry a high charge potential. The risk of later leakage of these early structures is very high in the area of the Launceston Tertiary Basin where the Cretaceous/Tertiary faulting is dominant. The pre-dolerite structures may survive in the Central Highlands. Traps developed by Tertiary tectonic events were formed after the Middle Jurassic to Late Cretaceous thermal maximum. The existing thermal models do not suggest petroleum generation has occurred since these structures were developed.

Analysis of the petroleum systems events for onshore Tasmania indicates the prospectivity for the province is low. There is doubt regarding quality, distribution and generative potential of source rocks in both petroleum systems. The Larapintine System depends on the existence of a reservoir with secondary porosity or palaeokarst. No potential reservoir has been found. In the Gondwana System while there has been local generation of hydrocarbons, no evidence of migrated hydrocarbons has been found during drilling in the main basin. However our knowledge of these systems is not mature. Future deep drilling through the Tasmania Basin and into the basement will do much to improve our understanding. Several potential hydrocarbon trap styles are present in onshore Tasmania. However, the timing of trap formation in relation to later structural development and the predicted maturation and migration of hydrocarbons is problematic.

FRONTISPIECE

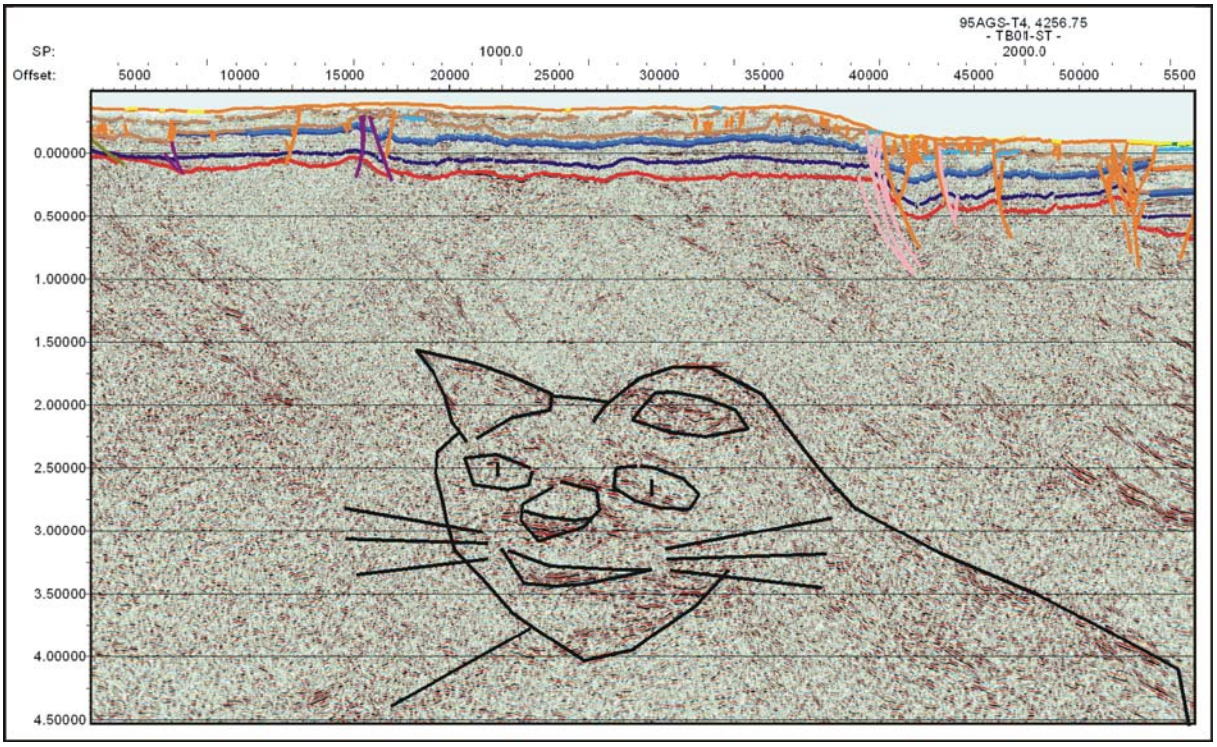

“Some days you’ve just got to get loose with your data”! ***L. Ross, 1999.***

ACKNOWLEDGEMENTS

This research was supported by an Australian Postgraduate Award (Industry), the University of Tasmania and Great Southland Minerals Limited.

I would like to thank Malcolm Bendall and Dr. Clive Burrett of Great Southland Minerals (GSLM) for their courage in conceiving the project and for their material and financial support throughout. I wish them and the staff of GSLM every success with their future exploration program.

My thanks to my supervisors Assoc. Prof. Ron Berry and Dr. Michael Roach. Ron, many thanks for your ideas, support and patience in seeing this thesis through. It is undoubtedly better for your input. Mike, thanks for your support, especially in computational matters and with the velocity survey, which was ultimately so important to the seismic interpretation. I must also thank Assoc. Prof. Leonid Danyushevsky and Dr. Trevor Falloon for plucking me from obscurity and allowing me to become involved in some "big science", and Dr's Peter McGoldrick and Garry Davidson for taking me again and again (and again) on the East Coast Excursion, an experience both enjoyable and educational. To all the academic, general staff and past and present students of the School of Earth Science and CODES, my thanks for your input over the years, whether it be intellectual, practical, physical or administrative, you have all in some way contributed to the success of this endeavour.

My co-conspirators on this project were Dr. Catherine Reid, Allan Chester and Jubo Lui, my thanks to you all for your help and interest and opinions on my part of our research and for the many discussions on Tasmania and its petroleum potential.

Many started a similar journey at the time I did, some have finished some are still labouring on. To the "usual suspects" Kate Bull, Nicky Pollington, Lee Evans, Jubo Lui, Allan Chester, Russell Fulton and Mawson Croaker, thanks folks for your friendship, support and advice over the past five years. To those who made it to the light – congratulations, and to those still going "hang in there, you'll make it"!

Finally, my thanks to Bron, without whose love and undying support, I may not have made it! And to Mary, for helping me finally get it all "done and dusted"!

TABLE OF CONTENTS

CHAPTER 1

INTRODUCTION

CHAPTER 2

REGIONAL GEOLOGY

CHAPTER 3

THE PETROLEUM GEOLOGY OF ONSHORE TASMANIA

CHAPTER 4

DIGITAL ELEVATION MODEL

CHAPTER 5

SEISMIC DATA AND INTERPRETATION METHODOLOGY

CHAPTER 6

SEISMIC INTERPRETATION – DESCRIPTTION

CHAPTER 7

SEISMIC INTERPRETATION – RESULTS

CHAPTER 8

CONCLUSIONS

LIST OF FIGURES

CHAPTER 1
INTRODUCTION

1.1: PREAMBLE

Concerted exploration in pre-Carboniferous rocks of Tasmania's west and northeast has yielded significant mineral discoveries, while exploration in the late Mesozoic to Cenozoic offshore basins have also shown significant potential and yielded hydrocarbons. In contrast, whether discouraged by the complex geology, the attitude of government or by poor results, there has only been intermittent exploration for hydrocarbons in onshore Tasmania, with many considering onshore Tasmania unprospective.

The main exploration interest lies in the Permo-Triassic Tasmania Basin, whose eroded remnant, often expressed as "Mesozoic cover sequences" on geological maps of Tasmania, covers more than 30 000 km^2 across central and eastern Tasmania. The depth of erosion and the ubiquitous dolerite intrusions are a major risk. Other potential plays lie in the Early to Middle Palaeozoic fold-thrust belt beneath the basin. Our current understanding of petroleum systems in Tasmania has been gleaned mainly from outcrop at the margins of the basin and from a very few deep drill holes. The knowledge base is very limited. Onshore Tasmania has not been extensively explored using modern commercial and scientific methods and thus remains very much a frontier exploration province.

The research presented in this thesis forms part of a broader SPIRT project, "Petroleum Systems Modelling Onshore Tasmania" jointly funded by the Australian Research Council and Great Southland Minerals (GSLM). The goal of this project is to substantially increase our understanding of Onshore Tasmania in terms of structural evolution, source potential, maturation, migration and timing of the events that may lead to the formation of viable petroleum systems and the accumulation of commercial hydrocarbons.

1.2: AIMS OF THIS STUDY

The main aims of this thesis are to:

1. identify the geometry and timing of folds and faults that affect the Permo-Triassic Tasmania Basin and the underlying Early-Middle Palaeozoic fold thrust belt,
2. examine the distribution of these structures,
3. identify potential hydrocarbon traps styles, and
4. discuss the structural history in terms of its implications for hydrocarbon prospectivity.

1.3: DATASETS, METHODS AND SOFTWARE TOOLS

The main datasets analysed were :

1. 662 line kilometres of regional 2D seismic data supplied by Great Southland Minerals,
2. Digital Elevation Model (DEM) at 25 m resolution supplied to the University of Tasmania by the Department of Primary Industry, Water and Energy, Tasmania,
3. drill hole data sourced from reports and the Tasmanian Drill Hole Database (DORIS) by Mineral Resources Tasmania (MRT),
4. regional geological mapping at 1: 250 000, 1;50 000 and 1;63 360 scales, and
5. the measured gravity field over northern Tasmania.

These datasets were analysed using the following software products:

- The seismic data was supplied in segy format and interpreted using Kingdom Suite™ software,
- the pre-gridded DEM image was manipulated using ER Mapper™ image processing software,
- base-maps of the seismic survey area were prepared using Petrosys™, while ArcView™ has been used to view the DORIS database and create several other maps and images, and
- Potent™ was used to model how changes in the thickness of dolerite sills affected the gravity field.

1.4: LOCATIONS, MAPS AND SEISMIC SECTIONS

All maps presented in this thesis were produced using Universal Transmercator Projection, the datum is AGD 66 and AMG Zone 55. Grid references, where used are produced using this system. All the localities mentioned in the text are shown on Figure 1.1, a table of grid references for all of these localities is located in Appendix 1. In many instances a general geographic location is given rather then a specific locality, these geographic locations are presented in Figure 1.2.

All geological maps presented use the stratigraphic nomenclature and legend used by the 1: 250 000 scale geological maps produced by Mineral Resources Tasmania (Brown et al., 1995, Calver et al., 1995, Forsyth et al., 1995, McClenaghan and Calver, 1994). A modified version of this legend has been created, which applies to all geological maps included in this thesis. A copy of this legend (Figure 1.3) is located with Map 5.1.

A complete set of the interpreted seismic sections is provided as a paper copy and in digital form (see Appendix 2 for section ranges and file names). The seismic sections are of the migrated data and are scaled such that V:H = ~1, based on velocities at the RG-145 and Hunterston 1 drill holes. The colours used to represent the various horizons and faults interpreted are presented in Figure 5.10, for convenience a copy of this figure is placed with the seismic sections.

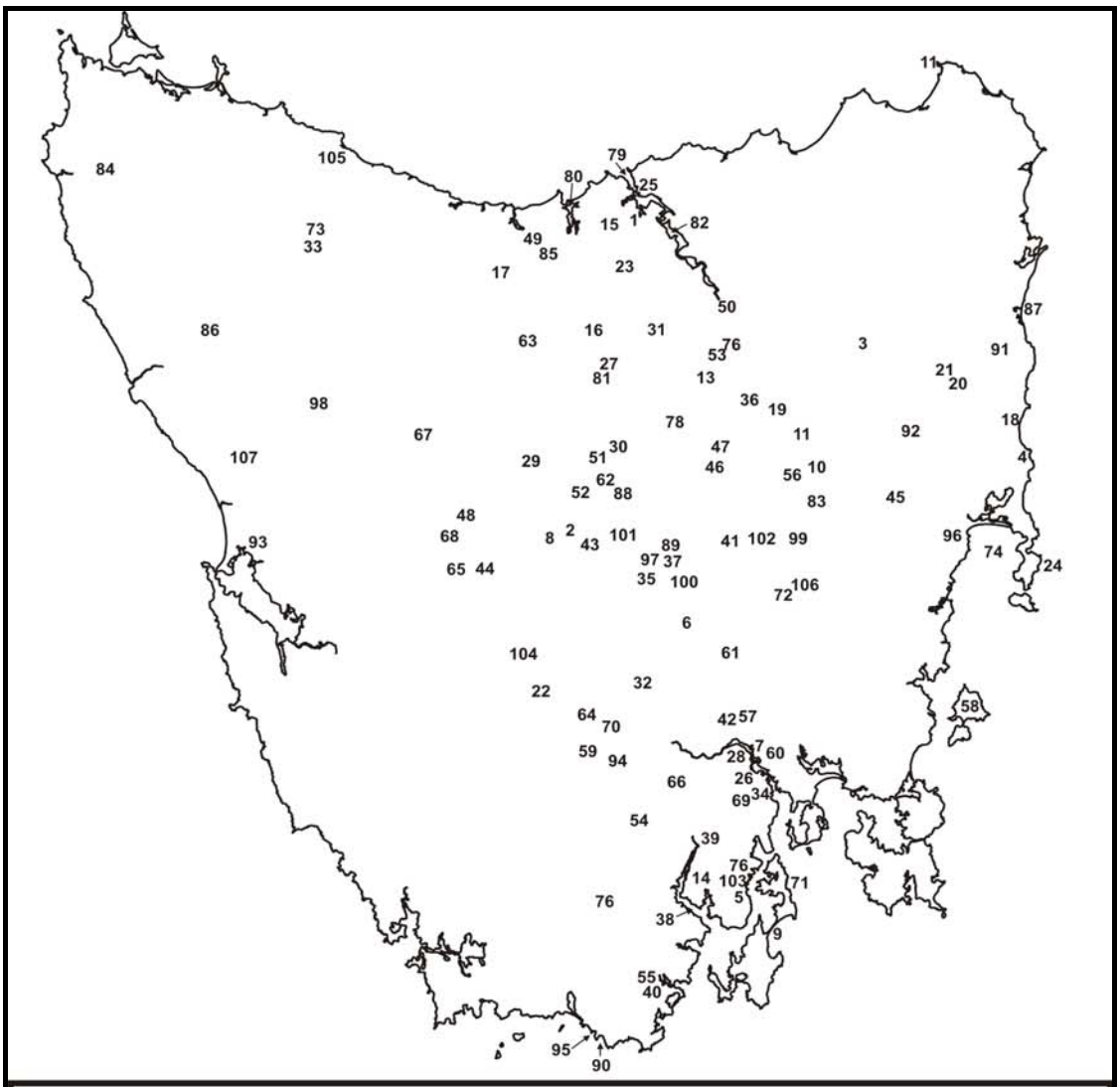

Localities mentioned in the text

1	Beaconsfield	28	Granton	55	Lune River	82	River Tamar
2	Bellevue Tier	29	Great Pine Tier	56	Macquarie Tiers	83	Ross
3	Ben Lomond	30	Great Lake	57	Mangalore	84	Salmon River
4	Bicheno	31	Hagley	58	Maria Island	85	Sassafras
5	Birches Bay	32	Hamilton	59	Maydena	86	Savage River
6	Bothwell	33	Hellyer Gorge	60	Meehan Ranges	87	Scamander
7	Bridgewater	34	Hobart	61	Melton Mobray	88	Shannon Lagoon
8	Bronte Park	35	Howells Sugerarloaf	62	Miena	89	Shannon Tier
9	Bruny Island	36	Hummocky Hills	63	Mole Creek	90	Shoemaker Bay
10	Campbell Town	37	Hunterston	64	Mt Field East	91	St Marys
11	Cape Portland	38	Huon River	65	Mt King William 1	92	St Pauls River
12	Conara	39	Huonville	66	Mt Lloyd	93	Strahn
13	Cressy	40	Ida Bay	67	Mt Pelion	94	Styx Valley
14	Cygnet	41	Interlaken	68	Mt Rufus	95	Suprise Bay
15	Dazzler Range	42	Jordan River	69	Mt Wellington	96	Swansea
16	Deloraine	43	Lake Echo	70	National Park	97	Synnots Creek
17	Don River	44	Lake King William	71	North Bruny Island	98	Tullah
18	Douglas River	45	Lake Leake	72	Oatlands	99	Tunbridge
19	Epping Forrest	46	Lake River	73	Oonah	100	Tunbridge Tier
20	Fingal Tier	47	Lake River Inlier	74	Oyster Bay	101	Waddamanna
21	Fingal Valley	48	Lake St. Clair	75	Oyster Cove	102	Weasel Plains
22	Florentine Valley	49	Latrobe	76	Perth	103	Woodbridge
23	Frankford	50	Launceston	77	Picton River	104	Wylds Craig
24	Freycinet Peninsula	51	Liawenee	78	Poatina	105	Wynyard
25	Georgetown	52	Little Pine Lagoon	79	Port Dalrymple	106	York Plains
26	Glenorchy	53	Longford	80	Port Sorell	107	Zeehan
27	Golden Valley	54	Lonnavale	81	Quamby Bluff		

Figure 1.1: Locations mentioned in the text.

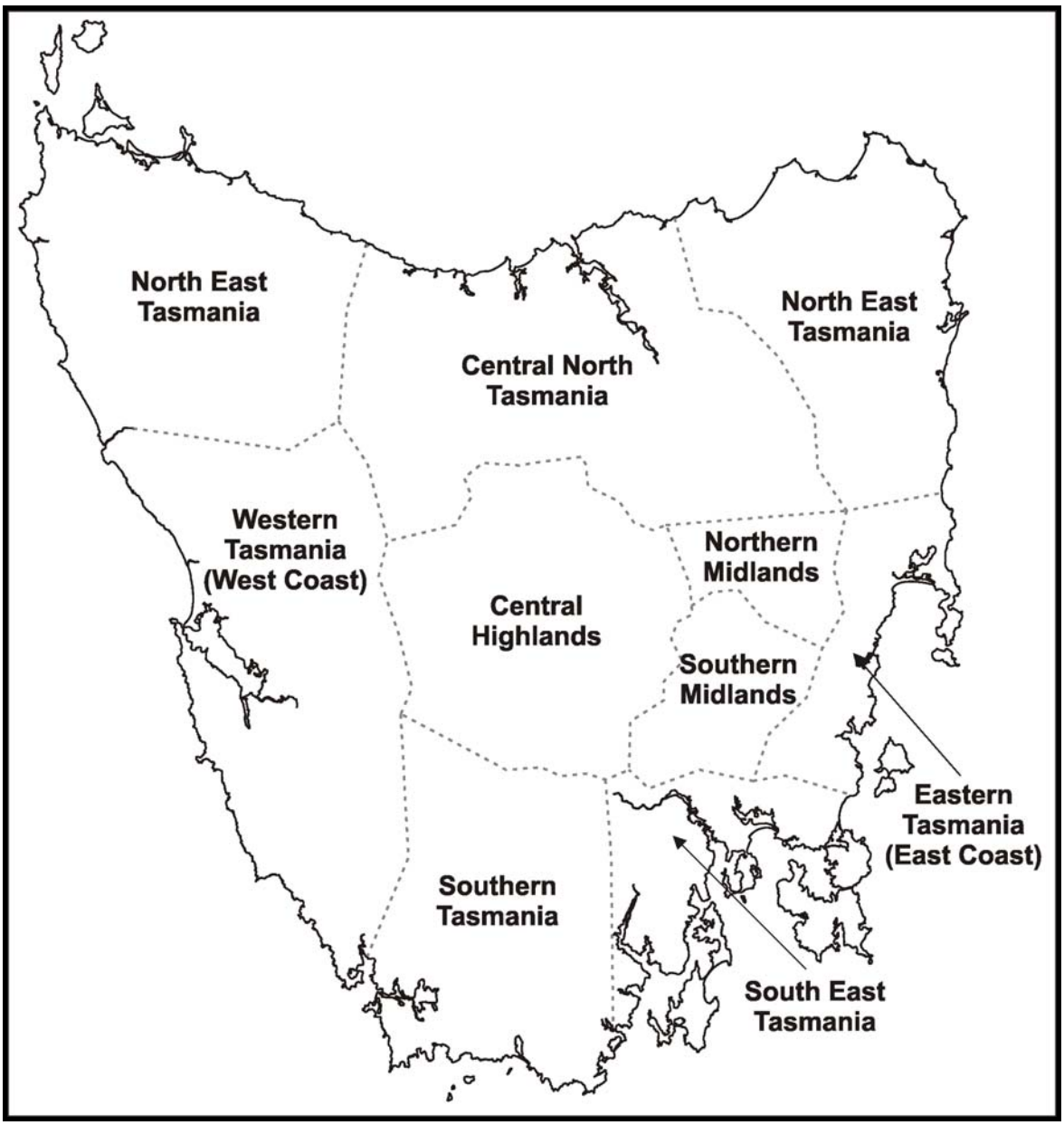

Figure 1.2: Major geographical areas mentioned in the text.

1.5: EXPLORATION HISTORY

The first assessment of Tasmania's petroleum potential was made by Twelvetrees (1917). Even though there were "no undoubted surface indications of oil and gas", he indicated the Tertiary basins and the "Gondwanaland beds" (Parmeener Supergroup of the Midlands region were prospective, recommending prospecting for surface seeps followed by "geologically correct" drilling. A later government geologist, Hills (1921, 1922) stridently believed as Tasmania appeared to not have been affected by compressional tectonics, which at that time was thought necessary for the development of hydrocarbons, that there was absolutely no chance of finding hydrocarbons in Tasmania.

1:250,000 Geology of the TB01 Seismic Survey Area (Figure 1.3)

CAINOZOIC

QUATERNARY — PLEISTOCENE HOLOCENE

TQ — Q — Qp

Qh — *Sand, gravel and mud of alluvial, lacustrine and littoral origin* (Qh).

Qpt, Qpg, Qps, Qpl — *Glacial, periglacial and fluvial sediments including till and interglacial deposits* (Qp), *Talus, vegetated and active* (Qpt), *glacial and glaciogene deposits* (Qpg), *coastal sand and gravel* (Qps) *and limestone* (Qpl) *indicated.*

Erosional Surface

TERTIARY — Tm, Ts, Tf, Tb — *Dominantly non-marine sequences of gravel, sand, silt, clay and regolith* (Ts); *marine limestone* (Tm); *ferricrete, laterite and derived lag deposits* (Tf); *basalt (tholeiitic to alkalic) and related pyroclastic rocks* (Tb).

MESOZOIC

TRIASSIC — R, Rv, Rvc, Rvv, Rq — *Undifferentiated fluviolacustrine sequences of sandstone, siltstone and mudstone* (R); *dominantly lithic volcaniclastic sandstone* (Rv); *lithic sandstone, siltstone, mudstone and felsic tuff with some coal and basal quartz sandstone* (Rvc); *dominantly siltstone, lithic sandstone and mudstone* (Rvv); *dominantly quartz sandstone* (Rq).

PERMIAN - LATE CARBONIFEROUS — P, Pu, Pc, Pf, Pl, Pt — *Undifferentiated glacial, glaciomarine and non-marine sedimentary rocks* (P); *freshwater sandstone with coal measures* (Pc); *upper glaciamarine sequences of pebbly mudstone, pebbly sandstone and limestone* (Pu); *freshwater and paralic sandstone and mudstone with some coal measures* (Pf); *lower glaciomarine sequences of mudstone, pebbly mudstone, pebbly sandstone, minor limestone and Tasmanite oil shale* (Pl); *basal tillite* (Pt).

UPPER PARMEENER SUPERGROUP / LOWER PARMEENER SUPERGROUP

IGNEOUS ROCKS

TERTIARY — Tb — *Basalt (tholeiitic to alkalic) and related pyroclastic rocks* (Tb).

JURASSIC — Jd — *Dolerite (tholeiitic) and locally developed granophyre* (Jd).

LATE - EARLY DEVONIAN — Dgaf, Dgafs — *Dominantly alkali-feldspar granite, I-type*(Dgaf); *S-type* (Dgafs).

Dgn — *Dominantly granodiorite/adamellite, (I-Type)* (Dgn).

Dgr — *Dominantly granodiorite, I-type* (Dgr).

Strike and dip of bedding: right way up; overturned; facing unknown; vertical with facing unknown.

Strike and dip of cleavage: dipping; vertical.

Strike and dip of crenulation cleavage: dipping; vertical.

Strike and dip of schistosity or metamorphic foliation: dipping; vertical.

Direction and plunge of hinge line of minor folds: unspecified age; folding, cleavage or schistosity.

Strike and dip of igneous mineral foliation: dipping; vertical; trend of foliation trace on horizontal surface.

Geological boundary.

Fault.

Wrench fault with relative displacement indicated.

Concealed fault.

Fault with relative downthrown side indicated.

Thrust or reverse fault, teeth on upper plate.

Axial trace of major antiform.

Axial trace of major synform.

WESTERN TASMANIA

Angular unconformity.

EARLY DEVONIAN - SILURIAN — SD, SDb, SDf, SDa, SDc — ELDON GROUP, TIGER RANGE GROUP

ORDOVICIAN — Ol, €Ou, €Ouc, €Ol, €Oh, €O, €On, €Os — DENISON GROUP, OWEN GROUP & CORRELATES

WURAWINA SUPERGROUP

Angular unconformity in some areas, apparent conformity in others.

MIDDLE CAMBRIAN — €dsv, €a, €as, €aq, €ac

WEST OF THE TAMAR RIVER

Angular unconformity.

SDb — *Undifferentiated shallow marine quartz sandstone, siltstone and shale* (SD); *siltstone, shale and fine-grained sandstone* (SDb).

Shallow marine quartz sandstone (SDf).

Siltstone, shale and minor quartz sandstone (SDa).

Faulted Contacts

Shallow marine quartz sandstone and pebbly conglomerate (SDc).

Ol — *Dominantly shallow marine limestone with minor siltstone and sandstone (Gordon Group)* (Ol).

€Ou, €Ouc — *Undifferentiated or poorly constrained conglomerate sequences* (€O). *Undifferentiated or poorly constrained, dominantly quartz sandstone sequences with rare fossils* (€Ou). *Dominantly calcareous sandstone and siltstone* (€Ouc). *Thin bedded quartz sandstone, siltstone and minor conglomerate* (€Ol). *Dominantly thick bedded siliceous conglomerate* (€Oh). *Dominantly marine sandstone, micaceous siltstone and minor conglomerate* (€On). *Dominantly siliceous conglomerate and pebble sandstone near Queenstown; dominantly quartzwacke turbidite and minor conglomerate near Adamsfield* (€On).

WURAWINA SUPERGROUP

Angular unconformity.

€ds, €da, €dsv — *Undifferentiated conglomerate - sandstone sequences* (€a). *Dominantly conglomerate and lithic sandstone* (€as). *Dominantly quartzwacke and lithicwacke turbidite with rare fossils in some sequences* (€aq). *Dominantly siliceous conglomerate and sandstone* (€ac). *Dominantly sedimentary sequences with minor volcanic material* (€ds); *some dominantly andesitic volcanics indicated* (€da); *dominantly felsic volcanosedimentary sequences* (€dsv).

Angular unconformity.

Ptp, Pts — *Undifferentiated metasedimentary sequences, with greenschist facies metamorphism* (Pt). *Dominantly quartzite sequences* (Pts). *Platy or schistose micaceous quartzite* (Ptsl). *Garnetiferous quartzite* (Ptsg).

Dominantly pelitic sequences, mainly phyllite (Ptp).

Dolomite (Ptd).

EAST OF THE TAMAR RIVER

Angular unconformity.

OD, ODq, ODp — MATHINNA GROUP — *Early Ordovician to Early Devonian micaceous quartzwacke turbiditic sequences* (ODq); *mudstone sequences* (ODp).

Pdv — *Mafic volcanoclastic rocks* (Pdv).

PROTEROZOIC

Pt — Pts, Ptsl, Ptsg, Ptp, Ptd

Modified from: McClenaghan, M. P. & Calver, C. R. (1994), Calver, C. R., Corbett, K. D., Everard, J. L., Goscombe, B. A. Pemberton, J & Seymour, D. B. (1995), Forsyth, S. M., Clarke, M. J., Calver, C. R., McClenaghan, M. P. & Corbett, K. D. (1995), Brown, A. V., Calver, C. R., Corbett, K. D., Forsyth, S. M., Goscombe, B. A., Green, G. R., McClenaghan, M. P., Pemberton, J. & Seymour, D. B. (1995).

To date the only hydrocarbons recovered from onshore Tasmania have been produced from the retorting of oil shale. Small deposits of Late Carboniferous Tasmanite Oil Shale have been mined intermittently in northern Tasmania since the 1860's. A variety of fuels and fuel products were retorted during the 1930's, without long term commercial success as the high production costs and high sulphur content made these products uncompetitive with imported oil.

Since 1915, over 200 licenses have been issued to search for oil and gas in Tasmania. Historically, exploration was been driven by reports of bitumen strandings and oil and gas seeps. Over 130 reports of seeps have been registered, the majority caused by agents other than naturally occurring hydrocarbons. Only one example, the seep at Lonnavale in southern Tasmania, has been confirmed as migrated hydrocarbons generated by a Tasmanian source. Over 40 holes have been drilled in the search for oil and gas, most drilled in the vicinity of seeps without detailed knowledge of stratigraphy or structure. Most of these wells were shallow, generally less then 350 m deep and bottom in Jurassic Dolerite.

The peak in exploration activity occurred in the 1920's when the Commonwealth Government offered a £10 000 reward for the discovery of a payable oil deposit anywhere in Australia. This led to a number of holes being drilled in northern Tasmania. Gas was reported at 350 m in Bore 8 drilled near Sassafras by the Adelaide Oil Exploration Company (Bacon et al., 2000), however exploration was generally unsuccessful and the individuals and companies involved eventually turned their attention to oil-bearing substances such as oil shale and "Pelionite".

By the late 1920's interest had faded, exploration was limited and only two holes, one at Bruny Island and another near Launceston were drilled over the next forty years. The next major phase of exploration began in 1965 when Esso Australia, the Nudec Petroleum Exploration Company and the Electrolytic Zinc Company explored the north, west and southwest coasts and south-western Tasmania without success (Lucarelli, 1965, Bacon et al., 2000). In 1966, Mr C. G. Sulzberger imported a drilling rig from Gippsland and from 1967 to 1974 he drilled eight wells ranging in depth from 50 to 831 m in northern Tasmania (Bacon et al., 2000). All were dry, bottoming in dolerite. In 1974 the Amoco Australia Petroleum Company explored the Macquarie Harbour Graben in western Tasmania. Concluding the area was unprospective they relinquishing the ground in 1975 (Bacon et al., 2000). Meekatharra Minerals Ltd, held several licences in eastern Tasmania between 1978

and 1981 (Bacon et al., 2000). Interested in the Tertiary sequences they acquired gravity and seismic data, however, their interpretations indicated the thicknesses were insufficient to have generated hydrocarbons from any basal Tertiary sequence (Shaw, 1985).

Since 1984, GSLM and its predecessors have held several licenses in Tasmania. These companies have carried out numerous geochemical analyses on source rocks, seeps, tars and bitumens, acquired significant quantities of infill gravity and reconnaissance magnetic data over southern Tasmania and an experimental reflection seismic survey was conducted on North Bruny Island in 1987. From 1997, GSLM has acquired 662 line kilometres of seismic data in the TB01 survey and completed over 6000m of drilling a 8 locations including the stratigraphic holes on North Bruny Island (Shittim 1, 1751 m in 1997) and the Central Highlands (Hunterston 1, 1324 m in 2002). Initially, their exploration concentrated on oil generated from the Gordon Group. However, from their work two petroleum system concepts have evolved: a Larapintine Petroleum System in the Ordovician to Devonian Wurawina Supergroup and a Gondwana Petroleum System in the Permo-Triassic Parmeener Supergroup.

The generally poor exploration results achieved thus far suggest that onshore Tasmania is indeed unprospective. However as many wells have been drilled without any knowledge of stratigraphy or subsurface structure, such results are not surprising. In addition to Bore 8 at Sassafras, gas has also been reported from two holes drilled by the Department of Mines at Conara in 1963 and 1990. All these holes were drilled in Tertiary sediments and the gas is speculated to have originated from bands of decomposing vegetable matter (Bacon et al., 2000). Gas was also reported from another Mines Department hole at Douglas River, however analysis indicated the methane was biogenic. Methane and C_2-C_6 hydrocarbons, hydrogen and helium have been detected in varying quantities from cuttings in the GSLM wells Shittim 1 and Jericho 1 drilled on Bruny Island and at Lonnavale 1 and Pelham 1 drilled in southern Tasmania (Burrett and Tanner, 1997).

1.6: PREVIOUS WORK

Tasmania is covered by 1:250 000 scale geological mapping, while about half of the island is covered by more detailed 1:50 000 and 1:63 360 maps with much of the structural interpretation contained in the explanatory notes accompanying these maps. The Tasmanian stratigraphy is well understood, as is the structure of Pre-Tasmania Basin rocks. The Geology and Mineral Resources of Tasmania (Burrett and Martin, 1989) presents an comprehensive

stratigraphic summary of the Parmeener Supergroup (Banks, 1989a, Clarke, 1989, Forsyth, 1989b). Whether because of ubiquitous dolerite outcrop, a lack interest by minerals and hydrocarbon explorers or both, the previous analysis of structures affecting the Tasmania Basin has generally been concentrated on the Launceston Tertiary Basin and the Tertiary grabens in southern of Tasmania. This section aims to present the previous work relating primarily to the structures affecting the Tasmania Basin, other work directly related to the analysis of the Digital Elevation Model and acquisition of seismic data is presented in Chapters 4 and 5.

In northern Tasmania, Johnston (1874) used the name Launceston Tertiary Basin to describe the trough containing Tertiary sediments, which he interpreted as a Tertiary rift. A detailed structural study was made by Carey (1947), who concluded the rift consisted of two, Early Miocene graben separated by a central horst and that both the Tiers and Mt Arnon were pre- to syn-dolerite, i.e. Middle Jurassic or older.

The later structural interpretations in northern Tasmania are based on mapping and gravity data. Hinch (1965) was the first to conduct a gravity survey in the Cressy Area, interpreting two half-graben divided by a central horst. He concluded that faulting had begun in the Jurassic and continued through to the Tertiary when the grabens developed. Longman (1966) and Longman and Leaman (1971) generally agree with this model, while Mathews (1983) interprets a more symmetrical graben structure. All these workers agree that the major basin bounding faults have a Jurassic history, while the major faults within the basin were formed during the Tertiary.

In the Longford Sub-basin region, Direen (1995) integrated potential field data and a regional stratigraphic analysis, interpreting a complex fault history. He concluded the major faults underlying the Tertiary section were at least Middle Jurassic age and were all reactivated in the Albian or Palaeocene to form the basin. He also interpreted several Late Eocene faults. Given the control on Devonian thrusting he concluded the Tiers Fault is probably pre Devonian. He interpreted the basin geometry as neither a simple graben nor half-graben, but rather an asymmetric depression developed on multiple blocks, most with half-graben rotation.

Using newly acquired seismic data Lane (2002) concluded the Longford Sub-basin comprised a graben in the west and a half-graben in the east, separated by a central high along strike from Hummocky Hills. The basin was formed by Tertiary extension creating major northwest striking faults and minor northeast striking faults, which compartmentalise the basin. The western graben is interpreted to have formed first followed by the eastern half-graben.

Mapping commissioned by the Hydro-Electric Commission of Tasmania in the late 1940's in the Central Highlands region is the first systematic evaluation of the geology and structure of the Tasmania Basin in this area. The Parmeener Supergroup in the areas around Great Lake, Arthur's and Lake River was interpreted as flat-lying, broken up by steep normal faults of Early Miocene age (Voisey, 1948a, Voisey, 1948b). Fairbridge (1948) completed a more complex interpretation for the area around Waddamana, producing a cross-section showing tilting, steep normal and reverse faulting and folding of the Parmeener Supergroup and Jurassic Dolerite. The faults were interpreted to have both a pre- and post-dolerite history (Fairbridge, 1948).

Extensive, geological mapping by MRT and its predecessors from the mid 1960's to the mid 1980's in northern and central Tasmania confirms the Parmeener Supergroup is generally flat-lying throughout the region and has been affected by two major phases of faulting, one pre-dolerite and a later Cretaceous to Tertiary phase. The authors all recognised faults with pre-dolerite movement, faults that were truncated by or intruded by sills, they also recognised faults which offset the dolerite sills (Longman, 1966, Pike et al., 1973b, Leaman, 1976, Forsyth, 1984, Mathews et al., 1996, Pike et al., 1973a, Forsyth et al., 1989).

In the Hobart area of southern Tasmania, Leaman (1971, 1972 and 1976), concluded major structures (Derwent and Coal River Grabens) resulted from Jurassic faulting, which was probably contemporaneous with the intrusion of dolerite. These structures were overprinted later by faulting mainly of Tertiary age. There is evidence of faults active before the mid-Jurassic intrusion of dolerite affecting the Parmeener Supergroup in southern Tasmania. By far the best example is the strong transpressional zone along the Maydena-National Park corridor. This zone has the appearance of a dextral positive flower structure and is truncated at the eastern end by a major dolerite dyke (Dunster, 1981). From fault striations measured in the Hobart region, Berry and Banks (1985) developed numerical models of the regional stress systems. From these models they concluded the area was affected by a major north-northwest compressional event that produced strike-slip striking 100° and 170° and reverse faults

striking northeast. This event was active before and after the Middle Jurassic dolerite intrusion. The models also indicate a subsequent phase of faulting produced by east to northeast extension in the early to middle Tertiary.

In summary, from numerous, well distributed studies the majority of workers report the Parmeener Supergroup as flat-lying with steep dips only occurring locally in the vicinity of faults. They also generally agree that the sequence has been affected by at least two major phases of faulting. The first occurring either prior to or concomitant with the intrusion of dolerite in the Middle Jurassic and resulting in normal, reverse and strike-slip movement, and the second in the Tertiary resulting in down to the east, normal faulting.

1.7: THESIS STRUCTURE

This thesis comprises eight chapters, two appendices and a series of maps and interpreted seismic sections in a separate map folder.

Chapter 1 is a general introduction to this work. It contains a background and states the reasons for and aims of this research. A description of the datasets, resources and tools utilised, an exploration history and an account of previous structural interpretations.

In Chapter 2, a detailed account of the regional geology is presented. This account includes new work on the Tasmania Basin which places the basin into its Gondwana context. The position of the basin in Gondwana and its relationship to adjacent basins is shown, with a new model for the basin presented. A summary of the stratigraphy of the Tasmania Basin has been undertaken. The stratigraphy and stratigraphic names vary across the basin and a detailed understanding is required to integrate stratigraphic data of different sources and vintage into a basin wide interpretation. This account is detailed and shows how the numerous stratigraphic units can be brought together in a simplified stratigraphic nomenclature that is applied to the entire basin.

A summary of the current knowledge regarding the petroleum geology of onshore Tasmania is presented in Chapter 3. The Gondwana and Larapintine Petroleum Systems predicted for onshore Tasmania are described, as is the maturation, migration and generative potential of both systems. This chapter serves as background to future discussions in this thesis regarding the implications of the structural history of the hydrocarbon potential.

Chapter 4 describes the use of high resolution Digital Elevation Model (DEM) with state-wide coverage to predict the pattern of Tertiary faulting in the Tasmania Basin. The resultant fault pattern is then used to make predictions regarding the nature of structures in the basement, especially in the region of the Tamar Fracture System. The DEM has been an important constraint to the seismic interpretation.

Chapters 5, 6 and 7 are concerned with the interpretation of the seismic dataset. The nature of the dataset and the methodology employed to interpret it, is outlined in Chapter 5. This chapter includes information on acquisition and processing, and suggestions as to why there is such variability in seismic data quality. The chapter also contains a description of the stratigraphic controls and constraints applied to the interpretation, including the results of a velocity survey undertaken as part of this research. Finally, Chapter 5 contains a thorough description of the nomenclature used in the seismic interpretation.

Chapter 6 is a detailed description of the seismic interpretation. The level of detail presented here is a reflection of the quality of the seismic data and the care taken during the interpretation process. This chapter aims to show the reasoning and constraint applied to the interpretation, especially in the many areas where the seismic data is ambiguous.

In Chapter 7 the results of the seismic interpretation are presented. The distribution and history of fault and fold generation in the Tertiary and Tasmania basins is described, while the basement is described in terms of three structural domains. The geometries of the Longford Sub-basin and Tasmania Basin derived from the seismic interpretation are compared with previous interpretations that were primarily based on outcrop and drill-hole data. Dolerite is recognised on all of the seismic sections and the intrusion geometry is described. Finally, the structures interpreted are described in terms of petroleum geology, i.e. the style of potential hydrocarbon traps and their distribution.

The overall conclusions are presented in Chapter 8, these include the model for the Tasmania Basin, the structural history of Tasmania and the implications of the structural history for the petroleum prospectivity of onshore Tasmania.

CHAPTER 2:
REGIONAL GEOLOGY

2.1: INTRODUCTION

The ?Mesoproterozoic basement of Tasmania is overlain by a Neoproterozoic passive margin sequence. Deposition was interrupted by a major Cambrian arc-continent collision. Ordovician to early Devonian, shallow-water sedimentation dominated across the Western Tasmanian Terrane, while a turbidite succession built rapidly across eastern Tasmania (Eastern Tasmania Terrane).

The eroded vestiges of the Late Carboniferous to Triassic Tasmania Basin cover approximately half of Tasmania. The Late Carboniferous to Early Permian Lower Parmeener Supergroup consists largely of glaciomarine sediments overlain by Triassic non-marine sandstones and coal measures of the Upper Parmeener Supergroup. Large volumes of tholeiitic dolerite intruded the Tasmania during the Middle Jurassic mainly as sills in the Parmeener Supergroup.

The Sorell, Bass and Durroon basins were initiated in the latest Jurassic to Early Cretaceous by extension related to rifting between Australia and Antarctica. By the Late Cretaceous, spreading had begun in the Tasman Sea. The Bass Basin continued to propagate southwards, extending onshore, opening the Tamar Graben in the latest Cretaceous, the Devonport-Port Sorell Sub-basin in the Early Paleocene, and the Longford Sub-basin in the Late Paleocene. On the west coast, the Sorell Basin extended onshore with the development of the Macquarie Harbour Graben in the Late Paleocene. During the Late Paleocene-Early Eocene, Tasmania was moving north along a left-lateral transform against Northern Victoria Land. In the Eocene, Australian-Antarctic motion became more divergent along this margin (Royer and Rollet, 1997) and the most active extension migrated to the Derwent and Coal River Graben.

2.2: PROTEROZOIC

Zircon inheritance in granites on King Island demonstrates that the basement of the Western Tasmania Terrane is 1600 Ma old (Black et al., 2004a), although the western King Island section may be an allochthonous element with no relationship to the larger scale history of Tasmania. The Eastern Tasmania Terrane did not exist at this stage and Black et al. (2004) identified the lower crust as less than 1000 million years old.

The early Neoproterozoic stratigraphy of northwest Tasmania is dominated by shallow water siliciclastics (Rocky Cape Group in the north west, Clark Group in the south) and turbidites (Burnie and Oonah Formations, Badger Head Block in the north) (Seymour and Calver, 1995). The age of these units is poorly constrained. The internal stratigraphy of the early Neoproterozoic siliciclastic sequences varies dramatically. In the northwest there are three basic facies varying from deep shelf through storm dominated shelf to massive quartzite deposited above fair weather wave base. The Clark Group includes similar shallow marine orthoquartzite units but has more carbonate units (Seymour and Calver, 1995). The deep-water facies (Burnie and Oonah Formations) shallow up from classical turbidites to storm-affected siliciclastics and carbonates.

A second extensional phase followed in the late Neoproterozoic, and possibly started as early as 740 Ma (Adams et al., 1985, Calver and Walter, 2000). The base of the late Neoproterozoic section is a regional-scale low angle (20˚) unconformity (Calver, 1998). A more intense deformation (Wickham Orogeny) is recorded from King Island where there was polyphase deformation and extensive granitoid intrusion at about 760 Ma (Cox, 1989, Turner et al., 1998). The granites have intensely deformed aureoles, but are not linked to any larger scale deformation features and may be related to rifting and the break-up of Rodinia (Holm et al., 2003). The Wickham Orogeny may correlate with the low angle unconformity observed on mainland Tasmania.

The late Neoproterozoic rift sequence (e.g. Togari Group in northwest Tasmania) has an initial siliciclastic shallow water section, followed by a lower dolomite and diamictite. Subsequent widespread intrusion of tholeiitic dolerite dykes (Rocky Cape dyke swarm), extrusion of tholeiitic basalt and associated volcanogenic sediments were followed by a second dolomite section and finally marine siliciclastics (Brown, 1989, Turner, 1989, Crawford and Berry, 1992, Calver and Walter, 2000). The most complete example of the late

Neoproterozoic rift sequence is in northwest Tasmania, and elsewhere only parts of the section are known (Seymour and Calver, 1995, Calver, 1998). Calver & Walter (2000) correlated the early dolomite with the Sturtian glaciation and the later dolomite with the Marinoan glaciation. The late Neoproterozoic sequence is interpreted as a rift-drift facies associated with the break-up of Rodinia (Crawford and Berry, 1992) or a second stage rift event (Direen and Crawford, 2003).

The Neoproterozoic sequence in Tasmania has largely been considered "unmetamorphosed", but detailed petrographic descriptions of the basalt commonly include pumpellyite and to a lesser extent prehnite. These units are best regarded as very low-grade metamorphic rocks. The age of this metamorphism is problematic. No structural model developed so far explains the inferred depth of burial (~10 km) of these rocks during either the Cambrian or the Devonian orogeny.

2.3: EARLY TO MIDDLE CAMBRIAN

The Tyennan Orogeny in Tasmania was a complex event. The locus and style of deformation changed very rapidly. At 520 Ma, Tasmania collided with an oceanic arc, and major slices of fore-arc lithologies were thrust over the Proterozoic sedimentary rocks. The only allochthonous element specifically identified by Berry & Crawford (1988) was the mafic/ultramafic complexes. Other possible allochthonous elements identified since are the Forth, Badger Head, Port Davey, Franklin, Mersey River and Arthur Metamorphic Complexes (Meffre et al., 2000), and the Wings Sandstone (Black et al., 2004a). These blocks are scattered across Tasmania lying structurally above the late Neoproterozoic rift facies and are unconformably overlain by late Middle Cambrian and younger sedimentary rocks. The Arthur Lineament was formed during the Tyennan Orogeny (Turner et al., 1998), but its tectonic significance remains in doubt (Turner, 1989, Holm and Berry, 2002). This lineament forms the western limit to allochthonous blocks in Tasmania and appears to mark the maximum extent of the thrust complex. The early part of the thrust emplacement is recorded in high temperature mylonites, and indicates thrusting towards the west (Berry 1989b). A major phase of thrusting to the south is recorded in the amphibolite facies metamorphic rocks and widespread cataclasites in western Tasmania (Berry et al., 1990, Findlay and Brown, 1992, Findlay, 1993, Holm and Berry, 2002) and is interpreted as a second component of the obduction process.

The second stage of the Tyennan Orogeny was a Middle Cambrian extensional event that produced rapid subsidence, active syn-orogenic deposition and major post-collisional felsic-dominated volcanism (Mt Read Volcanics). East-west extension is recorded in the hydrothermal vein geometry and the Henty dyke swarm. The extensional phase was closely followed, or may be coincident with, a north-south compressional event that produced east-west-trending folds to the east of the Mt Read Volcanics.

Most of the folding in the Neoproterozoic rocks in Tasmania is correlated with the Tyennan Orogeny. Two generations of early recumbent folding are recognised in allochthonous blocks and high strain underlying elements. These are overprinted by upright north-south (e.g. northwest Tasmania) or east-west (e.g. Tyennan block) folding and related high angle reverse faults. West of the Arthur Lineament, upright folding and thrusting dominated the Proterozoic (Seymour and Calver, 1995). The allochthonous units are scattered across the rest of Tasmania and overly a variably deformed Neoproterozoic section.

2.4: LATE CAMBRIAN TO EARLY DEVONIAN

2.4.1: WURAWINA SUPERGROUP

In the Late Cambrian, the last phase of the Tyennan Orogeny inverted earlier extensional faults (e.g. Henty Fault). Major reverse faults and upright, open, north trending folds were formed in western Tasmania. This phase also caused uplift of the Tyennan block with syn-orogenic sediments (Owen Conglomerate) accumulating in synclinal cores and other structural depressions (Berry, 1994).

Following the Late Cambrian basin inversion western Tasmania was peneplained and a new cycle of deposition began in the Middle Ordovician. This cycle has a thin basal sheet sand followed by widespread intertidal to shallow marine tropical carbonate (Gordon Group) that is overlain by a Silurian to Early Devonian shallow marine siliciclastic sequence (Tiger Range Group) (Banks, 1989b).

2.4.2: MATHINNA SUPERGROUP

The Mathinna Supergroup was deposited in northeast Tasmania. The earliest unit, Stoney Head Sandstone, is a proximal turbidite and is overlain by Middle Ordovician deep-water mudstone unit. The Silurian and Early Devonian section is a highly variable turbidite section with rapid facies variations, derived from a quartzose, cratonic source to the southwest

(Baillie et al., 1989a). However, detrital zircon dating indicates this source was not the Western Tasmania Terrane (Black et al., 2004b).

2.5: MIDDLE DEVONIAN TO LATE CARBONIFEROUS

Middle Devonian deformation (Tabberabberan Orogeny) (390 Ma: Black et al. 2004b) is characterised by the complexity of fold orientations. In many areas, the fold geometry is controlled by the Cambrian fold trends, which tightened during the Devonian (Figure 2.1). This led to Devonian cleavage orientations that are not parallel to the axial plane of the folds with which they are associated. In the north, east-west Cambrian folds were tightened. In the west, north trending Cambrian folds were tightened with an associated north-northwest-striking Devonian cleavage. North-northeast-trending folds, north of Tullah, are controlled by the reactivation of the Henty Fault. This region acted as a transfer zone in the Devonian and the north-northeast fold trend is probably a rotated north-trending Cambrian trend.

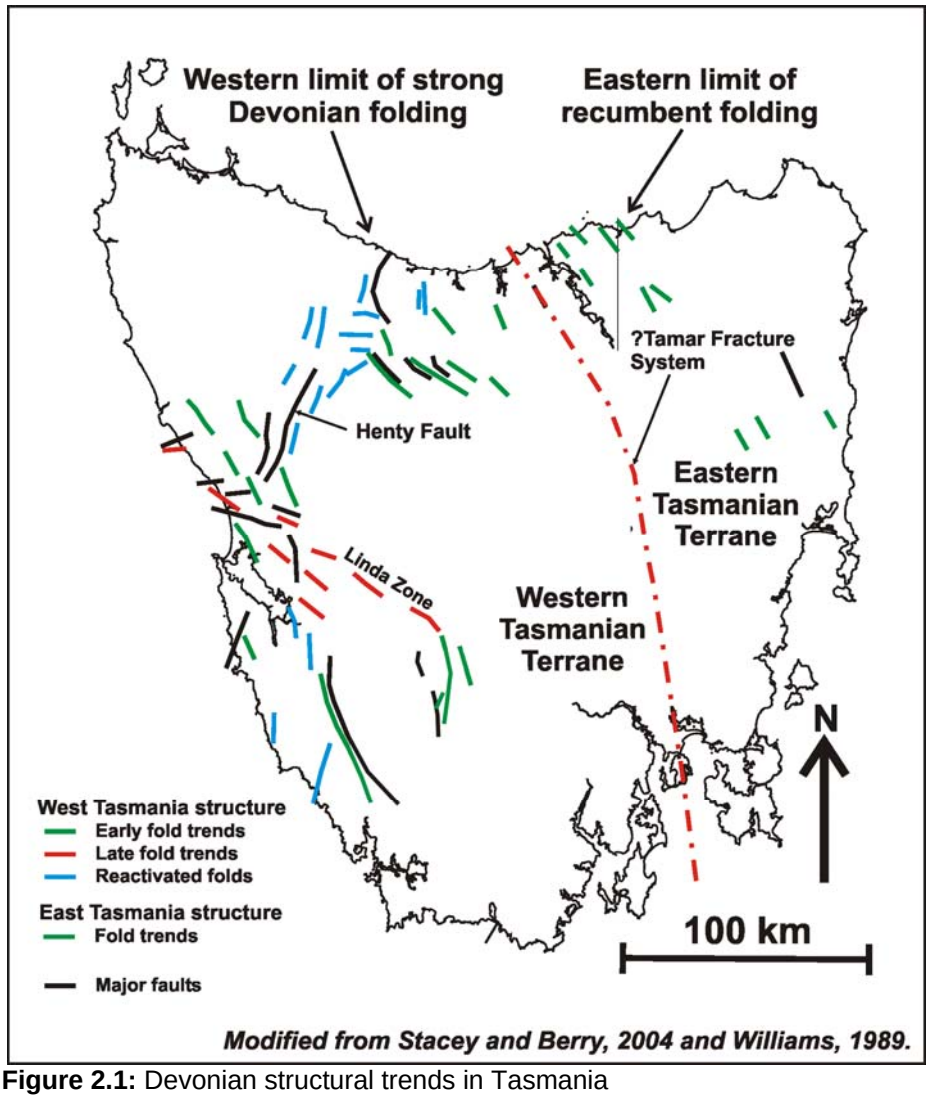

Figure 2.1: Devonian structural trends in Tasmania

The subsequent north- to north-northeast-trending compression produced west-northwest-trending folds and thrusts in the south, and northwest-striking thrusts and associated folds in the north. On the west coast, there is an associated phase of brittle strike slip faulting dominated by north-northeast-striking sinistral movement on the Henty Fault (Berry, 1989a).

In northeast Tasmania, the early phase of deformation thrust the shallow-water West Tasmania stratigraphy east across the deep-water section with recumbent folds in the Georgetown area. This was followed by back thrusting, especially strong in the Beaconsfield zone. A late stage of north-trending compression produced strike slip movement on some faults and large-scale kinks (Goscombe et al., 1994).

The regional metamorphic grade associated with the Devonian orogeny is prehnite-pumpellyite with local zones of greenschist facies in the vicinity of late syn- to post-orogenic granites. Areas of very low grade metamorphism survive in the Western Tasmania Terrane at Surprise Bay (Burrett, 1992) and in the Mathinna Supergroup on the far east coast at Scamander (Patison et al., 2001).

Large-scale granitoid intrusion in northeast Tasmania started before the Devonian deformation and continued after (400-380 Ma). The more restricted granite intrusions scattered throughout western Tasmania and King Island, post-date peak deformation (375-350 Ma: Black et al. 2004b).

2.5.1: TABBERABBERAN OROGENY AND THE TAMAR FRACTURE SYSTEM

Deposition of the Early Ordovician to Early Devonian Mathinna Supergroup in eastern Tasmania was approximately coeval with the deposition of the Wurawina Supergroup in western Tasmania (Seymour et al., 2006). The Mathinna Supergroup comprises turbiditic sandstone and mudstone deposited in deepwater, while the Wurawina Supergroup comprises shallow marine carbonates and siliciclastics. Folds in northeast Tasmania verge northeast, while west of the Tamar Valley Devonian folds in the Sheffield Element verge southwest (Williams, 1979, Williams, 1989, Seymour and Calver, 1995). Furthermore, the age of granitoid intrusions in the is are generally younger than those of the granitoid batholiths in the east (Williams et al., 1989). Current models suggest that eastern and western Tasmania may have been substantially separated at the time of deposition of these two units (Seymour et al., 2006).

During the Tabberabberan Orogeny the Western and Eastern Tasmania Terranes were amalgamated along an interpreted major crustal dislocation known as the Tamar Fracture System (Williams, 1979, Williams, 1989). The proposed suture is roughly coincident with the axis of the Launceston Tertiary Basin in northern Tasmania, the distribution of contrasting rock types continues to the south southeast, indicating the structure passes between Hobart and Maria Island (Figure 2.1).

The geological evidence for the Tamar Fracture System is however somewhat circumstantial. The boundary between the two terranes is nowhere exposed, concealed beneath a 20 km wide strip of the Tasmania Basin and younger cover in the Tamar Valley and by the Tasmania Basin to the south-southeast. A major, crustal scale boundary should be geophysically visible; however there is little convincing geophysical evidence for the existence of such a boundary (Leaman, 1994). A conductivity anomaly has been reported coinciding with the proposed Tamar Fracture System in the Tamar Valley and extending southwards to Maria Island (Parkinson and Hermanto, 1986, Parkinson et al., 1988, Parkinson and Richardson, 1989).

2.6: LATE CARBONIFEROUS TO LATE TRIASSIC

2.6.1: TASMANIA BASIN

The Tasmania Basin contains both marine and non-marine sedimentary rocks deposited from the Late Carboniferous to the Late Triassic and known as the Parmeener Supergroup (after Mount Parmeener, 447 540 mE, 5 388 990 mN) (Banks, 1973). The sequence is generally flat-lying and approximately 1.5 km thick in the deepest parts of the basin, lying with pronounced unconformity on Late Devonian granites and older folded rocks. The unconformity surface has a relief of approximately 1000 m (Banks, 1989a). The thickest parts of the basin are thought to be coincident with zones of structural weakness in the basement, such as the Tamar Fracture System, the Linda Disturbance and the Arthur Lineament (Banks and Clarke, 1987, Clarke, 1989). Large volumes of tholeiitic dolerite intruded the Tasmania Basin during the Middle Jurassic and occur mainly as sills. The Tasmania Basin currently covers an area greater than 30,000 km^2 (Figure 2.2), and is best preserved in northern and south-eastern Tasmania, often capped and protected from erosion by thick dolerite sills. The present basin margins are erosional, rather than depositional, indicating the basin was once much larger (Bacon et al., 2000).

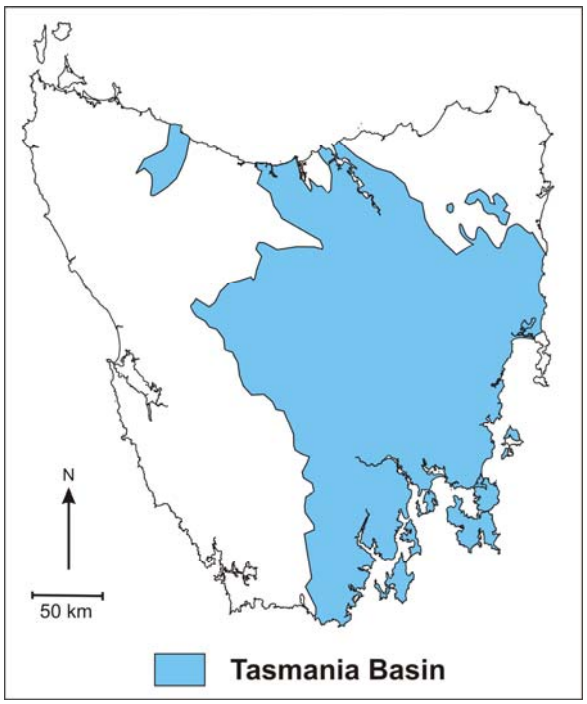

Figure 2.2: Current extent of the Tasmania Basin

Tectonic setting and basin style

Until its break-up at 95 ± 5 Ma, Tasmania and Antarctica were united as part of Gondwana for at least 500 million years. The Late Carboniferous to Late Triassic Tasmania Basin was developed 500 to 1000 km inboard of a convergent plate boundary that stretched over 10 000 km along the Panthalassan margin of Gondwana from western Argentina to northern Queensland (Figure 2.3).

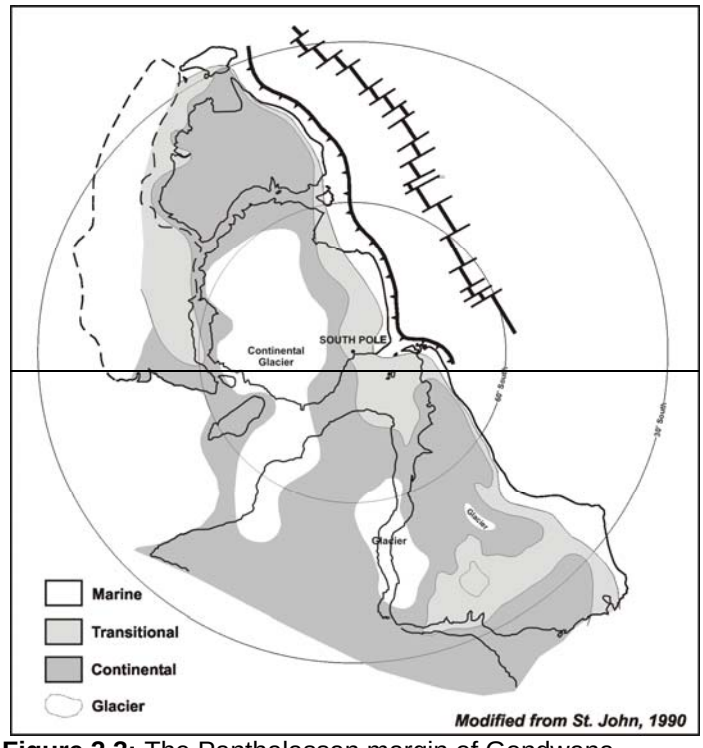

Figure 2.3: The Panthalassan margin of Gondwana

The Tasmania Basin has been variously labelled a sag basin (Veevers, 1984), a foreland basin (Collinson et al., 1987) or a continental margin ("pericratonic") basin (Stacey and Berry, 2004). The accumulation of 1.5 km of sediment in 100 m.y. is an order of magnitude slower than classic foreland basins (Schwab, 1986). There is evidence for minor normal faulting early in the basin history, but the limited nature of such faulting and the relatively slow sediment accumulation rate is not typical of rift basins. In reconstructions of Gondwana, Tasmania is juxtaposed against Northern Victoria Land (Figure 2.4). Collinson et al. (1994) describes the development of an extensive foreland basin system along the Antarctic sector of the Panthalassan margin from the Late Carboniferous to Triassic; the most distal part of this system is a shallow, 200 – 300 km wide, epi-cratonic basin, developed in Victoria Land (Figure 2.5). DeCelles and Giles (1996) define foreland basin systems in terms four discrete depozones, the wedge-top, foredeep, forebulge, and back-bulge (Figure 2.5). Comparison of the orogen normal cross-section (Collinson et al., 1994) and the schematic cross-section for a foreland basin system (DeCelles and Giles, 1996), shows that the features of idealised system correspond extremely well with the features of the Transantarctic Basin, with the Victoria epi-cratonic sub-basin (Victoria Land Basin) corresponding to the back-bulge depozone (Figure 2.5). The sedimentary package of back-bulge depozones is relatively thin in comparison to the foredeep depozone (Figure 2.5), and comprises sediment which accumulates in a shallow, broad zone on the cratonward side of the forebulge (Figure 2.5) (DeCelles and Giles, 1996). Subsidence due to loading at the continental margin is not significant this far inboard of the margin. However, subducting oceanic slabs have been shown to cause rapid subsidence and uplift in the overriding continental plate more than 1000 km from the trench (Mitrovica et al., 1989, Gurnis, 1992).

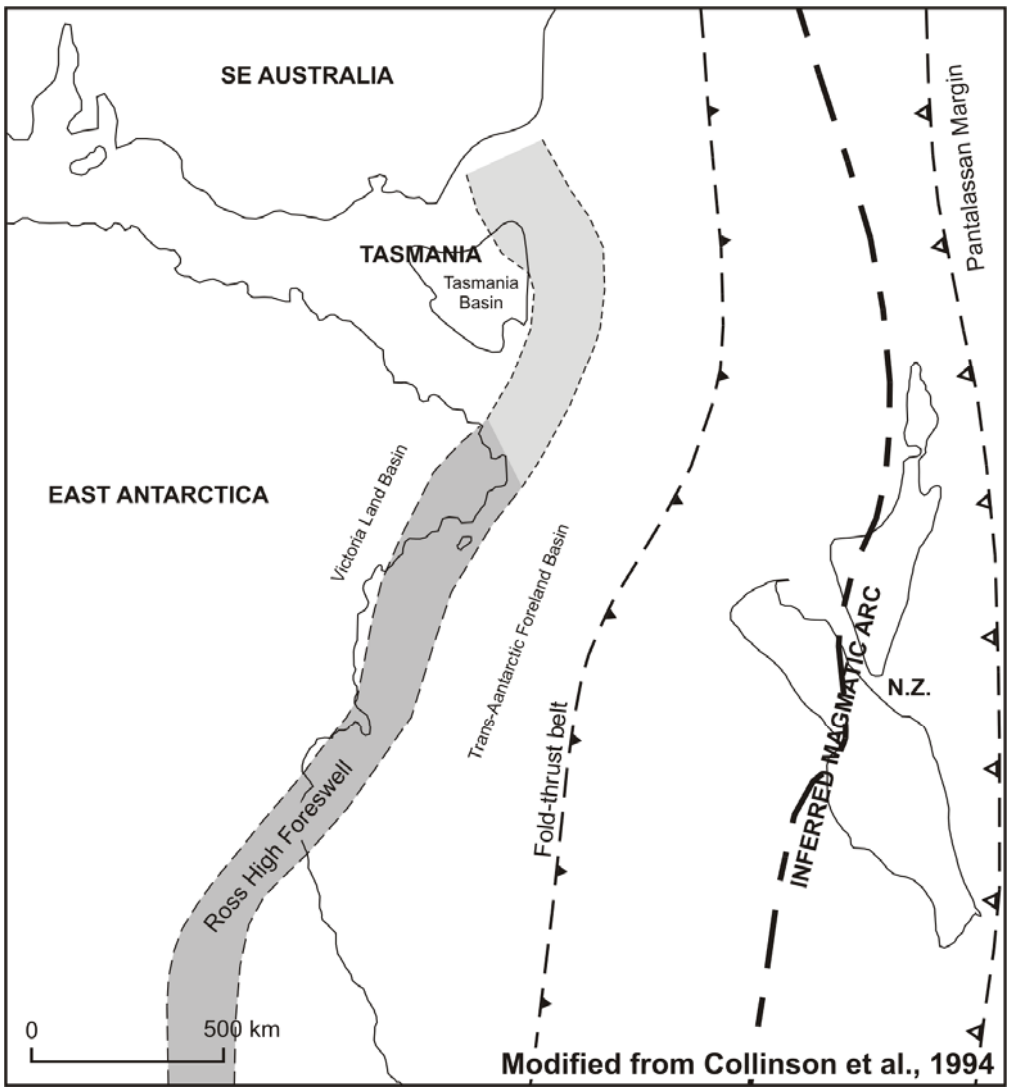

Figure 2.4: The Panthalassan margin between Australia and Antarctica

The tectonic development and depositional history of the Late Carboniferous to basins in Late Triassic Victoria Land and Tasmania are similar. Veevers (2000) describes the development of the Panthalassan margin between the Late Carboniferous and Triassic in terms of seven stages. Stage A (Late Carboniferous to Early Permian) involved extension across the platform after the amalgamation of Pangea, with the easternmost parts of Australia subjected to dextral transtension and widespread volcanism (Veevers, 2000c). Extension resulted in the widespread deposition of glacigenic sediments across Gondwana. In the Tasmania Basin isostatic loading by ice resulted in the initial deposition of diamictites in glacial valleys, fiords and in topographic lows, followed by mudstone, siltstone and sandstone of the Lower Marine sequence of the Lower Parmeener Supergroup (Banks and Clarke, 1987, Clarke, 1989, Hand, 1993). Meanwhile, in the Victoria Land Basin the terrestrial Darwin, Metschel Tillite (Barrett and McKelvey, 1981) and a 350 m thick unnamed diamictite deposited in subaerial to shallow marine conditions east of the Rennick Glacier (Laird and Bradshaw, 1981) are preserved in glacial valleys (Collinson et al., 1994).

A. Schematic cross-section of a foreland basin system (Modified from DeCelles and Giles, 1996)

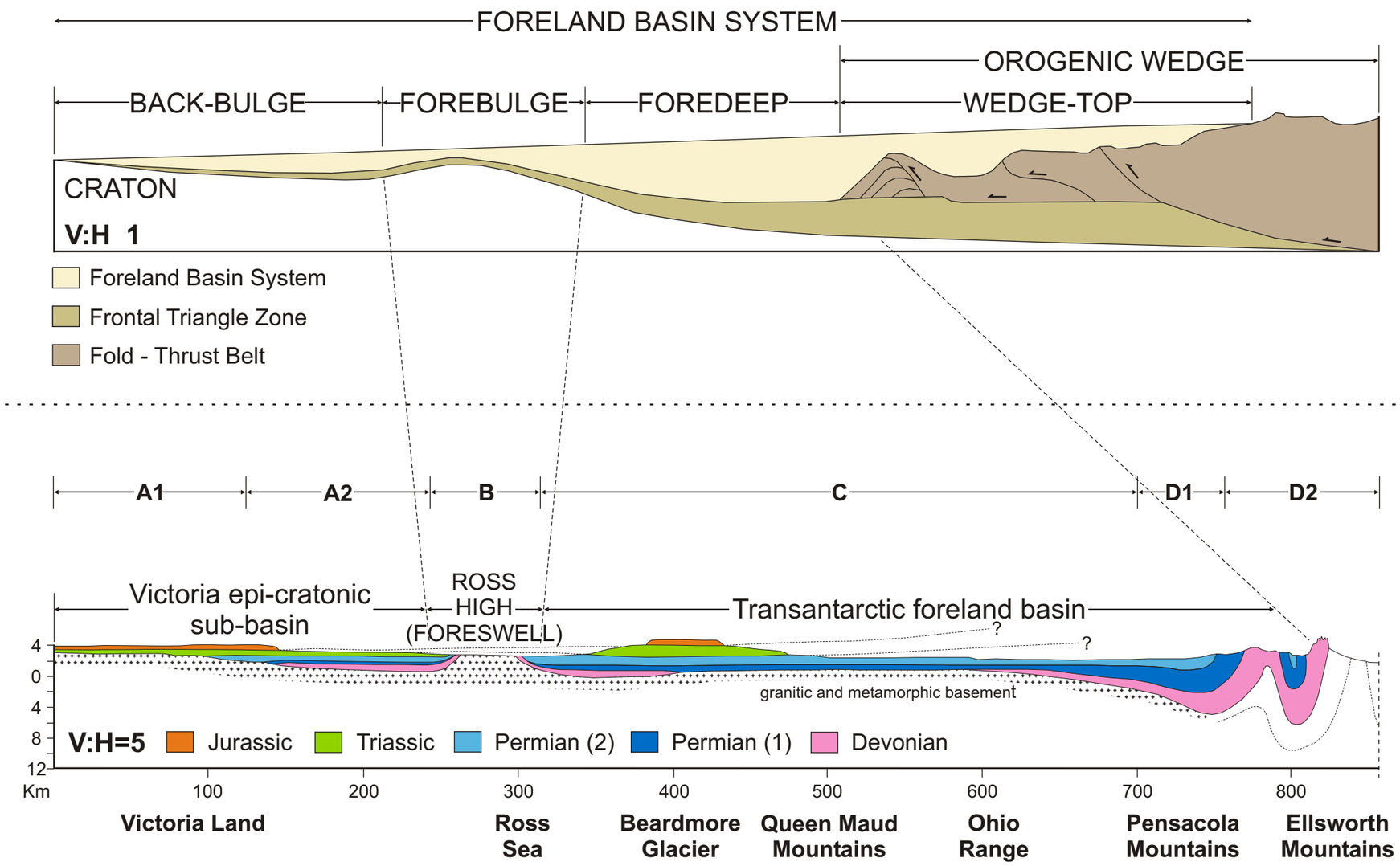

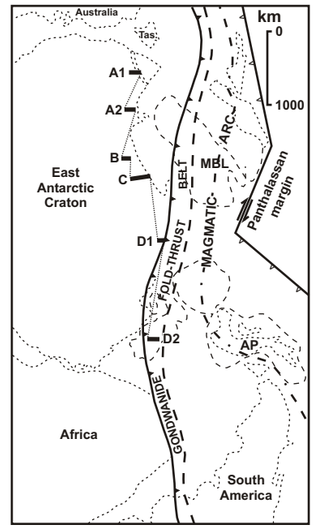

Late Triassic (230 Ma) Recomstruction

B. Orogen normal cross-section west to east Antarctica, just before Late Jurassic rifting (Modified from Collinson et al., 1994)

Figure 2.5: Comparison of the schematic cross-section for a foreland basin system (DeCellesand Giles, 1996) with the orogen normal cross-section of the Transantarctic Basin (Collinson et al., 1994)

During Stage B (Early Permian to Late Permian) the Ross High, possibly the continuation of the Australia Foreswell 1, extended almost to the present South Pole, separating Tasmania and Victoria Land from the foreland basin (Figure 2.4) (Veevers, 2000c). In Tasmania, the Upper Marine Sequence of the Lower Parmeener Supergroup was deposited in shallow marine conditions, while in Victoria Land, which lay slightly further inboard of the foreland basin and above sea level, coal measures were deposited after a period of isostatic uplift (Collinson et al., 1994). The period of uplift in the Victoria Land Basin (Collinson, et al., 1994, Fig. 8) roughly corresponds to the depositional hiatus identified in western and central Tasmania (Figure 2.6). Thin layers of metabentonite (275 Ma) near Hobart are the first indications of the convergent magmatic arc seen in the Tasmania Basin (Veevers, 2000b).

By the Late Permian (Stage C) the foreland basin stretched from northern Queensland to the South Pole (Veevers, 2000c). In Tasmania, the foreswell ran through the northeast, then probably towards the south along the east coast, marking the eastern limit of deposition of Unit 1 of the Upper Parmeener Supergroup. Late Permian sedimentary rocks are absent from Northern Victoria Land (Collinson et al., 1994), as northeast Antarctica was elevated at this time forming the Beardmore-Ross Upland (Veevers, 2000c). The tectonics of Stage D (Early Triassic) is similar to Stage C with a changed surface environment resulting in the deposition of redbeds in the major basins along the margin. In Tasmania, quartz sand (Unit 2) was deposited by rivers flowing towards southeast from a presumed upland in the Tyennan region, while the northeast remained elevated in the foreswell (Veevers, 2000c). At this time, northern Victoria Land remained elevated, while quartzose sandstone was deposited in southern Victoria Land from a source to the south and from the foreswell to the east, while volcaniclastic sandstone and tuff are recorded in the Central Transantarctic Mountains, which lay on the arcward side of the forebulge.

Stage E (early Middle Triassic) involved the deposition of volcanolithic sandstone in the foreland basin in Antarctica, Tasmania and Eastern Australia (Veevers, 2000c), representing a change of source from the Beardmore-Ross Upland to the magmatic arc. This change in provenance signals the westward migration of the foreland basin towards the craton and the demise of the foreswell (Collinson et al., 1994), or using the scheme of DeCelles and Giles (1996), the migration of the foredeep depozone over the forebulge. At this time the Hawkesbury Sandstone in the Sydney Basin swept northeast from a voluminous source in the Beardmore-Ross region, which also fed another quartz sandstone in Tasmania (Veevers, 2000c).

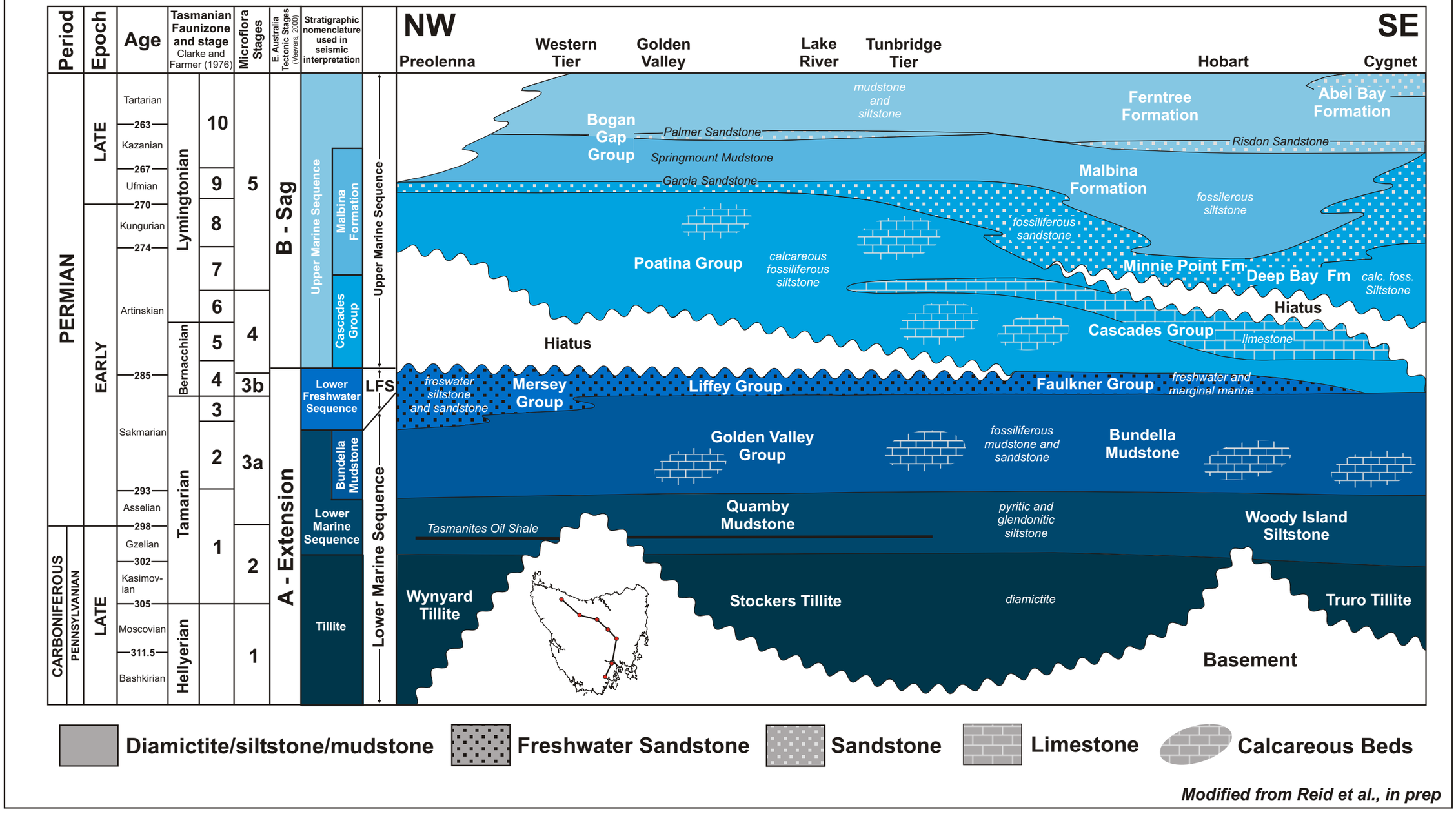

Figure 2.6: The generalised stratigraphy of the Lower Parmeener Supergroup.

Other than the intrusion of basalt at St Marys, the complex events of Stage F (late Middle Triassic to early Late Triassic) seem to have affected Tasmania little. At this time, the margin was being deformed from South America as far as the Ellsworth and Pensacola Mountains in Antarctica, while the final pulse of sediment into the foreland basin was shed from the New England Fold Belt, which itself underwent right lateral displacement (Veevers, 2000b). In Tasmania, quartzose sandstone dominates; however these vary laterally from quartzose to lithic or feldspathic indicating varying provenance and that the interval may be a transitional facies between craton and arc derived sediments.

Mid-Triassic thrusting along the margin was followed by extension (Veevers, 2000c). From the middle Late Triassic until the end of the period (Stage G), fluvial volcanolithic sandstone sourced from the magmatic arc and coal was deposited in the central Transantarctic Mountains, Victoria Land and Tasmania, in a single elongate basin by streams flowing from Antarctica towards Tasmania (Collinson et al., 1987, Veevers, 2000b). These sediments comprise the uppermost, and therefore are the youngest unit, recorded in the Tasmania Basin.

The Tasmanian and Victoria Land Basins were developed side by side, behind the convergent Panthalassan Margin in the Late Carboniferous to Late Triassic. The Permian history of the Tasmania Basin differs from the Victoria Land Basin in that deposition during this time was dominantly marine. This discrepancy is explained by a Permian drainage basin that extended from highlands in Victoria Land to a coastal and marine area in Tasmania (Barrett and Fitzgerald, 1985). Deposition was not always contemporaneous in both basins, which were also separated by the Beardmore-Ross Upland from the Late Permian until the Early Triassic (Stages C and D). The rocks of the Tasmania and Victoria Land basins share a similar history from the Early Triassic. Overall, the Tasmania and Victoria Land basins share a similar tectonic and depositional history. They were probably formed behind a forebulge (Ross High, Australia Foreswell 1) in a back-bulge depozone, the most distal part of a major foreland basin system, which developed along the Panthalassan margin in the Late Carboniferous to the Triassic.

Stratigraphy, palaeogeography, depositional environment and age

The Late Carboniferous to Late Triassic rocks that fill the Tasmania Basin are known as the Parmeener Supergroup (Banks, 1973). The Parmeener Supergroup is divided into two broad lithological and environmental associations, the Lower and Upper Parmeener Supergroups (Forsyth et al., 1974). The Late Carboniferous to Permian, Lower Parmeener Supergroup

consists of glacial, glaciomarine and fluvial sedimentary rocks, while the Upper Parmeener Supergroup comprises, non-marine sedimentary rocks, Late Permian to Late Triassic in age, both units containing subordinate coal measures (Figure 2.6) (Forsyth et al., 1974). The Lower and Upper Parmeener Supergroups are lithostratigraphic units, their boundary does not correlate with the Permian-Triassic biostratigraphic boundary, which is located in the lower part of the Upper Parmeener Supergroup (Forsyth et al., 1974).

2.6.2: LOWER PARMEENER SUPERGROUP

During the Late Palaeozoic, Gondwana was subjected to widespread glaciation (Crowell and Frakes, 1973). During the Late Carboniferous (Stephanian) much of the Tasmanian region was covered by an ice sheet (Banks and Clarke, 1987). At this time the Tasmania Basin was a broad, north-south striking basin with low areas concentrated along passive zones of structural weakness in the basement, the Arthur Lineament (Savage River to Wynyard), the Linda Disturbance (south of Zeehan to north of Wylds Craig) and the Tamar Fracture System (east of Beaconsfield to east of Mangalore) (Banks and Clarke, 1987, Clarke, 1989). High areas extended from the Ducane and Mackintosh regions in the middle of the basin (Reid et al., 2003), and in northeast, northwest, southwest and eastern Tasmania (Clarke, 1989, Hand, 1993, Reid et al., in prep), are indicated by the distribution, age and facies of the earliest marine beds (Banks and Clarke, 1987, Hand, 1993). Ice flowed into Tasmania from the present west; ice movement direction derived from glacial abrasion features and from the imbrication direction of clasts, indicates the ice dispersed northeast and southeast around the central high into the low-lying areas (Figure 2.7) (Banks and Clarke, 1987, Clarke, 1989, Hand, 1993). The north-easterly lobe occupied a deep depression in the Wynyard-Hellyer Gorge area, while the southern lobe covered much of central and northern Tasmania, a deep depression in the Maydena-Cygnet-Woodbridge area and possibly parts of the east coast highlands (Figure 2.7) (Clarke, 1989).

Basal Tillite

Diamictite

(Wynyard Tillite, Stockers Tillite, Truro Tillite)

The onset of marine conditions in the Tasmania Basin probably resulted from isostatic loading during ice advance (Hand, 1993). As the ice retreated westwards, glacigenic sediments, mostly of glaciomarine origin were deposited (Clarke, 1989, Hand, 1993, Reid et al., in prep). The thickest of these deposits were developed in the areas of the deep basement depressions (Figure 2.7) (Clarke, 1989, Hand, 1993, Reid et al., in prep).

Late Carboniferous → *Early Permian* →

Basal Tillite
(Wynyard,Tillite, Stockers Tillite, Truro Tillite)

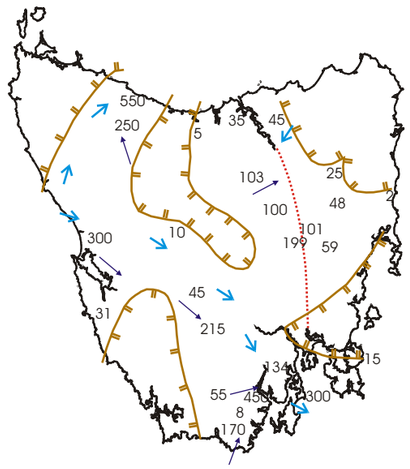

Direction of ice movement (Clarke and Banks, 1987)

Direction of ice movement (Hand, 1993)

Lower Marine Sequence
(Woody Island Siltstone, Quamby Mudstone)

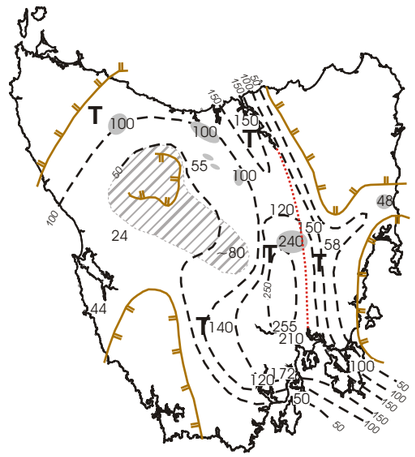

Tasmanite Oil Shale

T Dispersed *Tasmanites*

Conglomeratic Facies

(Bundella Mudstone, Golden Valley Group)

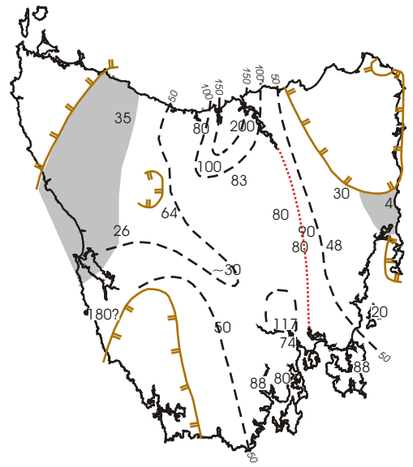

Earliest development of freshwater environments

Lower Freshwater Sequence
(Liffey Group, Faulkner Group, Mersey Group)

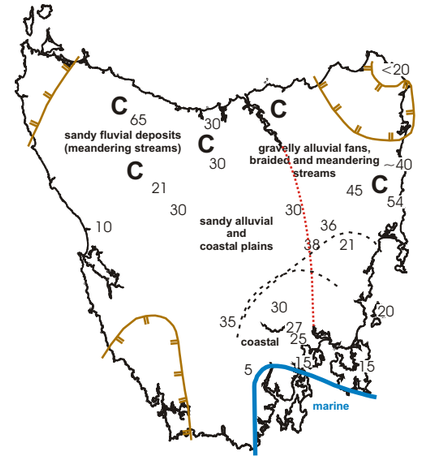

C Coal development

Extent of brief marine incursions

Late Permian →

Upper Marine Sequence
(Cascades Group, Poatina Group)

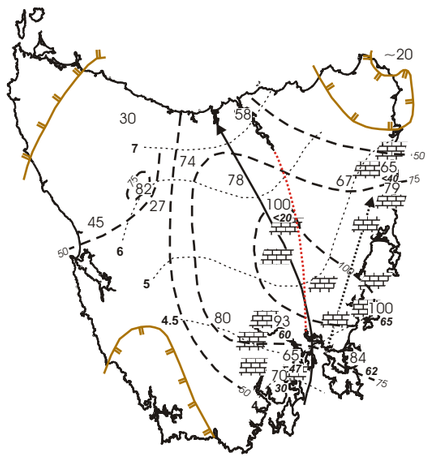

(Deep Bay & Minnie Point Formations, Malbina Formation; MarraFormation; Garcia Sandstone, Springmount Mudstone & Palmer Sandstone)

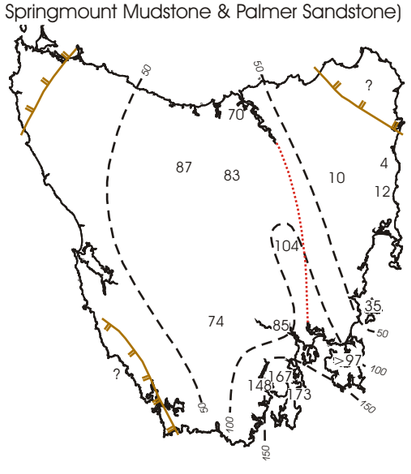

(Ferntree Formation, Bogan Gap Formation)

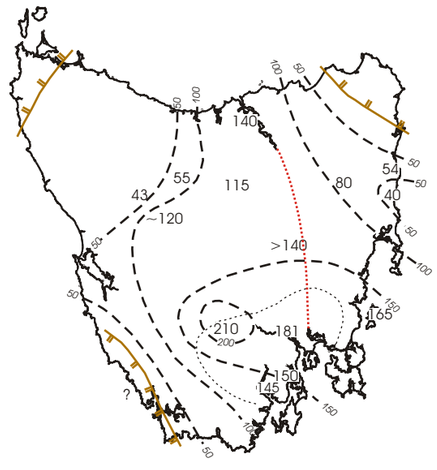

Extent of Risdon Sandstone deposition

Limestone - approx thickness in metres

5 Faunizone age at the base of the calcareous units

Younging direction of calcareous beds

Younging direction of limestone

156 Thickness (metres)

100 Isopachs (metres)

Topographic highs

Tamar Fracture Zone

Modified from Reid et al., in prep

Figure 2.7: Palaeogeographic reconstructions of the Tasmania Basin during the deposition of major units of the Lower Parmeener Supergroup.

The basal units of the Parmeener Supergroup are the Wynyard Tillite (north-western Tasmania), the Stockers Tillite (central Tasmania) and the Truro Tillite (south-eastern Tasmania). They comprise debris flow diamictite, dropstone diamictite, glacial outwash conglomerate and sandstone, pebbly mudstone and rhythmite (Clarke, 1989, Hand, 1993, Reid et al., in prep). The thicknesses of these units vary considerably across the basin. The thickest sequence (Wynyard Tillite) exceeds 500 m near Wynyard in northern Tasmania; other substantial developments are found north of Strahan (300 m), Maydena (215 m), Cygnet-Woodbridge (Truro Tillite, 450 m) and Poatina (Stockers Tillite, 100 m) (Figure 2.7) (Clarke, 1989, Reid et al., in prep). In the Northern Midlands region, the Stockers Tillite thins towards the east in drill holes RG-145 at Tunbridge (199 m), RG-146 at Ross (101 m) and at The Quoin (59 m) (Map 5.1). The Truro Tillite thins rapidly to the north of Woodbridge and is absent from the Glenorchy drill hole (Reid et al., in prep). Elsewhere in Tasmania, the tillite sequences are considerably thinner, rarely exceeding 50 m, or completely absent (Figure 2.7) (Reid et al., in prep).

The bulk of the tillite units' thickness is monotonous diamictite, with conglomerate, and minor discrete sandstone beds and rhythmite (Clarke, 1989). The basal unit is usually diamictite; however conglomeratic beds closely followed by monotonous diamictite are also known (Reid et al., in prep). Clasts are angular to rounded, range from small pebble to cobble size and are supported by a matrix of silt and clay. The clast lithotypes include quartzite, schist, phyllite, volcanic rocks and granites. Silt and sand sizes grains are of quartz and feldspar, with common hornblende and mica grains sourced from volcanic rocks (Clarke, 1989, Reid et al., in prep). Lithologies dominated by rounded clasts may result from the remobilisation or entrainment of material by ice from a depositional setting, or from the reworking of glacigenic material from a previous glacial episode (Hand, 1993).

Lithological indicators and fossil evidence indicate that the majority of the glacigenic sediments found in Tasmania are of marine origin (Hand, 1993). The common dropstone diamictite requires a relatively large body of open marine or lacustrine water, for deposition (Hand, 1993). Rhythmite is found throughout the basin and their deposition is dependent on considerable tidal fluctuation, indicating marine conditions (Banks and Clarke, 1987, Clarke, 1989). Trace fossils in rhythmite in the Eaglehawk Neck and The Quoin drill holes are characteristic of shallow marine conditions (Hand, 1993). However, near Hellyer Gorge, rhythmite contains seed ferns, arthropod tracks and an insect indicating deposition under glacilacustrine conditions in this area (Reid et al., in prep). Marine macrofossils are present at

Shoemaker Bay on the south coast and at Maydena in the central south (Truswell, 1978, Clarke and Banks, 1973).

Age diagnostic fossils are rare in these rocks. Stage 1 microflora are recorded in rhythmite at Hellyer Gorge and at Strahan, while Stage 2 microflora were tentatively identified in diamictite at Lake River (Hand, 1993). The presence of Stage 1 and 2 microflora indicates Late Carboniferous to Early Permian (Asselian) ages. Marine macro-fossils found at Maydena and Shoemaker Bay fall into Faunizone 1, giving an age of latest Carboniferous to earliest Permian (Clarke and Banks, 1973, Hand, 1993). The age ranges derived from fossils indicate Late Carboniferous (Stephanian) to earliest Permian (Asselian) age for the basal tillites (Banks and Clarke, 1987, Hand, 1993).

Lower Marine Sequence

Pebbly siltstone (and Tasmanite Oil Shale)

(Woody Island Siltstone, Quamby Mudstone)

Glacial retreat was closely followed by a marine transgression resulting in marine conditions over most of Tasmania (Clarke, 1989, Domack et al., 1993). Almost everywhere the basal tillite is succeeded by a thick sequence of uniform, organic-rich, massive-bedded siltstone and mudstone, containing ubiquitous pyrite, abundant glendonites and rare marine fossils (Domack et al., 1993, Reid et al., in prep). These rocks contain a variable ice rafted component characterised by ubiquitous sand sized particles and scattered pebbles and cobbles that decrease in abundance upwards (Clarke, 1989, Domack et al., 1993). These dropstones were modified by fluvial or beach processes, and none show evidence of transport by ice (Domack et al., 1993). In northern Tasmania, this sequence is known as the Quamby Mudstone, while in southern Tasmania it is known as the Woody Island Siltstone.

In some parts of the basin, an approximately 2 m thick interval of oil shale formed from flattened sphaeroids of the green alga *Tasmanites punctatus*, occurs in the basal part of the sequence (Figure 2.7) (Domack et al., 1993). With the exception of the Bonney's Plains borehole and the far southeast, *Tasmanites* is found dispersed throughout the sequence across the entire basin; however, distinct intervals of Oil Shale are only produced when the concentration of algal spores exceeds 10% (Reid et al., in prep). Banks and Clarke (1987) explained the distribution of the oil shale as resulting from algal blooms accumulating about the shoreline of the main basin, around islands in northern Tasmania, and in the narrow gulf at Douglas River, while away from these shorelines, the alga was diluted rapidly by faster rates

of sedimentation. However, Domack et al. (1993) considered that *Tasmanites* recorded a period of enhanced primary productivity coupled with ice rafting within the basin, and that the distribution of oil shale was controlled by local conditions rather than by distance from the palaeo-shoreline.

The contact between the basal tillite and the overlying siltstone and mudstone is generally thought to be sharp; however examples of transitional or interbedded contacts are found in the basin (Domack et al., 1993). In the RG-146 drill hole at Tunbridge Tiers the contact occurs over 3 m of interbedded thin diamictites and dark grey mudstone, followed by a sandy mudstone, which marks the base of the Quamby Mudstone (Domack et al., 1993). Similar interbedded contacts are observed at The Quoin drill hole near Ross, and at Oonah where interbedded diamictite and mudstone occur over a 10 m interval (Reid et al., in prep). At Golden Valley, Douglas River and near Cygnet, a transitional contact is observed as a gradual decrease in pebble abundance occurs as the poorly sorted matrix of diamictite changes to the fine matrix of a pebbly mudstone (Clarke, 1989, Domack et al., 1993). At Maydena and Picton River in the south of the island, Hand (1993) observed the Woody Island Siltstone occupying positions laterally equivalent to the basal tillite, and suggested that a diachronous boundary may exist in areas beyond the maximum extent of glaciation.

Deposition took place along a NNW-SSE striking trough, coincident with the buried Tamar Fracture System (Reid et al., 2003). The thickest deposits occur along the trough axis and exceed 265 m, while elsewhere the thickness is generally 80 – 100 m (Figure 2.7) (Reid et al., 2003). The Woody Island Siltstone and the fossiliferous lower Bundella Mudstone facies are absent from the Hunterston 1 DDH in the Central Highlands, replaced by conglomerate, conglomeratic siltstone and pebbly siltstone (Domack et al., 1993). The absence of this sequence at Hunterston and similar sequences close by in the Mackintosh and Du Cane areas indicates a persisting regional high in the centre of the basin (Domack et al., 1993).

The Lower Marine Sequence is dominantly fine to medium siltstone, with poorly sorted, angular grains in a clay matrix. Pebble sized clasts occur throughout the sequence, although their abundance decreases up-section (Reid et al., in prep). Bedding is generally massive, with rare thin laminae (Domack et al., 1993). Carbonaceous material is present in the rocks either as fragments or as small carbonaceous clay lenses (Domack et al., 1993).

Glendonites are found in Tasmanite Oil Shale, but are more common above this level (Suess et al., 1982). They become larger and more abundant up-section, their size and abundance decreasing close to the top of the sequence (Shearman and Smith, 1985). To precipitate glendonites requires easily metabolised organic matter (Domack et al., 1993); an undisturbed, unconsolidated mud substrate and temperatures close to freezing (Domack et al., 1993), their presence is therefore indicative of deposition in a deep marine setting with cold bottom waters (Domack et al., 1993).

Fossils are rare in both variety and distribution in this sequence. They generally occur towards the top of the sequence where the rocks become coarser with bioturbated pebble horizons, indicating shallowing of the basin (Calver et al., 1984). Spores are found throughout the sequence; however their diversity, abundance and preservation vary, depending on the stratigraphic position (Domack et al., 1993). Stage 2 microflora occur in and around the Tasmanite Oil Shale in the Douglas River Borehole and at Hellyer Gorge and Latrobe (Calver et al., 1984, Banks and Clarke, 1987), while, Truswell (1978) reported Stage 2 and lower Substage 3a microflora in the Golden Valley drill hole indicating latest Carboniferous to earliest Permian age. Marine macro-fossils are reported in the lower part of the sequence at Latrobe and indicate an early Tamarian age (Clarke, 1989).

Fossiliferous siltstone

(Bundella Mudstone, Golden Valley Group)

Deposition of the Woody Island and Quamby Mudstone filled the NNW-SSE striking trough, resulting in the development of a shallow open shelf sea environment rich in benthic faunas (Banks and Clarke, 1987, Clarke, 1989). The rocks formed in this environment are known as the Golden Valley Group in northern Tasmania and the Bundella Mudstone in the south. The transformation from a shallow to deeper water environment is attributed to another marine transgression, resulting in onlap of older sediments and inundation of previously emergent areas in the east of the basin (Banks and Clarke, 1987, Reid et al., in prep). Evidence of the relative sea-level rise is seen on Maria Island and in the Ben Lomond area where richly fossiliferous siltstone and conglomerate directly overly basement rocks (Clarke, 1989).

Characteristic lithologies include alternations of richly fossiliferous siltstone, calcareous siltstone, sandstone and subordinate micritic limestone formed in the lower parts of the sequence; large, ice rafted dropstones are common (Banks and Clarke, 1987, Reid et al., in prep). The siltstone is usually well-bedded, medium to coarse grained and poorly sorted

(Reid et al., in prep). It is thickest along the axis of the trough, reaching about 200 m at Beaconsfield in the north, and 117 m at Granton in the south, while elsewhere they are about 80 m thick (Figure 2.7) (Banks and Clarke, 1987, Clarke, 1989). The lower parts of the Golden Valley group comprise fossiliferous siltstone; and sandstone, micritic limestone are commonly richly foraminiferal, while the upper part of the sequence is generally fine grained (Banks and Clarke, 1987, Reid et al., in prep). The lower parts of the Golden Valley Group and the Bundella mudstone are richly fossiliferous, dominated by brachiopods, molluscs and bryozoans; fenestrate bryozoans are common in finer grained beds (Clarke, 1989). Most faunas show evidence of some reworking; however biocoenotic assemblages of strophalosiids and spiriferids are relatively common, indicating quiet-water conditions (Banks and Clarke, 1987, Clarke, 1989).

Upper Tamarian rocks (Figure 2.6) indicate a gradual marine regression towards the south and southeast, leading to increasingly brackish deposits over north and central Tasmania (Banks and Clarke, 1987, Clarke, 1989). Laminated mudstone and siltstone with abundant hydroplastic structures dominate, and loadstones decrease, while the carbonaceous and pyritic content increases, e.g. Macrae Mudstone (Banks and Clarke, 1987, Clarke, 1989, Reid et al., in prep). Contemporaneous deposits at Douglas River are of carbonaceous mudstone, minor coal and coarse-grained, cross-bedded quartz sandstone, these developments are the earliest proof of the onset of non-marine conditions anywhere in the Tasmania Basin (Clarke and Banks, 1973, Clarke and Farmer, 1973).

The abundance and diversity of fauna in the sequence provides sound biostratigraphic control. The Tamarian Faunizones 1-3, based on bivalves and gastropods can be confidently correlated with the Allandale Fauna of the Sydney Basin (Clarke, 1990). The basal Golden Valley Group and Bundella Mudstone, both contain *Strophalosia concentrica* belonging to Faunizone 1 (Reid et al., in prep), which gives way up-section to *Strophalosia subcircularis* which is confined to Faunizone 2 (Clarke and Banks, 1973). The basal beds on Maria Island also contain *Strophalosia subcircularis* (Reid et al., in prep). Finally, the appearance of *Sulciplica stutchburii* and the absence of *Eurydesma cordatum* near the top of the Golden Valley Group, Bundella Mudstone and the basal beds on Maria Island indicate Faunizone 3 (Banks and Clarke, 1987, Clarke, 1989).

Lower Freshwater Sequence

Freshwater and marginal marine siltstone and sandstone

(Liffey Group, Faulkner Group, Mersey Group)

Marine regression in the earliest Bernacchian, developed first in the northeast and probably the northwest and spread southward resulting in the deposition of fluvial sediments across a broad plain, while in the southeast, marine conditions persisted (Farmer, 1985, Banks and Clarke, 1987, Reid et al., in prep). These fluvial deposits are generally known as the Lower Freshwater Sequence, comprising the Liffey Group in the north, the Faulkner group in the south and in the central north coal measures known as the Mersey Group (Figure 2.6). South of Hobart freshwater facies are absent and the marine to marginal marine Hickman Formation, the lower part of which is a time equivalent of the Faulkner Group, conformably overlies the Bundella Mudstone (Clarke, 1989).

At the time of deposition, the basin was bordered by high ground in the southwest, northwest and in the northeast (Figure 2.7) (Banks and Clarke, 1987, McClenaghan and Calver, 1994, Reid et al., in prep). In many parts of northeast Tasmania the Lower Freshwater Sequence lies directly on basement rocks (Figure 2.8) (Clarke, 1989). Marked, but local decreases in thickness probably represent pinch-outs against residual basement highs (Banks and Clarke, 1987, Reid et al., in prep). Overall, the sequence is relatively thin with the thickest units found in north-western and north-eastern Tasmania (Figure 2.7). The thickness of the sequence generally decreases towards the centre of the basin, where it is about 25 m on average, and from the centre of the basin the sequence thins towards the far southeast (Figure 2.7).

Figure 2.8: Angular unconformity between the Mathinna Supergroup and the Lower Freshwater Sequence, Lower Parmeener Supergroup, Pepper Hill, north-eastern Tasmania (570 934 mE, 5 390 283 mN).

The Freshwater Sequence is characterised by well sorted, quartz-rich, cross-bedded sandstone, with conglomerate and carbonaceous siltstone and mudstone (Clarke, 1989). Sandstone is coarser around the margins of the basin and finer in the southeast where siltstone dominates (Banks and Clarke, 1987, Clarke, 1989). Coal developed around the landward margins of the basin, in up to four seams, generally a little more than a metre thick (Mersey Coal Measures, north; Preoleena Coal Measures, northwest; Mt Elephant Sandstone, northeast) (Figure 2.7) (Clarke, 1989, Reid et al., in prep). Coarse, clean, quartz-rich sandstone is typical of the Liffey Group, while the Faulkner Group tends to be finer grained with fine sandstone and micaceous and carbonaceous siltstone common in the Hobart region (Banks and Clarke, 1987). At its maximum extent the fluvial plain reached just south of Hobart, as indicated by the presence of the marine Hickman Formation in the Margate area south of Hobart (Clarke, 1989). In south-eastern and central Tasmania, freshwater deposits contain thin intercalations on marine sediments in two cyclothems (Martini and Banks, 1989), indicating two short-lived marine incursions.

The distribution and association of certain facies indicate that coarse gravelly alluvial fans, braided and meandering streams, dominated deposition in the northeast (Figure 2.7) (Martini and Banks, 1989). In north and north-western Tasmania, sandy fluvial facies were deposited primarily in meandering streams, with minor deposition occurring in braided streams (Figure 2.7) (Martini and Banks, 1989). In south-eastern and central Tasmania, sandy alluvial and coastal plains facies dominate (Figure 2.7) (Clarke, 1989). In Hobart region, the depositional environment was coastal, with shallow subtidal and possibly inertial zones indicated (Clarke, 1989).

In the deposits resulting from marine incursions, fragments of *Etheripecten* and *Eurydesma* are found in addition to rare specimens of the large *Paraconularia derwentensis* (Truswell, 1978). Further south, the Hickman Formation is rich in faunas, characterised by an abundance of the linoproductid *Cancrinella farleyensis* and *Tomiopsis branxtonensis* (Calver et al., 1984). Age diagnostic microflora are present in the Lower Freshwater Sequence, which always yield Substage 3b microflora (Turner and Calver, 1987). In the Douglas River Borehole, Substage 3a microflora are identified in the lowest parts of the 56 m thick sequence (Clarke, 1989). While a 70 m thick section at Huntsmans Creek near St Marys, yields Substage 3a microflora (Lower Tamarian) at the base of the sequence and Stage 4 microflora at the very top, indicating the Lower Freshwater Sequence on the east coast may extend to both older and younger age limits than elsewhere in Tasmania (Banks and Clarke, 1987).

Upper Marine Sequence

Calcareous fossiliferous siltstone and limestone

(Cascades Group, Poatina Group)

In the late Early Bernacchian, marine sedimentation was renewed in the Tasmania Basin, resulting in the deposition of fossiliferous calcareous siltstone and limestone in a shallow, cold-water environment (Clarke, 1989). In the earliest Bernacchian the sea, which had been restricted to an area south of Margate, transgressed northwards (Banks and Clarke, 1987, Clarke, 1989). Marine rocks were deposited first in the Hobart region, with deposition progressing northwards over time resulting in the further burial of the previously emergent areas in the east and northeast (Clarke, 1989). Age diagnostic flora and fauna indicate the development of a depositional hiatus between the Lower Freshwater Sequence and the basal units of the Upper Glaciomarine Sequence in the northern and central parts of the basin as the sea transgressed in an arc towards the north-northwest from its original position in the southeast (Figure 2.6) (Reid et al., in prep).

The stratigraphy of the carbonaceous rocks overlying the Lower Freshwater Sequence is variable as are the stratigraphic names applied in different regions. Reid et al.(in prep) generally defines calcareous siltstone overlain by thick limestone in the southeast of Tasmania as the Cascades Group, while in central and northern Tasmania, limestones are generally subordinate and these rocks are collectively referred to as the Poatina Group (Figure 2.6).

In the southeast of Tasmania marine deposition continued in the Hickman Formation and as the sea moved northwards through the Hobart region, a 30 m thick, calcareous fossiliferous grey-black siltstone was deposited at the base of the Cascades Formation (Nassau Siltstone) (Turner and Calver, 1987). A similar thickness of calcareous siltstone interbedded with thin argillaceous limestones are observed in the east on Maria Island (Skipping Ridge Formation) (Calver et al., 1984). In the St Marys area in the northeast of Tasmania, fossiliferous mudstone with subordinate medium to thick beds of limey sandstone and sandy calcarenite occupy the basal 30 m of the sequence (Reid et al., in prep). In the Douglas River borehole the calcareous siltstones are thin and interbedded with medium- to thick-bedded, fossiliferous limestone, and 78 m thick (Reid et al., in prep).

In south-eastern Tasmania, the calcareous siltstone is overlain by thick limestone sequences (Harts Hill Limestone, Margate; Berriedale Limestone, Hobart; Counsel Creek Limestone; Maria Island) (Figure 2.6) (Rao, 1981). The limestone is calcarenite and calcilutites, and

richly fossiliferous with small, infrequent dropstones (Rao, 1988). Trace element and oxygen isotopic analysis of the calcitic micrite and spar from the Berriedale Limestone indicates precipitation from seawater at <3°C and <4°C respectively (Clarke and Banks, 1973, Turner and Calver, 1987). In the northeast around St Marys, the limestone is pale grey to off-white, thick-bedded to massive, fine to very coarse grained bioclastic calcarenite, with interbeds of fossiliferous trigonous lithologies (usually mudstone), generally about 35 to 40 m thick (Clarke and Banks, 1973). The greatest thickness of limestone is found along the south-eastern and east coast of Tasmania (Figure 2.7). The limestone thins towards the centre of the basin and ceases to be a significant part of the sequence north and northwest of the RG-145 Tunbridge Tier drill hole (Figure 2.7).

Age diagnostic faunas indicate the calcareous siltstone in the Hobart region (Nassau Siltstone) correlates with Faunizone 4, Early Bernacchian in age (Reid et al., in prep). The overlying limestone contains abundant *Terrakea pollex* (gp.) and *Taeniothaerus subquadratus* indicative of Faunizone 5 (Late Bernacchian (Calver et al., 1984). The sequence at Douglas River contains Stage 4 Microflora (Calver et al., 1984). The thin calcareous siltstone at the base of the sequence is tentatively identified just above the base of the Stage 4 Microflora interval and of late Early Bernacchian age (Reid et al., in prep), while the top of the limestone at Douglas River is probably coincident with the top of the Stage 4 Microflora interval and therefore of Early Lymingtonian age (Calver et al., 1984, Forsyth et al., 1989). Taxi indicative of Faunizone 5 (Late Bernacchian) are found in the fossiliferous mudstone near the base of the sequence in the St Marys area, while elements of Faunizone 9 are present in limestone immediately below the top of the formation indicating late Middle Lymingtonian age (Reid et al., in prep). The biostratigraphy indicates that both the calcareous siltstone and the limestone are diachronous (Reid et al., in prep). The calcareous siltstone generally youngs towards the northwest, while limestone youngs in a north-north-easterly direction (Reid et al., in prep).

In central Tasmania, the Lower Freshwater Sequence is immediately overlain by a glaciomarine sequence, containing poorly fossiliferous siltstone, grading up to a poorly sorted sandstone, richly fossiliferous siltstone and limestone (Forsyth et al., 1989, Reid, 2003). The sequence is intersected by the RG-145 (Tunbridge Tier) and the RG-146 (Ross) drill holes and is 105.5 m and 99 m thick respectively (Forsyth et al., 1989). Bryozoan faunas indicating Faunizone 5 (Bernacchian) are found at the base of the richly fossiliferous siltstone in the Tunbridge drill hole (Reid et al., in prep). Brachiopod faunas, found in an outcrop

(probably from higher in the sequence) of impure limestone, one kilometre NNW of Ross indicate Faunizone 6-7 (Bravo and Pike, 1969, Mathews et al., 1996).

The term Poatina Group was introduced to describe the rocks lying directly above the Liffey Group (Lower Freshwater Sequence) at Poatina (Mathews et al., 1996). These rocks are recognised along the Great Western Tiers flanking the Central Highlands. In general the Poatina Group is variably fossiliferous, comprising mudstone at its base, followed by sandy siltstone, sandstone and pebbly sandstone (Mathews et al., 1996). The Poatina Group is 80 – 90 m thick around Poatina and about 90 m thick northwest at Quamby (Figure 2.7) (Farmer, 1985).

Fossiliferous siltstone and sandstone

(Deep Bay and Minnie Point Formations, Malbina Formation; Marra Formation; Garcia Sandstone, Springmount Mudstone and Palmer Sandstone)

As deposition of calcareous rocks of the Cascades and Poatina Groups progressed northwards, fossiliferous sandstone and siltstone beds were deposited in a deepening basin in the south. These are thick and well developed in the southern part of the Tasmania Basin, while towards the north sandstone decreases and less fossiliferous siltstone is more prevalent (Figure 2.6) (Reid et al., in prep).

In the south, these rocks are known as the Deep Bay Formation, which is about 100 m thick and typically consists of alternating, thin- to medium-bedded, poorly sorted, indurated siltstone, fine-grained sandstone with subordinate mudstone and occasional thin impersistent pods and stringers of feldspathic granule conglomerate and shaley partings (Farmer, 1985). Most of the formation is richly fossiliferous, bioturbation is common and dropstones are abundant throughout the sequence (Farmer, 1985). The Deep Bay Formation is paraconformable on the Bundella Mudstone at Cygnet with the Lower Freshwater Sequence and overlying calcareous rocks absent; however to the north and northwest, the formation progressively oversteps the Bundella Mudstone, the Hickman Formation and the Harts Hill Limestone (Farmer, 1985). Clarke and Banks (1973) assigned the Deep Bay Formation to their Faunizones 6 – 8, indicating an Early to Middle Lymingtonian age.

The Minnie Point Formation overlies the Deep Bay Formation and consists of medium- and massive-bedded, poorly sorted, pebbly sandstone, with subordinate dark grey, poorly sorted, thin- to medium- to massive-bedded pebbly siltstone in the upper part of the section

(Farmer, 1985). Granule sized feldspathic and other clastic detritus is found in many of the sandstone beds (Farmer, 1985). Bioturbation is common in the upper part of the formation and pebble- to cobble sized clasts are abundant throughout, both in scattered and in winnowed concentrations (Farmer, 1985). Faunas corresponding to Faunizone 9 and 10 are found in the formation indicating a late Middle Lymingtonian to Late Lymingtonian age (Farmer, 1985).

The equivalent of the Deep Bay and Minnie Point Formations in the Hobart region is the Malbina Formation which is about 90 m thick and consists of alternating sandstone and siltstone resting disconformably on the Berriedale Limestone (Figure 2.6). Some of the sandstone beds are poorly sorted and graded, with grainsizes ranging from fine to coarse, fossils are generally present but not abundant until the very top of the formation, while ice rafted lonestones remain ubiquitous (Banks and Read, 1962, Banks and Clarke, 1987). The base of the Malbina Formation is the lateral equivalent of the Minnie Point Formation (Reid et al., in prep), but Malbina Formation (Member A) contains faunas indicative of at least upper Faunizone7 and no younger than Faunizone 8 (Reid et al., in prep). This diachronism indicates that the Deep Bay Formation transgressed northward and was quickly superseded by the Malbina Formation in the Hobart region before deposition of siltstone in the south (Reid et al., in prep). The uppermost fossiliferous siltstone of the Malbina Formation (Member E) contains fossils indicative of Faunizone 10 (Clarke and Banks, 1973).

The equivalents of the Malbina Formation thin towards the northeast (Reid et al., in prep). On Maria Island, the 35 m thick Marra Formation conformably overlies the Counsel Creek Limestone. The formation comprises thin- to thick-bedded sandstone with subordinate siltstone and becomes increasingly sandy and fossiliferous up-section (Clarke and Baillie, 1984). Towards the top of the formation the sandstone becomes increasingly arkosic and glauconitic, possibly indicating slow or discontinuous deposition (Clarke and Baillie, 1984). The formation can be traced further north where it is found at Douglas River and in the St Marys area, where it thins to about 5 m and is glauconitic (Reid et al., in prep). The distribution of fossils through the Marra Formation indicates that the formation represents a substantial period of time, ranging from the Early Lymingtonian to the late Middle Lymingtonian (Faunizones 6 – 9) (Clarke and Baillie, 1984).

In central and northern Tasmania, equivalents to the fossiliferous siltstone and sandstone of the south are not easily distinguished. In central Tasmania a pebbly sandstone (Garcia Sandstone), followed by thin sandy beds, then nearly 80 m of wispy siltstone and mudstone

with granule and pebble rich beds and foraminifera in some horizons are considered equivalent to the Malbina Formation by Reid et al. (in prep).

Poorly fossiliferous mudstone and siltstone

(Ferntree Formation, Bogan Gap Group, Middle Arm Group)

The fossiliferous sandstone and siltstone of the Malbina Formation and its equivalents were followed by a brief marine transgression and the deposition of generally fine-grained siltstone and mudstone, with sandstone persisting to the north (Banks and Clarke, 1987, Reid et al., in prep). Preceding the deposition of fine-grained sediments in the south, regression led to the formation of an offshore barrier bar facies (Risdon Sandstone), which is a well-washed quartz sandstone with a pebbly base and cross-bedding indicating derivation from the south and southwest (Farmer, 1985, Banks and Clarke, 1987, Clarke, 1989, Reid et al., in prep). Deposition of the Risdon Sandstone is only recognised in the Hobart region (Reid et al., in prep). Behind the barrier bar, a dark bioturbated siltstone containing sporadic marine fossils and often carbonaceous (Ferntree Formation) was accumulated in a shallow, brackish estuarine or lagoonal environment (Banks and Clarke, 1987, Clarke, 1989). The Ferntree Formation of southern Tasmania is a 145 – 210 m thick, generally monotonous sequence of non-fossiliferous siltstone and mudstone, with rare fossiliferous and conglomeratic horizons (Reid et al., in prep). To the south of Hobart at Birches Bay the higher part of the sequence contains a high proportion of silicic volcanic ash (Clarke, 1989).

In central and northern Tasmania, the poorly-fossiliferous sequence is referred to as the Bogan Gap Group, comprising the Springmount Mudstone at the base, followed by the Palmer Sandstone, Drys Mudstone, Blackwood Conglomerate and the Eden Mudstone (Bravo and Pike, 1969). The fine-grained units are generally fossiliferous to sparsely fossiliferous, thick-bedded, mudstone, siltstone, sandy siltstone and muddy sandstone with sparse pebbles/dropstones. Between the fine-grained units are two prominent coarse-grained beds, the Palmer Sandstone and the Blackwood Conglomerate, which are used as marker beds as they can be mapped continuously across most of the central and northern Tasmania. The Palmer Sandstone interval is characterised by poorly sorted, unfossiliferous sandstone, pebbly sandstone and sandstone conglomerate (Pike et al., 1973, Farmer, 1985, Forsyth et al., 1989), and is thought to be the lateral equivalent of the Risdon Sandstone (Forsyth et al., 1989). The Blackwood Conglomerate lying approximately 120 m above the Palmer Sandstone is an unfossiliferous, conglomeratic sandstone to conglomerate. A similar sequence, known as the Middle Arm Group is recognised at Beaconsfield, and includes

correlates of the Springmount Mudstone, Palmer Sandstone and Blackwood Conglomerate (Gee and Legge, 1979).

The thickness of the Bogan Gap Group and its correlates at Beaconsfield ranges between 180 and 250 m thick (Pike et al., 1973, Gee and Legge, 1979, Farmer, 1985, Forsyth et al., 1989). *Warthia micromphala* found in the Palmer Sandstone correlate and *Etheripecten leniusculus* found in the Blackwood Conglomerate correlate in the Interlaken Quadrangle indicate late Middle to Late Lymingtonian age (Faunizone 8 – 10) for the Bogan Gap Group (Forsyth et al., 1989). Fossils demonstrate a Late Lymingtonian age (Faunizone 10) for the Bogan Gap Group in the Lake River Region (Farmer, 1985). In all areas the topmost beds, where not eroded, are muddy and carbonaceous, representing marginal marine conditions before the beginning of freshwater deposition (Reid et al., in prep).

Summary

The Lower Parmeener Supergroup was deposited under glaciomarine conditions from the Late Carboniferous to the Late Permian, except for a period of freshwater deposition in the Early Permian (Sakmarian). The basal units are tillite (diamictite), deposited during ice retreat to the west on a glaciated basement surface with significant relief (Clarke, 1989, Hand, 1993, Reid et al., in prep). The thickness of the tillite varies across the basin, with the thickest developments along passive zones of structural weakness in the basement (Banks and Clarke, 1987, Clarke, 1989). Almost everywhere these rocks are overlain by a thick sequence of organic-rich siltstone and mudstone containing pyrite, abundant glendonites and dropstones (Woody Island Siltstone, Quamby Mudstone) (Banks and Clarke, 1987, Clarke, 1989, Domack et al., 1993, Hand, 1993). These rocks were deposited in a cold water environment during a marine transgression (Banks and Clarke, 1987, Domack et al., 1993, Hand, 1993). In some parts of the basin, a thin (2 m) interval of oil shale formed near the base of the sequence.

Marine regression in the earliest Bernacchian resulted in the deposition of fluvial sediments across a broad plain (Liffey Group, Faulkner Group, Mersey Group), with the exception of the far southeast where marine conditions persisted (Banks and Clarke, 1987, Clarke, 1989, Reid et al., in prep). In the late Early Bernacchian, marine sedimentation was renewed as the sea transgressed northwards from its previous position in the far southeast. Fossiliferous, calcareous siltstone and limestone were deposited in a shallow, cold-water environment (Cascade Group, Poatina Group). These rocks overstepped older rocks as the sea transgressed northwards resulting in a diachronous boundary with underlying units (Reid et al., in prep).

An offshore barrier bar was developed in the south (Risdon Sandstone), behind which a thick sequence of poorly fossiliferous bioturbated, dark siltstone (Ferntree Formation) accumulated in a restricted, brackish estuarine or lagoonal environment (Banks and Clarke, 1987, Clarke, 1989). In central and northern Tasmania, similar sequences of poorly fossiliferous rocks are known as the Bogan Gap and Middle Arm Groups.

2.6.3: UPPER PARMEENER SUPERGROUP

The Late Permian (Ufimian/Kazanian?) to Late Triassic (Norian) Upper Parmeener Supergroup represents all the units deposited in freshwater that lie above the dominantly glaciomarine Lower Parmeener Supergroup. The change from rocks of a glaciomarine origin to those deposited in a fluvial environment is abrupt and may result from eustatic sea-level fall or regional uplift in Eastern Australia (Forsyth, 1987, Forsyth, 1989b). Across most of Tasmania the boundary between the Lower and Upper Parmeener Supergroups is probably transitional (Forsyth, 1987, Forsyth, 1989b). The transitional facies are usually partly eroded and abruptly overlain by coarse-grained often pebbly Upper Parmeener sandstone (Forsyth, 1987, Forsyth, 1989b). In north-eastern Tasmania the Upper and Lower Parmeener Supergroup are separated by a hiatus lasting at least as long as the Early Triassic epoch (Williams, 1989).

The Upper Parmeener Supergroup consists predominantly of sandstone, siltstone, mudstone and coal measures, with subordinate conglomerate and tuff usually found in lenses (Forsyth, 1987, Forsyth, 1989b). The sequence, which is less than one kilometre thick, was deposited in fluvial and fluviolacustrine environments by both low and high sinuosity rivers (Forsyth, 1987, Forsyth, 1989b).

Formal stratigraphic names have not been applied to the Upper Parmeener Supergroup on maps produced by the state government geological survey since 1963. Prior to 1963, the application of different lithostratigraphic names to various parts of the sequence in different locations by different authors had resulted in a confusing proliferation of local stratigraphic names. Since 1963, quadrangle maps produced by Mineral Resources Tasmania and its predecessors use a system of letters descriptive of rock type or lithofacies. The simplest and most widely applied scheme, subdivides the sequence into four units (one to four) using features such as the sandstone lithology, proportion and the nature of lutite and the presence or absence of coal measures and other carbonaceous rocks (Table 2.1) (Forsyth, 1987).

An extensive correlation between this scheme and those used on lithostratigraphic maps is provided in Forsyth (1978).

Table 2.1: Subdivisions within the Upper Parmeener Supergroup (Forsyth, 1987).

Top	Unit 4	Volcanic lithic sandstone and coal measures (Karnian)
	Unit 3	Quartz and lithic sandstone (Pre-Anisian? - Ladinian)
	Unit 2	Quartz sandstone (Griesbachian - pre-Anisian?)
Base	Unit 1	Carbonaceous rocks and coal measures (Wuchiapingian? - Griesbachian)

Unit 1

Carbonaceous rocks and coal measures

(Cygnet Coal Measures, Jackey Formation, Clog Tom Sandstone)

Carbonaceous rocks and coal measures progressively overly the glaciomarine rocks at the top of the Lower Parmeener Supergroup (Figure 2.9). In northern Tasmania this sequence is known as the Clog Tom Sandstone (Green, 1959) and the Jackey Shale (Formation) (McKellar, 1957), while in southern Tasmania coal measures and laterally equivalent rocks are known as the Cygnet Coal Measures (Farmer, 1985).

The carbonaceous rocks and coal measures are associated with interbedded, well-sorted, cross-bedded or ripple laminated sandstone and lutite (Forsyth, 1987, Forsyth, 1989b). In southern and western, but not in northern Tasmania, discontinuous lenses of quartz pebble conglomerate or pebbly sandstone, comprising clasts of quartzite, schist, slate and granite, usually comprise the first few metres of the sequence (Forsyth, 1987, Forsyth, 1989b). In southern and central Tasmania, sandstone is characteristically carbonaceous, arkosic or richly feldspathic, while carbonaceous, micaceous, quartz sandstone is common in northern Tasmania (Forsyth, 1987, Forsyth, 1989b). Lutite is common in the upper part of the sequence, in coal measures and in areas of the Great Western Tiers, it is usually micaceous, and beds may be shaley, massive or interbedded to interlaminated with sandstone (Forsyth, 1987, Forsyth, 1989b). Lutite associated with coal measures is usually medium- to dark-grey and paler elsewhere. Coal measures associated with this sequence occur in the far south and northwest of the Tasmania Basin (Figure 2.10). The seams are thin and small in number and, although mined in the past, they currently have little economic value. The main source of detritus for these rocks was probably granitic; however metamorphics, including high grade (eclogitic) rocks have also contributed (Forsyth, 1987, Forsyth, 1989b).

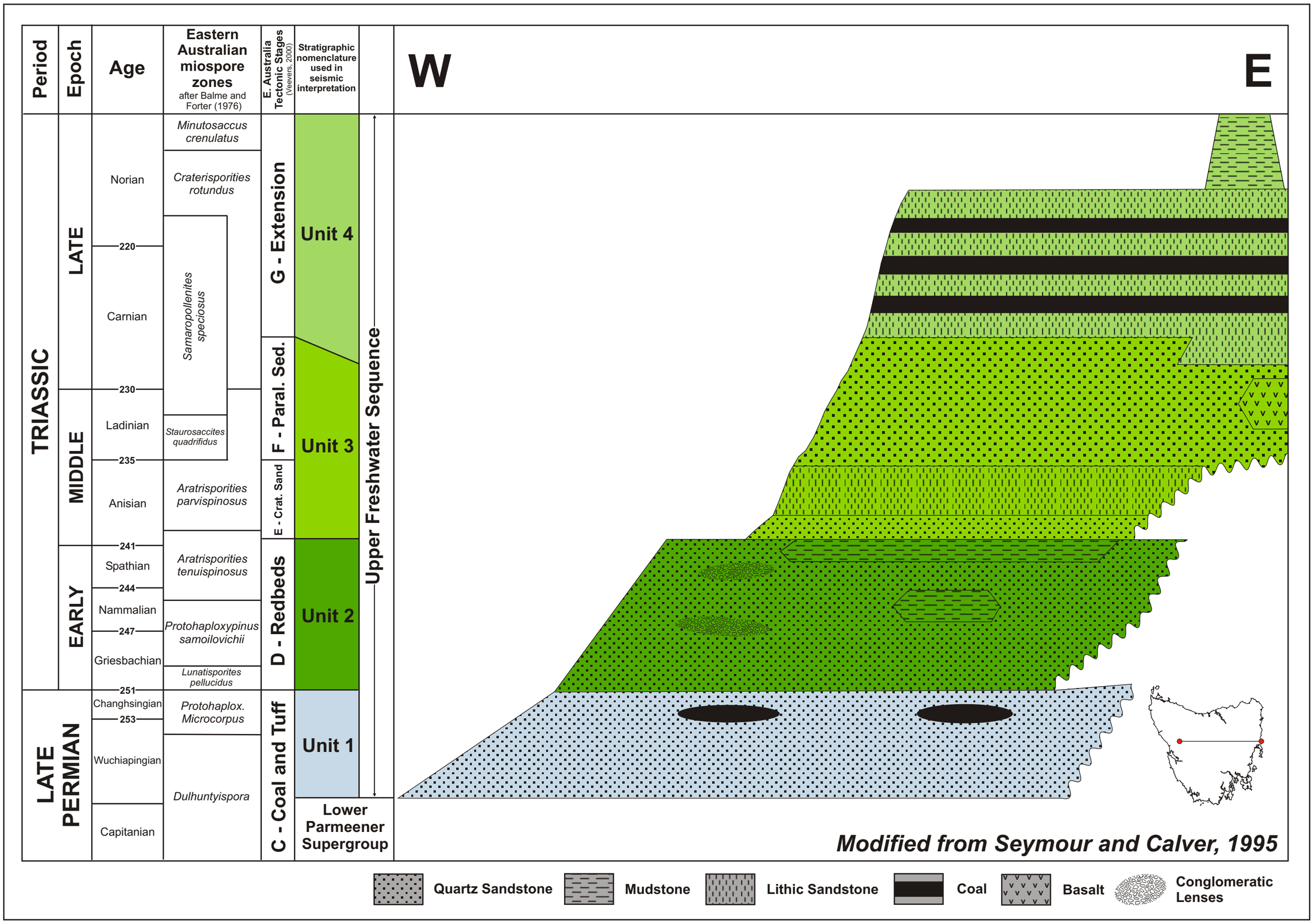

Figure 2.9: The generalised stratigraphy of the Upper Parmeener Supergroup.

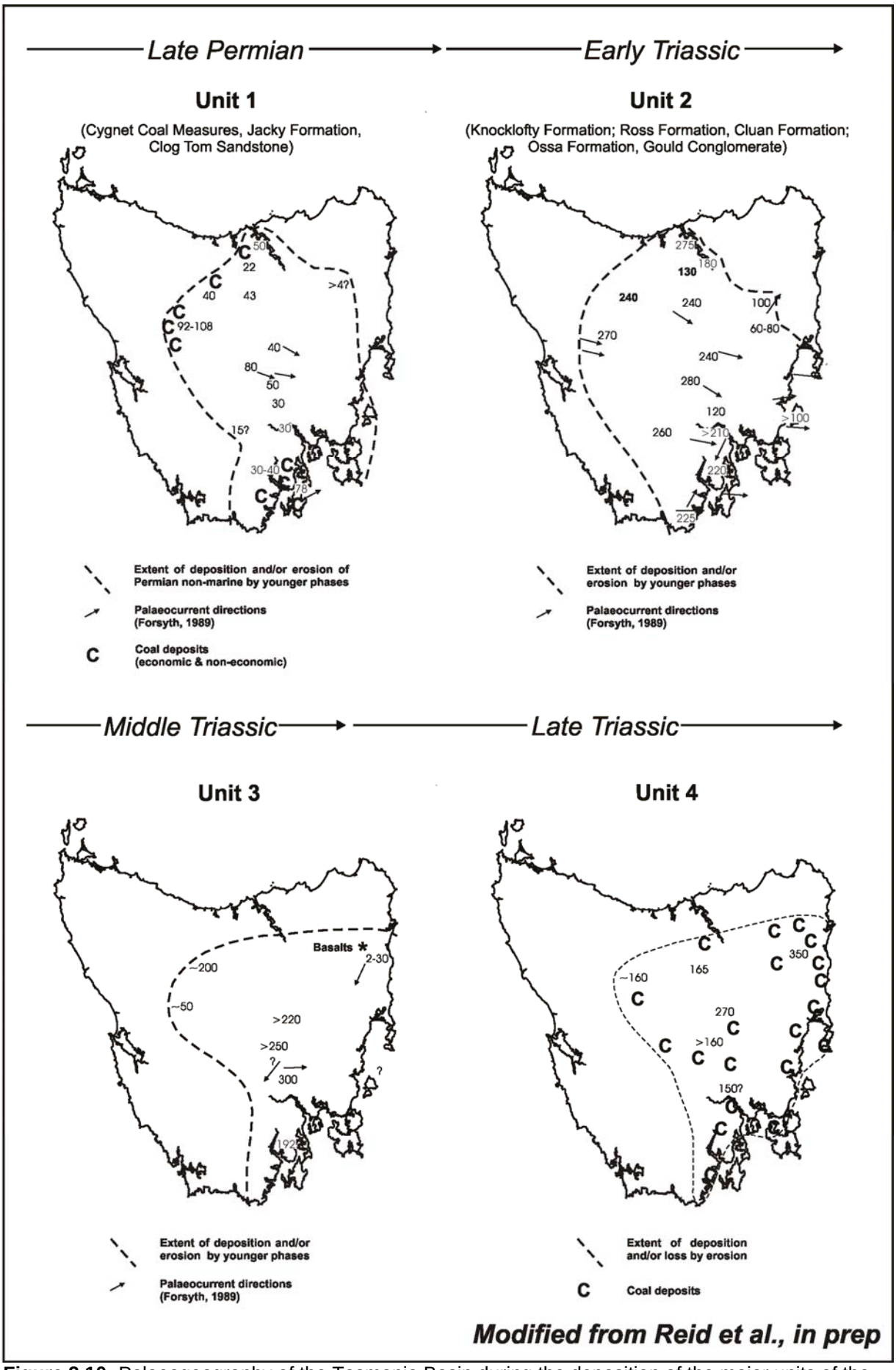

Figure 2.10: Palaeogeography of the Tasmania Basin during the deposition of the major units of the Upper Parmeener Supergroup

The depositional environment is generally regarded as a coastal plain, where the sequence was deposited over the marginal marine facies at the top of the Lower Parmeener Supergroup by sand-laden rivers, rapidly prograding towards the east and southeast (Figure 2.10) (Forsyth, 1987, Forsyth, 1989b). Deltaic conditions prevailed in the far southeast, while in central Tasmania fluvial conditions existed with sediment deposited by broad, low-sinuosity rivers (Forsyth, 1987, Forsyth, 1989b). Conditions suitable for peat formation probably existed from the time marine deposition ceased (Gee and Legge, 1979). The low sulphur content of the coals indicates they were probably formed in lacustrine or flood-basin type environment (Forsyth, 1987, Forsyth, 1989b). Combinations of flora indicating a Late Permian age for the sequence are found throughout the basin (Forsyth, 1987, Forsyth, 1989b).

Unit 2

Quartz Sandstone

(Knocklofty Formation; Ross Formation, Cluan Formation; Ossa Formation, Gould Conglomerate)

An abrupt change in depositional environment is reflected by the development of a thick, dominantly quartz sandstone sequence, which rests on Late Permian coal measures or in the east where they are absent, on the Lower Parmeener Supergroup (Figure 2.9) (Forsyth, 1987, Forsyth, 1989b). The sequence consists predominantly of well-sorted, commonly cross-bedded quartz sandstone, and feldspathic quartz sandstone, with subordinate lutite (Forsyth, 1987, Forsyth, 1989b). The sequence is regionally divisible into a lower interval, dominated by sandstone with lenses of lenticular lutite and a thinner upper interval consisting predominately of lutite (Forsyth, 1987, Forsyth, 1989b). The sequence is between 200 and 300 m thick over much of Tasmania, thinner in the northeast and absent near St Marys and Cranbrook (Figure 2.10) (Forsyth, 1987, Forsyth, 1989b).

The quartz sandstone of the lower interval comprises 45 - 100% quartz, 0 - 47% feldspar and 0 - 18% lithics (Eggert, 1983). Quartz grains are both strained and clear, unstrained and lithic grains are mostly siliceous metasedimentary; in some beds locally derived rock fragments are common (Forsyth, 1987, Forsyth, 1989b). Sandstone in the upper lutite rich interval can be feldspathic quartz sandstone to less quartzose micaceous rock with a rich ferruginous matrix (Forsyth, 1987, Forsyth, 1989b). Lutite is generally micaceous, fissile to massive and silty and occurs dispersed in the sandstone or as 20 – 60 m thick intervals at or near the top of the sequence (Forsyth, 1987, Forsyth, 1989b). Some layers within the lutite-rich layer are bioturbated, and locally silicified, and mudcracks maybe present (Forsyth, 1987,

Forsyth, 1989b). Source rocks include granite pegmatite, and probably some sedimentary and volcanic rocks probably derived from western Tasmania or beyond in Antarctica or south-eastern Australia (Forsyth, 1987, Forsyth, 1989b).

Overall the sequence fines upwards from medium- and coarse-grained sandstone to very fine-grained sandstone (Forsyth, 1987, Forsyth, 1989b). Granules or small quartzose pebbles forming conglomeratic lenses are dispersed in the sandstone. The conglomerates are common in the basal few metres of the sequence and become rare in higher horizons, where they occur mainly at the base of major cycles (Forsyth, 1987, Forsyth, 1989b). Individual sandstone beds are commonly <600 mm and form thick intervals (60 – 80 m) consisting almost entirely of sandstone with isolated, randomly distributed, lenticular beds of lutite (Forsyth, 1987, Forsyth, 1989b). The intervals are composed of cycles, or eroded cycles, that fine upwards from medium- to coarse-grained sandstone to finer, rarely muddy rocks with mud pellet conglomerate and uncommon quartz granules at the base (Forsyth, 1987, Forsyth, 1989b). The basal beds of a cycle may be massive tabular cross-bedded and in places coset with festoons; they may also include planar-laminated scour fills (Forsyth, 1987, Forsyth, 1989b). Low-angle cross-bedding occurs both high and low in the cycles; fine-scale planar lamination and ripple cross-lamination occur in the high cycles and current-drag overturned cross-bedding is very common (Forsyth, 1987, Forsyth, 1989b).

Deposition of the sandstone was primarily by low sinuosity rivers, which average palaeocurrent directions indicate flowed towards the east or southeast (Figure 2.10). Lutite was deposited in abandoned channel, slack-water, lacustrine and overbank environments (Forsyth, 1987, Forsyth, 1989b).

A variety of fossils is found in the sequence, and include macro and microflora and macrofauna including freshwater fish, amphibians, reptiles and insects (Forsyth, 1987, Forsyth, 1989b). Microflora from the lower parts of the sandstone sequence correlate with Perth, Sydney and Bowen Basin assemblages, indicating Greisbachian to Nammalian (Early Triassic) age. Cluan Formation microflora from the upper part of the sequence correlate with parts of the *A. tenuispinosus* zone of the Sydney Basin and the *T. playfordii* zone in Western Australia indicating Nammalian to early Anisian (late Early Triassic to early Middle Triassic) age (Forsyth, 1987, Forsyth, 1989b, Reid et al., in prep).

Unit 3

Quartz and lithic sandstone

A broad, basin wide change in sandstone composition followed the quartz sandstone dominated sequence, with the deposition of dominantly lithic sandstone and some coal measures (Figure 2.9). In some areas, the sequence is interrupted by hiatuses and by two distinct quartz sandstone intervals, a basal interval that is often absent and an upper interval, which on a sub-regional scale is lenticular and diachronous (Forsyth, 1987, Forsyth, 1989b). Due to the periods of non-deposition, the upper quartz sandstone interval in northeast Tasmania commonly occupies the basal stratigraphic position and rests on Lower Triassic sandstone, Lower Parmeener Supergroup or older rocks (Forsyth, 1987, Forsyth, 1989b).

The sequence is best known from the Southern Midlands area (Forsyth, 1984). In this region a discontinuous granule sandstone marks the base of the sequence containing both quartz and lithic sandstone (Forsyth, 1984, Forsyth, 1987, Forsyth, 1989b). The granule sandstone is probably a shoe-string deposit by an erosive, low sinuosity river flowing towards the north-northwest (Forsyth, 1987, Forsyth, 1989b). The overlying quartz and lithic sandstone unit is about 20 m thick and contains several lenticular quartz sandstone units interbedded with lithic sandstone and lutite (Forsyth, 1987, Forsyth, 1989b). The quartz sandstone is very mature, white, with sharply defined laminations and thin silicified layers (Forsyth, 1987).

In the Southern Midlands, the basal interval containing quartz sandstone is succeeded by an 80 m thick interval of interbedded quartz-rich lithic sandstone and lutite (Forsyth, 1987, Forsyth, 1989b). The sandstone comprises 25 – 45% quartz, feldspar, chert and other quartzose lithic grains, some fine-grained felsic igneous grains and rare basaltic grains (Forsyth, 1987, Forsyth, 1989b). The lutite occurs in mainly upward fining cycles, with a basal fine- to medium-grained sandstone (0.1 – 1 m) overlain by lutite (Forsyth, 1987, Forsyth, 1989b). Carbonate concretions, bioturbated horizons and possible palaeosols are observed, and water escape structures are common, but desiccation cracks are not observed (Forsyth, 1984, Forsyth, 1987, Forsyth, 1989b). A lack of mudcracks suggests deposition in a humid environment, such as a swamp (Forsyth, 1987, Forsyth, 1989b). Major channels transporting sand were either uncommon or rarely migrated far from the flood plain (Forsyth, 1987, Forsyth, 1989b). The basal sandstone beds in the lutite dominated cycles are generally non-erosive and are interpreted as deposits from sluggish water moving through the swampy environment (Forsyth, 1984, Forsyth, 1987, Forsyth, 1989b).

The upper interval of quartz sandstone reaches a thickness of 100 m in the Southern Midlands region, but is thinner at Mt Lloyd to the south, Poatina to the north and at St Marys (Forsyth, 1987, Forsyth, 1989b). In the St Marys area the thickness varies (0 – 60 m), approximately corresponding to basement topography (Turner and Calver, 1987). The interval can show considerable variation, containing quartz and lithic sandstone, lutite and thin coal seams in some areas. The sandstone varies laterally from quartzose to lithic or feldspathic; the lithic sandstone is, in places quartz- or chert rich and often contains biotite (Forsyth, 1987, Forsyth, 1989b). Two conformable basalt horizons, up to 30 m thick occur north of St Marys (Figure 2.9, 2.10) (Turner and Calver, 1987). These basalts exhibit features indicating that the were either very shallowly intrusive or extrusive (Turner and Calver, 1987). The main sandstone units of the upper interval are fluvial in origin, while some lutite units were channel-fill or flood-basin deposits (Forsyth, 1984, Forsyth, 1987, Forsyth, 1989b).

Fossils present throughout the sequence indicate an overall Anisian to Ladinian (Middle Triassic) age (Reid et al., in prep). Microflora from the basal quartz sandstone interval approximately correlate with the *Aratrisporites tenuispinosus – A. parvispinosus* (Forsyth, 1987, Forsyth, 1989b). Macroflora recorded about 40 m from the top of the lithic sandstone and lutite interval in the Southern Midlands indicate a post-Middle-Anisian age (Forsyth, 1984, Forsyth, 1987, Forsyth, 1989b). Palaeontological data suggest the upper quartz sandstone interval is late Anisian to Ladinian in age (Forsyth, 1987, Forsyth, 1989b), which is supported by the minimum radiometric age (233 ± 5 Ma) of the lower basalt near St Marys (Calver and Castleden, 1981).

Unit 4

Volcanic lithic sandstone and coal measures

Unit 4 consists predominantly of volcanic lithic sandstone, lutite and coal seams, with rare tuff and conglomerate beds (Figure 2.9) (Forsyth, 1987, Forsyth, 1989b). The sequence is about 270 m thick in the Midlands area (Forsyth, 1984), and up to 350 m thick in the coal field near St Marys (Bacon, 1991) (Figure 2.10), and is preserved beneath Jurassic or Tertiary igneous rocks or in graben (Forsyth, 1987, Forsyth, 1989b).

Sandstone comprises about 70% of the sequence, lutite and coal measures making up the remainder (Forsyth, 1987, Forsyth, 1989b). Lutite is generally light-grey to black and occurs finely interbedded with sandstone (Forsyth, 1987, Forsyth, 1989b). Sandstone occurs as parts of fining-up fluvial cycles; the basal beds are coarse-grained sandstone that rapidly pass up

into cross-bedded sandstone then ripple-laminated fine-grained sandstone and lutite in complete cycles (Forsyth, 1987, Forsyth, 1989b). Throughout the sequence, sandstone is generally less quartzose or less feldspathic, containing a higher proportion of very-fine igneous grains then older, Upper Parmeener Supergroup sandstone. The sandstone commonly contains about 5 – 35% quartz and 6 – 18% feldspar; however, quartz content can be >50 % and feldspar content can be as high as 80 % (Forsyth, 1989b). Opinion on what constitutes the major part of the lithic fraction differ; however volcanic grains, lutite and chert appear to be the most common. Igneous grains are often trachytic, some are flow-banded and some have a spherulitic fabric; composition ranges from acid to basic with intermediate grains most common (Forsyth, 1987, Forsyth, 1989b). Other rock fragments include schist, slate, phyllite, chalcedony and coal (Forsyth, 1987, Forsyth, 1989b). Palaeocurrent evidence suggests provenance from the east. Source rocks include the Lower Parmeener Supergroup; the sandstone is generally sourced from calcalkaline volcanics and plutonic rocks probably from a magmatic arc (Eggert, 1983).

Extrabasinal clasts of pebble and cobble size occur as channel lags and in conglomerate beds, while boulder sized clasts are found in the northeast and in the Midlands (Forsyth, 1987, Forsyth, 1989b). Clast lithologies reflect lower Palaeozoic rocks of western Tasmania and the Mathinna Supergroup and Devonian dykes of eastern Tasmania are also recognised as are contemporaneous Triassic tuffs (Forsyth, 1987, Forsyth, 1989b); however, many of the igneous rocks have no known source (Forsyth, 1987, Forsyth, 1989b).

Coal is found throughout the sequence (Figure 2.10); however the occurrences are isolated and no effective regional stratigraphic subdivision of the major coal-bearing interval has been achieved (Forsyth, 1987, Forsyth, 1989b). In the northeast, where coal is currently mined, local coal seam stratigraphy names eight seams or groups of seams (A to H from top to bottom) over a 220 m vertical interval (Bacon, 1991). The seams range from 0.5 to 3 m thick. The coals are generally dull, with only a small (10 %) component of bright coal, and are of medium rank with a high ash and low sulphur content (Bacon, 1991).

The volcanic lithic sandstone is a channel deposit, laid down by high sinuosity rivers forming continuous sheets of sandstone over areas of tens, perhaps hundreds of square kilometres, that in places contain finer-grained deposits, probably constituting channel fill (Forsyth, 1987, Forsyth, 1989b). Coal seams, continuous over tens of square kilometres were developed in areas sufficiently isolated from the main channels for peat swamps to form; however peat

formation was often terminated by the reappearance of major channels (Forsyth, 1987, Forsyth, 1989b).

Extensively altered, rhyolitic to rhyodacitic pyroclastic rocks, confined to the upper parts of the sequence, are observed near Bicheno in north-eastern Tasmania (Bacon and Everard, 1981), and in drill core from the Fingal Tier (Bacon et al., 1989). The distribution of these rocks is erratic, horizons are generally >1 m thick, but may occur closely spaced within a very short stratigraphic interval, indicating intermittent, explosive volcanic activity (Bacon et al., 1989). The relict vitroclastic texture is slightly deformed, indicating the rock is a poorly welded ash-fall tuff (Bacon et al., 1989). Minor lateral and vertical variations in grainsize and mineralogy are attributed to aeolian sorting.

The sequence is broadly Carnian in age (Forsyth, 1987, Forsyth, 1989b). The biotite age of the ash-fall tuff near Bicheno is 214 ± 1 Ma, which lies close to the Carnian–Norian boundary of Webb (1981) (Bacon and Green, 1984). Immediately underlying the tuff, a broad interval from H seam to above A seam, may be correlated with the *Craterisporites rotundus* zone (De Jersey, 1973) indicating a Carnian age (Forsyth, 1987, Bacon et al., 1989, Forsyth, 1989b), while a microflora referred to the lower *Polycingulatisporites crenulatus* zone (Norian) occurs about 20 m above the tuff (Bacon et al., 1989, Forsyth, 1989b).

Summary

In the Late Permian, deposition of the Upper Parmeener Supergroup began in a non-marine environment. The first rocks deposited were carbonaceous and coal measures associated with sandstone and lutite (Forsyth, 1987, Forsyth, 1989b). These progressively overly the glaciomarine rocks of the Lower Parmeener Supergroup. Deposition was along a sandy coastal plain by low sinuosity, sand laden rivers prograding towards the east and southeast (Forsyth, 1987, Forsyth, 1989b). The source of the sediments was probably granitic; however metamorphic rocks have also contributed (Forsyth, 1987, Forsyth, 1989b). An abrupt change in depositional environment is reflected by the development of a thick dominantly quartz sandstone sequence deposited by low sinuosity rivers flowing towards the east and southeast (Forsyth, 1987, Forsyth, 1989b). The source was in western Tasmania or beyond and included granite and probably some sedimentary and volcanic rocks (Forsyth, 1987, Forsyth, 1989b).

A basin-wide change in sandstone composition to a dominantly lithic variety followed. Two conformable basalt horizons are found in the upper interval north of St Marys, and these are a useful constraint on the age of the sequence. Above the lithic sandstone lies a thick sequence of predominately volcanic lithic sandstone. Palaeocurrent data suggest a source to the east that included the Lower Parmeener Supergroup and calcalkaline igneous rocks (Eggert, 1983). Isolated occurrences of coal, some economic, are distributed throughout the sequence. A poorly welded ash-fall tuff is found in the east, indicating contemporaneous explosive volcanism, probably from a magmatic arc east of Tasmania.

2.7: LATE JURASSIC TO RECENT

Multiple periods of extension related to the break-up of the eastern margin of Gondwana affected the Tasmanian region from the Late Jurassic. Stress in the upper crust resulted from three main regional events: 1). an easterly propagating rift between Australia and Antarctica to the west of Tasmania, 2). rifting associated with the formation of the Tasman Basin to the east and 3). the prolonged fragmentation, separation and clearance of the Australian and Antarctic plates along Tasmania's western margin (Blevin, 2003). These stresses resulted in the formation of north-westerly trending continental rift basins, the Bass and Durroon Basins in the Bass Strait and a series of north-northwest trending transtensional basins along the western margin of Tasmania collectively known as the Sorell Basin (Figure 2.11).

Apatite fission track (AFT) ages from inland Tasmania record a rapid cooling episode in the middle Cretaceous (~ 100 – 85 Ma), indicating km scale uplift and denudation (O'Sullivan et al., 1998, O'Sullivan et al., 2000a). No Late Jurassic to middle Cretaceous sedimentary rocks are found in Tasmania, while thick Late Cretaceous to middle Tertiary deposits are located in the offshore basins. O' Sullivan et al. (1998) suggests following shallow intrusion, the dolerite was deeply buried by a Late Jurassic to middle Cretaceous sedimentary succession (>~2.5 – 4 km) which may have covered much of Tasmania prior to middle Cretaceous rifting and subsequent extension.

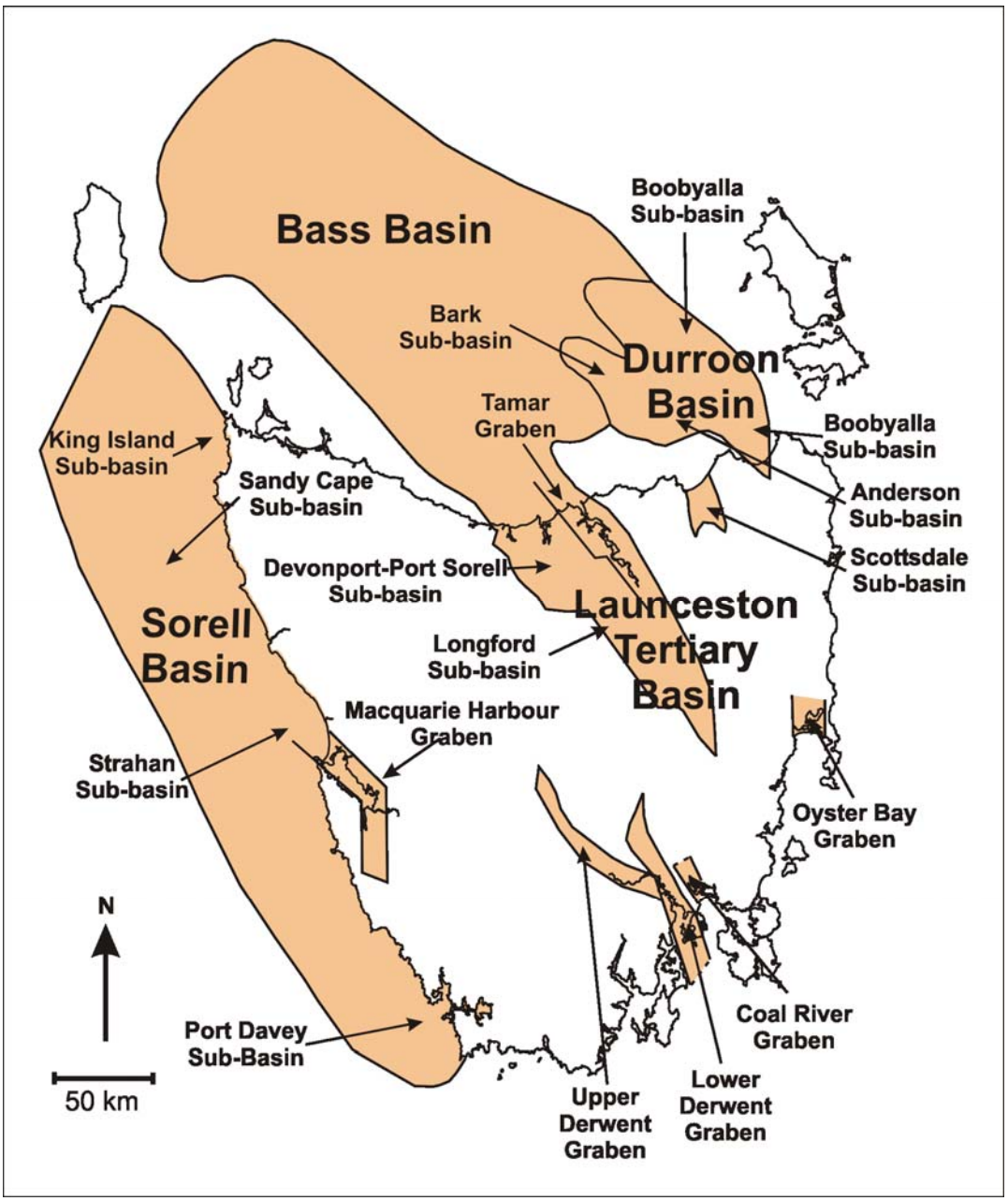

Figure 2.11: Mesozoic basins of Tasmania

In the latest Cretaceous, a series of extensional structures began to develop across NE Tasmania. The Bass Basin propagated onshore, beginning with the Tamar Graben and ultimately resulting in development of the Launceston Tertiary Basin (Figure 2.11). During the Late Paleocene to Early Eocene Tasmania was moving NNE along the left-lateral transform, which ran along the eastern margin of Antarctica. About this time, an extension of the Strahan Sub-basin, the Macquarie Harbour Graben, developed on the west coast of Tasmania (Figure 2.11). In southeast Tasmania, the Derwent Graben began forming in the Paleocene to Early Eocene and the adjacent Coal River Graben probably before the early Miocene (Figure 2.11) (Baillie and Leaman, 1989). Spreading in the Tasman Sea ceased in the Early Eocene (55-50 Ma) (Royer and Rollet, 1997). Major structuring related to these events ceased by the end of the Eocene.

A phase of strike slip faulting is prominent in western and southern Tasmania. These faults are widespread but largely minor in nature. No major faults of this age have been recognized on the Tasmanian mainland. The faults affect rocks as young as 100 Ma and predate the normal faulting in the Derwent Graben (Berry and Banks, 1985). The faults increase in intensity towards the southwest and no faults or fractures of this style are known in northeast Tasmania. Cretaceous reconstructions for Gondwana place Tasmania very close to Northern Victoria Land. Rosetti et al. (2003) record a major dextral transpressional zone along the Rennick Glacier, which correlates with western Tasmania. This belt was interpreted as a Late Cretaceous deformation zone by Fleming et al. (1993), although Rosetti et al. (2003) argued that the dextral faulting was active at 50 Ma. Further south, a dextral transtensional zone in Marie Byrd Land is well dated at 95 Ma (Siddoway et al., 2004a, Siddoway et al., 2004b) and this is the most likely age for the dextral faulting in the Rennick Glacier and in western Tasmania. This short period of dextral transtension during break-up contrasts with the Late Jurassic to Eocene sinistral movement generally interpreted along this margin. The deformation associated with this event may correlate with Cenomanian inversion in the Sorell Basin.

Mio-Pliocene compressional tectonics is widely recognized in Victoria and measurements of the modern stress field indicate that Tasmania is also affected by northwest compressional stress (Hillis and Reynolds, 2000). However, there is very little evidence for neotectonic structures in Tasmania. The only known active fault in Tasmania is the Lake Edgar Fault. Movement was originally thought to be a regional response to high heat flow (Murray-Wallace and Goede, 1995); however recent work indicates the fault is susceptible to reactivation under conditions imposed by the current Australian intraplate stress field (Clark et al., in press). The vertical displacement of the late Tertiary faults can still be recognised in the modern topography.

2.7.1: OFFSHORE BASINS

Bass Basin

The Bass Basin is northwest trending intracratonic rift basin lying beneath the Bass Strait between Tasmania and Victoria (Figure 2.11) (Blevin, 2003). The formation of the basin was strongly controlled by the underlying Proterozoic and Palaeozoic basement terranes (Blevin, 2003) which correlate with the Western and Eastern Tasmania Terranes.

Proposed north-northeast extension has resulted in the development of a series of west-northwest trending half-graben along northeast and southwest dipping basement controlled normal faults (Etheridge et al., 1985, Hill et al., 1995, Blevin, 2003). These faults generally have throws of 3 to 5 km, with the total sedimentary succession reaching thicknesses of 8 to 10.5 km (Williamson et al., 1987, Young et al., 1991). Etheridge et al. (1985) observed that these normal faults can terminate abruptly at transverse zones that span the basin. They interpreted these transverse zones were transfer faults similar to oceanic transforms.

Initial deposition took place in terrestrial to marginal marine environments from the Early Cretaceous to the Middle Eocene; widespread marine flooding occurred from the late Middle Eocene, with deepening marine environment becoming dominant from the Late Miocene (Blevin, 2003). Six phases of deposition are recorded in the basin correlating to three periods of extension, a rift-transition phase, and two phases of subsidence (Blevin, 2003).

Durroon Basin

The Durroon Basin comprises three sub-basins (Baillie and Pickering, 1991), the Bark, Anderson and Boobyalla sub-basins (Figure 2.11). The basin adjoins the southeast Bass Basin and its earliest development is related to the same extensional event, but has a different structural history (Baillie and Pickering, 1991). Deposition of Otway Group correlates probably began in the Early Cretaceous in a broad linear depression with fault bounded margins (Baillie and Pickering, 1991).

Extension coupled with lithospheric cooling in the Durroon Basin split the basin into northwest trending graben and half-graben separated by major listric faults (Baillie and Pickering, 1991). Graben development in the basin is asymmetrical with fault blocks tilted southwest (Seymour and Calver, 1995). The Durroon Basin experienced increased geothermal gradients (up to 55ºC/km) from 100 Ma to 90 Ma, followed by Cenomanian uplift and erosion (Duddy, 1992). A 110 Ma to 90 Ma cooling event is recorded throughout eastern Tasmania. This is partly in response to kilometre scale erosion of a thick overlying succession, probably including Jurassic to Early Cretaceous stratigraphy (O'Sullivan and Kohn, 1997, Kohn et al., 2002, O'Sullivan et al., 2000b), but also influenced by cooling after the Cretaceous magmatic pulse.

By the Late Cretaceous there was significant growth on northeast-trending extensional faults resulting in thick (up to 2.5 km) wedges of Durroon Formation, unconformably overlain by a Campanian to Maastrichtian sag sequence (Hill et al., 1995). Baillie and Pickering (1991) report, that by the latest Cretaceous, subsidence in the basin had diminished with regional subsidence migrating towards the present day depocentre of the Bass Basin.

Sorell Basin

Sediments of the Sorell Basin cover the western continental margin of Tasmania (Willcox et al., 1989). The basin contains four depocentres, the King Island, Sandy Cape, Strahan and Port Davey Sub-basins (Figure 2.11), each with over 4 km sediment thickness. These sub-basins were probably developed in the latest Jurassic to earliest Cretaceous (Hill et al., 1997), and have been interpreted as “relieving bends” on a major left-lateral, strike-slip fault, associated with extension along Australia’s southern margin (Moore et al., 1992). The eastern edges of the sub-basins are bounded by strike-slip faults, except for the King Island Sub-basin that lies inboard of the major fault. They are separated by basement highs.

Both the King Island and Sandy Cape Sub-basins were initiated in or before the Early Cretaceous, and contain Early Cretaceous Otway Group correlates (Moore et al., 1992). The King Island Sub-basin is a perched half-graben, apparently formed by extension (Moore et al., 1992), that deepens eastward to a high angle northwest dipping normal fault (Willcox et al., 1989). The Strahan Sub-basin is a north-northwest-striking slot comprising two east-west-trending half-grabens, which shallow to the southwest from a northern depocentre (Moore et al., 1992). Moore et al. (1992) considered the basin boundary faults and the extensional faults bounding the tilt-blocks to be a linked fault system responsible for basin formation. Opinion remains divided on the timing of the earliest deposition in the Strahan Sub-basin, in spite of its close seismic coverage, and a single exploration well that only just penetrates the upper Cretaceous (Cape Sorell-1). In Moore et al. (1992), the junior authors argue the basin was formed along a strike-slip zone during the Late Jurassic and was contemporaneous with the formation of the Eyre Sub-Basin and the Great Australian Bight Basin. In contrast, Moore (1991) argues that the basin is unlikely to contain any Lower Cretaceous section and with the Port Davey Sub-basin is the product of strike-slip and transform plate interaction in the Late Cretaceous to Paleocene. The latter case is consistent with the age of basin formation decreasing southwards, and links their relative age of

formation to the northward movement of Tasmania with respect to the Antarctic Plate (Moore et al., 1992).

2.7.2: ONSHORE BASINS

Launceston Tertiary Basin

The term Launceston Tertiary Basin was first used by Johnston (1874) to describe the trough containing Tertiary age sediments in the north of the island (Figure 2.11). Areas such as Ross, Tunbridge, York Plains and the Fingal Valley were included in his interpretation (Mathews, 1983). Here, the Launceston Tertiary Basin is interpreted as the 140 km long, north-westerly striking trough. Where the structure meets Bass Strait it is approximately 40 km wide between Devonport and the eastern side of Port Dalrymple and tapers to about 20 km wide in the Northern Midlands. The areal extent of the basin is recognisable on the digital elevation model of Tasmania (Figure 2.12). The basin contains the largest area of unconsolidated Tertiary sediments in Tasmania (Mathews, 1983) The thickest deposits occur in three main depocentres, the Tamar Graben, Devonport-Port Sorell Sub-basin and the Longford Sub-basin, which are separated by basement highs (Figure 2.13).

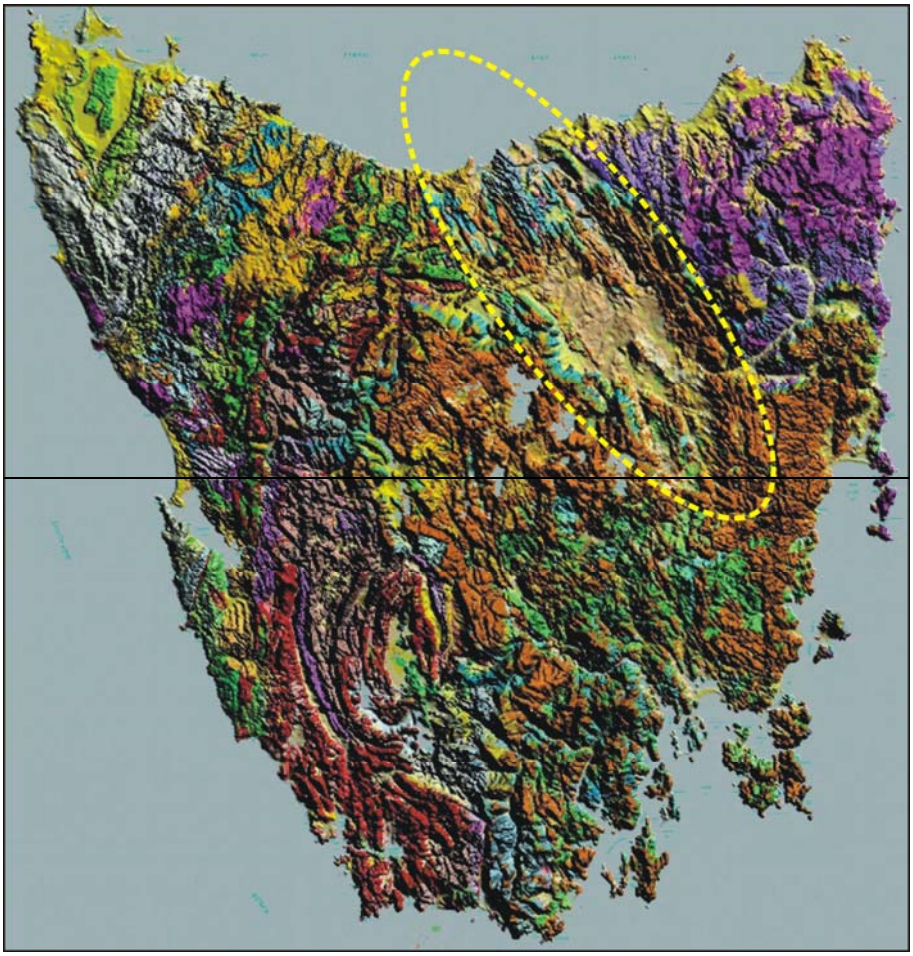

Figure 2.12: Location and extent of the Launceston Tertiary Basin

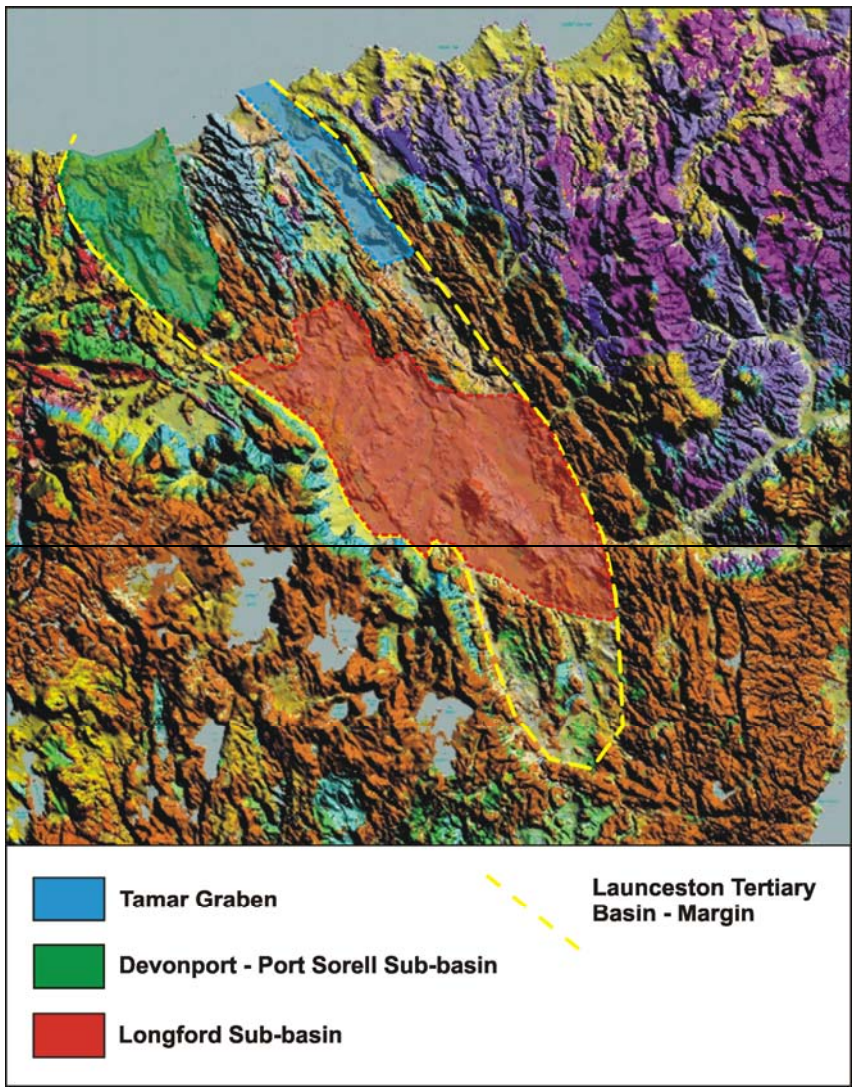

Figure 2.13: Sub-basins of the Launceston Tertiary Basin

Tamar Graben

The Tamar Graben is a relatively small northwest striking trough located at the seaward end of the Launceston Tertiary Basin (Figure 2.11, 2.13). Deposits in the Tamar Graben are predominantly non-marine and include sand and clay with granule beds, siliceous to doleritic conglomerate, carbonaceous beds, lignite, tuff and associated basalt (Forsyth, 1989a). Some of the sandstone and conglomerate exhibits features characteristic of deposition in a fluvial environment; open-framework doleritic conglomerates may be slope deposits; finer grained sediments are interpreted as lacustrine, while some marine or brackish-water sedimentation may have occurred in restricted areas (Forsyth, 1989a). The oldest sediments lie in the south of the structure. These contain microflora assignable to the Latest Cretaceous and Paleocene (Forsyth, 1989a). At the seaward end of the structure the basement is overlain by sediments of latest Paleocene to Eocene age (Seymour and Calver, 1995). The youngest sediments are probably post-basalt siliceous gravels from Beauty Point in the north of the structure, estimated to be late Pliocene in age (Forsyth, 1989a).

Devonport – Port Sorell Sub-basin

The Devonport-Port Sorell Sub-basin is a continental fracture, structurally related to the offshore Bass Basin (Figure 2.11, 2.13) (Cromer, 1989), and has been previously called the Mersey Basin (Johnston, 1888) and the Mersey Graben (Burns, 1964). The basin is exposed as a belt of Permian rocks, Jurassic Dolerite and Tertiary sediments that stretch from the Don River in the west to Port Sorell in the east and to the south just beyond Sassafras. The Tertiary sediments are interpreted as basin infill of second order and fault controlled structures within the first order, Mersey Graben (Burns, 1964). The western boundary of the basin is a series of major faults and associated en echelon fractures that strike towards the northwest (Burns, 1964, Cromer, 1993), and link to the Tiers Fault System in the south. The total pre-Tertiary relief on these structures is about 300 m (Cromer, 1993). The eastern boundary of the basin is marked by a fault with a throw about 200 m that extends the length of the Port Sorell estuary (Burns, 1964, Cromer, 1993), then continues southeast in an en echelon fashion through Frankford and Sassafras (Cromer, 1993).

The Devonport-Port Sorell Sub-basin contains interbedded non-marine sediments separated by two basalt flows, the sequence collectively is at least 350 m, and possibly up to 500 m thick (Cromer, 1989, Cromer, 1993). The sediments are generally claystone, mudstone, sandstone and minor conglomerate deposited under fluviatile to lacustrine conditions (Cromer, 1989, Cromer, 1993). The >250 m thick Harford beds at the base of the sequence contain Paleocene microflora near their base and Eocene (probably Early Eocene) microflora at their top (Cromer, 1989, Cromer, 1993). These are overlain by the 175 m thick, Late Eocene Thirlstane Basalt (Cromer, 1980, Cromer, 1993). Above this are the weakly consolidated, 75 m thick, Wesley Vale Sands which contain Early Oligocene to Early Miocene microflora (Cromer, 1980, Cromer, 1989, Cromer, 1993). The Moriarty Basalt is no more than 50 m thick and forms shallow leads and thin plateau cappings over the Wesley Vale Sand (Cromer, 1989, Cromer, 1993) K-Ar dating indicates a Late Oligocene age (26 Ma) for the basalt (Baillie, 1986).

Longford Sub-basin

The structure of the Longford Sub-basin (Figure 2.11, 2.13) has been described as a graben with a central horst (Mt Arnon and Hummocky Hills, Carey, 1947), while later gravity surveys indicate the basin comprises south-westerly dipping beds fractured by normal faults down-thrown to the east (Longman and Leaman, 1971, Longman, 1966). Direen and Leaman (1997) considered the basin to be an asymmetrical depression developed on multiple, fluvially

incised blocks, most of which exhibit half-graben rotation. Interpretation of recent regional seismic data by Lane (2002), suggested a northwest trending basin composed of a western graben and an eastern half-graben separated by a central horst. These structures developed sub-parallel to the basin bounding Tiers and Castle Carey Faults. Lane (2002) interpreted the western graben to have formed at the onset of rifting, with a series of north-easterly trending transfer faults active during the initial extension. Reactivation of the transfer structures initiated the development of the eastern half-graben (Lane, 2002). Many of these faults were continuously active during deposition. Lane (2002) interpreted several hundred metres of growth on the western sides of the western graben and eastern half-graben.

The Tertiary sediments of the Longford Sub-basin are disconformable and unconformable on the Parmeener Supergroup and Jurassic Dolerite. The terrestrial basin fill is largely derived from the erosion of basement rocks and were deposited under lacustrine/fluviatile conditions. The sediments are dominantly clay and silty clay interbedded with well-sorted fine- to medium-grained quartz sand, sandy clay, coarse sand to granule horizons, siliceous cobble beds and conglomerate consisting mainly of rounded dolerite boulders (Mathews, 1989). Basalt flows and associated tuffs occur towards the top of the succession (Mathews, 1989). Sediments from the deepest part of the basin near Hagley are Paleocene in age, while palynological data indicate the majority of the sediment in the basin were deposited in the Eocene (Mathews, 1983).

Macquarie Harbour Graben

The Macquarie Harbour Graben is an onshore extension of the Strahan Sub-basin (Figure 2.11) containing up to 500 m of early Eocene to Plio-Pleistocene sediment (Baillie and Hudspeth, 1989). The early Eocene succession contains interbedded sandstone, siltstone and minor coal all deposited in a marginal marine setting. These are overlain by cross-bedded sandstone of fluvial origin (Baillie et al., 1986). In the Strahan region, Plio-Pleistocene sediments lie unconformably on the early Eocene sediments (Baillie and Corbett, 1985).

Derwent Graben

The Derwent Graben consists of two linked structures, the lower and upper Derwent Graben (Figure 2.11). The Lower Derwent Graben is a narrow northwest-trending structure, bounded on the west by the Cascades Fault system and by the Meehan Ranges in the east. The structure contains only a few hundred metres of sediment, the oldest being of Paleocene age, indicating

faulting initiated in the early Tertiary (Colhoun, 1989). Analysis of the digital elevation model of Tasmania indicates the Derwent Valley follows the structure as far north as Bridgewater. The Lower Derwent Graben continues towards the north-northwest, containing the Jordan River, and terminating near Melton Mowbray. The throw on the Cascades system decreases to the north.

The Upper Derwent Graben is bounded on its south-western side by a strongly curved normal fault, down to the northeast that approaches the Cascades Fault near Hobart. The fault follows the upper Derwent Valley before dying out in a horsetail splay on the Central Plateau. The intersection between the two faults is a lateral ramp, with no direct intersection between the two structures. Curved, non-linked faults as identified here are indicative of a regime of low extension, while the overall complexity of the observed pattern may indicate oblique extension (McClay et al., 2002), although the influence of basement structures cannot be discounted (Chapter 4 and 7).

Coal River Graben

The Coal River Graben (Figure 2.11) contains three main depocentres which contain the largest exposure of Tertiary sediments in southern Tasmania (Leaman, 1971). Controlling faults strike towards the north and north-northwest and deposition has been largely controlled by the erosion of overlapping grabens and half-grabens (Baillie and Leaman, 1989).

Other Tertiary Structures

Oyster Bay Graben

The Oyster Bay Graben is a north-south trending structure containing up to 300 m of Tertiary sediments that lies between the Freycinet Peninsula and Swansea on Tasmania's east coast (Figure 2.11) (Baillie et al., 1989b).

Scottsdale Sub-basin

The Scottsdale Sub-basin forms a distinctive lowland area in north-eastern Tasmania (Figure 2.11), and contains up to 225 m of Tertiary sediment (Moore, 1989). The 22 km wide basin is bounded to the east and west by two conspicuous scarps; however the present basin is a remnant of a thicker Tertiary sequence where the higher sediments have been removed by erosion (Moore, 1989).

2.8: IGNEOUS ROCKS

2.8.1: JURASSIC DOLERITE

The fragmentation of Gondwana began in the Early to Middle Jurassic and was associated with the emplacement of over 3 000 000 km^3 of dominantly basaltic magma. Evidence for a magmatic mega-province in pre-break-up reconstructions of Gondwana is recorded in igneous rocks from South America, southern Africa, Antarctica, New Zealand, southeast Australia and Tasmania (Figure 2.14). The origin of the magma has been linked to either active plume-driven processes (Duncan and Richards, 1991), or to passive upwelling of the mantle resulting from lithospheric stretching, the process enhanced by the presence of a plume (White and McKenzie, 1989).

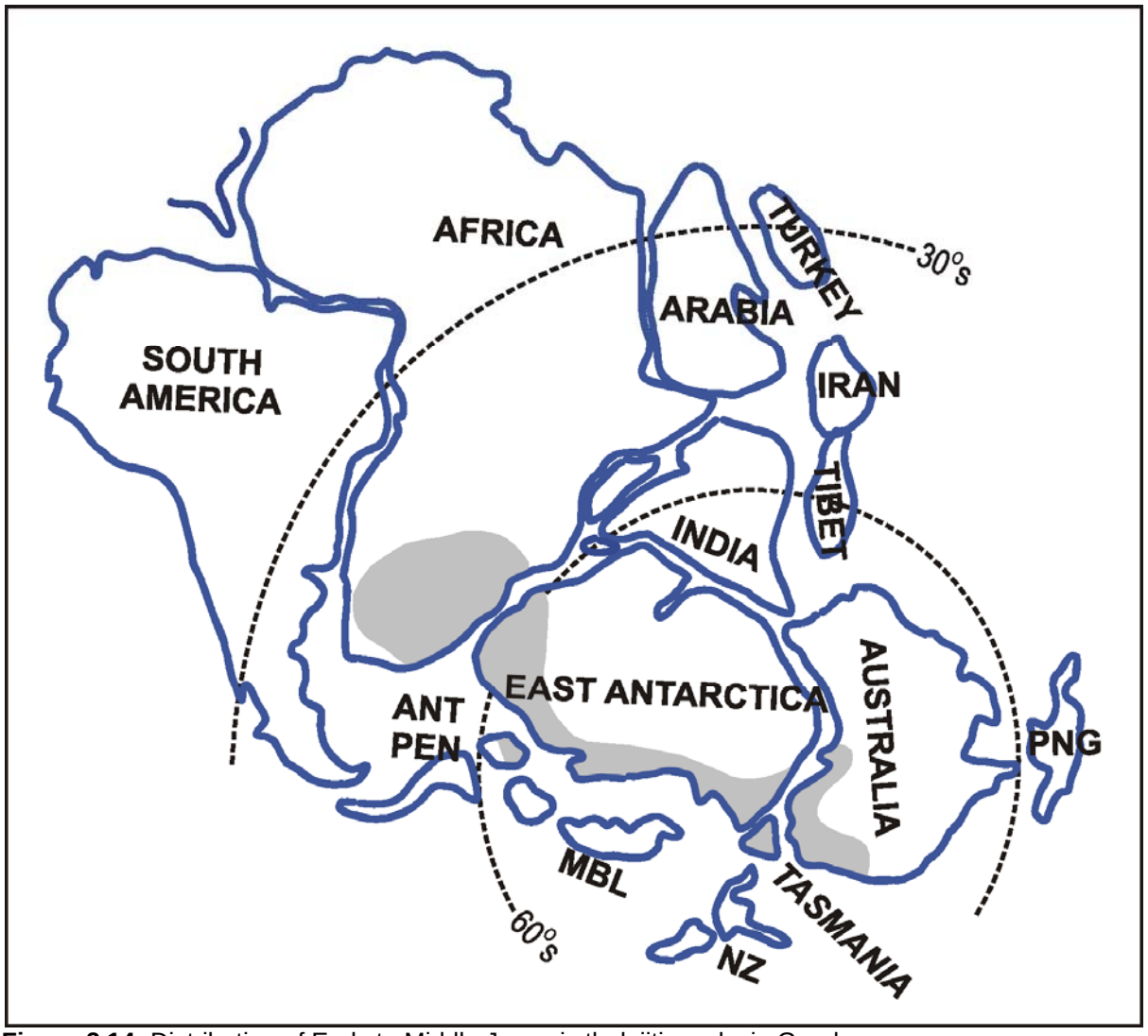

Figure 2.14: Distribution of Early to Middle Jurassic tholeiitic rocks in Gondwana.

By the early Jurassic, the Parmeener Supergroup formed a 1.5 km thick, generally sub-horizontal succession. Large volumes of tholeiitic dolerite were intruded into the Tasmanian crust during the Middle Jurassic (175.1 ± 5.4 Ma, Brauns et al., 2000). Dolerite rose through the basement into the Parmeener Supergroup forming mainly as sills (Hergt et al., 1989). Extrusive basalts are only known from limited areas at Lune River. The Lune River Basalts are associated with sediments containing plant fossils, probably of Jurassic age, and are comagmatic with dolerite on petrographic, geochemical and isotopic evidence (Hergt et al., 1989).

In Tasmania, dolerite is currently exposed over an area of 30,000 km^2, and has an estimated volume of 15,000 km^3 (Figure 2.15) (Hergt et al., 1989). Dolerite has been a major deterrent to petroleum exploration, with nearly every part of the basin being intruded by at least one dolerite sill. Many dolerite intrusions have the form of a flattened cone connected to a source or sources at the deepest point, the limbs are concordant (sills) or approximately concordant with abrupt transgressions when rising to higher levels (Figure 2.16) (Leaman, 1976). The metamorphic effects resulting from dolerite intrusion are usually confined to within a few metres of the intrusion margin, the effect being more severe at the roof of the intrusions. In the Hobart area, two or three sills are commonly present. The sills are usually either less than 1 m, or 300 m to 400 m thick. The thick sills in middle or lower Permian rocks are typically 30 km^2 in area, while sills in Triassic rocks are more extensive (Leaman, 1975). In contrast, only a single sill, intruding the Upper Parmeener Supergroup, has been recognised in the northern part of the basin (Central Highlands, Ben Lomond and the Fingal Tier) (Bacon et al., 2000). A single, 650 m thick, sill was intersected near the Upper – Lower Parmeener Supergroup boundary in the Hunterston-1 DDH (Reid et al., 2003). Interpretations of the current seismic data (Chapter 6 and 7) indicate this sill covers many hundreds of square kilometres.

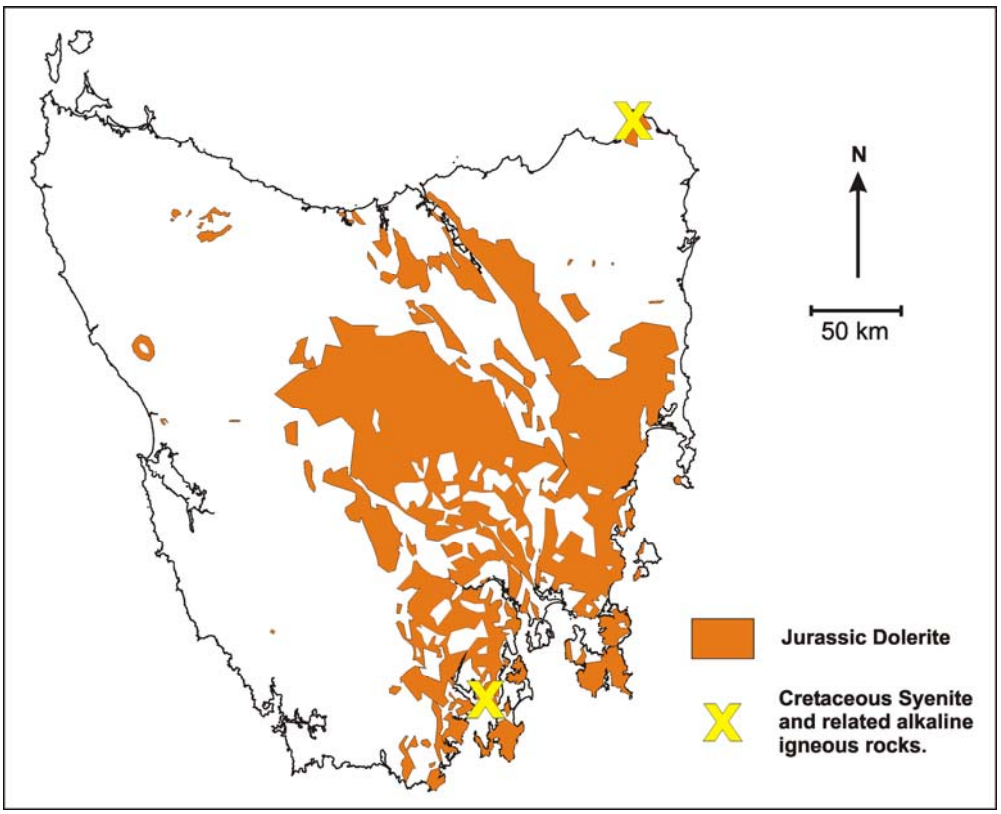

Figure 2.15: Distribution of Jurassic Dolerite and Cretaceous Alkaline igneous rocks in Tasmania.

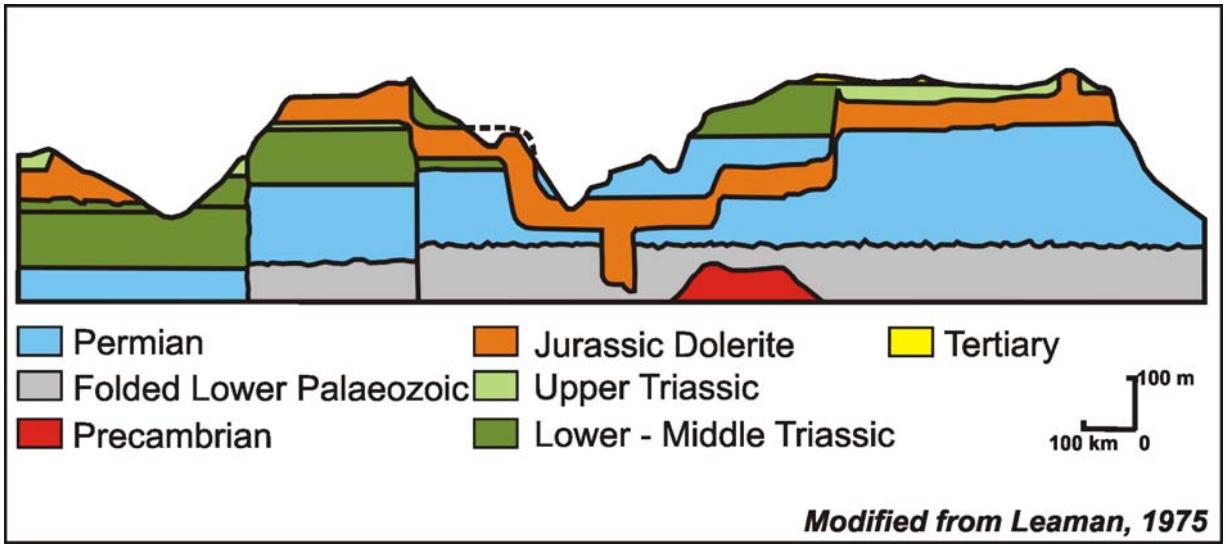

Figure 2.16: Generalised dolerite intrusion forms observed in Tasmania

2.8.2: CRETACEOUS ALKALINE ROCKS

Intrusions of alkaline igneous rocks occur in the southeast (Cygnet-Oyster Cove area) and in the far northeast (Cape Portland) (Figure 2.15). The Cygnet Syenites occur as a series of sheet-like bodies and sills a few tens of metres thick, and as numerous widely dispersed smaller sills, dykes and pipes (Farmer, 1985). They mainly intrude the lowermost units of the Lower Parmeener Supergroup. At Cygnet, the Lower Parmeener Supergroup is domed above a 750 m thick laccolith lying close to the surface (Leaman, 1990). The alkaline rocks near

Cape Portland occur in a series of small flows, dykes and irregular plugs (Jennings and Sutherland, 1969). K-Ar ages indicate the age of emplacement of the Cygnet intrusion is 100.5 ± 3 Ma (Evernden and Richards, 1962, McDougall and Leggo, 1965), and the rocks at Cape Portland are dated at 102 ± 3 Ma (McDougall and Green, 1982).

Tasmania experienced a peak in the geothermal gradient in the Middle to Late Cretaceous. Organic matter taken from the Parmeener Supergroup in the Cygnet area has been totally carbonised by regional heating associated with the intrusions (Farmer, 1985) while the Gordon Group at Ida Bay has been remagnetised by a Late Cretaceous heating event that persisted for about 10 million years (Sharples and Klootwijk, 1981). The Parmeener Supergroup yields apatite ages indicating rapid cooling from elevated palaeotemperatures (>95°C) in the middle Cretaceous at the earliest (O'Sullivan and Kohn, 1997). This Cretaceous thermal event is widely recognised across the adjacent parts of Antarctica and New Zealand (Tessensohn, 1994, Veevers, 2000a).

2.8.3: TERTIARY BASALT

Tertiary basalts are common throughout Tasmania. Tertiary drainages were filled by sub-aerial flows from numerous scattered eruptive centres. About 400 km^2 of basalt is distributed across northern and eastern Tasmania, while no occurrences are known from south-western Tasmania (Sutherland, 1989). The most extensive occurrences are found in northwest Tasmania where early Tertiary drainages were overtopped forming lava plains (Sutherland, 1989). Less voluminous zones are common in the Central Highlands, Launceston Tertiary Basin and to lesser extent in the southeast and northeast.

The basalts were erupted from the Palaeocene to the late Miocene, significantly later than the uplift and extension of the latest Cretaceous to early Tertiary (Sutherland, 1989). Many eruptive centres are located in or near faults, fault intersections and the margins of dolerite intrusions, some aligning along fault and graben systems, while others are aligned beside (but not intruding) major dolerite feeders(Sutherland, 1989). Major basement features appear to control the distribution of the eruptive centres over considerable distances.

CHAPTER 3
THE PETROLEUM GEOLOGY OF ONSHORE TASMANIA

3.1: INTRODUCTION

Onshore Tasmania is a frontier petroleum province. There has been intermittent exploration for oil and gas since the late 1800's, with efforts generally focused on reported oil and gas seeps. Little exploration using modern methods, such as seismic reflection surveys, potential field methods and electronic logging of drill holes, has been undertaken thus far.

There have been many reports of bitumen (inland and coastal strandings) and of oil and gas seeps in Tasmania; almost all have proved to be erroneous. Trace amounts of hydrocarbons are found in various rocks in Tasmania. However, there are no known examples of either inactive oil or gas seeps found onshore in Tasmania. Pyrobitumen is recorded in a number of rock units and bitumens are found in Ordovician limestone, coal measures in the Upper Parmeener Supergroup and in fractured dolerite at Lonnavale, approximately 42 km WSW of Hobart. A number of exploration wells have been drilled in Tasmania, however other than small scale retorting of Tasmanites Oil Shale in the 1920's - 1930's at Latrobe in the states north, there have been no discoveries of commercial quantities of oil and gas onshore in Tasmania.

Since 1984, Great Southland Minerals Limited (GSLM) and its predecessor companies have operated petroleum exploration licences over several parts of the Tasmania Basin. The exploration licence operated during the bulk of this research, SEL 13/98 covered an area of 30,356 km^2 and until 2005 was the largest petroleum exploration licence held in Australia, covering most of the Tasmania Basin (Figure 3.1). Part of the licence area was relinquished in 2005, the new licence covering an area of 15,035 km^2 (Figure 3.1). The exploration program is predicated on two potential hydrocarbon plays that are thought to form a stacked petroleum system. These are an intra-Tasmania Basin play based on a potential Gondwana Petroleum System in the Parmeener Supergroup and a Lower Palaeozoic play based on an interpreted Larapintine Petroleum System in the Wurawina Supergroup. To date data collected include a limited gravity survey, 659 line kilometres of seismic data in the Central Highlands and Northern Midlands areas and a stratigraphic drill hole at Hunterston. Further seismic acquisition and wildcat drilling is planned for 2007/2008.

The following is a summary of the available data sourced from thesis's, published papers and reports. For a more comprehensive review of the petroleum geology of onshore Tasmania the reader is directed to Bacon, 2000, Reid, 2004 and Chester, 2006. Many of the stratigraphic names mentioned in this chapter are local names and their position in the broader stratigraphy is shown in figures 2.6 and 2.9.

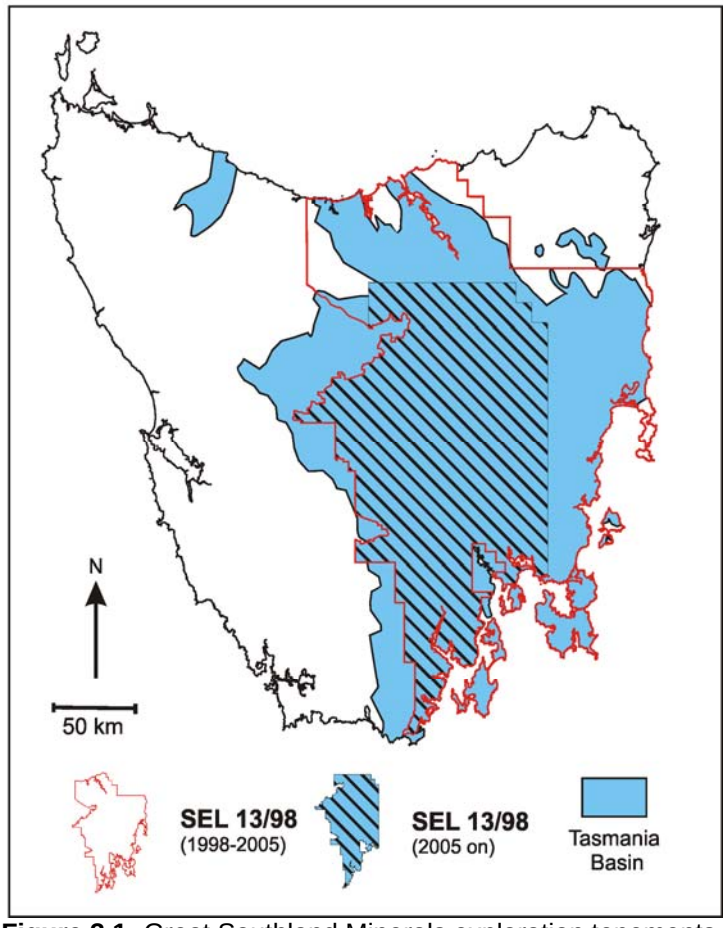

Figure 3.1: Great Southland Minerals exploration tenements, 1998 – present

3.2: TASMANIA BASIN – PARMEENER SUPERGROUP – GONDWANA PETROLEUM SYSTEM

Gondwana Petroleum Systems comprise sequences of Late Carboniferous to Middle Triassic age and are dominated by coarse glacigenic clastic sediments resulting from major Permo-Carboniferous glaciation of the Gondwana Supercontinent (Bradshaw, 1993). The Gondwanan Petroleum System interpreted for the Tasmania Basin contains source, reservoir and seal rocks within the Lower Parmeener Supergroup (Figure 3.2). Potential source, reservoir and seal rocks exist in the Upper Parmeener Supergroup (Figure 3.2), however dolerite intrusions and the erosion of much of the Upper Parmeener Supergroup makes the potential accumulation of hydrocarbons from these rocks far less likely.

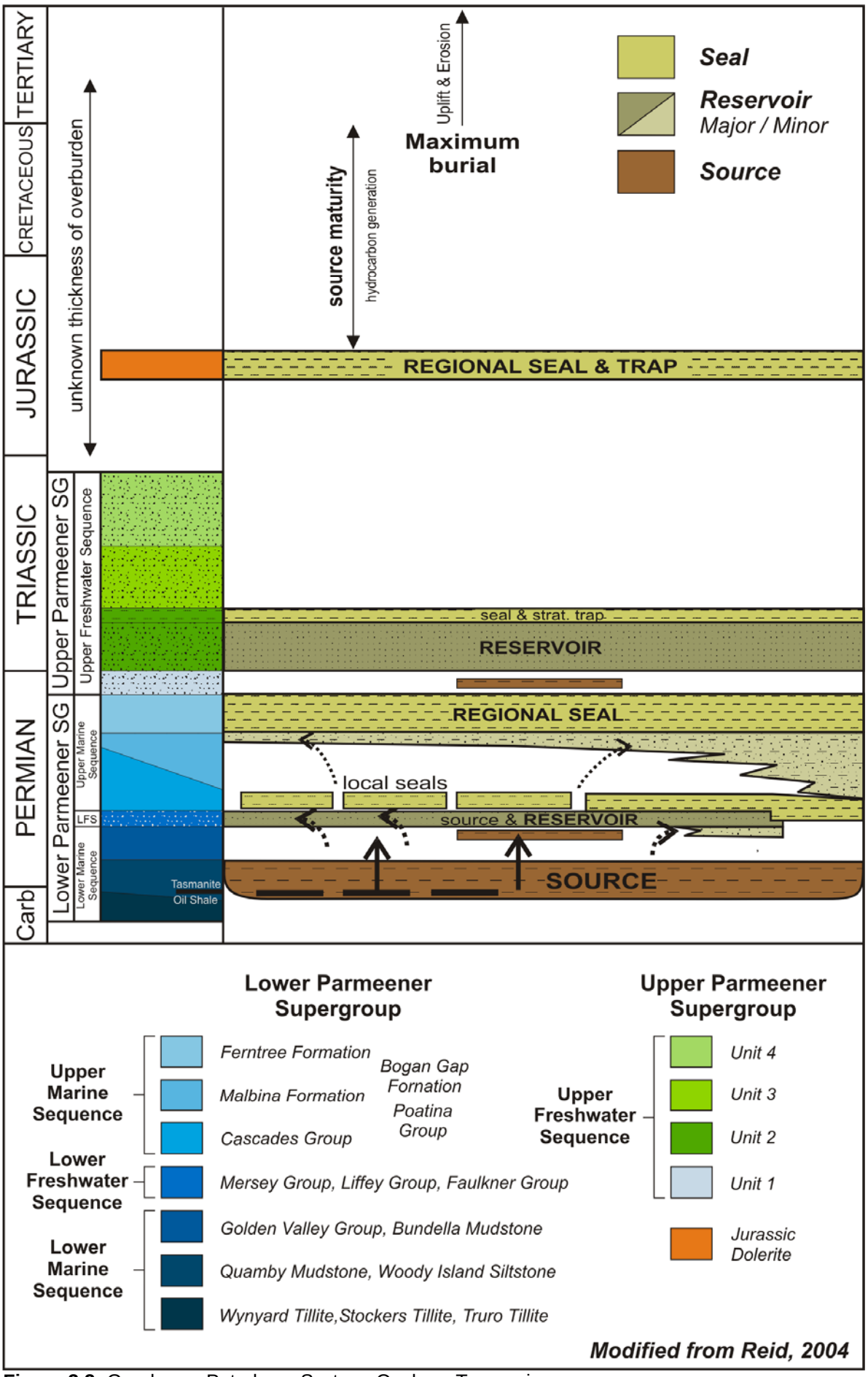

Figure 3.2: Gondwana Petroleum System, Onshore Tasmania

3.2.1: SOURCE ROCKS

Several possible source rock units are found within the Lower Parmeener Supergroup. The major source sequence includes the high grade but thin and laterally impersistent Tasmanites Oil Shale and the low grade, but thick and laterally extensive Woody Island Siltstone and correlates (Figure 3.2). Sparse evidence indicates the Macrae Mudstone (top of the Golden Valley Group) and coals within the Lower Freshwater Sequence are potentially good, but volumetrically minor source rocks (Figure 3.2) (Bacon et al., 2000).

Tasmanite Oil Shale

The Tasmanite Oil Shale generally occurs as a 2 m thick interval between 5 and 20 m above the base of the Quamby Mudstone. Approximately 10 to 70% of the silty shale is composed of the compacted cysts of the alga *Tasmanites punctatus* (Bacon et al., 2000). With Total Organic Carbon (TOC) content up to 44.3% (James, 1950), the oil shales is a rich potential source rock. Until recently, major known occurrences of Tasmanite Oil Shale were limited to the northern part of the basin and a discrete occurrence in the Douglas River Borehole. Bitumen dominated by biomarkers indicating a *Tasmanites* rich source have been recovered from joints in Jurassic Dolerite at Lonnavale (Revill, 1996, Wythe and Watson, 1996), which demonstrates the presence of migrated hydrocarbons and the previously unknown development Tasmanite Oil Shale in subsurface in the southern part of the basin (Bacon et al., 2000).

A high Hydrogen Index (HI) and low Oxygen Index (OI) values indicate Type I kerogen, while low S_1 (free hydrocarbons contained in the sample) and T_{max} (temperature at maximum rate of hydrocarbon generation) indicate the known occurrences in northern and eastern and Tasmania are immature to marginally mature (Reid, 2004). Maturity parameters for the Lonnavale bitumen indicate derivation from a mature source rock well within the oil generation window (Reid, 2004), however whether the presence of hydrocarbons here has resulted from burial, local heating by intruding dolerite or by both is unclear.

Woody Island Siltstone and Quamby Mudstone

The Woody Island Siltstone and its correlates are both laterally extensive and thick, up to 265 m in the deepest part of the basin. The TOC is low (0.5 – 1.5%), and while *Tasmanites* tests are found dispersed throughout the sequence, the bulk of the organic matter is derived from disseminated material rather than from a discrete algal source (Reid, 2004).

Rock-eval analyses from across the basin indicate the Woody Island Siltstone and its correlates contain Type III to Type II/III kerogens, which are generally more gas than oil prone (Bacon et al., 2000). Pyrolysis assays indicate these rocks have a low Hydrocarbon Generative Potential (=S_1 + S_2 (free hydrocarbons contained in the sample + hydrocarbons generated by pyrolysis)) and therefore, though voluminous, would be poor source rocks for oil because expulsion is inefficient (Bacon et al., 2000). When the hydrocarbon generative potential is less than 5 kg/t, the expulsion efficiency is likely to be less than 50% (Bacon et al., 2000). Viable source rocks are characterised by a generative potential of at least 2.5 kg/t (Bacon et al., 2000). The average generative potential (S_1 + S_2) for 45 samples of the Woody Island Formation and correlates taken from drill holes dispersed across the basin (Bacon et al., 2000, appendix 5) is 1.61 kg/t, indicating very poor oil expulsion potential. Reid (2004) agrees, indicating that if the Woody Island Siltstone and its correlates were producing any oil, it is unlikely to be expelled. The formation is generally massive and unfractured, and may therefore be restricting the migration of oil produced by the Tasmanite Oil Shale as well. This restriction does not apply to the expulsion of gas, although across most of the basin these rocks are not mature for gas (Reid, 2004).

Macrae Mudstone

The Macrae Mudstone is a dark shale, up to 49 m thick that underlies the Lower Freshwater Sequence at Golden Valley and Frankford in the central north of the state. A single sample from the Golden Valley 1 drill hole has a TOC of 4.25% and a generative potential of 4.11 kg/t, the sample comprises immature to marginally mature Type III kerogen (Bacon et al., 2000). While this is a good local source, the unit is not laterally extensive.

Lower Freshwater Sequence: Mersey Group, Liffey Group, Faulkner Group

In the north of the basin, potential hydrocarbon sources in the Lower Freshwater Sequence (LFS) are carbonaceous sandstone and siltstone and coal horizons. Coals appear to be good potential source rocks with TOC up to 65%. The coal horizons contain oil prone Type II kerogen with an average generative potential (S_1 + S_2) of 98.6 kg/t (Reid, 2004, Bacon et al., 2000, appendix 5). However, to be an efficient source rock, coals must have sufficient hydrocarbon saturation to overcome the absorption of the remaining carbon in the rock matrix, consequently many coals are poor source rocks despite their high TOC (Bacon et al., 2000). Carbonaceous rocks have a TOC of less than 5% and contain wet-gas prone Type III kerogen derived from disseminated organic matter (Reid, 2004).

A sample of Pelionite from Mt Pelion in the northwest of Tasmania, has source quality parameters similar to those of the Tasmanite Oil Shale, while T_{max} indicates the sample has just entered the oil window (Reid, 2004, Bacon et al., 2000). However, the distribution of this horizon is unknown as outcrop distribution is poor and no drilling has been undertaken in this part of the basin (Reid, 2004).

Unit 1: Cygnet Coal Measures

Bitumen sourced from the Cygnet Coal Measures has been identified in sandstone south of Zeehan and at the Comstock mine (Chester, 2006), both locations are in northwest Tasmania. An average vitrinite reflectance of 0.76% indicates these rocks are in the oil window (Cook, 2004) and bitumen observed in sandstone demonstrate both production and migration (Chester, 2006). Other samples from this unit correlate well with maturity boundaries for the Tasmania Basin calculated by Reid (2004) (Figure 3.3).

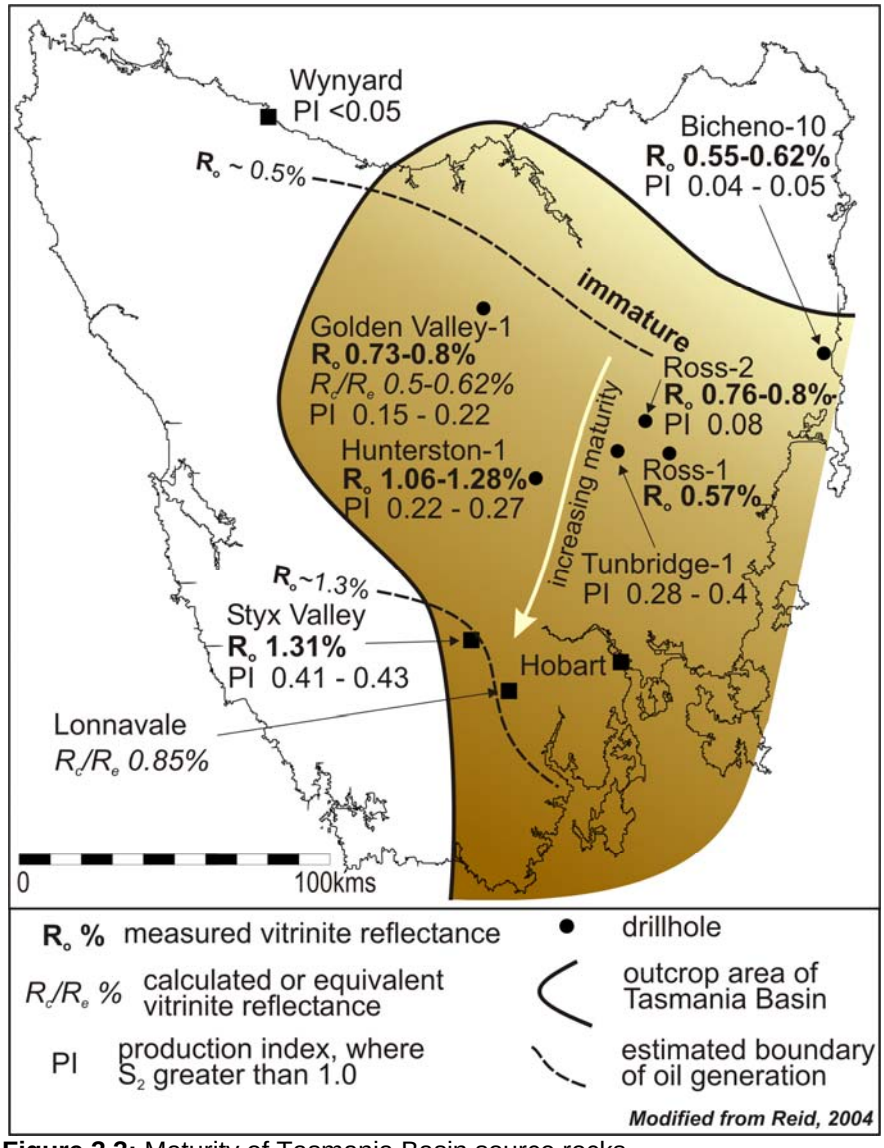

Figure 3.3: Maturity of Tasmania Basin source rocks

Thermal History and Maturity

By the Late Triassic the Tasmania Basin was probably about 2 km thick. In the Middle Jurassic it was intruded by at least one 600 – 800 m thick dolerite sill, which was overlain by at least a further 800 m of Late Triassic to Middle Jurassic sediment (Turner and Calver, 1987). The extra heat resulting from the intrusion of dolerite has probably locally enhanced the maturity of source rocks. Thermal conductivity of the country rocks is not only a function of the size of the intrusion, but also their water content (Chester, 2006, Bacon et al., 2000). This coupled with differing intrusion geometries makes predicting the effects difficult. The Hunterston 1 DDH drill hole intersects a 650 m thick dolerite sill, where alteration was limited to about 45 m beneath the sill (Reid et al., 2003).

Apatite Fission Track (AFT) data records a major cooling event at ~ 100 – 85 Ma throughout eastern Tasmania. This is partly in response to km scale erosion of a thick overlying succession, probably including Jurassic to Early Cretaceous stratigraphy (Kohn et al., 2002, O'Sullivan et al., 2000b, O'Sullivan and Kohn, 1997), but also influenced by a mid-Cretaceous magmatic pulse resulting in the intrusion of alkaline igneous rocks occur in the southeast (Cygnet-Oyster Cove area) and in the far northeast (Cape Portland). Offshore the Durroon Basin experienced increased geothermal gradients (up to 55ºC/km) from 100 Ma to 90 Ma (Duddy, 1992).

It is most likely that hydrocarbons in the Tasmania Basin were generated during this Jurassic to Cretaceous thermal maximum. Permo-Triassic source rocks of the Tasmania Basin are immature in the northeast, in the oil window in the central part of the basin and entering the gas window in a zone between the Huonville and the Styx Valley on the south (Figure 3.3) (Chester, 2006, Reid, 2004, Bacon et al., 2000).

3.2.2: RESERVOIR ROCKS

The most promising potential reservoir rocks occur in the Lower Freshwater Sequence, which is generally found throughout the basin (Figure 3.2). Other, more restricted, potential reservoir rocks in the Lower Parmeener Supergroup are found in marine sandstones and limestones in the southern part of the basin (Figure 3.2). The quartz sandstone of Unit 2 in the Upper Parmeener Supergroup also has very good reservoir properties and is quite extensive, although it is often in close proximity to intruded dolerite (Figure 3.2).

Lower Freshwater Sequence

The Lower Freshwater Sequence (LFS) occurs throughout the basin and is characterised by fluvial to paralic, quartz rich sandstone, with conglomerate and carbonaceous siltstone and mudstone and coal. Siltstone is dominant in the southeast, while coal is developed around the landward margins of the basin (Banks and Clarke, 1987, Clarke, 1989). The thickness of the unit varies from 6 to 50 m, generally decreasing from north to south and averaging 25 m in the central part of the basin.

The reservoir quality varies both laterally and vertically across the basin (Maynard, 1996). The average porosity for the unit is 10.9% (Bacon et al., 2000). The porosity of the sandstone varies depending on grainsize. In the central Tasmania the porosity ranges from 1 – 18% (Reid, 2004), while where the sandstone is interbedded with, or contains laminations of carbonaceous material, the overall porosity is reduced (Reid, 2004). In southeast Tasmania where siltstone is dominant, the porosity is less than 5% (Reid, 2004). The permeability of the unit is generally poor, ranging from 0.01 – 0.1 mD (Reid, 2004).

Other potential reservoir rocks in the Lower Parmeener Supergroup

In the southeast of the basin, other potential, although geographically restricted reservoirs are located within the Upper and Lower Marine Sequences of the Lower Parmeener Supergroup. In the Lower Marine Sequence, the Bundella Mudstone (Figure 3.2) comprises fossiliferous siltstone with minor sandstone and granule conglomerate and has porosities ranging from 7.4 -22.3% and permeabilities of 0.07 – 9 mD, measured from samples in the Shittim-1 drill hole on Bruny Island (Farley, 1995, Woods, 1995). In the Upper Marine Sequence the Minnie Point Formation and the Risdon Sandstone have porosities of 14.1 – 16.6% and 13.7 – 14.7% respectively (Woods, 1995).

Unit 2

Unit 2 of the Upper Parmeener Supergroup is fluvial sandstone, which is generally 200 m thick and occurs across the basin. The unit consists predominantly of quartz sandstone, which is well-sorted with a porosity of 22% and a permeability of 9.7 mD (Bedi, 2003). The sandstone is clean with little interbedded shale or coal (Bacon et al., 2000). Wiltshire (1980) indicated that lithologically, these are probably the best potential reservoir rocks in the basin.

3.2.3: SEALS AND TRAPS

Potential seals are the Ferntree Formation and correlates in the Upper Marine Sequence of the Lower Parmeener Supergroup and the Jurassic Dolerite, while local seals are probably provided by clay and mudstone rich zones in the lower part of the Cascades and Poatina Groups (Figure 3.2).

Ferntree Formation and Correlates

The Ferntree Formation and correlates lie at the top of the Upper Marine Sequence of the Lower Parmeener Supergroup, enclosing all the reservoir units of the Tasmania Basin with the exception of Unit 2 (Figure 3.2). The unit is characterised by poorly fossiliferous mudstone and siltstone, which is generally 100 -200 m thick and laterally extensive, covering almost the entire basin. Across the basin the Ferntree Formation and correlates are often exposed at or lie within a few hundred metres of the surface. In outcrop the formation is always well fractured, with open horizontal and vertical joints, raising questions of its integrity as a seal. Groundwater investigations indicate that the fractures are closed below a depth of about 30 m and therefore should not be a source of leakage (Bacon et al., 2000).

Jurassic Dolerite

The generally thick Jurassic Dolerite may provide an effective regional seal. Usually intruding the Parmeener Supergroup in a zone between the base of the Ferntree Formation and the top of Unit 2, it is likely to encompass all the reservoir units of the Tasmania Basin in some areas (Figure 3.2). All rocks in contact with dolerite show clay alteration (Reid, 2004). Helium was present in cuttings gas samples from below dolerite sills in the Shittim-1 well on Bruny Island (Burrett, 1997). The presence of helium is significant, as it has the smallest effective atomic/molecular diameter of any gas, and its occurrence suggests that the dolerite has provided a very effective seal (Bacon et al., 2000).

Cascades and Poatina Groups

The potential of the Cascades and Poatina Groups to act as an effective seal is not well defined. Its stratigraphy is variable and is therefore less likely to act as a regional seal like the generally monotonous Ferntree Formation and correlates. The rocks are characterised by calcareous, fossiliferous siltstone and limestone. Mudstones at the base of the Poatina Group in the north and northwest of Tasmania and thin metabentonite layers present in the Cascades Group in the Hobart area may act as local seals (Figure 3.2).

Traps

Traps in Gondwanan Petroleum Systems are predominantly structural (Bradshaw, 1993). Suitable hydrocarbon traps may have been formed in the Tasmania Basin by folding and faulting during a Mesozoic (pre-Middle Jurassic) compressional phase, Middle Jurassic dolerite intrusion and an Early to Middle Tertiary extensional phase. Folded structures are rare in the Tasmania Basin and the most likely traps are probably formed by fault offsets. With maturation and migration most likely the result of a Jurassic to Cretaceous thermal maximum, the most likely charged structures are those formed prior to or during the intrusion of dolerite in the Middle Jurassic. Many Jurassic faults were sealed by intruding dolerite, reactivation and further faulting during the Tertiary represents a significant risk to the integrity of these structures (Bacon et al., 2000). Tertiary fault bounded structures may be exploration targets if charged by secondary migration. Steep faults and vertical feeder and dyke systems associated with Jurassic Dolerite may provide migration pathways to stratigraphically higher reservoirs such as the Risdon Sandstone and Unit 2 (Bacon et al., 2000). Stratigraphic traps may include the lutite of Unit 2 and pinch outs beneath dolerite seals (Bedi, 2003).

The complex stratigraphic relationship between the dolerite intrusions and the Parmeener Supergroup, in addition to dolerite and later sediment concealing the underlying Tasmania Basin rocks makes the accurate identification of structures from surface mapping alone difficult. Therefore, the style and distribution of possible hydrocarbon traps in the Tasmania Basin is currently not well understood. One of the aims of this thesis to use the TB01 Seismic Survey data and other methods to identify the timing, geometry and distribution of structure within the Tasmania Basin to better target exploration.

3.3: WURAWINA SUPERGROUP – LARAPINTINE PETROLEUM SYSTEM

Larapintine Petroleum Systems are characterised by carbonates, evaporates and shallow marine clastic sediments (Bradshaw, 1993). The system generally encompasses rocks of Late Proterozoic to Middle Carboniferous age, although basins in eastern Australia usually only contain a Devonian to Carboniferous sequence (Bradshaw, 1993). In Tasmania, the interpreted Larapintine Petroleum System comprises rocks of the Late Cambrian to Early Devonian Wurawina Supergroup (Figure 3.4). The Wurawina Supergroup contains source, reservoir and seal rocks in the Gordon and Eldon Groups. Structural and stratigraphic traps

are proposed in the Gordon and Eldon Groups and at the unconformity at the base of the Tasmania Basin. Maturation and structural traps are most likely the product of high heat flows and folding during the Tabberabberan Orogeny (Bacon et al., 2000).

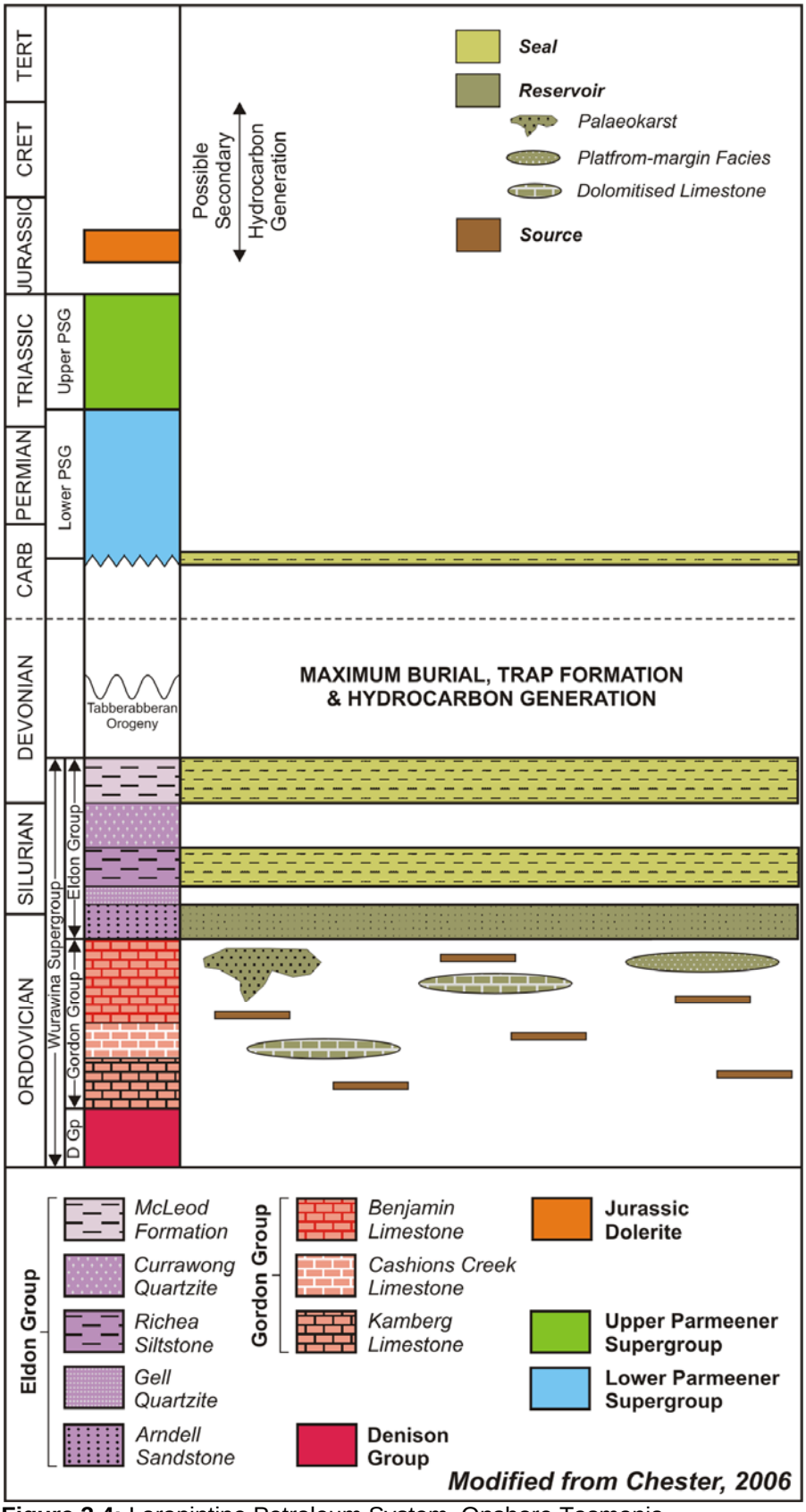

Figure 3.4: Larapintine Petroleum System, Onshore Tasmania

3.3.1: SOURCE ROCKS

Gordon Group

The only potential source rocks known in the Wurawina Supergroup are the Ordovician Gordon Group (Figure 3.4). The Gordon Group is approximately 1.5 km thick, consisting predominantly of micritic limestone, deposited in a shallow marine, warm water environment.

Recent studies indicate the source potential of the Gordon Group is poor (Chester, 2006, Bacon et al., 2000). These data however come from outcrop samples from around the margins of the Tasmania Basin, as no drilling within the basin has sampled the Gordon Group. Sparse Rock-Eval data collated by Mineral Resources Tasmania (Bacon et al., 2000, Appendix 5) have an average TOC of 0.14 ± 0.07% and probably contain poor quality kerogen, while analysis of 15 samples of Gordon Group, taken from outcrop on the margins of the Tasmania Basin by Chester (2006) have an average TOC of 0.78%. Source beds within the Gordon Group are thin (<200 mm) and discontinuous, organic matter is amorphous, Type III or Type IV kerogen, which is gas prone and has a very low generative potential (Chester, 2006). The Gordon Group is tight, and unless fractured, very high generation pressures would be required to migrate hydrocarbons, which is highly unlikely considering its maturity and generative potential (Chester, 2006).

Limited outcrop sampling of the Gordon Group around the south-western edge of the Tasmania Basin indicate the Gordon Group lies in the gas window in southern Tasmania (Burrett, 1992, Chester, 2006). In western and northern Tasmania the Gordon Group is overmature, with deep burial (>5 km) occurring during the Tabberabberan Orogeny (Burrett, 1992). In southern Tasmania, Colour Alteration Index (CAI), biomarker maturation indices and Rock-Eval pyrolysis all indicate maturities close to that of the Tasmania Basin, indicating the Gordon Group was probably less deeply buried in the south (Burrett, 1992, Bacon et al., 2000, Chester, 2006). Maturity modelling by Woods (1995) indicates that most of the Gordon Group in southern Tasmania had entered the oil window during the Devonian, only locally entering the gas window. If the effect of the Jurassic-Cretaceous thermal maximum exceeds that of the Tabberabberan Orogeny in southern Tasmania, then additional hydrocarbons may have been produced, charging unconformity traps below the Tasmania Basin in addition to structures within the Wurawina Supergroup (Bacon et al., 2000).

3.3.2: RESERVOIR ROCKS

Gordon Group

Several potential reservoir scenarios are thought possible in the Gordon Group (Figure 3.4), although any data on such units is scarce. Palaeokarst reservoirs are a possibility. Modern karst features are widespread throughout the Gordon Group and it is likely that the unit was karstified if sub-aerially exposed in the past (Kiernan, 1995), and palaeokarst sediments ranging from Devonian to Late Carboniferous age have been found in Gordon Group outcrop across the state. With much of the Gordon Group lying beneath the Tasmania Basin, there is potential for the formation of palaeokarst reservoirs at the base of the Parmeener Supergroup. Reservoirs may also lie within dolomitised sections of the Gordon Group. Dolomitisation results in a loss of volume, increasing porosity. Another potential setting is a calcarenitic, platform-margin facies, which in the uppermost parts of the Gordon Group are expected to initially have high intergranular porosities (Bendall et al., 2000). Such rocks occur in an east-southeast trending belt through Precipitous Bluff in far southern Tasmania, and may continue beneath the Tasmania Basin (Burrett, 1986).

Eldon/Tiger Range Groups

Little data on the porosity and permeability is available for sandstone units within the Eldon and Tiger Range Groups. Chester (2006) assessed the reservoir potential of the Tiger Range Group in the Florentine Valley area. The only promising potential reservoir rocks were the Arndall Sandstone (Figure 3.4). However, these rocks have an apparent porosity of 2%, are fine-grained with little permeability and are considered unviable as reservoir rocks (Chester, 2006).

3.3.3: SEALS AND TRAPS

Seals

Mudstones from 60 to 500 m thick in the Eldon Group are likely to create effective seals for reservoir in the upper Gordon Group (Bendall et al., 2000). While, the tillite and mudstone at the base of the Tasmania Basin is likely to seal palaeokarst reservoirs (Bendall et al., 2000) (Figure 3.4).

Traps

A range of structural and stratigraphic traps are possible within the Wurawina Supergroup. Structural traps such as anticlines and traps sealed by fault offsets or trusts were possibly created during the Tabberabberan Orogeny. Stratigraphic traps within the Gordon Group might also have been charged at this time. Tertiary migration of pre-Carboniferous hydrocarbons or maturation during the Jurassic-Cretaceous thermal maximum makes sub-unconformity traps beneath the Tasmania Basin another possibility.

The style and distribution of potential traps is not well understood. When pre-Carboniferous rocks outcrop, their structure is often complex. Some broad, folded structures, such as in the Florentine Valley and at Mole Creek are known from the margins of the Tasmania Basin.

3.4: PROTEROZOIC HYDROCARBONS

Trace quantities of bitumen, probably sourced from Proterozoic rocks are found in north-western Tasmania. Bitumen is observed in amygdales in basalts of the Spinks Creek Volcanics and in association with the Black River Dolomite (Figure 3.5) in the Forest 1 DDH. The Black River Dolomite is thought to be the source from both occurrences, although samples analysed by Chester (2006) indicate it has low potential as a source rock. Other potential source rocks in the area are the Salmon River Siltstone and the Cowrie Siltstone (Figure 3.5). The Salmon River Siltstone has a fair TOC (0.85%), but is both stratigraphically higher and younger than the basalts and is therefore an unlikely source. The Cowrie Siltstone has the best potential of any of the Proterozoic rocks in northwest Tasmania with fair to good TOC (0.64% - 1.37%).

These potential source rocks are all now overmature, however they were probably immature during the Proterozoic and it is probable that intruding basalts generated the hydrocarbons which were then trapped in the amygdales (Chester, 2006). If related to the intrusion of the Spinks Creek Volcanics, generation would have occurred in the late Neoproterozoic (~600 – 650 Ma) (Logan et al., 1999). The Neoproterozoic sequence in Tasmania has largely been considered as “unmetamorphosed” but detailed petrographic descriptions of the basalts commonly include pumpellyite and to a lesser extent prehnite. These units are best regarded as very low-grade metamorphic rocks. The age of this metamorphism is problematic.

There are no reservoir sequences in the known Proterozoic sequences nor are any traps likely. However, drilling and geophysical evidence suggest that these sequences extend below the Tasmania Basin (Leaman, 2001, Reid et al., 2003) where reservoirs and traps may be present, although the potential for generating significant hydrocarbons from these rocks is remote.

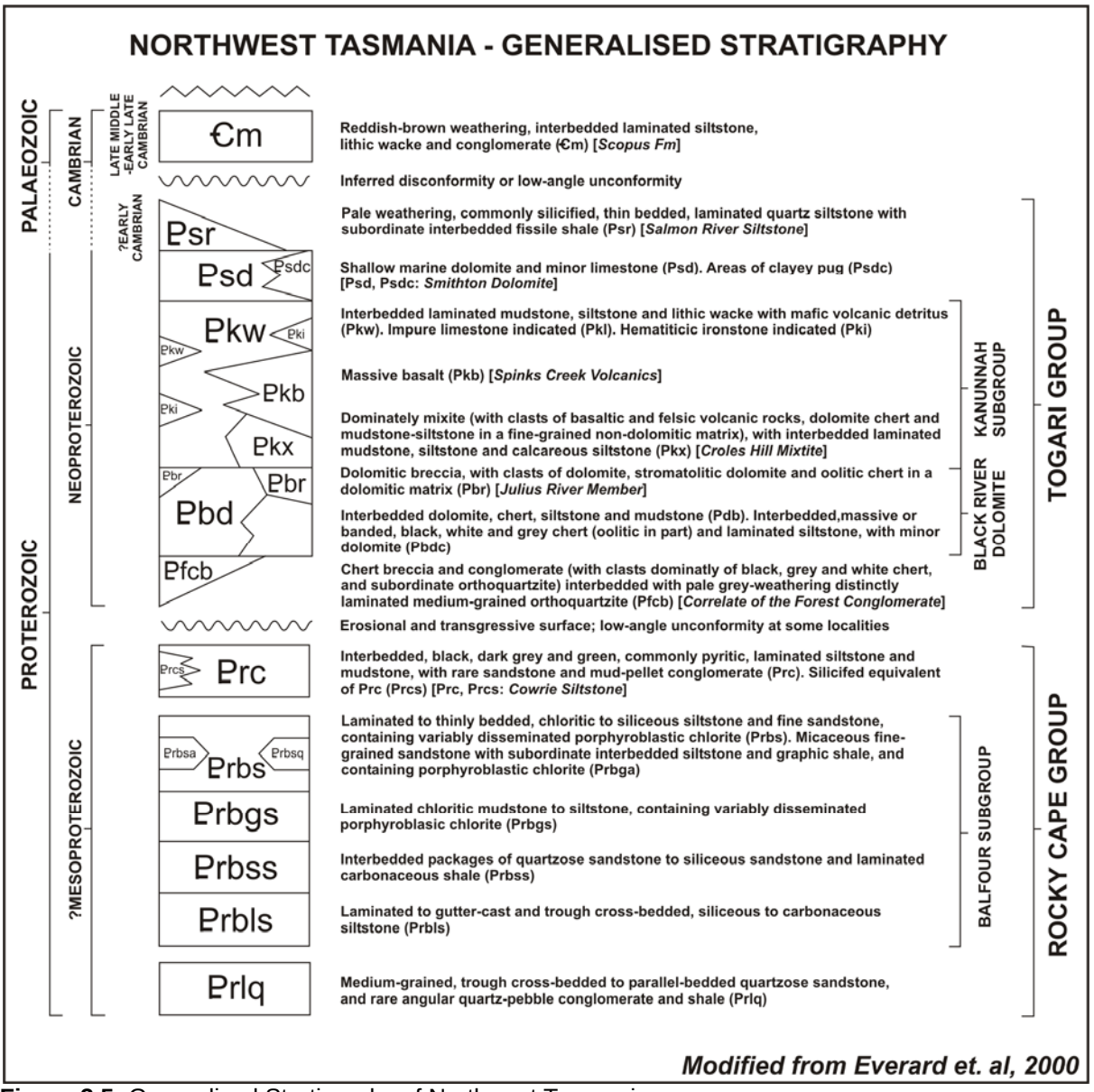

Figure 3.5: Generalised Stratigraphy of Northwest Tasmania

CHAPTER 4
DIGITAL ELEVATION MODEL

4.1: INTRODUCTION

Contemporary Tasmanian topography is the product of early Tertiary tectonic processes, subsequently modified by erosion. It is presumed that linear features identified in the present topography result primarily from geological controls such as faults, joints, sills and dykes, and lithological boundaries. In Tasmania, large changes in topography probably result from early Tertiary tectonic processes, while other, subtle linear features may be a reflection of older basement structures.

The Digital Elevation Model (DEM) used in this study covers the entire island and was derived from 1:25 000 contours at 25 m intervals (Figure 4.1) (DPIWE, 2002). The DEM represents a continuous, unbiased image of the geomorphologic response to environmental conditions, active geological processes and the underlying geology and can be interpreted in a qualitative sense similar to the process of interpreting a gravity or magnetic image (Rice, 1997).

The DEM used in this study is a raster dataset which was viewed using the digital image processing software, ER Mapper™, with various other processing steps being carried out using Surfer 7™ and ArcView™ software. In this study the DEM is used to develop a model of the Tertiary topography (Peneplain Analysis), which is aimed at predicting possible Tertiary migration pathways and prospective areas. As part of this process a reconnaissance lineament analysis was conducted. Lineaments are linear features in the DEM that cut across primary topographic features e.g. conspicuous, linear breaks in mountain chains or long stretches of major watercourses that are visibly linear.

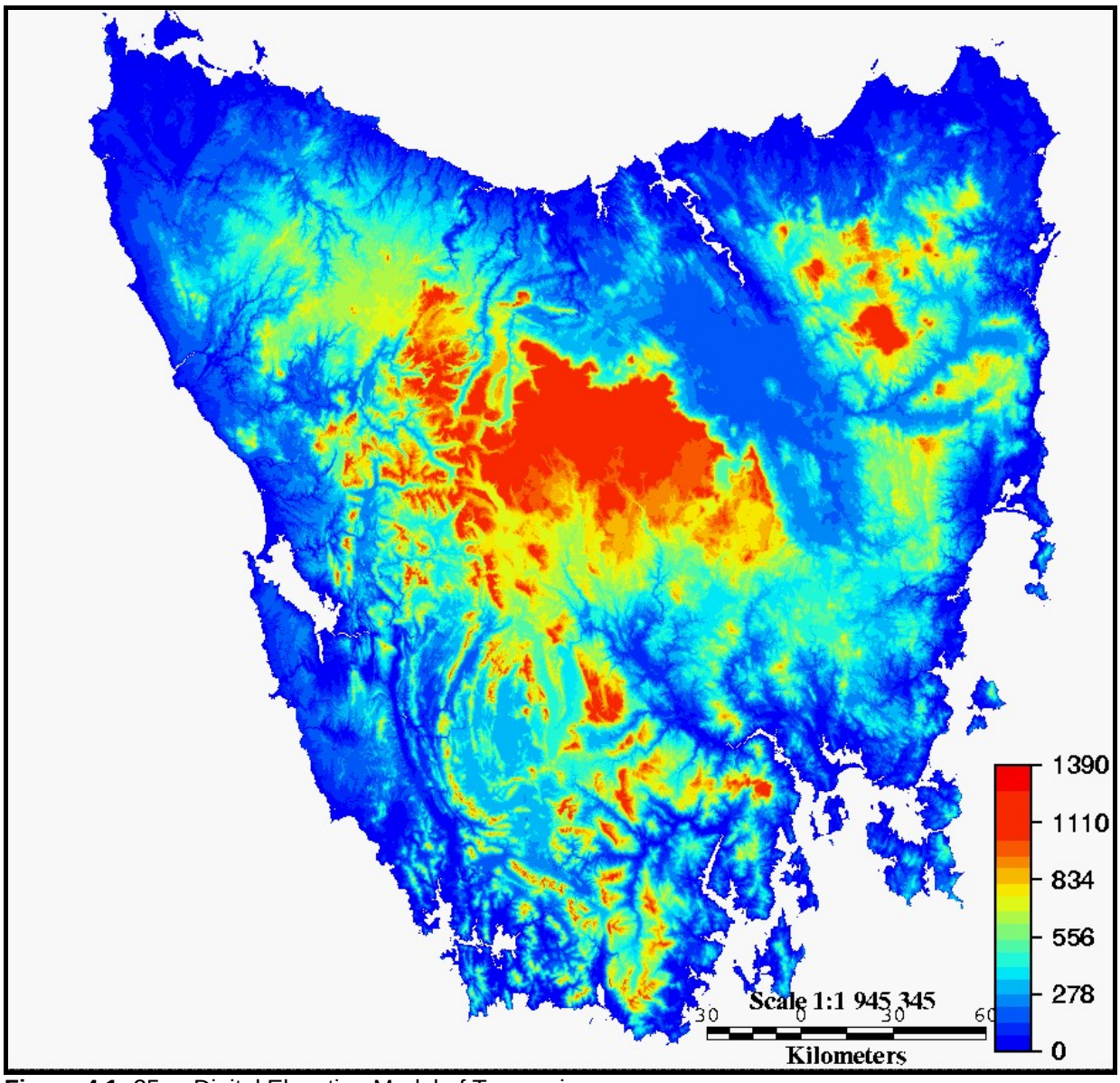

Figure 4.1: 25 m Digital Elevation Model of Tasmania

The DEM was also used to assist the interpretation of data from the TB01 Seismic Survey. Well control is sparse in the area of the seismic survey. The DEM draped with the 1:250 000 geology (Figure 4.2) was used to constrain the seismic stratigraphy at depth via the calculation of the thickness of stratigraphic units from exposures of those units in scarps and on hillsides. This representation of the data was especially useful for identifying unmapped faults in extensive areas where only dolerite outcrops. A previously unmapped fault along the eastern margin of Lake Echo is a good example of the power of the data for identifying such structures (Figure 4.3). Overall, the DEM draped with the 1:250 000 geology provides a window into the broad geologic framework of the region as well as an extra constraint to the seismic interpretation.

Figure 4.2: DEM draped with 1:250 000 Geology

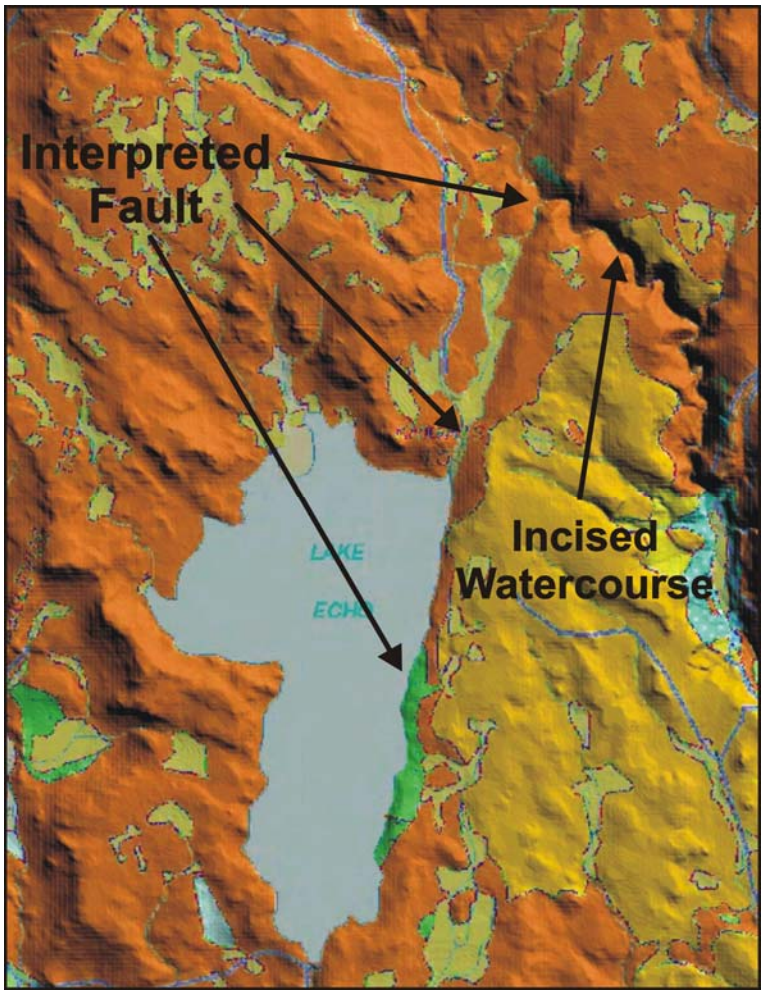

Figure 4.3: DEM used to identify an unmapped fault in dolerite

4.2: PREVIOUS WORK

O'Driscoll (1980) and Campbell (1989) described many continental and sub-continental scale geophysical, geological and topographic lineaments, and although not treated in any detail, several of theses were traced into Tasmania. Leaman and Richardson (1990) produced a map summarising regional structures and trends based on analysis of magnetic and gravity data. Most studies of lineaments in Tasmania have been restricted to geophysical datasets.

To date the most comprehensive analysis of topographic lineaments in Tasmania has been produced by Rice (1997), who tested their spatial association to primary copper, gold and tin deposits. His analysis utilised a DEM generated from 1:250 000 contours at 100 m intervals and drainage data, from which he classified topographic lineaments into four types according to azimuthal frequency, persistence and temporal relationships.

4.3: PENEPLAIN ANALYSIS

4.3.1: AIMS

The aim of this study was to create a model showing the orientation, location and vertical offset of major faults developed during the Late Cretaceous and early Tertiary. Secondary migration of hydrocarbons within the Tasmania Basin is a distinct possibility. The resultant model should highlight block rotation which may influence possible Tertiary migration pathways and up-dip areas within the fault-bounded blocks that may be prospective. The models were constructed by combining interpretations of major lineaments and topographic breaks, mainly for the area east of longitude 145°, as this is the part of Tasmania occupied by the Tasmania Basin.

4.3.2: METHODOLOGY

Figure 4.4, shows the processing steps followed to generate the Tertiary Fault Pattern and the model of the Tertiary topography.

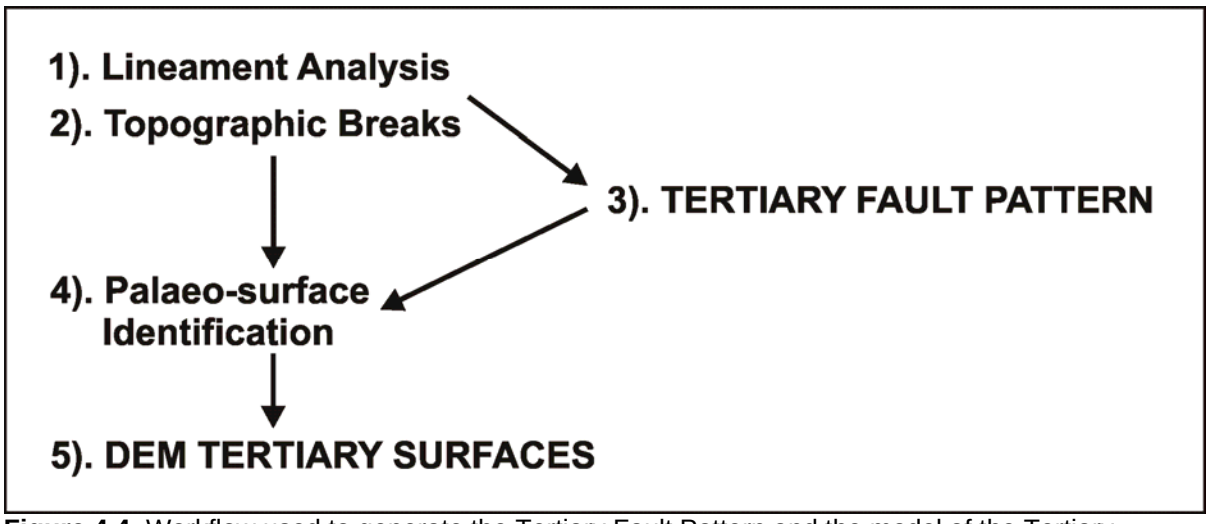

Figure 4.4: Workflow used to generate the Tertiary Fault Pattern and the model of the Tertiary topography

Lineament Analysis

Lineaments were identified and manually plotted on the DEM. The greyscale image of the DEM was found to be the most effective image on which to identify linear features (Figure 4.5). The image was examined at several different scales (zoomed in and out), with the interpreted lineaments manually digitised over the DEM as a separate vector layer. Many of the major structures strike towards the northwest, artificial illumination (sun-angle) was initially directed from the northeast to highlight these features. The process was repeated with illumination from the southeast, this repetition at 90° to the initial interpretation ensures that all the major lineaments are identified regardless of their orientation. Lineaments interpreted with the illumination from the northeast are shown in white, illumination from the southeast in yellow and where the two overlap in red (Figure 4.5). The interpreted lineaments were used as a guide to the placement of the Tertiary faults.

Topographic Breaks

In the northern Tasmania, sediments in the Launceston Tertiary Basin range from Latest Cretaceous at the base of the Tamar Graben to Paleocene in the other sub-basins, while the Derwent Graben in the south also contains Paleocene aged sediments. The age of the earliest basin fill sediments indicates these structures were formed by the early Tertiary. The tectonics responsible for the formation of these grabens also left areas of high ground, such as the Central Highlands and Ben Lomond in the north and Mt Field East and Mt Dromedary-Mt Wellington in the south. The tectonic history of Tasmania suggests that most of the components of the present landscape originated in the Tertiary (Colhoun, 1989), consequently large-scale, linear breaks in the modern topography probably result from Tertiary movement.

Major topographic breaks were recognised from rapid changes in elevation (changes in colour) on the pseudocolour rendered DEM image (Figure 4.6).

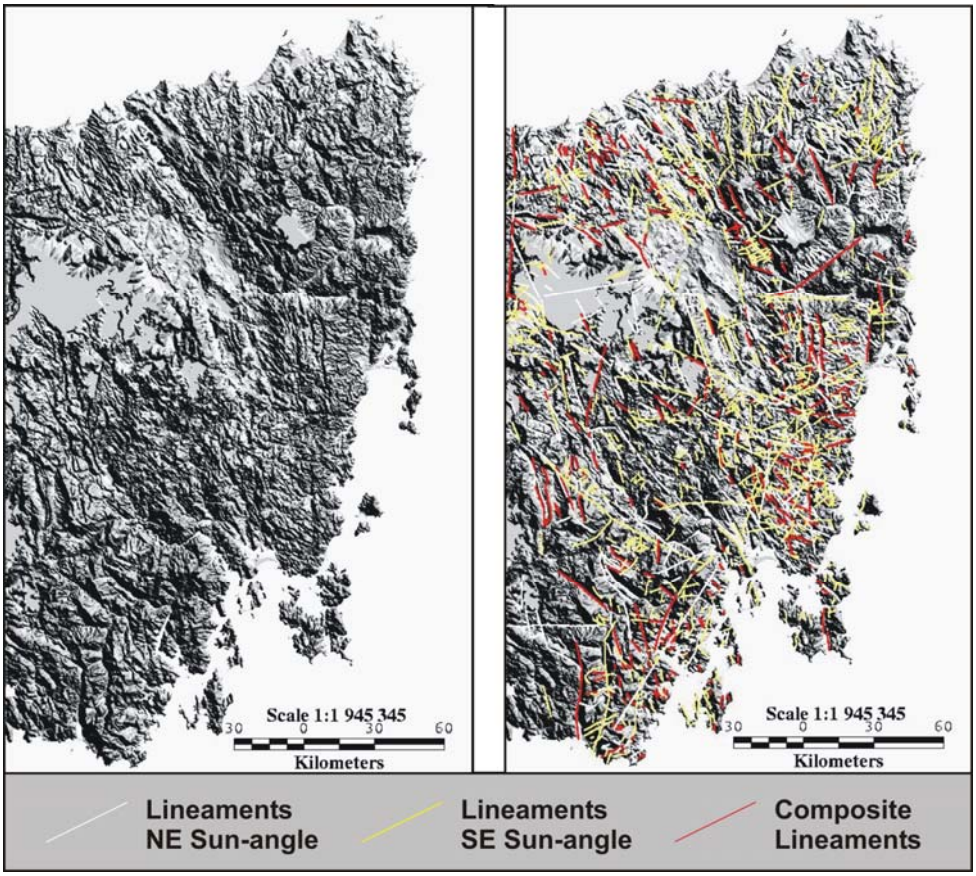

Figure 4.5: Greyscale DEM image used to identify lineaments

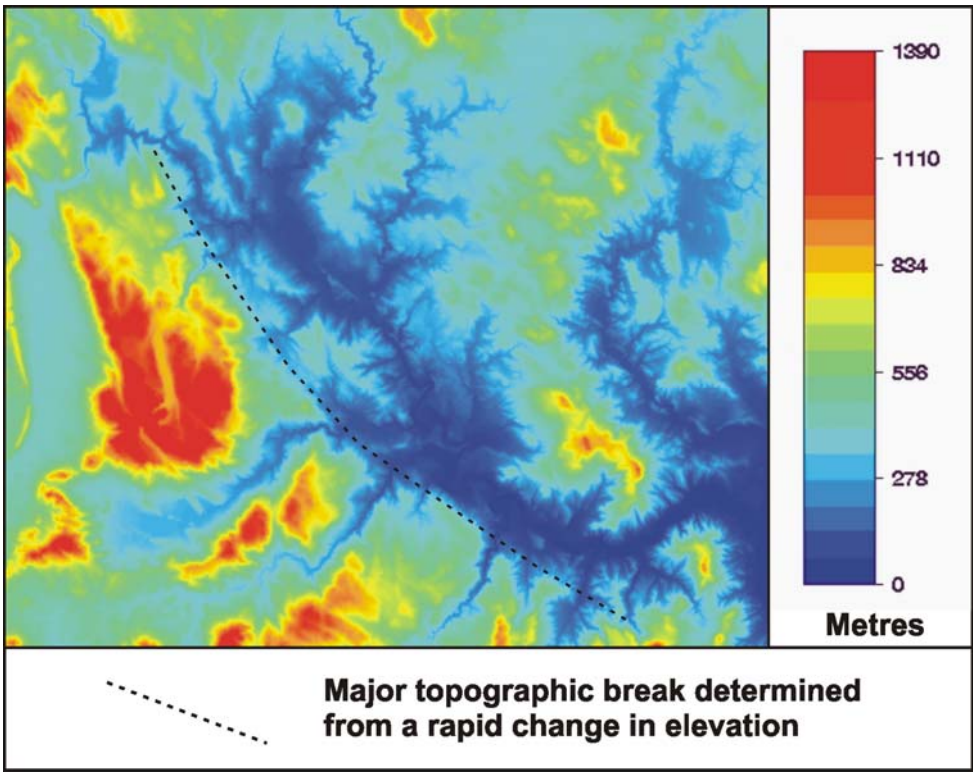

Figure 4.6: Major topographic breaks are recognised from rapid changes in elevation on the pseudocolour rendered DEM image.

Tertiary Fault Pattern

The interpretation of the Tertiary Fault Pattern combines the major topographic breaks with the results of the lineament analysis. Here the pseudocolour rendered DEM was overlain by the lineaments layer using it as a guide to the placement of the Tertiary faults. This was especially useful where changes in elevation were relatively small. The resultant Tertiary Fault Pattern (Figure 4.7) was plotted manually as a separate vector layer over the DEM. The throw of the faults was determined from the DEM draped by the 1:250 000 geology, where the direction and magnitude of offsets can be confidently determined from the stratigraphy (Figure 4.8).

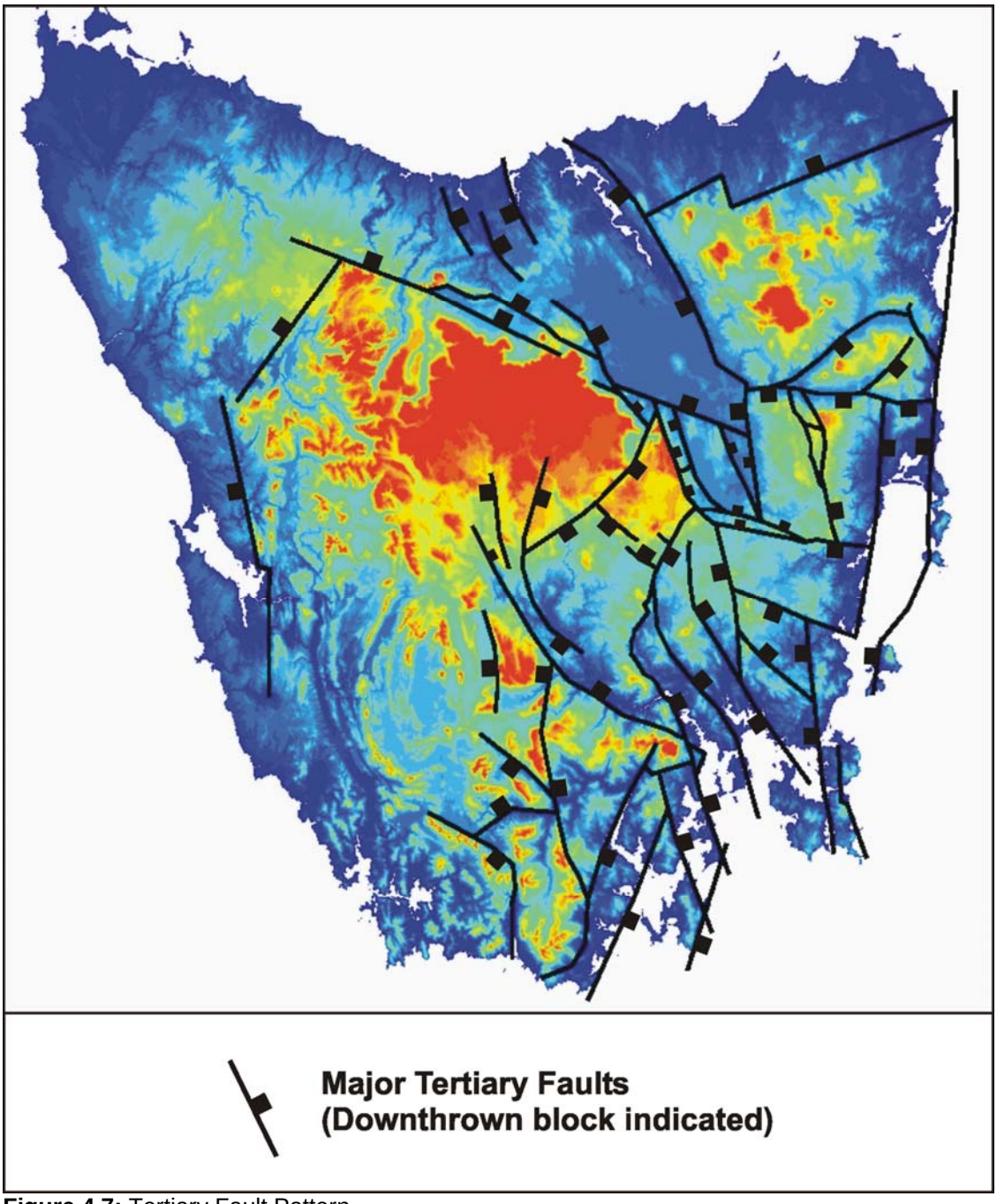

Figure 4.7: Tertiary Fault Pattern

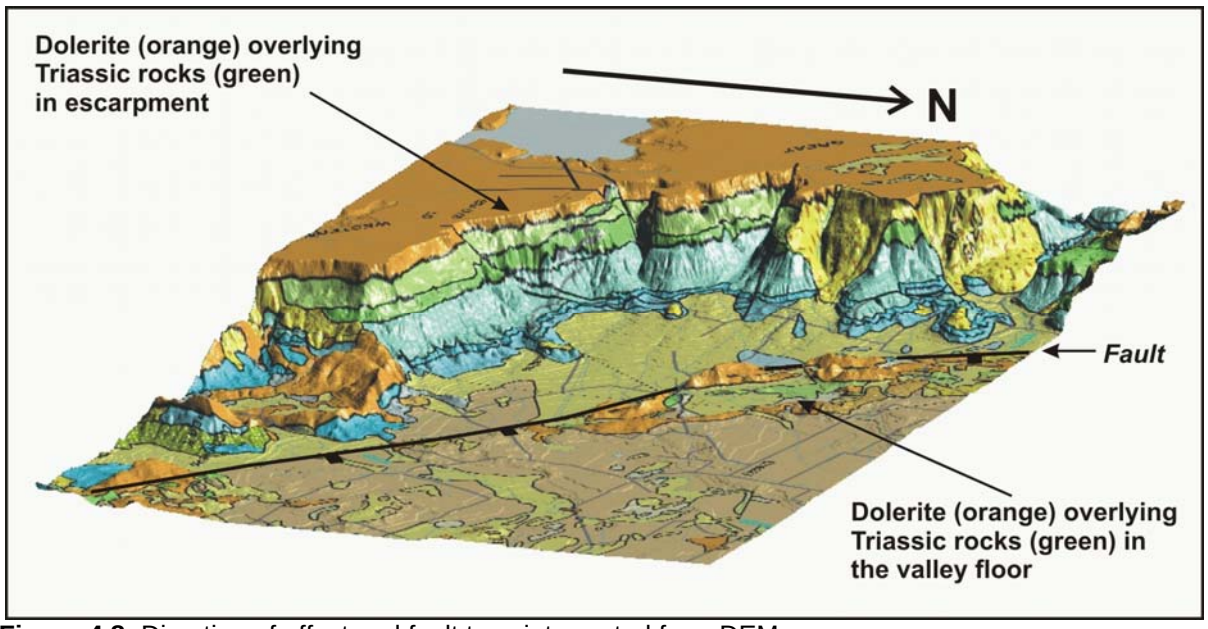

Figure 4.8: Direction of offset and fault type interpreted from DEM.

Coordinate (easting and northing) information characterising each fault of the Tertiary Fault Pattern was recorded. Each fault is made up from a series of segments connected at nodes, thus the coordinates for the beginning and end of the fault, and for all of the nodes were recorded. These data were later used to create "blanking files" that are used during the gridding process used to create the Tertiary DEM.

Palaeo-Surface Identification

This process aims to produce data that can be used to identify the degree of tilting of each of the fault blocks. This data will be used to produce a surface analogous to the post-faulting Tertiary land surface. The basic assumption here, is that the contemporary topography represents the Tertiary topography minus erosion, and while it is difficult to access the degree of erosion since the early Tertiary, it is assumed that high points in the topography have been eroded least. These high areas are usually capped by dolerite and usually form either plateaux or monadnocks (Figure 4.9). A planar surface that passes through the highest points in each block therefore should be approximately analogous to the orientation of the land surface during the Tertiary.

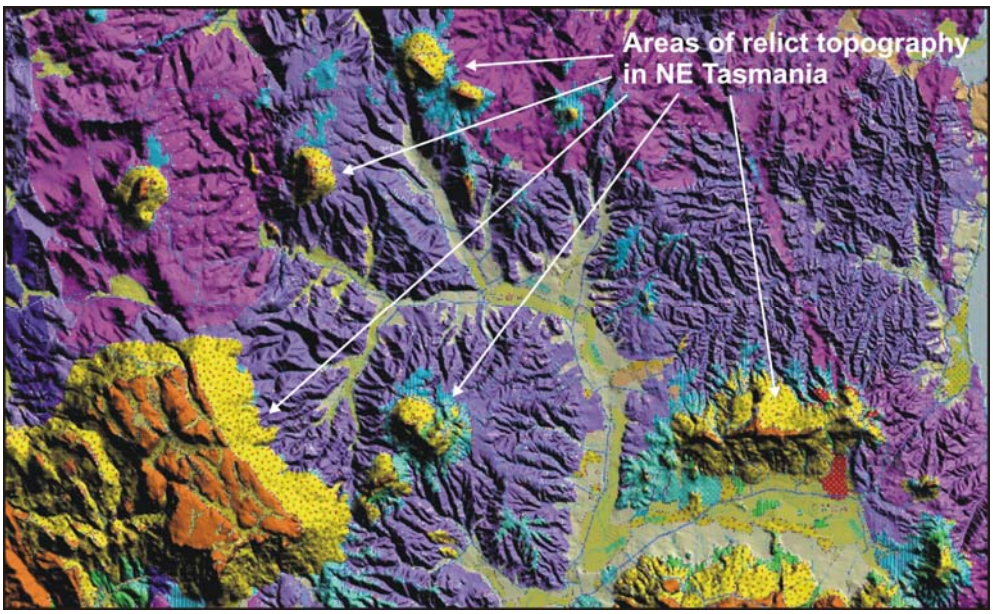

Figure 4.9: Examples of Relict topography in NE Tasmania.

Tertiary Topography

The orientation of Tertiary surfaces was determined by choosing several of the high points from within each block from the DEM draped with the 1:250 000 geology and recording their easting, northing and elevation. This process is subjective and wholly dependant on the distribution of the high points, where possible an attempt was made to uniformly select the points from across the whole fault block. Points on or near the coast were avoided as a partial marine incursion in the Holocene has resulted in lower coastal surfaces (Colhoun, 1989, Rice, 1997).

These data were then gridded in combination with the Tertiary Fault Pattern (blanking files) determined earlier. In Surfer, a fault is a two-dimensional blanking file defining a line that acts as a barrier to information flow when gridding, i.e. during the gridding process, data on one side of a fault is not used when calculating grid node values on the other side of the fault (Golden Software, 2001). If the fault lines form a closed polygon, the gridding algorithm uses only the data from the interior of the polygon (Golden Software, 2001). If the fault line doesn't form a closed polygon, the gridding algorithm can search around the end of the fault to see a point on the other side of the fault, but this longer distance reduces the weight of the point in interpolating the grid node value (Golden Software, 2001). The gridding process employed uses a minimum curvature algorithm with spacing of 1000 m, generating a unique grid for each fault block. When contoured, these grids indicate the approximate slope of the palaeo-surface within each block (Figure 4.10). The model of the Tertiary topography is produced when all the blocks are combined with the Tertiary Fault Pattern (Figure 4.11).

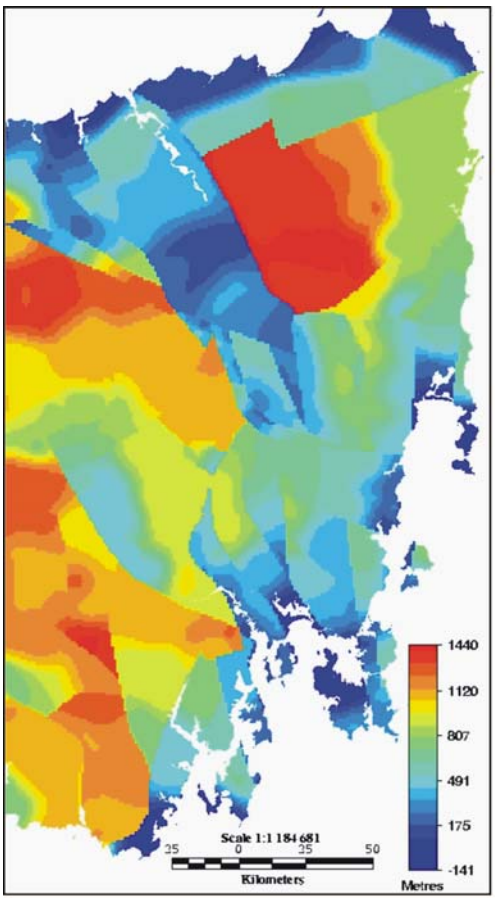

Figure 4.10: Tertiary Palaeo–Surfaces

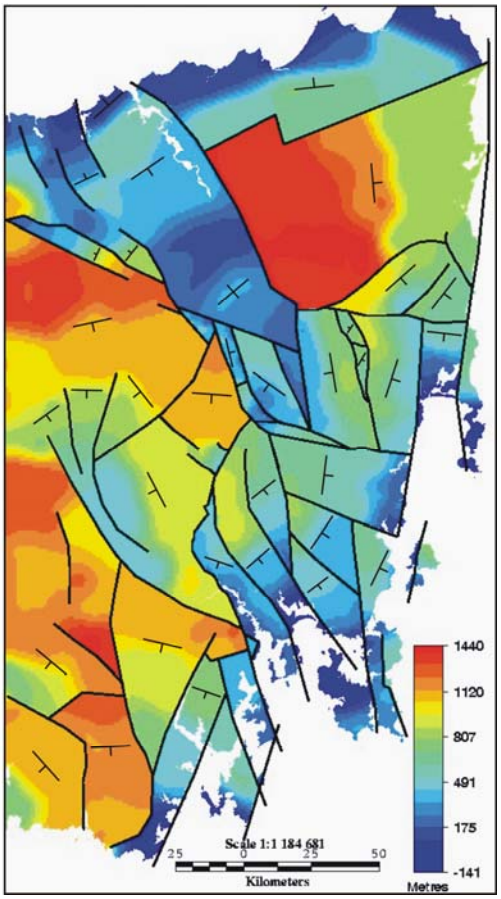

Figure 4.11: Tertiary Palaeo-Surfaces combined with the Tertiary Fault Pattern

4.3.3: OBSERVATIONS

The combined Tertiary Fault Pattern and Palaeo-surface diagrams (Figure 4.11) reveal a series of fault blocks in the eastern half of Tasmania, the complexity of their organisation increases towards the south. Based on complexity, size and orientation of the bounding faults, these structures are grouped into five geographical domains i.e. the central north, northeast, central, southeast and southern (Figure 4.12).

Central Northern Domain

In northern Tasmania, the primary structures are delineated by faults striking towards the northwest and north-northwest. The throw of the north-northwest striking faults is variable, while the northwest striking faults are all down towards the northeast (Figure 4.13).

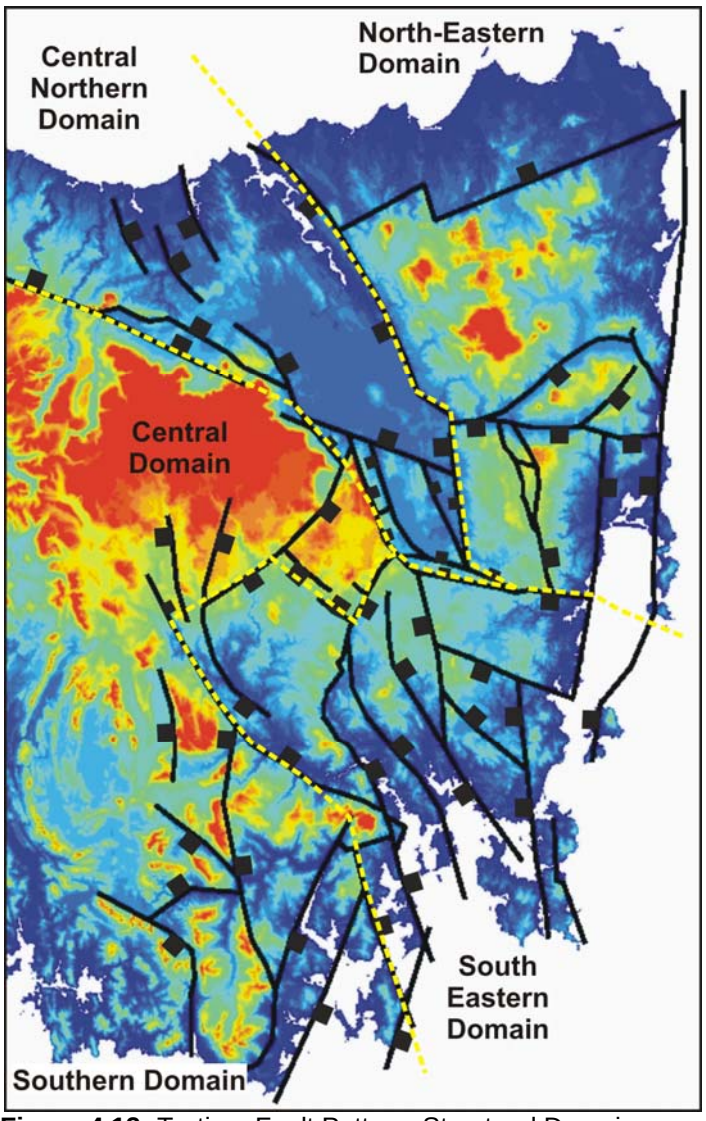

Figure 4.12: Tertiary Fault Pattern, Structural Domains

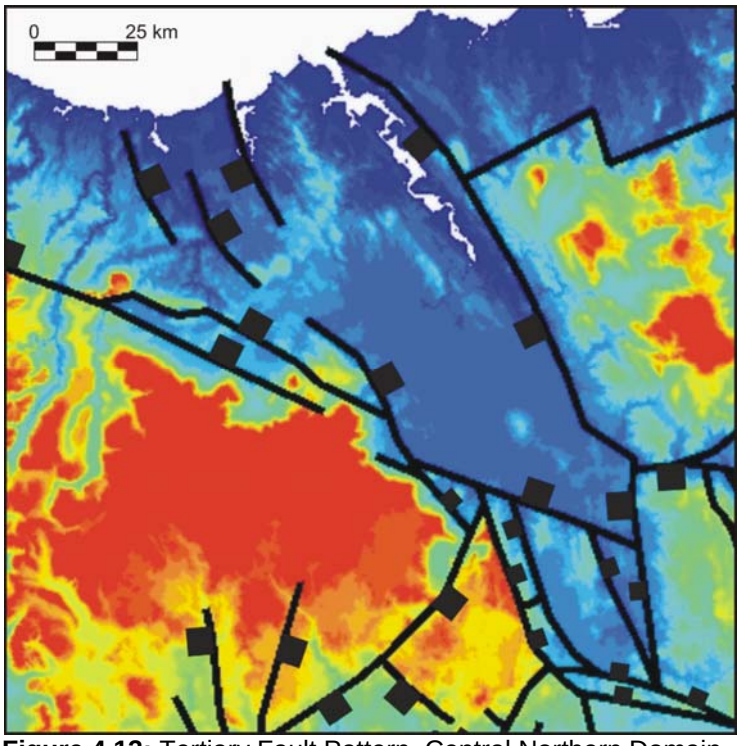

Figure 4.13: Tertiary Fault Pattern, Central Northern Domain

The primary feature observed is a large northwest trending graben, which is crosscut by northwest striking faults (Figure 4.13). The graben is approximately 40 km wide x 130 km long, it is open to Bass Strait in the northwest and is truncated by an east – west striking feature in the southwest. The graben and its fill correspond to the Launceston Tertiary Basin (Figure 4.14). The deepest part of the graben cuts through an east-northeast trending high, on the eastern flank is the North-Eastern Highlands and on the western flank the Central Highlands (Figure 4.13, 4.14). In the north a small graben (25 x 25 km) corresponding to the Devonport–Port Sorell Sub-basin is defined by north-northwest striking faults (Figure 4.13, 4.14). To the south of the Devonport–Port Sorell Sub-basin, northwest striking faults define the scarp which is the northern boundary of the Central Highlands (Great Western Tiers) (Figure 4.13, 4.14). The deep area in the central part of the graben corresponds to the Longford Sub-basin (Figure 4.13, 4.14).

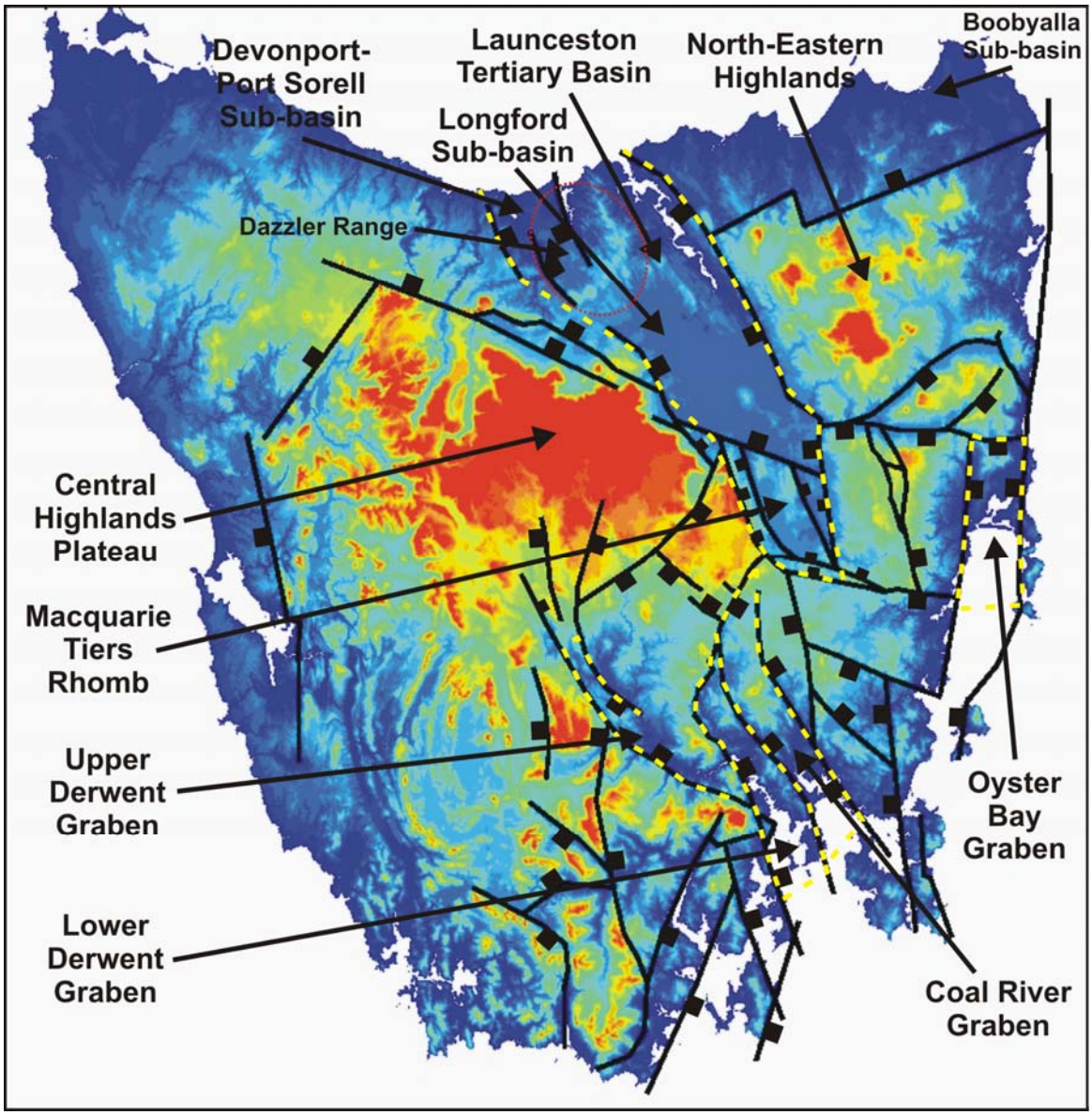

Figure 4.14: Known Tertiary structures in Tasmania

A rhomb formed by the Macquarie Tiers lies at south-eastern end of the graben (Figure 4.14). The fault pattern in this region is more complicated than that for the rest of the graben, including faults that strike several different directions (Figure 4.13). It could be argued that this region is in fact separate from the rest of the graben, however the general orientation and shared boundary faults indicate that the region in the broadest sense is part of the overall structure. The elevated area of the Macquarie Tiers Rhomb is bounded in the north by a down to the north, northwest striking fault, which corresponds to the major Marrawah-Liffey Lineament of Rice (1997). The rhomb block is bounded to the east by a north striking fault, representing a change in the strike of the eastern bounding fault (Figure 4.13). In the west and south, the rhomb is defined by a fault that begins striking towards the northwest, bending sharply in the southwest corner of the rhomb to join a west-northwest striking fault (Figure 4.13, 4.14). The basin is apparently truncated by this east-west structure, the observed fault pattern changes markedly south of this structure.

North-Eastern Domain

The North-Eastern Domain (Figure 4.12) differs substantially from the Central Northern Domain in that the fault blocks defined by the analysis are generally larger and rectangular (Figure 4.7). In the north and central part of the area, faults striking east-northeast bound the large (100 x 50 km) North-Eastern Highlands block (Figure 4.15). Two smaller similarly orientated faults, follow major, relatively linear, northeast trending watercourses in the south of the North-Eastern Highlands block. These structures are truncated by an east-west feature following the course of the St Pauls River (Figure 4.15).

In the region south of the St Pauls River, the elevation of the blocks is less than those to the north. The orientation of faults in this area is strongly north-south and east-west, with the exception of two north-northwest faults that bisect the main block (Figure 4.15). The easternmost of these faults is an unmapped extension of a fault mapped through Avoca (Figure 4.16). The structure follows a lineament identified on the DEM corresponding to strongly linear watercourses north and south of Lake Leake (Figure 4.16).

The Oyster Bay Graben, Tertiary, is located in the south-eastern corner of the domain (Figure 4.14). The onshore part of the structure is defined by north striking faults truncated by the east-west fault.

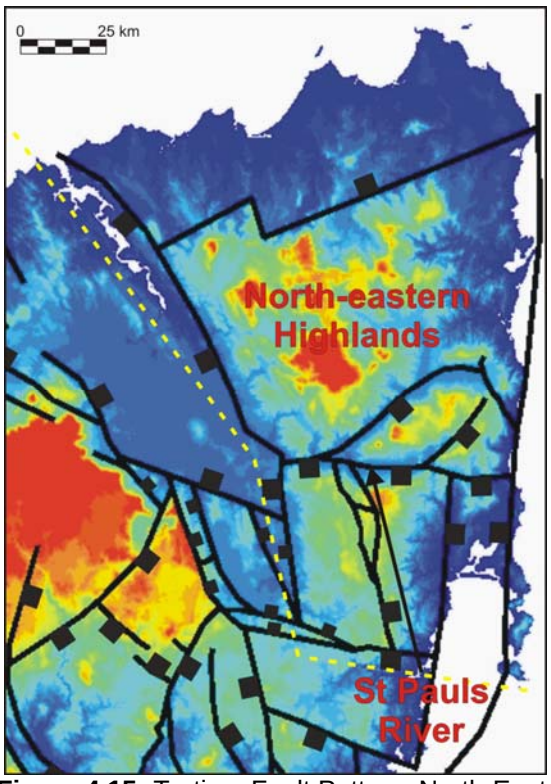

Figure 4.15: Tertiary Fault Pattern, North-Eastern Domain

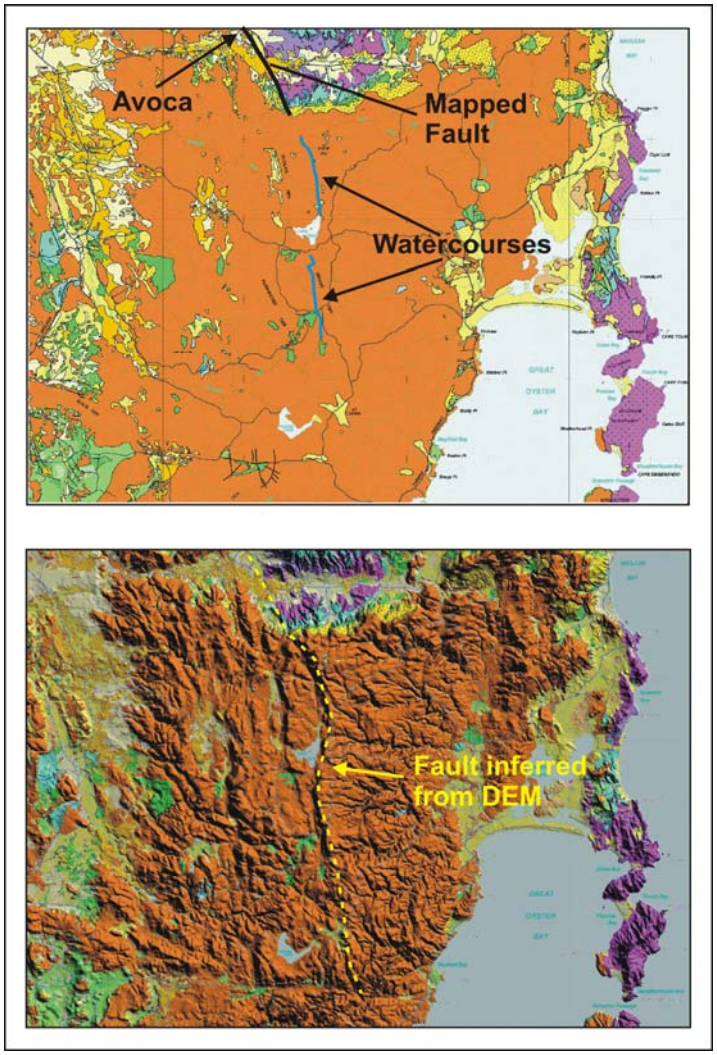

Figure 4.16: Major unmapped fault in the St Pauls River region interpreted from the DEM.

Central Domain

The boundaries of the Central Domain are interpreted at the major topographic breaks that mark the edge of the Central Highlands region (Figure 4.12). Structuring in the Central Domain is relatively simple, faults occur mainly at the boundaries and several faults splay into the region from the South-Eastern Domain (Figure 4.12). The general lack of structure in the region indicates it probably acted as a competent block during Tertiary extension.

South-Eastern Domain

The South-Eastern Domain is considerably more complex than that of the Northern and Central domains (Figure 4.12). Fault bounded blocks similar to those in the North-Eastern Domain are observed in the east of the region, while narrow, northwest striking grabens feature in the centre and west of the domain (Figure 4.17). On the eastern side of the region the northern and southern bounding faults have a different strike. These fault strike nearly east west in the north of the region, while in the south of the region they strike towards the north-northwest (Figure 4.17).

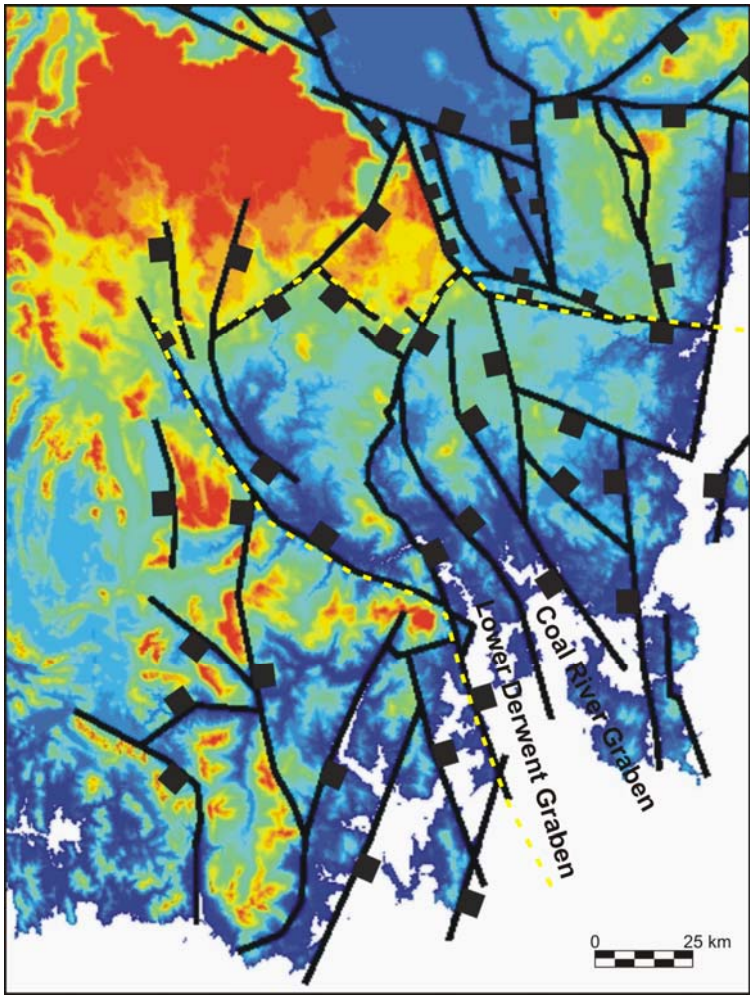

Figure 4.17: Tertiary Fault Pattern, Central, South-Eastern and Southern Domains

The western boundary faults of north-easterly striking Tertiary structures such as the Lower Derwent Graben and the Coal River Graben are concave towards the northeast, curving northwards and joining into a single fault in the centre of the region (Figure 4.14, 4.17). In the west of the region, the Upper Derwent Graben is bounded on its south-western side by a strongly curved fault that strikes northwest from Hobart, turning more towards the north-northwest at the base of the Central Highlands where the structure dies out in a horsetail splay (Figure 4.14, 4.17).

Southern Domain

A very different fault pattern is observed in the Southern Domain as compared with the South-Eastern Domain (Figure 4.12). In this region three north-easterly striking, down to the southeast faults were recognised along the east coast. The westernmost of these faults controls the course of the Huon River (Figure 4.18). In the west of the region, blocks are more equidimensional (Figure 4.18).

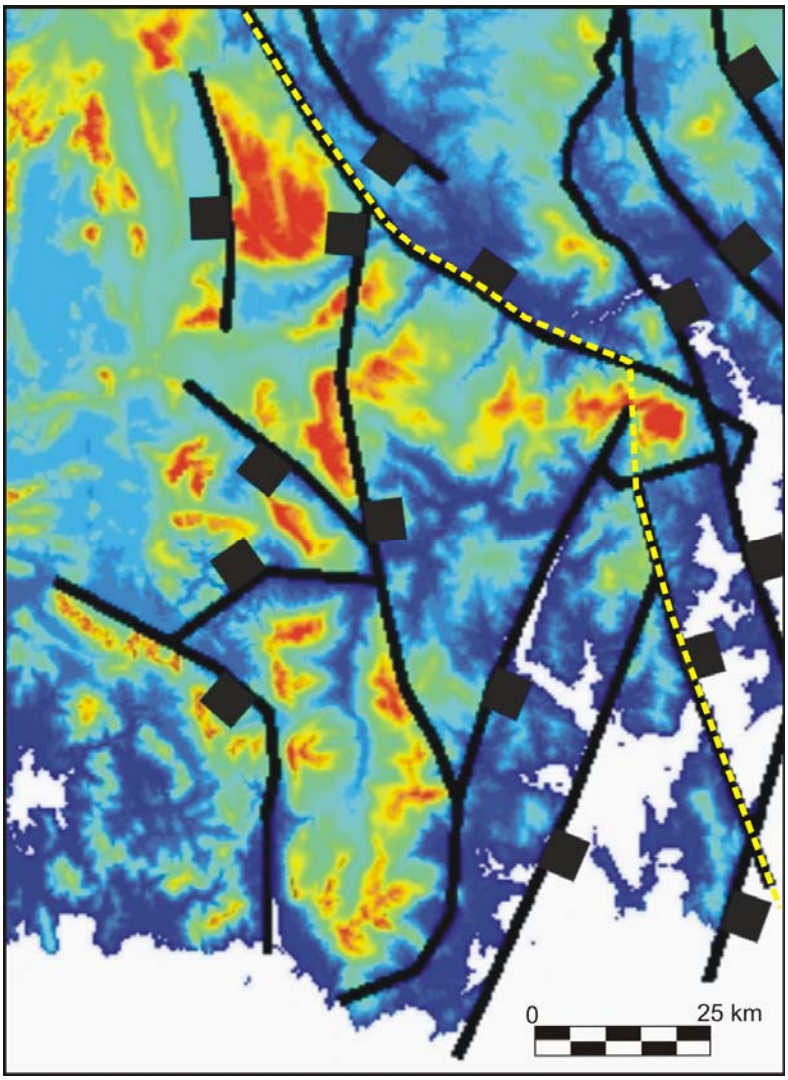

Figure 4.18: Tertiary Fault Pattern, Southern Domain

4.3.4: DISCUSSION

Previous attempts to structurally delineate Tertiary depocentres and to describe structures influencing Tasmania's Cenozoic geomorphologic development are shown in Figure 4.19. The overall structural pattern revealed by the analysis presented here is significantly more complex than those produced previously and highlights a relatively structurally simple northern zone and a significantly more complex zone to the south (Figure 4.7). The new analysis shows that there are soft linkages between the grabens.

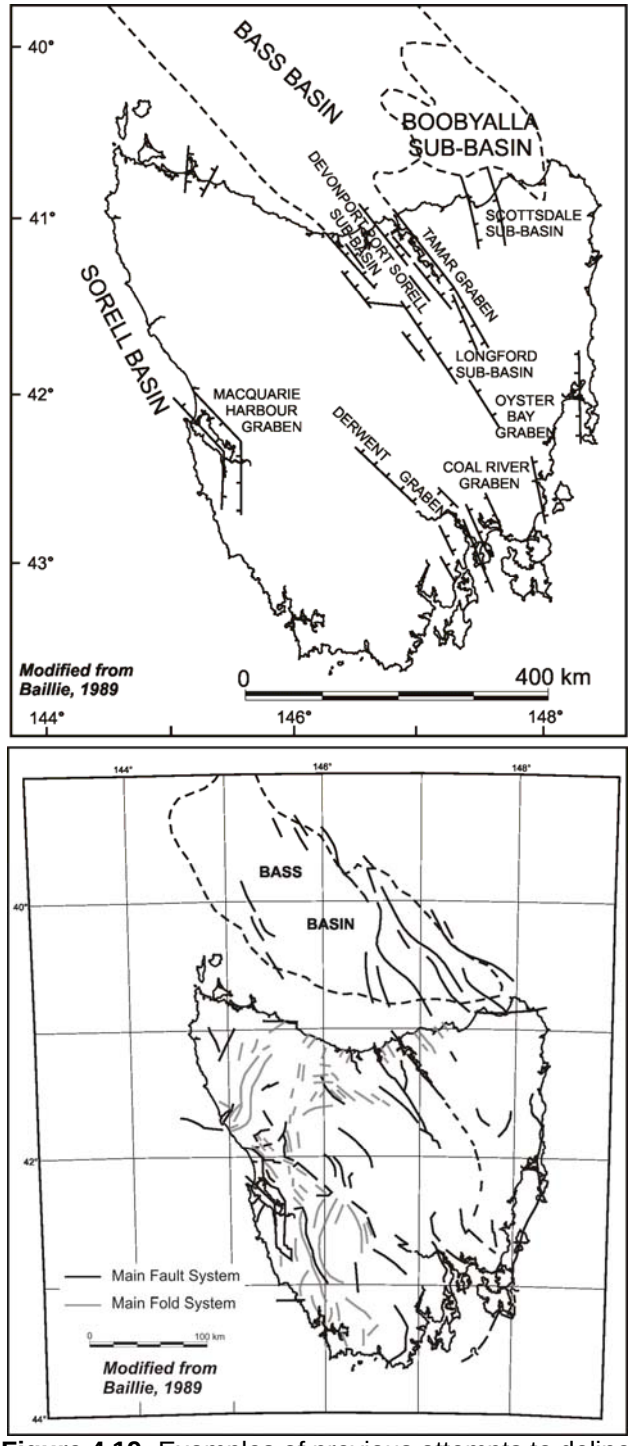

Figure 4.19: Examples of previous attempts to delineate Tertiary depocentres and to describe structures in Tasmania.

Numerous workers have noted the fault geometry of extensional domains is heavily influenced by pre-existing basement fabrics (McClay and White, 1995, Morley, 1995, Morley, 1999a, Morley, 1999b, McClay et al., 2002, Michon and Sokoutis, 2005). Experimental evidence suggests that where extensional stress is orthogonal to basement fabric, simple, linear structures are produced, and where extensional stress becomes oblique to the basement fabric more complex structures result (McClay and White, 1995, McClay et al., 2002, Michon and Sokoutis, 2005). Many of the structures developed in Tasmania trend from northwest to southeast and are related to extension that operated in an east-northeast to a northeast direction in the late Mesozoic to early Tertiary (Colhoun, 1989). The extension was related to spreading along an east-northeast to west-southwest ridge during the opening of the Tasman Sea between 79 Ma and 83 Ma (Sutherland, 1999)

In northern Tasmania the basement fabric strikes northwest or north-northwest. At the north-western end of the Launceston Tertiary Basin Neoproterozoic rocks outcrop in the Dazzler Range (Figure 4.14). The Neoproterozoic rocks are dissected by northwest to north-northwest striking, north-easterly dipping thrust faults, and subsequent reactivation of these faults has produced a similarly oriented fabric in the overlying Parmeener Supergroup and Jurassic Dolerite (Figure 4.20). Basement rocks outcrop extensively throughout northeast Tasmania. The region is characterised by Ordovician to Early Devonian turbidite sequences of the Mathinna Supergroup. These sequences are extensively intruded by Devonian granitoids. Folding in the Mathinna Supergroup rather than faults produce the fabric observed in the northeast (Figure 4.21). The fabric observed is considerably less pervasive than that associated with thrust faults to the west (Figure 4.21). In most of northeast Tasmania the trend of foliations and their associated fold hinges is towards the northwest, however in the southern part of the region this trend becomes more northerly (Figure 4.22).

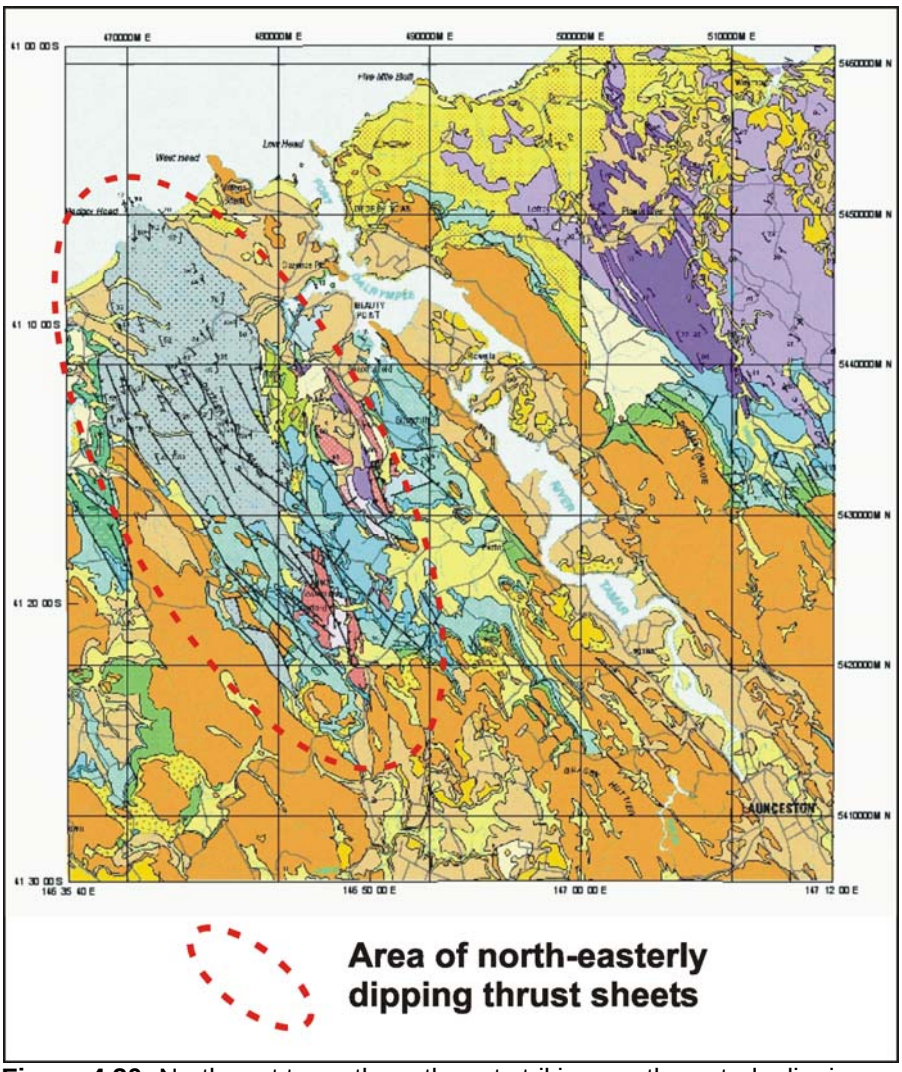

Figure 4.20: Northwest to north-northwest striking, north-easterly dipping thrust faults in the Dazzler Range region, Northern Tasmania.

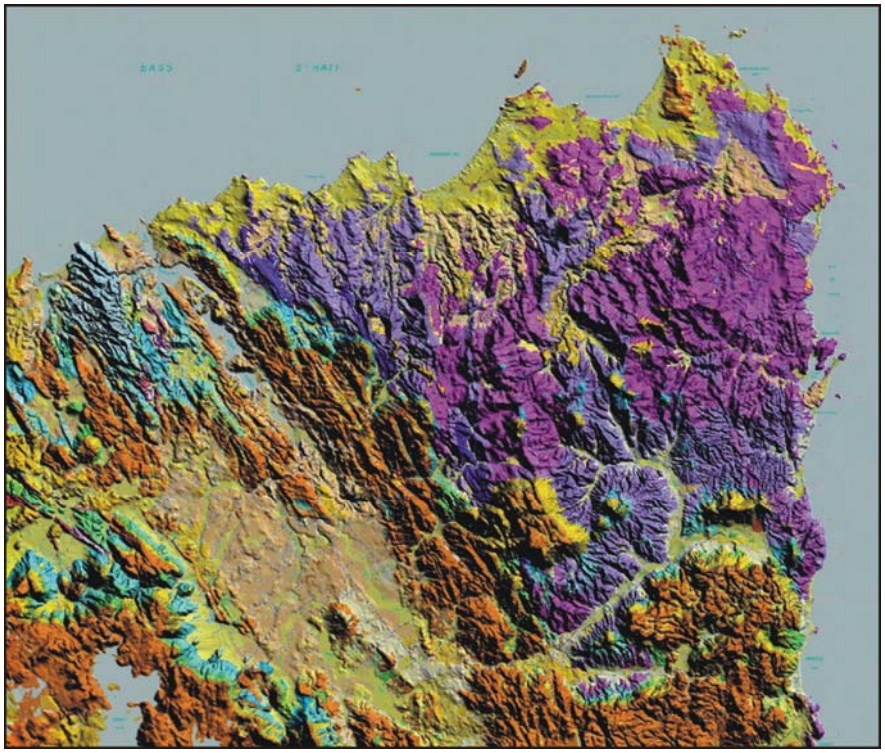

Figure 4.21: Strong NNW striking fabric observed in North Eastern Tasmania.

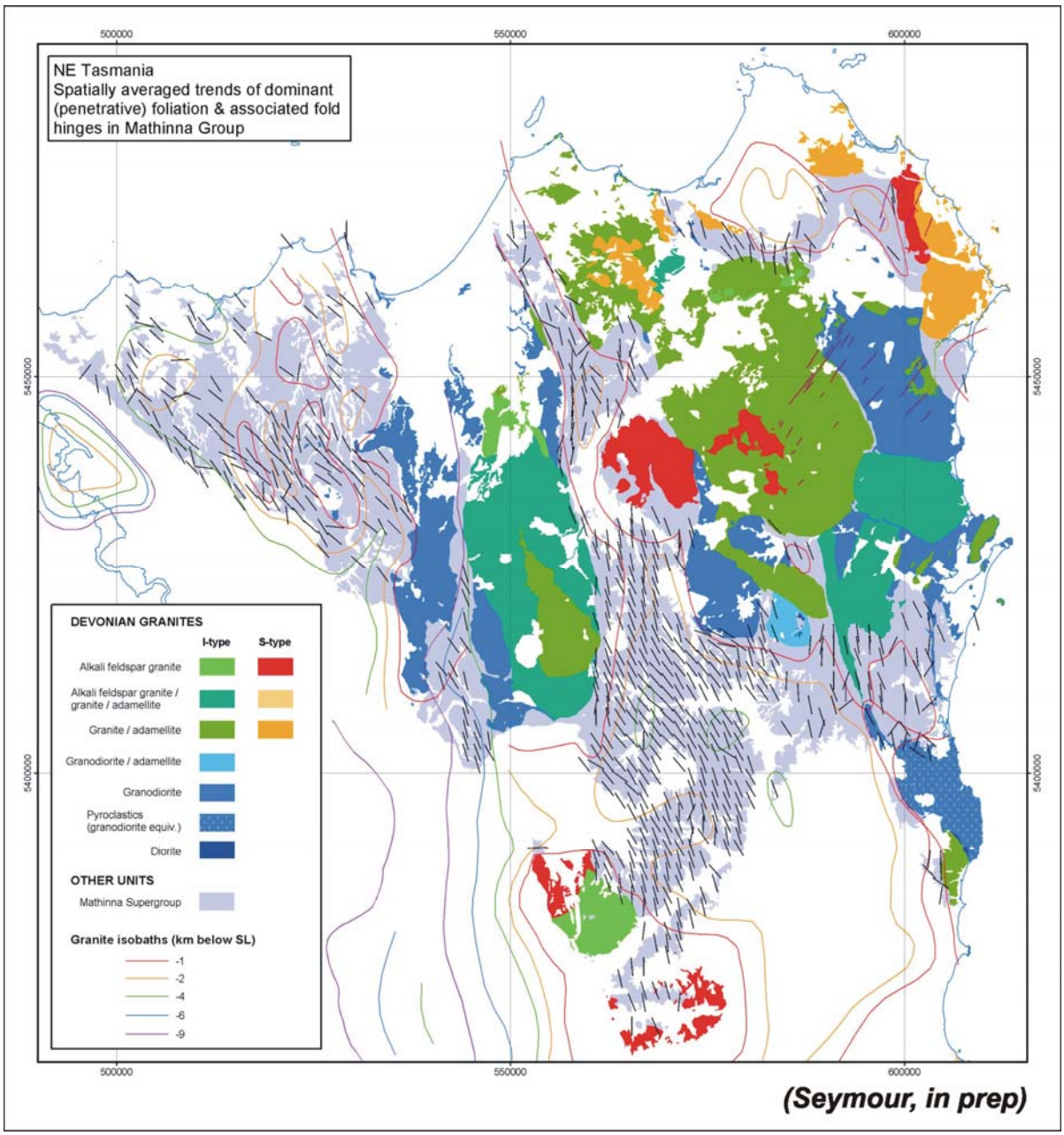

Figure 4.22: Trend of foliations and their associated fold hinges in North Eastern Tasmania.

The distribution of Tertiary depocentres, the generally linear basin boundaries and topographic highs on its south-western and north-eastern sides indicate extension was concentrated in the Launceston Tertiary Basin and has little affected the areas to the west and east (Figure 4.23). During east-northeast directed extension, stretching was accommodated through reactivation of thrust faults rather than through modification of structures in the Mathinna Supergroup and associated granites. The orientation of the basin generally is parallel to the basement fabric. The linear basin boundary faults and internal simplicity are typical of basins where extension was near orthogonal to the basement fabric. The size and extent of the basin indicates these basement structures extend to the southeast at least as far as the Macquarie Tiers region (Figure 4.14).

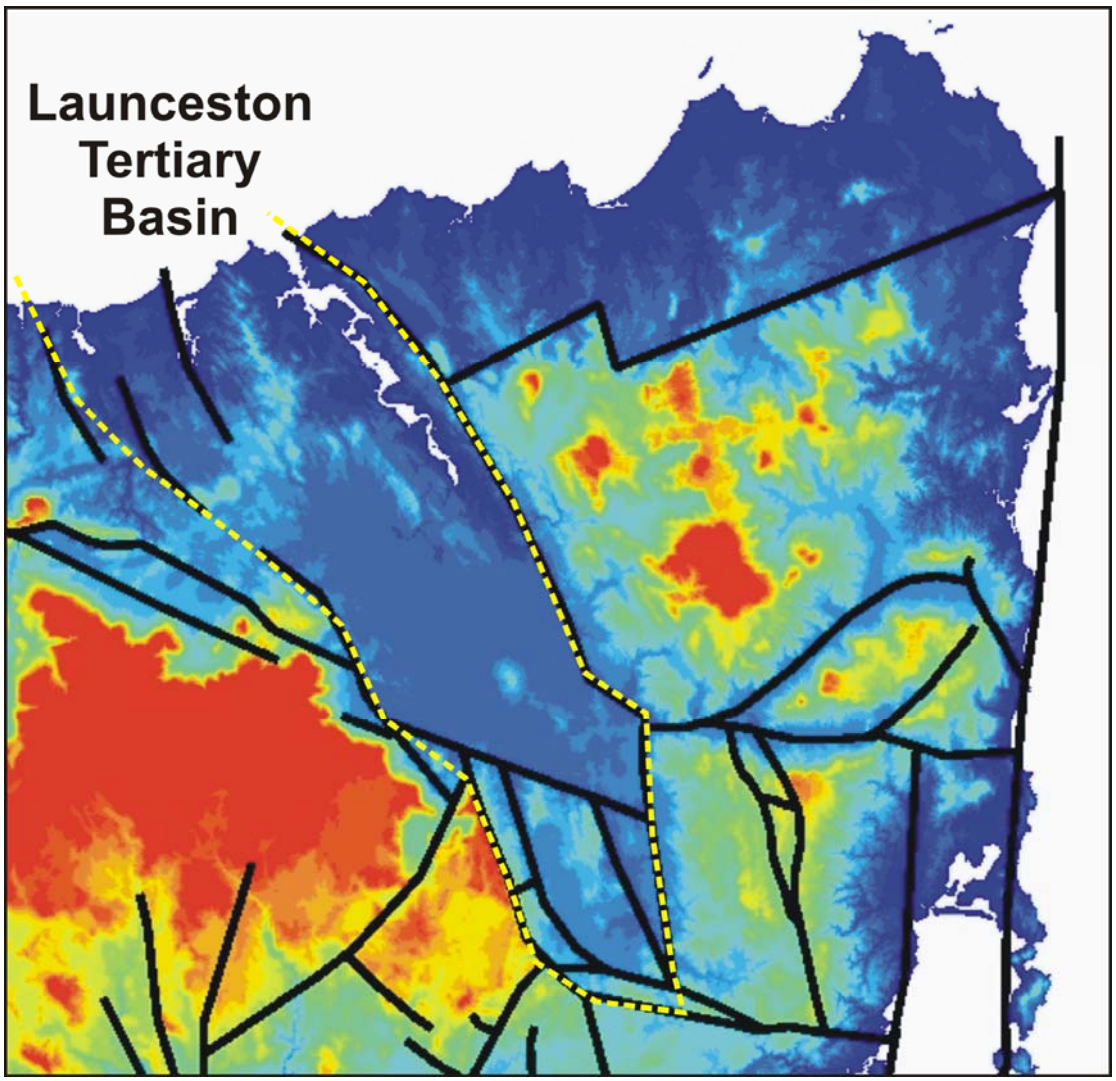

Figure 4.23: Pseudocolour rendered DEM image indicating the extent of the Launceston Tertiary Basin.

The fault pattern south of the Macquarie Tiers marks a rapid increase in complexity (Figure 4.14). The increase in complexity is coincident with a change in the strike of the structural fabric of the Mathinna Supergroup from northwest to north (Figure 4.22), thus the basement fabric is oblique to the extension direction in this zone.

Further south, on Maria Island, the trend of structures in the Mathinna Supergroup is towards the north-northeast (Figure 4.24). The Mathinna Supergroup and associated granites are confined to the east coast region, and even though basement fabric is even more oblique to extension here the structures formed are still very blocky, the only difference between north and south is the size of the blocks and the orientation of their boundary faults (Figure 4.25).

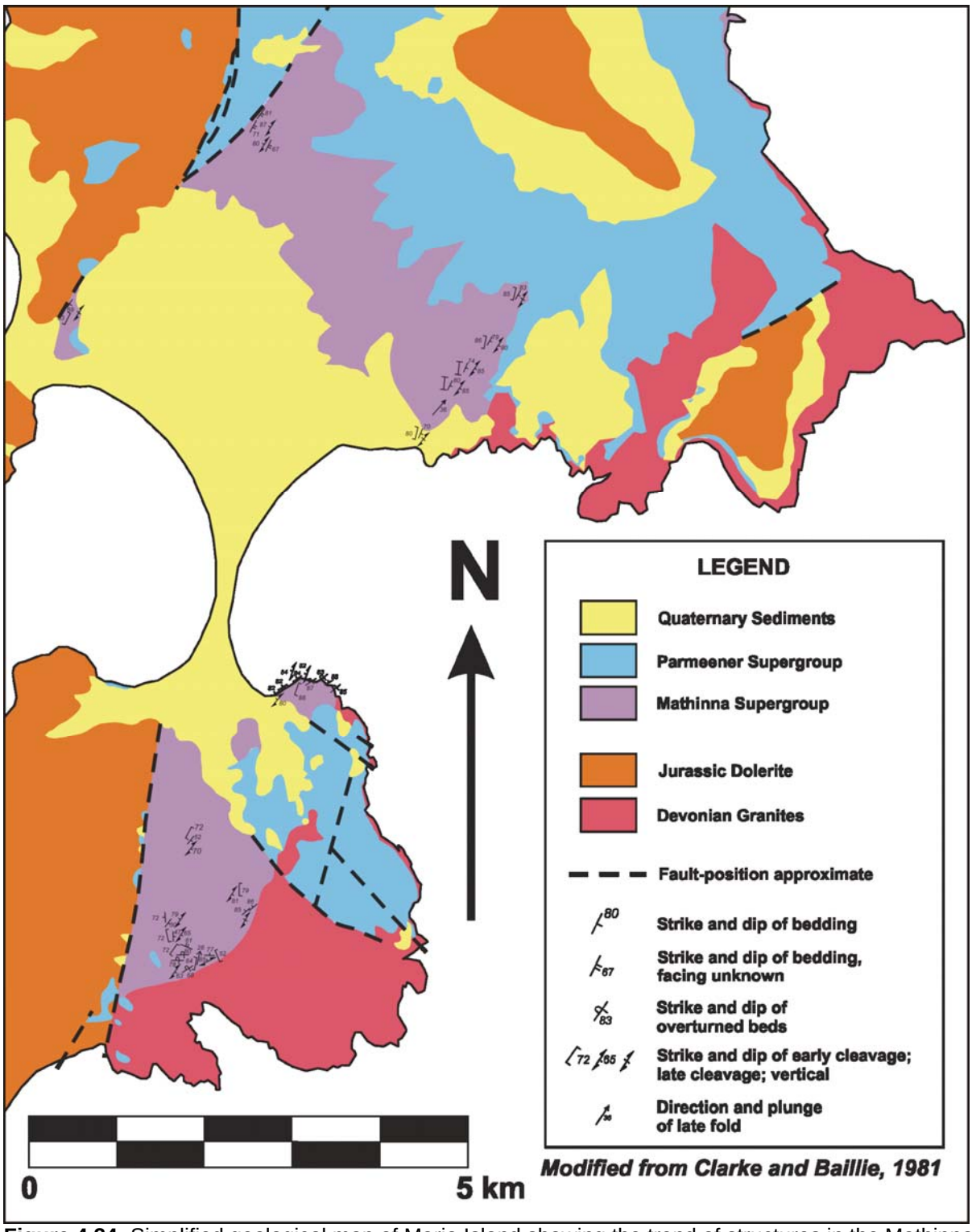

Figure 4.24: Simplified geological map of Maria Island showing the trend of structures in the Mathinna Supergroup.

The basement rocks to the west of the Mathinna Supergroup boundary belong to the Western Tasmania Terrane. The nearest exposures of Western Tasmania Terrane rocks are found in south-western Tasmania, therefore the fabric of the rocks immediately west of the Mathinna Supergroup boundary is unknown. Structures formed in the overlying rocks are more diverse and disorganized than those to the east (Figure 4.7). Some indications of orientation and type of structures may be deduced from the Tertiary Fault Pattern.

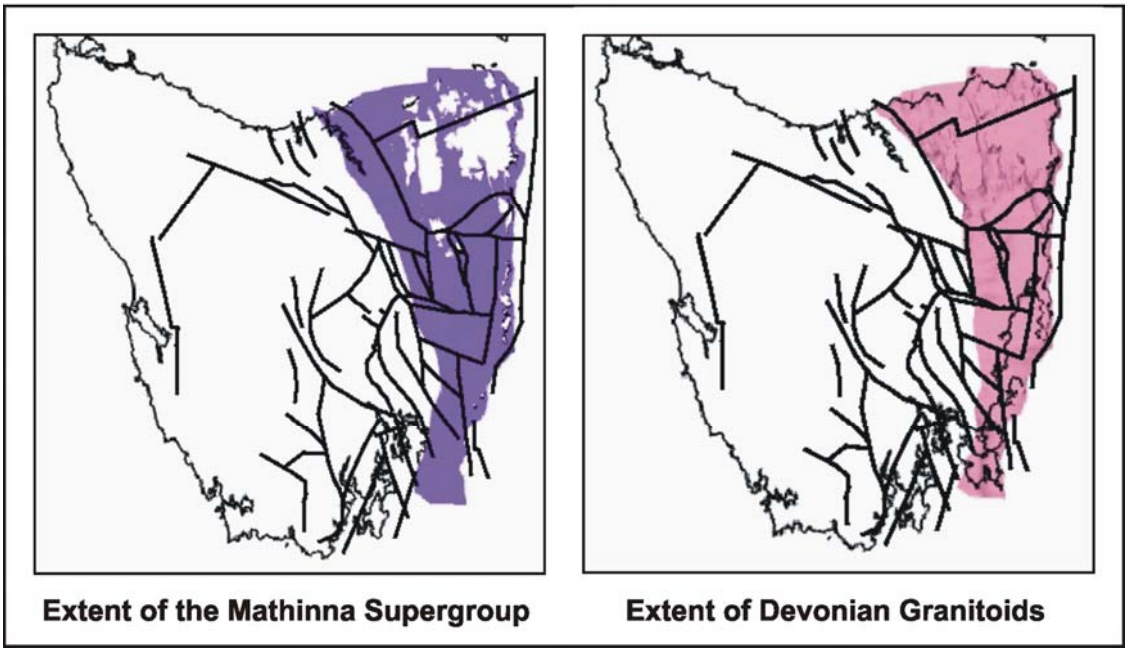

Figure 4.25: The extent of the Mathinna Supergroup and Devonian Granitoids compared to the Tertiary fault pattern developed above them.

The Lower Derwent, Coal River Grabens and an adjacent fault to the north are all sub-orthogonal to the extension direction and anastomose into a single northeast trending fault (Figure 4.17). This pattern is typical of an accommodation or transfer structure formed over an active pre-existing fabric. Active fabrics result in a strike- or oblique-slip fault zone that lies sub-parallel to the regional extension direction while normal faults are developed sub-orthogonal to regional extension (Morley, 1999b, McClay et al., 2002) (Figure 4.26). The fault pattern interpreted for the grabens implies they terminate at a basement structure that strikes northeast, which acts as a transfer structure during the extension.

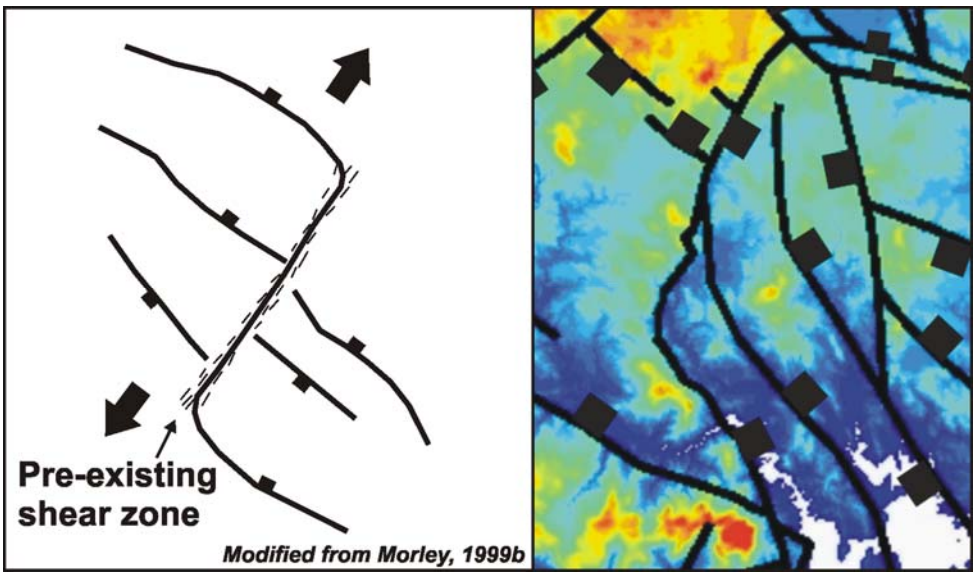

Figure 4.26: Comparison of an accommodation/transfer structure with the fault pattern interpreted for the north-western ends of the Lower Derwent and Coal River Grabens.

The southern part of the Upper Derwent Graben strikes west-northwest, parallel to, and along strike from, structures in the Linda Zone of western Tasmania (Figure 4.27). Whether this structure is developed on an extension of the Linda Zone is not known, the graben is parallel to the trend for about half its length before turning toward the northwest, an orientation similar to that of the Lower Derwent Graben, dying out in a horsetail splay in the Central Highlands. Faults along the coast in the far southeast are orientated towards the north-northeast, orthogonal to the Upper Derwent Graben (Figure 4.17). These structures and the Upper Derwent Graben are all truncated by the Lower Derwent Graben (Figure 4.17).

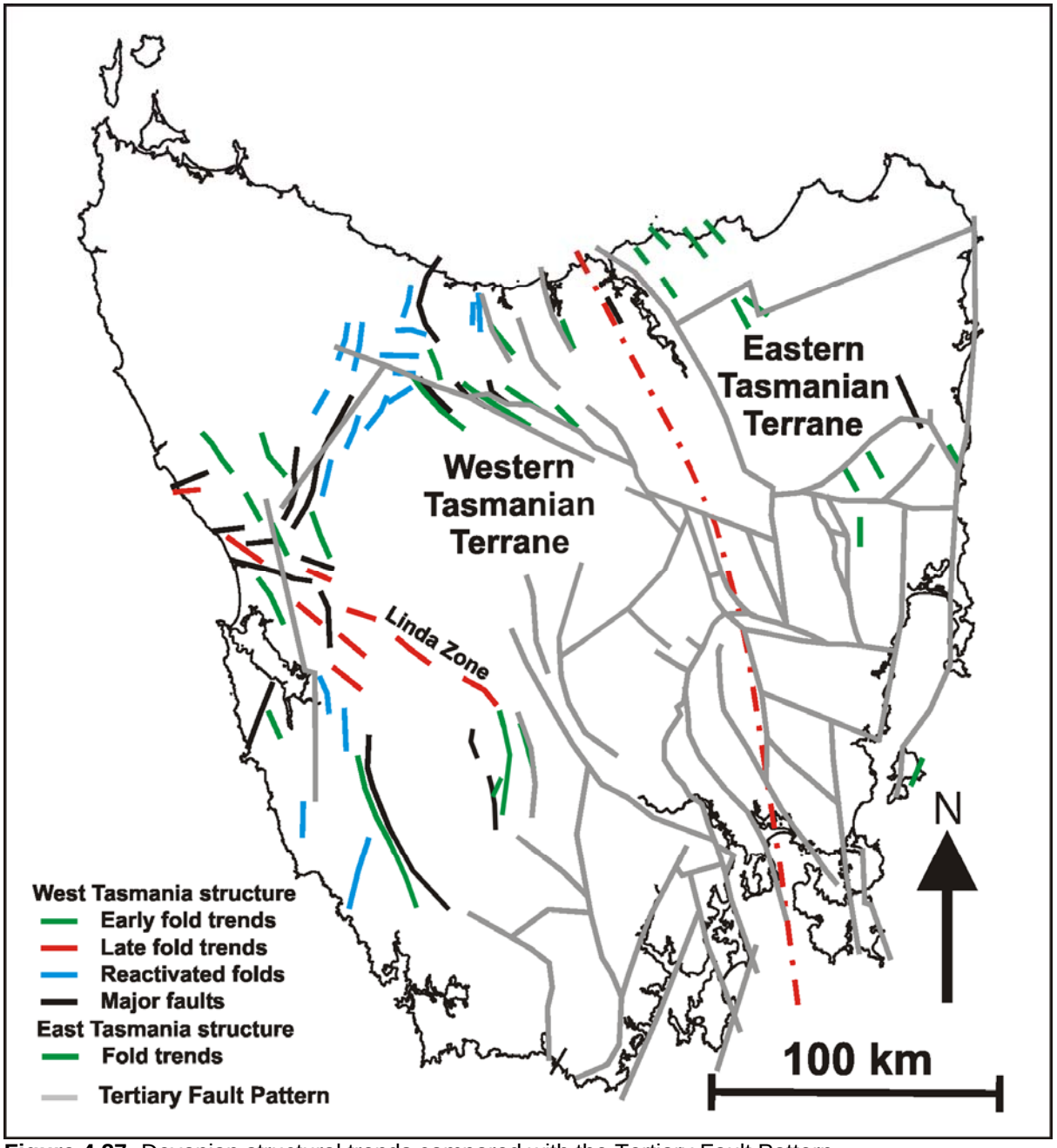

Figure 4.27: Devonian structural trends compared with the Tertiary Fault Pattern.

The model of the Tertiary topography shows the majority of the fault blocks dip away from central Tasmania. A dip for each of the blocks was calculated from the DEM and these were found to be, in general extremely small (Figure 4.11). The small dips imply that extension was in most places limited and block rotation was small on this scale. Larger rotations, up to 20°, are common in small blocks (<1 km) along the Lower Derwent Graben (Leaman, 1976).

4.4: CONCLUSIONS

The Tertiary fault pattern can be sub-divided into a northern and southern zone based on the complexity of the structures observed. The northern zone is structurally simple. Extension was concentrated along a 35 km wide, 100 km long zone to form the Launceston Tertiary Basin. Stretching was probably accommodated by reactivation of northwest striking, east dipping thrust faults underlying this zone, while the Central and Northeast Highlands acted as competent blocks and remained relatively unaffected by the extension. Further south as the strike of the basement structures becomes more oblique to extension, the resulting Tertiary fault pattern markedly increases in complexity.

CHAPTER 5
SEISMIC DATA AND INTERPRETATION METHODOLOGY

5.1: INTRODUCTION

Prior to the TB01 survey, no major industry-standard, multi-line seismic data has been acquired onshore in Tasmania. It is in itself an experiment, building on the lessons of previous surveys. Following is a review of the dataset: where and why it was acquired, how it was processed, what some problems with the data are and what caused them.

The Tasmania Basin is a frontier exploration province and lacks the constraints and controls on interpretation found in mature exploration areas. For this interpretation, stratigraphic control is provided by a very few wells and from outcrop in the escarpments fringing the Central Highlands region and new velocity data were used to correlate between wells and the seismic sections. The seismic stratigraphy and nomenclature used has been modified from scheme used by MRT on their 1:250 000 scale geological maps.

5.2: PREVIOUS WORK

A number of small commercial and experimental reflection seismic surveys have been conducted in Tasmania with varying success. The commercial surveys were generally conducted by mineral explorers and aimed at detecting the thickness of cover and while adequate for the task, these surveys were small, low fold and not extensively processed (Leaman, 1996).

The Department of Mines (now Mineral Resources Tasmania - MRT) has conducted several experimental surveys. These are short and generally of a higher standard and resolution than industry long-line surveys, due to fine tuning of signal and adjustment for online conditions (Leaman, 1996). Several of these have been over coalfields and are thus generally shallow. While successful at proving seam thickness and structure, they did not penetrate deep enough or have sufficient resolution to successfully define units within the Lower Parmeener Supergroup (Richardson and Leaman, 1980, Richardson and Leaman, 1981). At the request of Conga Oil, a single traverse was conducted on North Bruny Island to test whether the reflection seismic method was applicable to the Tasmania Basin conditions

(Richardson, 1987). While, the test was considered successful, the data quality was extremely poor, being both vertically and laterally incoherent.

Meekatharra Minerals Limited acquired 19.7 km of data in a three line survey at the northern end of Oyster Bay (Shaw, 1982). While the survey was experimental, trying to access the applicability of the method to the area. It was also aimed at assessing the thickness of the Tertiary section and highlighting structure. The resulting processed section probably represents the best data to come from onshore Tasmania up to that time, clearly showing the base of the Tertiary section and a thick dolerite sill.

The Australian Geological Survey Organisation (AGSO, now Geoscience Australia) recorded five seismic lines in Tasmania during 1995. These lines represent the first modern, industry standard seismic surveys onshore in Tasmania. Of the five lines recorded only seismic line 95AGS-T4 is in the region of the Tasmania Basin Seismic Survey (TB01), intersecting line TB01-ST (shot-point 1997) (Map 5.1). The line was recorded across an area of variable geology and parallel to, and above, a major basement structure (Leaman, 1996). The resultant unmigrated data is poor quality, adding little to the interpretation of the current survey.

5.3: 2001 TASMANIA BASIN SEISMIC SURVEY (TB01)

5.3.1: INTRODUCTION

In 2001 Great Southland Minerals Ltd (GSLM) acquired 662 km (23 lines) of seismic data in northern Tasmania, the Tasmania Basin Seismic Survey (TB01). This was the first major commercial seismic survey undertaken onshore in Tasmania, and was designed to define the regional structure of the Tertiary, Permo-Triassic and pre-Carboniferous basement units and to locate exploration targets. The lines were recorded across the Central Highlands, Northern Midlands and Longford Sub-basin regions of Tasmania (Map 5.1), with several short seismic lines recorded to more accurately define potential structures identified by a limited gravity survey carried out by GSLM in 2000.

Not all of the lines acquired as part of the TB01 survey have been fully interpreted as part of this research. In the Longford Sub-basin only lines TB01- PF, PG, PM, PT, PU, PW and TE (Map 5.1) were interpreted as these lines are either relatively orthogonal to regional structuring and show the effects of Late Cretaceous to Tertiary extension, or are strike lines that tie with the other lines. Detailed work on the Longford Sub-basin seismic lines was

completed by Lane (2002). The lines comprising the Central Highlands and Northern Midlands regions (TB01 – TB, TI, PB, TA, TH, PA, PD and ST) have all been fully interpreted, while lines line TB01-TC and 95AGST4 have only received cursory attention because of their location and poor quality data (Map 5.1).

5.3.2: ACQUISITION

The seismic data was acquired for GSLM by Trace Energy Services using the Vibroseis method between the 10th of March and 25th of June 2001 (Table 5.1). The data was mainly recorded along existing roads, which were not always straight.

Table 5.1: Acquisition parameters for the TB01 survey.

Key Seismic Survey Recording Parameters	
Data Recorded by:	Trace Terracorp
Date Recorded:	10 March - 25 June 2001
Seismic Source	Vibroseis Litton LRS-15
Number of Vibrators	Four
Number of sweeps per VP	2 sweeps each station no move up (standing sweeps)
Vibrator Spacing	Vibrators centred on station 12.5 m pad to pad
Source Array Length	37.5 m
Sweep Length	8 secs
Sweep Frequency	6-80 Hz sweep
Sweep Type	Linear
Recording System:	I/O System Two
Format	IEEE SEGD
Record Length	14 secs
Sample Interval	2 ms
Low Cut Filter	5.5 Hz
High Cut Filter	Out
Receivers:	
Geophone Type	Sensor SM4 10 Hz
Group Interval	25 m
Number of Groups	240 or 360
Spread Type	Split Spread
Spread 360 Channel	4487.5-12.5-X-12.5-4487.5
Spread 240 Channel	2987.5-12.5-X-12.5-2987.5

5.3.3: PROCESSING

The data was processed by Robertson Research (Australia) Pty Ltd using a conventional processing stream (Table 5.2). Final stack and migrated data are available with the migrated data being used for the interpretation. The data is minimum phase, normal polarity i.e. negative values represented by a trough, which is shown on the seismic sections in red.

Table 5.2: Typical processing stream for the TB01 survey.

PROCESSING STREAM FOR SEISMIC LINE TB01-ST		
SEQUENCE	**PROCESSING PARAMETERS**	
	FINAL STACK	**MIGRATION STACK**
Transcription	Transcribe SEGD to Robertson's internal format	Transcribe SEGD to Robertson's internal format
Phase Conversion	Convert to minimum phase Velocity cuts: +/- 1500 m/s in shot domain	Convert to minimum phase Velocity cuts: +/- 1500 m/s in shot domain
Amplitude Recovery	Gain (dB) = 3.0t + 26log(t) + 110	Gain (dB) = 3.0t + 26log(t) + 110
Statics	Floating Datum Correction Green Mountain Refraction Statics	Floating Datum Correction Green Mountain Refraction Statics
CDP Sort	180 Nominal Fold	180 Nominal Fold
Deconvolution	16 msec gapped decon using 2 windows 0.1% white noise 120ms Operator Length Design (near) : 150-2400 2000-4000 ms (far) : 1000-3000 2800-4200 ms	16 msec gapped decon using 2 windows 0.1% white noise 120ms Operator Length Design (near) : 150-2400 2000-4000 ms (far) : 1000-3000 2800-4200 ms
Velocity Analysis	Preliminary Velocity Analysis Approximately 2.5 km intervals	Preliminary Velocity Analysis Approximately 2.5 km intervals
Residual Statics	7 Trace pilot Correlation window 100-3800 ms	7 Trace pilot Correlation window 100-3800 ms
Velocity Analysis	Secondary Velocity Analysis Approximately 1.25 km intervals	Secondary Velocity Analysis Approximately 1.25 km intervals
DMO	Dip Move Out by integral method 180 equal offset planes	Dip Move Out by integral method 180 equal offset planes
Velocity Analysis	Final Velocity Analysis Approximately 1.0 km intervals	Final Velocity Analysis Approximately 1.0 km intervals
NMO Corrections	Velocity functions referenced to surface	Velocity functions referenced to surface
Mute	Offset : 200 300 800 1700 4500 m Time : 0 200 500 1200 2000 ms	Offset : 200 300 800 1700 4500 m Time : 0 200 500 1200 2000 ms
Scaling	500 ms AGC	500 ms AGC
Statics	Floating datum to sea level correction New time of origin -700 ms	Floating datum to sea level correction New time of origin -700 ms
CDP Trim Statics	CDP consistent residual statics 7 Trace plot Correlation window 100-5200 ms	CDP consistent residual statics 7 Trace plot Correlation window 100-5200 ms
Stack	CDP stack	CDP stack
Spectral Balance	Zero phase deconvolution after stack Desired output 10 - 65 Hz	Zero phase deconvolution after stack Desired output 10 - 65 Hz
Migration		F.D Migration - Second Order Solution 20 ms step size 80% smoothed stacking velocities
Band Pass Filter	Application Time (ms) Frequency (Hz) 700 8/12 - 65/75 1300 8/12 - 55/65 3700 8/12 - 35/45	Application Time (ms) Frequency (Hz) 700 8/12 - 65/75 1300 8/12 - 55/65 3700 8/12 - 35/45
Scaling	Dual window AGC with lengths of 1000 and 400 ms 50% application	Dual window AGC with lengths of 1000 and 400 ms 50% application
TAUP	Tome variant dip and coherency filter Mix back: 70%	Tome variant dip and coherency filter Mix back: 70%

In general, the quality of the data in the resultant seismic sections is highly variable, with the seismic data often degraded both horizontally and vertically. Reflections that are laterally coherent over a significant distance are rare. In part, this variation probably results from the crooked line geometry, the variable topography and complex geology. The presence of Jurassic Dolerite sills creates a significant velocity inversion within the Parmeener

Supergroup sequence and has a significant affect on seismic energy and velocity. It is the major cause of the poor quality of the processed data.

Most of the data was recorded along existing roads and required processing using crooked line techniques. Events in seismic data acquired along lines that are straight are more easily ascribed to geologic features, while with crooked line geometries events may represent changes in line direction rather than geological structures. Processing techniques generally assume a straight line profile with uniform fold and even offsets, crooked line acquisition results in variable fold and uneven offsets (Wu, 1996). Specialised processing with careful initial and residual statics corrections and frequent velocity analyses are required, and even with crooked line processing methods applied, problems such as seismic transparent zones and coherent noise can still result where there are changes in survey line direction (Wu, 1996). Many of the roads used in this survey were windy, some containing many tight bends over short distances. Therefore, even with the application of crooked line processing techniques, variably degraded seismic data can be expected.

The geology and structure of the Tasmania Basin is very different to that of the basement, imposing unique problems during processing. The Tasmania Basin comprises mainly flat lying sedimentary rocks and dolerite sills. Dips rarely exceed 10° and are on average less than 5°. The structure of the basement is more complicated. Deformation during Middle Devonian Tabberabberan Orogeny resulted in folds and thrusts that verge southwest, west of the River Tamar, while folds verge northeast in northeast Tasmania (Seymour and Calver, 1995, Reed et al., 2002). Dips in the basement are normally steep, with dips less than 30° very rare.

The presence of Jurassic Dolerite has caused substantial problems in previous surveys of the Tasmania Basin. It has resulted in either total absorption or loss of signal or produced a seismic shadow up to one second below the intrusion, the reasons for this are not well understood (Leaman, 1996). Throughout the TB01 survey significant degradation of the seismic record occurs where dolerite outcrops, while seismic events beneath dolerite sills that lie some distance from the surface are often better resolved (Figure 5.1).

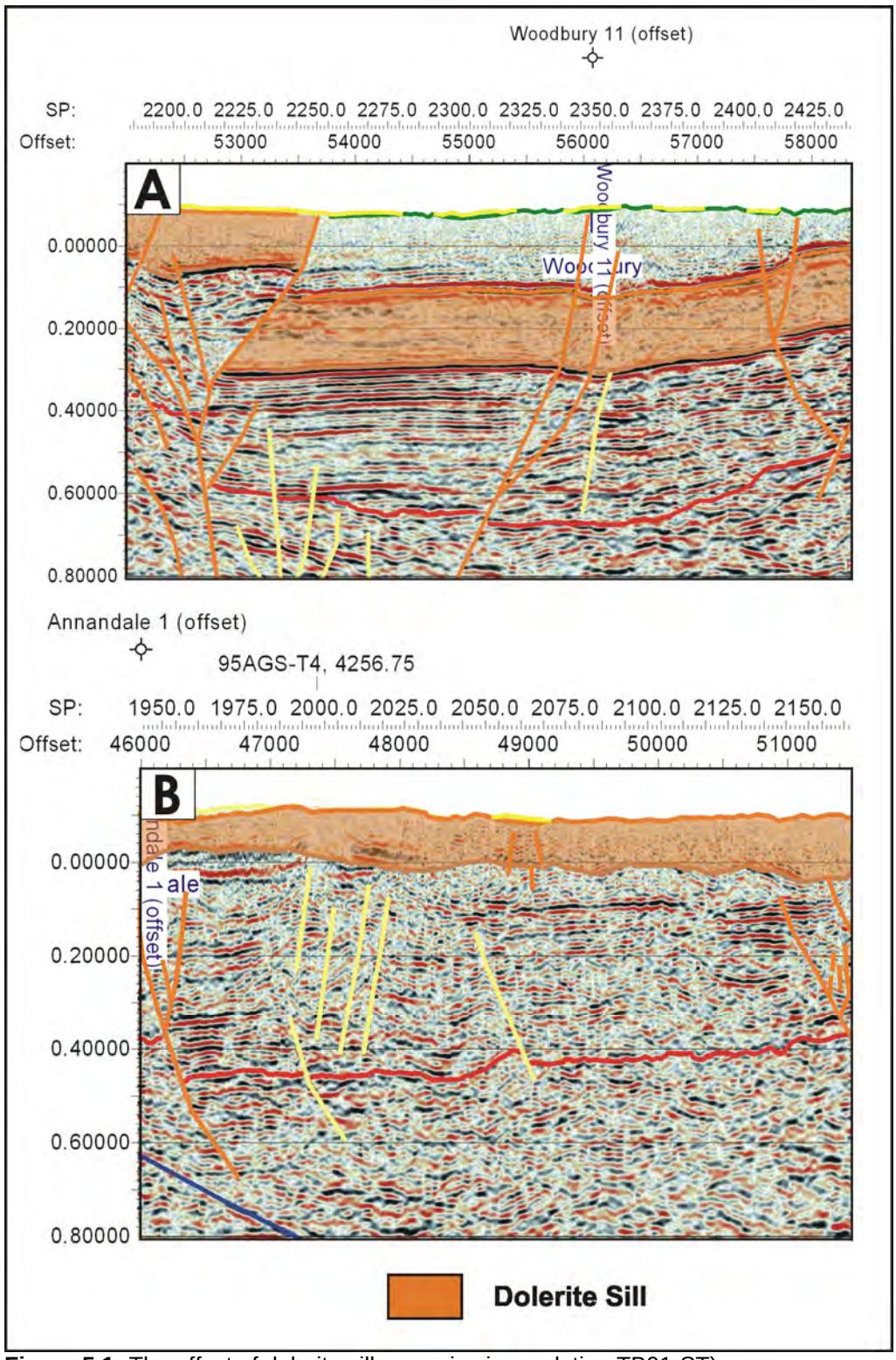

Figure 5.1: The effect of dolerite sills on seismic resolution TB01-ST):
A). where the sill is at depth, B). where the sill outcrops.

A high seismic velocity layer near to the surface may result in much of the energy input being reflected from either the upper or the lower interface and energy may even be multiply reflected within the layer resulting in reverberations at later times that could be confused with real features or obscure those features. The effect on seismic data quality of high velocity layers at or near the surface is well documented for areas such as the Parana Basin of

South America, the Mesozoic basins of Northern Ireland (Papworth, 1985) and Columbia Plateau in North America (Pujol et al., 1989, Withers et al., 1994). The large velocity and density contrasts between the high density basalts (5800 m/s) and interbedded clay layers (1700 m/s) of the Columbia Plateau have a major effect on wave generation and propagation (Pujol et al., 1989).

In the Tasmania Basin the velocities within the dolerite are extremely high. Velocities recorded for dolerite as part of this research exceeded 7000 m/s for one interval with an average velocity across the dolerite section of 6250 m/s, while the average velocity of the underlying Permian Strata is 4500 m/s. For outcropping dolerite, velocities greater than 5500 m/s at 50 m are typical (Leaman, 1996). These must be taken into account during processing. High initial velocities are required if the dolerite is at or very near to the surface or when at depth the velocity inversions must be similarly managed. For the TB01 survey, stacking velocities applied to the dolerite intervals during processing were low. Incorrect velocities used during processing can have a significant affect on the quality of the stacked section. Velocity enters into the processing sequence at two stages:

1. It is required for normal moveout correction, which is applied prior to stacking. An incorrect velocity estimate at this stage will have the effect of smearing the reflected energy out over a time interval rather than having a clear single reflection.
2. Velocity is used in migration and in general an incorrect velocity will result in "de-focussing" of the section. A bad velocity estimate can also have significant affects on the appearance of dipping reflections and features such as diffractions.

The complex geometry and generally steeply dip of the basement poses other problems in processing. The seismic data has been migrated using the Finite-difference method. Steep dips were recognised during processing and a 65° second order solution was used (Curran, 2003). However, steep dips and the structural complexity mapped in outcrop is not observed in the seismic section indicating that the basement section is probably under-migrated.

The crooked line geometry of the survey may also have an effect on the imaging of events in the basement. Truly dipping events should be easily recognised in seismic lines that are relatively straight and orthogonal to the regional strike of the basement, for example line TB01- ST (Map 5.1). On lines that are sub-parallel to the strike, line TB01-TH for example (Map 5.1), the dip of events is apparent. On roads where the direction of the line changes the dip of the basement events should also change, which is generally not observed.

Onshore Tasmania is a difficult area to record seismic data due to issues of access, complex topography and geology. If the data quality of future surveys of the Tasmania Basin is to improve, careful acquisition and processing, that compensates for the high seismic velocity of the ubiquitous dolerite is required. While, properly imaging structure in the basement will require careful orientation of future lines.

5.4: STRATIGRAPHIC CONTROL AND CORRELATION

5.4.1: STRATIGRAPHIC CONTROL

Introduction

The stratigraphic and structural data provided by mapping and drill holes provides important support for the interpretation of the TB01 Seismic Survey. The outcrop geology of the TB01 survey area is covered by geological mapping at 1:250 000, 1:50 000 and 1:63 360 scales. The mapping and accompanying explanatory notes has provided information on the location and orientation of stratigraphic units, faults and other structures. Outcrop data is also used as a substitute for drill hole data in areas where there is an absence of deep drilling. Mapped outcrop along the escarpment of the Great Western Tiers and escarpments to the west of Lake St. Clair and Lake King William are useful, especially where no drill hole data is available, to determine the occurrence and local thickness of units. These abrupt changes in relief expose significant thicknesses of Parmeener Supergroup section, where individual unit thicknesses can be calculated using topographic contours or electronically from the Digital Elevation Model (Figure 5.2).

The survey area is covered by regional gravity and magnetic datasets. The magnetic data is of little use due to the variably magnetic character of the dolerite. The entire Tasmania Basin is covered by a several generations of gravity surveys, which have been acquired at varying line spacing. The spacing of the gravity stations and the variable basement lithology makes the data generally unsuitable for mapping the depth, extent or structures in the sedimentary sequence. However, the dataset has proven a useful tool for estimating changes in the thickness of dolerite sills.

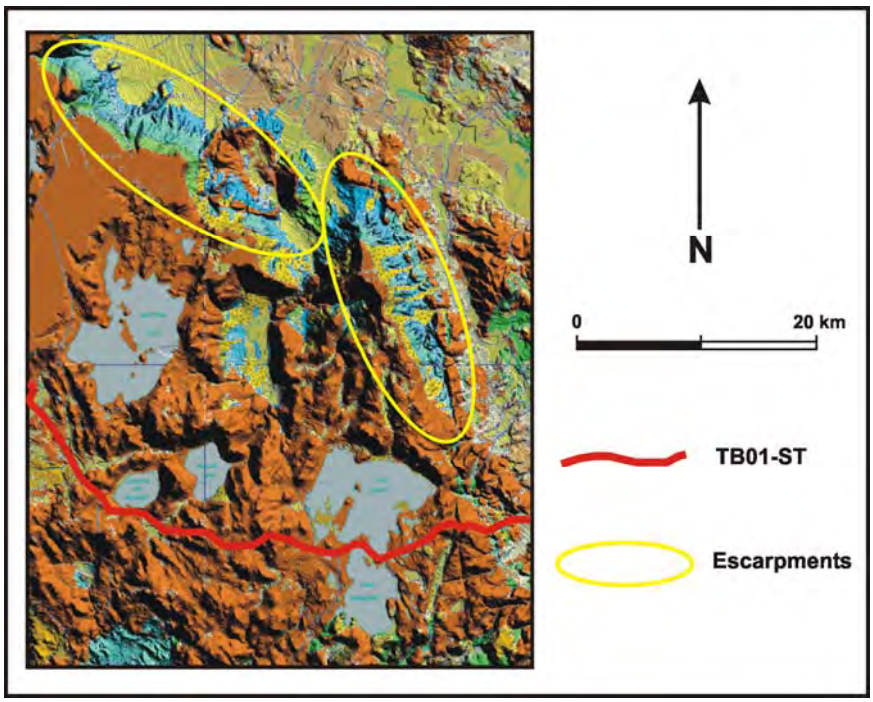

Figure 5.2: The Parmeener Supergroup is exposed in the escarpments fringing the Central Highlands. The thickness of stratigraphic units could be calculated from such areas and used to constrain the seismic interpretation.

To date a single exploration well (Hunterston 1) has been drilled by GSLM as a tie to the seismic data, therefore much of the interpretation has been reliant on open file information gathered from MRT. The initial source of information was the Tasmanian Drill Hole Database (DORIS) supplied by MRT. This database provides such important information as location, depth and location of supporting documentation.

In the region covered by the TB01 survey, numerous drill holes are recorded, the vast majority of these occur in the Northern Midlands/Longford Sub-basin region with a smaller number of holes in the Central Highlands. The holes in the Northern Midlands/Longford Sub-basin region are mostly shallow and were drilled as water bores and for coal exploration. Most holes terminate at the dolerite contact. There are some reasonably deep engineering holes in the Central Highlands; however, these are far from the seismic lines. The holes of most use are the deep, stratigraphic holes drilled by the Department of Mines (MRT). Several of these holes are reasonably close to seismic line TB01-ST (RG-145, RG-146 and The Quoin) and a hole drilled at Golden Valley (GV 1) is adjacent to seismic line TB01-TH (Map 5.1). The exploration holes, Hunterston 1 and MPT 1 Dungrove constrain the interpretation at the beginning of seismic line TB01-PB (Map 5.1). None of these drill holes has been electronically logged or has an accompanying velocity survey. Consequently, while the Hunterston 1 hole was open, a velocity survey was conducted using equipment built at the

University of Tasmania. The velocity data collected was used to correlate seismic events and stratigraphic events for the whole survey area.

Well Control

Hunterston 1 DDH

The Hunterston 1 DDH (Diamond Drill Hole) is a stratigraphic hole drilled by GSLM north of the township of Bothwell in the Central Highlands (Map 5.1). Located on seismic line TB01-PA (495 500 mE, 5 326 400 mN), Hunterston 1 is the only drill hole in the Central Highlands to pass through the Parmeener Supergroup and terminate in the basement. It is also the only hole drilled since the TB01 Seismic Survey was conducted, and was open allowing a velocity survey to be completed. This drill hole has been extremely important for correlating litho- and seismic-stratigraphy and as a control on the seismic interpretation.

The hole was drilled to investigate a structure known as the Hunterston Dome. The Hunterston Dome was first described by Fairbridge (1949), during regional geologic mapping of the Waddamana region for the Hydro-Electric Commission (HEC). This structure occurs in a "window" in the dolerite where Fairbridge (1949) interpreted a possible closure in the Lower Parmeener Supergroup with an absence of dolerite in the section, making it an attractive target for hydrocarbon explorers in the Tasmania Basin.

The drill hole was pre-collared in August 1997 to a depth of 336 m, encountering dolerite at 135 m (Figure 5.3). Diamond drilling commenced in July 2002 (HQ, 63 mm diameter to 974 m followed by NQ, 45 mm diameter), continuing through the dolerite and rocks of the Lower Parmeener Supergroup to terminate in Precambrian Dolomite at a depth of 1324 m (Figure 5.3). No significant hydrocarbons were encountered during drilling.

Drilling revealed differences in the Lower Marine Sequence of the Lower Parmeener Supergroup from that found elsewhere in the Tasmania Basin. The thick basal tillites are completely absent and while the first 6 m of Bundella Mudstone are typical, the main body of the correlate is a bioturbated grey siltstone which becomes increasingly pebbly down hole (Reid et al., 2003). The lower Bundella Mudstone facies and Woody Island Siltstone are absent, replaced by conglomerates, conglomeratic siltstones and pebbly siltstone (Reid et al., 2003). Several sub-horizontal, highly brecciated fault zones occur around 900 m (Figure 5.3). These zones have high porosity and permeability, which led to a loss of circulation during drilling.

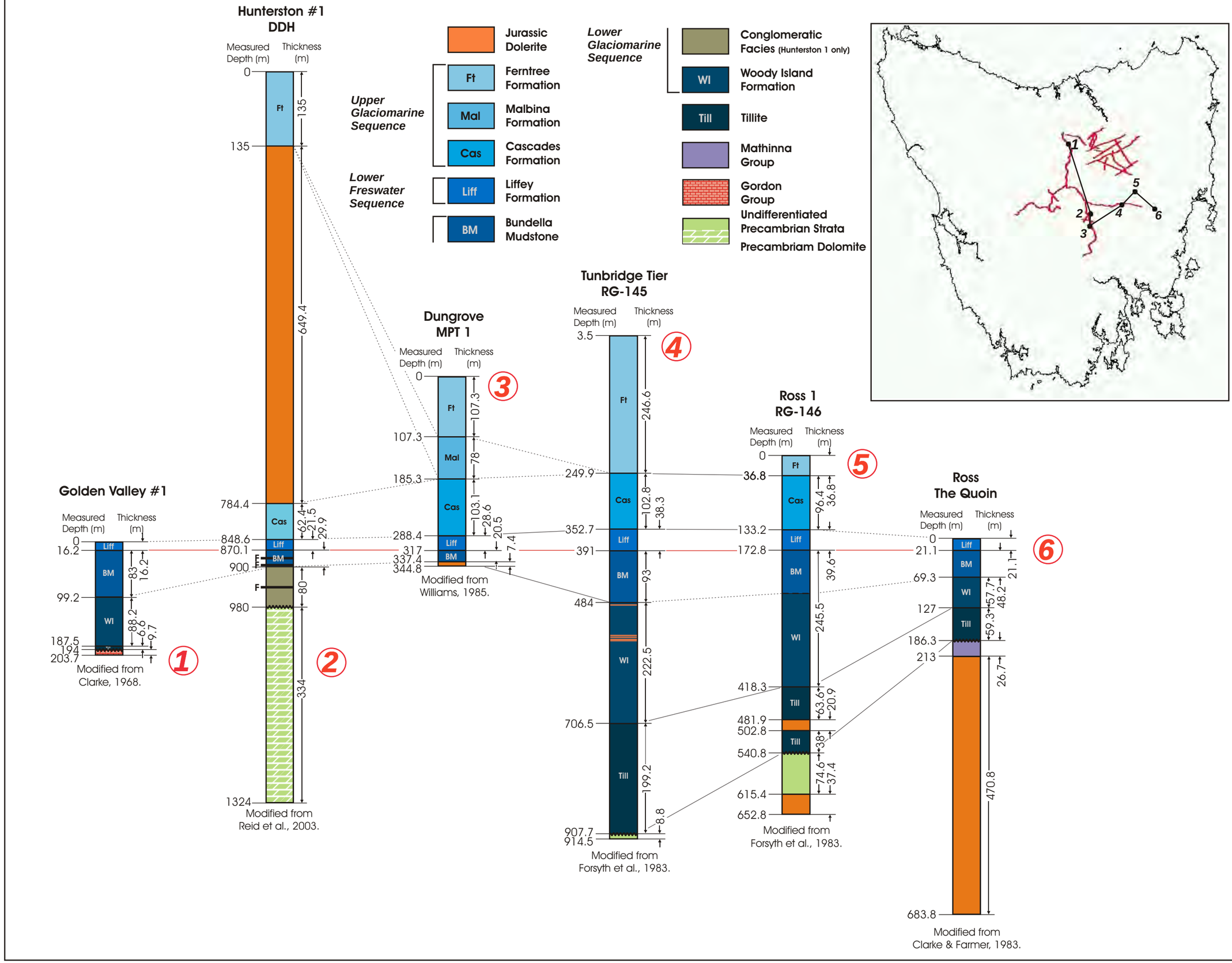

Figure 5.3: Drill holes used to constrain the seismic interpretation.

RG-145 Tunbridge Tier

The RG-145 drill hole at Tunbridge Tier (Map 5.1) is a 914 m deep, fully cored stratigraphic hole drilled by the Mines Department (MRT) in 1983. Located approximately 1000 m south of seismic line TB01-ST (SP 1725) (524 510 mE, 5 334 870 mN) this drill hole has also been important in linking the seismic survey to the local stratigraphy.

The drill hole is collared in the Upper Marine Sequence (Ferntree Formation) and passes through a complete section of the Lower Parmeener Supergroup. A series of thin (<1 m) sills intrude the Lower Marine Sequence (Woody Island Siltstone) between 490 m and 550 m (Figure 5.3). These sills have been variously interpreted as Tertiary Basalt (Forsyth et al., 1989) or as Jurassic Dolerite (Domack, 1991). The drill hole terminates in folded rocks, which are probably Precambrian in age (Figure 5.3). These folded rocks have low grade metamorphism and the degree of tectonic/metamorphic modification is similar to the Precambrian sequences of Western Tasmania rather than the Ordovician – Silurian rocks (Mathinna Supergroup) of north-eastern Tasmania (Forsyth et al., 1989).

GV1 Golden Valley

The GV 1 drill hole at Golden Valley is a fully cored stratigraphic hole, drilled to a depth of 204 m by the Department of Mines (MRT) in 1967. The drill hole is approximately 500 m west of seismic line TB01-TH (SP 675) (474 911 mE, 5 391 332 mN) (Map 5.1). The drill hole was positioned on the hanging-wall of a normal fault, while the seismic line is recorded the on the footwall side. The line is useful for determining the presence and thickness of sub-Liffey Group units in the area, but not used to correlate the seismic data.

The drill hole was collared in the Lower Freshwater Sequence (Liffey Group) and passes down through the Lower Marine Sequence (Golden Valley Group and Quamby Mudstone) and Tillite (Stockers Tillite) terminating in Gordon Limestone (Ordovician) (Figure 5.3).

Other Wells

RG-146 Ross

The 652.8 m deep RG-146 stratigraphic hole, located approximately 12 km north of seismic line TB01-ST (SP 2200) (586 282 mE, 5 347 165 mN) (Map 5.1), was drilled by the Tasmania Department of Mines (MRT) in November 1983. Although some distance from a seismic line, this drill hole constrains the interpretation of the thickness of Lower Parmeener

Supergroup units that lie between the RG-145 and The Quoin drill holes on the eastern end of seismic line TB01-ST (Map 5.1).

The drill hole was collared in the Upper Marine Sequence (Ferntree Formation) and passes through a complete sequence of Lower Parmeener Supergroup and hornfelsed, folded rocks probably of Precambrian in age, terminating in Jurassic Dolerite (Figure 5.3). A second dolerite sill between 481.9 m and 502.8 m intrudes the tillite at the base of the Parmeener Supergroup (Figure 5.3). The folded basement rocks display features commonly developed in pre-Middle Devonian sedimentary sequences of western Tasmania, no similar sequences are known in the Mathinna Supergroup of north-eastern Tasmania (Forsyth et al., 1989).

The Quoin - Ross

The 470 m deep drill hole at The Quoin located 15 km southeast of the township of Ross (554 738 mE, 5 331 162 mN)is a fully cored stratigraphic hole drilled by the Department of Mines (MRT) in 1983 (Map 5.1). The purpose of the hole was to ascertain the nature of the pre-Parmeener Supergroup basement, which in this location should occur at a relatively shallow depth (Clarke and Farmer, 1983). Drilled approximately 12 km southeast of the end of seismic line TB01-ST, the drill hole was used to determine if any major stratigraphic changes (primarily thickness changes) occur in the Lower Parmeener Supergroup between the RG-145 (Tunbridge Tier) drill hole and the end of the line.

The drill hole was collared in the Lower Freshwater Sequence (Liffey Group), passing down through the Lower Marine Sequence (Golden Valley Group, Quamby Mudstone) and the Stockers Tillite. The hole intersected folded and cleaved Mathinna Supergroup at 186.3 m, followed by Jurassic Dolerite at 213 m which continued until termination at 683.8 m (Figure 5.3).

Annandale 1

The Annandale 1 drill hole is a shallow (116 m) percussion hole, drilled in January 1982 by the Northwest Bay Company P/L who were exploring the Northern Midlands area for Triassic coal (Summons, 1982). The drill hole samples unconsolidated sediments to 62 m followed by siltstones with some mudstones interpreted as the Upper Marine Sequence (Ferntree Formation). The proximity of the drill hole to seismic line TB01-ST (SP 1950) (529 270 mE, 5 336 820 mN) (Map 5.1) confirms the Ferntree Formation and not Triassic sandstones lie beneath Quaternary cover in this area.

Woodbury 11

The Woodbury 11 drill hole is another shallow (96 m) hole drilled by Victor Petroleum and Resources Limited as part of an exploration program for coal and lignite (Summons, 1981a). The hole lies approximately 2 km south of seismic line TB01-ST (SP 2350) (538 786 mE, 5 333 200 mN) (Map 5.1) and samples Upper Marine Sequence rocks (Triassic sandstone and some mudstone) to 50 m where it intersected dolerite, constraining the stratigraphic position of the dolerite in the area.

MPT 1- Dungrove

The MPT 1 hole at Dungrove was drilled to a depth of 345 m by Mobil Minerals Australia Inc in October 1983 (Williams, 1985). The drill hole lies 10 km northwest of the township of Bothwell and 2 km southwest of seismic line TB01-PB (SP 450) (494 550 mE, 5 315 000 mN) in the southern part of the "window" where the Hunterston 1 DDH was drilled (Map 5.1).

The hole was collared in the Upper Marine Sequence (Ferntree Formation), passing down through the Malbina, Cascades and Lower Freshwater Sequence (Liffey Group) and a section of Lower Marine Sequence (Bundella Mudstone), which is truncated by Jurassic Dolerite at 337 m. The hole terminates in dolerite at 345 m (Figure 5.3). The hole constrains the interpretation of the south-eastern end of line TB01-PB.

5.4.2: SEISMIC- LITHO-STRATIGRAPHIC CORRELATION

Velocity Survey

Introduction

Velocity data provides a means of correlating seismic- and litho-stratigraphic events. To date, a conventional velocity survey of the Lower Parmeener Supergroup sequence has not been performed. All previous velocity assumptions are based on refraction data (Leaman, 1996) (Table 5.3).

Table 5.3: Seismic velocities based on refraction surveys.

Summary of velocity information for the Tasmania Basin (Leaman, 1996)	
Tertiary sediments	1750 - 2000 m/s
Jurassic dolerite	5000 - 6000 m/s
Triassic rocks	3500 - 4200 m/s
Permian rocks	4000 - 4500 m/s

The aim of the velocity survey was to confirm the above assumptions by using a sonde (Fournier, 2000) to acquire velocity data at multiple levels within the Hunterston 1 DDH. Data was acquired at or as near as possible to formation boundaries (identified from core). This data is intended to be used to correlate seismic- and litho-stratigraphic events between the drill hole and the adjacent seismic line, TB01-PA (Map 5.1). The velocity data can also be applied to other drill holes with similar stratigraphy enabling the identification of seismic events on other seismic sections in the TB01 survey.

Equipment

The system used to conduct the survey was developed by Patrick Fournier as part of an Honours project at the University of Tasmania (Fournier, 2000). The system consists of two main elements; a sonde housing a temperature sensor, a geophone, their associated electronics and power supply (Figure 5.4) and a flat top trailer which mounts a drum of communications cable, a separate drum of strength cable and a 12 volt winch (Figure 5.5). The communication cable comprises two 500 m lengths of 4-core underground telephone wire, joined to create a single 1000 m cable. The cable is labelled every 25 m beginning at the tail of the sonde allowing the position of the sonde down hole to be estimated. The position of the sonde in the drill hole was controlled by a separate 1000 m of strength cable attached to the 12 volt winch. The strength cable runs through a counter, used to double-check the position of the sonde (Figure 5.5). Seismic energy was provided by explosives using zero delay detonators, the seismic data was recorded with a Geometrics ES-1225 seismograph, and the records for each shot were then downloaded onto a laptop computer using *Seisview*™ seismic refraction interpretation software.

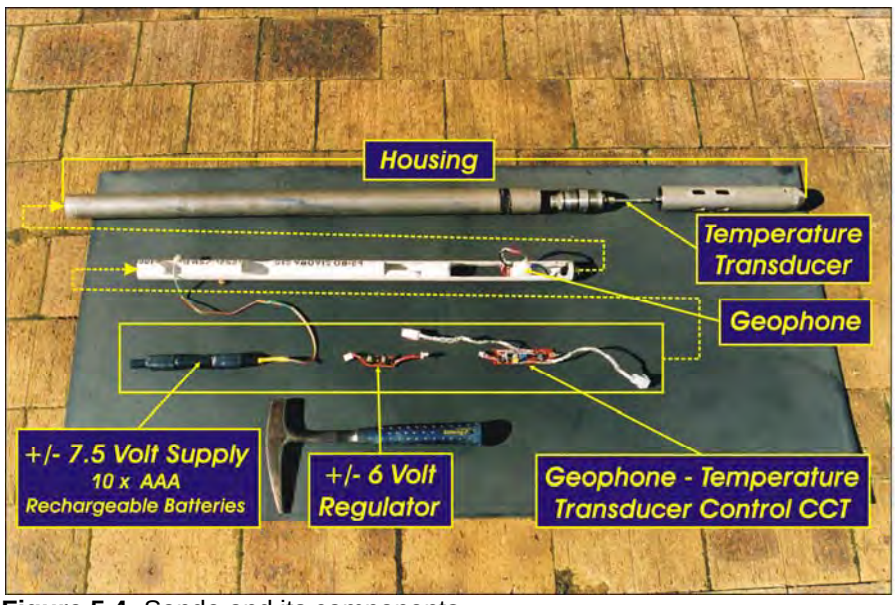

Figure 5.4: Sonde and its components.

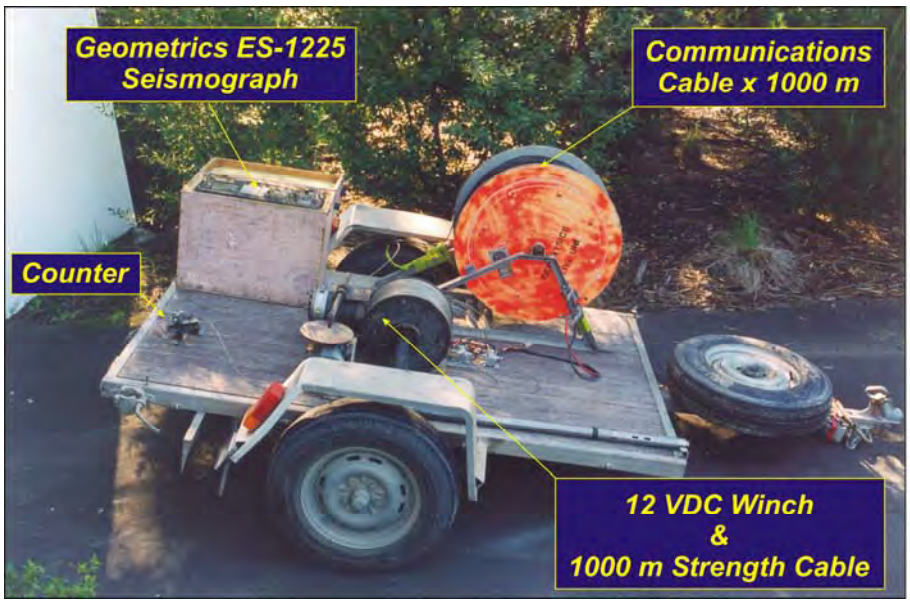

Figure 5.5: Trailer mounted equipment.

Procedure

Data Acquisition

The drill rods were cracked at the collar allowing the sonde to be lowered through the rods into the open drill hole. The trailer with the communications and strength cable was positioned adjacent to the drill hole, the cables running through pulleys slung from the derrick, guiding the communications and strength cables vertically into the drill hole. The energy source was fired 50m from and 6m below the collar in an adjacent pond (Figure 5.6), providing excellent coupling between the seismic energy source and the ground. As the sonde was lowered into the drill hole, the distance below the collar was calculated to the nearest metre by using the labels on the cable and the counter on the strength cable. When the desired depth was reached (usually a formation boundary), the cables were clamped at the top of the drill hole and the tension between the collar and cable drums eased to reduce the risk of cable induced noise.

The seismograph was then connected to the communications cable (this connection could not be maintained while the cable drum was moving) and the charge readied for the shot. The seismograph was triggered by a signal sent from the shot-box as the shot is fired. On completion of the shot, the seismograph was checked to ensure the data was recorded successfully, the data was then downloaded onto a laptop computer and the seismograph cleared and readied for the next shot. The cable connecting the seismograph to the communications cable is then removed, the clamps at the collar removed and the sonde lowered into position for the next shot.

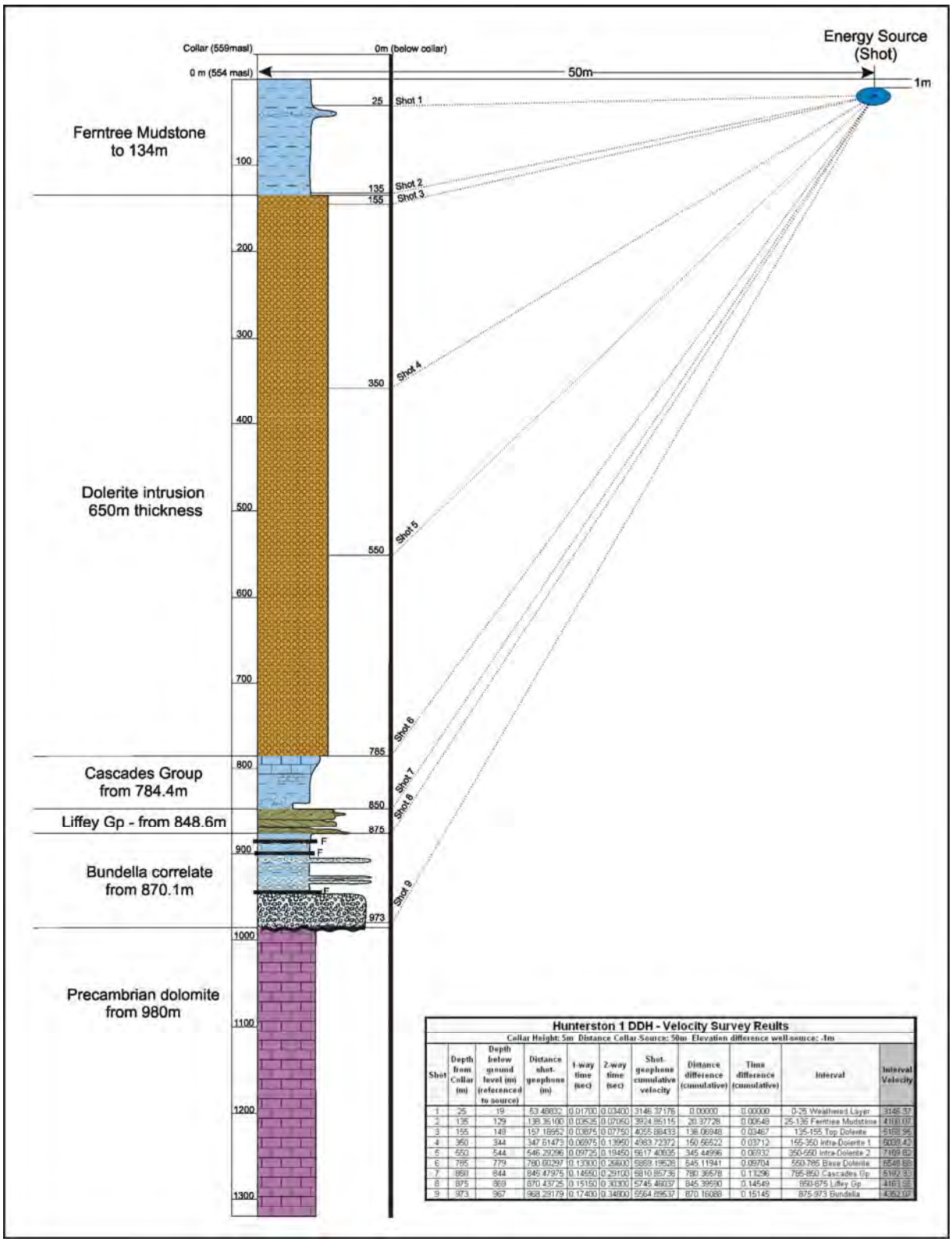

Hunterston 1 DDH - Velocity Survey Reults

Collar Height: 5m Distance Collar-Source: 50m Elevation difference well-source: -1m

Shot	Depth from Collar (m)	Depth below ground level (m) (referenced to source)	Distance shot-geophone (m)	1-way time (sec)	2-way time (sec)	Shot-geophone cumulative velocity	Distance difference (cumulative)	Time difference (cumulative)	Interval	Interval Velocity
1	25	19	53.48832	0.01700	0.03400	3146.37176	0.00000	0.00000	0-25 Weathered Layer	3146.37
2	135	129	138.35100	0.03535	0.07050	3924.85115	20.37728	0.00649	25-135 Ferntree Mudstone	4161.07
3	155	149	157.18952	0.03875	0.07750	4055.88433	138.06948	0.03467	135-155 Top Dolerite	5168.95
4	350	344	347.61473	0.06975	0.13950	4963.72372	150.66522	0.03712	155-350 Intra-Dolerite 1	6038.42
5	550	544	546.29296	0.09735	0.19450	5617.40635	345.44996	0.06932	350-550 Intra-Dolerite 2	7169.62
6	785	779	780.60297	0.13500	0.26800	5869.19526	545.11941	0.09704	550-785 Base Dolerite	8549.82
7	850	844	845.47975	0.14550	0.29100	5810.85736	780.36578	0.11296	785-850 Cascades Gp.	5192.93
8	875	869	870.43725	0.15150	0.30300	5745.46037	845.39590	0.14549	850-875 Liffey Gp.	4161.98
9	973	967	968.29179	0.17400	0.34800	5564.89637	870.16088	0.15145	875-973 Bundella	4362.07

Figure 5.6: Schematic of the set up of the Hunterston 1 DDH velocity survey.

Shots were taken at varying intervals in the drill hole to best ascertain the velocities across and within the formations identified in the Hunterston 1 DDH. Nine shots were taken in all. Shot 1 was taken to ascertain the velocity of the weathering layer, shot 2 for the velocity in the Upper Marine Sequence (Ferntree Formation), shots 3-6 to ascertain the variation in velocity variation in the Jurassic Dolerite, shot 7, 8 and 9 to ascertain the velocity of the

Upper Marine Sequence (Cascades Group), Lower Freshwater Sequence (Liffey Group) and the Lower Marine Sequence (Bundella Mudstone correlate) respectively (Figure 5.6).

Interpretation

The critical data recorded was the arrival times or first breaks, which represent the time taken for the seismic energy to move via the shortest distance from source to receiver through the earth (one-way time). The first breaks for this data set are troughs, the times are picked as the first negative deflection of the signal into the first large trough of the seismic record (Figure 5.7).

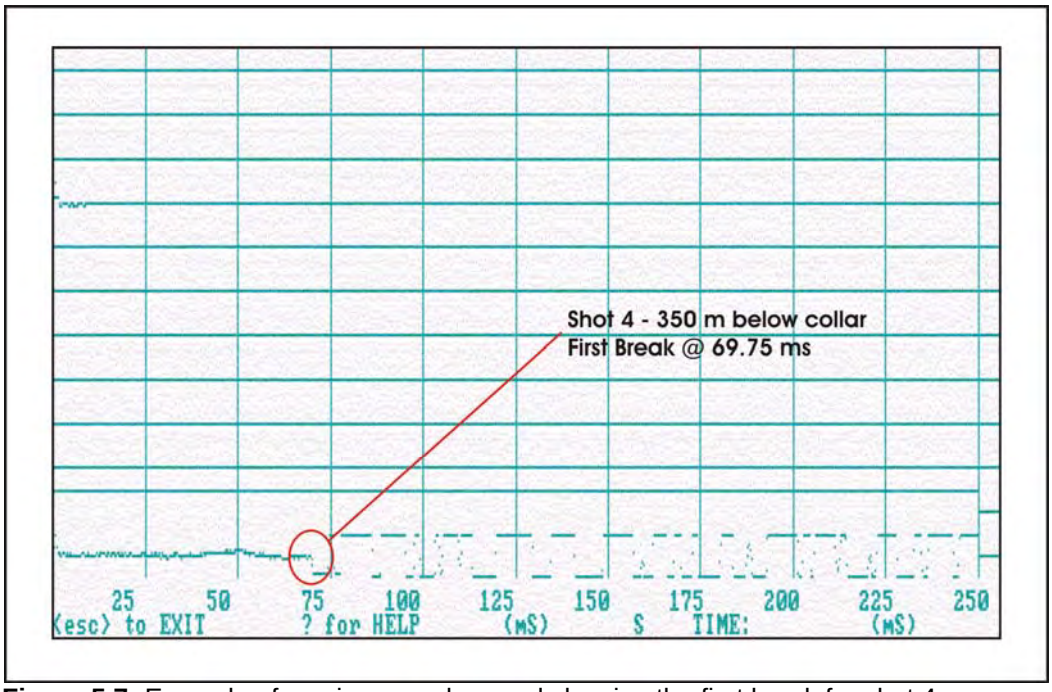

Figure 5.7: Example of a seismograph record showing the first break for shot 4.

The relationships between velocity, distance and time are summarised by the equation:

$v=d/t$ v = velocity (m/s), d = distance (m) and t = time (seconds),

where time is given by the first break, distance is the distance down hole from the surface or from the last measurement.

Cumulative velocity is calculated by adding the times and distances down hole and applying them to the equation. To calculate the interval velocity, the times and distances that apply all of the preceding intervals need to be subtracted from the interval under consideration, in order that the velocity for the interval is calculated using only the time taken and distance covered by the seismic energy in that particular interval.

Results

The average velocities of the rocks of the Tasmania Basin have been calculated using the results of the velocity survey (Table 5.4). These results compare favourably with the velocity estimates of Leaman (1996) (Table 5.3).

Two interesting features are observed in the data. Firstly, that there is a considerable variation in velocity within the Jurassic dolerite, this variation was explored by Fournier (2000) who found that coarse-grained dolerite was slower (~6200 m/s) than finer grained varieties. Secondly, that the velocity of the Cascades Formation in this drill hole was considerably higher than other Permian strata. However, this unit is in contact with dolerite and metamorphosed for about 30 m (Reid et al., 2003). The contact metamorphism contributes to this result.

Hunterston 1 DDH - Velocity Survey Results										
Collar Height: 5m Distance Collar-Source: 50m Elevation difference well-source: -1m										
Shot	**Depth from Collar (m)**	**Depth below ground level (m) (referenced to source)**	**Distance shot-geophone (m)**	**1-way time (sec)**	**2-way time (sec)**	**Shot-geophone cumulative velocity**	**Distance difference (cumulative)**	**Time difference (cumulative)**	**Interval**	**Interval Velocity**
1	25	19	53.48832	0.01700	0.03400	3146.37176	0.00000	0.00000	0-25 Weathered Layer	3146
2	135	129	138.35100	0.03525	0.07050	3924.85115	20.37728	0.00648	25-135 Ferntree Formation	4100
3	155	149	157.16552	0.03875	0.07750	4055.88433	136.06948	0.03467	135-155 Top Dolerite	5169
4	350	344	347.61473	0.06975	0.13950	4983.72372	150.56522	0.03712	155-350 Intra-Dolerite 1	6039
5	550	544	546.29296	0.09725	0.19450	5617.40835	345.44996	0.06932	350-550 Intra-Dolerite 2	7190
6	785	779	780.60297	0.13300	0.26600	5869.19528	545.11941	0.09704	550-785 Base Dolerite	6549
7	850	844	845.47975	0.14550	0.29100	5810.85736	780.36578	0.13296	785-850 Cascades Gp	5192
8	875	869	870.43725	0.15150	0.30300	5745.46037	845.39590	0.14549	850-875 Liffey Gp	4164
9	973	967	968.29179	0.17400	0.34800	5564.89537	870.16088	0.15145	875-973 Bundella	4352
Average velocity (Dolerite) = 6237 m/s **(6250 m/s)** Average velocity (Parmeener) = 4452 m/s **(4500 m/s)** Average velocity (Weathered Rocks) = 3146 m/s **(3150 m/s)**										

Table 5.4: Hunterston 1 velocity survey results.

5.4.3: REGIONAL GRAVITY DATA

The TB01 survey area is covered by several generations of gravity data (Figure 5.8). The spacing of the gravity stations and the variable basement lithology means the data is not suitable for mapping the depth, extent or structures in the sedimentary sequence. However, the dataset has proven useful in estimating changes in the thicknesses of dolerite. This has been achieved by locating an area where the thickness can be accurately predicted, calculating the change in gravity across a boundary between the known and unknown thickness of dolerite and modelling the change across the boundary to give an estimate the thickness change. Figure 5.9 shows a section of seismic line where dolerite is mapped at the surface and where there is a marked change in the gravity data (Figure 5.9, A). The gravity data shows the dolerite appears to be thickening to the west, which can be reliably interpreted on the western half of the section shown in Figure 5.9, B. Figure 5.9, C shows readings from the gravity stations on either side of the boundary, the difference between these readings is 3.15 mgal. This difference is then modelled using Potent software, using a 10 x 10 km domain, with a density of 2.9 t/m^3 for dolerite in a background body with a density of 2.5 t/m^3 simulating the Parmeener Supergroup. For this model a gravity reading of 3.15 mgal (Figure 5.9, D) requires a thickness of 190 m of dolerite. Therefore, a thickness change of about 200 m is interpreted on the seismic section (Figure 5.9, B).

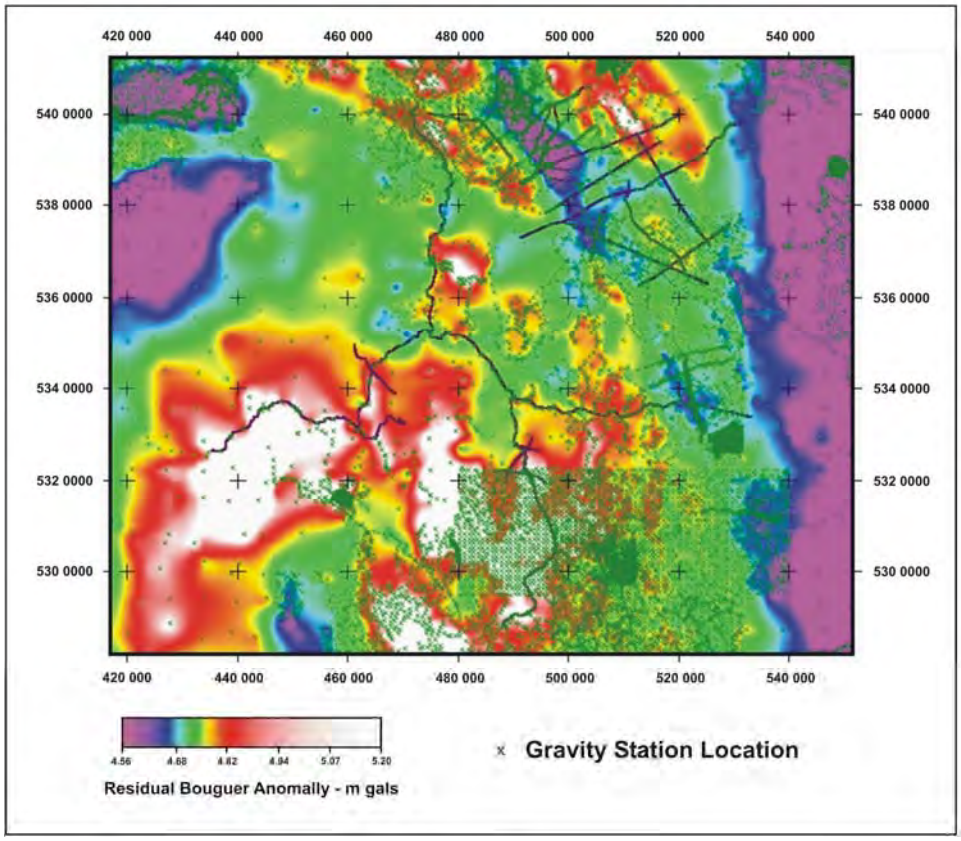

Figure 5.8: Gravity station location in the TB01 survey area.

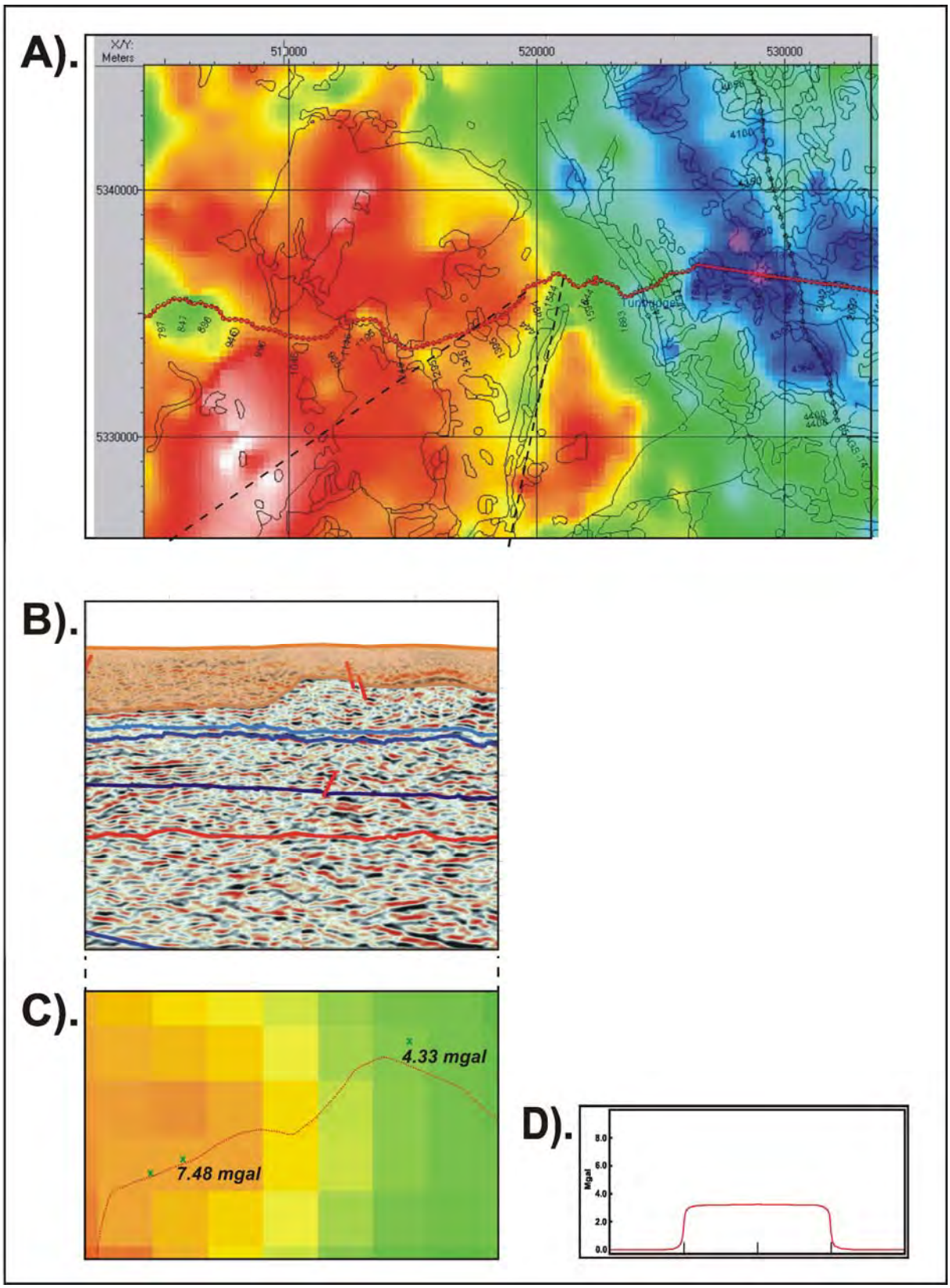

Figure 5.9: Modelling variations in the measured gravity field to predict thickness changes in dolerite sills.

5.5: SEISMIC STRATIGRAPHY, NOMENCLATURE, HORIZON AND FAULT PICKS

5.5.1: INTRODUCTION

The stratigraphic nomenclature found on geologic maps and in literature used to describe the rocks of the Parmeener Supergroup and basement units is generally inconsistent across the survey area; this is especially true of the Parmeener Supergroup. A confusing proliferation of stratigraphic names has resulted from different authors giving rock units different names in different locations across the basin. Therefore, a simplified stratigraphic nomenclature has been devised for the seismic interpretation (Figure 5.10). This working stratigraphy generally follows the stratigraphic nomenclature used in 1:250 000 scale geologic mapping. The system is broad enough to include all the rock units of the Parmeener Supergroup, while having sufficient resolution to identify the relative timing of events. The working stratigraphy used for the basement is extremely simple, because no drilling sufficiently penetrates the basement to allow an accurate stratigraphy to be interpreted. Seismic-stratigraphic events are indicated on the interpreted sections by coloured lines that unless otherwise stated corresponding to the top of a stratigraphic unit (Figure 5.10).

The variation in quality of the seismic data set means that there are no marker horizons and few coherent events that can be followed over much distance on any of the seismic lines. The discontinuous nature of reflections in this dataset often means it is difficult to identify stratigraphic boundaries by character or away from constraining drill hole or outcrop data. When interpreting in zones away from stratigraphic control, the position of a stratigraphic boundary is generally estimated by using thicknesses determined from the closest drill hole, outcrop or confident seismic interpretation referenced to reliably identifiable events, such as the Base Parmeener Unconformity. If the data is so poor that no seismic events can be recognised then the interpretation is advanced across these areas by extrapolating from either better quality data or from areas that are more constrained by outcrop of well data. Other stratigraphic boundaries are identified in the seismic record by changes in character, such as the upper and lower boundaries of the dolerite.

Seismic Stratigraphy

QUATERNARY

- Undifferentiated Quaternary (Q).
- Sand, gravel and mud (Qh).
- Glacial, periglacial and fluvial sediments including till and interglacial deposits (Qp).
- Talus, fan and slope deposits (Qpt).
- Glacial and glaciogene deposits (Qpg).

TERTIARY

- Basalt (Tb).
- Laterite (Tf).
- Non-marine sequences of gravel, sand, silt and clay (Ts).
- Base Tertiary Unconformity.

JURASSIC

- Top Dolerite (tJd).
- Base Dolerite (bJd).

LATE CARBONIFEROUS - TRIASSIC

- Upper/Lower Parmeener Supergroup boundary.
- Unit 4 (TRvc).
- Unit 3 (TRvv).
- Intra Unit 2 Horizon.
- Unit 2 (TRq).
- Unit 1 (Pc).
- Upper Marine Sequence (Pu).
- Malbina Formation
- Cascades Formation
- Lower Freshwater Sequence (Pf).
- Conglomeratic Beds (Hunterston 1 DDH).
- Lower Marine Sequence and Tasmanites Oil Shale (Pl).
- Base Bundella Mudstone.
- Tillite (Pt).
- Base Parmeener Unconformity

PRE - LATE CARBONIFEROUS

- Undifferentiated Basement Events
- Bellevue Antiform - Hanging wall
- Bellevue Antiform - Footwall

Faults

POST - JURASSIC (POST - DOLERITE)

- Later Tertiary
- Early Tertiary
- Undifferentiated Tertiary

PRE - JURASSIC (PRE - DOLERITE)

- Not Intruded - Normal
- Not Intruded - Reverse
- Intruded - Normal
- Intruded - Reverse

- Indeterminate

Figure 5.10: Seismic stratigraphy and nomenclature

At the top of each seismic section, a zone of incoherent data bounded at its base by a series of high amplitude, low frequency reflections is common (Figure 5.11). It is not clear what causes these; however, the data becomes coherent directly below these strong reflections. There is no evidence that these first high amplitude events are related to geological reflections as they occur consistently across the sections regardless of the lithology or structure present at surface (Figure 5.11).

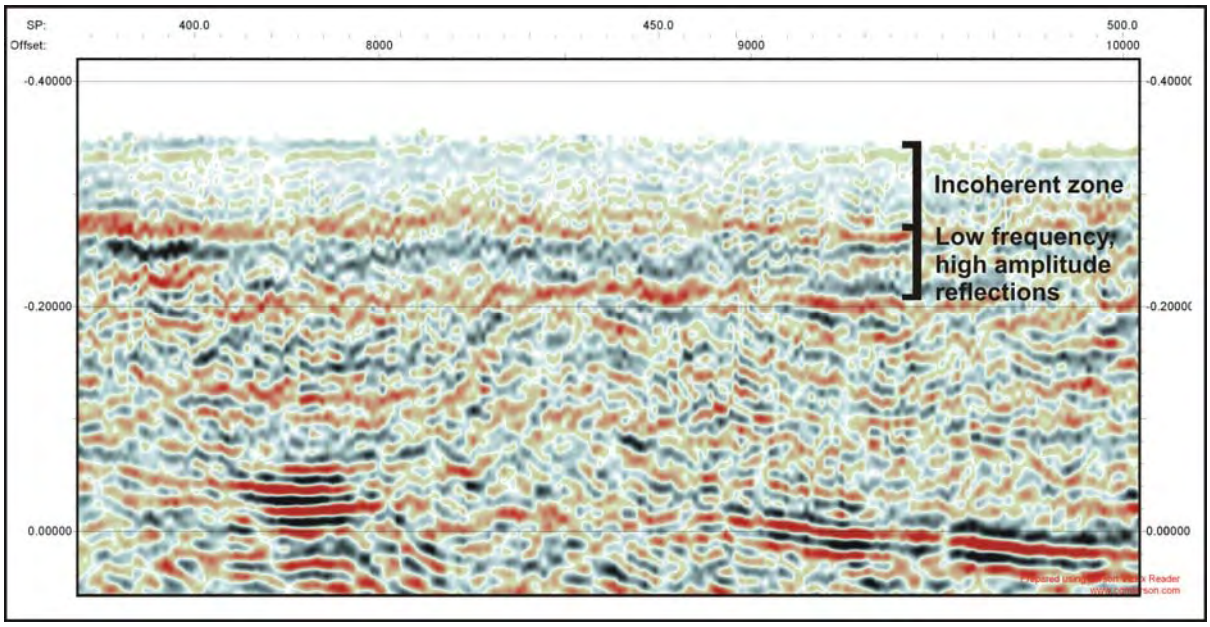

Figure 5.11: Example of the zone of incoherent, low frequency, high amplitude data that typically occurs at the top of most sections.

5.5.2: QUATERNARY SEISMIC STRATIGRAPHY

Quaternary rocks and sediments occur as cover sequences over many parts of the survey area. They are generally unrelated to structure, but have been picked mainly as an aid to locate positions on a line.

5.5.3: TERTIARY SEISMIC STRATIGRAPHY

Four horizons are interpreted (Figure 5.10), three are in the cover sequence and the fourth is the unconformity surface at the base of the Tertiary sedimentary sequence. The Tertiary sedimentary sequence is seen only in the lines that were acquired across the Launceston Tertiary Basin (Figure 2.11). The character of the unconformity surface highlights the geometry and timing of structures in the Parmeener Supergroup sequences in the area. Only lines TB01- PT, PG, PU, PM and PW (Map 5.1) that are acquired roughly perpendicular to the strike of these structures, have been included in this interpretation.

The Base Tertiary Unconformity Horizon is interpreted at a significant change in seismic character. The Tertiary sequence is identified by a series of coherent events at top of the section. The unconformity surface is picked at a strong negative event (trough, red) at the base of these coherent events. The horizon is indicated by a violet coloured line (Figure 5.12).

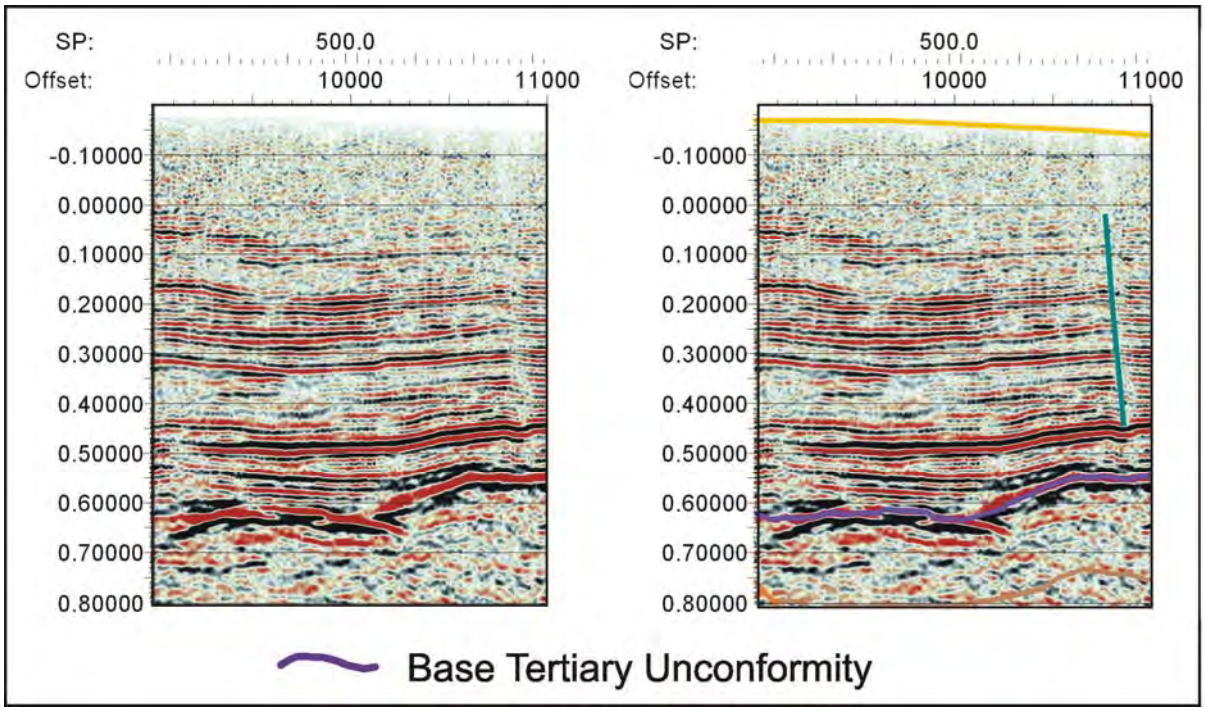

Figure 5.12: An example of the Base Tertiary Unconformity Horizon pick (TB01-PM).

5.5.4: JURASSIC DOLERITE SEISMIC STRATIGRAPHY

Jurassic Dolerite is seen on all of the interpreted lines of the TB01 Survey, either as outcrop or as a thick sill at depth. The Top Dolerite Horizon is picked at the last strong positive reflection (peak, black) that overlies a zone of incoherent, low amplitude reflections. This horizon is indicated by an orange coloured line on the interpreted sections (Figure 5.13). The Base Dolerite Horizon is interpreted at a negative to positive zero-crossing event at the base of the zone of incoherent reflections; this is often underlain by a series of coherent seismic reflections. On the interpreted sections, a brown coloured line indicates the Base Dolerite horizon (Figure 5.13). The position of the Top and Base Dolerite horizons calculated using velocity and depth data acquired in the Hunterston 1 DDH, correlate well with the character based picks on the adjacent TB01-PA (Figure 5.14).

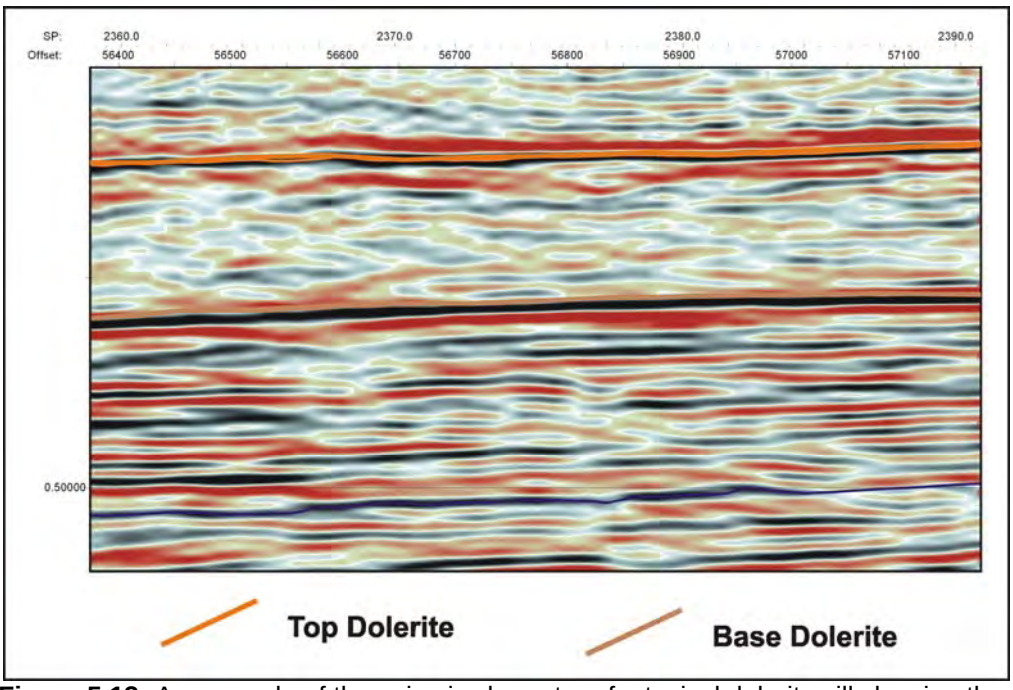

Figure 5.13: An example of the seismic character of a typical dolerite sill showing the Top and Base Dolerite Horizon picks (TB01-ST).

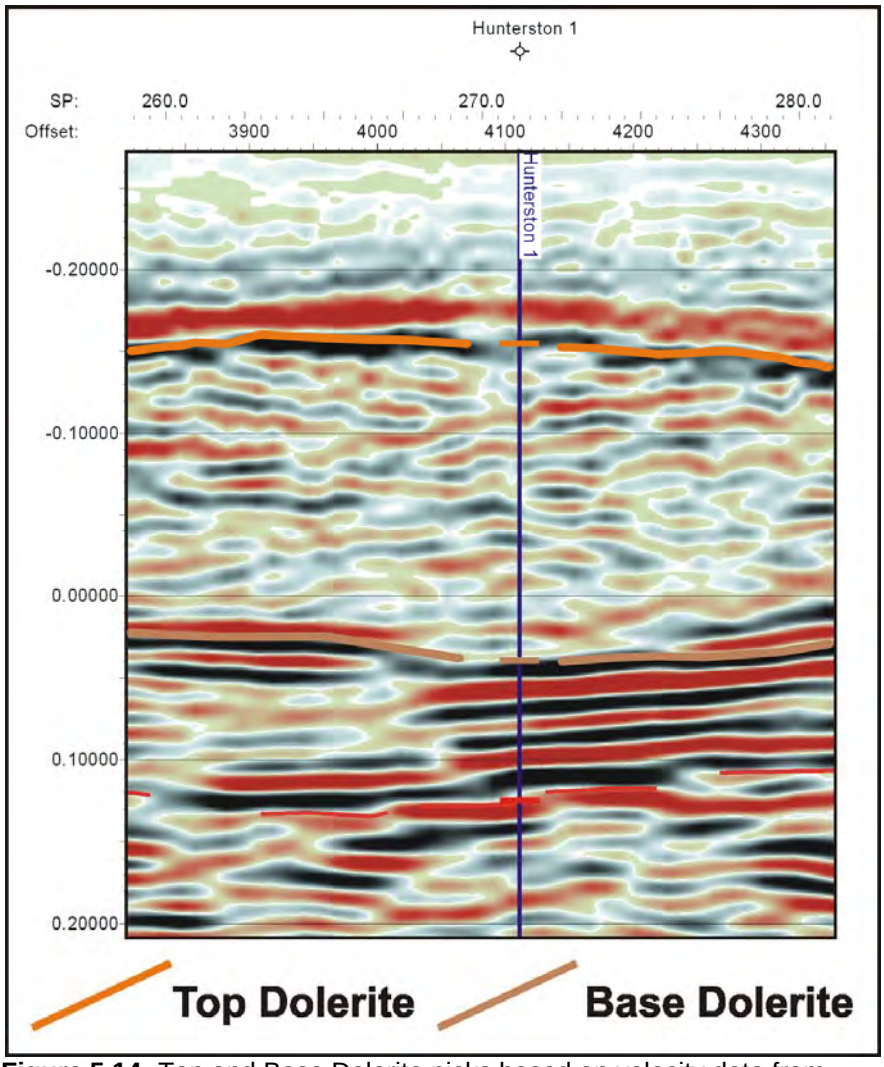

Figure 5.14: Top and Base Dolerite picks based on velocity data from Hunterston 1, correlate well with the character based picks (TB01-PA).

5.5.5: LATE CARBONIFEROUS TO TRIASSIC (PARMEENER SUPERGROUP) SEISMIC STRATIGRAPHY

Unit 4

The youngest unit interpreted within the seismic sections is Unit 4, which is identified in 1: 250 000 scale mapping between shot-points 3525 – 3650 on the western end of line TB01-PB. The unit is only identified where it outcrops; it has not been interpreted within any of the sections. A light green line at the top of the section (Figure 5.10) indicates outcropping Unit 4.

Unit 2

The Top Unit 2 Horizon is interpreted near or at the top of the section where it is often truncated by dolerite. The unit is interpreted on lines TB01-TH as outcrop, while at the western end of line TB01-PB and the eastern end of line TB01-ST the horizon is interpreted near the top of the section. The horizon is picked on a positive event (peak, black), and indicated by a dark green line on the interpreted section (Figure 5.15). A coherent reflection rarely defines this horizon and its position above the Upper Marine Sequence horizon is generally based on estimates of its thickness from drill holes and outcrop.

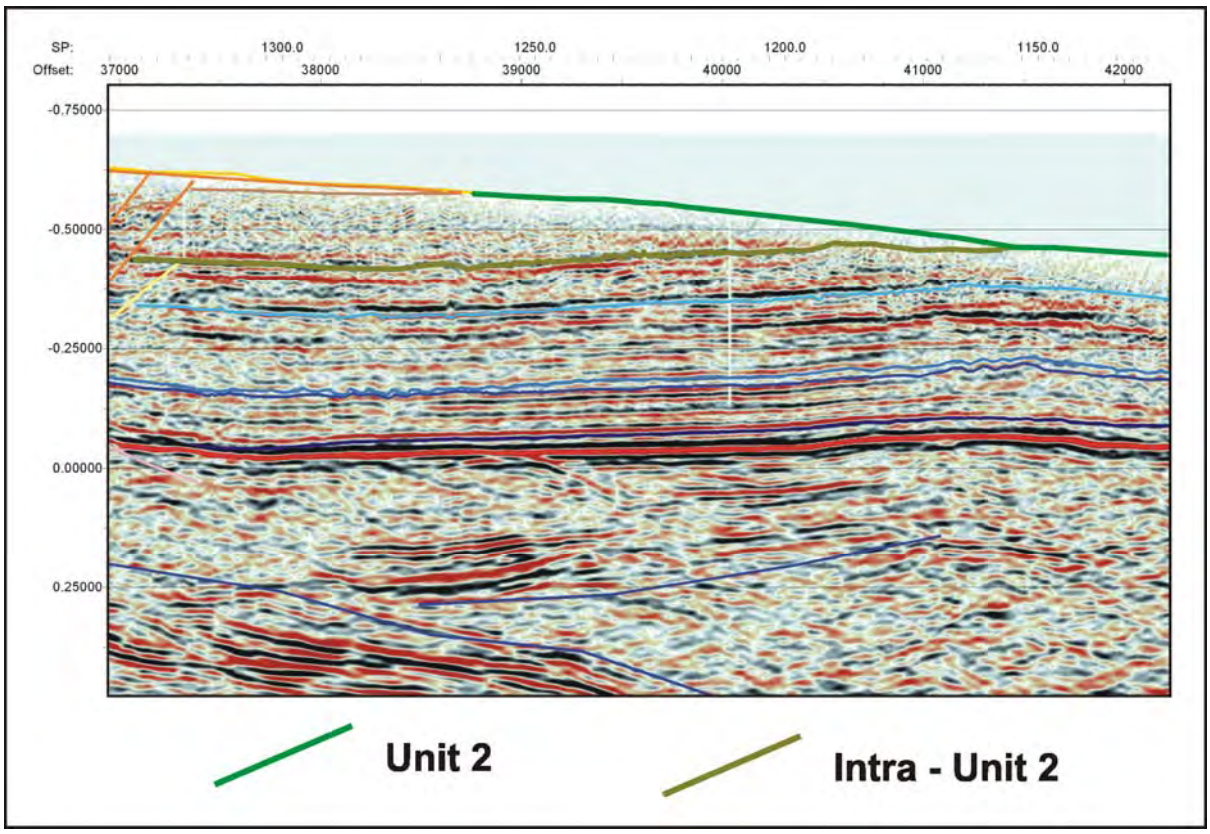

Figure 5.15: Examples of the Top Unit 2 and the Intra-Unit 2 horizon picks (TB01-TH).

A strong Intra Unit 2 reflection is identified on the northern end of line TB01-TH (Figure 5.15). This horizon is picked on a distinctive positive event (peak, black) that can be followed with confidence over 5-6 line kilometres. The horizon is a useful marker as reflections below are generally less coherent and more difficult to follow.

Upper Marine Sequence

The Upper Marine Sequence is seen in drill holes and outcrop through out the survey area. The horizon is interpreted on most lines in the Central Highlands and on line TB01-ST. As the unit generally lies at or close to the surface, the top of the formation is not seen in any of the constraining drill holes, however the base is recognised in a number of the holes (Figure 5.3), and its thickness can often be determined from nearby mapped outcrop. The interpreted top of the formation generally occurs near the top of the section or in close proximity to dolerite that is at the top of the section, consequently the reflection representing the top Upper Marine Sequence horizon is often poorly defined. The Top Upper Marine Sequence Horizon is picked on a negative event (trough, red), and indicated on the interpreted section by a light blue line (Figure 5.16). Generally, the position of the horizon is based on estimations of formation thickness rather than from an obvious change in the seismic character.

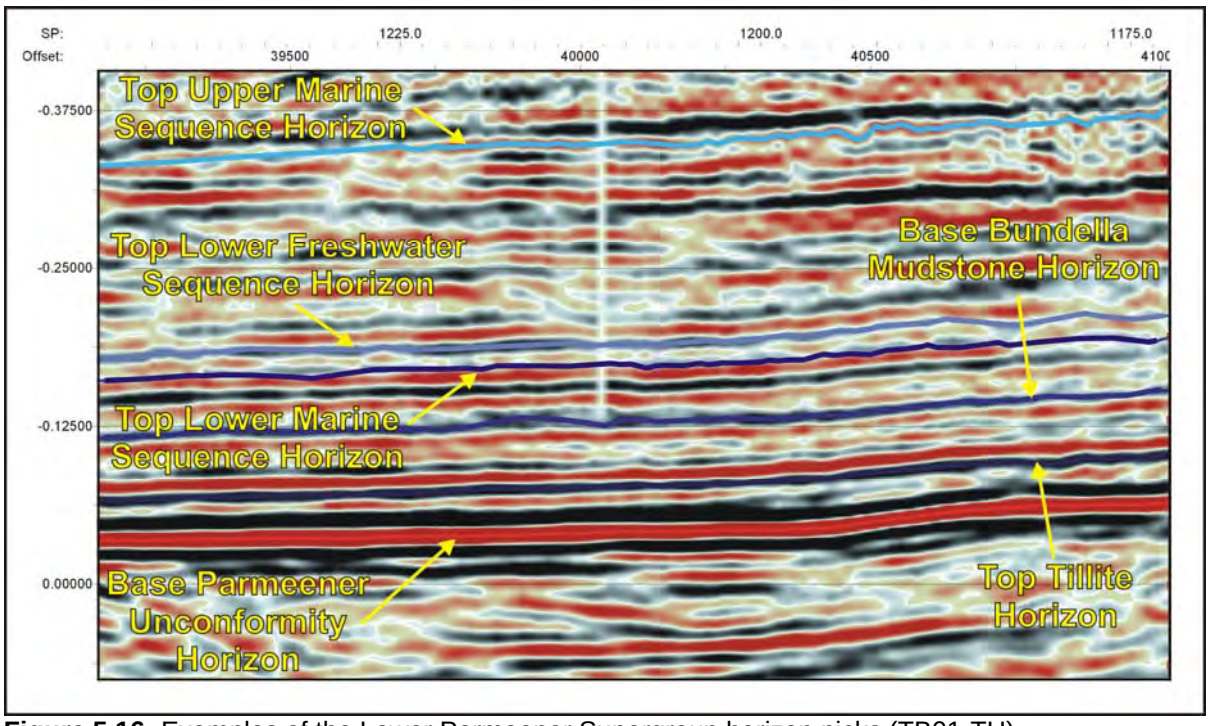

Figure 5.16: Examples of the Lower Parmeener Supergroup horizon picks (TB01-TH).

Cascades Formation

The Cascades Formation does not fall into the nomenclature defined by 1:250 000 scale geological mapping and is not identified by any mapping in the western part of the survey area. However, the unit is identified in the Hunterston 1 DDH (Reid et al., 2003) and in the MPT 1 drill hole at Dungrove (Williams, 1985) and correlates (Poatina Group) are identified in the RG-145 (Forsyth et al., 1989) and the GV1 (Clarke, 1967) drill holes (Figure 5.3). The stratigraphic control makes the unit a useful a reference point within the Upper Marine Sequence aiding the accuracy of the interpretation. The unit has been interpreted on lines TB01-ST, PA, PD, TD and on line TB01-PB south of the intersection with line TB01-ST. The Top Cascades Formation Horizon pick is based on its calculated position in the Hunterston and RG-145 (Tunbridge) drill holes. The horizon is picked at a positive event (peak, black), and indicated by a violet-red line in the interpreted section (Figure 5.17). The position of the horizon away from well control is estimated by thickness rather than based on seismic character.

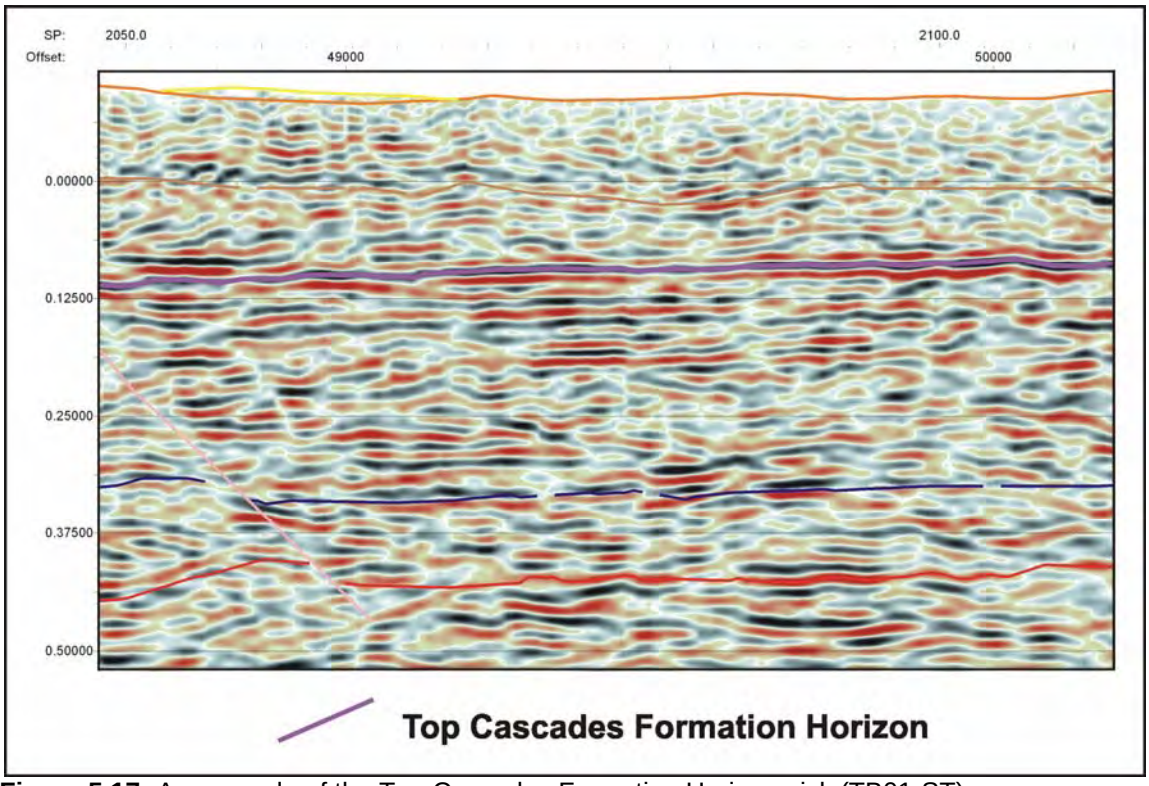

Figure 5.17: An example of the Top Cascades Formation Horizon pick (TB01-ST).

Lower Freshwater Sequence

The Lower Freshwater Sequence is mapped and observed in all the drill holes used for correlation in the TB01 Survey area (Figure 5.3). While the unit is thin, the top of the formation is well constrained by drill hole data (Figure 5.3), while the thickness is generally

consistent, approximately 25 m in the Central Highlands and 38 m in the Northern Midlands. The interpreted position of the horizon in the sections is based on its position relative to other units in the Hunterston 1 and RG-145 (Tunbridge) drill holes. The Top Lower Freshwater Sequence Horizon is picked on a strong positive event (peak, black) and indicated by a blue line in the interpreted section (Figure 5.16).

Lower Marine Sequence

The Lower Marine Sequence is recognised in all the drill holes used to constrain the interpretation (Figure 5.3) and on 1:250 000 scale geological mapping across the entire survey area. The Top Lower Marine Sequence Horizon is picked at a positive to negative (black to red) zero-crossing event and indicated by blue line on the interpreted section (Figure 5.16). This horizon is generally picked using thickness estimates rather than on distinctive character changes. The thickness of the unit is estimated from mapped outcrop in the west and north, and from drill hole data in the east of the survey area.

Base Bundella Mudstone

Correlates of the Bundella Mudstone are recognised in all the constraining drill holes (Figure 5.3). The unit is not identified by mapping at 1:250 000 scale and not identified in smaller scale mapping in the western part of the TB01 survey area. The base of the formation is indicated where there is sufficient constraining data and provides a useful reference point within the Lower Marine Sequence. The base of the formation is indicated rather than the top, as the top would be coincident with the Top Lower Marine Sequence Horizon. The horizon is picked on a positive event (peak, black), indicated by a dark blue line in the interpreted section (Figure 5.16).

Tillite

The Tillite is mapped at the base of the escarpments in the east, west and north and is present in drill holes in the east and north of the survey area. The Top Tillite Horizon is picked at a positive event (peak, black) and indicated on the interpreted sections as a dark blue line (Figure 5.16). In the absence of constraining data the position of the horizon is based on the estimates of thickness of the overlying Lower Marine Sequence.

Base Parmeener Unconformity

The unconformity surface at the base of Parmeener Supergroup is generally identified by an interface between flat-lying reflections (Parmeener Supergroup) and underlying dipping

reflections associated with basement rocks. Where the basement rocks appear to be flat-lying, the horizon can usually be identified by differences in seismic character. The horizon is picked on the first negative (trough, red) reflection above the dipping events or character change and is indicated on the interpreted sections by a red line (Figure 5.16).

Basement

The basement units underlying the Tasmania Basin form part of a fold-thrust belt. Tectonic transportation from the northeast has resulted in structures that strike towards the northwest and north-northwest, with thrust sheets that dip towards the northeast. Examples of basement structure are observed around the margins of the basin in areas where these units outcrop. The most prominent of these areas are the Florentine Valley in the south, the Dazzler Range and Deloraine to Mole Creek in the north, and west of Mount King William. The rocks in these areas are generally highly faulted and steeply dipping, where seismic data is available over these areas it does not reflect the structure seen in outcrop, raising doubt as to how accurately complex basement structures are being imaged by the seismic.

The interpretation of seismic data corresponding to the basement has been divided into Undifferentiated Basement Events and the Bellevue Anticline (footwall and hanging wall). Both sets of events are essentially undifferentiated as the stratigraphic arrangement of basement below the Tasmania Basin is unclear, the Bellevue Anticline is a faulted antiform and is singled out because it has been flagged as a possible exploration target.

Undifferentiated Basement Events are indicated on the sections by a dark blue line (Figure 5.10). These events have been interpreted at marked changes in seismic character (Figure 5.18). Consideration must be given during interpretation to the difference in orientation of the seismic lines (or segments of lines) and the orientation of the basement structure. The best data and therefore the more confident interpretation is restricted to straighter lines striking towards the northeast, i.e. dip parallel. The reflections generally dip northeast to east, and the seismic event picked are probably attributable to changes in lithology, either between thrust sheets or within them (i.e. thrust faults). However, deeper in the section where the data is poorer the interpretation of these events is much more tenuous.

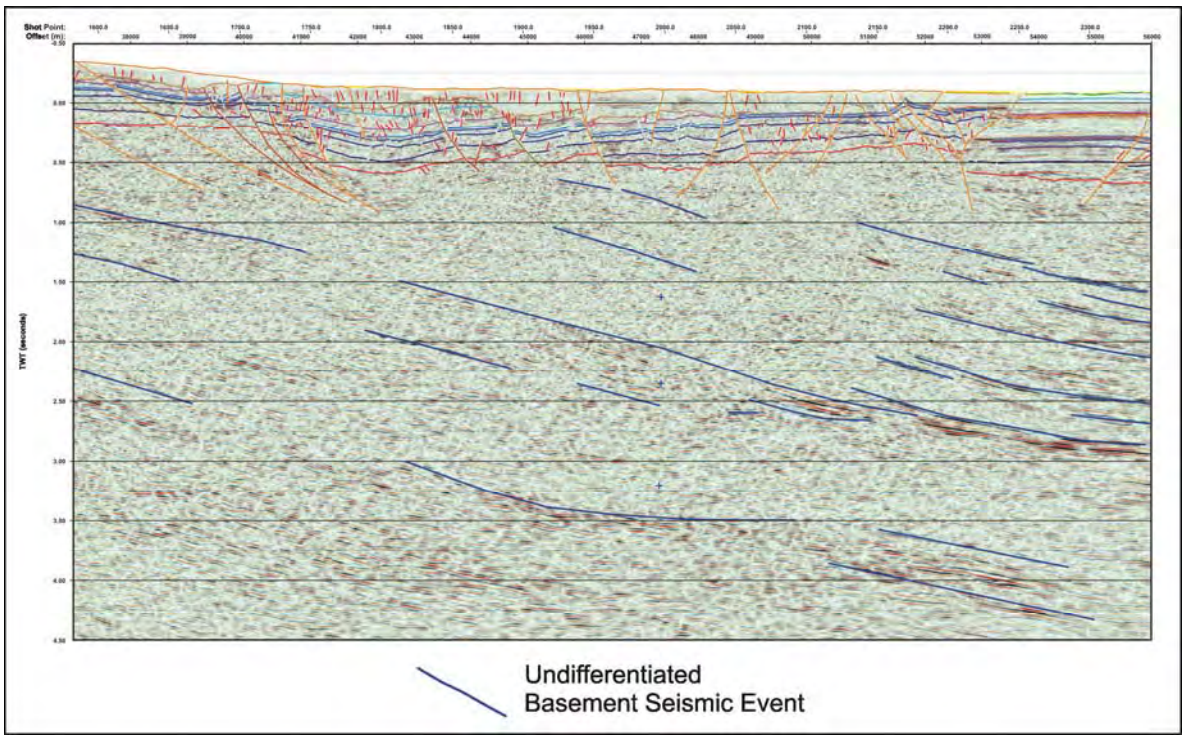

Figure 5.18: Examples of Undifferentiated Basement Seismic Events (TB01-ST).

A faulted antiform is recognised on the western side of the survey area, mainly on line TB01-PB near the Bellevue Tiers (Figure 5.19). The "Bellevue Antiform" is defined by changes in seismic character. The hanging wall of the structure is indicated on the interpreted section by medium blue lines, while green-blue lines define the footwall of the structure (Figure 5.10).

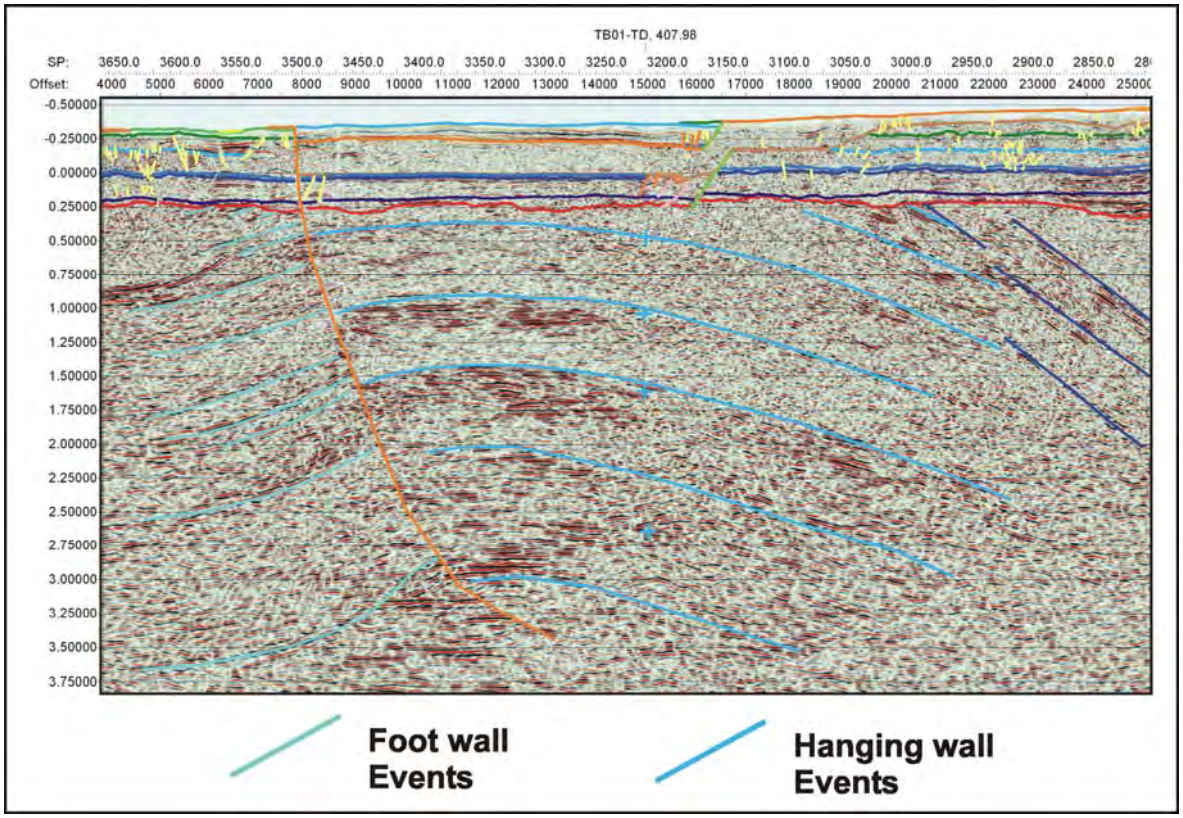

Figure 5.19: Basement events associated with the Bellevue Anticline (TB01-PB).

5.5.6: FAULTS

Problems similar to those encountered while interpreting stratigraphic events, which arose from the variability of the seismic data, affect the interpretation of faults. The lack of coherency and the often diffuse nature of the reflections may either disguise faults or conversely, indicate faults that may not exist. Primary evidence for faulting is distinctive displacement of reflections (picked horizons). The best horizons with which to pick displacement, or offsets, were the Base Parmeener Supergroup Unconformity and the Top and Base Dolerite horizons, as these are generally the most confidently picked horizons across the survey. Often where the offsets are subtle or the data quality poor, secondary evidence was used to prove the existence of a fault. Geological mapping already identifies the position of many of the faults and other evidence to support the interpretation of a fault was found in gravity data and the DEM.

Dolerite sills are the most easily identifiable unit in the Parmeener Supergroup section and displacements related to faulting are most easily identified where they affect dolerite. The nomenclature chosen to describe the faults interpreted in this section is broadly divided into two major classes, pre- and post-Jurassic (pre- and post-dolerite) (Figure 5.10). These are sub-divided further. The Post-Jurassic class is divided into Later, Early and Undifferentiated Tertiary Faults (Figure 5.10). These faults generally displace dolerite, and are interpreted to have resulted from latest Cretaceous to early Tertiary extension. Some faults interpreted in this class (particularly Undifferentiated Tertiary Faults) do not displace dolerite, but due to their proximity and genetic relationship to major post-Jurassic faults, are included. Pre-Jurassic Faults are divided into normal and reverse faults, which are either intruded or not intruded by dolerite. The timing of the intruded faults is clear, while evidence for the timing of the “not-intruded” faults is not always certain. Several “not intruded” reverse faults have been placed in this class because they occur low in the section and are interpreted to have resulted from pre-Jurassic compressional tectonics.

Post - Jurassic (Post – Dolerite) Faults

Movement on post-Jurassic faults is probably associated with extension in the early to middle Tertiary and many are likely to have been reactivated. Displacements in the Parmeener Supergroup, the Base Tertiary Unconformity Horizon and reflections within the Tertiary section aid in identifying faults in this class. This class is further subdivided, into Later Tertiary, Early Tertiary and Undifferentiated Tertiary Faults (Figure 5.10).

Later Tertiary Faults

Later Tertiary Faults are those, which affect only the Tertiary sequence and its base. This class of fault is only recognised in the Longford Sub-basin sections where thick Tertiary sequences occur. Both normal and reverse faults have been recognised. The vast majority of these faults are short, less than 500 m long in section, steeply dipping and have throws in the 10's of metres (Figure 5.20). Larger normal faults of this class are interpreted on line TB01-PG. Most of the larger faults are down to the northeast. On average, they are 1000 m long in section with throws of 200 m. One example, approximately 6000 m long (shot-point 1425), dips shallowly towards the northeast and displaces Tertiary, dolerite and Parmeener Supergroup sequences by 125 m (Figure 5.20).

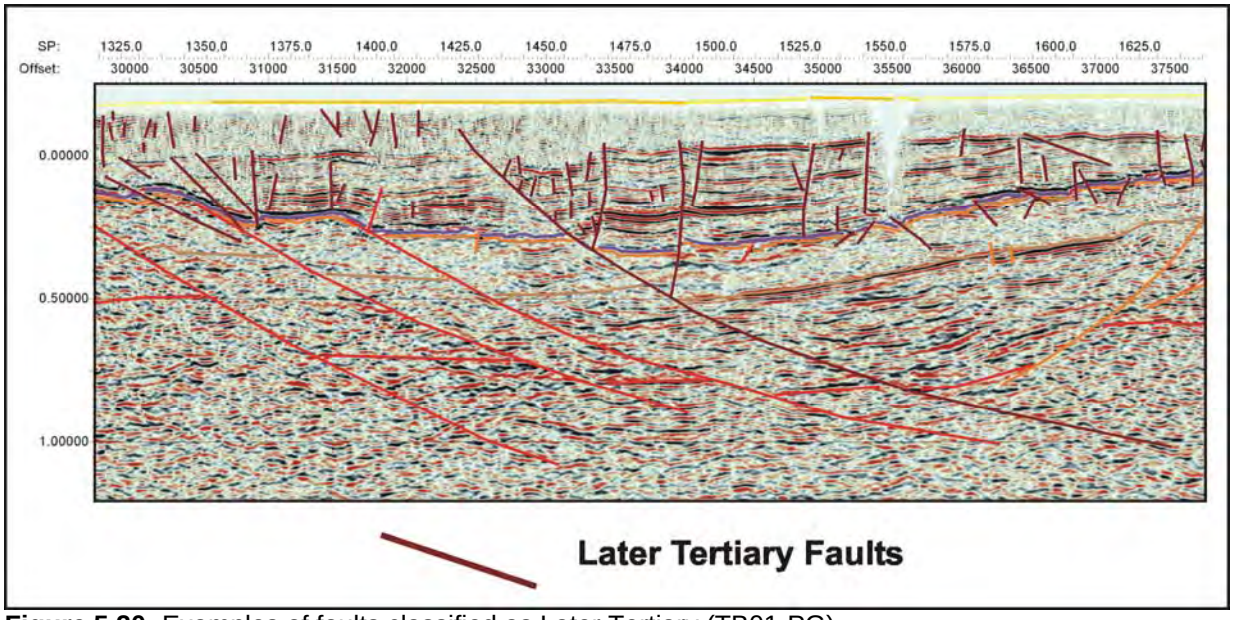

Figure 5.20: Examples of faults classified as Later Tertiary (TB01-PG).

A single, large reverse fault is interpreted at about shot-point 988 (TB01-PG). This fault is approximately 2000 m long with a throw of about 60 m (Figure 5.21). There are also numerous smaller reverse faults interpreted indicating compression, probably late in the Tertiary basins history. No growth is associated with these faults, indicating they were active after early deposition and after the Early Tertiary Faults, which exhibit growth. On the interpreted sections, a red-brown coloured line indicates these faults (Figure 5.10).

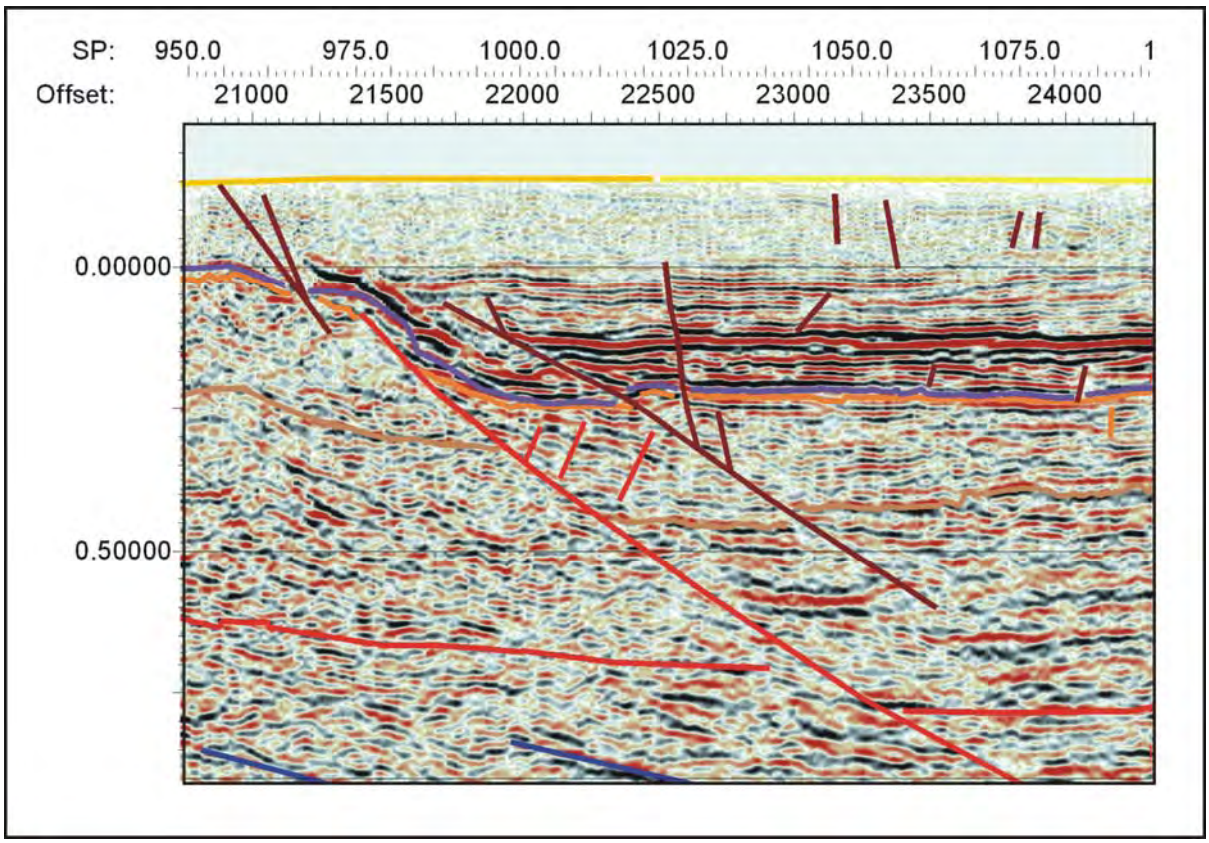

Figure 5.21: A Later Tertiary reverse fault is interpreted at shot-point 988 on TB01-PG.

Early Tertiary Faults

Early Tertiary Faults are all normal faults, which affect the Tertiary sequence, Jurassic Dolerite and the Parmeener Supergroup. This class of fault is only recognised in the Longford Sub-basin sections. These are significant structures, dipping towards the northeast, generally at low angles, affecting several kilometres of strata with throws averaging about 200 m (Figure 5.22). The basin bounding fault of the Tertiary sequence, which is recognised on several lines, has throws exceeding 1000 m (Figure 5.22). It is probable that many of these faults are extensions of reactivated basement structures. The early Tertiary faults are generally associated with growth in the basal part of the Tertiary sequence. These faults were likely produced by extension in latest Cretaceous to early Tertiary and are indicated by a red coloured line on the interpreted sections (Figure 5.10).

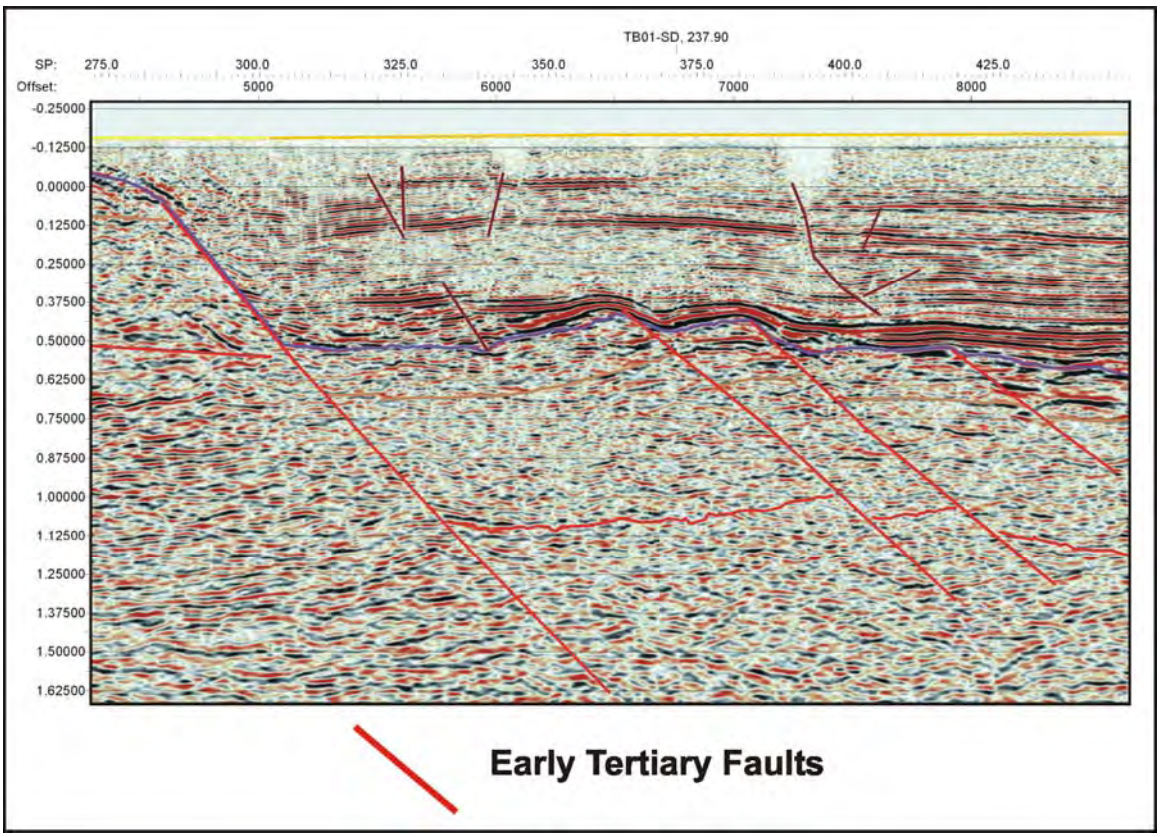

Figure 5.22: Examples of faults classified as Early Tertiary (TB01-PM).

Undifferentiated Tertiary Faults

The term Undifferentiated Tertiary Faults describes faults that offset Jurassic Dolerite and the Parmeener Supergroup and are interpreted in areas without Tertiary cover. Many faults in this class can be followed deep into the basement. They are most likely to have resulted from movement in the Tertiary. Many have similar geometry to the Tertiary faults described above, however, the lack of younger cover makes their timing more difficult to constrain.

Of all the faults interpreted, these are the most numerous. This class can be further subdivided based on relative size into small, medium and large faults. Small Undifferentiated Tertiary faults are less than 500 m long in section, with throws ranging from metres to a few 10's of metres. Small faults are interpreted mainly within or at the boundaries of dolerite sills (Figure 5.23). Medium Undifferentiated Tertiary faults with normal and reverse movement are interpreted in about equal numbers. These faults can be up to 2000 m long in section (Figure 5.24). They are common in the Tasmania Basin sequence in the Central Highlands region, especially near Hunterston. Normal faults dip between 42° and 88° (65° av.) with throws up to 20 m, while reverse faults have dips ranging from 46° to 88° (68° av.) and throws up to 50 m. Many medium sized faults have a synthetic or antithetic relationship with large faults (Figure 5.25).

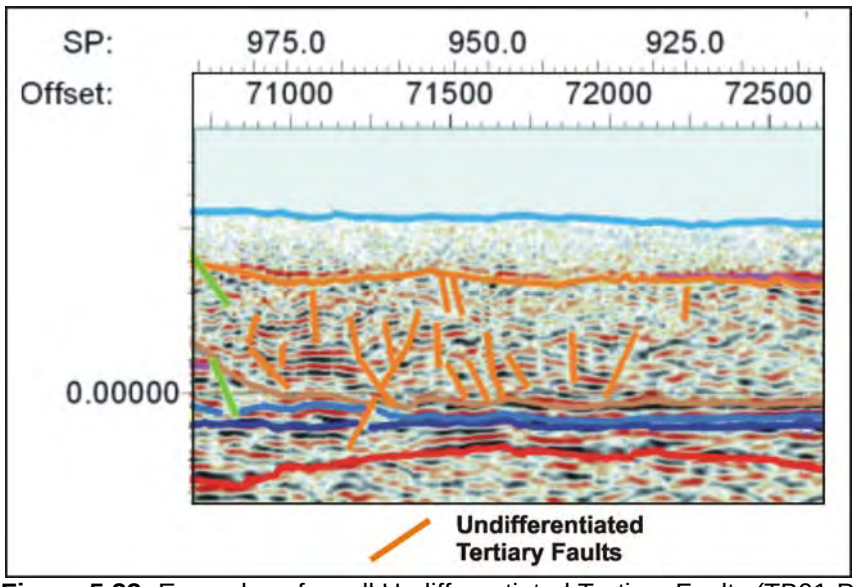

Figure 5.23: Examples of small Undifferentiated Tertiary Faults (TB01-PB).

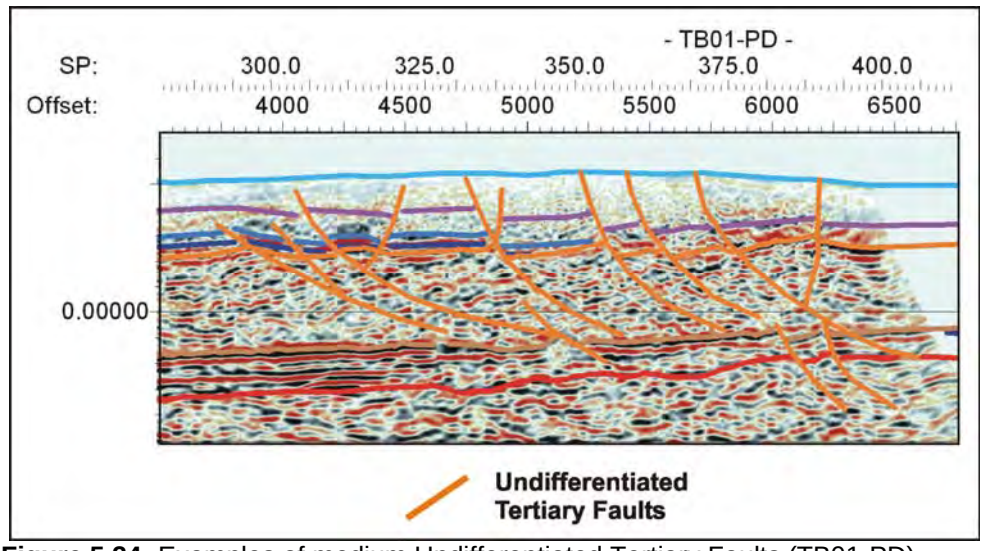

Figure 5.24: Examples of medium Undifferentiated Tertiary Faults (TB01-PD).

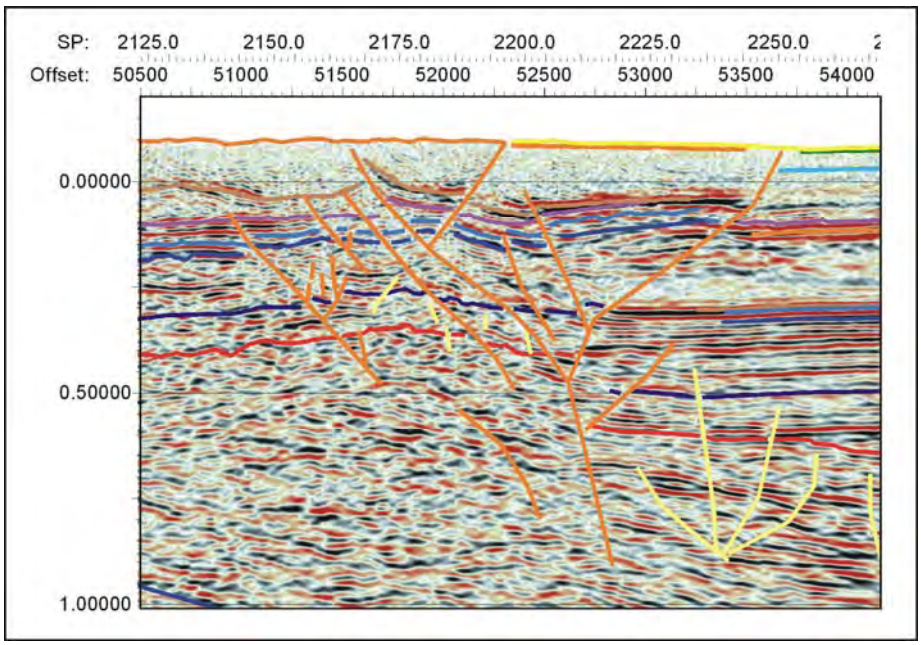

Figure 5.25: Synthetic and antithetic, medium Undifferentiated Tertiary Faults (TB01-ST).

Large Undifferentiated Tertiary faults are mainly normal, though many reverse faults were also observed. These faults range up to 4500 m in length and penetrate into the basement (Figure 5.26). Many of the normal faults probably formed as extensions of basement faults reactivated during Tertiary extension. Reverse faults may result from Late Tertiary compression. Normal faults dip between 28° and 74° (50° av.) with throws from 5 m to 450 m, while reverse faults have dips ranging from 20° to 70° (42° av.) and throws up to 200 m. These faults are interpreted in both the Central Highlands and the Northern Midlands/Longford Sub-basin regions. On the interpreted sections, an orange coloured line indicates these faults (Figure 5.10).

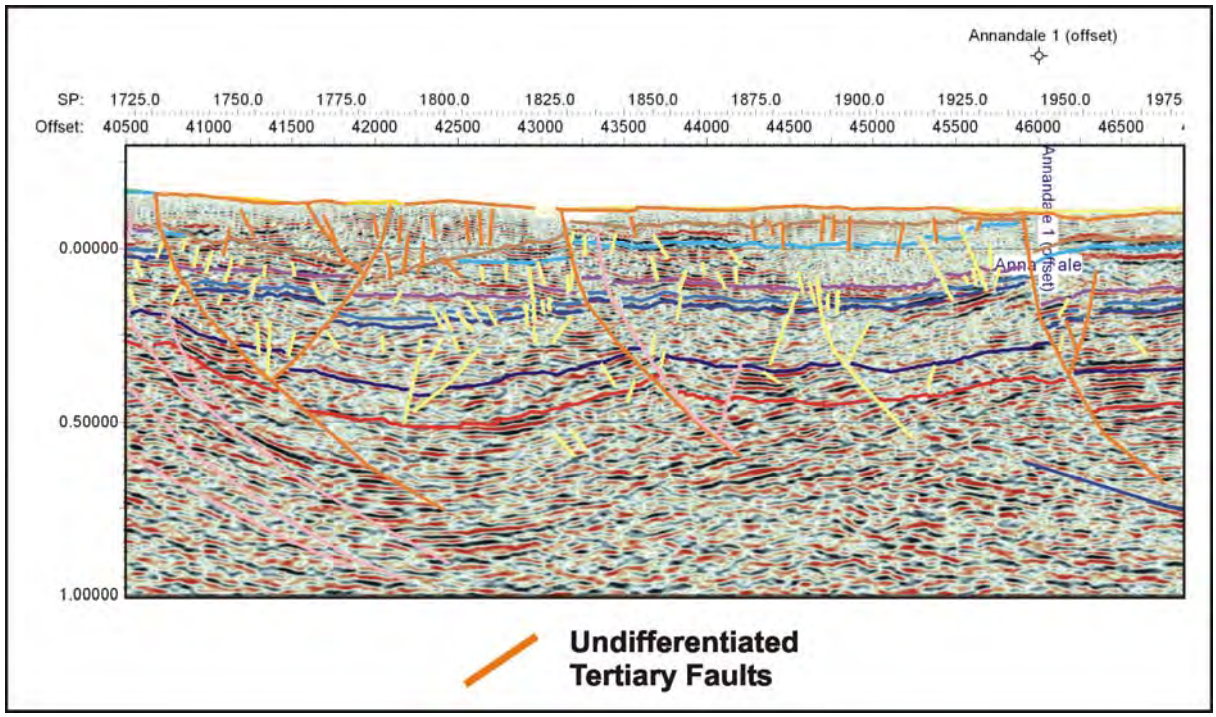

Figure 5.26: Examples of large Undifferentiated Tertiary Fault (TB01-ST).

Pre - Jurassic (Pre – Dolerite) Faults

Pre-Jurassic Faults are indicated where the latest movement is interpreted to have occurred either during or prior to the intrusion of dolerite in the Middle Jurassic. Both normal and reverse faults are interpreted; these are subdivided into two classes: those, which are intruded by dolerite, and those, which are not (Figure 5.10). Pre-Jurassic Faults are much less common across the survey area than Post-Jurassic Faults.

"Not Intruded" Faults

These faults that only affect the Parmeener Supergroup and basement, they do not displace the Jurassic Dolerite nor have they been intruded by Jurassic Dolerite. They are recognised in the

basal part of the Parmeener Supergroup where they displace the Base Parmeener Unconformity. Several faults of this class are truncated by dolerite sills, which clearly constrains their age (Figure 5.27). However, many are not. These are mainly interpreted in zones where the data is poor therefore they are not interpreted with confidence. It is assumed that because they are limited to the base of the section and/or because of their style that they are pre-Jurassic.

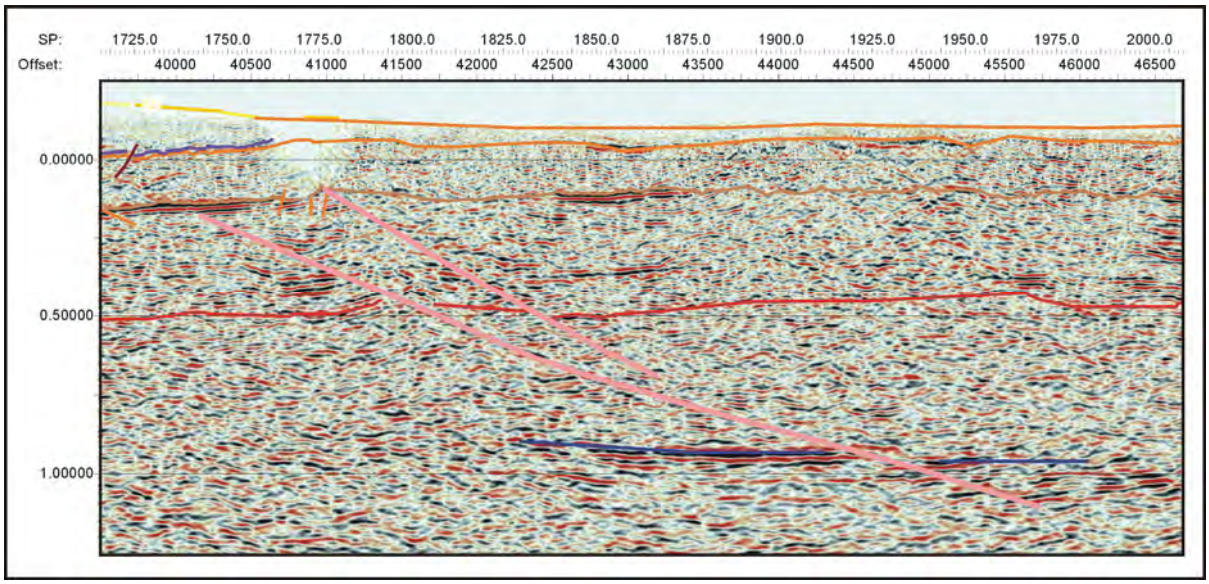

Figure 5.27: Pre-Jurassic Not Intruded, Normal Faults truncated by Jurassic Dolerite (TB01-PG).

Reverse and normal faults occur in approximately equal numbers, although overall, faults of this class are not numerous. Normal faults in this class were observed in both the Central Highlands and Northern Midlands/Longford Sub-basin regions, although mainly in areas of poor data. These faults are generally quite long in section (2645 m av.) and shallowly dipping (42° av.) and have throws ranging from 5 m to 135 m (Figure 5.28). Reverse faults were only observed in the Central Highlands region, the most convincing of these are a series of thrusts interpreted on line TB01-TH (Figure 5.29). The majority of these faults are 750 m to 1500 m long, dip less than 45° (37° av.) and have throws less than 40 m. “Not Intruded” – Normal Faults are indicated on the interpreted section by a pink line, while a purple line indicates “Not Intruded” – Reverse Faults (Figure 5.10).

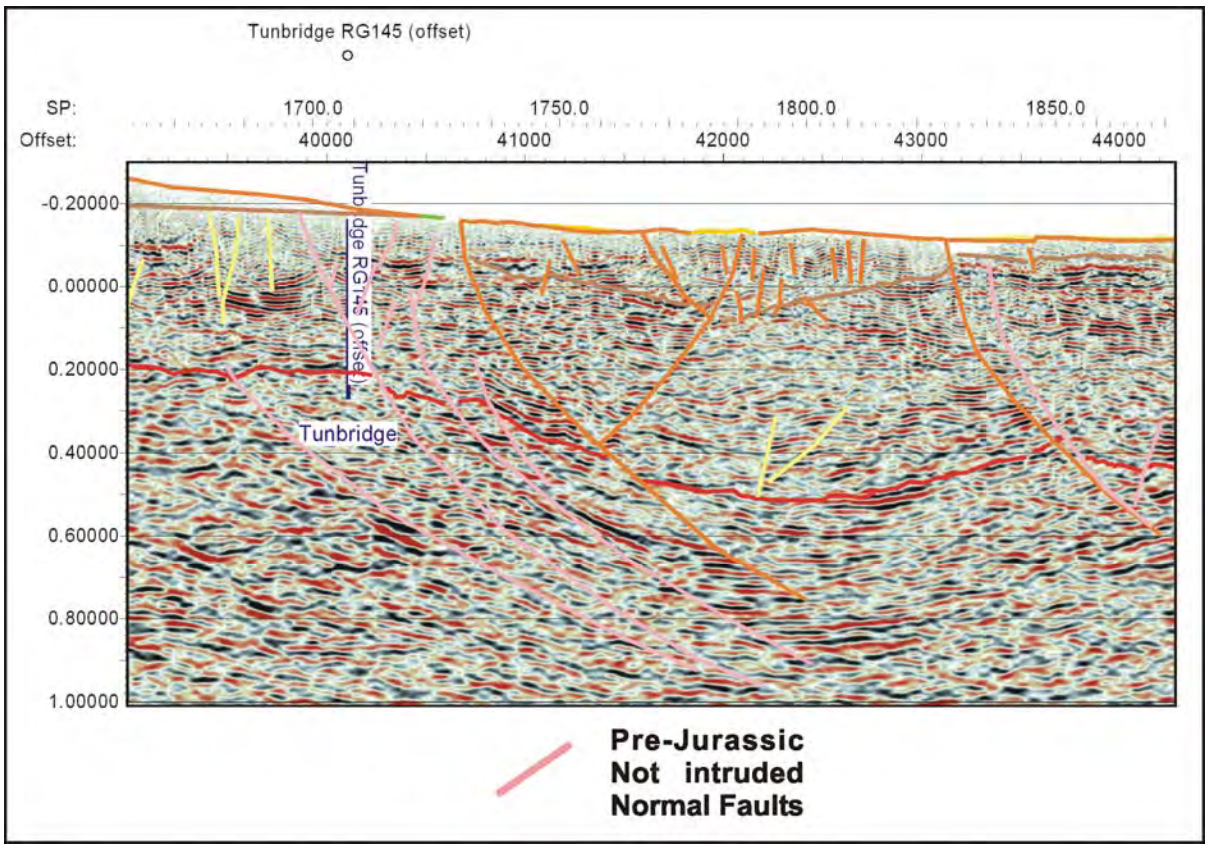

Figure 5.28: Examples of faults classified as Pre-Jurassic, "Not Intruded", Normal (TB01-ST).

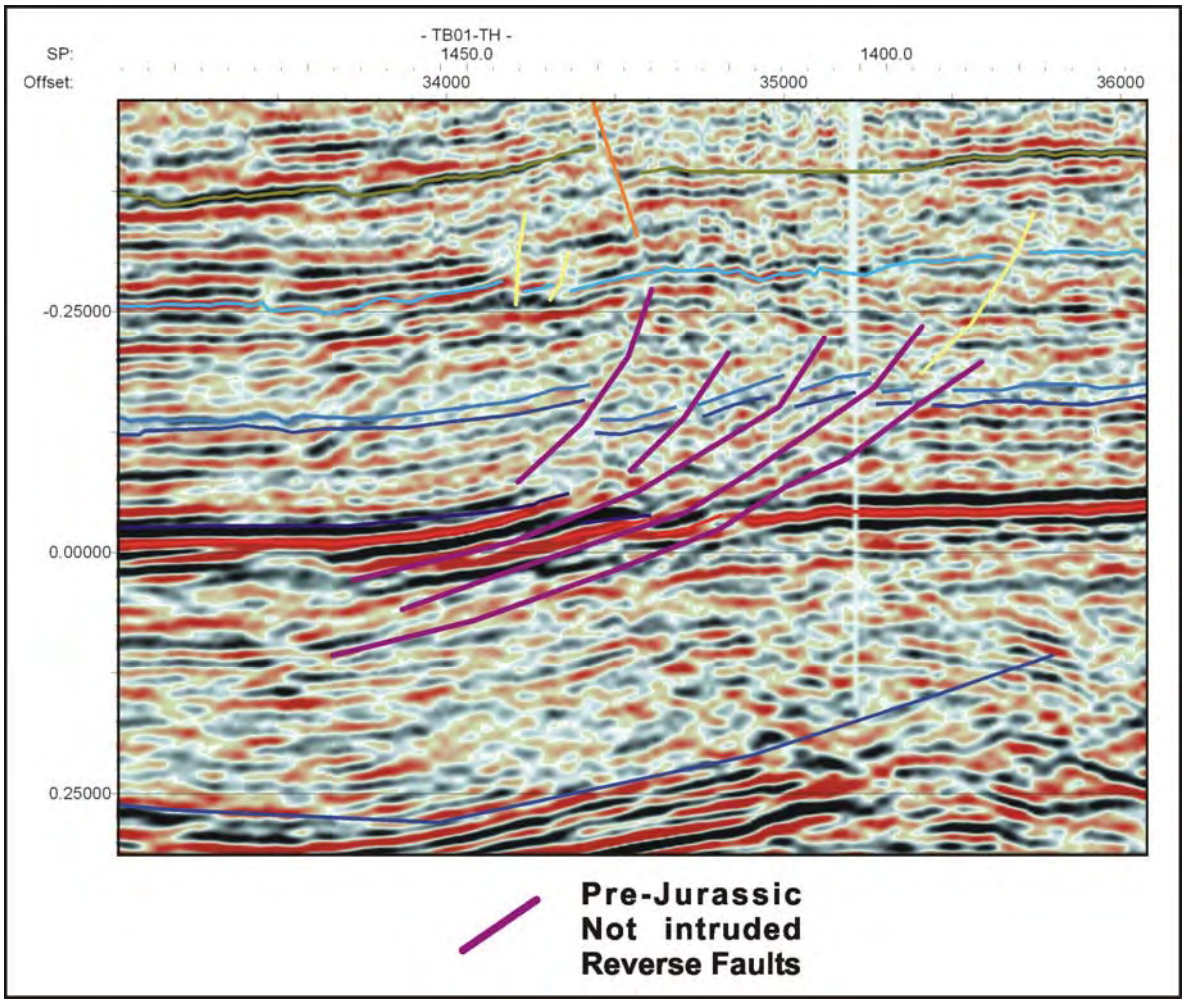

Figure 5.29: Examples of faults classified as Pre-Jurassic, "Not Intruded", Reverse (TB01-TH).

"Intruded" Faults

The term is applied to pre-Jurassic faults that have been intruded by dolerite. Fault planes above and below transgressing dolerite sills are identified, indicating the fault has provided a path for the intruding dolerite. Initial faulting probably took place prior to the intrusion of dolerite and during intrusion, dolerite moved along the weak fault planes to new stratigraphic levels. Faults of this class are rare. A single "Intruded" - Reverse Fault is interpreted on line TB01-ST (Figure 5.30), while several examples of "Intruded" – Normal Faults are interpreted in the Central Highlands region, occurring mainly at the margins of the windows in the dolerite (Figure 5.31). "Intruded" – Normal Faults are indicated on the interpreted section by a light green line, while an olive green line indicates Intruded – Reverse Faults (Figure 5.10).

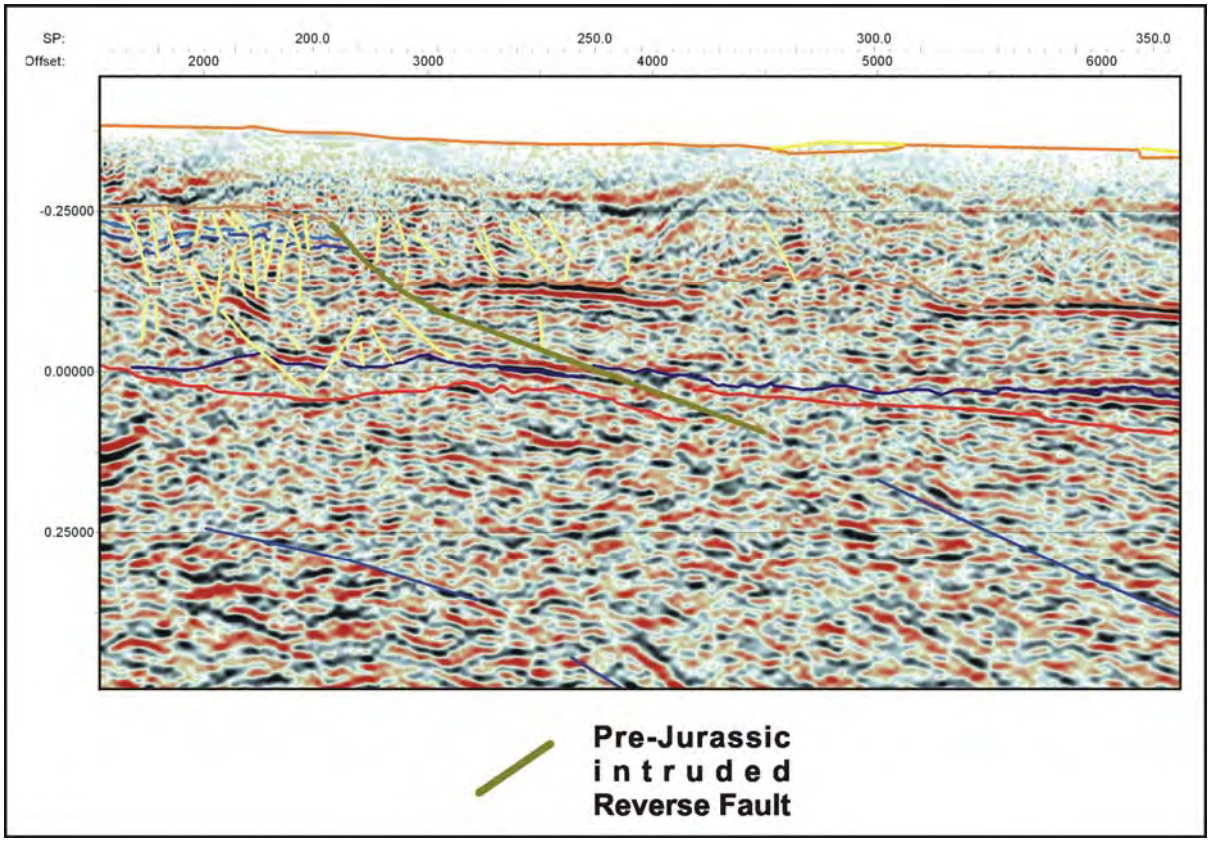

Figure 5.30: An example of a Pre-Jurassic, "Intruded", Reverse Fault (TB01-ST).

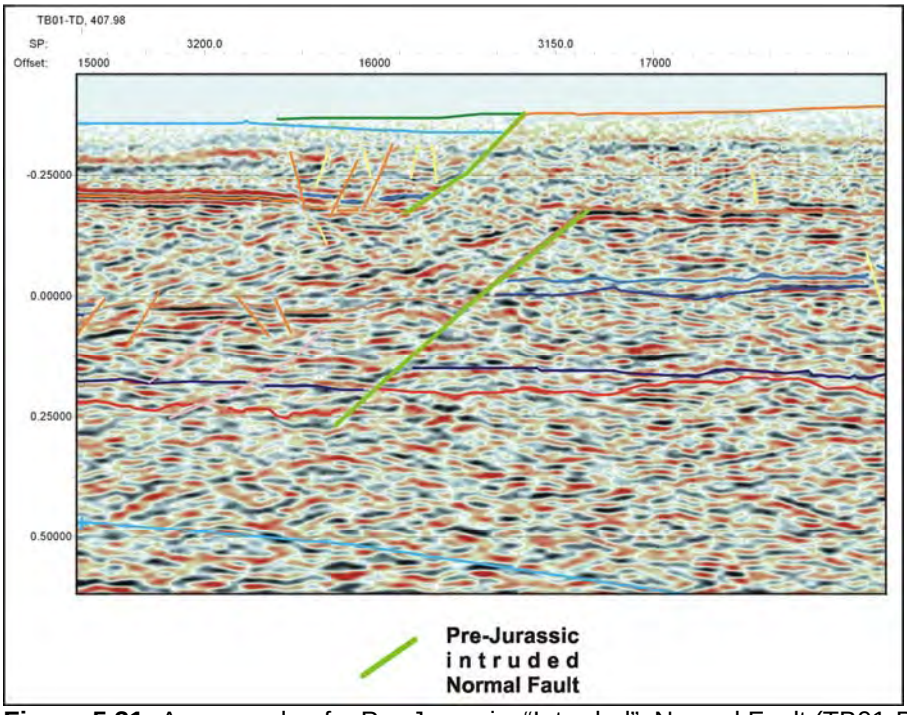

Figure 5.31: An example of a Pre-Jurassic, "Intruded", Normal Fault (TB01-PB).

Indeterminate Faults

Other faults are interpreted in the Tasmania Basin section are ambiguous. They probably have histories ranging from the earliest deposition in the basin right through to the recent. These faults are numerous. They have both normal and reverse offsets (Figure 5.32). However, many of these faults are small, with negligible displacements. Some of the offset between reflections may result from diffractions or other noise and may not represent a genuine displacement. Indeterminate Faults are represented on the on the interpreted sections by a yellow line (Figure 5.10).

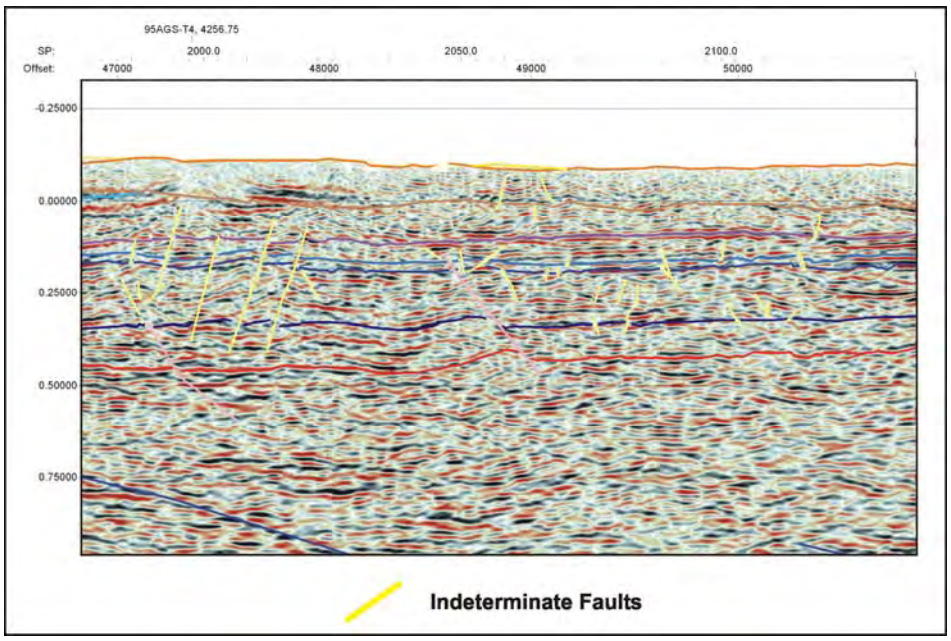

Figure 5.32: Examples of variously sized Indeterminate Faults (TB01-ST).

CHAPTER 6
SEISMIC INTERPRETATION - DESCRIPTION

6.1: INTRODUCTION

The following chapter presents a detailed description of the rationale used and the various constraints applied to the interpretation of the seismic dataset. Due to the variable quality of the seismic data, this detailed explanation of the interpretation process was thought necessary to explain how and why horizons and faults were recognised, especially in zones where the quality of seismic data is poor.

The TB01 Seismic Survey was acquired over two geographical areas, the Central Highlands and the Longford Sub-basin, with seismic line TB01-ST extending from the Central Highlands over the Northern Midlands region. The descriptions that follow are organised firstly by region then alphabetically by line name.

6.2: CENTRAL HIGHLANDS

6.2.1: TB01-PA

(Figure 6.1)

Seismic line TB01-PA has been acquired across the northern end of a window in the outcropping dolerite in the Highlands region of Central Tasmania (Map 5.1, Figure 6.2). The line is 6.20 km long, and was acquired west to east commencing at 491 462 mE, 5 327 252 mN and ending at 497 348 mE, 5 326 096 mN (Map 5.1). The line is positioned along with lines TB01-PB, PD and TA to define geological structure known as the Hunterston Dome (Fairbridge, 1948) (Figure 6.3). This line is important to the overall interpretation as the Hunterston 1 DDH was located to tie to the line and target the crest of the Hunterston Dome. Although the overall quality of the seismic data is quite good, typically the top 0.1 seconds TWT of the section consists of incoherent, low amplitude reflections (Figure 6.4).

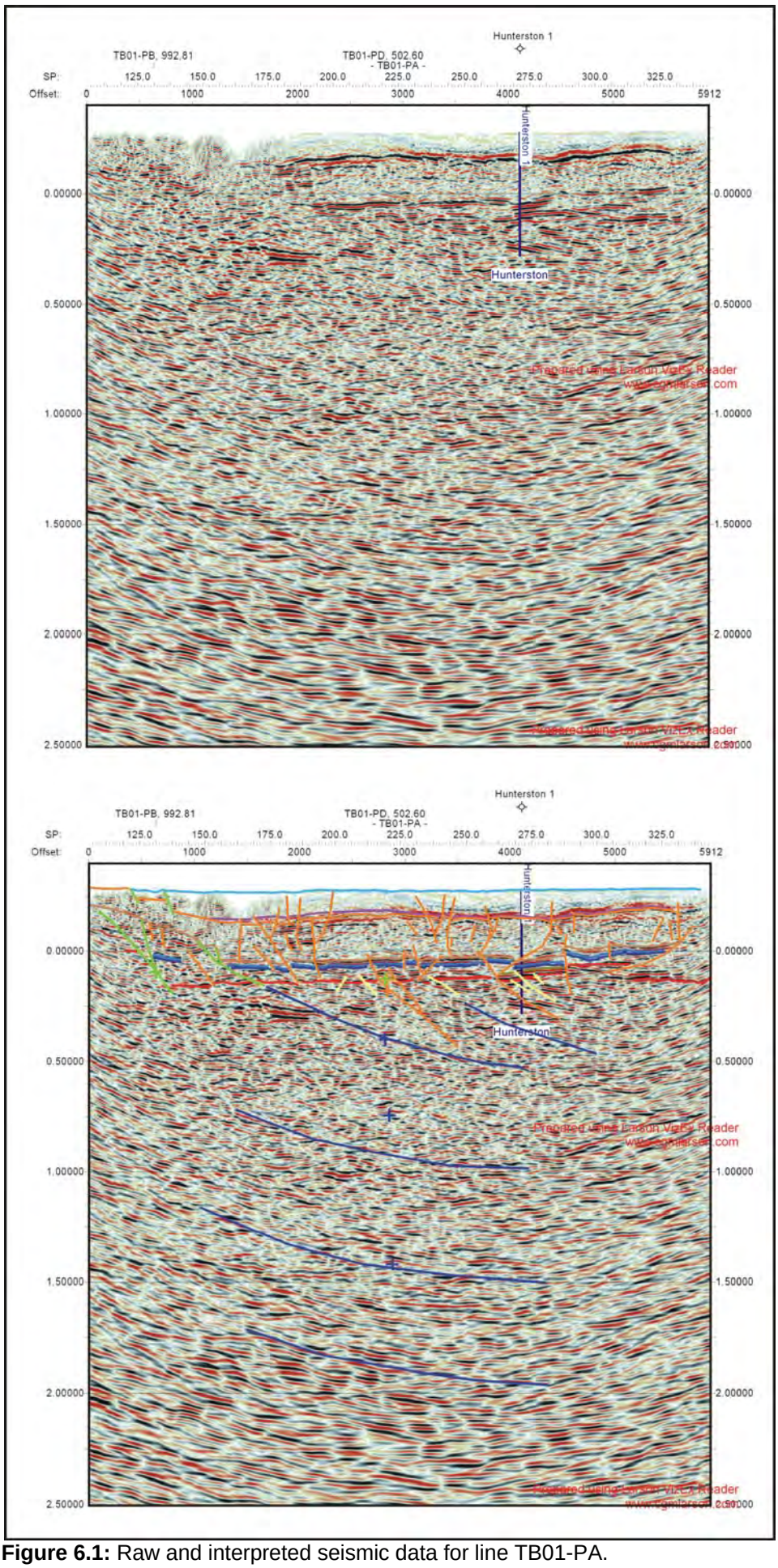

Figure 6.1: Raw and interpreted seismic data for line TB01-PA.

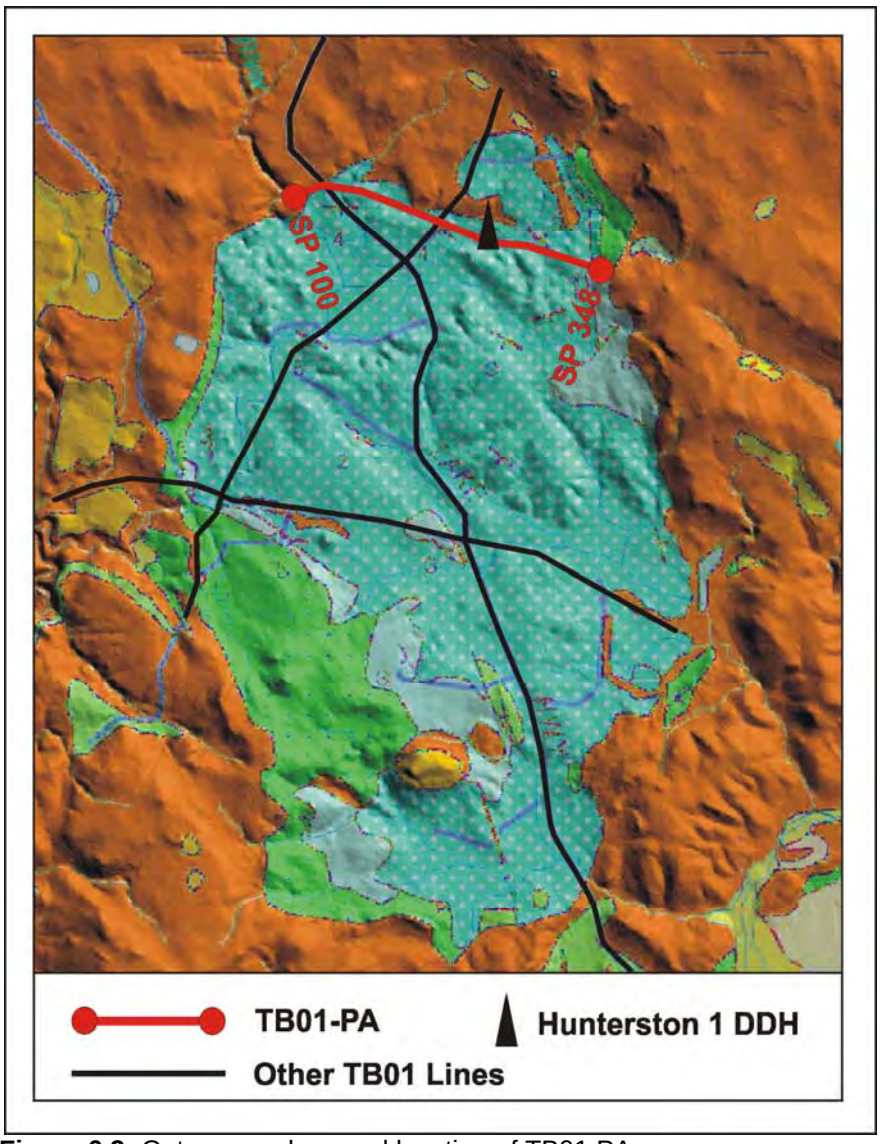

Figure 6.2: Outcrop geology and location of TB01 PA.

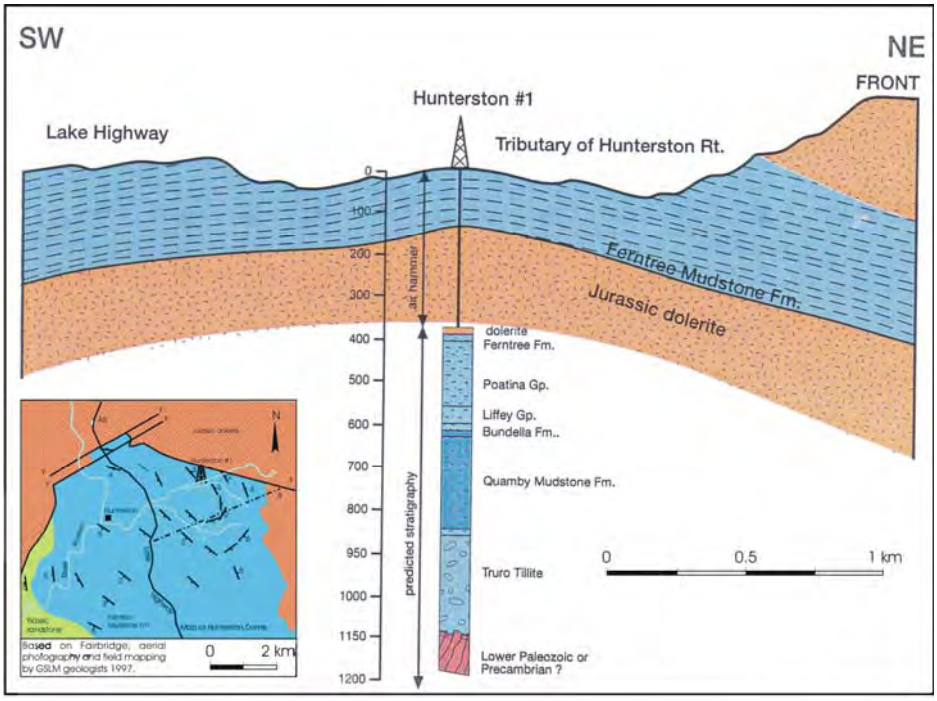

Figure 6.3: Pre-seismic interpretation of the geometry of the Hunterston Dome.

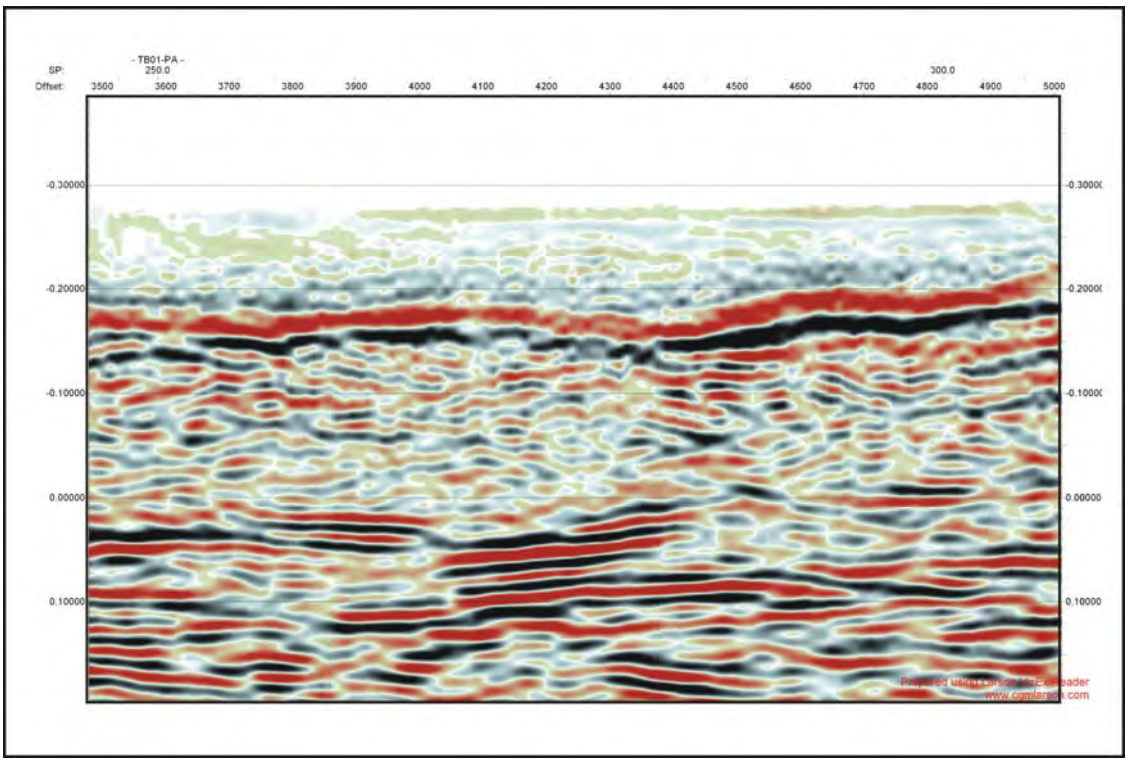

Figure 6.4: Incoherent and high amplitude, low frequency reflections occur commonly at the top of the seismic sections across the entire survey area (TB01-PA).

Line TB01-PA is the only location in the survey area where accurate lithological and velocity data have been acquired in a drill hole adjacent to a seismic line. A velocity survey was conducted at the Hunterston 1 DDH (see Chapter 5, section 5.4.2). The data obtained is used to establish the position of lithological boundaries within the drill hole, and this information has then been extrapolated to the seismic section. This line is essentially the "seismic type-section" for the survey, where the many of the correlations between litho- and seismic-stratigraphic events were initially made.

The position, in TWT of the top of the dolerite sill in the drill hole is calculated using the velocity survey data and correlates with a strong (high amplitude), positive reflection (black) when projected onto the seismic section (Figure 6.5). Similarly, the positions of the other lithologic boundaries identified in the drill hole are recalculated in TWT and based on the velocity information, projected onto the seismic section.

The Upper Marine Sequence (Ferntree Formation) is mapped at the surface (Forsyth et al., 1995). The 650 m thick dolerite sill (Reid et al., 2003) is easily distinguished by a zone of incoherent, low amplitude reflections from -0.20 to 0.05 seconds TWT (Figure 6.5). The interpretation shows the dolerite sill intruding the Upper Marine Sequence at the contact between the Ferntree and Cascades Formations (Figure 5.10).

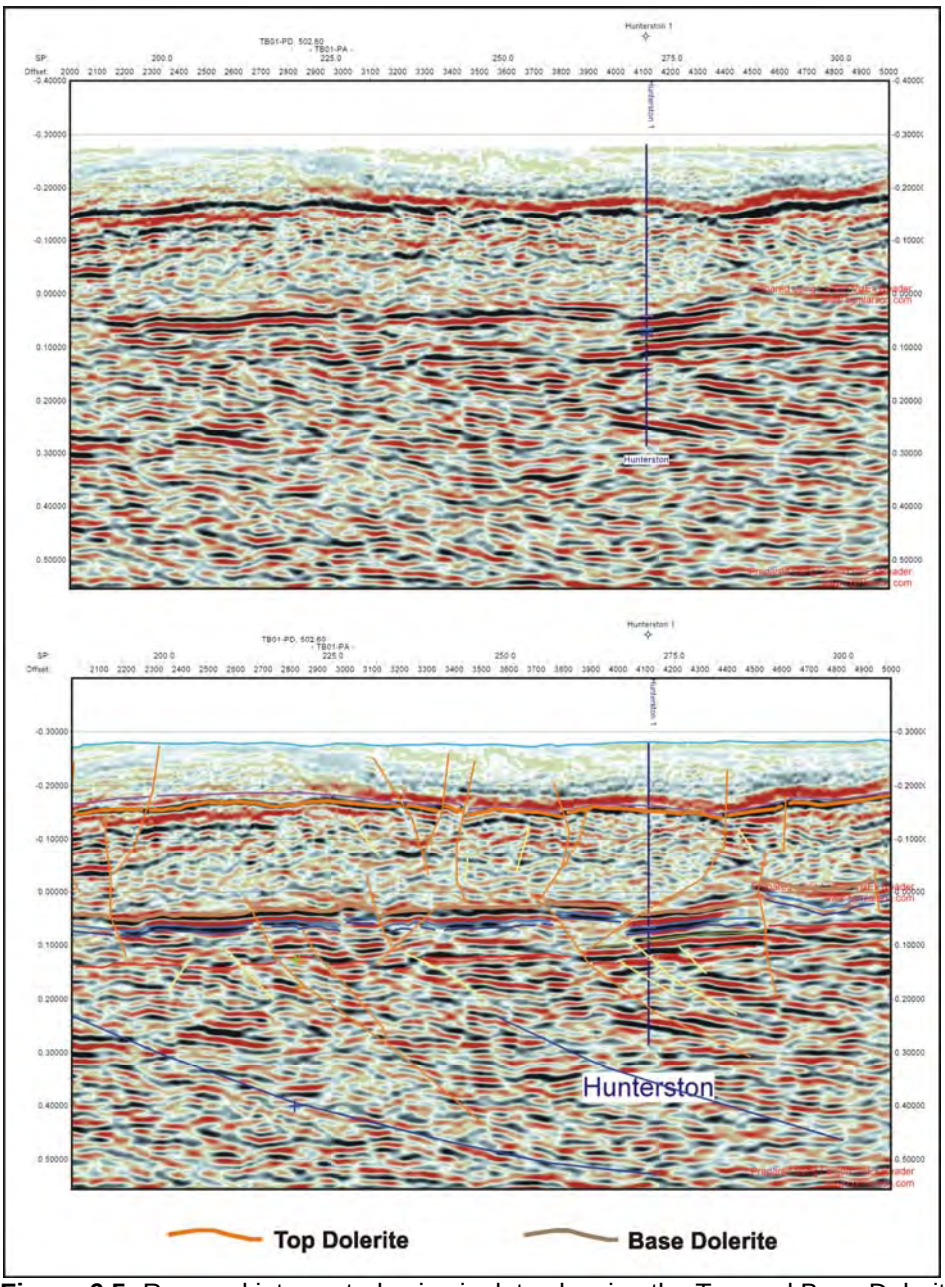

Figure 6.5: Raw and interpreted seismic data showing the Top and Base Dolerite Horizon picks, constrained by the Hunterston drill hole (TB01-PA).

The Lower Parmeener Supergroup section below the dolerite sill is incomplete, with recognised stratigraphic units finishing around 120 m below the base of the sill, below these lies a 80 m thick conglomeratic unit not previously recognised (Figure 5.3) (Reid et al., 2003). The position of the Base Parmeener Unconformity horizon is based on drill hole data and most easily distinguished in the greyscale image, where it appears as a bright (high amplitude) reflection (Figure 6.6). The interpretation of the unconformity's position is further aided by a series of east dipping reflections truncated by the horizon between shot-points 200 and 250 (Figure 6.7). The position interpreted for the Lower Freshwater Sequence and Lower Marine Sequence horizons away from the constraint of the drill hole are based on the thickness observed in the Hunterston drill hole.

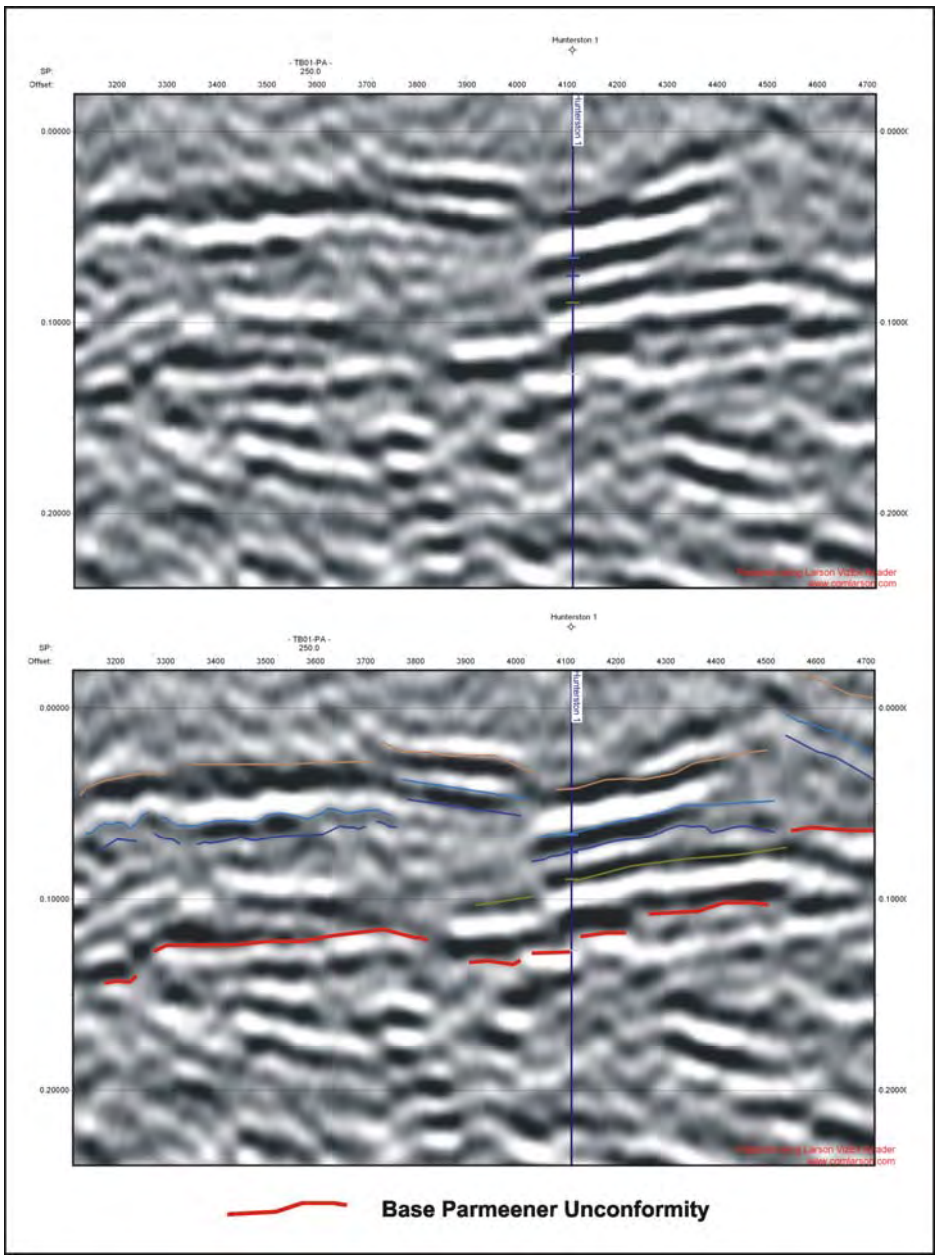

Figure 6.6: Raw and interpreted, greyscale seismic data, showing the position of the Base Parmeener Unconformity Horizon pick (TB01-PA).

The line crosses the north-western boundary of the window where the mapped outcrop changes from dolerite to Upper Marine Sequence rocks (Ferntree Formation) (Map 5.1, Figure 6.2). This change occurs across a linear boundary that has been mapped as a series of north-easterly striking faults (Figure 6.8) (Reid et al., 2003, Fairbridge, 1948). These faults have been interpreted on the seismic section as Pre-Jurassic, "Intruded", normal faults (Figure 6.9). These faults were active prior to the intrusion of dolerite and subsequently acted as barriers forcing the dolerite sill up to a new stratigraphic level. The intrusion can be followed across the faults by using the differences in the seismic character of the dolerite sill and the Parmeener Supergroup (Figure 6.9). The sill thins substantially to the west across these faults, an interpretation supported by measured gravity field (Figure 6.10).

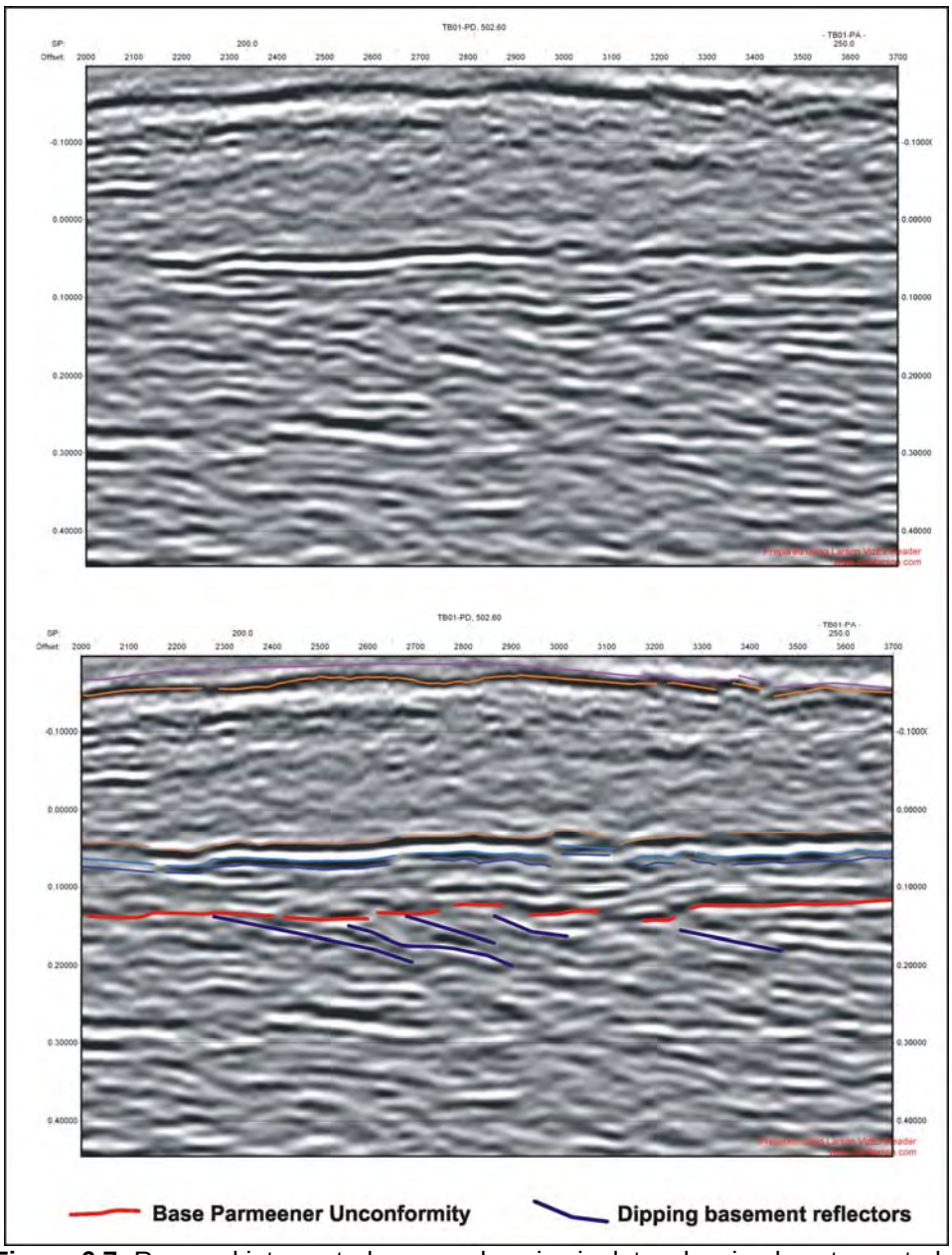

Figure 6.7: Raw and interpreted, greyscale seismic data, showing how truncated reflections indicate the position of the Base Parmeener Unconformity Horizon away from the Hunterston drill hole (TB01-PB).

The Parmeener Supergroup section contains many faults that are interpreted to have occurred after the intrusion of dolerite (Undifferentiated Tertiary Faults) (Figure 6.1). These faults dip towards the east near the western end of the line and west at the eastern end of the line. An Undifferentiated Tertiary Fault within the dolerite sill appears to cut through Hunterston drill hole (Figure 6.1), however as the dolerite section of the drill hole was not cored, no evidence for this fault has been recorded. On this line the Undifferentiated Tertiary Faults are mainly reverse with displacements in the 10's of metres, indicative of a compressional event sometime after the intrusion of dolerite. Several sub-horizontal faults were recorded around 900 m depth in the drill hole (Reid et al., 2003), however these are not resolved by the seismic data.

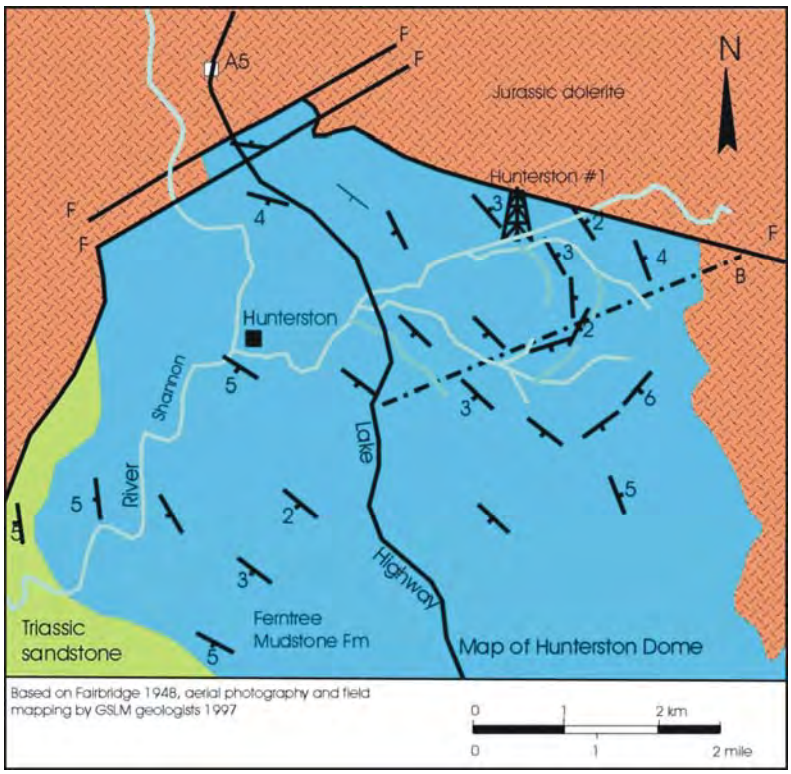

Figure 6.8: North-easterly striking faults are mapped at the northern boundary of the “window” in the dolerite.

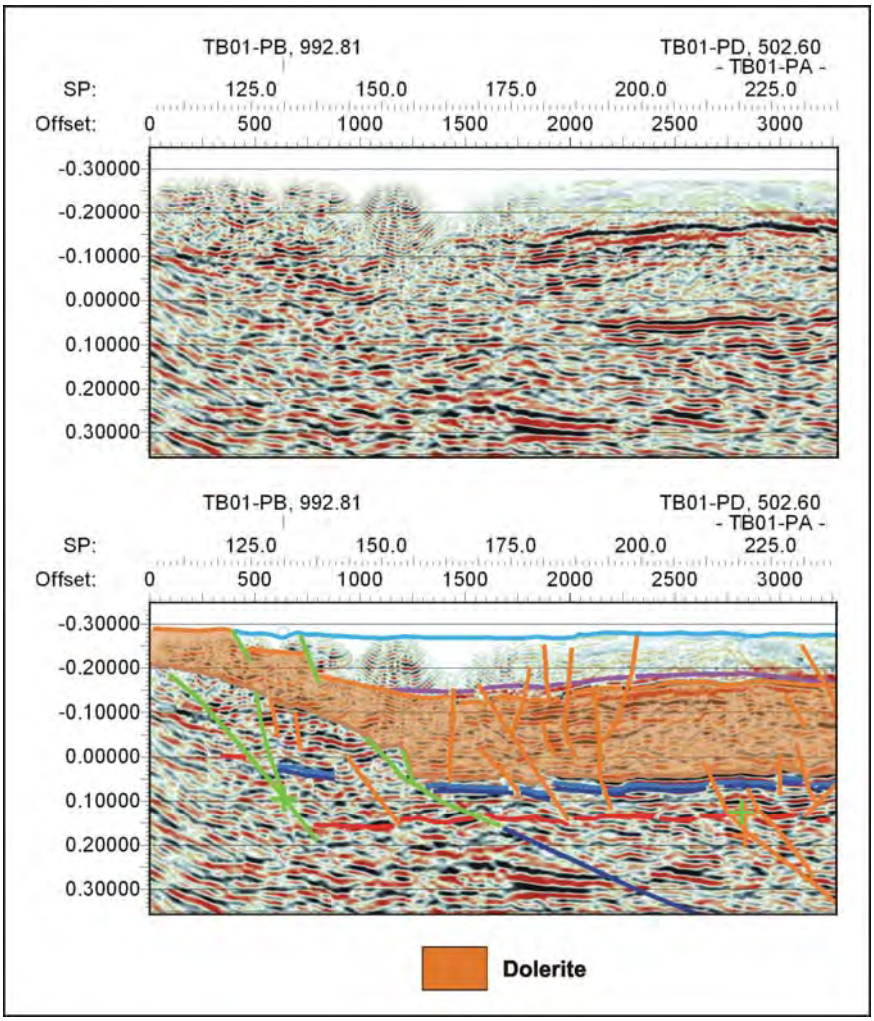

Figure 6.9: Interpretation of the path of the Jurassic Dolerite over the faults forming the northern boundary of the “window” near Hunterston (TB01-PA).

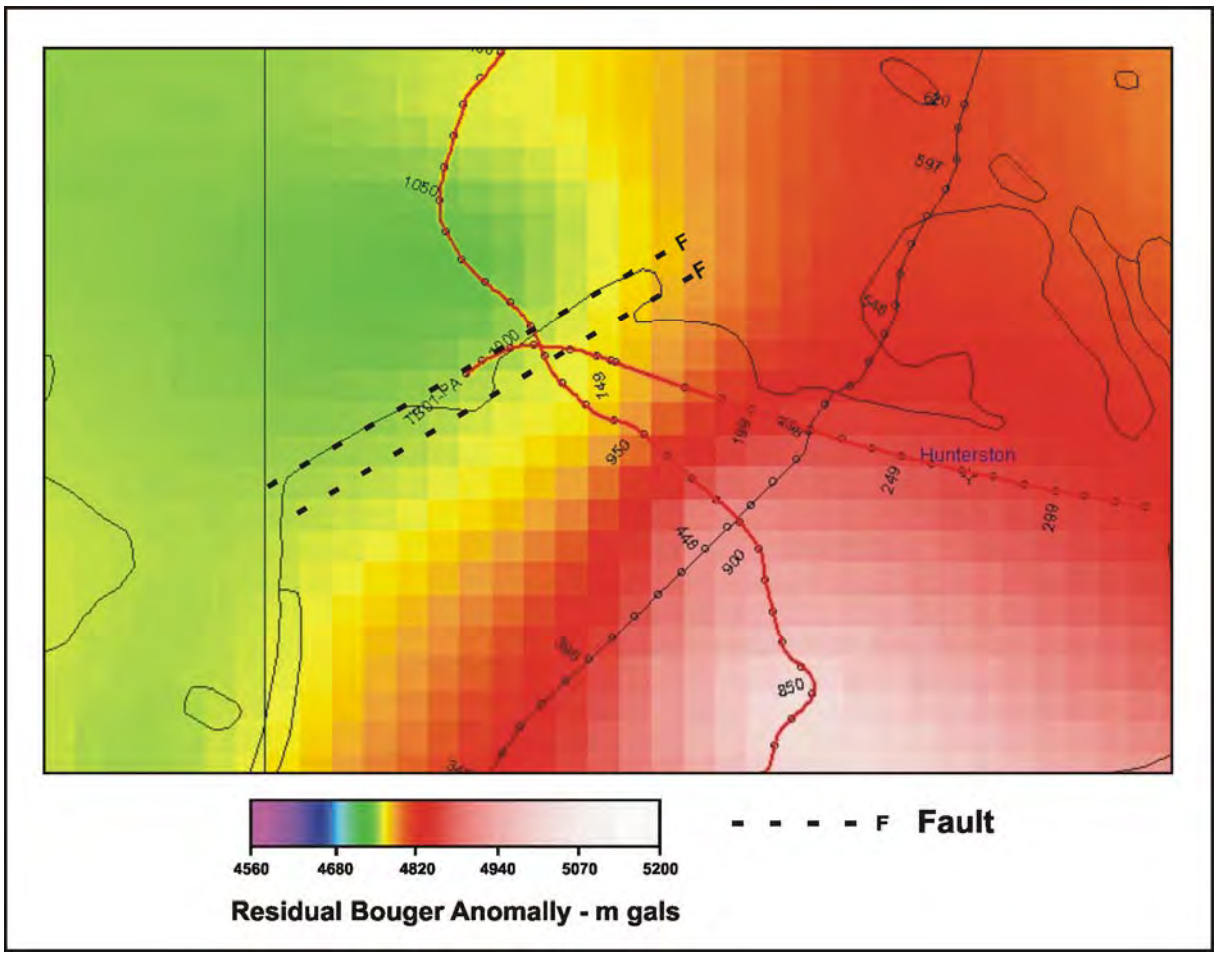

Figure 6.10: Variation in the measured gravity field at the boundary faults supports the interpretation of a thinning dolerite sill.

On this line, seismic events that may represent lithologic events or boundaries within the basement are difficult to reliably pick. Reflections in the basement are incoherent and changes in seismic character are subtle. The events that have been interpreted in the basement, dip shallowly to the east and become steeper towards the base of the Parmeener Supergroup.

6.2.2: TB01-PB

Seismic line TB01-PB is the longest line in the survey at 92.84 km and confined to the Central Highlands region of Tasmania. The line begins in the town of Bothwell (499 838 mE, 5 308 232 mN), follows the Lake Highway north then north-west to Miena (475 800 mE, 5 351 124 mN) where the line diverts south-west then south along the Marlborough Highway finishing at Bronte Park (456 972 mE, 5 330 405 mN) (Map 5.1). The quality of the data along this line is highly variable, however, considering the length of the line this is to be expected.

Shot-points 100 – 500

(Figure 6.11)

The relationship between dolerite and the Parmeener Supergroup in the south-western part of the Central Highlands (the area southwest of the Hunterston 1 DDH) is more complex than elsewhere in the survey area (Map 5.1). Interpretation of the section of the line between shot-points 100 and 500 is limited by the complex geology and poor seismic data (Figure 6.11). The data on line TB01-TC, intersecting TB01-PB and continuing south is similarly poor, making it very difficult to advance the interpretation further in that direction.

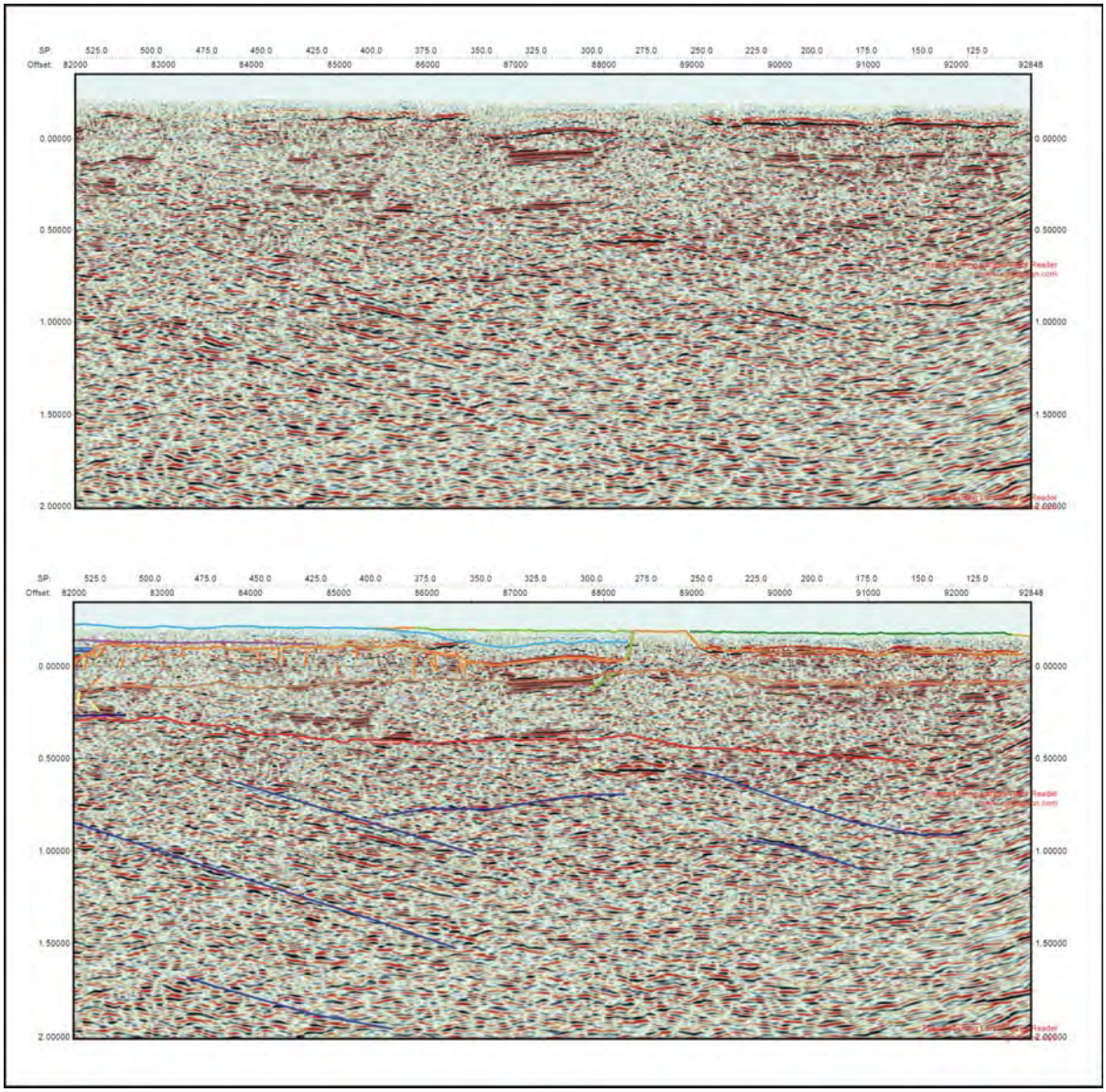

Figure 6.11: Raw and interpreted seismic data from shot-point 101 to 500 (TB01-PB).

Dolerite is the most distinguishable unit in this section and the geometry of the sill is considerably more complex than elsewhere in the survey (Figure 6.11). Between shot-points 100 and 250, the dolerite sill lies 200 m below the surface (Figure 6.11). At shot-point 250 a dolerite dyke rises steeply through the section (Figure 6.11), and corresponds to mapped dolerite outcrop between shot-points 257 and 280 (Figure 6.12). This dyke may have been a feeder to a sill higher in the original section. The northern side of the dyke is bounded by a fault where the adjacent rocks may have acted as a barrier forcing the intrusion upwards (Figure 6.11). The dolerite sill to the north of the feeder is much thinner than the sill to the south (Figure 6.11), an interpretation supported by the gravity data, shows a reduction in the measured gravity field from shot-point 300 (Figure 6.13). The sill begins to thicken from shot-point 350, from 350 m to 800 m thick by shot-point 450 (Figure 6.11).

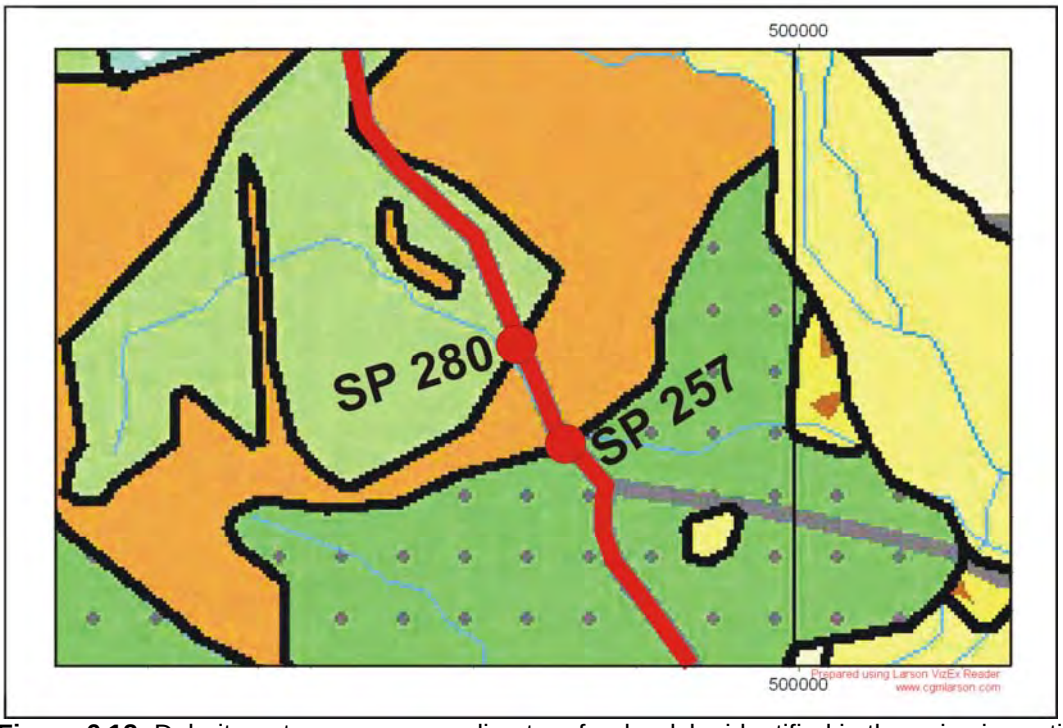

Figure 6.12: Dolerite outcrop corresponding to a feeder dyke identified in the seismic section. (Modified from Forsyth et al., 1995)

The MPT 1 Dungrove drill hole lies 2 km west of the line across a north – south striking fault (Figure 6.14). The dolerite sill is much deeper in the section recorded at the Dungrove drill hole (Figure 5.3) on the west side of the fault than interpreted in the seismic section to the east. Consequently, while useful to constrain the thickness of individual units the drill hole data cannot be directly correlated with seismic section.

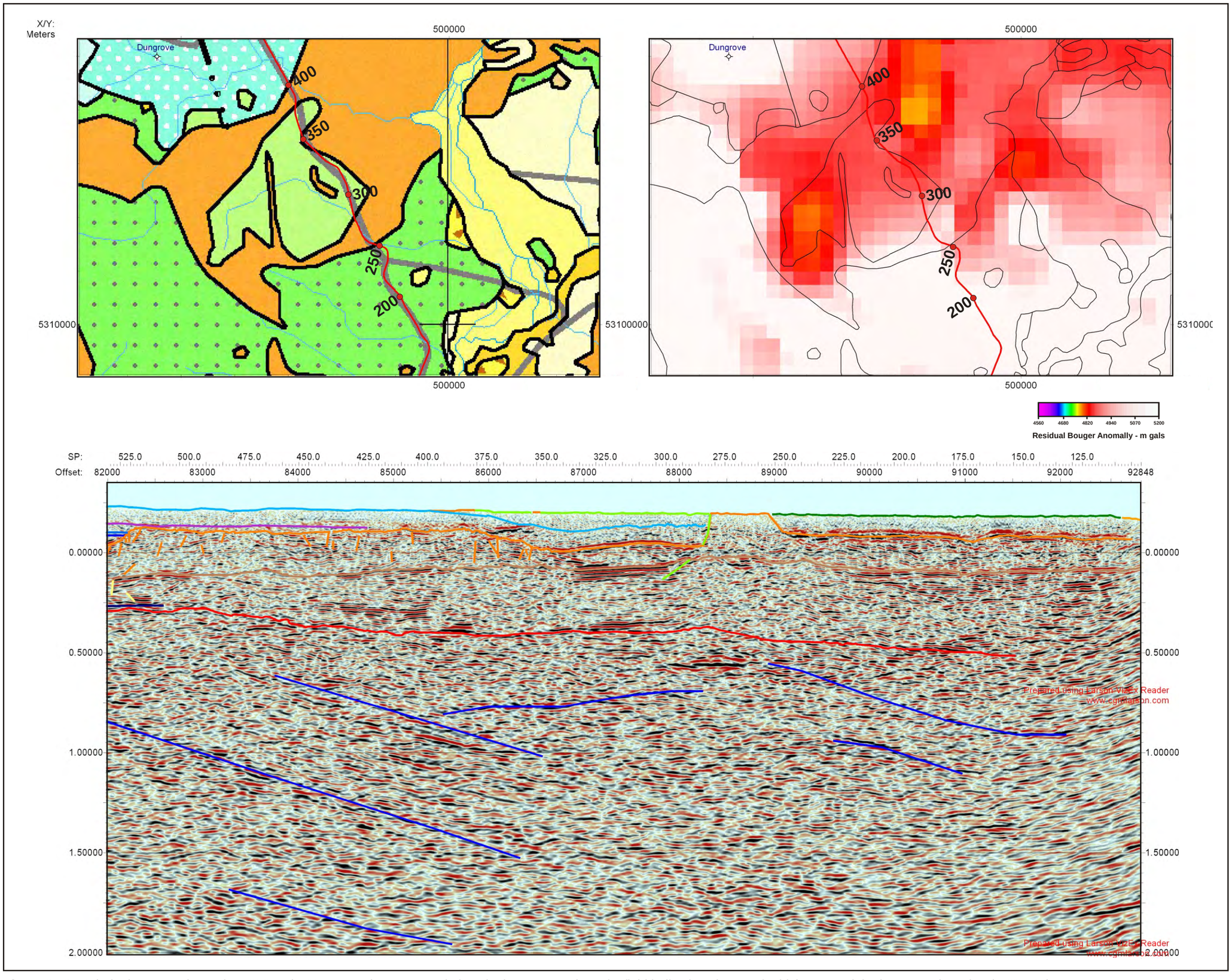

Figure 6.13: Dolerite between shot-points 200 and 400, mapped outcrop, variations in the measured gravity field indicating changes in thickness and the interpreted section (TB01-PB).

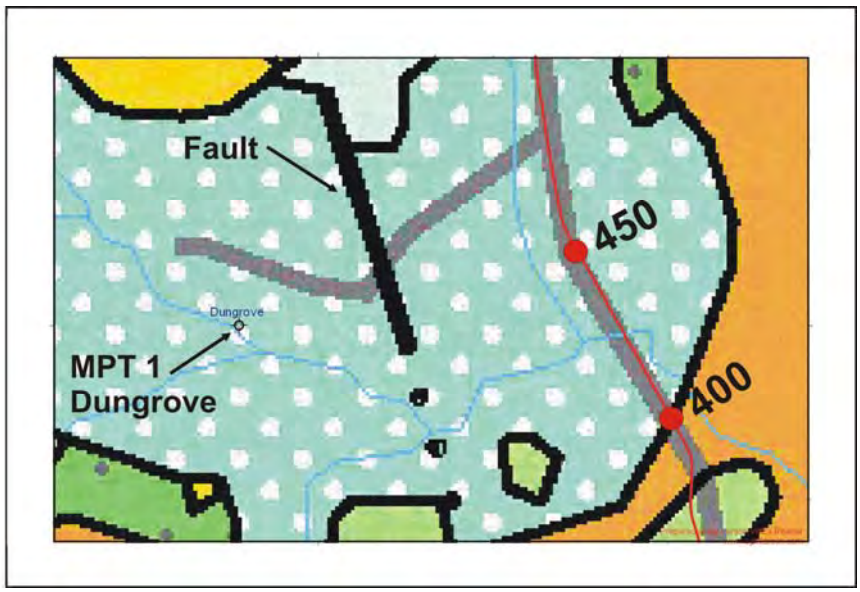

Figure 6.14: Location of the Dungrove MPT 1 drill hole, west of TB01-PB. (Modified from Forsyth et al., 1995)

The Base Parmeener Unconformity horizon is difficult to pick in this part of the section and has been extrapolated south from shot-point 500, where it can be picked with some confidence (Figure 6.11). The pick follows an intermittently strong (high amplitude) reflection from shot-point 500 to 100 that is best viewed on the greyscale image (Figure 6.15). The horizon moves deeper into the section towards the south, indicating thickening of the Parmeener Supergroup section (Figure 6.11).

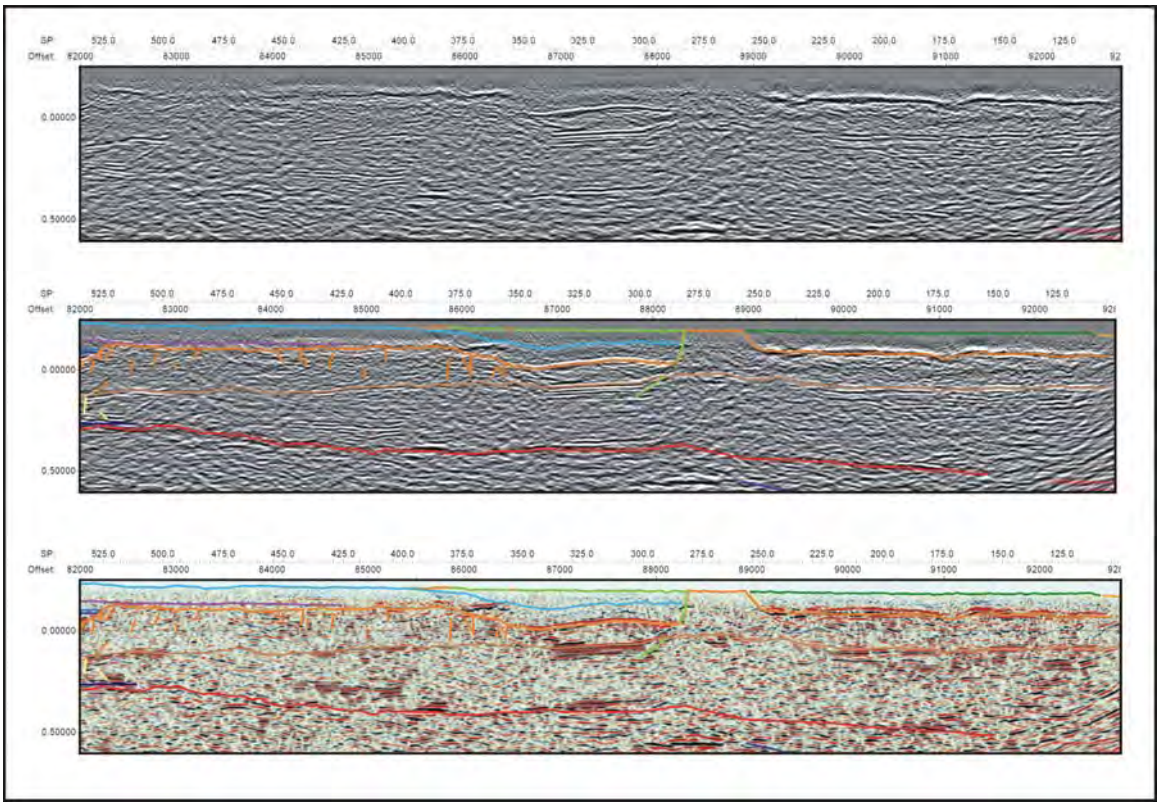

Figure 6.15: Raw and interpreted, greyscale and colour rendered seismic data, showing the Base Parmeener Unconformity Horizon pick between shot-points 500 and 100 (TB01-PB).

Shot-points 400 – 1000

(Figure 6.16)

From shot-points 400 to 1000 the seismic line has been acquired over a “window” in outcropping dolerite (Figure 6.17), where Upper Marine Sequence (Ferntree Formation) is mapped (Forsyth et al., 1995). The interpretation indicates that the geometry of the dolerite sill is far less complex across the window than it was between shot-points 100 – 400. The quality of the seismic data improves from shot-point 500.

From shot-point 400 to 525, the top of the dolerite sill (Top Dolerite Horizon) is interpreted to lie 300 m below the surface, dipping steeply towards the north from shot-point 525 it lies 600 m below the surface by shot-point 550 (Figure 6.18). There is no evidence observed in the seismic data to explain the sharp change in the stratigraphic position of the sill. At shot-point 550 the dolerite sill locally thickens to 900 m on the footwall side of a pre-Jurassic fault, thinning rapidly to a more typical 600 m thickness by shot-point 600 (Figure 6.18).

The single dolerite sill is defined in this section by the strong reflections associated with its upper and lower surfaces. A strong (high amplitude) positive reflection (black) defines the Top Dolerite horizon, while a strong (high amplitude) negative to positive zero-crossing event (red – black) defines the Base Dolerite horizon (Figure 6.16). The reflections, while not continuous occur regularly enough to interpret the path of the dolerite sill (Figure 6.19). At shot-point 600 the sill is 600 m thick and lies 450 m below the surface (Figure 6.19). The sill gradually rises up through the stratigraphic section, maintaining its thickness. By shot-point 975 it lies 200 m below the surface (Figure 6.19). Units of the Parmeener Supergroup interpreted above the sill at shot-point 600, lie below the sill by shot-point 975 (Figure 6.19). The position of units of the Lower Parmeener Supergroup interpreted between shot-points 525 and 900 is based on the unit thicknesses recorded in the Dungrove drill hole, the position of the dolerite sill was guided by groups of weak reflections between shot-points 525 and 850 (Figure 6.20). Below the sill groups of strong reflections that are coherent over short distances, define the Parmeener Supergroup section. The Base Parmeener Unconformity horizon is picked where the seismic character changes at the base of these reflections (Figure 6.20).

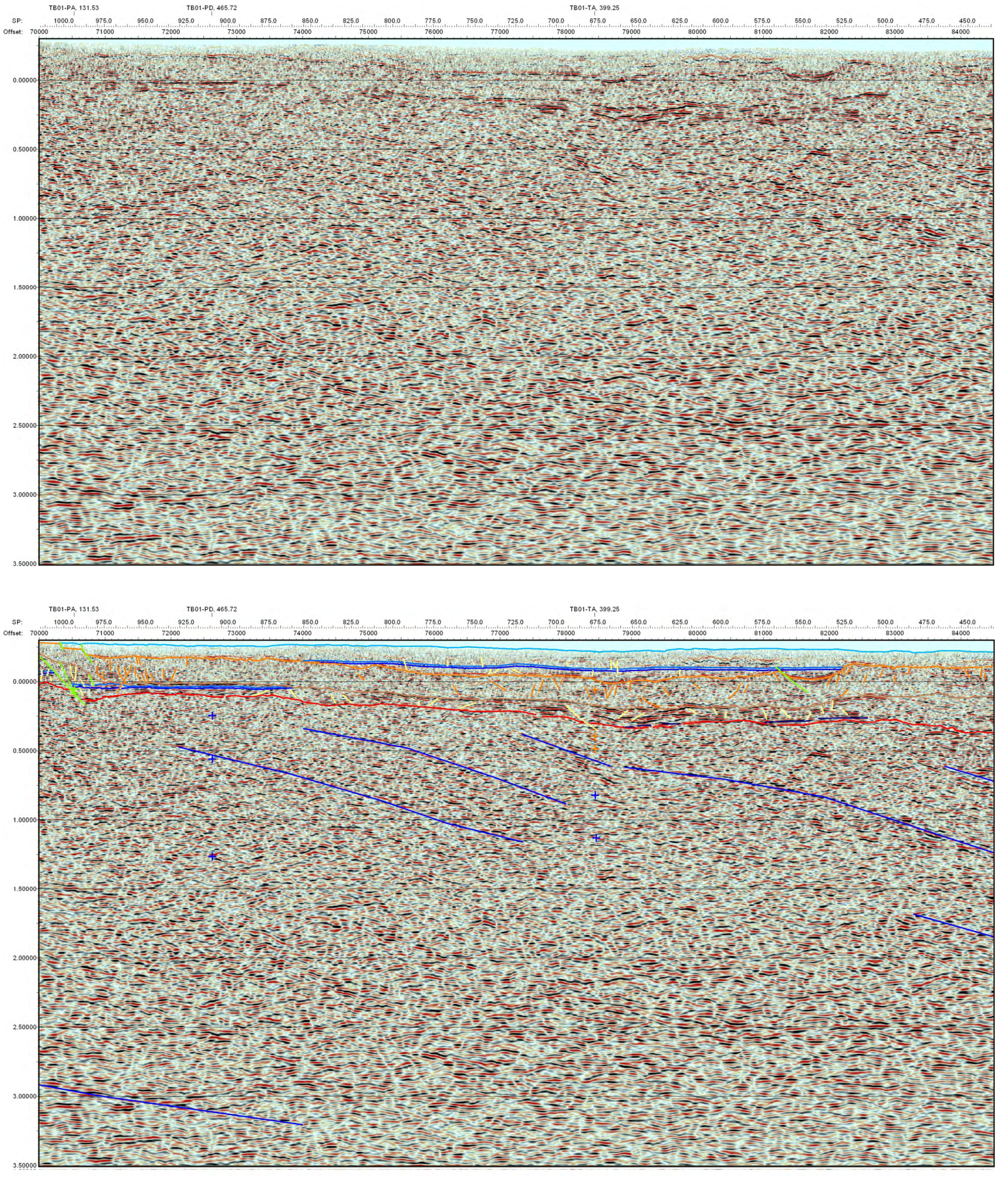

Figure 6.16: Raw and interpreted seismic data from shot-point 400 to 1000.

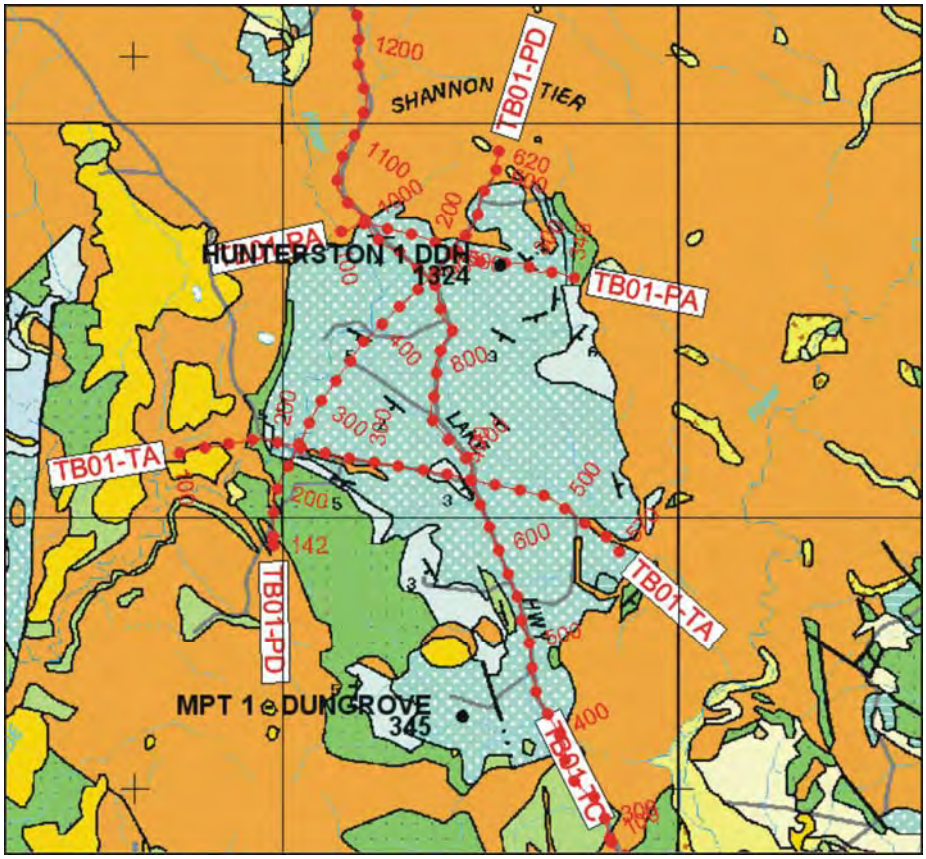

Figure 6.17: Outcrop geology and location of TB01-PB between shot-points 400 and 1000. (Modified from Forsyth et al., 1995)

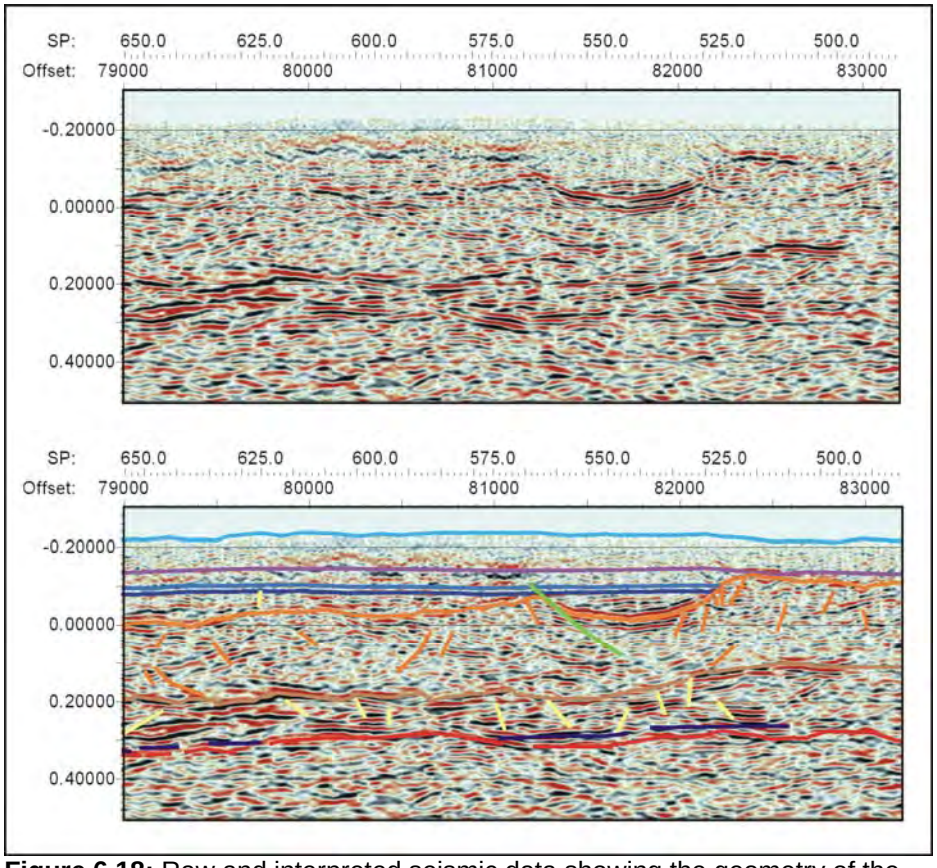

Figure 6.18: Raw and interpreted seismic data showing the geometry of the dolerite sill between shot-points 500 and 650 (TB01-PB).

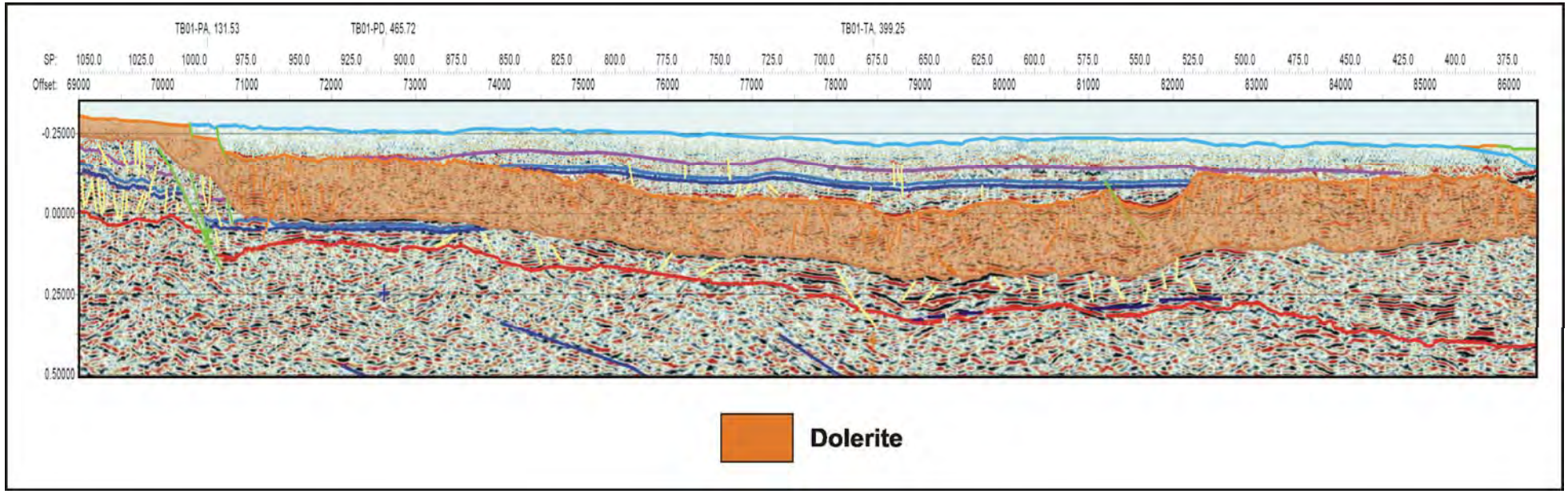

Figure 6.19: Interpreted seismic data showing the dolerite sill gradually rising towards the north between shot-points 400 and 1000 (TB01-PB).

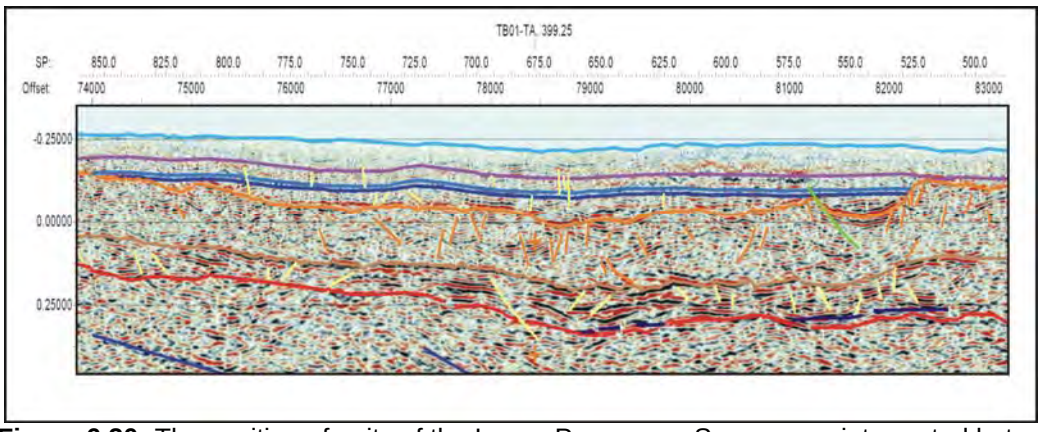

Figure 6.20: The position of units of the Lower Parmeener Supergroup interpreted between shot-points 525 and 900 is based on the unit thicknesses recorded in the Dungrove drill hole, the Base Parmeener Unconformity horizon is picked at the base of group of strong reflections between shot-points 525 and 725 (TB01-PB).

The Lower Parmeener Supergroup and dolerite are relatively unstructured in the section of the line that coincides with the window in the outcropping dolerite (Figure 6.16). The interpretation shows the dolerite sheet gradually cutting upwards through the Parmeener Supergroup section until it reaches the faults interpreted at shot-point 1000 (Figure 6.19). Apart from the pre-Jurassic fault that affects the dolerite sill at shot-point 550, no other major faults affecting the section are observed. Faults, indeterminate in age are interpreted below the dolerite sill between shot-points 500 and 800 (Figure 6.16). Collectively these faults appear to have no preferential orientation. They have only small displacements and their concentration near the site of a sharp change in the geometry of the dolerite sill, where the sill is thickening, suggests that these faults may be associated with the intrusion of the dolerite (Figure 6.21).

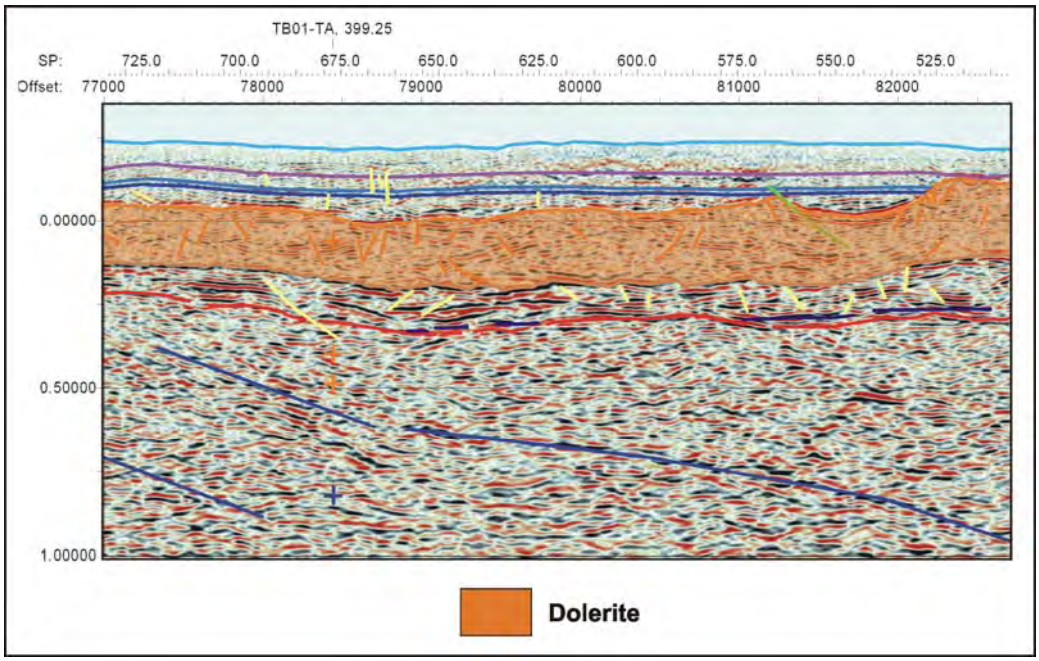

Figure 6.21: Numerous faults of indeterminate age are interpreted below the dolerite sill. Their concentration near a major change in the sill's geometry suggests their formation may be associated with the intrusion of dolerite (TB01-PB).

The basement between shot-points 100 and 1000 consists of incoherent reflections (Figure 6.16). These have a consistent frequency and amplitude that makes the recognition of events on the basis of differences in seismic character difficult (Figure 6.16). The events picked with the most confidence occur between 0.5 and 2.0 seconds TWT (Figure 6.16). These events dip towards the southeast at ~10°, with a possible roll over structure between shot-point 250 and 400 (Figure 6.16).

A series of faults interpreted by Fairbridge (1948) mark the north-western boundary of the window. The relationship between the faults, Parmeener Supergroup and the dolerite sill is complex. The dolerite sill rises through the section and the measured gravity field indicates that it thins rapidly across these faults (Figure 6.10). These faults are interpreted as Pre-Jurassic, "Intruded" faults, where the dolerite sill steps upwards by 300 m through the Parmeener Supergroup section to outcrop at the surface on the footwall side (Figure 6.16, 6.19). The Base Parmeener Unconformity is displaced by about 150 m across the fault, while the dolerite rises 450 – 500 m (Figure 6.22).

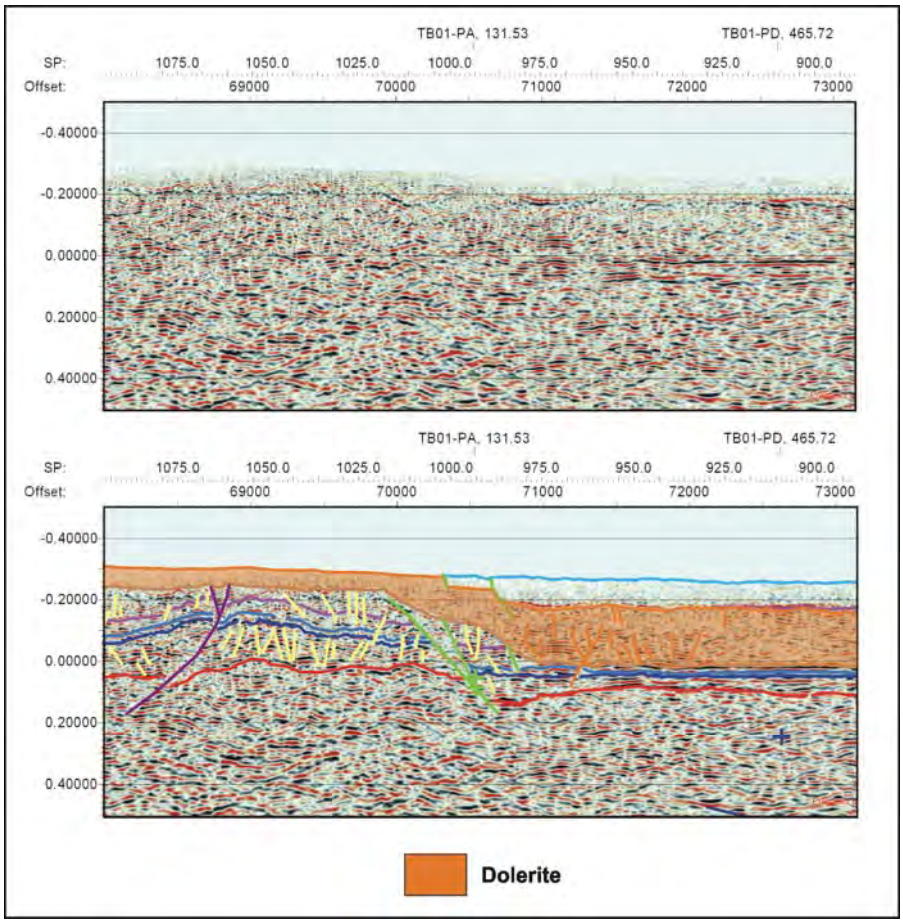

Figure 6.22: Raw and interpreted seismic data showing the displacement of the Base Parmeener Unconformity with respect to the change in the position of the dolerite sill, indicating these faults were probably active prior to the intrusion of the dolerite sill (TB01-PB).

Shot-points 1000-2200

(Figure 6.23)

Aside from scattered outcrops of Tertiary Basalt, outcropping dolerite is mapped from shot-point 1000 to 3150, a distance of 54 km (Map 5.1, Figure 6.24). Between shot-points 1025 to 2200 the data is highly incoherent making accurate interpretation difficult (Figure 6.23). The interpretation of this section relies on ties to intersecting lines to help guide the placement of the horizons. Apart from a Pre-Jurassic, reverse fault interpreted at shot-point 1075 and other small faults the dolerite and Parmeener Supergroup appear to be largely unstructured (Figure 6.23). The thickness of the dolerite sill in this section of the line is 250 to 300 m, except for a region around the intersection with line TB01-ST where the dolerite thickens to around 400 m (Figure 6.25). The Base Dolerite horizon is picked on the first strong positive reflection (black) below the incoherent zone at the top of the section (Figure 6.23). This interpretation is constrained by the measured gravity field, which indicates that the thickness of the dolerite remains constant along this section of line (Figure 6.26).

The Base Parmeener Unconformity horizon is difficult to pick in this section due to the general poor quality of the seismic data and because reflections in the basement are flat lying, making no obvious intersection with the base of the Parmeener Supergroup (Figure 6.23). The section between shot-point 1025 and the intersection with line TB01-ST is particularly difficult to interpret and the horizons are interpolated from confident interpretations at either end of the section (Figure 6.27).

The Base Parmeener Unconformity in the section between TB01-ST and shot-point 2200 is more easily recognised. The resulting interpretation relies on short zones of coherent data and the tie with line TB01-ST (Figure 6.28). The zones of coherent data comprise the Parmeener Supergroup. The base of these zones where the character becomes less coherent is interpreted as the Base Parmeener Unconformity horizon (Figure 6.28). The interpretation shows the Parmeener Supergroup section thickening after the intersection with line TB01-ST (Figure 6.28). Reflections within the Lower Parmeener Supergroup are mostly horizontal and the interpreted horizons maintain the thicknesses at the tie with TB01-ST (Figure 6.28). At shot-point 1600, where the Parmeener Supergroup is at its thinnest the Top Tillite horizon is interpreted onlapping the Base Parmeener (Figure 6.28).

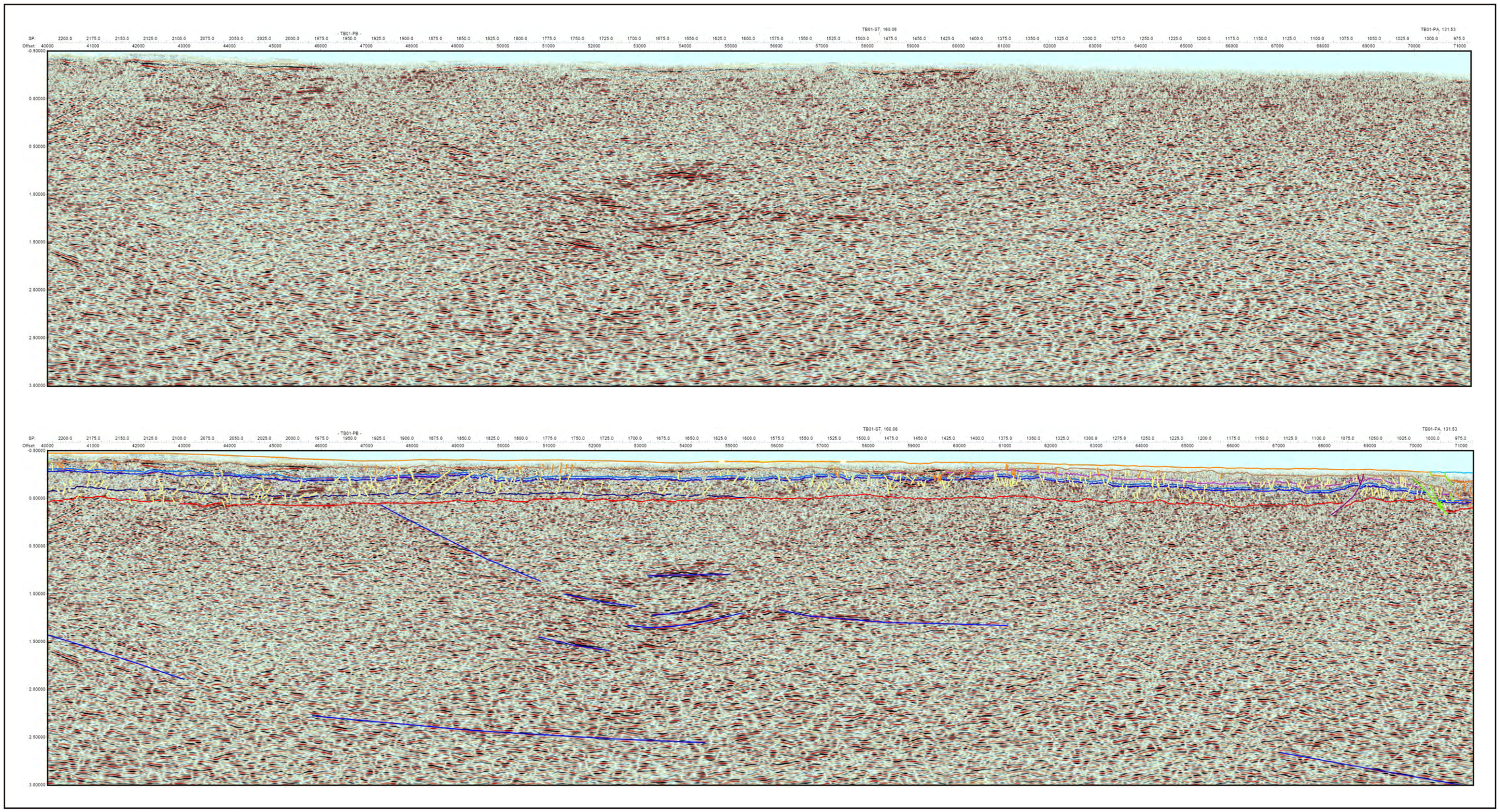

Figure 6.23: Raw and interpreted seismic data from shot-point 1000 and 2200 (TB01-PB).

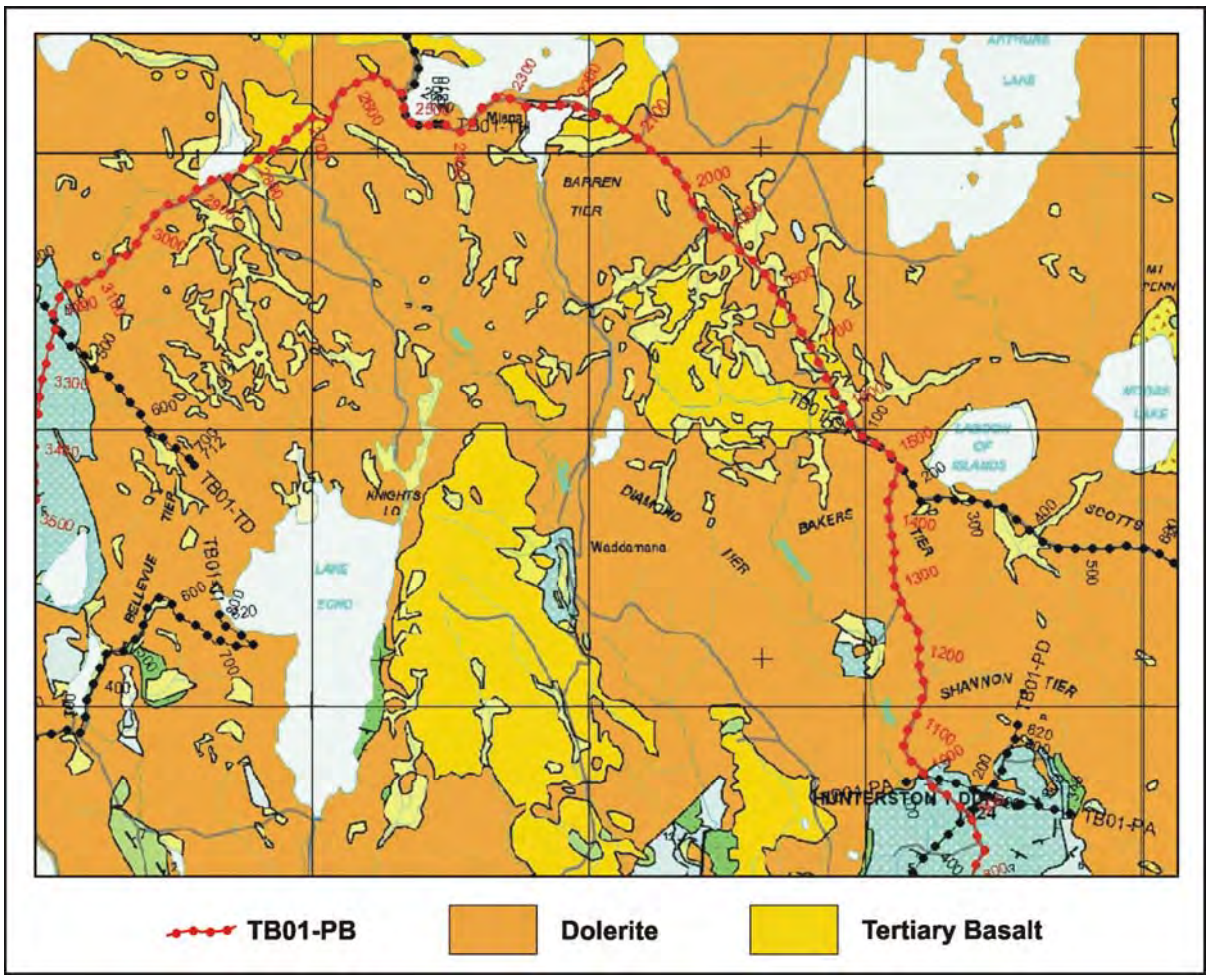

Figure 6.24: Outcrop geology and location of TB01-PB between shot-points 1000 and 2200. (Modified from Forsyth et al., 1995)

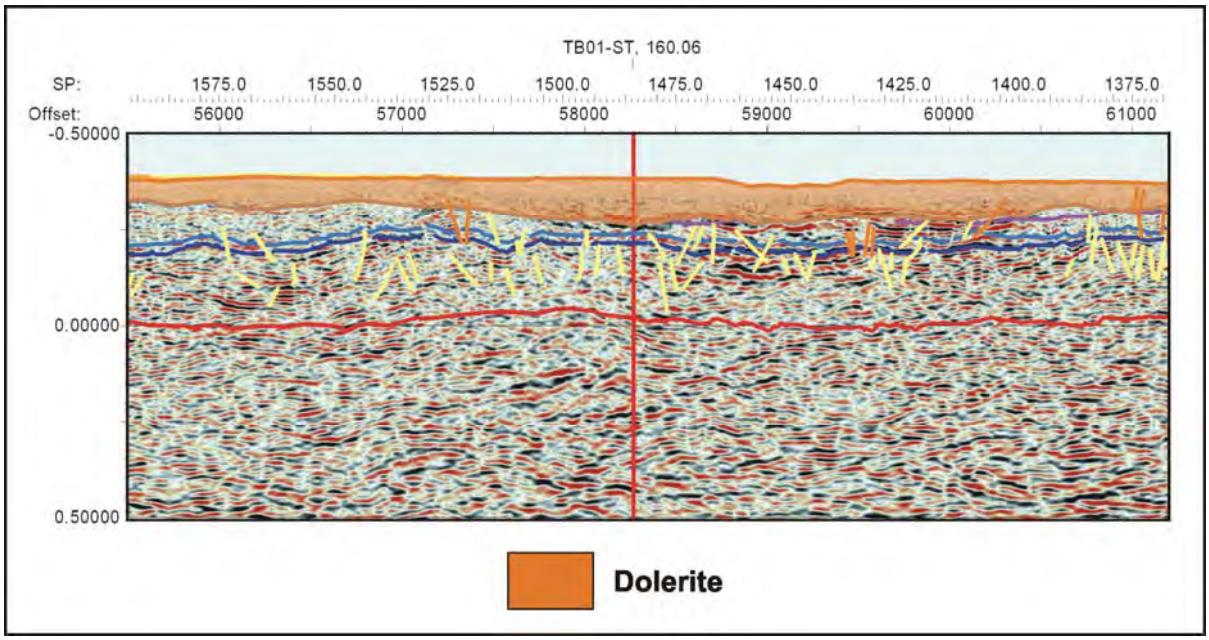

Figure 6.25: The thickness of the dolerite sill is 250 to 300 m in this section, except for a region around the intersection with TB01-ST where the dolerite thickens to around 400 m (TB01-PB).

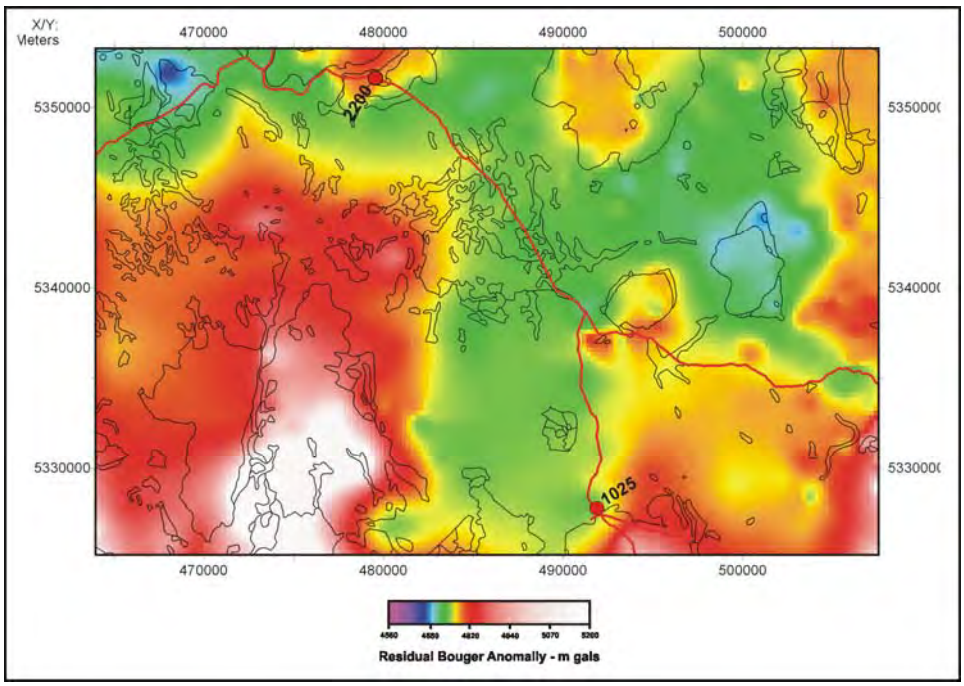

Figure 6.26: The measured gravity field indicates the thickness of the dolerite sill is relatively constant between shot-points 1025 and 2200.

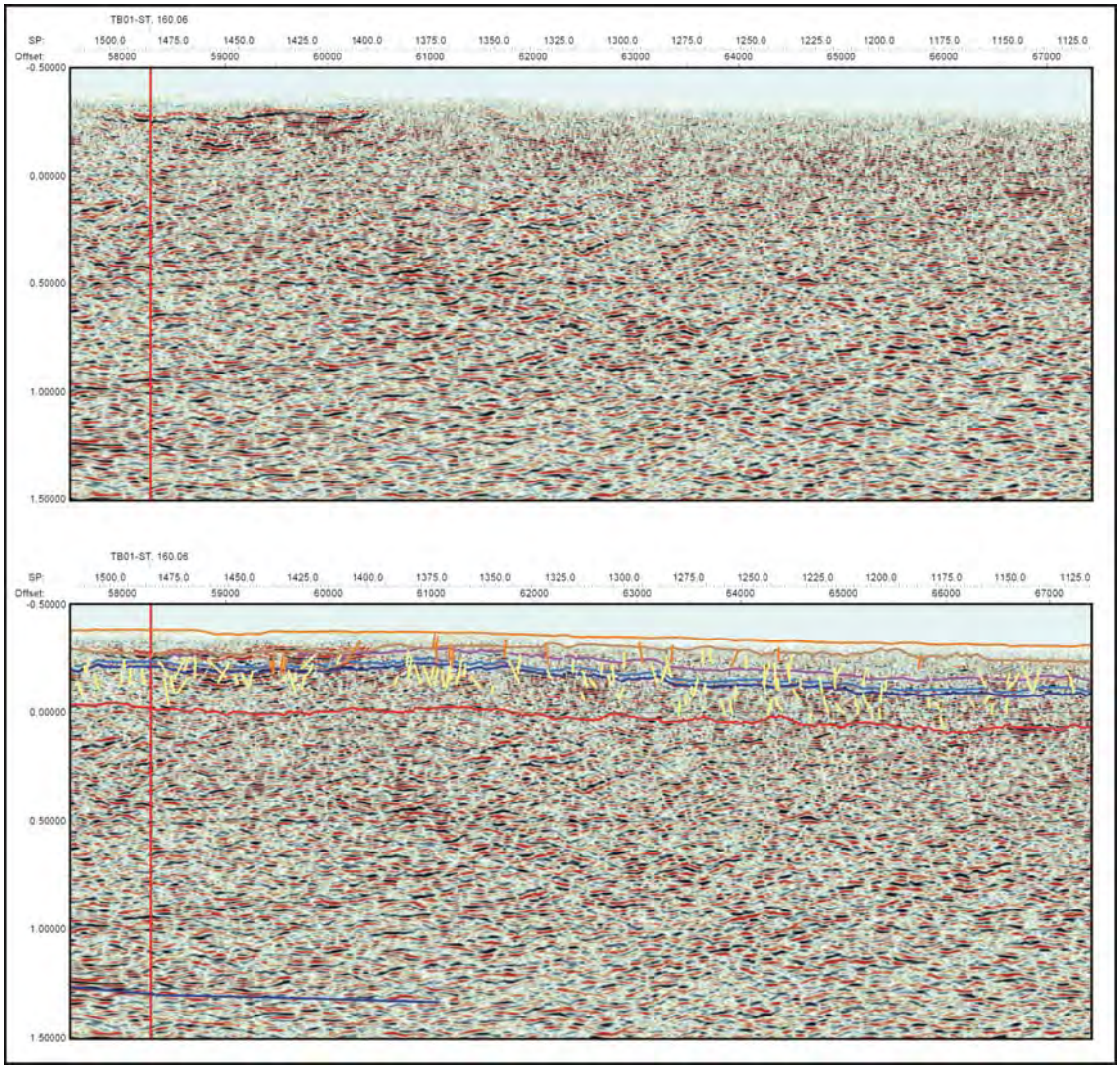

Figure 6.27: The seismic data between shot-point 1025 on TB01-PB and the intersection with TB01-ST is poor and the horizons are interpolated from more confident interpretations at either end of the section.

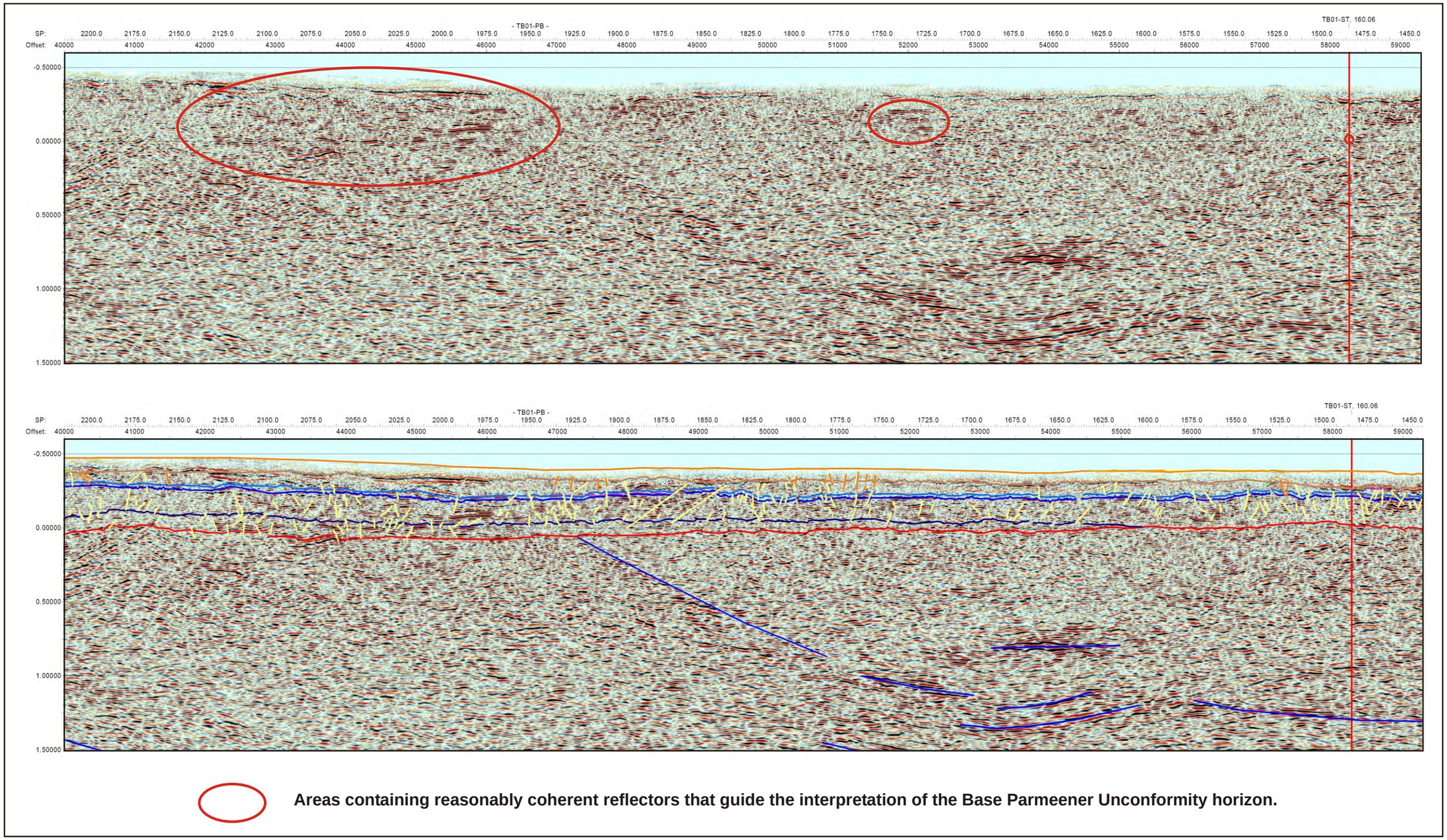

Figure 6.28: Line TB01-PB from the intersection with line TB01-ST to shot-point 2200, showing the rawdata and the areas of more coherent data that help guide the interpretation and the interpreted section.

Basement events in this section of line are interpreted at coherent reflections or at changes in the seismic character (Figure 6.23). There is no discernable pattern in this section. It includes sub-horizontal events, events that dip towards the south and others that dip north (Figure 6.23). This section of the line runs to the north and then to the north-west, sub-parallel then parallel with the anticipated strike of basement structures. Many of the events picked in the basement are difficult to reconcile with these proposed structures. The interpretation may relate more to poor quality seismic data, as seen in the overlying Parmeener Supergroup section rather than to geological structures. The interpretation of the basement structure in this area is unreliable.

Shot-points 2200 – 2350

(Figure 6.29)

The Parmeener Supergroup section interpreted between shot-points 2200 and 2350 is out of character with the seismic section on either side it. It contains a series of coherent, high amplitude reflections that appear abruptly and are not seen in the surrounding section. This short section runs mainly along a narrow strip of land between Great Lake and the Shannon Lagoon, east of Miena (Figure 6.30). The outcrop geology is mainly dolerite with Quaternary sediments along the northern shore of Shannon Lagoon. Quaternary sediments lying close to a large body of water may afford better acoustic coupling. A similar local improvement in data quality is observed at shot-point 2850 where the data is acquired over Quaternary sediments adjacent to Little Pine Lagoon (Figure 6.31).

The interpretation of this section of line owes much to the ties with lines TB01-ST to the east and TB01-TH to the west (Map 5.1). This section is along strike from a major fault identified on the DEM. However, the fault is not recognised in the seismic data and probably dies out before it reaches the line (Figure 6.32). Projected along strike the fault should intersect the line at shot-point 2275, where no displacement can be seen or interpreted in the seismic section (Figure 6.29). A normal fault, down to the west is interpreted at shot-point 2325, where a series of strong reflections are offset by 0.05 seconds TWT (100 m) (Figure 6.29). The trace of this fault is difficult to determine. The fault occurs where the seismic line rapidly changes direction by 90° and the data at this bend is chaotic (Figure 6.29). The measured gravity field indicates that the dolerite is thickening across the section, and then thins on the downthrown side of the fault (Figure 6.33). There is no evidence in the seismic data that the dolerite sill has been affected by the fault, therefore, the fault is interpreted to have occurred prior to the intrusion of the dolerite.

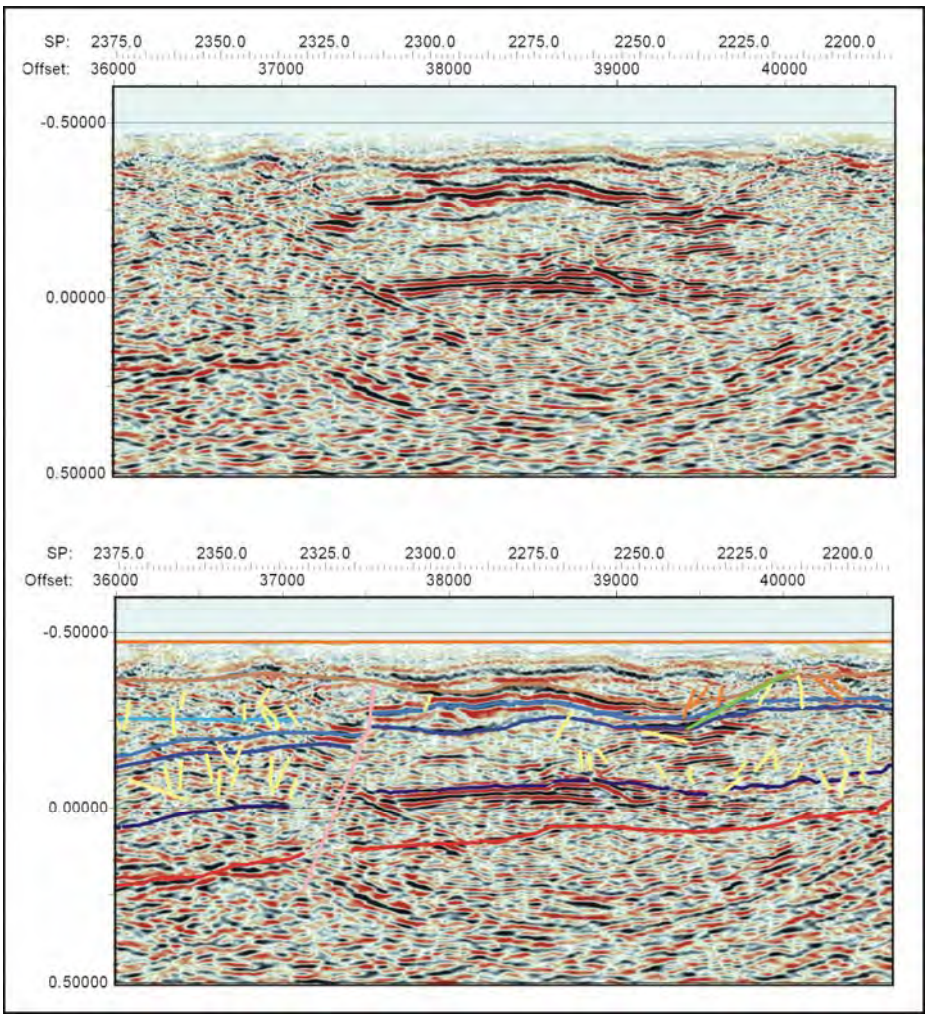

Figure 6.29: Raw and interpreted seismic data from shot-point 2200 to 2350 (TB01-PB).

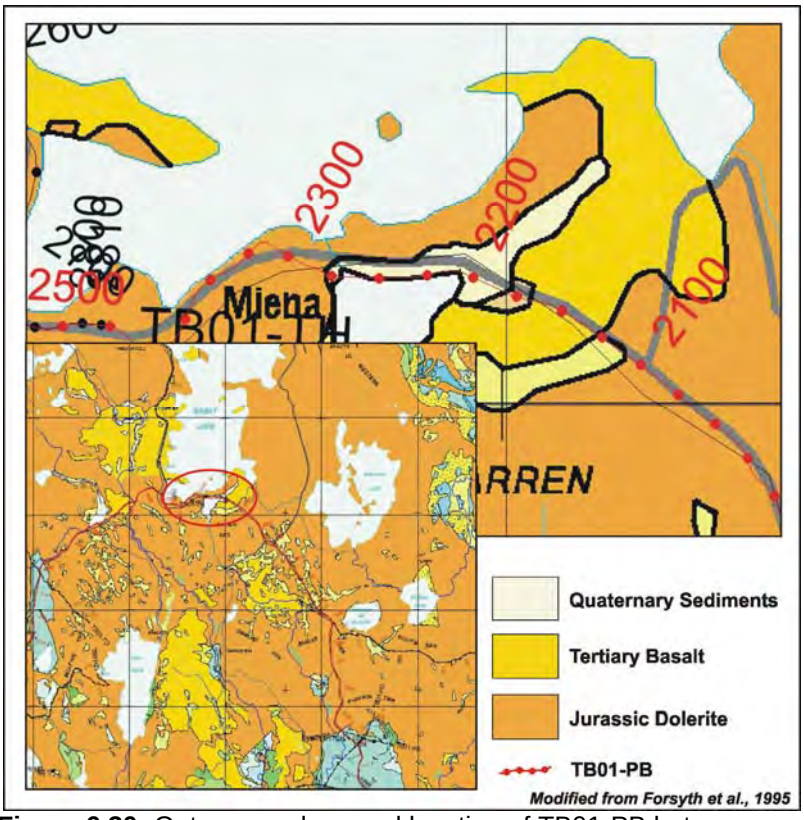

Figure 6.30: Outcrop geology and location of TB01-PB between shot-points 2200 and 2350.

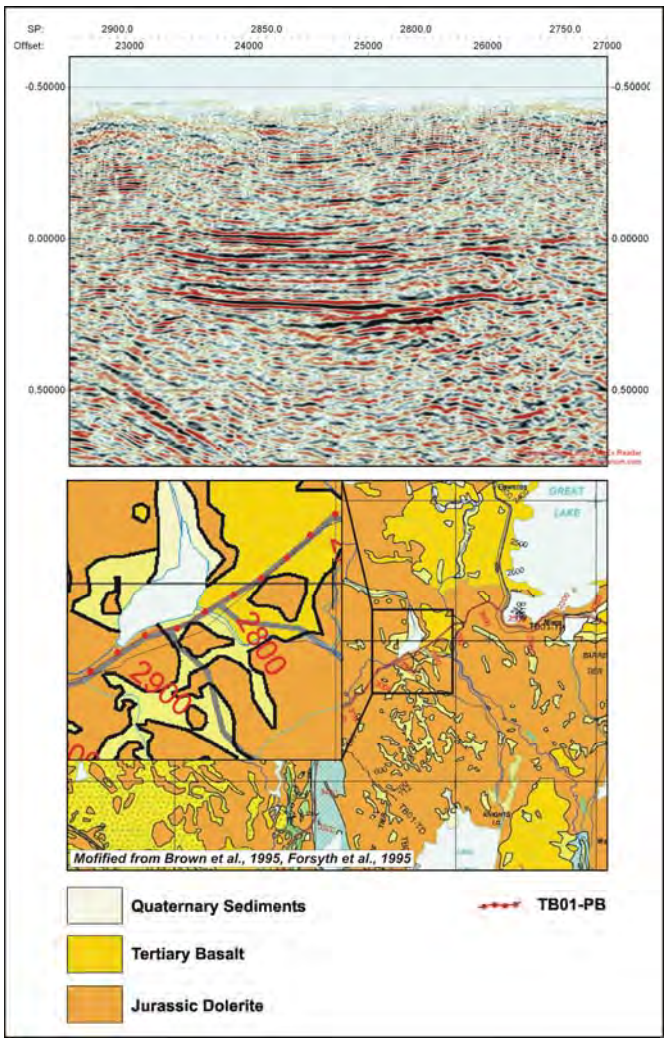

Figure 6.31: Local improvement in seismic data quality is observed at shot-point 2850 where the data is acquired over Quaternary sediments adjacent to Little Pine Lagoon.

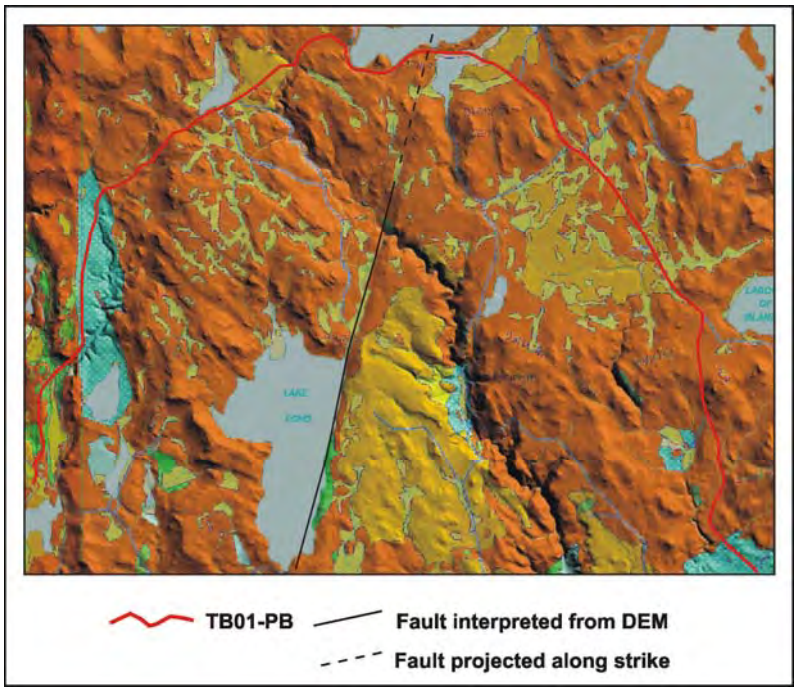

Figure 6.32: The section between shot-points 2200 and 2350 is along strike from a major fault identified on the DEM, which is not recognised in the seismic data and probably dies out before it reaches the line.

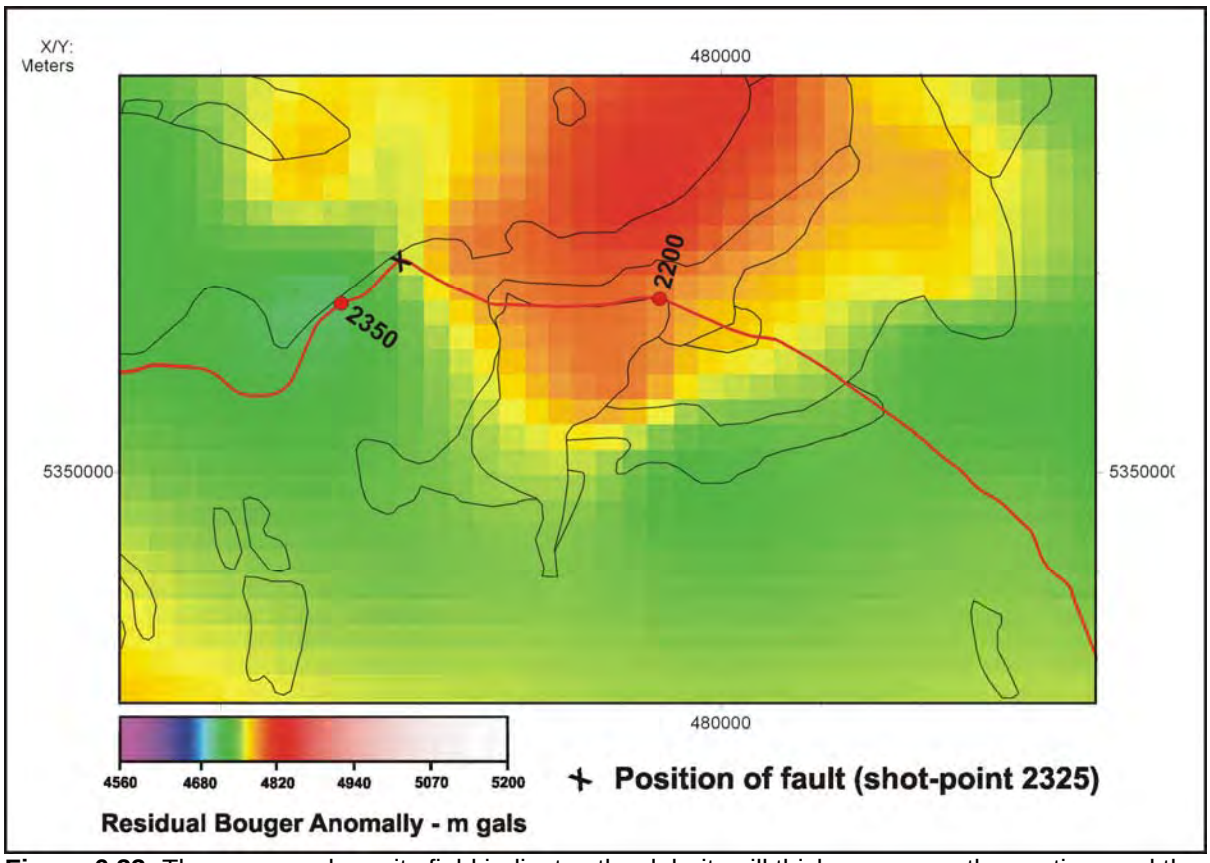

Figure 6.33: The measured gravity field indicates the dolerite sill thickens across the section, and then thins on the downthrown side of the fault interpreted at shot-point 2325 (TB01-PB).

Shot-points 2350 – 3150

(Figure 6.34)

The seismic data in the Parmeener Supergroup section contains many zones of incoherent data. From shot-points 2775 to 2875 and 2925 to 3000 the seismic data is sufficiently coherent to indicate that units within the Parmeener Supergroup are flat lying (Figure 6.34). The Base Parmeener Unconformity horizon in the east is tied to line TB01-TH (Figure 6.34). While at the western end of the section the position of the unconformity surface is easily picked between shot-points 2975 and 3100 at an intersection between flat-lying and dipping and reflections (Figure 6.34). Between the intersection with line TB01-TH and shot-point 2975 the lower part of the section contains numerous high amplitude reflections, the change in seismic character at the base of these reflections (0.25 seconds TWT) guides the placement of the Base Parmeener Unconformity horizon (Figure 6.34).

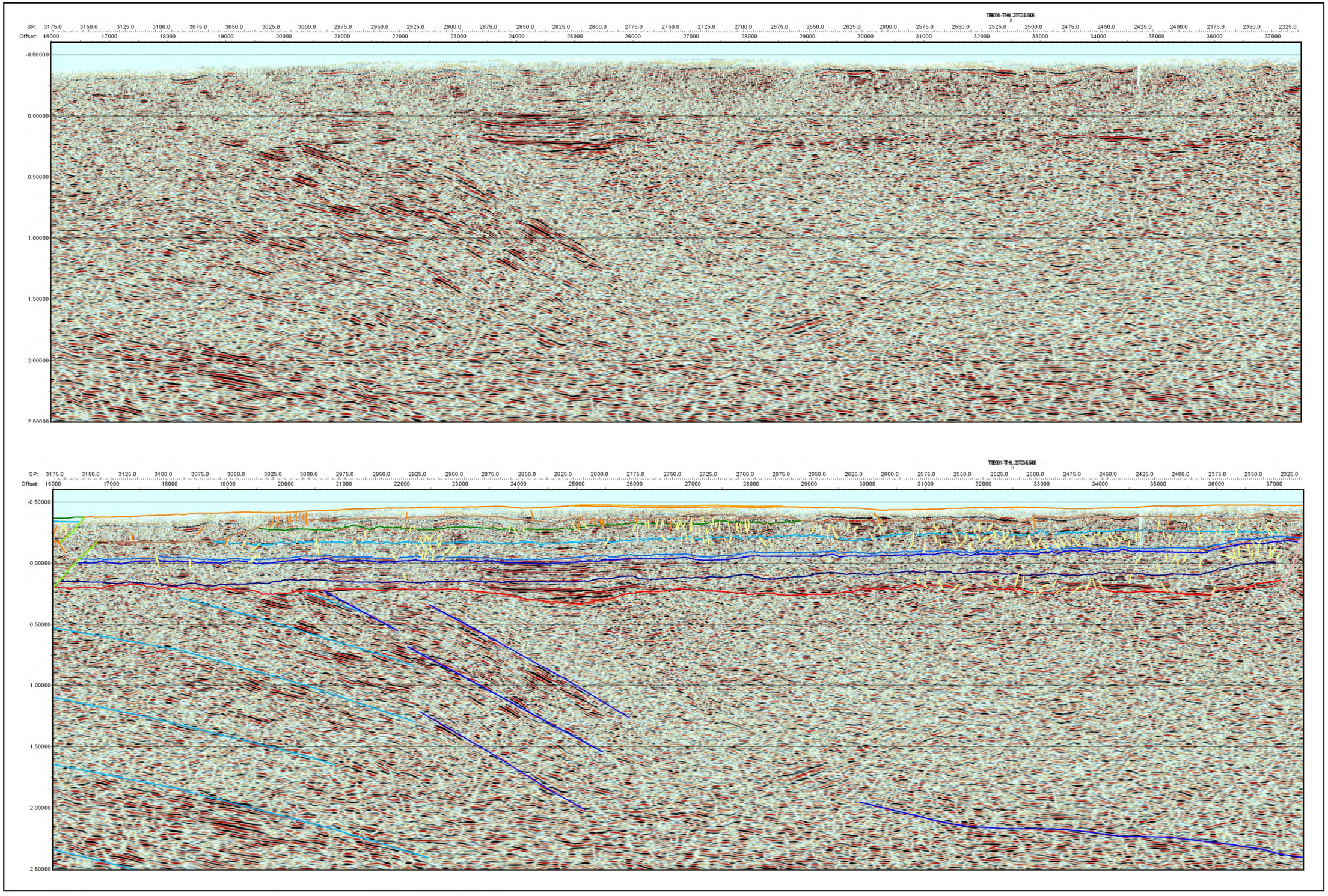

Figure 6.34: Raw and interpreted seismic data from shot-point 2350 to 3150 (TB01-PB).

Tertiary Basalt and Jurassic Dolerite outcrop along this entire section of line (Map 5.1, Figure 6.35). With the exception of the area between shot-points 2700 – 2750, the measured gravity field indicates the thickness of the dolerite remains relatively constant across the section until shot-point 3025 where it thickens rapidly (Figure 6.36). The Base Dolerite horizon is picked at the tie with line TB01-TH. The dolerite is only 350 m thick with the bottom interpreted at the base of the highly incoherent zone at the top of the section (Figure 6.34). The Base Dolerite horizon loosely follows the base of the incoherent zone, maintaining a relatively constant thickness (Figure 6.34).

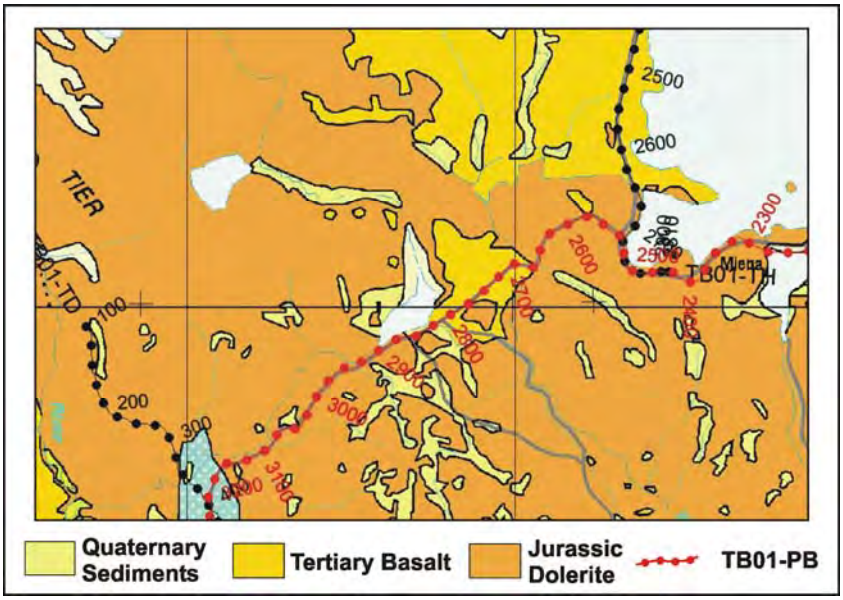

Figure 6.35: Outcrop geology and location of TB01-PB between shot-points 2350 and 3150. Modified from Forsyth et al., 1995)

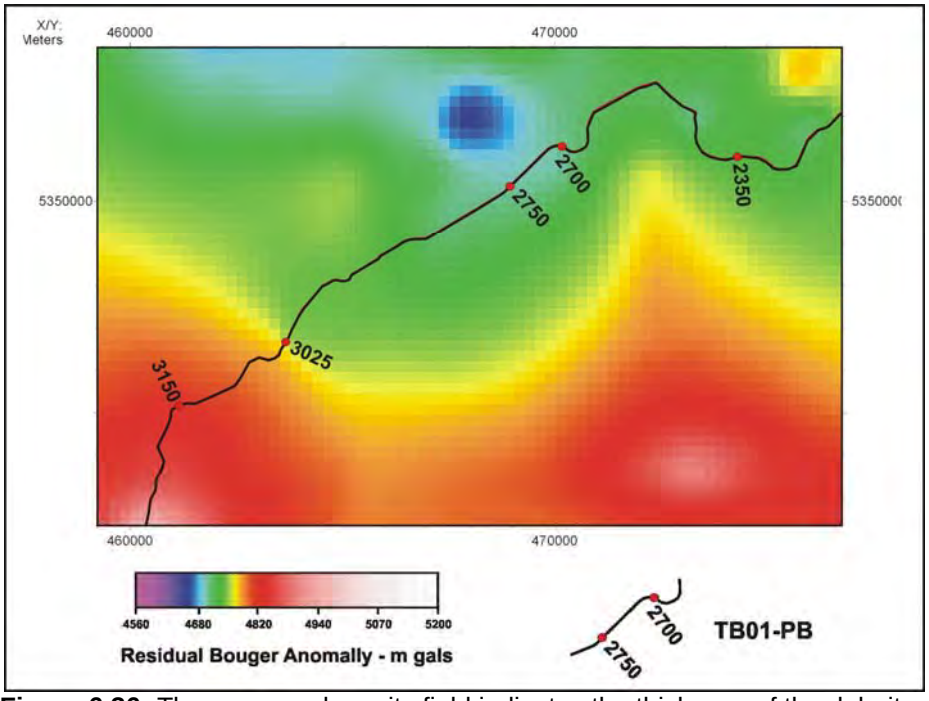

Figure 6.36: The measured gravity field indicates the thickness of the dolerite sill remains constant across the section until shot-point 3025, where it rapidly thickens.

The area between the Base Dolerite and the Base Parmeener Unconformity horizons is sufficiently thick to accommodate a 1400 m thick Parmeener Supergroup section, 900 m of Lower Parmeener Supergroup and 350 m of Upper Parmeener Supergroup (Figure 6.34). The interpretation of these horizons is based on the unit thicknesses interpreted at the southern end of line TB01-TH. The thicknesses of these units is interpreted to remain relatively constant, with the exception of the tillite unit at the base of the Parmeener Supergroup which thins from shot-point 3050 over a basement high, while the Upper Parmeener Supergroup is truncated by thickening dolerite at shot-point 3025 (Figure 6.34).

No major faults were detected in the Parmeener Supergroup in this section of line. Numerous indeterminate faults are interpreted (Figure 6.34), however the incoherent nature of the data on this section may disguise or result in the misinterpretation of many faults.

In the basement, between shot-points 2350 and 2550, events are difficult to recognise (Figure 6.34). This is probably because the road, along which the data has been acquired, winds around the southern end of Great Lake (Map 5.1, Figure 6.35). After shot-point 2650 the road heads towards the southwest and is much straighter. Between shot-points 2700 and 3150 a series of high amplitude reflections, dipping relatively steeply towards the northeast are observed in the basement (Figure 6.34).

Shot-points 3150-3500

(Figure 6.37)

This section of the line tends more towards the south, crossing another “window” in the outcropping dolerite between shot-points 3150 and 3500 (Figure 6.38). Between shot-points 3150 and 3200, the dolerite sill steps up across a fault (Pre-Jurassic “Intruded”) by 500 m to the surface (Figure 6.37). The boundary between the Upper Marine Sequence rocks and the outcropping dolerite is linear supporting the presence of the fault (Figure 6.39). This fault probably had normal offset prior to the intrusion of dolerite. Several Undifferentiated Tertiary and two Pre-Jurassic faults are interpreted in the hanging wall adjacent to the main fault (Figure 6.37). The timing of these faults is uncertain, they are either associated with the original normal fault, the intrusion of the dolerite sill or a product of both.

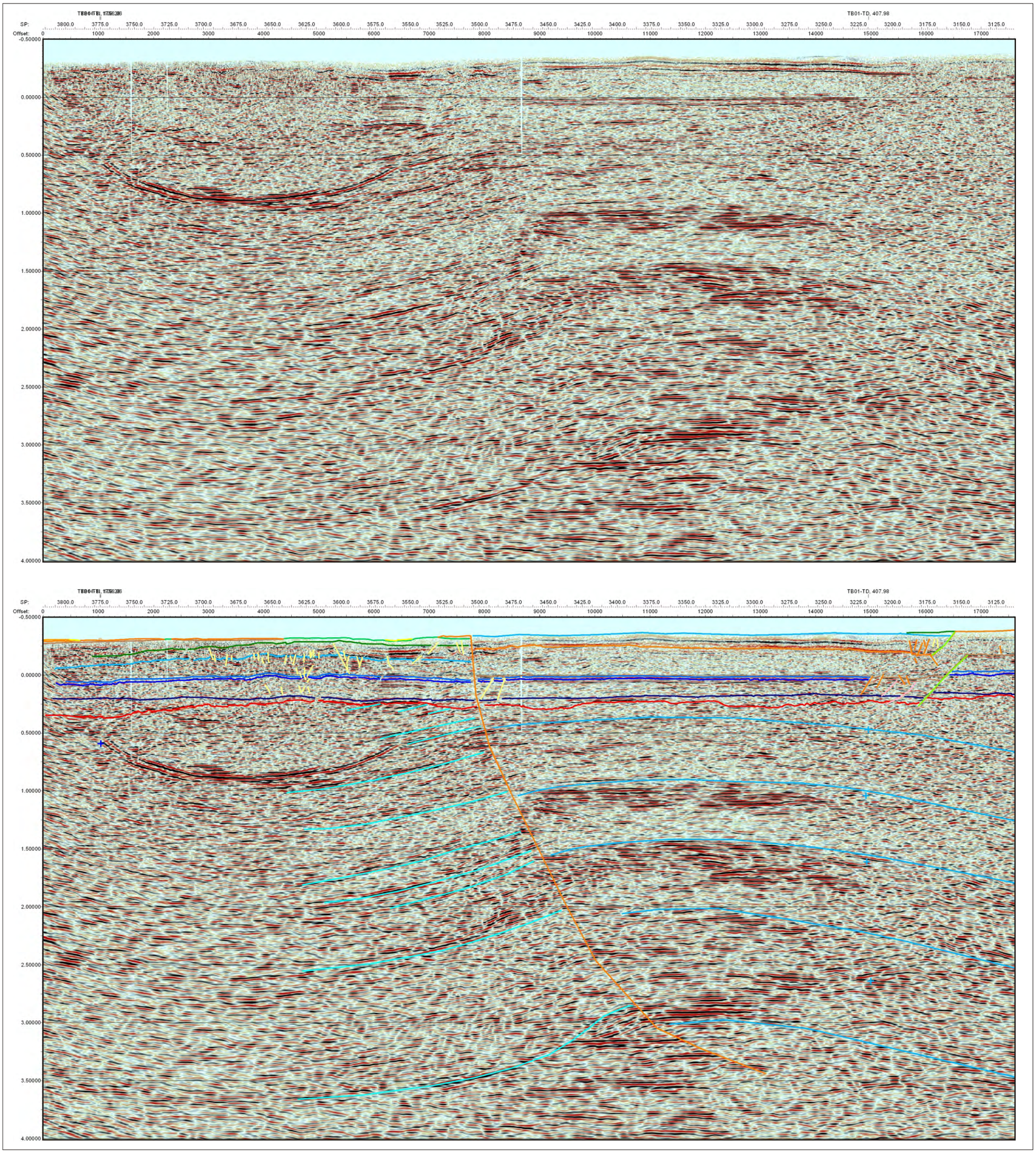

Figure 6.37: Raw and interpreted seismic data from shot-point 3150 and 3800.

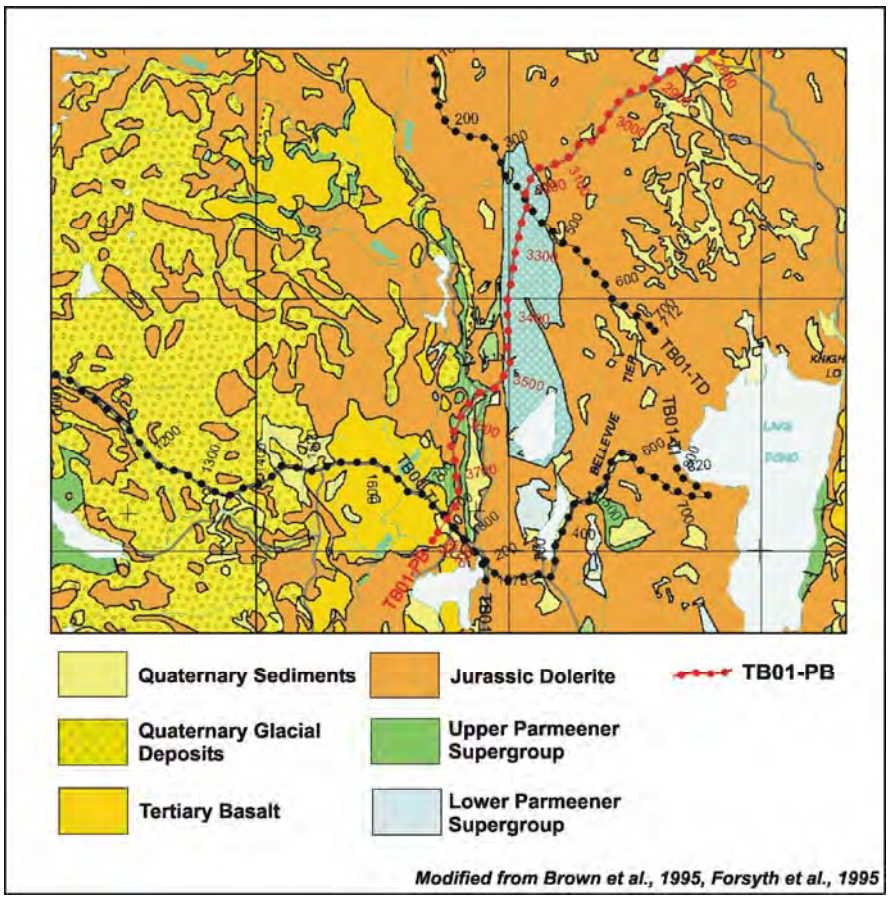

Figure 6.38: Outcrop geology and location of TB01-PB between shot-points 3150 and 3800.

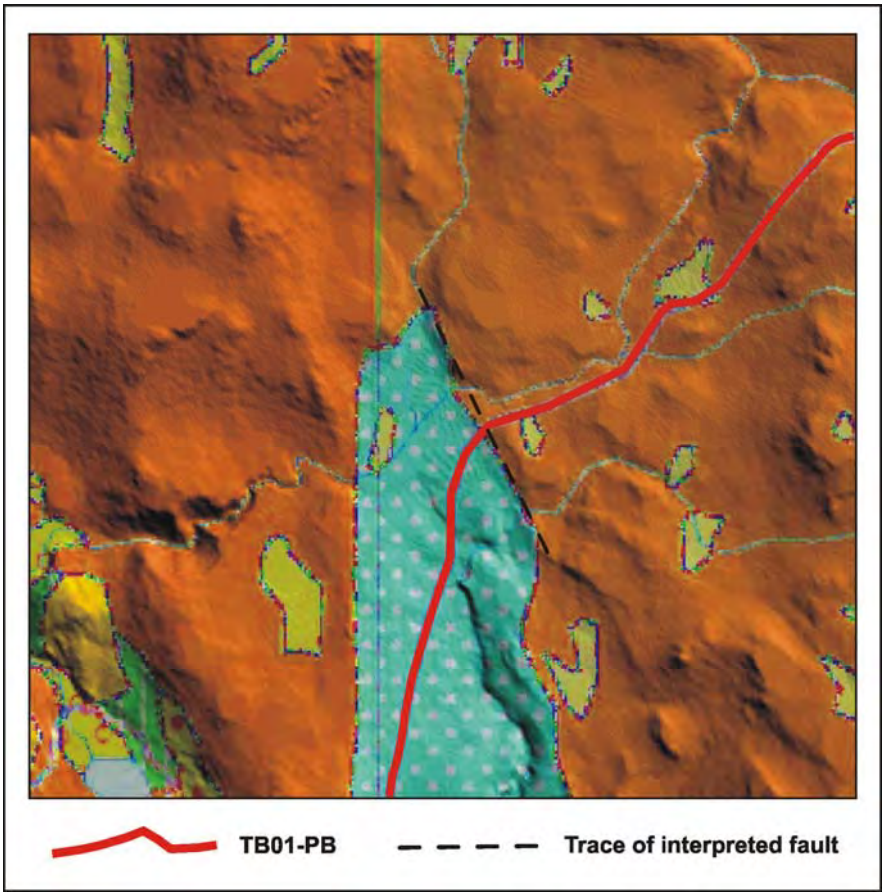

Figure 6.39: The boundary between the Upper Marine Sequence rocks and dolerite is linear suggesting the presence of the fault.

West of the Pre-Jurassic “Intruded” fault, a thin band of Unit 2 (Triassic Quartz Sandstone) outcrop is identified; however Upper Marine Sequence rocks outcrop in the “window” between shot-points 3150 and 3500 (Figure 6.38). Here the dolerite sill lies 250 m below the surface and is interpreted to have intruded near or along the contact between Upper Marine and Lower Freshwater sequences (Figure 6.37). The sill thickens towards the west, reaching a maximum thickness of 800 m at shot-point 3425 (Figure 6.37). The Top Dolerite horizon is picked at a strong (high amplitude) positive reflection (black), easily identified at -0.2 seconds TWT at shot-point 3200 (Figure 6.37). This reflection can be reliably followed to shot-point 3450, after which the interpretation becomes more difficult (Figure 6.37). Reflections within the dolerite sill are typically weak and incoherent, allowing the Base Dolerite horizon to be reliably picked at a negative to positive zero-crossing event at the base of this incoherent zone (Figure 6.37).

The location of Lower Freshwater and Lower Marine Sequence horizons southwest of the Pre-Jurassic “Intruded” fault between shot-points 3150 and 3200 is based on their positions below the Upper Marine Sequence horizon northeast of the same fault (Figure 6.40). The resulting interpretation places the Lower Freshwater and Lower Marine Sequence horizons just above the dolerite between shot-point 3175 and 3200, and after shot-point 3225, below the south-westerly thickening sill (Figure 6.37).

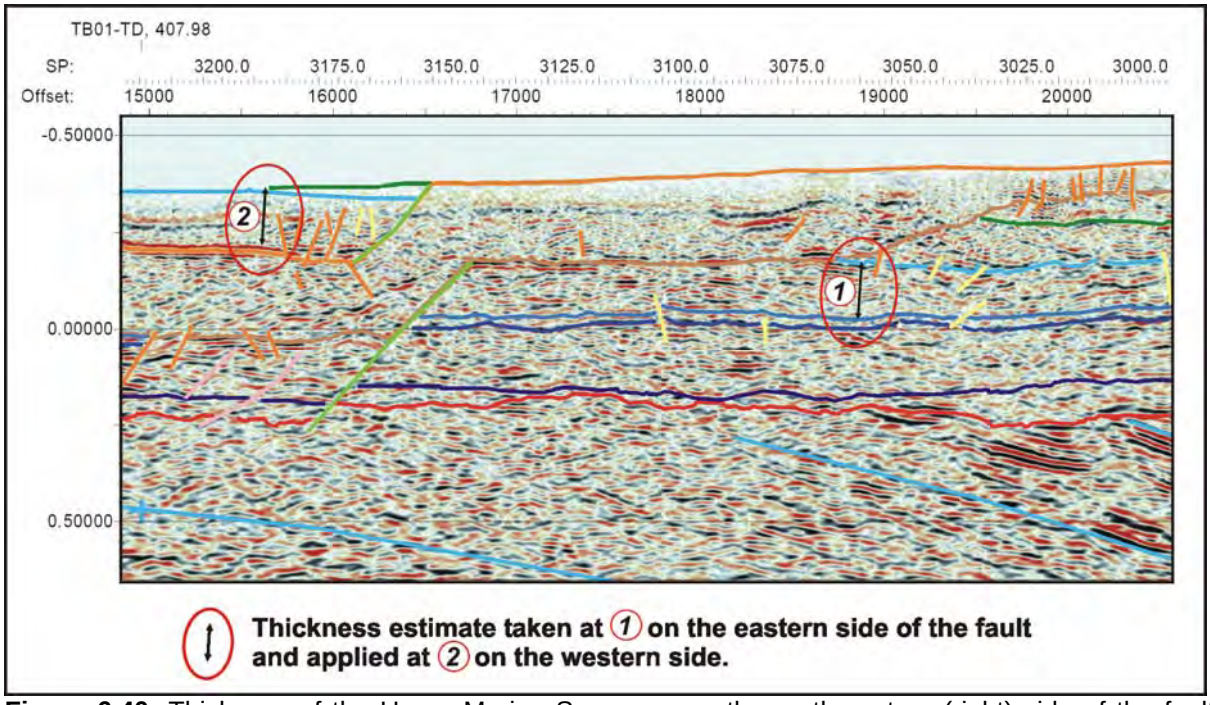

Figure 6.40: Thickness of the Upper Marine Sequence on the north-eastern (right) side of the fault used to interpret the position of horizons to the southwest (TB01-PB).

The position of the Base Parmeener Unconformity horizon is difficult to pick in this section. Reflections in the basement are sub-parallel with those of the Parmeener Supergroup section, consequently there is no intersections to guide the placement of the horizon, nor is there a distinctive change in seismic character evident (Figure 6.37). The position of the horizon in this section of line relies on the estimated thickness of the Lower Freshwater, Lower Marine and Tillite sequences picked on the eastern side of the fault at shot-point 3150. These thicknesses are applied to the sequence on the western side of the fault, assuming that the dolerite sill has intruded at the contact between the Upper Marine Sequence and Lower Freshwater Sequence (Figure 6.37).

Shot-points 3500-3800

(Figure 6.37)

The geometry of the contact that forms the boundary between dolerite and the Lower Parmeener Supergroup on the western side of the window (between shot-points 3500 and 3525) is very difficult to decipher (Figure 6.37). The seismic data between shot-points 3500 and 3550 is poor, making identification of faults and horizons west of the contact difficult. Literature accompanying 1:63 360 scale geological mapping indicates that this contact forms the boundary between the simple geometry of a single dolerite sill intruding the Parmeener Supergroup to the east in the Central Highlands, and a more complex relationship between the dolerite and the Parmeener Supergroup to the west (Gulline et al., 1963). Immediately west of the contact Gulline (1963) reports complex and numerous dolerite intrusions that have left isolated patches and probably rafted blocks of sedimentary rocks, the position of these in the overall Triassic section cannot be accurately ascertained. To the north in the Du Cane quadrangle, the Parmeener Supergroup and dolerite have been disturbed by north to northwest trending, steeply dipping normal faults that are probably Tertiary in age (Macleod et al., 1961). The displacement along this contact is thought to be the continuation of the Great Pine Tier uplift (Gulline et al., 1963) (Figure 6.41), itself interpreted as a continuation of a fault, downthrown to the west, that traverses the Mersey Valley. Locally the contact strikes north – south, and is linear (Figure 6.42). The mapped units in the “window” are Late Permian, Upper Marine Sequence, these lie 100 m higher than the Late Triassic Unit 4 (?Brady Formation (Gulline et al., 1963)) mapped in the valley to the west (Figure 6.42). An incised creek on the eastern side of the contact indicates that the uplift of that side has been relatively recent (Figure 6.42).

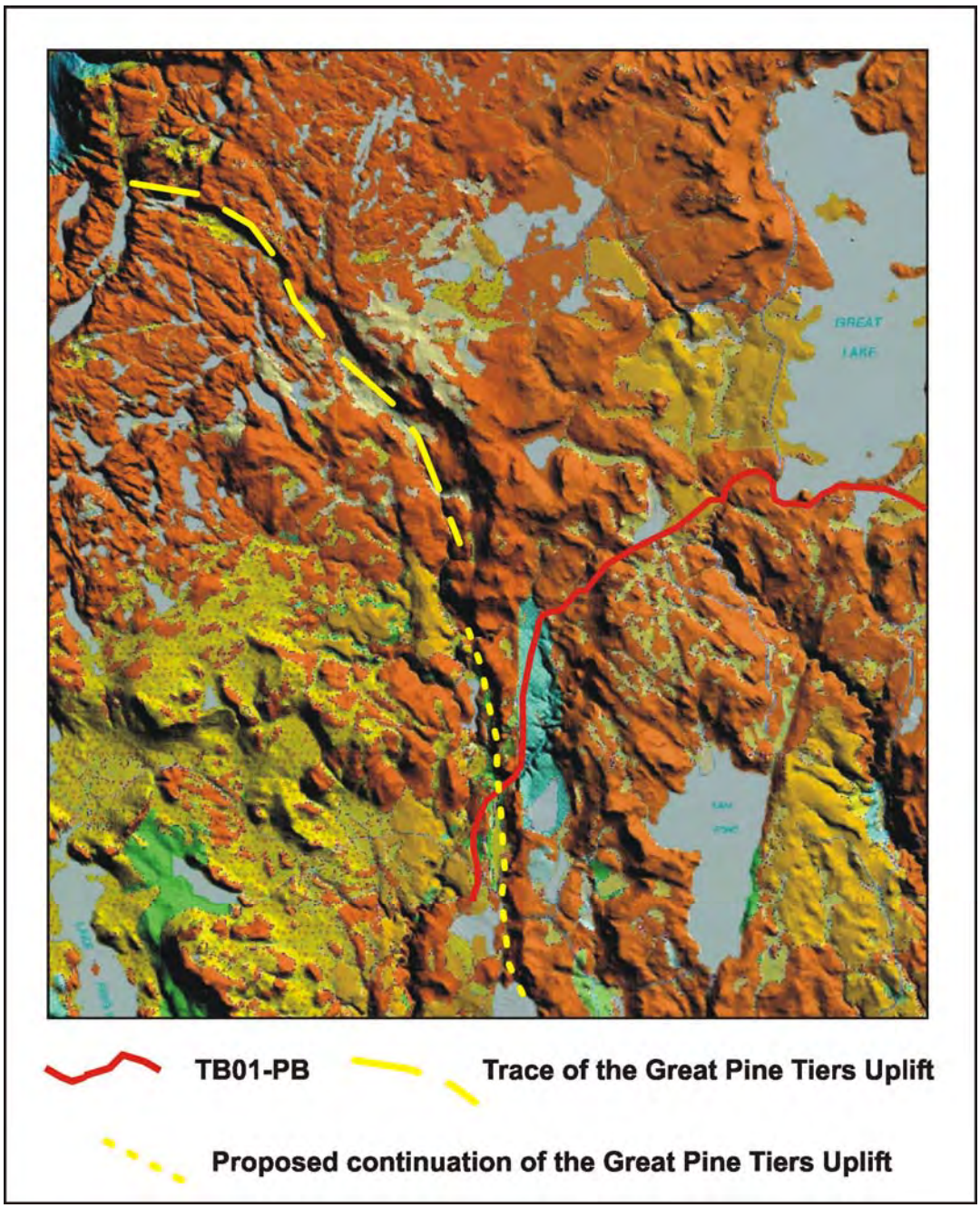

Figure 6.41: Location of the proposed continuation of the Great Pine Tiers Uplift.

The seismic data from shot-point 3500 to the end of the line is variable. Between shot-point 3500 and 3530 the data is quite vague, the data improves until shot-point 3600, before becoming very poor and difficult to interpret with confidence to the end of the line (Figure 6.37). The vagaries of the data, complicated by intruding dolerite, allows for a number of different interpretations of the contact between Upper Marine Sequence and dolerite at shot-point 3500. Previous interpretations of faulting in the Du Cane and St. Clair quadrangles indicate that the block between Bronte Park and Lake St. Clair is down thrown by 450 m (Gulline et al., 1963).

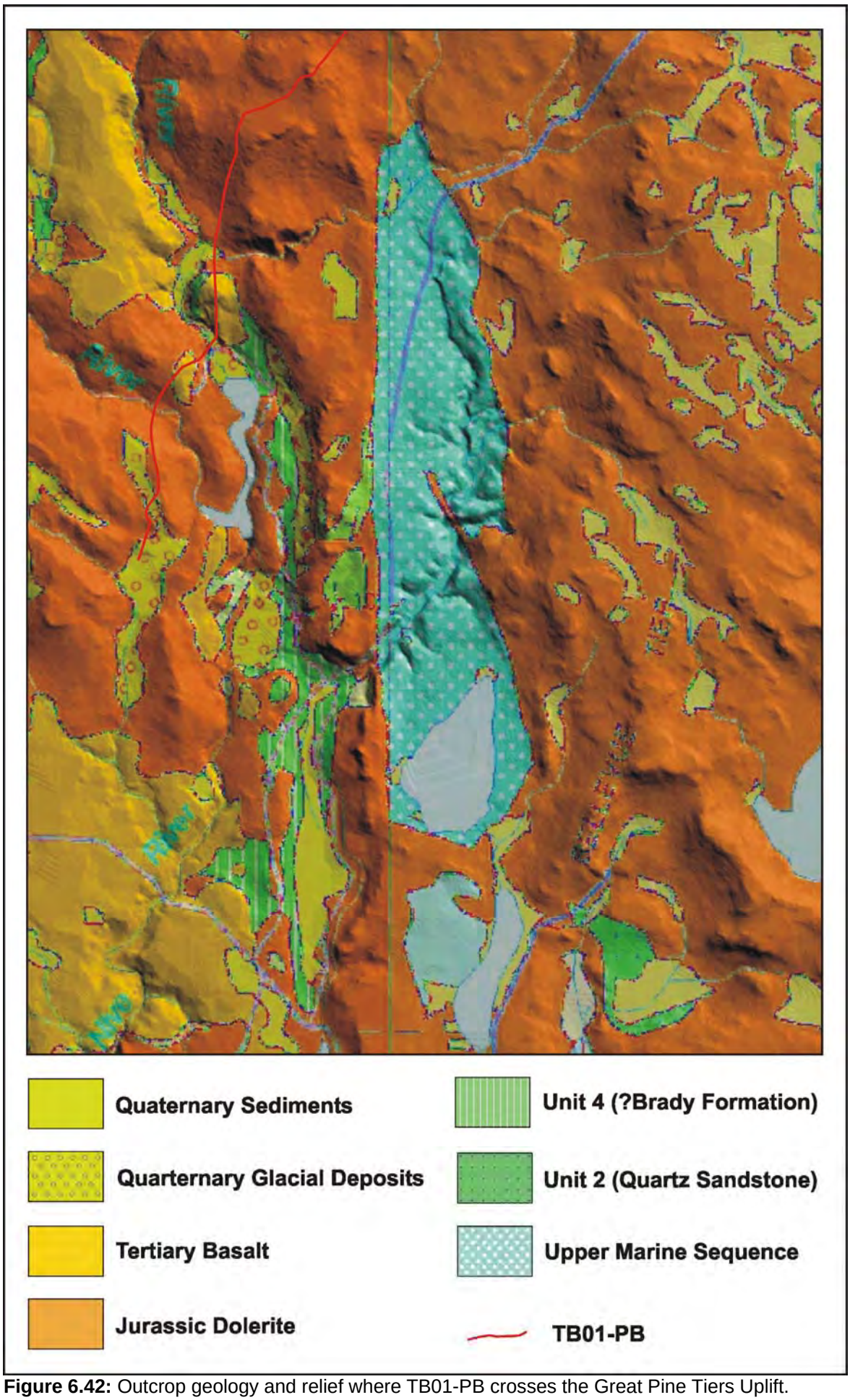

Figure 6.42: Outcrop geology and relief where TB01-PB crosses the Great Pine Tiers Uplift.

The interpretation provided here is the simplest, honouring both the seismic and outcrop data. The contact is interpreted to result from a major west-dipping fault, starting at the boundary between the Upper Marine sequence and the dolerite and following an intersection between dipping and flat lying reflections in the basement, terminating at 3.50 seconds (Figure 6.37). The Base Parmeener Unconformity horizon can be reliably interpreted to the southwest of the fault where flat-lying and dipping reflections intersect (Figure 6.43). If the thickness of the Parmeener Supergroup units (minus the dolerite sill) has not changed dramatically since shot-point 3000, then contrary to the interpretation of Gulline (1963) the dolerite is thin to the west of the fault. A 100 m thick remanent, identified outcropping between 3500 and 3550 at the top of the section is the only dolerite recognised in this interpretation (Figure 6.37). Assuming that the dolerite on either side of the fault results from a single sill, then the footwall must have been downthrown by 800 – 1000 m at the time dolerite was intruded (Figure 6.44, A and B). The fault was subsequently reactivated bringing the Triassic rocks in the footwall to the surface (Figure 6.44, C). Finally, there must have been some recent uplift of the footwall by 50-80 m to account for the incised creek on the eastern side of the fault (Figure 6.42). From shot-point 3600 to the end of the line the Parmeener Supergroup horizons are extrapolated from the picks between shot-point 3500 to 3600 to the tie with line TB01-TB (Figure 6.37). A more complex interpretation could be made with a dolerite dyke at the boundary, however, it is difficult to reconcile such a structure with the seismic data.

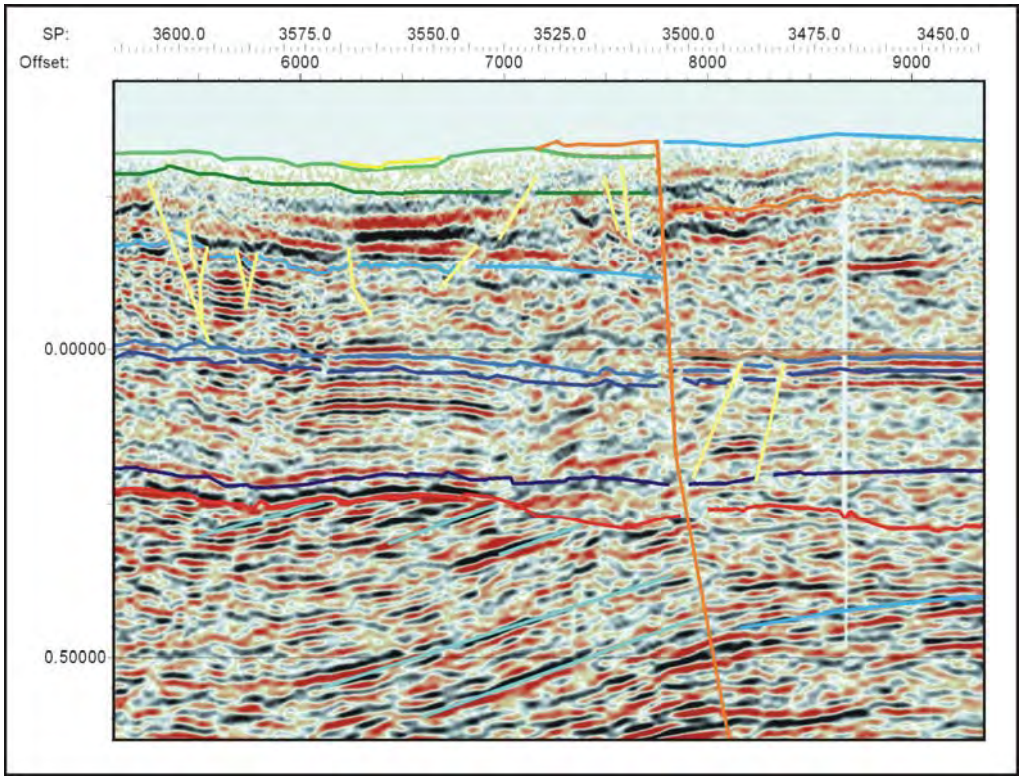

Figure 6.43: The Base Parmeener Unconformity horizon can be reliably interpreted to the southwest of the fault where flat-lying and dipping reflections intersect (TB01-PB).

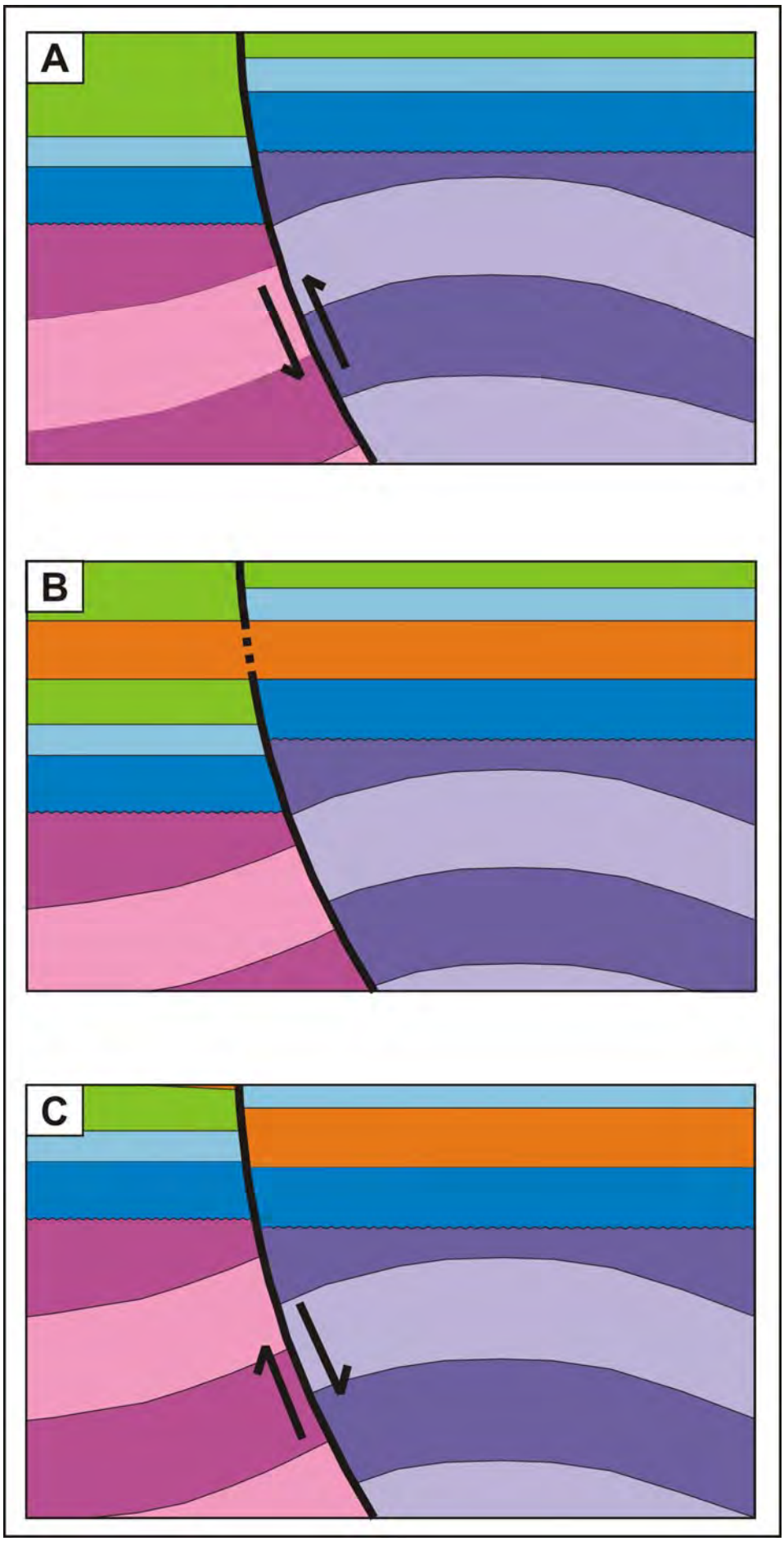

Figure 6.44: Cartoon describing the movement history of the Undifferentiated Tertiary Fault described at shot-point 3500 on TB01-PB.

Shot-points 2800 – 3800 (Basement)

(Figure 6.45)

Between shot-points 2800 and 3800, numerous dipping reflections are identified within the basement (Figure 6.45). The interpretation shows a group of steeply dipping events (dark blue) between shot-point 2800 and 3000 and a faulted anticline (light blue and cyan) between shot-points 3000 and 3650 (Figure 6.45). The road along which the data has been acquired is relatively straight, from shot-points 2600 to 3150 the line turns towards the southwest, turning more towards the south-southwest between shot-points 3150 and 3500, then back towards the southwest until the end of the line (Figure 6.46).

Events within the basement are picked at changes of seismic character. The steeply dipping events, shown in dark blue between shot-point 2800 and 3000 are picked at a change from incoherent, confused reflections to coherent, higher amplitude reflections (Figure 6.47). These events truncate the light blue events of the anticline. The events in the hanging-wall of the anticline (shot-points 3000 – 3500, light blue) are picked at the boundary between incoherent, weak reflections and sets of coherent, high amplitude reflections in the crests of the interpreted anticlines. The boundary indicates a small amount of rollover to the left and more extensive rollover to the right. To the right the interpreted events are extrapolated, following the trend of the most confidently picked event. The best example of the pick for this event is seen at 1.4 seconds TWT (Figure 6.48).

Changes in character in the footwall section of the anticline are more subtle than those in the hanging wall (Figure 6.45), and events are picked on laterally coherent reflections. There are no obvious similarities in seismic character across the fault that would indicate events interpreted in the hanging wall have direct equivalents in the footwall i.e. individual beds cannot be traced across the fault, therefore throw cannot be estimated. The fault through the anticline is interpreted to pass through the point where the events in the hanging wall can no longer be traced. At this point events to the right appear convex up, while events to the left are more concave (Figure 6.45). Between shot-points 3550 and 3790, a distinctive “smile” is observed in the seismic data at 0.75 seconds TWT (Figure 6.37). This feature is not an artefact, as a similar feature can be seen in the same position in the data along strike on line TB01-TD between shot-points 100 and 225 (Figure 6.91).

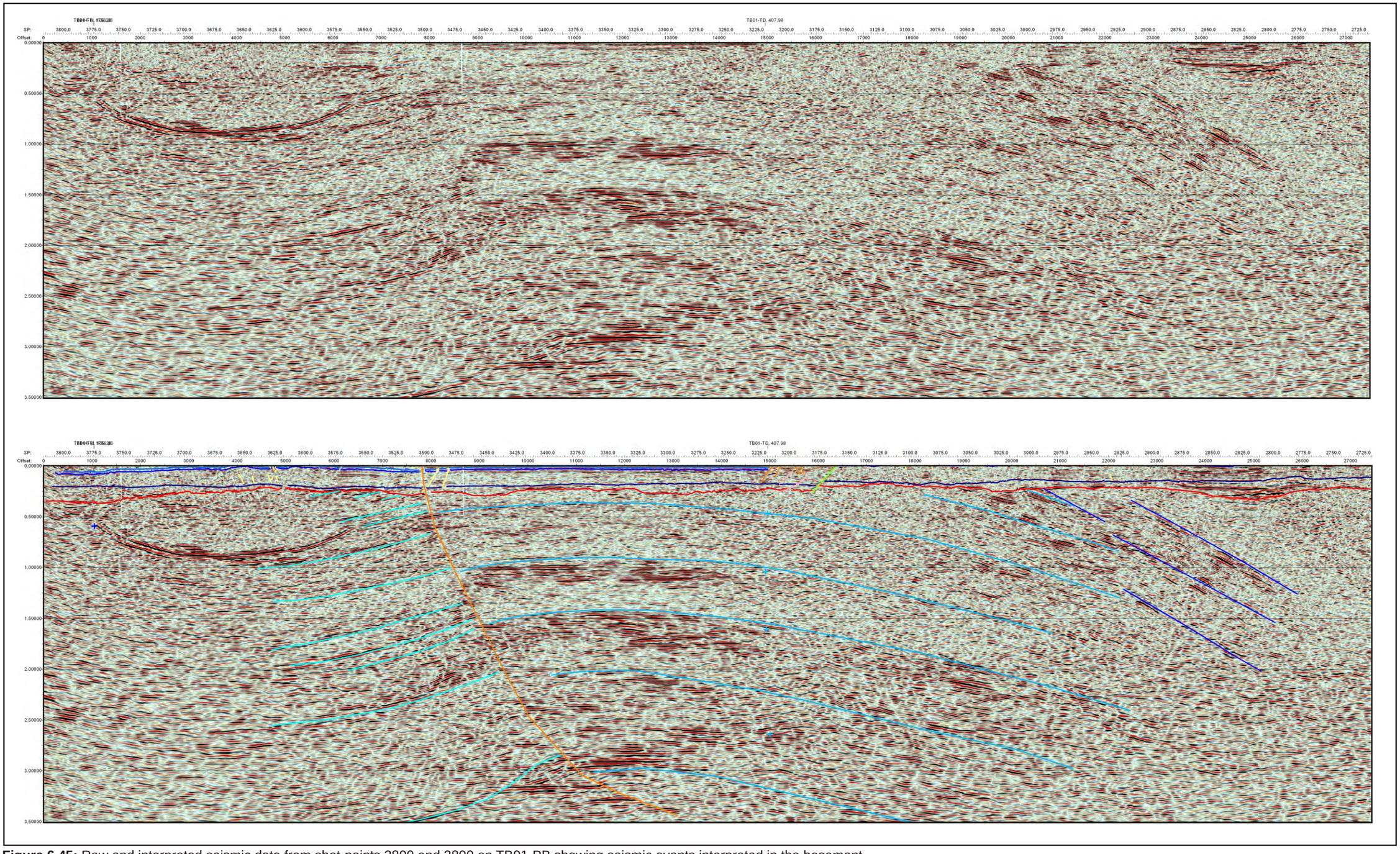

Figure 6.45: Raw and interpreted seismic data from shot-points 2800 and 3800 on TB01-PB showing seismic events interpreted in the basement.

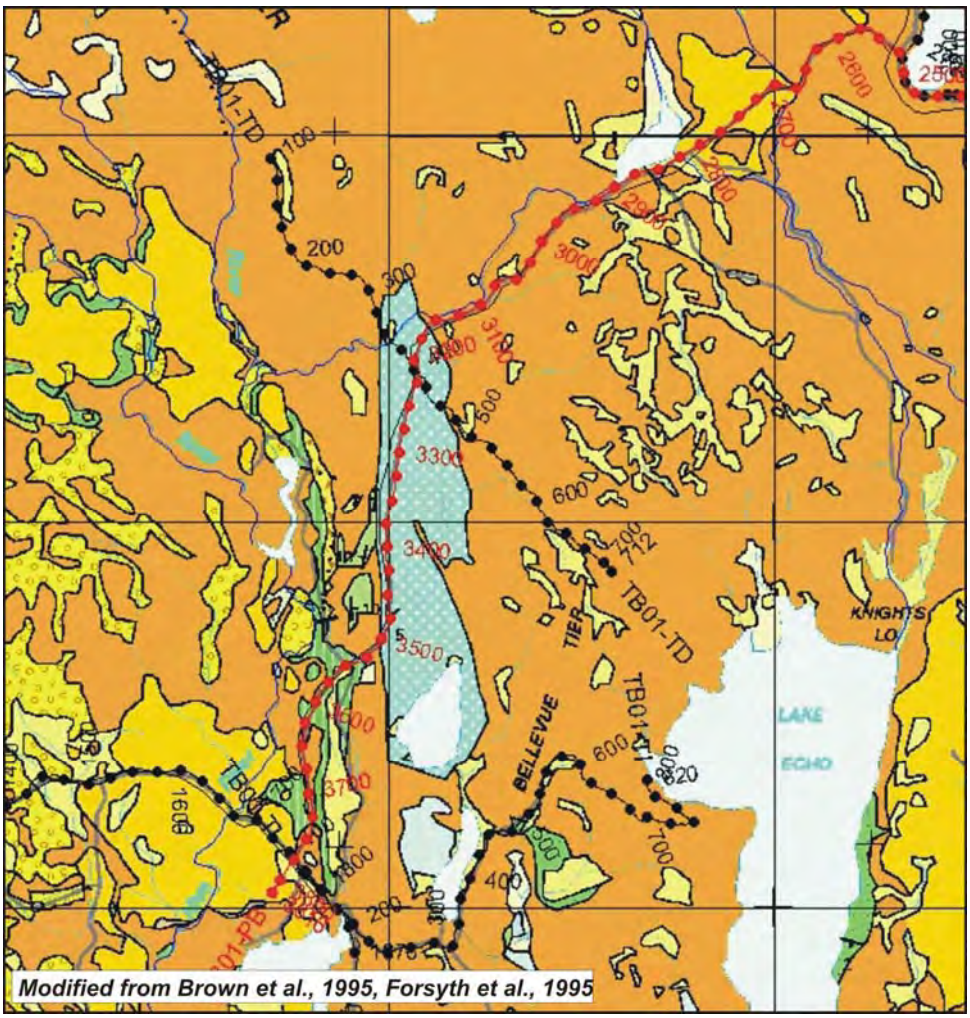

Figure 6.46: Orientation of TB01-PB between shot-points 3150 and 3500.

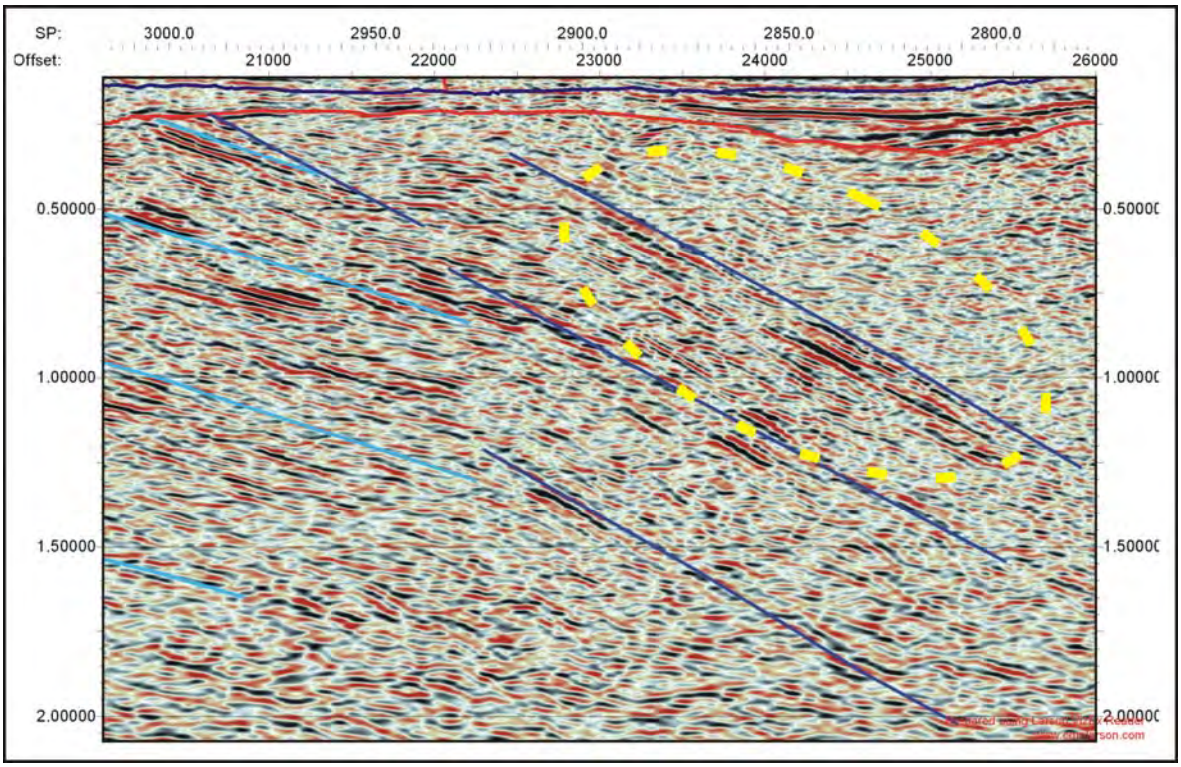

Figure 6.47: Events within the basement are picked at changes of seismic character. The steeply dipping events, shown in dark blue between shot-point 2800 and 3000 are picked at a change from incoherent, confused reflections to coherent, higher amplitude reflections (TB01-PB).

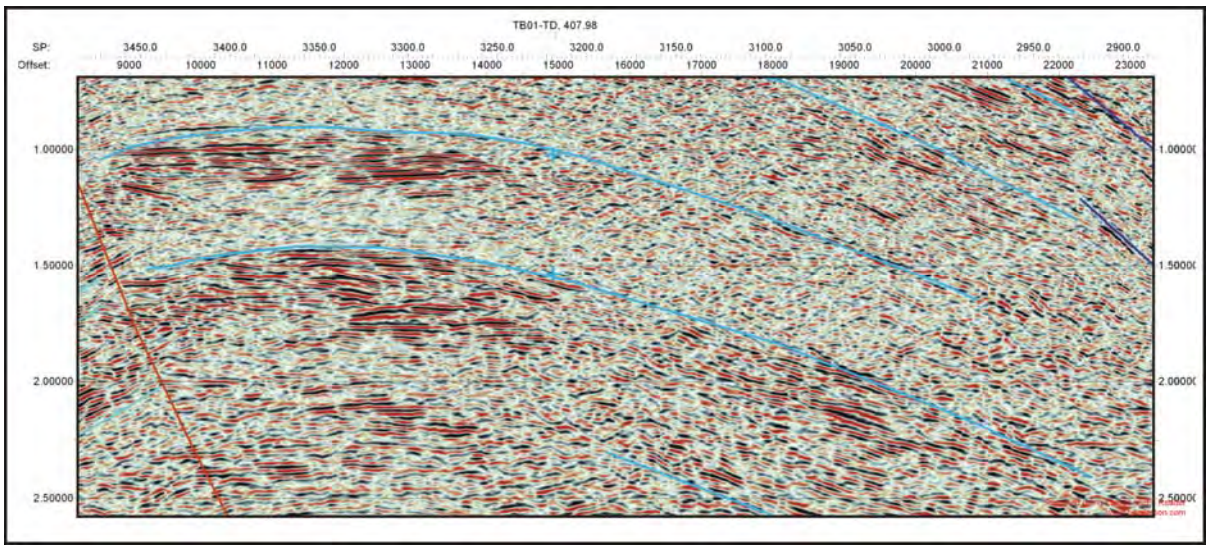

Figure 6.48: Seismic events picked in the hanging wall of the Bellevue Anticline (TB01-PB).

6.2.3: TB01-PD

Seismic line TB01-PD has been acquired across the window in the outcropping dolerite (Map 5.1, Figure 6.49). The line is 11.93 km in length and has been recorded roughly in a southwest to northeast direction. The line begins adjacent to Howells Sugarloaf (489 779 mE, 5 319 321 mN) and heads towards the northeast along Southernfield Road, across private property and along Glovers Road, finishing near Shannon Tier (495 465 mE, 5 329 313 mN) (Map 5.1, Figure 6.49).

The line has been acquired over a variety of outcropping lithologies. Starting at shot-point 142 on dolerite the line crosses onto Unit 2 (quartz sandstone) of the Upper Parmeener Supergroup at shot-point 150 (Figure 6.49). The line crosses into the Upper Marine Sequence of the Lower Parmeener Supergroup at shot-point 225, crosses over a tongue of dolerite between shot-points 520 and 538 and out of the "window" into the area dominated by dolerite at shot-point 575 until the end of the line at shot-point 620 (Figure 6.49). The line is straight and the overall quality of the seismic data is reasonable. The interpretation is well constrained by ties with lines TB01-PA, PB and TA. However, where the line crosses from Parmeener Supergroup sediments to dolerite the data is degraded. Whether this is a result of lithology change or from complex structures at these boundaries is not clear, consequently the geometry of these contacts is very difficult to interpret.

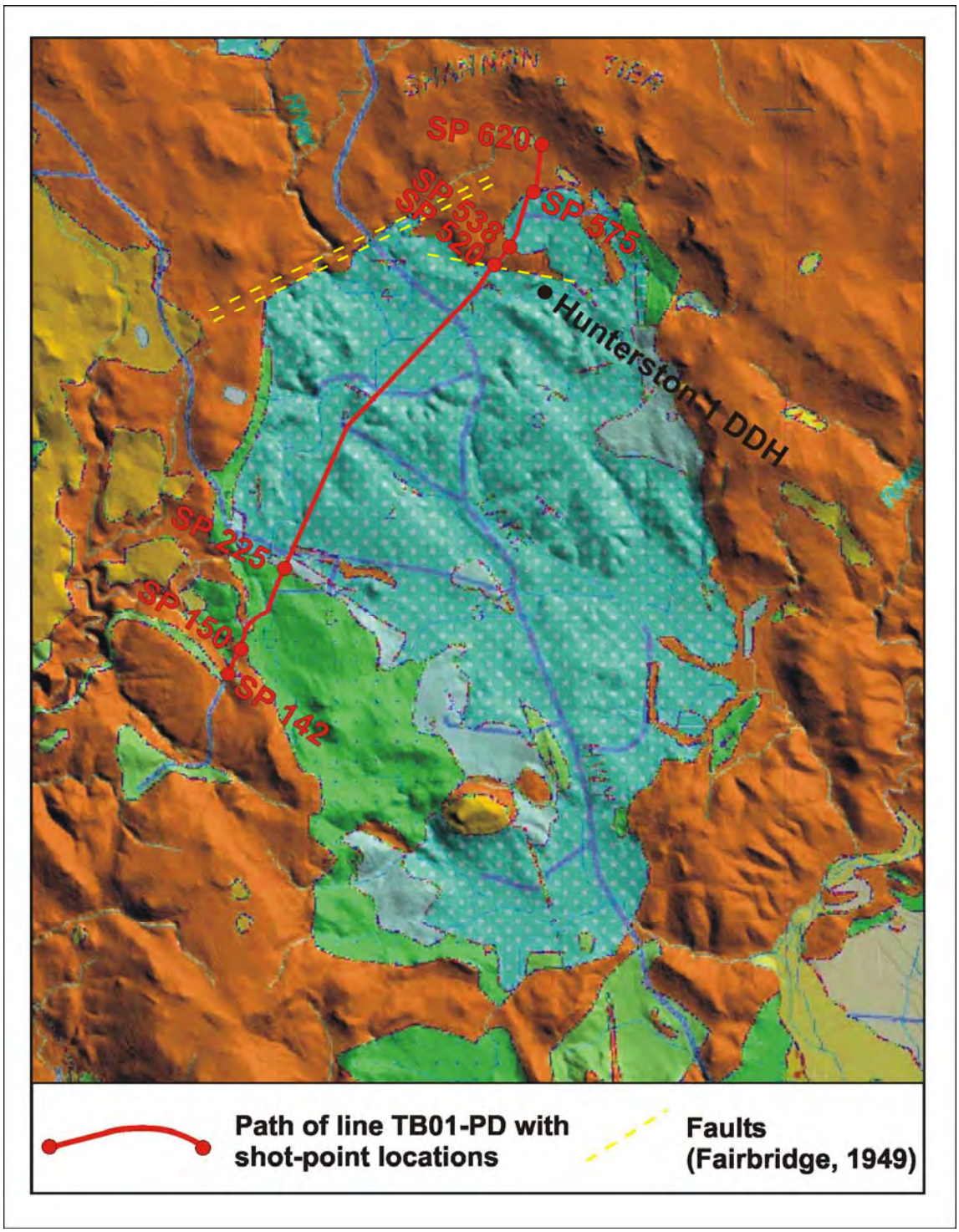

Figure 6.49: Outcrop geology and location of TB01-PD.

Shot-points 142 – 250

(Figure 6.50)

This section of line crosses the south-western boundary of the "window" between shot-points 150 and 250. In outcrop the boundary appears complex and in section the dolerite sill moves from 450 m below the surface to outcrop over a distance of 1 km (Figure 6.50). However, the seismic data here is quite poor, making it difficult to resolve the nature of the relationship between the Parmeener Supergroup and the dolerite sill across this contact (Figure 6.50).

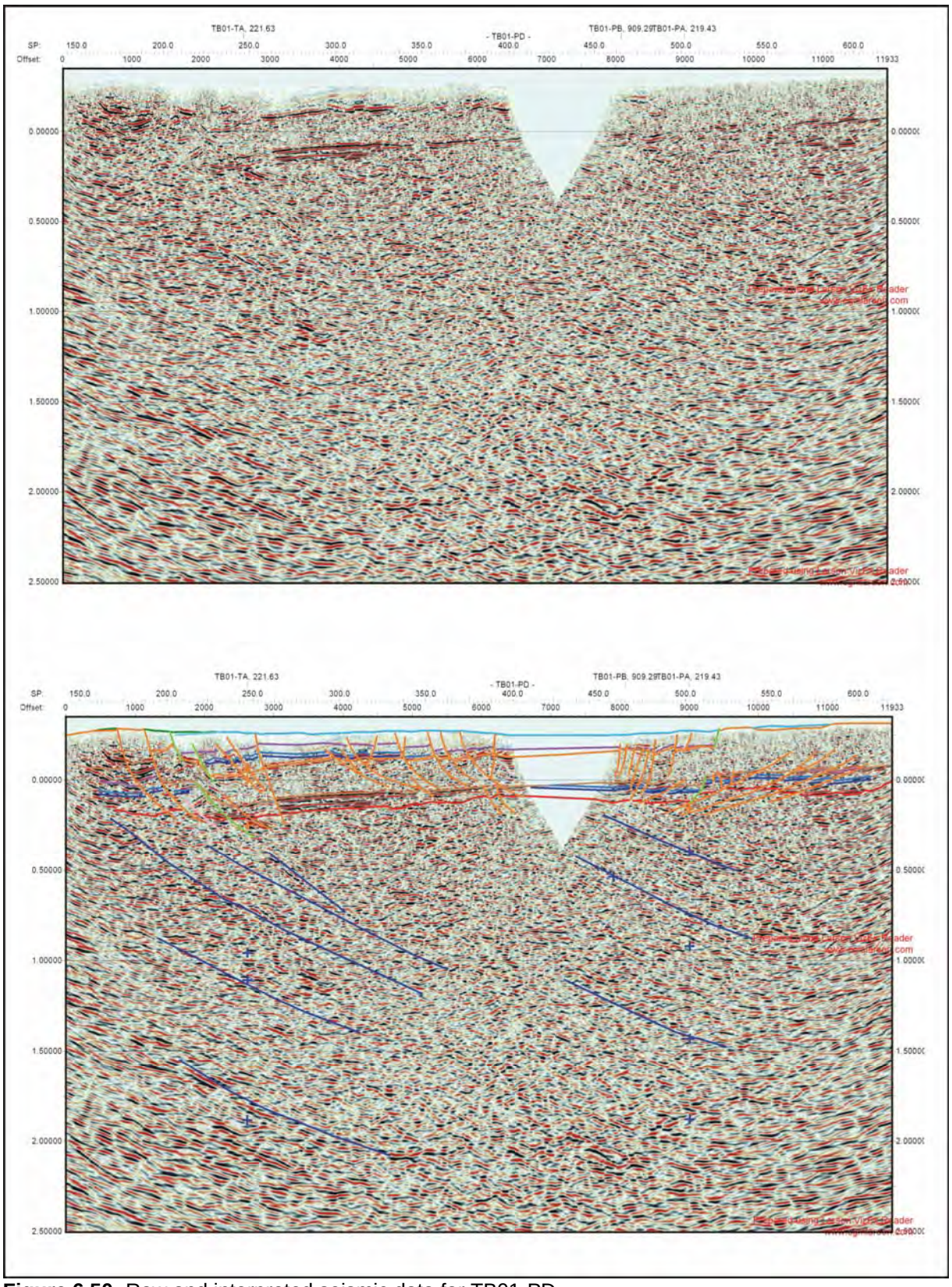

Figure 6.50: Raw and interpreted seismic data for TB01-PD.

The interpretations of the Parmeener Supergroup horizons in this section of the line are constrained by the tie to TB01-TA (Figure 6.65) and the better quality data north (right) of shot-point 250. The Base Parmeener Unconformity horizon is well constrained north of shot-point 250 at the base of a series of laterally coherent, strong reflections, similar reflections are

identified between shot-points 200 and 250 (Figure 6.50). The base of these reflections correlates with the pick for the horizon on line TB01-TA (Figure 6.50). The picks for the Top Dolerite and Base Dolerite horizons can be made reliably between shot-points 225 and 250. The Top Dolerite horizon is picked at a high amplitude, negative reflection, while the Base Dolerite horizon is picked on a negative to positive zero-crossing event (Figure 6.50). In between these two picks are weak, incoherent reflections, typical of the intra-dolerite character. The positions of the other Parmeener Supergroup horizons are primarily based on maintaining the thicknesses constrained by the tie with line TB01-TA.

Several major north-dipping faults are interpreted in this section of line (Figure 6.50). The main faults influencing the position of the dolerite are interpreted as Pre-Jurassic "Intruded" faults. Here the dolerite sill has stepped upwards through section by ~400 m across the faults from intruding the Lower Marine Sequence (Lower Parmeener Supergroup) to the north (right) of the faults zone to intrude Unit 2 of the Upper Parmeener Supergroup to the south (left) of the faults (Figure 6.51).

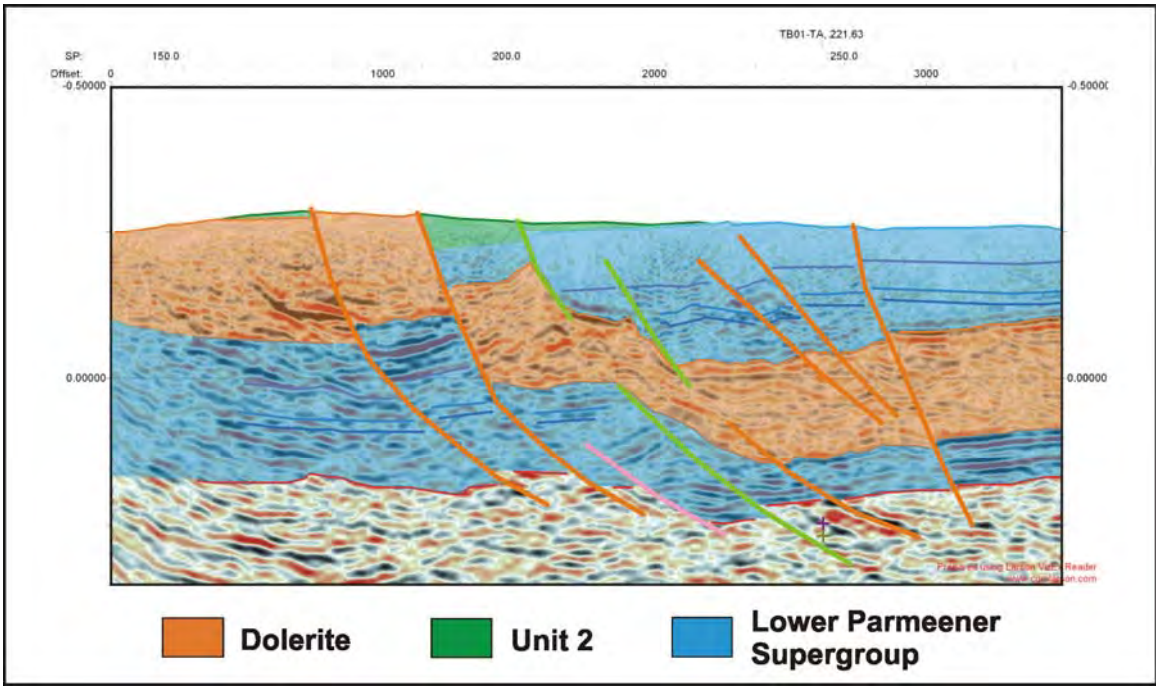

Figure 6.51: Path of the dolerite sill across the faults interpreted between shot-point 160 and 225 (TB01-PD).

To the south (left of section) of the Pre-Jurassic "Intruded" faults, two Undifferentiated Tertiary faults are interpreted penetrating through to the basement (Figures 6.50, 6.51). The interpretation of these faults has been made to account for the alternating Unit 2 and dolerite outcrops between shot-points 150 and 200 (Figure 6.50). However, there is little evidence in the degraded seismic data to support this interpretation

North (right of section) of the Pre-Jurassic “Intruded” faults a series of Undifferentiated Tertiary faults are interpreted (Figures 6.50, 6.51). The two smaller faults account for offsets in the Parmeener Supergroup and the top of the dolerite sill (Figures 6.50, 6.51). The northern most fault, which also accounts for offsets in the Parmeener Supergroup and the dolerite, can be traced through to the Base Parmeener Unconformity and also forms a boundary between good quality data in the hanging wall side and poorer data in its shadow on the footwall side (Figures 6.50, 6.51).

Shot-points 250 – 400

(Figure 6.50)

Upper Marine sequence rocks outcrop in this section of line (Figure 6.49), and a 650 m thick dolerite sill is interpreted 350 m below the surface (Figure 6.50). The section terminates at a gap in the data, where the line crosses two arms of the Hunterston Rivulet and no data was acquired.

The most obvious feature in this section of the line is the dolerite sill, easily identified between shot-points 250 and 300 the sill gently dips towards the south, cutting across units of the Lower Parmeener Supergroup (Figure 6.50). The Base Dolerite horizon is picked at the top of a series of strong, laterally coherent reflections, and can be followed as far as shot-point 400 (Figure 6.50). Above the Base Dolerite horizon the reflections are typically weak and incoherent (Figure 6.50). The Top Dolerite horizon is picked at the first strong (high amplitude), positive reflection above these incoherent reflections. The Base Parmeener Unconformity horizon is picked at the base of strong, coherent reflections that stop at shot-point 325 (Figure 6.52). Beyond this point the data becomes incoherent and the interpretation of the horizon roughly follows a bright event seen in the greyscale image (Figure 6.52).

In this section of line, the other Parmeener Supergroup horizons are located above the dolerite sill in the zone of incoherent data at the top of the section (Figure 6.50). As there are no reflections to guide the placement of the horizons, the interpretation relies on maintaining the thicknesses of the units identified at the tie TB01-TA. The Lower Marine Sequence and the Lower Freshwater Sequence horizons are interpreted to pinch out against the dolerite sill between shot-points 300 and 350 (Figure 6.50).

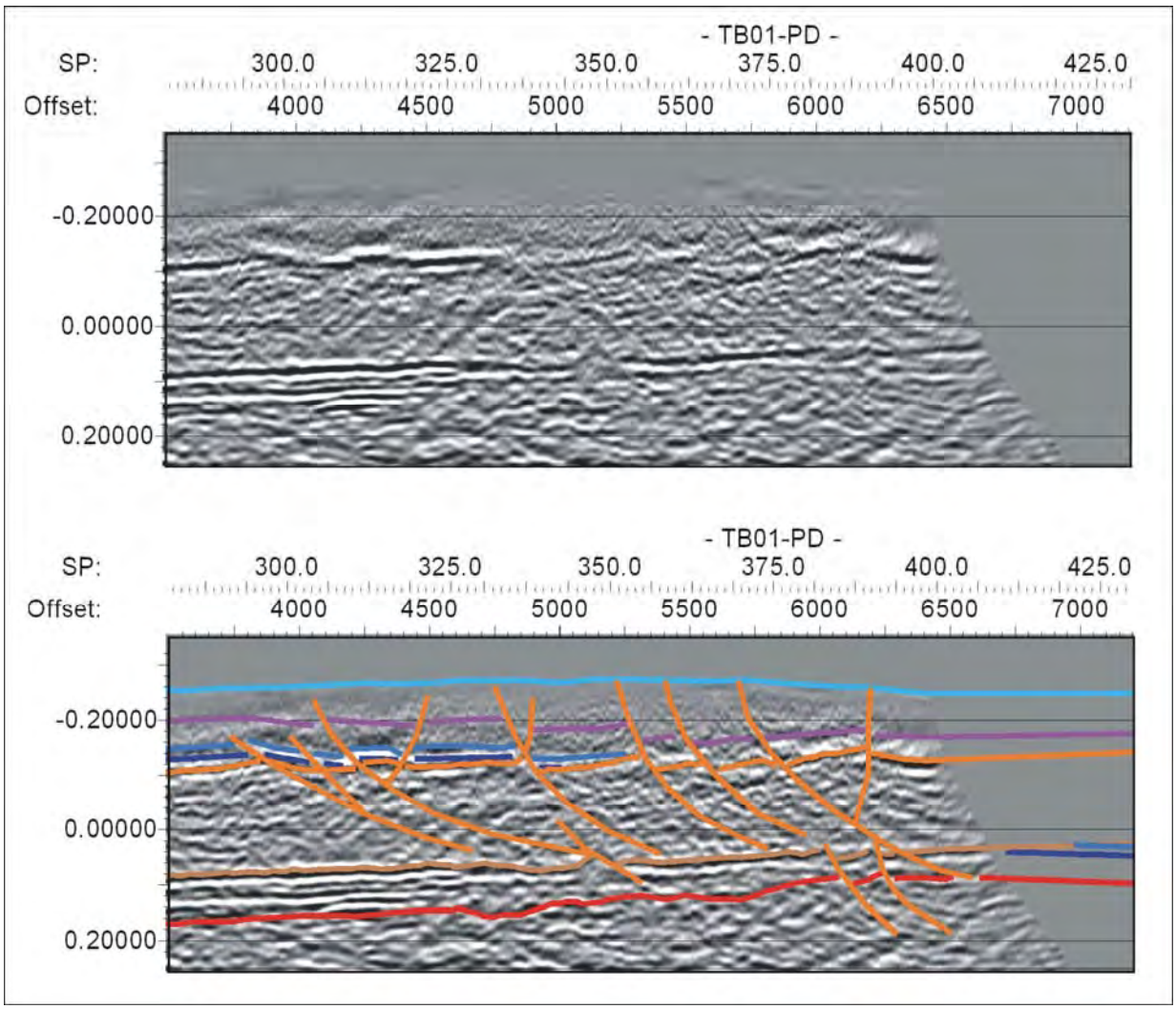

Figure 6.52: Raw and interpreted, greyscale seismic data showing the Base Parmeener Unconformity Horizon pick between shot-points 250 and 400 (TB01-PD).

Looking at the entire line, the dolerite sill dips gently towards the south cutting through bedding in the Parmeener Supergroup (Figure 6.50). The stratigraphic position of the sill is different in the east to west lines TB01-PA and TB01-TA that lie at the north and south ends of TB01-PD respectively. To the north, on line TB01-PA (Map 5.1, Figure 6.1) the dolerite sill has intruded at the level of the boundary between the Ferntree and Cascades formations (both sub-units of the Upper Marine Sequence – see Figure 2.6). This interpretation is constrained by the Hunterston 1 DDH (Reid et al., 2003). While to the south on line TB01-TA, the sill intrudes the Lower Marine Sequence (Map 5.1, Figure 6.65).

Between shot-point 300 and 400 several faults are interpreted (Figure 6.50). The faults in the dolerite sill and the overlying section are all interpreted as Undifferentiated Tertiary (post-dolerite) faults. These faults dip towards the north, are normal and have small displacements, with the exception of small pop-up structures at shot-points 300 and 375, suggesting a component of strike-slip movement. Several faults are interpreted below the

dolerite sill (Figure 6.50). The relative age of these faults in not clear, they have negligible displacements and mostly dip towards the south.

Shot-points 400 – 620

(Figure 6.50)

Upper Marine Sequence rocks continue to outcrop as far as shot-point 575, interrupted by a tongue of dolerite between shot-point 520 and 538 (Figure 6.49). At shot-point 520, Fairbridge (1948) interpreted at least one fault along the contact between the Upper Marine Sequence rocks and the dolerite (Figure 6.49). The quality of the seismic data is relatively poor after shot-point 450 and the ties with lines TB01-PA and PB guide the interpretation of this section of line.

The Base Dolerite horizon is the most easily interpreted horizon. Its path is defined at the top of a group of semi-coherent reflections at 0.05 seconds (TWT) between shot-points 450 and 500 and by similar groups of reflections at -0.95 seconds (TWT) around shot-point 525 and from shot-point 550 to the end of the line (Figure 6.50). The Top Dolerite horizon is more difficult to define. Based on its thickness the horizon is located in the highly incoherent zone at the top of the section.

The position of the Base Parmeener Unconformity horizon is not as well defined in this section of the line. Between shot-point 450 and 500 its position is constrained by line TB01-PA and PB (Figure 6.50). Between shot-points 550 and 620 the horizon is picked at the base of a series of strong coherent reflections (Figure 6.50).

The Lower Freshwater and Lower Marine Sequence horizons are interpreted below the dipping dolerite sill in this section of the line (Figure 6.50). This interpretation is based on the tie with line TB01-PA and the horizons are truncated by the dipping sill between shot-points 400 and 450 (Figure 6.50). From shot-point 525 to shot-point 620 there are no obvious reflections to correlate with these horizons, consequently they are picked the same distance above the Base Parmeener Unconformity horizon as at the tie with TB01-PA (Figure 6.53).

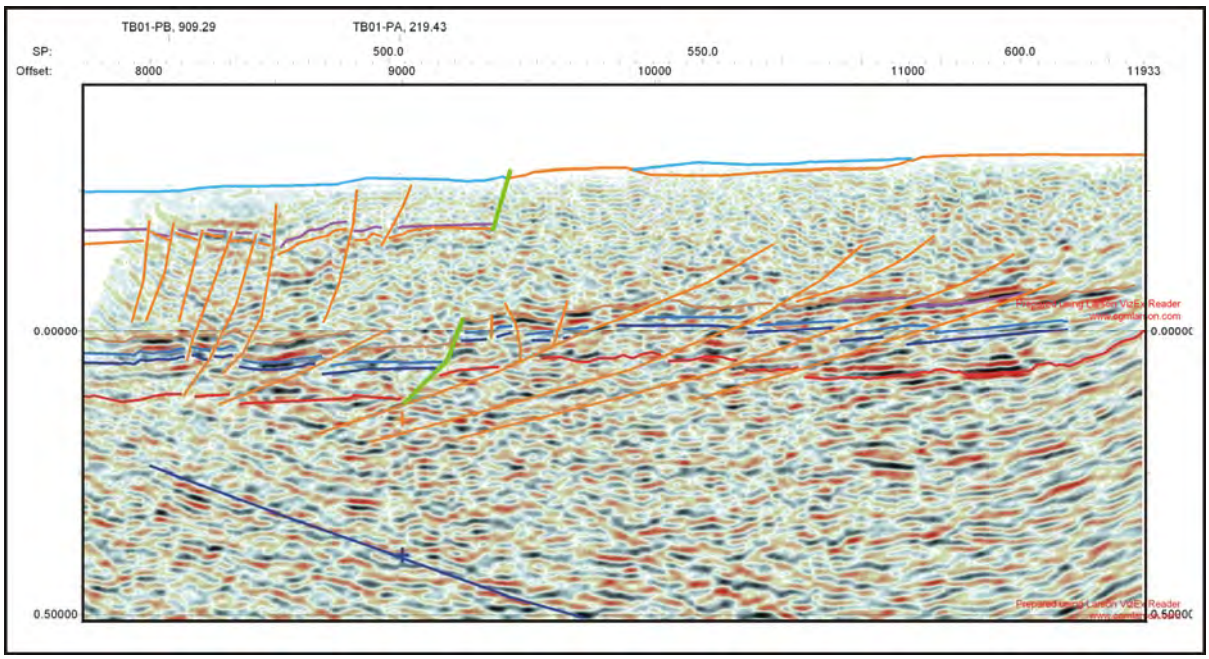

Figure 6.53: Faults and Parmeener Supergroup horizon picks at the northern end of TB01-PD.

The section between shot-points 450 and 620 (end of the line) is extensively faulted (Figure 6.53). Two, possibly three stages of faults are interpreted here. The oldest fault is the Pre-Jurassic “Intruded” fault at shot-point 520. This fault predates the dolerite sill, which steps up ~100 m across the fault and thickens on the footwall side to outcrop at the surface (Figure 6.53). The position of the dolerite sill on the southern (left) side of the fault is constrained by the interpretation of line TB01-PA (Figure 6.53). A Pre-Jurassic “Intruded” fault is interpreted here, because the dolerite sill has to thicken on the footwall side of the fault to outcrop at the surface. This situation cannot be easily resolved if the fault occurred post the dolerite intrusion, unless the outcrop represents a feeder to a higher level or the base of a second sill.

Between shot-points, 450 and 500 the dolerite is extensively faulted (Figure 6.53). These faults are interpreted to have occurred after the intrusion of the dolerite sill and have minor displacements in the Top Dolerite, Base Dolerite and Parmeener Supergroup horizons (Figure 6.53). These are reverse faults with steep dips towards the south (left of section

From shot-point 475 a series of shallowly south dipping faults are interpreted in the lower part of the Parmeener Supergroup section (Figure 6.53). With the exception of the fault between shot-points 500 and 550, these are all reverse faults with displacements in the 10’s of metres (Figure 6.53). These faults all displace the Base Dolerite, Lower Parmeener Supergroup and Base Parmeener Unconformity horizons and therefore must have occurred after the intrusion of dolerite.

Basement

(Figure 6.50)

The resolution of seismic events in the basement section of this line is very poor. The events are interpreted at subtle changes in character and are only recognised with any confidence towards the edges of the section, where they dip towards the north at ~20° (Figure 6.50).

6.2.4: TB01-ST

Line TB01-ST is a key line in the interpretation of this dataset, this is because of its proximity to a number of deep drill holes and other constraining data and since it traverses a number of differing structural domains. The line is 59.9 km long, beginning in the Highlands near the intersection of the Lake Highway and Interlaken Road (459 961 mE, 5 339 672 mN) and finishing east of Tunbridge (542 784 mE, 5 333 614 mN) (Map 5.1, Figure 6.54). The line has been acquired across the Central Highlands, the Great Western Tiers and the Northern Midlands. The line drops 650 m over 6.5 km towards the east, from the Great Western Tiers to the Northern Midlands across the Tiers Fault System (Figure 6.54). The overall quality of the seismic data is good. The line has been acquired roughly west to east making it sub-orthogonal to the inferred strike of the basement structure. The interpretation is well constrained east of the Great Western Tiers by several deep wells and excellent exposures along the scarp of the Tiers (Map 5.1, Figure 6.54). The line can be examined in terms of three distinct structural zones that are coincident with the Central Highlands (shot-points 100 – 1650) the Northern Midlands (shot-points 1950 - 2500) areas and the Tiers Fault system (shot-points 1650 – 1950).

In the Highlands the line has been acquired almost entirely on dolerite (Figure 6.54), with a resultant degradation of data in many areas. The geology across the Tiers Fault System and the Midlands is more complex. Here Tertiary rocks and Quaternary sediments (Figure 6.54) overlie dolerite and Parmeener Supergroup rocks. The change from Tertiary rocks to dolerite to Parmeener Supergroup rocks can be explained by extensive faulting across the Midlands section of the line. Where dolerite is at the surface there is an associated degradation of the data, however where dolerite is at depth the quality and coherency of the surrounding seismic data is improved.

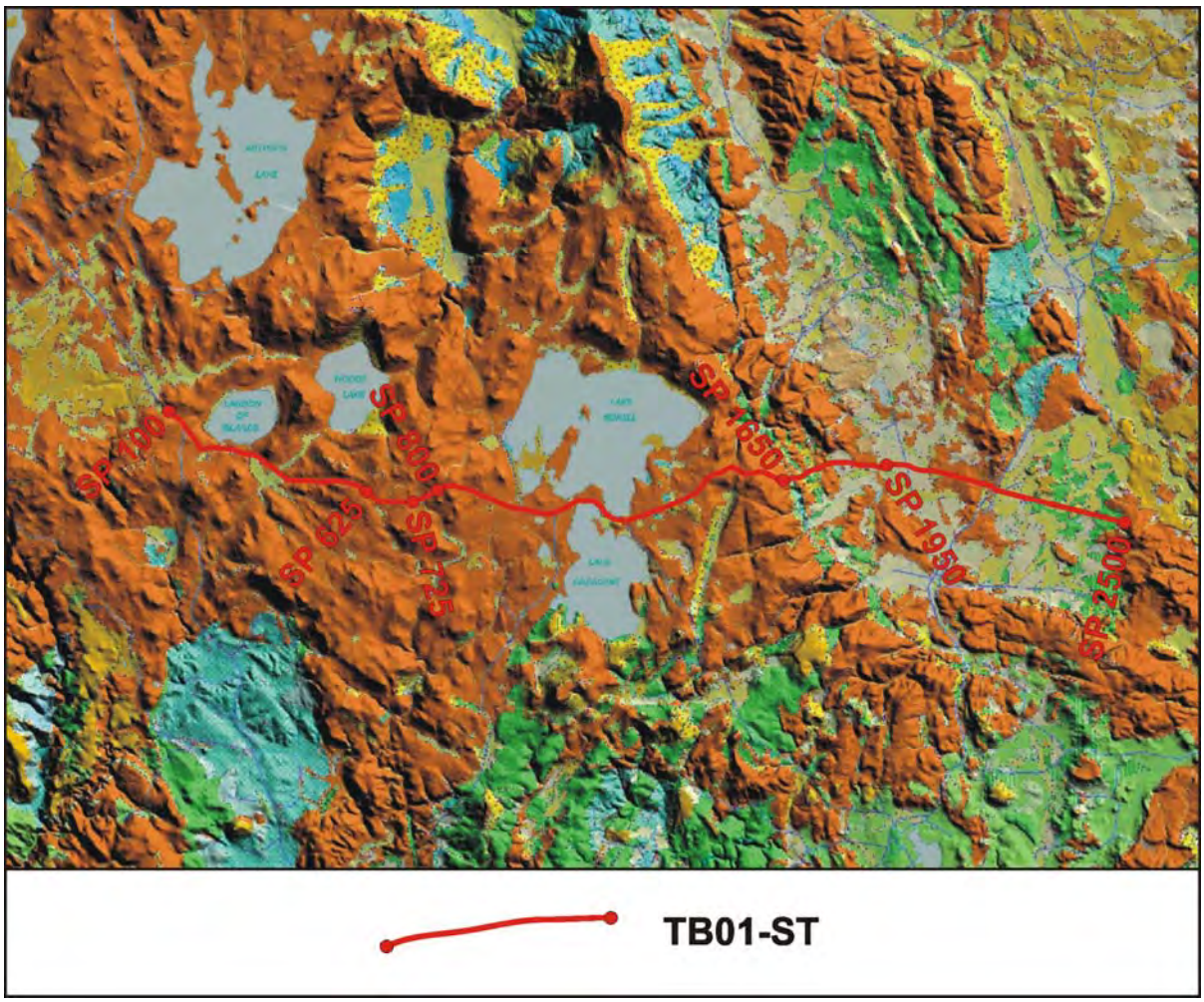

Figure 6.54: Outcrop geology and location of TB01-ST.

Shot-points 100-1650

(Figure 6.55)

The Highlands section of the line lies between shot-points 100 to 1650 (Figure 6.54). The overall structure of the Parmeener Supergroup in this section appears relatively simple, with few major faults either geologically mapped or interpreted in the seismic data. A dolerite sill outcrops across the whole of the Highlands section (Figure 6.54). The sill varies in thickness from 350 – 700 m (Figure 6.55). The thickness variations were determined using the measured gravity field (Figure 6.56). The variations observed in the measured gravity field are either associated with faulting, or the position of the dolerite sill in the section.

The Lower Parmeener Supergroup lies beneath the dolerite sill, which intruded at the boundary between the Upper and Lower Parmeener Supergroup, at or near the top of the Lower Marine Sequence (Figure 5.10). With the exception of the lowermost units, the thickness of the individual Parmeener Supergroup units remains relatively constant across the Highlands (Figure 6.55). The position of the Parmeener Supergroup horizons is based on the

Parmeener Supergroup stratigraphy established in the RG-145 drill hole at Tunbridge Tier using the velocity data acquired at the Hunterston 1 DDH. The Lower Marine Sequence thins and the top tillite horizon onlaps the Base Parmeener Unconformity horizon towards the west over a basement high (shot-point 170) (Figure 6.55). This feature may be a continuation of the basement high identified at the Hunterston 1 DDH (Reid et al., 2003) (Map 5.1).

Faults interpreted as Pre-Jurassic (not affecting the dolerite sill) that displace the Parmeener Supergroup section and penetrate through to basement, have been interpreted at shot-points 225 and 775. The movement of both faults has been interpreted as reverse. The fault interpreted at shot-point 225 is a Pre-Jurassic “Intruded” fault. The fault lies along trend from an event interpreted in the basement, which penetrates deep into the basement section, finishing at 1.5 seconds TWT (Figure 6.57). The proximity of a fault in the Parmeener Supergroup to the basement event suggest reactivation of the basement structure. The dolerite sill has been displaced only a by few faults between shot-points 575 and 825. The throw on these faults is at a scale of 10’s of metres and none of the faults have been recognised on the surface by mapping. However, they are coincident with small valleys at shot-point 625 and between shot-points 725 and 800 (Figure 6.54). Numerous meso-scale faults/fractures have been interpreted across the Highlands section. Most of these are concentrated in the footwalls of the larger faults and are probably related to them.

The Base Parmeener Unconformity horizon is confidently picked at the base of strong coherent reflections that occur regularly across the Central Highlands section (Figure 6.55). There are few other coherent events in the section that correspond to the horizons of the Lower Parmeener Supergroup. The interpretation of the position of these horizons is constrained by formation thicknesses established (in TWT) in the RG-145 Tunbridge Tier drill hole. In several locations across this section, a change in seismic character between relatively incoherent and coherent events is interpreted as the base of the Bundella Mudstone, a sub-unit of the Lower Marine Sequence (Figure 6.58). The consistency of this event provides extra confidence in the placement of the other Lower Parmeener Supergroup horizons. No major thickness changes are interpreted in the Lower Parmeener Supergroup section and no growth has been observed across any of the faults

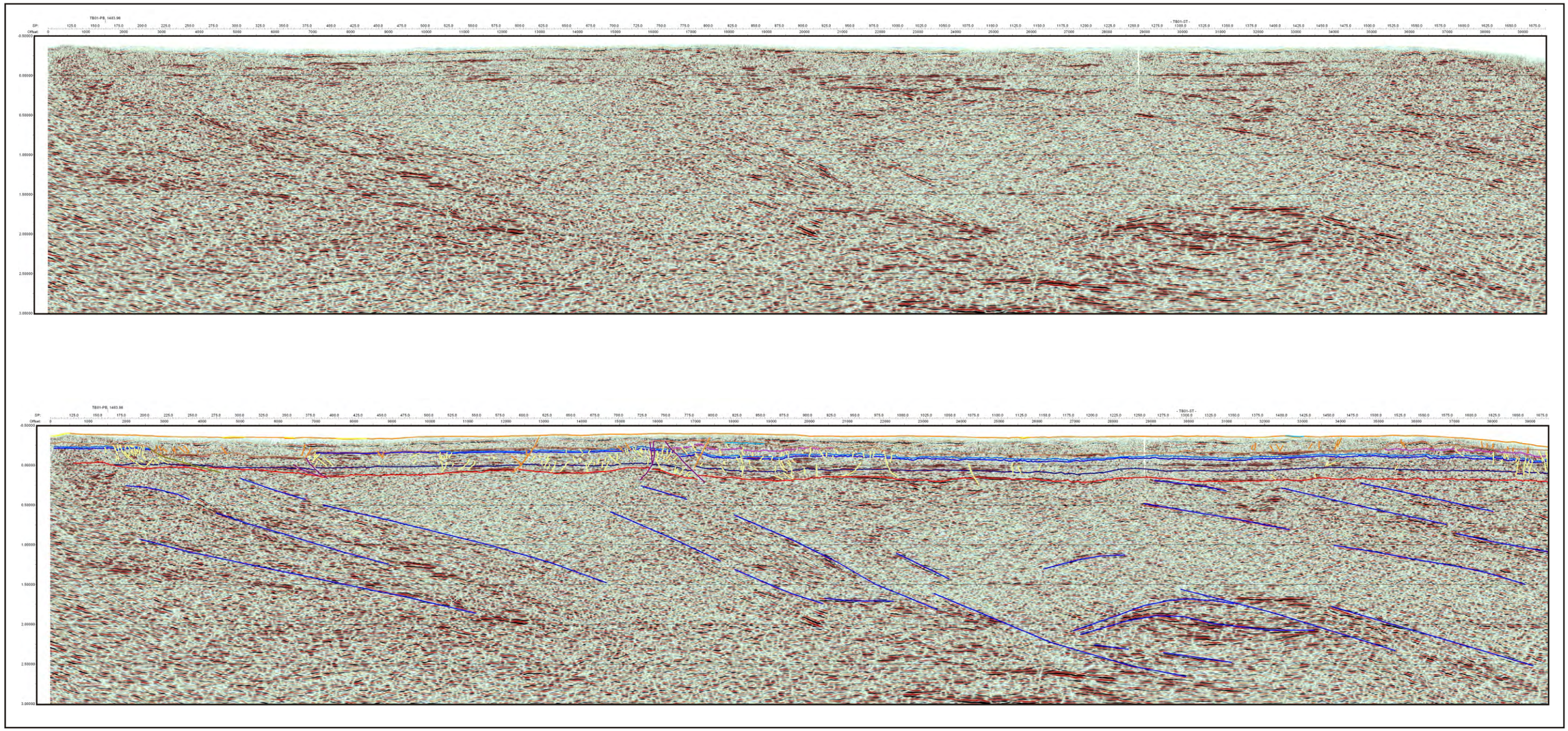

Figure 6.55: Raw and interpreted seismic data from shot-point 100 to 1650 (TB01-ST - Highlands section).

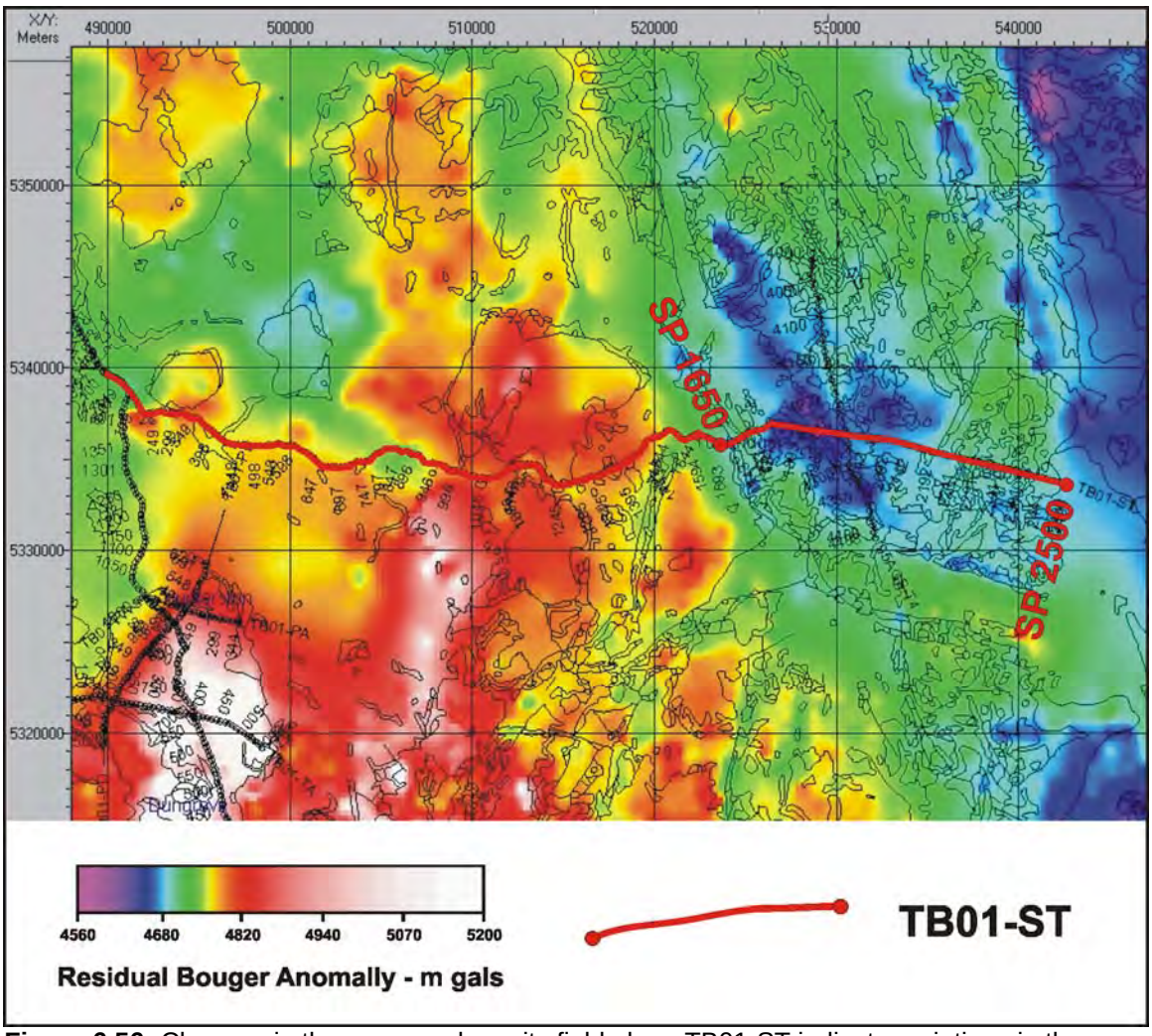

Figure 6.56: Changes in the measured gravity field along TB01-ST indicate variations in the thickness of the dolerite sill.

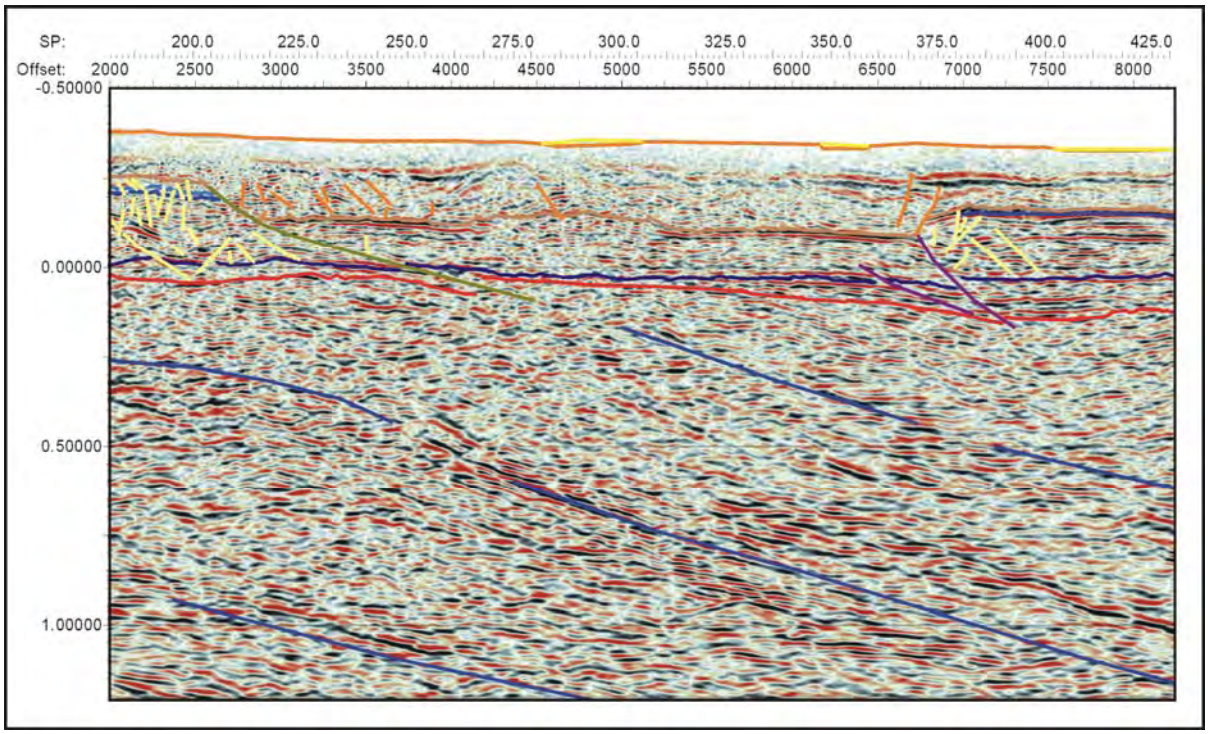

Figure 6.57: The pre-Jurassic reverse fault interpreted at shot-point 225 lies along trend from a major basement event (TB01-ST).

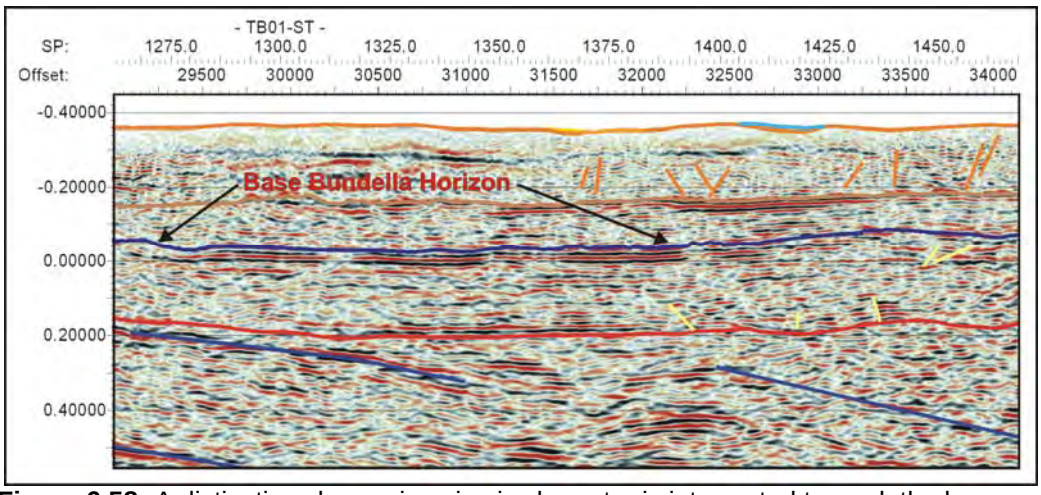

Figure 6.58: A distinctive change in seismic character is interpreted to mark the base of the Bundella Mudstone. This horizon is used as a marker to interpret the positions of other horizons in the Lower Parmeener Supergroup section (TB01-ST).

Events within the basement dip towards the east, events between shot-points 100 and 650 dip at ~20°, while events between shot-points 700 and 1200 dip more steeply at 30° to 40° (Figure 6.55). A series of events interpreted between shot-points 1200 and 1500, at 2.0 seconds TWT, show west directed thrusting over a folded structure (Figure 6.55).

Shot-points 1650 – 1950

(Figure 6.59)

The Tiers Fault System forms the western boundary of the Launceston Tertiary Basin (Figures 2.11, 4.14 and 4.23). The interpretation of the Parmeener Supergroup portion of the section shows a series of east dipping normal faults that have been active at different times (Figure 6.59). The combined displacement across these faults is 500 - 600 m, down to the east. The thickness of the Parmeener Supergroup units on this line is well constrained by the Tunbridge RG-145 drill hole and by outcrop along the escarpment of the Great Western Tiers (Map 5.1, Figure 6.54). The drill hole is 1 km south of the seismic line and its position on the seismic section is not strictly geologically correct, as it has been projected the shortest distance to the line. The drill hole lies in a gap in the outcropping dolerite, between shot-points 1720 – 1730, slightly east of its projected position on the section (Map 5.1, Figure 6.59).

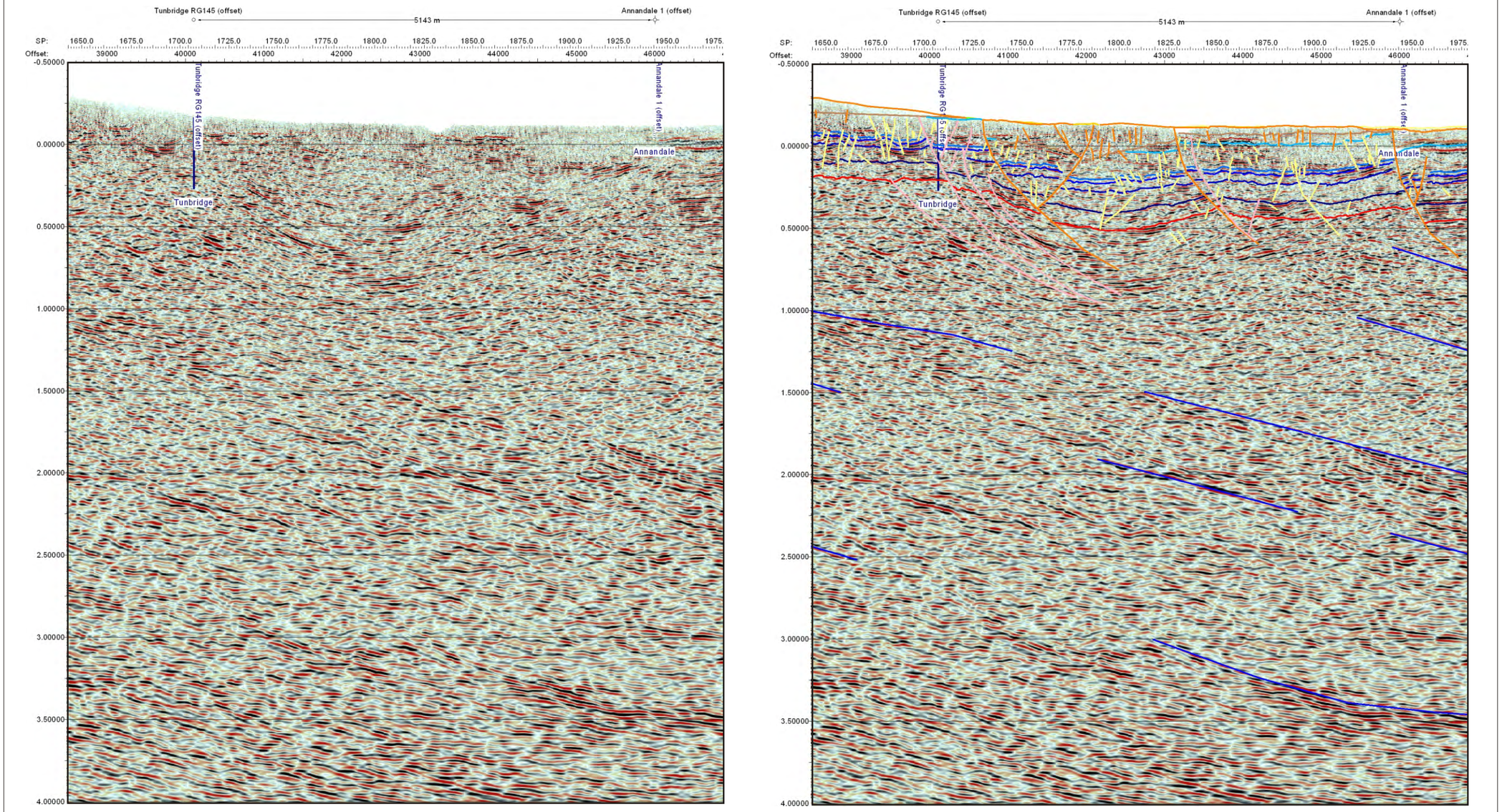

Figure 6.59: Raw and interpreted seismic data from shot-point 1650 to 1950 (TB01-ST).

The westernmost faults interpreted as part of the Tiers Fault System are a series of Pre-Jurassic, normal faults between shot-points 1675 and 1800 (Figure 6.59). There is no evidence from geological mapping, seismic data or in the DEM to suggest that these faults either penetrate the dolerite sill or reach the surface. Throw on these faults is less than 100 m. The interpretation shows these faults converging at depth, reaching 0.50 - 0.75 seconds (TWT) into the basement. However, there is no evidence in the seismic data to show that they link to structures in the basement (Figure 6.59). The timing of movement on these faults is difficult to determine as the seismic data is quite poor and evidence that would support syn-depositional movement such as growth, or the reactivation of basement structures affecting the overlying Parmeener Supergroup cannot be clearly observed.

East of the Pre-Jurassic faults, an Undifferentiated Tertiary fault is observed between shot-points 1730 and 1800 (Figure 6.59). The fault is inferred on the geological maps (Forsyth et al., 1995) and in the seismic section is interpreted as normal with an associated antithetic fault, dropping the section down to the east by ~100 m (Figure 6.59). No evidence was found for a pre-dolerite component of movement; however, the proximity of the fault to major Pre-Jurassic faults makes this a possibility.

Major, down to the east faults, become less common in the eastern portion of this section. An Undifferentiated Tertiary fault and an adjacent Pre-Jurassic fault are interpreted at shot-point 1835. The overall sense of movement across these faults is normal with a 50 m displacement. The easternmost structure on this section of the line is a major, down to the east, Undifferentiated Tertiary fault at shot-point 1940 with a throw of 225 m (Figure 6.59).

The overall coherency of seismic reflections is poor in this section. This may be a function of fault density, the variable thickness of the dolerite sill or the winding road down from the Central Highlands on which the data was acquired (Figure 6.59). Many of the faults have been interpreted based on lateral changes in seismic character.

The interpretation of horizons in the Parmeener Supergroup section relies on the RG-145 drill hole at Tunbridge Tier to constrain the thicknesses of the various sub-units of the Parmeener Supergroup. The Base Parmeener Unconformity, which can be confidently interpreted in the Highlands and Midlands sections of the line, cannot be as easily identified here. The position of the Base Parmeener Unconformity horizon is interpreted at shot-point 1725 (correct position for the RG-145 drill-hole) based on its position in the drill hole

(Figure 6.59). The interpretation of the horizon between shot-points 1650 and 1750 follows the base of strong and coherent reflections (Figure 6.60). Between shot-point 1750 and 1850 the horizon is much more difficult to interpret. In this short section the horizon is picked at the base of strong reflections at shot-point 1840 and follows weak, but coherent reflections back to shot-point 1750 (Figure 6.61). Beyond shot-point 1850 the Base Parmeener Unconformity horizon is interpreted with more confidence because of the intersection between horizontal and west dipping reflections (Figure 6.61). The west dipping reflections are observed between shot-points 1750 and 1900. The reflections dip in the opposite direction to events deeper in the basement section. An alternate interpretation could place the Base Parmeener Unconformity horizon at the base of these reflections, with the Parmeener Supergroup thickening across the large, Pre-Jurassic faults between shot-points 1700 and 1800 (Figure 6.59). However, this interpretation requires an 1800 m thick, Lower Parmeener Supergroup section. None of the constraining drill holes contain such a thick sequence, nor has such a thickness of Lower Parmeener Supergroup section been identified elsewhere in the Tasmania Basin.

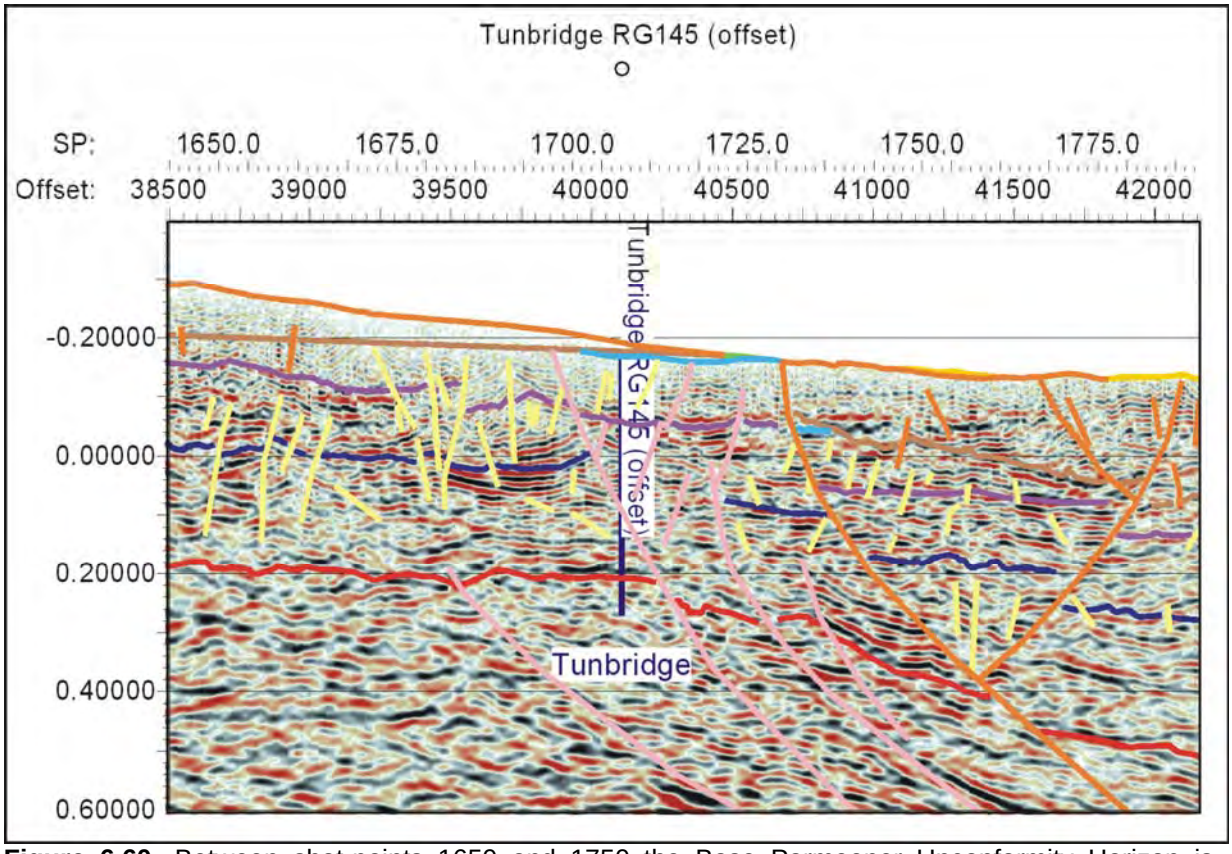

Figure 6.60: Between shot-points 1650 and 1750 the Base Parmeener Unconformity Horizon is interpreted at the base of a series of strong, coherent reflections (TB01-ST).

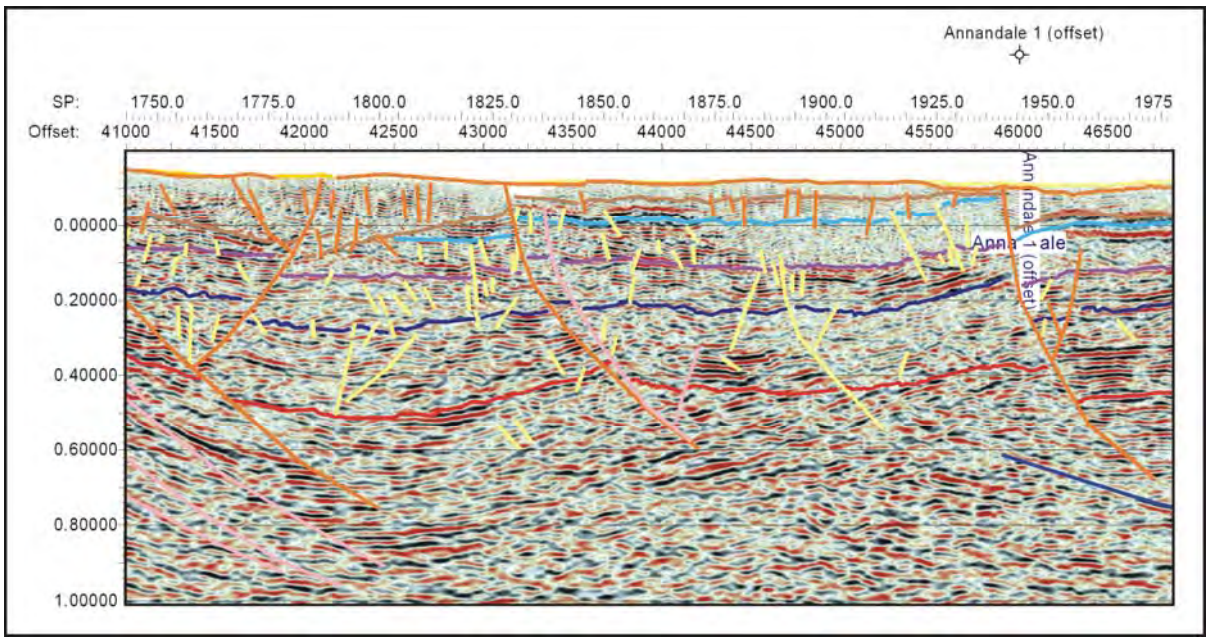

Figure 6.61: Beyond shot-point 1850 the Base Parmeener Unconformity horizon is confidently interpreted at the intersection between horizontal and west dipping reflections (TB01-ST).

The thickness of the dolerite sill is difficult to determine. Interpretation of the Base Dolerite horizon is extremely difficult because of the incoherent and weak reflections at the top of the section (Figure 6.59). The horizons position is approximated using changes in seismic character and the measured gravity field to indicate changes in thickness of the dolerite sill. The positions of other horizons within the Parmeener Supergroup are estimated from the thickness of the section between them and the Base Parmeener Supergroup Unconformity established in the RG-145 drill hole.

Seismic events interpreted in the basement in this section of line were interpreted from changes in seismic character. The events are the down dip continuation events interpreted to the west.

Shot-points 1950-2499

(Figure 6.62)

This section of line is bisected by a positive flower structure around shot-point 2200. West of shot-point 2200 the section is relatively unstructured, dolerite is mapped at the surface (Forsyth et al., 1995) and few large faults are interpreted in the section (Figure 6.62). The faults that have been interpreted mainly dip towards the east (Figure 6.62). To the east of the flower structure, dolerite does not outcrop and sub-surface structure again appears relatively simple, with faults that dip towards the west (Figure 6.62). The interpretation of this section is well constrained by deep drill holes in the vicinity of Ross (RG-146 and The Quoin).

Comparing the stratigraphy of these drill holes with the drill hole at Tunbridge Tier (RG-145) indicates that the thickness of the Cascades (Upper Marine Sequence) and Liffey Formation (Lower Freshwater Sequence) remain relatively constant, while the underlying Lower Marine Sequence (including the Bundella Mudstone) and Tillite thin towards the east (Figure 5.3).

The location of the Parmeener Supergroup horizons in the section to the west of the flower structure (western section) is constrained by the position of the Base Parmeener Unconformity, which is easily distinguished on the section as a bright event in the grey-scale image (Figure 6.63). While the seismic data in this section is incoherent in places, towards the top of the section a relatively coherent event is interpreted as the top of the Cascades Formation. The pick correlates well with estimations for the position of the horizon from drill hole data. The remaining Parmeener Supergroup horizons are interpreted between these two horizons using their thicknesses from drill hole data and rare coherent seismic reflections as a guide to their placement (Figure 6.63). For example, between shot-points 1950 and 2000 a series of coherent reflections coincide with the interpreted position (based on drill hole data) of the Base Bundella horizon (Figure 6.63) and between shot-points 2075 and 2150 the Top Liffey horizon is interpreted at the base of a series of coherent events (Figure 6.63).

The Base Dolerite horizon is difficult to pick, as it is located in the incoherent zone at the top of the section. Regional Gravity data indicates that the dolerite sill is thinner here than to the east of the flower structure, where the sill is extremely well resolved by the seismic data (Figure 6.62). The position of the Base Dolerite horizon between shot-points 1950 and 2200 is interpreted at a weak, but distinguishable reflection, 0.1 seconds TWT below the surface (Figures 6.62, 6.63). Based on this interpretation the dolerite in this region is 300 m thick.

The section west of the flower structure (shot-points 1950 – 2200) is relatively unstructured beyond the major fault at shot-point 1950, marking the boundary between the Tiers Faults System and the Northern Midlands sections (Figure 6.62). The faults interpreted in this section are short and have displacements in the tens of metres. The timing of movement is difficult to determine.

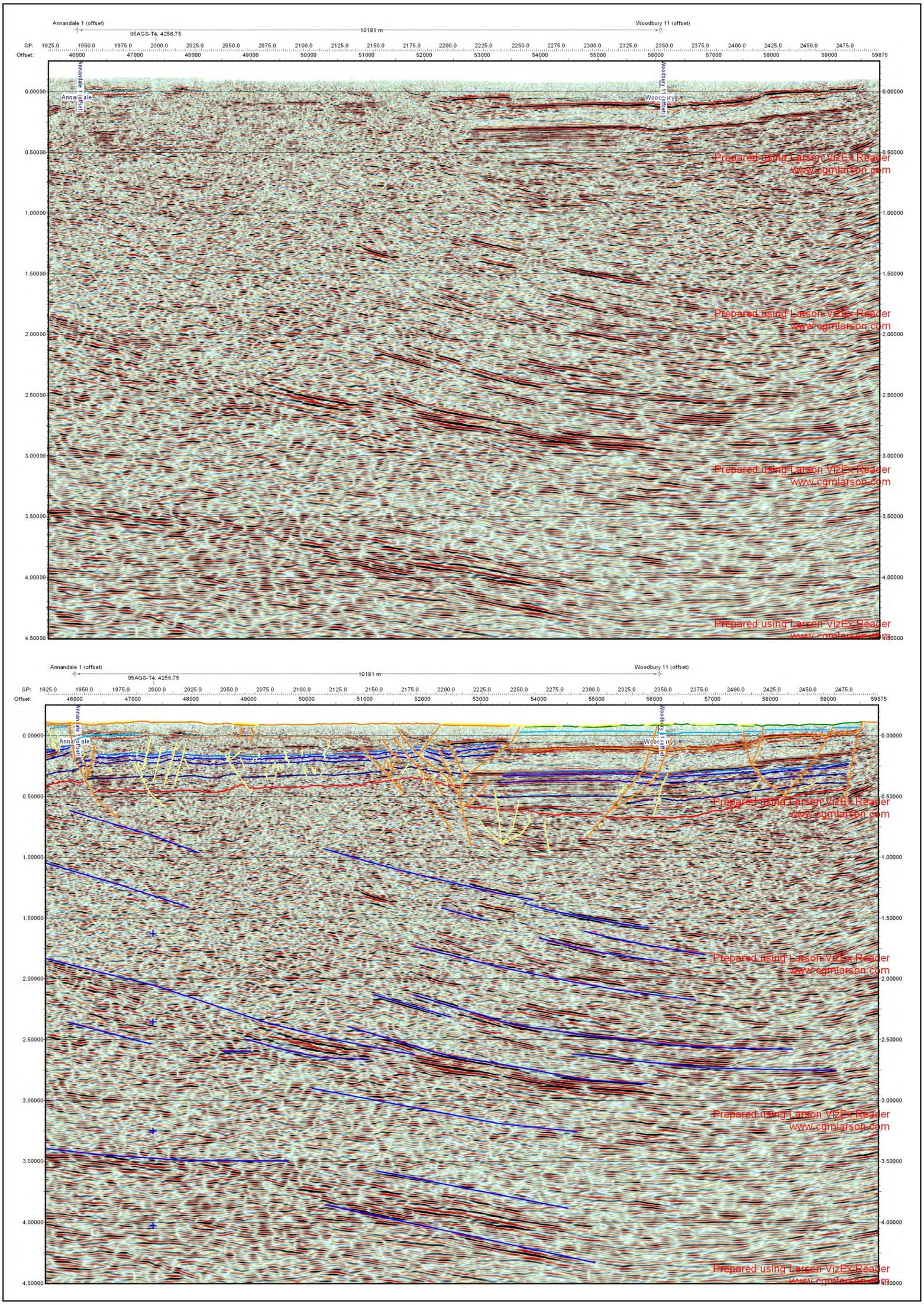

Figure 6.62: Raw and interpreted seismic data from shot-point 1950 to 2499.

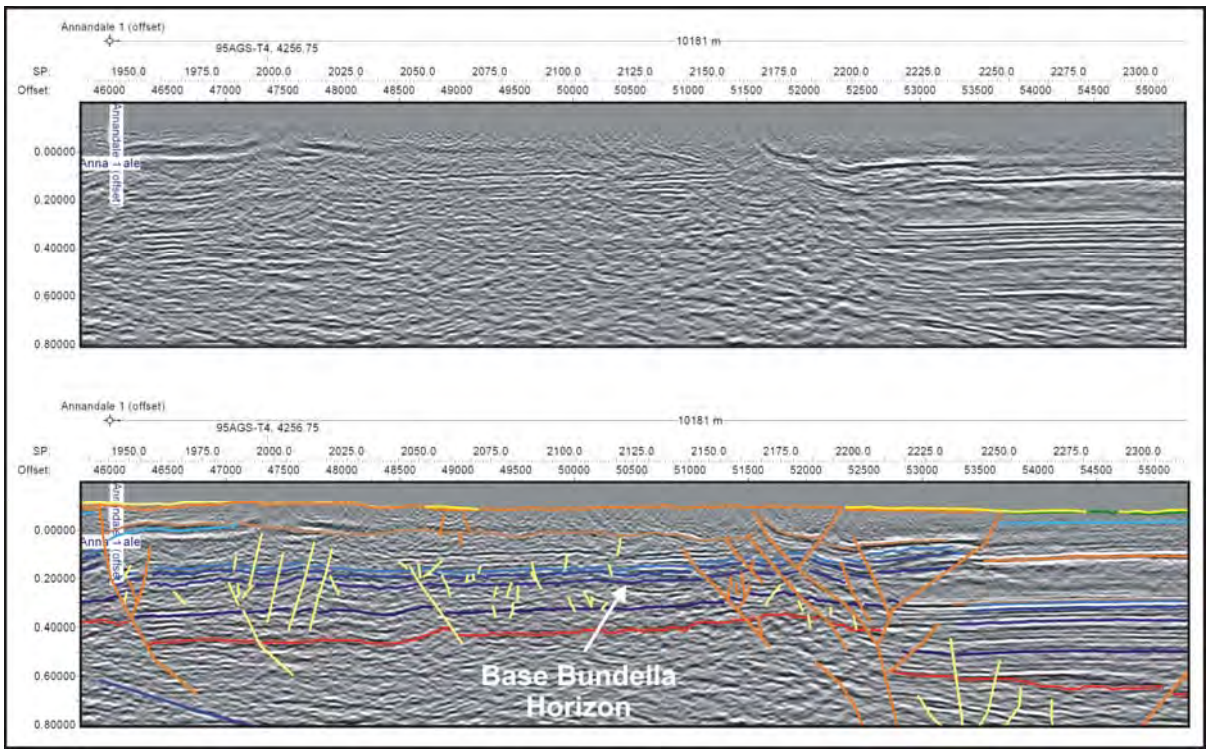

Figure 6.63: West of the flower structure several horizons can be intermittently picked and are used as references to pick the other horizons in the Lower Parmeener Supergroup section (TB01-ST).

The flower structure is a distinct boundary of dolerite outcrop. Dolerite does not outcrop again until a 5 km further east, at the end of the line. The location of the dolerite sill is extremely well resolved by the seismic data east of the flower structure (Figure 6.62), where it is distinguished by a zone of weak incoherent reflections, 300 m below the surface (Figure 6.62).

The interpretation of the flower structure is based on the changing position of the dolerite sill across several faults. The overall movement across the structure is normal, the Parmeener Supergroup section to the east of the flower structure is considerably deeper than the equivalent section to the west, indicating throw of 300–350 m down to the east (Figure 6.62). The dolerite sill gradually rises from east to west, intruding at the Liffey/Cascades Formation boundary on the east and moving above the Cascades Formation west of the structure (Figure 6.62). There is no evidence in the seismic data that these faults were active prior to the intrusion of the dolerite sill. While the overall movement is normal the wedges formed by the antithetic faults indicate a significant strike-slip component (Figure 6.62).

The section of line between shot-points 2225 and 2499 contains the best quality seismic data in the entire TB01 survey (Figure 6.62). The Base Parmeener Unconformity horizon is interpreted at a strong (high amplitude) reflection and the overlying events picked on

estimates of their thickness based on stratigraphic data from the RG-145, RG-146 and The Quoin drill holes. Several large, Undifferentiated Tertiary faults are interpreted in the section between shot-points 2225 and 2499. These faults all dip towards the west. These fault lie close to the eastern boundary of the basin and are probably synthetic to the main boundary fault.

Events in the basement in the section from shot-point 1950 to 2499 are picked at changes in seismic character. The basement events dip towards the east between 10°and 20° (Figure 6.62). Thrust slices become thinner and more horizontal towards the east and a possible décollement is identified at 3.0 seconds (TWT) after shot-point 2150 (Figure 6.62).

6.2.5: TB01-TA

Seismic line TB01-TA has been acquired in the Central Highlands across a window in the outcropping dolerite where the Parmeener Supergroup rocks are mapped at the surface (Map 5.1, Figure 6.64). The line is 11.75 km in length, recorded west to east across the central part of the window and intersects the north-south lines TB01-PA and PB (Map 5.1, Figure 6.64). The line begins west of the “window” (on dolerite) near Synnots Creek (487 400 mE, 5 321 659 mN) and finishes close to the eastern edge of the window on Weasel Plains (489 490 mE, 5 319 163 mN (Map 5.1, Figure 6.64).

The line crosses the western boundary of the window at shot-point 170, where dolerite is in contact with Unit 2 of the Upper Parmeener Supergroup (Figure 6.64), passing into the Upper Marine Sequence by shot-point 200 (Figure 6.64). The line remains in the Upper Marine Sequence rocks until it crosses a narrow, finger of outcropping dolerite between shot-points 520 and 555 (Figure 6.64).

The Parmeener Supergroup occupies the top half second (TWT) of the section. The data quality in the Parmeener Supergroup section is good, the single dolerite sill being the easiest unit to identify. The dolerite sill does not gradually cut through the Parmeener Supergroup as it does on line TB01-PA and PB, indicating that this line is probably sub-parallel to the strike of the dipping sill. The seismic data in the basement section is rather confused and there are no strong character changes or continuous reflections to indicate the presence of structure. Therefore, the events interpreted in the basement must be treated with some care, as they may not reflect the complexity of the actual geological structure.

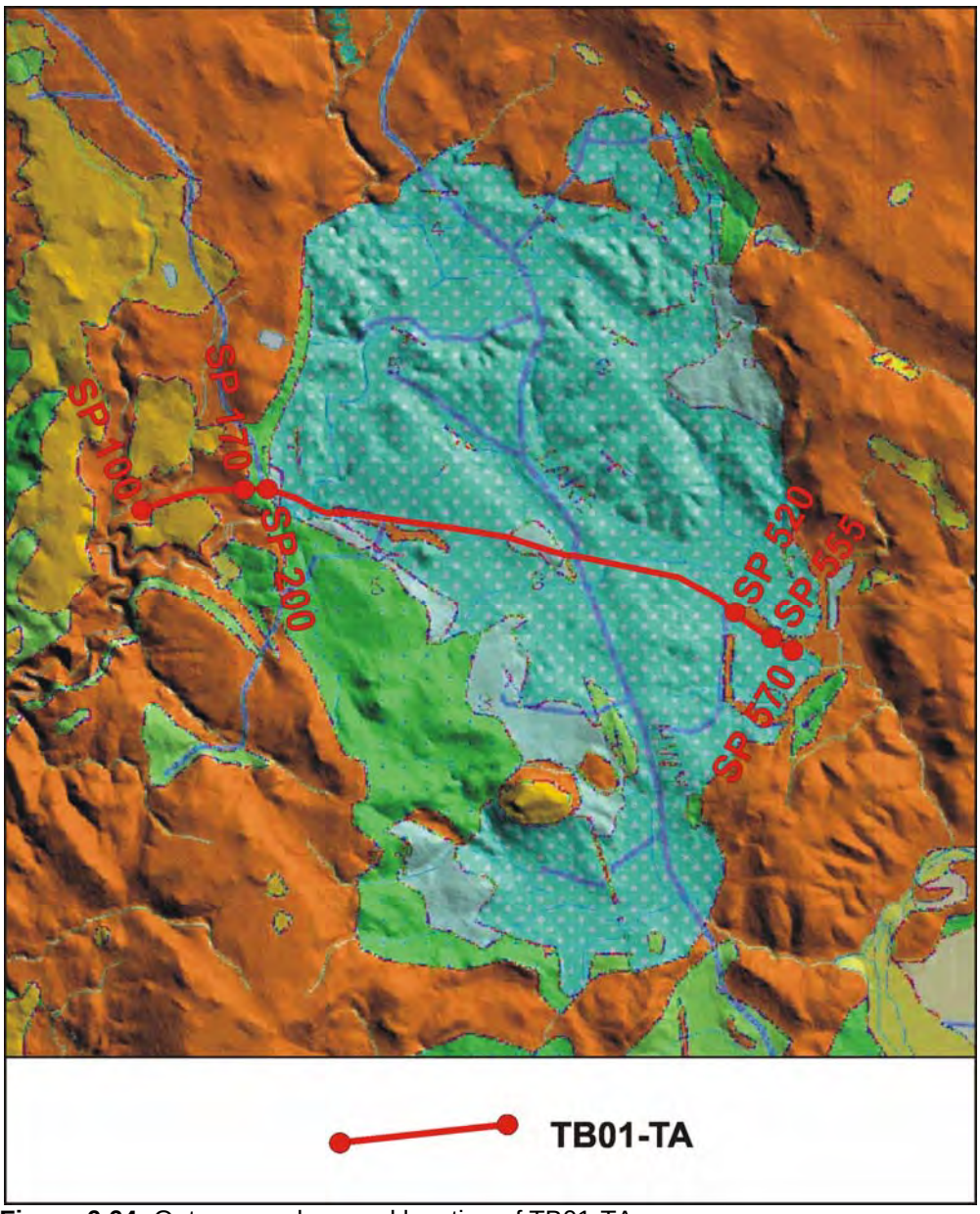

Figure 6.64: Outcrop geology and location of TB01-TA.

Shot-points 100 – 275

(Figure 6.65)

This section of line includes the boundary of the window, where the line crosses from an area dominated by outcropping dolerite to an area where Parmeener Supergroup rocks are dominant (Figure 6.64). The boundary occurs at shot-point 170, where the dolerite sill steps up section towards the west across two faults (Figure 6.66). These faults have been interpreted as Pre-Jurassic “Intruded”, Normal faults.

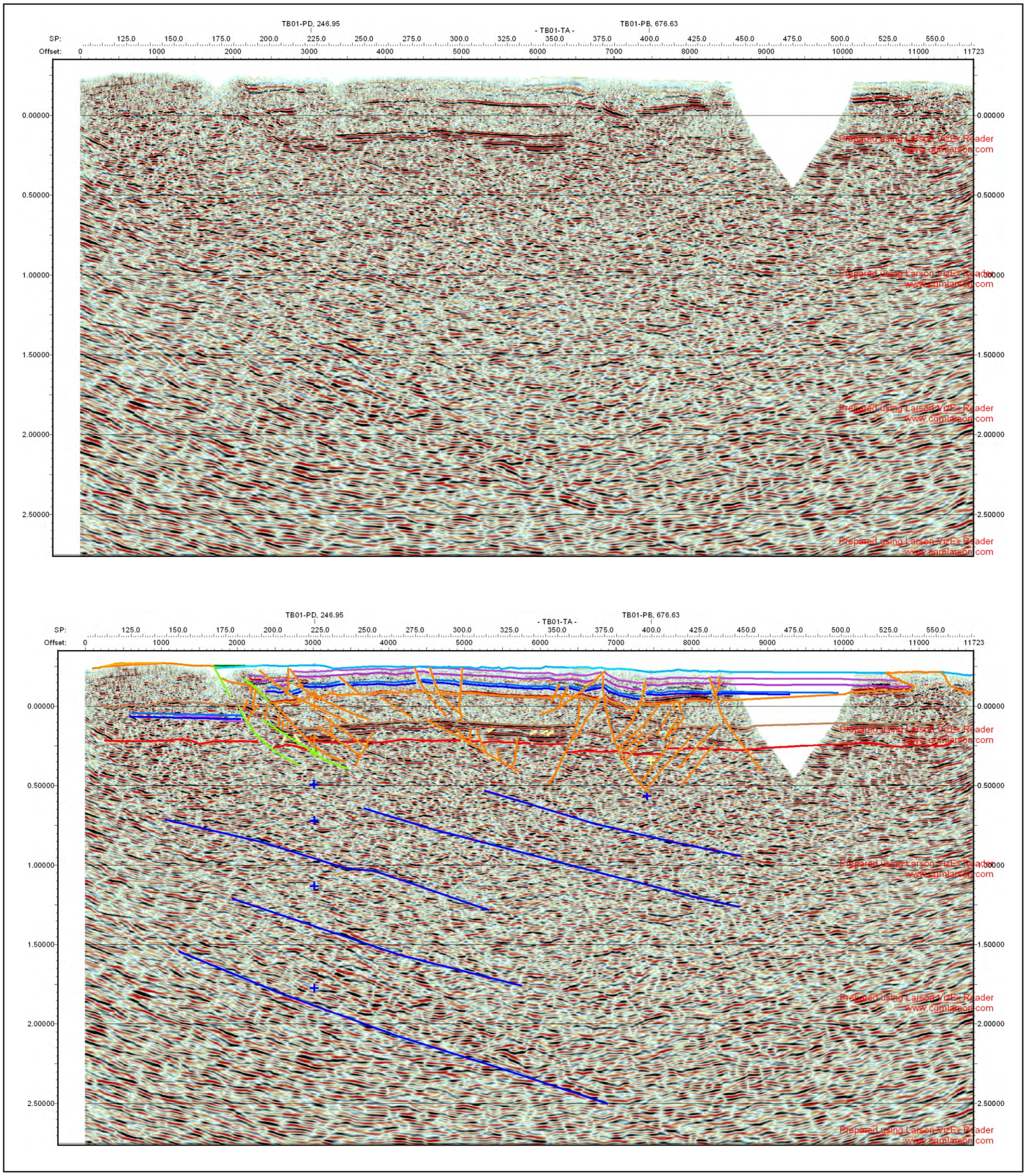

Figure 6.65: Raw and interpreted seismic data from shot-point 100 to 570.

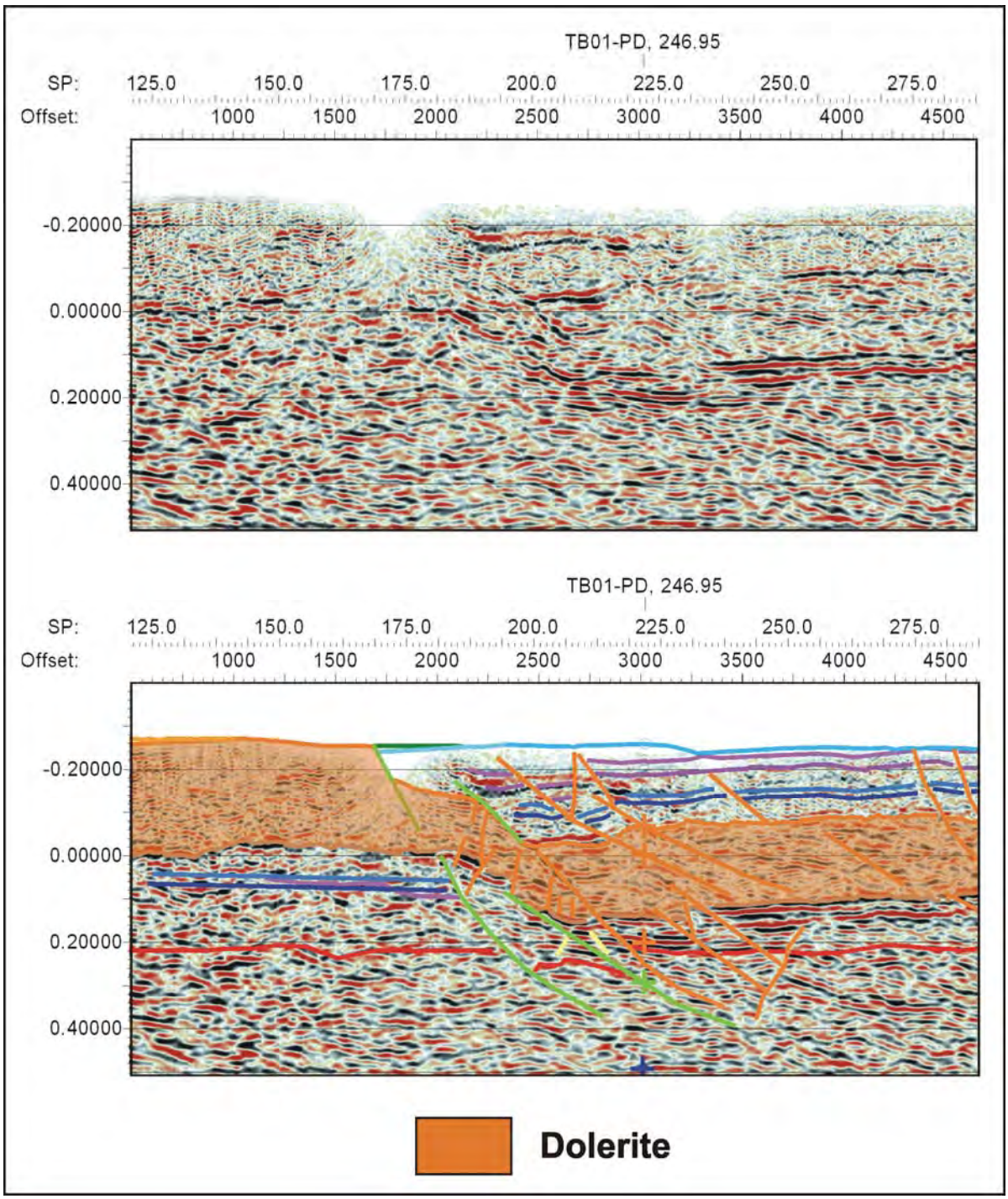

Figure 6.66: Western boundary of the "window" where the dolerite sill steps up across a series of Pre-Jurassic faults (TB01-TA).

On the eastern (right) side of Figure 6.66, the dolerite sill can be identified by its typical seismic character, strong reflections at the top, underlain by weak, incoherent and discontinuous reflections that terminate at another strong reflection. The Top Dolerite horizon is picked on the first strong, positive reflection above the incoherent data. The horizon can be confidently interpreted from shot-point 275, to where it intersects with the first Pre-Jurassic "Intruded" fault at shot-point 200 (Figure 6.66). From shot-point 200 to the outcrop at shot-point 175, the path of the horizon is less clear and its position between the faults is estimated

(Figure 6.66). The Base Dolerite horizon is interpreted at the base of the incoherent data and can be confidently picked from shot-point 275 to shot-point 220 where it intersects with the first Pre-Jurassic "Intruded" fault (Figure 6.66). The horizon is picked across the faults following strong reflections at the base of a zone of weak reflections (Figure 6.67). Between shot-point 180 and the start of the line the seismic data is relatively poor and the horizon is picked at the top of several strong, but intermittent reflections (Figure 6.66).

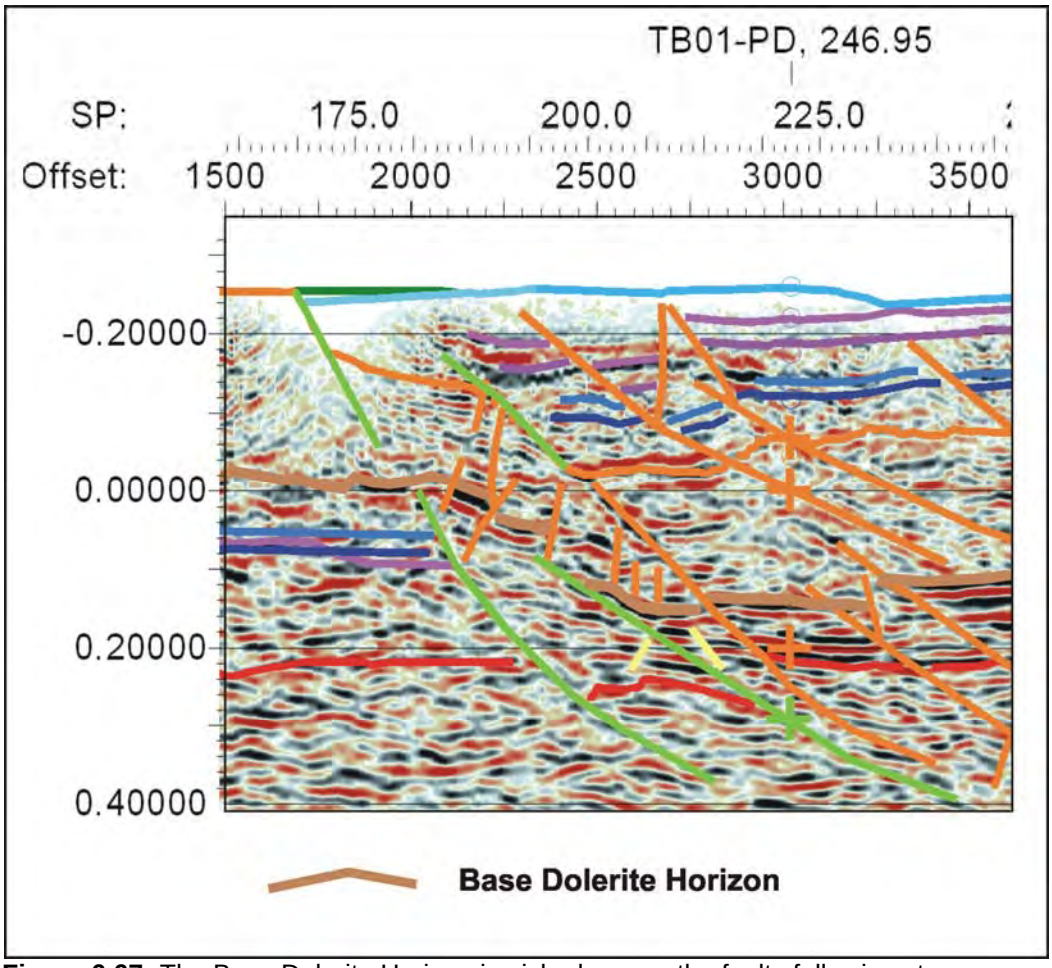

Figure 6.67: The Base Dolerite Horizon is picked across the faults following strong reflections at the base of a zone of weak reflections (TB01-TA).

The Base Parmeener Unconformity horizon is picked at the base of a series of strong, coherent and continuous reflections between shot-points 220 and 250 (Figure 6.65). After shot-point 250 the reflections have a much lower amplitude and the horizons are extrapolated to shot-point 275, maintaining the same thickness below the Base Dolerite horizon as established between shot-points 220 and 250 (Figure 6.65). To the west of the Pre-Jurassic "Intruded" faults between shot-points 150 and 225, the horizon is picked at a subtle character change, however the pick is not a reliable (Figure 6.65).

The positions of the Cascades, Lower Freshwater Sequence and Lower Marine Sequence horizons are extrapolated from the intersection with TB01-PB at shot-point 400 (Figure 6.65).

These horizons all occur in the top part of the section where the data is very incoherent. West of the Pre-Jurassic “Intruded” faults between shot-point 150 and 225, the Lower Freshwater and Lower Marine Sequence horizons are picked below the dolerite sill (Figure 6.65). Their positions are estimated from the thickness of the Lower Marine Sequence (minus dolerite) at shot-point 250 (Figure 6.65).

Several large, Undifferentiated Tertiary faults are interpreted east of the Pre-Jurassic “Intruded” faults between shot-points 200 and 250 (Figure 6.65). These faults are synthetic to the Pre-Jurassic “Intruded” faults, however they have small displacements and only effect the top or base of the dolerite sill, whether they have a shared history is not clear. A number of small antithetic faults are interpreted between the two Pre-Jurassic “Intruded” faults (Figure 6.65). These faults displace the Base Dolerite horizon and have been active post dolerite intrusion.

Shot-points 275 – 475

(Figure 6.65)

The major seismic-stratigraphic events of the Parmeener Supergroup are well defined in this section of the line. The dolerite sill is easily interpreted between shot-points 275 and 360 due to its typical character. Between shot-points 360 and 420 the path of the dolerite sill is disrupted by several faults and while the path of the sill is obscured, it can still be reliably followed (Figure 6.65). The Top Dolerite horizon is interpreted along a series of strong, discontinuous reflections between shot-points 360 and 420, and -0.1 and 0.0 seconds (TWT) (Figure 6.65). The path of the Base Dolerite horizon is more difficult to follow, but can be traced along a series of strong, discontinuous reflections at 0.2 seconds (TWT) (Figure 6.65). From shot-point 420 the dolerite sill regains its typical seismic character and can be easily picked (Figure 6.65).

The Base Parmeener Unconformity horizon is easily recognised at the base of strong, coherent and continuous reflections between shot-points 300 and 360 Figure 6.65). The position of the horizon becomes increasingly difficult to determine between shot-points 360 and 475 and is estimated by maintaining the thickness between the Base Dolerite and Base Parmeener Unconformity horizons established between shot-points 300 and 360 and further constrained by the tie with TB01-PB (Figure 6.65).

Similar to the previous section of line, the positions of the Cascades, Lower Freshwater Sequence and Lower Marine Sequence horizons are based on the intersection with TB01-PB and extrapolated across the section whilst maintaining the thicknesses established at the tie (Figure 6.65).

The section between shot-points 275 – 475 is highly faulted (Figure 6.65). The faults interpreted between shot-point 275 and 350, dip towards the east and are interpreted from minor displacements in the Top and Base Dolerite horizons (Figure 6.65). The displacements on these faults are small (10's of metres) and the movement usually reverse. These faults affect the dolerite sill are interpreted as Undifferentiated Tertiary faults. A major fault structure occurs between shot-points 350 and 400 (Figure 6.65). This structure is recognised in the measured gravity field as a weak linear anomaly that strikes north-northwest (Figure 6.68). Faults interpreted on the west side of the structure dip towards the west and faults on its eastern side dip east, forming a wedge with the central part down dropped by about 120 m relative the west across a single fault and 100 m relative to the east across several small antithetic faults (Figure 6.65). The dolerite sill has not thickened across any of the faults indicating that faulting probably took place after the sill was intruded.

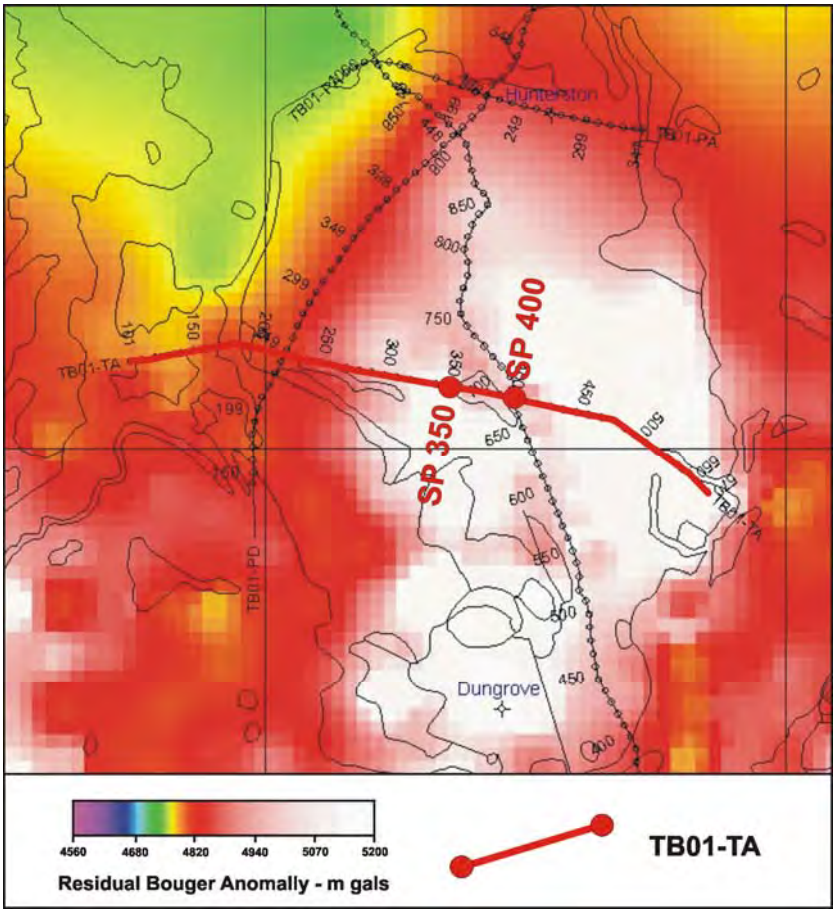

Figure 6.68: Variation in the measured gravity field between shot-points 350 and 400 corresponds to a fault complex interpreted at the same location.

Shot-points 475-570

(Figure 6.65)

This section of line occurs on the eastern side of a 1650 m "V" shaped gap in the data resulting from a suspension in acquisition as the line crossed a creek junction. The section is 1.7 km long with the horizons picked in a similar manner to the previous sections. The dolerite sill dips gently towards the northwest in this short section (Figure 6.65). Consequently, the sill truncates the Parmeener Supergroup horizons interpreted above the sill in the previous section of the line, as it rises towards the east. Dolerite outcrops between shot-points 525 and 550 (Forsyth et al., 1995), however the top and base of the sill can still be interpreted directly below this outcrop (Figure 6.65). The dolerite outcrop is mapped as a thin, finger protruding out from the main body (Figure 6.65), this geometry indicates that it is probably a small dyke.

Basement

(Figure 6.65)

The resolution of seismic events in the basement section of this line is very poor. The line is relatively straight, but the extensive faulting interpreted in the Parmeener Supergroup section may affect the quality of the data deeper in the section and consequently the resolution of the deep structure. The interpretation of basement events in this line is made at changes in seismic character. Between the base of the Parmeener Supergroup and 1.5 seconds (TWT) reflections dip towards the east (right of section) at 10° to 20° (Figure 6.65). These truncate steeper, east dipping events that originate at 2.5 seconds (TWT) (Figure 6.65).

6.2.6: TB01-TB

Seismic line TB01-TB is located on the western edge of the Central Highlands. The line has been acquired along the Lyell Highway, starting to the north of Mt King William 1 (426 054 mE, 5 326 242 mN) on the western, erosional margin of the Tasmania Basin and finishing to the south of Bronte Park (459 104 mE, 5 328 864 mN) (Map 5.1, Figure 6.69). The line is 44.37 km long, the first (western) half trends towards the northeast. While the eastern half is orientated in an east-southeast direction, intersecting lines TB01-PB and TB01-TI at its eastern end (Map 5.1). Part of the line has been acquired over Quaternary glacial and glacigene deposits that obscure any evidence of underlying structure. These deposits occur in the low ground between the surrounding ranges where older rocks outcrop (Brown et al., 1995) (Map 5.1, Figure 6.69).

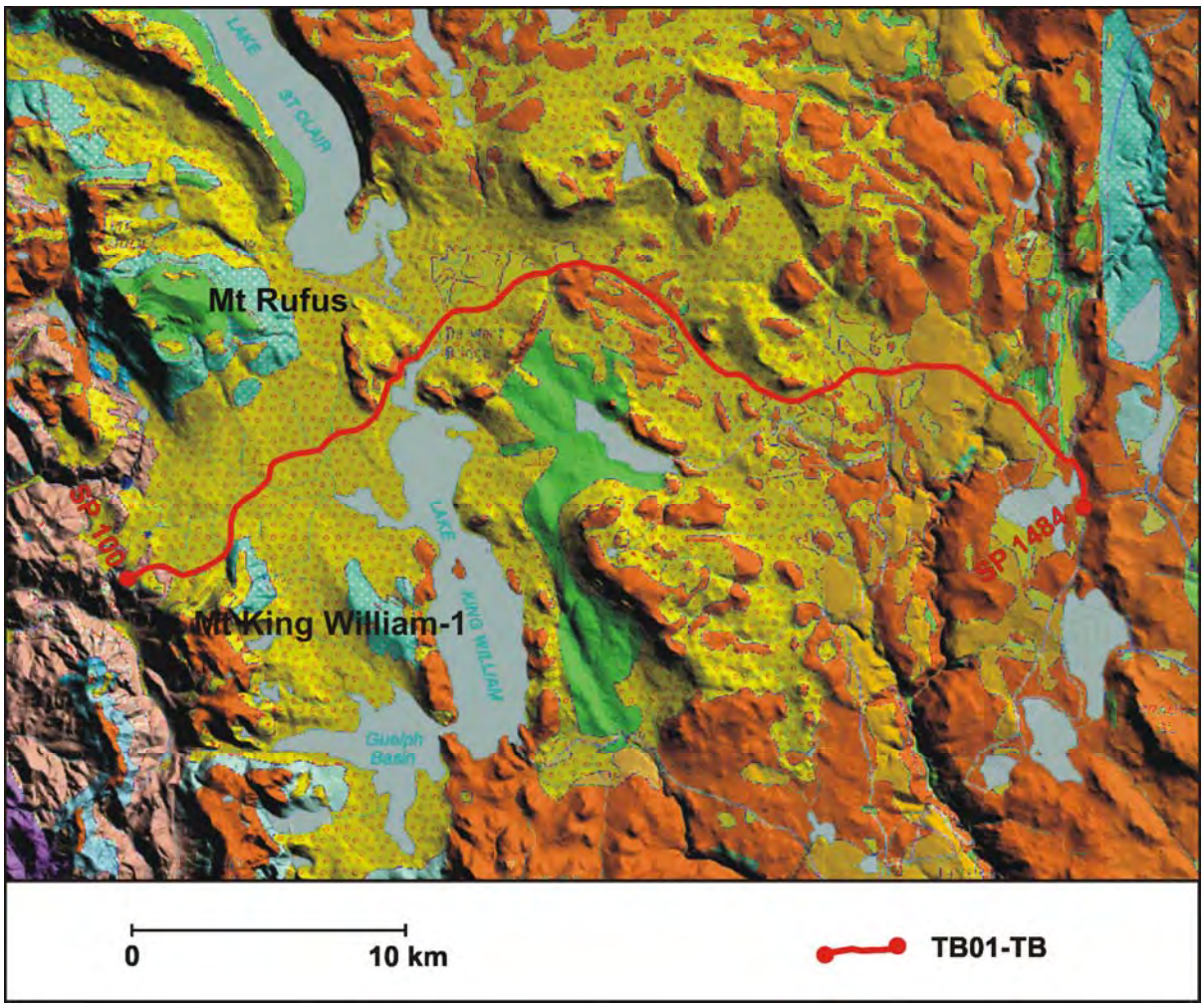

Figure 6.69: Outcrop geology and location of TB01-TB.

Although the seismic data has been acquired along the highway, the road is sufficiently straight to have caused few problems (Map 5.1, Figure 6.69). The seismic data quality across the whole section is variable with a zone of incoherent data in the top 0.2 seconds TWT (Figure 5.11). In the top half second of the section where the Parmeener Supergroup is interpreted to lie, the seismic data is incoherent. However, there are enough zones of coherent data to enable a confident interpretation of the Parmeener Supergroup section across the full length of the line.

The basement between shot-points 100 and 1000 is confused. Sets of reflections dip to the left and to the right of the section, these changes in dip do not correspond closely to changes in the direction of the road. From shot-point 1000 to the eastern end of the line, the data is less chaotic with all the interpreted events dipping towards the west (left of the section).

Shot-points 100 – 280

(Figure 6.70)

The line begins in Precambrian rocks with the first outcrop of Parmeener Supergroup occurring at shot-point 150. At this small outcrop, 1:63 360 geological mapping indicates a contact between Basal Conglomerate and Wallace River Group (Tillite and the Lower Marine sequence in the seismic stratigraphic nomenclature used here) and that these basal units of the Parmeener Supergroup dip towards the east at 4° (Gulline et al., 1963). The contact between these units, the Top Tillite horizon, has been projected into the incoherent zone to the east (right of the section) dipping at 4° (Figure 6.70).

The Top Lower Marine Sequence horizon is been picked parallel to the Top Tillite horizon (Figure 6.70). The thickness calculated for the Lower Marine Sequence is based on the thickness of mapped outcrop around Mt Rufus (Brown et al., 1995, Gulline et al., 1963).

The Base Parmeener Unconformity horizon intersects the surface at shot-point 160 (Figure 6.70). This intersection is concealed on geological maps by overlying Quaternary deposits. Its position at this surface intersection, is based on the thickness of the Basal Conglomerate calculated from adjacent outcrop where the unconformity, the Basal Conglomerate and the overlying Wallace River Group (Lower Marine Sequence) have been mapped (Gulline et al., 1963). The path the Base Parmeener Unconformity horizon follows is a strong (high amplitude), but intermittent reflection (best viewed on the greyscale image) (Figure 6.71). The reflection truncates several dipping reflections, terminating at a fault at shot-point 300 (Figure 6.71).

Basement seismic events for this part of the line are distinguished by character changes and by the presence of coherent reflections. Events dip relatively uniformly towards the right of the section (Figure 6.70). However, geological mapping in the vicinity of this line shows basement rocks dipping 48° to east and 37° to the west (Gulline et al., 1963), indicating the seismic data has been ineffective at resolving complex structures in the basement.

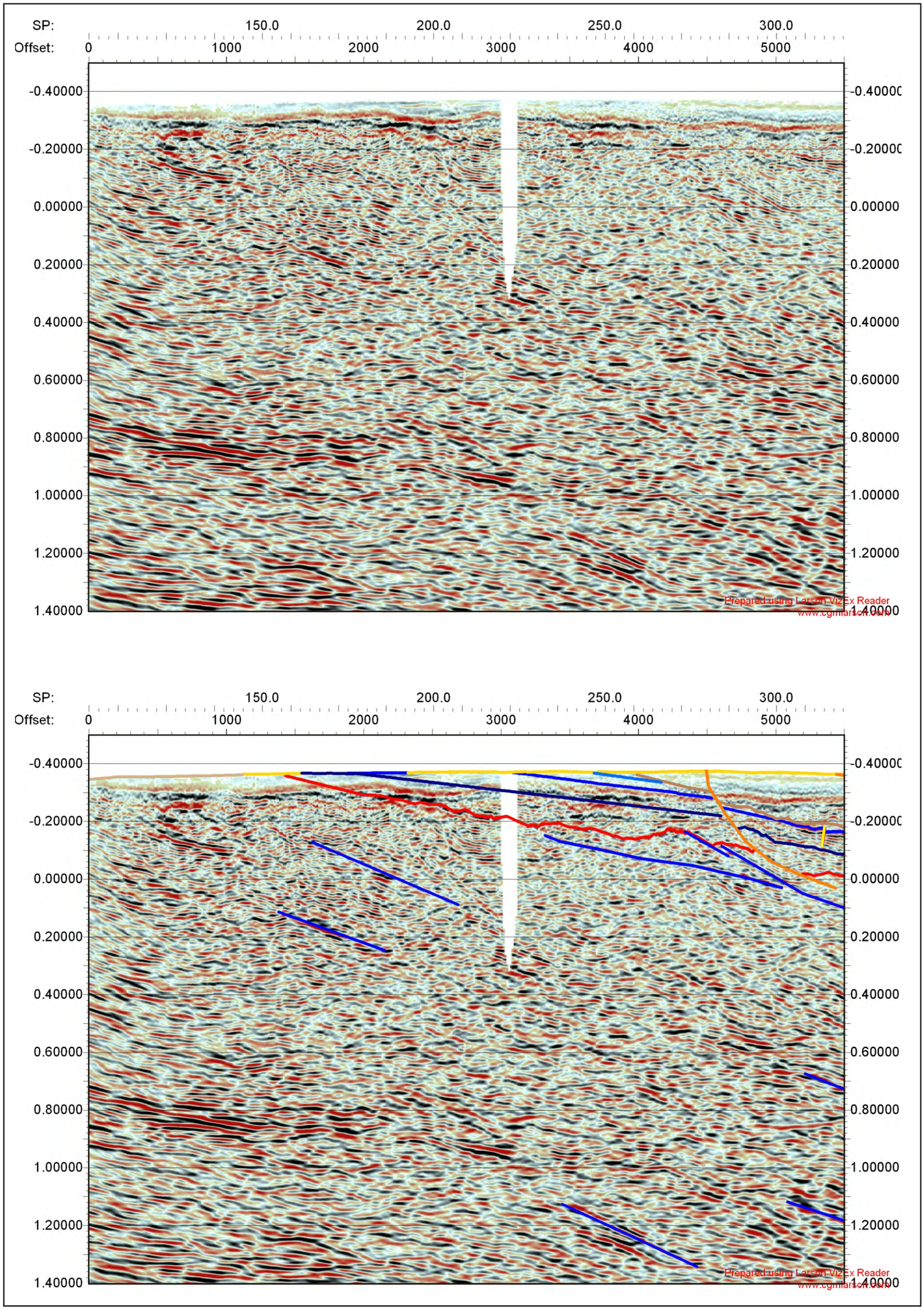

Figure 6.70: Raw and interpreted seismic data from shot-point 100 to 280.

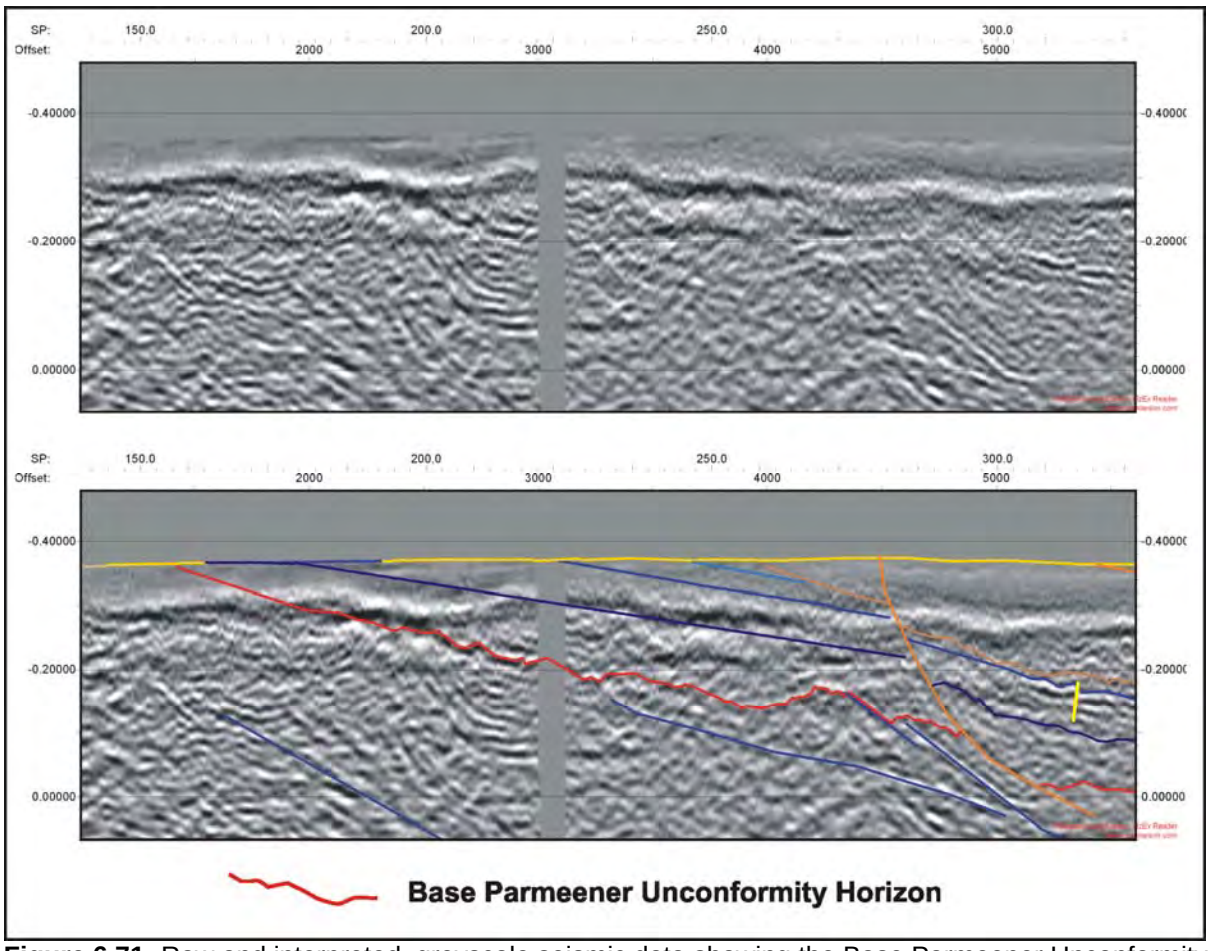

Figure 6.71: Raw and interpreted, greyscale seismic data showing the Base Parmeener Unconformity Horizon pick from shot-point 100 to 300 (TB01-TB).

Shot-points 280 – 900

(Figure 6.72)

The Parmeener Supergroup section in this portion of the line forms a graben, controlled by faults interpreted at shot-points 280 and 900 (Figure 6.72). There is no evidence for the fault at shot-point 280 in the topography (Figure 6.69). However, dolerite mapped at the summit of Mt King William 1 is higher than the Upper Marine Sequence mapped directly to its east (Brown et al., 1995, Gulline et al., 1963) (Figure 6.69). Assuming the stratigraphic position of the dolerite sill remains the same on both sides of the fault, then the east (right) is down with respect to the west (left), with the latest movement occurring after the emplacement of the dolerite sill.

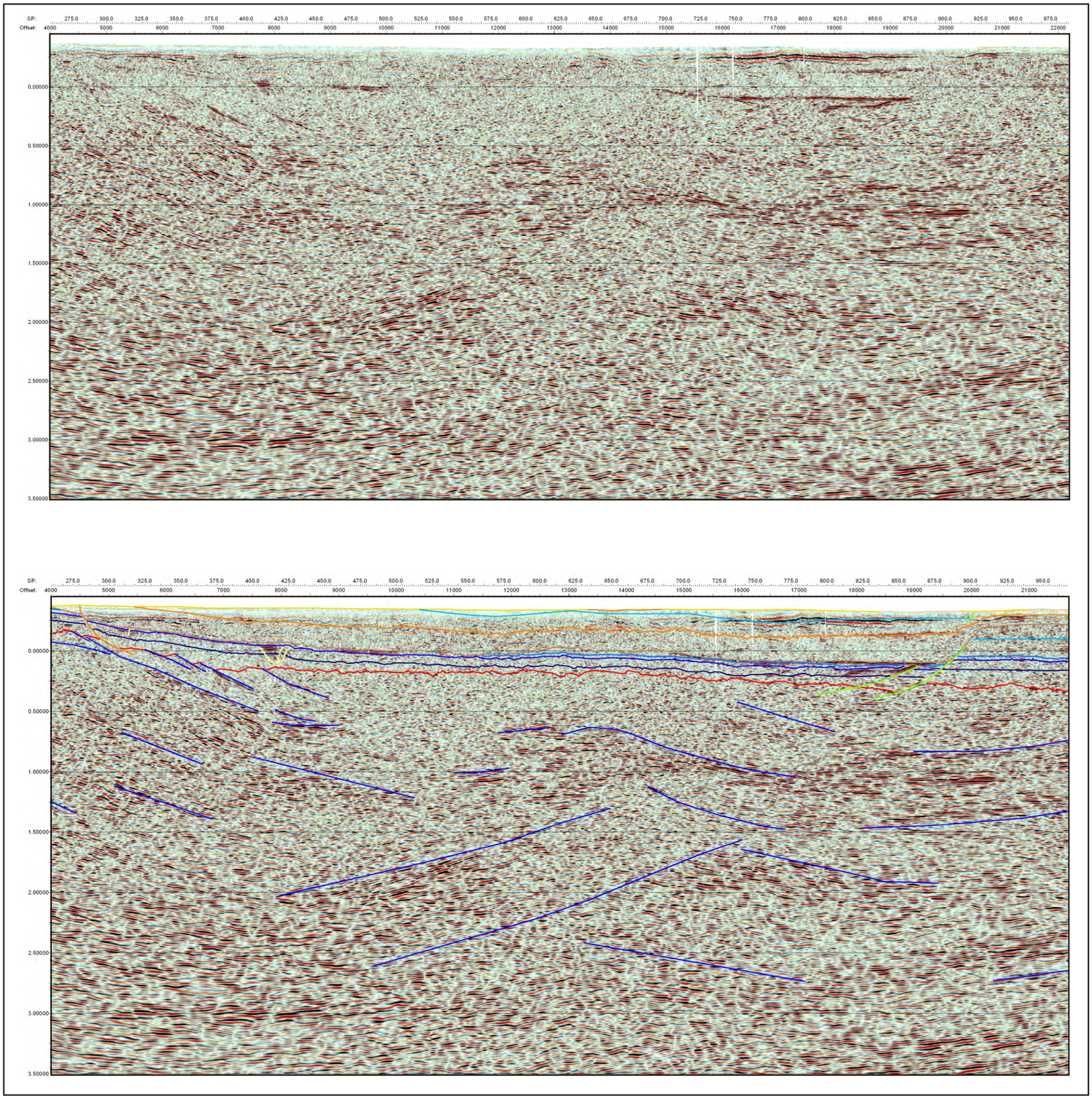

Figure 6.72: Raw and interpreted seismic data from shot-point 280 to 900.

A thick dolerite sill is interpreted intruding the Lower Parmeener Supergroup in this part of the line. The interpretation of the dolerite sill is based on the distinctive seismic character observed between shot-points 700 and 900 (Figure 6.73). Between shot-points 825 and 875 a group of coherent, strong reflections distinguish the top of the dolerite sill at -0.15 seconds TWT (Figure 6.73). Below these are 0.25 seconds (TWT) of weak, incoherent reflections (Figure 6.73). The base of the dolerite sill is picked at another group of coherent, strong reflections at -0.10 seconds TWT (Figure 6.73). This interpretation corresponds to the well constrained example of the seismic character of a dolerite sill seen at the intersection of seismic line TB01-PA and the Hunterston 1 DDH (Figure 6.3). The path of the dolerite sill is constrained by other coherent, strong (high amplitude) reflections between shot-points 450 and 500 and at shot-point 425 (Figure 6.72). These reflections are interpreted as the base of the dolerite sill because of the weak, incoherent reflections above, and the group of reflections indicative of layered rocks observed at shot-point 425 (Figure 6.72). From shot-point 425 to the fault at shot-point 280 the path of the Base Dolerite horizon tracks a distinctive, negative reflection (red) that dips towards the east at a similar angle to the Lower Parmeener Supergroup units interpreted to the west of the fault (Figure 6.72). Outcropping dolerite is mapped (Brown et al., 1995, Gulline et al., 1963) between shot-points 630 and 680, probably indicating the base of a higher sill.

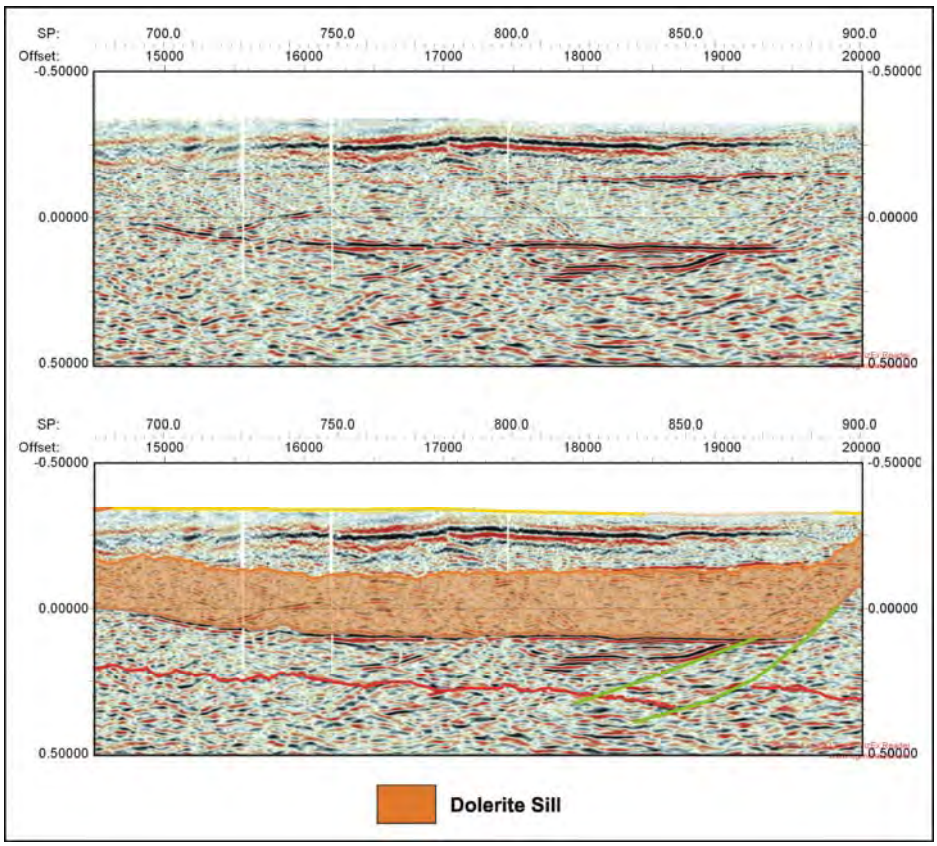

Figure 6.73: Based on seismic character, a thick dolerite sill is interpreted between shot-points 700 and 875 (TB01-TB).

East of the fault at shot-point 280, reflections that are horizontal, albeit incoherent can be picked down to 0.0 seconds TWT (Figure 6.74). The unconformity horizon is picked below these reflections, where the seismic character changes to reflections that are more incoherent and weaker (Figure 6.74). The unconformity horizon is picked to shot-point 400, from dipping basement events truncated by horizontal reflections (Figure 6.74). The lowest part of the sequence thickens above these truncated reflections indicating growth (Figure 6.74). The last of these truncated, dipping basement events is at shot-point 400, where the unconformity horizon is confidently picked at the base of a group of horizontal reflections (Figure 6.74). From shot-point 400 to shot-point 750, the seismic data is highly incoherent (Figure 6.74) and the pick for the unconformity horizon is unreliable. After shot-point 750, a more confident pick is made for the horizon at a strong (high amplitude) reflection, which truncates several dipping events in the basement and is most easily seen in the greyscale image (Figure 6.75).

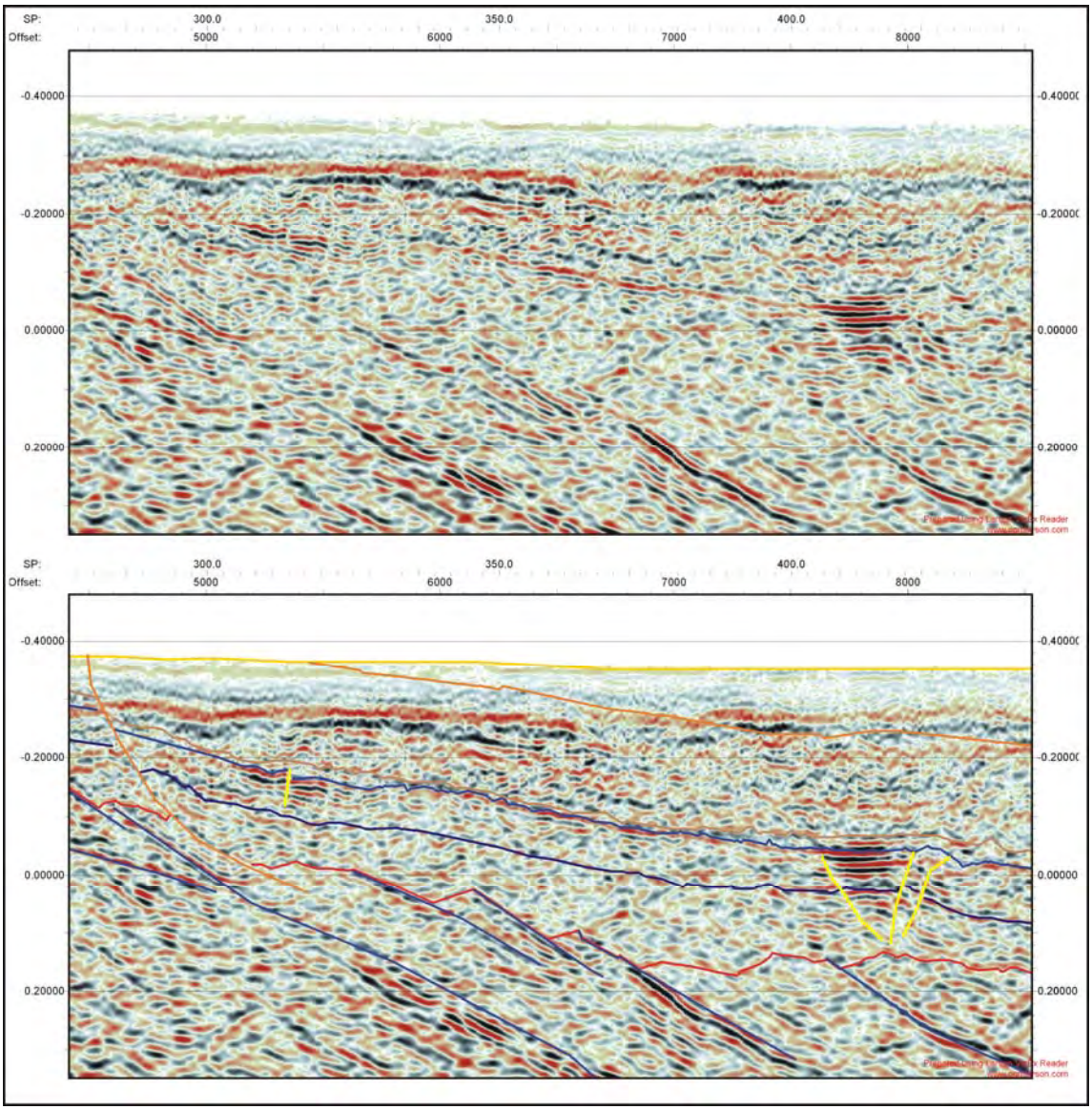

Figure 6.74: Raw and interpreted seismic data east of shot-point 280 showing the Base Parmeener Unconformity Horizon pick in red (TB01-TB).

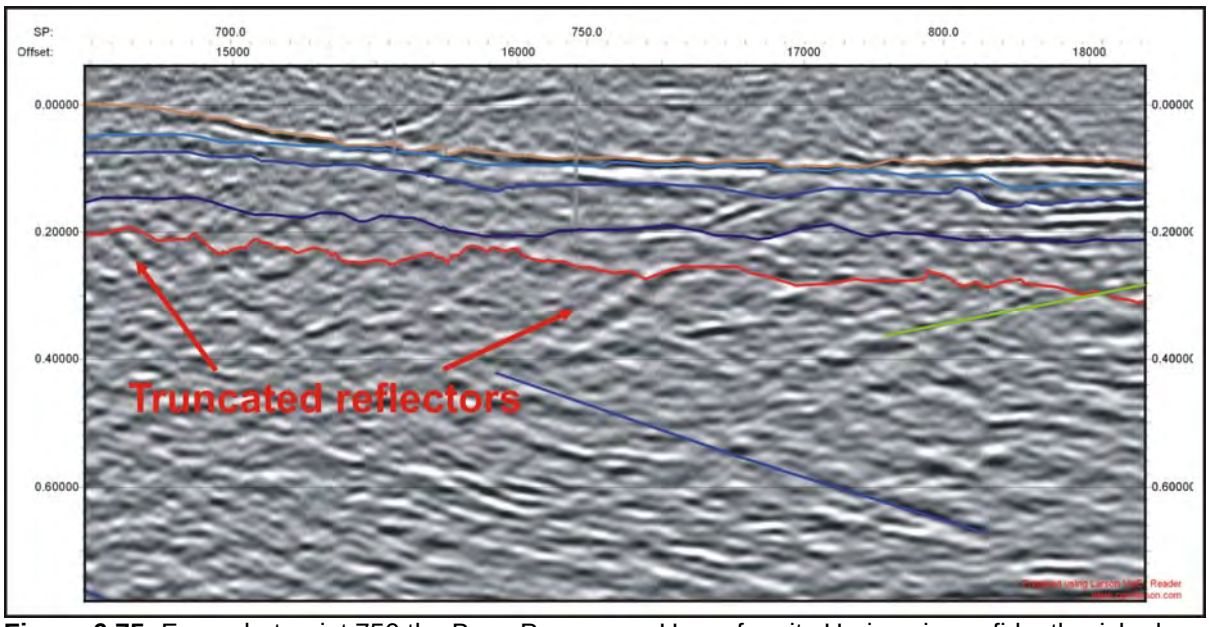

Figure 6.75: From shot-point 750 the Base Parmeener Unconformity Horizon is confidently picked on a strong reflection that truncates underlying events (TB01-TB).

The Top Tillite horizon is interpreted at the base of a group of layered, coherent reflections that occur around shot-points 425 and 825 (Figure 6.72). The horizon is interpolated between these two shot-points through the zone of incoherent data. To the west (left) of shot-point 425, the horizon is picked roughly parallel to the Base Dolerite horizon (Figure 6.72). The Top Lower Marine Sequence horizon is picked at the top of the coherent reflections and is interpreted parallel to the Top Tillite horizon across the areas of incoherent data (Figure 6.72). The thickness of the Lower Marine Sequence interpreted at shot-points 425 and 825 is consistent with the thickness indicated by mapped outcrop on the flanks of Mt Rufus (Figure 6.69). Similarly, the position of the Upper Marine Sequence pick is based on the assumption that the dolerite sill is conformable, while the thickness of the sequence is constrained by outcrop on Mt Rufus (Figure 6.69).

The faults that form the eastern boundary of the graben are interpreted as Pre-Jurassic "Intruded", normal faults (Figure 6.76). This interpretation assumes these faults were active prior to dolerite intrusion and acted as a zone of weakness allowing the dolerite to step up to a higher level in the sequence. This interpretation is made based on there being semi-coherent, horizontal reflections on the eastern (right) side of the fault from -0.2 to 0.15 seconds TWT, indicative of layered rock rather than dolerite (Figure 6.77). The occurrence of these reflections and their location at the same level as the dolerite sill to the left (west) of the fault indicate that the dolerite sill is not at the same level and has jumped to a position higher in the section.

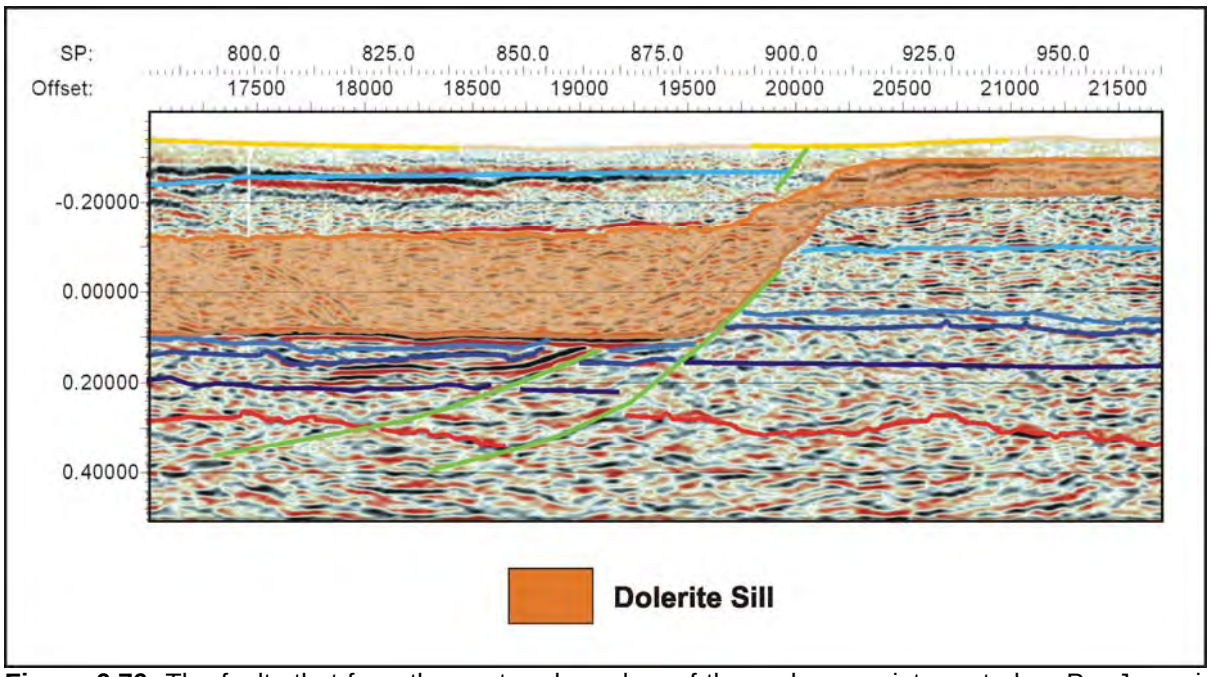

Figure 6.76: The faults that form the eastern boundary of the graben are interpreted as Pre-Jurassic normal faults that have been intruded by the dolerite sill (TB01-TB).

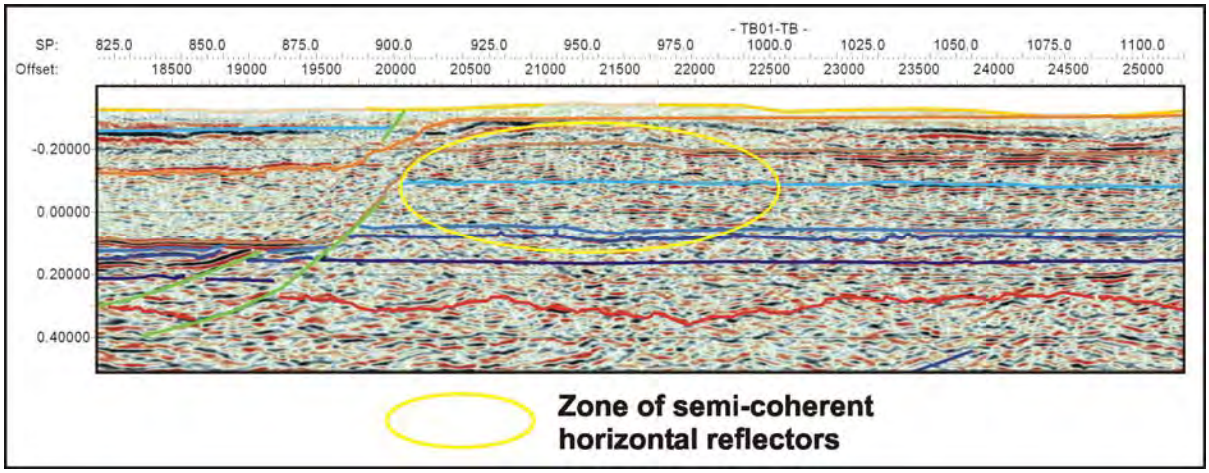

Figure 6.77: Semi-coherent horizontal reflections on the eastern side of the fault indicate the presence of layered rocks, not dolerite (TB01-TB).

The basement section between shot-points 280 and 900 contains zones of reflections that dip both left and right (Figure 6.72). Seismic events in this section have been interpreted at changes in seismic character, where relatively strong (high amplitude), and more coherent reflections change to reflections that are less coherent and are much weaker (have a lower amplitude). However, geological mapping indicates more complex basement structure to the west (Gulline et al., 1963). It is likely that the interpretation under represents the actual complexity of basement structure. The overlapping events and the event that rolls over at shot-point 650 may result from under migration of the basement section and in an alternative interpretation these events could represent either an antiform with a very steep western limb or a reverse fault (Figure 6.78).

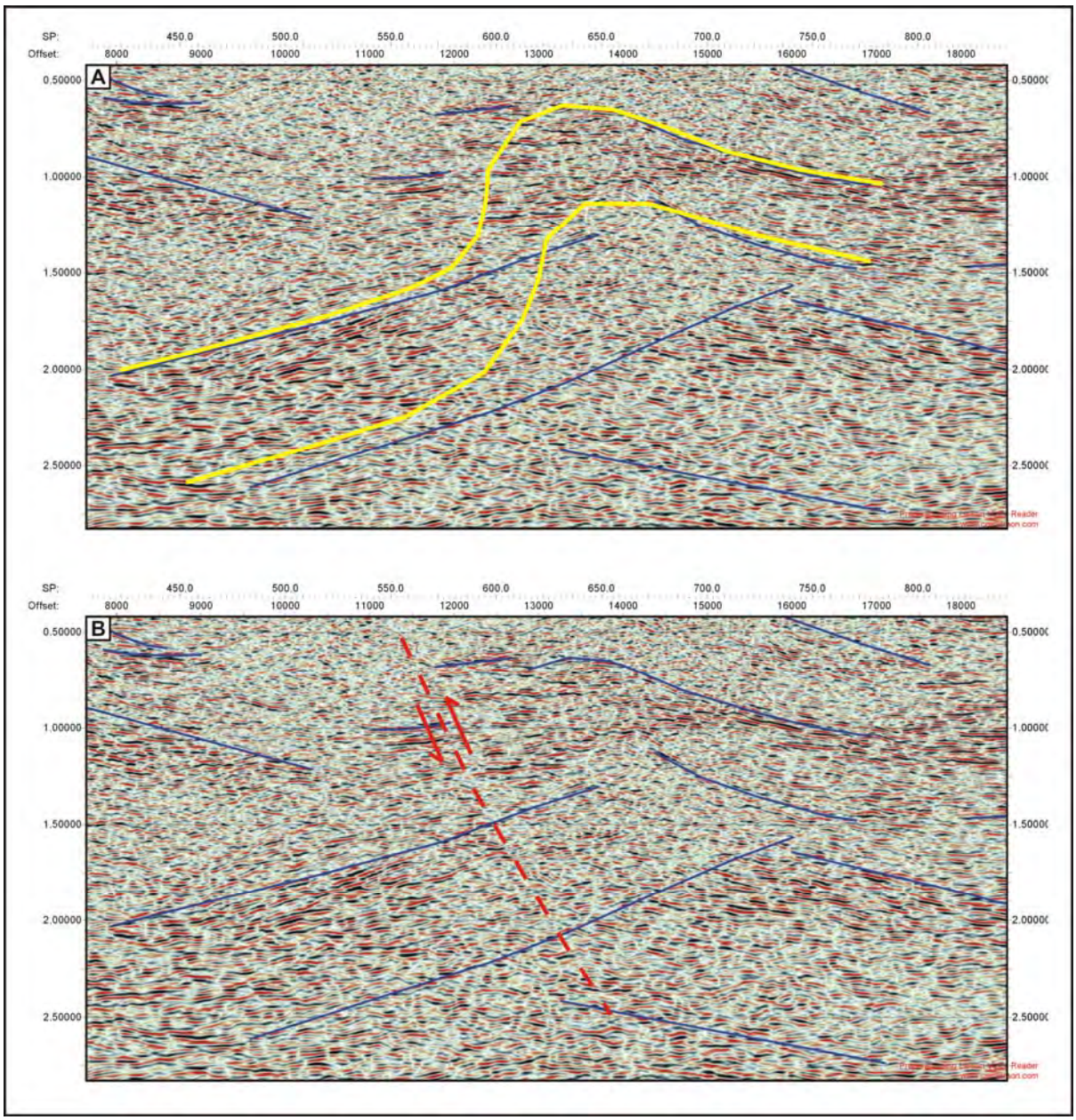

Figure 6.78: Alternative interpretations for basement events between shot-points 400 and 850 (TB01-TB): A). an antiform with a steep western limb, B). a reverse faulted antiform.

Shot-points 900-1650

(Figure 6.79)

The portion of the line between shot-points 900 and 1650 trends towards the east-northeast for 2000 m, then turns towards the southwest from shot-point 1000 (Map 5.1). Quaternary glacial sediments conceal outcrop and structure, making the interpretation of this section of line difficult to constrain.

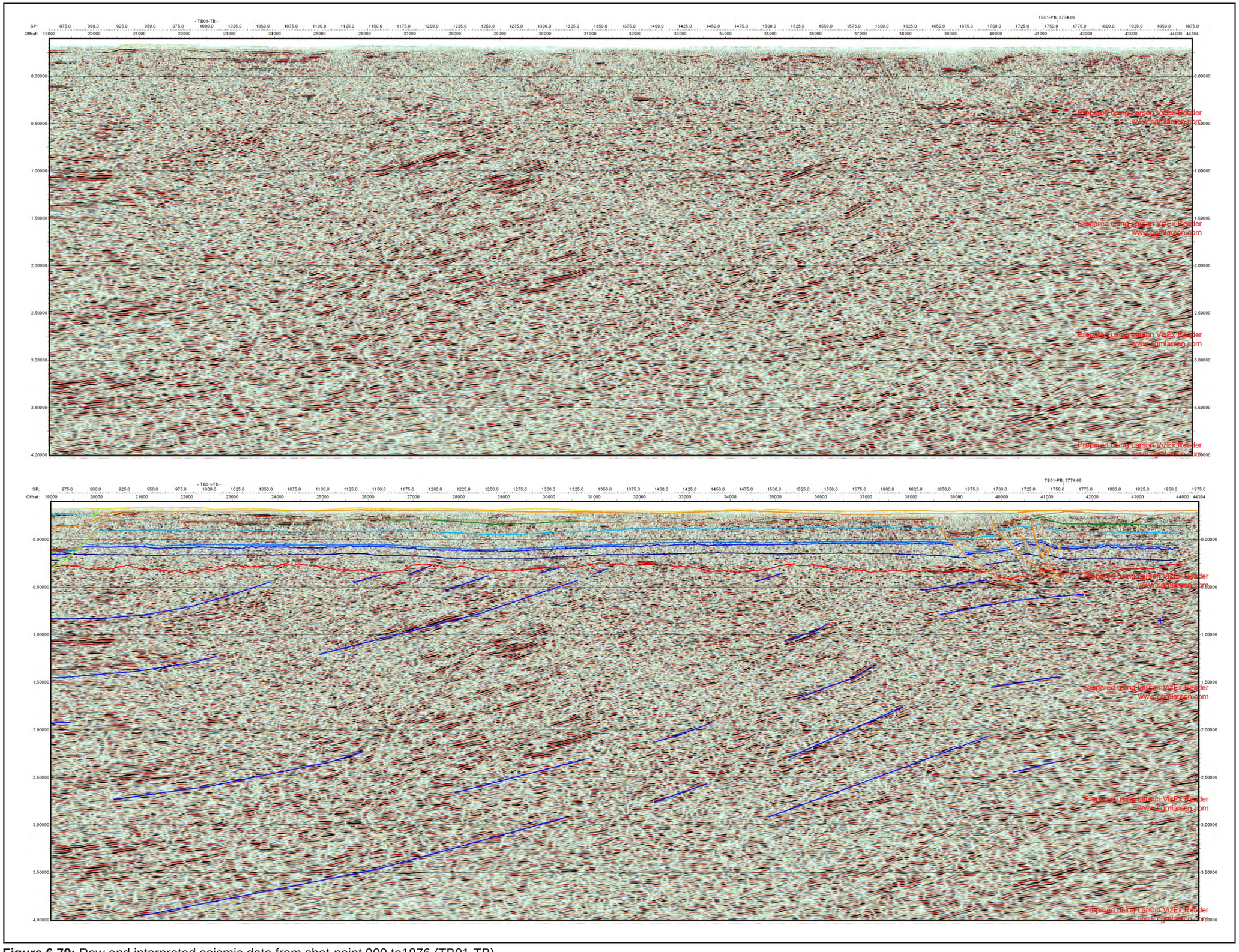

Figure 6.79: Raw and interpreted seismic data from shot-point 900 to1876 (TB01-TB).

In the part of the section interpreted as the Parmeener Supergroup, the seismic data is often incoherent. The Base Parmeener Supergroup Unconformity horizon pick is constrained by several dipping reflections between shot-points 1200 and 1350 that appear truncated by the horizon (Figure 6.79). Between shot-points 900 and 1350 the horizon is picked at the base of a series of subtle, coherent, horizontal reflections, which occur at the same time as the truncated dipping reflections between shot-points 1200 and 1350 (Figure 6.80). Confidently interpreting the horizon from shot-point 1350 to the fault at shot-point 1650 is more difficult. The interpretation is based on an extremely subtle change in amplitude across the unconformity, where reflections in the basement appear stronger (have slightly higher amplitudes) and are more coherent than those in the overlying Parmeener Supergroup (Figure 6.81).

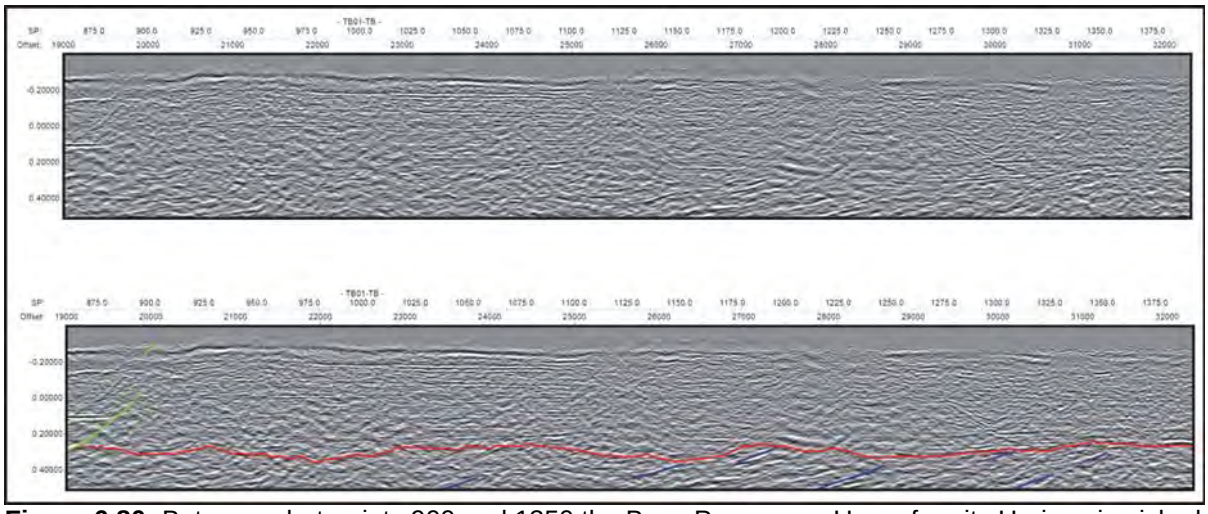

Figure 6.80: Between shot-points 900 and 1350 the Base Parmeener Unconformity Horizon is picked at the base of a series of subtle, coherent, horizontal reflections (TB01-TB).

The Base Dolerite horizon is interpreted at the top of groups of horizontal reflections between shot-points 925 and 1100, 1150 and 1200, 1250 and 1350 and from 1500 to 1650 (Figure 6.79). The interpretation assumes the base of the sill is relatively horizontal allowing the horizon to be extrapolated between these zones.

The horizons interpreted for the Lower Parmeener Supergroup units are fixed at shot-point 900, where the interpretation to the west is used to constrain the positions of the horizons, while at shot-point 1650 the tie with line TB01-PB provides further constraint (Figure 6.79). The incoherent seismic data between shot-points 900 and 1650 make it difficult to interpret the position of these horizons with any accuracy. The horizons have been extrapolated across this section of line, using the more coherent reflections as a guide (Figure 6.79).

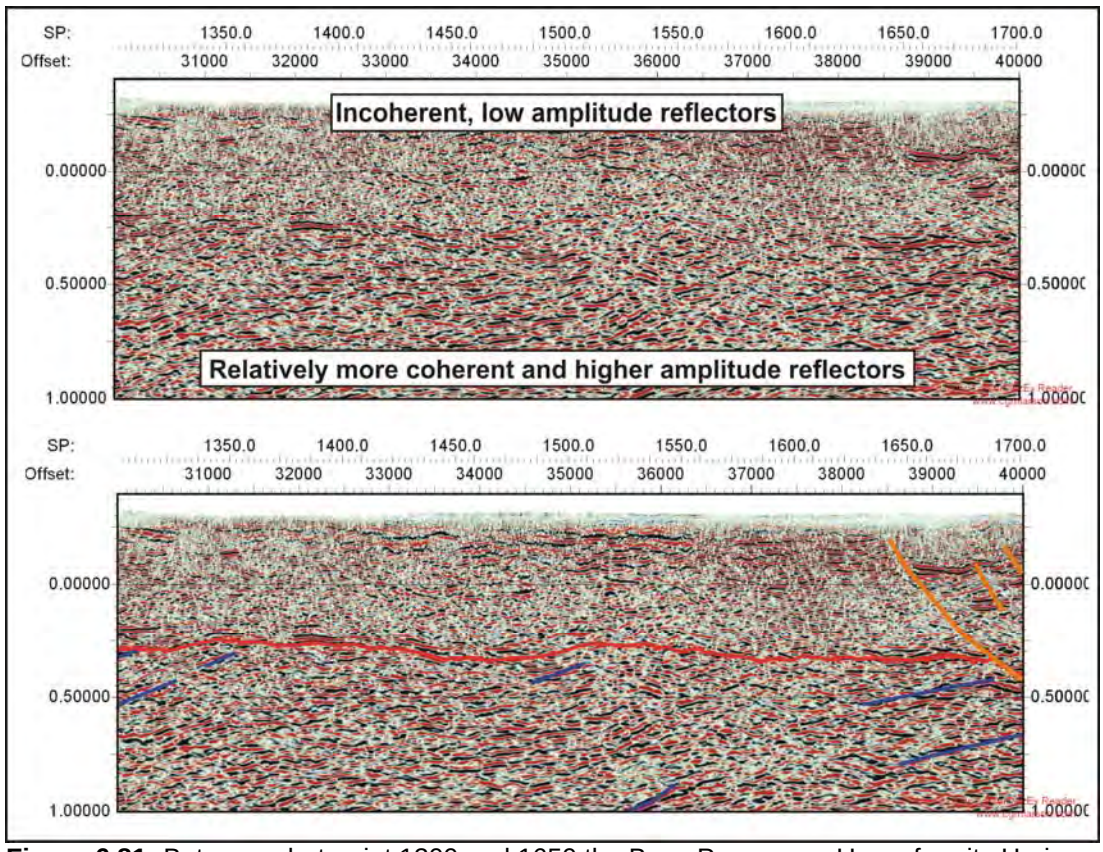

Figure 6.81: Between shot-point 1300 and 1650 the Base Parmeener Unconformity Horizon is picked at a subtle change in coherency and amplitude (TB01-TB).

The interpretation of basement events between shot-points 900 and 1650 is based largely on changes in character and coherency. In this section of line the interpreted events, uniformly dip at about 20° towards the west (left of section) (Figure 6.79). The incoherent zone between shot-points 1350 and 1450 possibly results from a change in direction of the line from southeast to northeast (Map 5.1).

Shot-points 1650 – 1876

(Figure 6.79)

A zone containing several Undifferentiated Tertiary faults is interpreted between shot-points 1650 and 1725, where the dolerite sill appears to thicken rapidly towards the west (Figure 6.82). This interpretation of the dolerite sill and the main fault at shot-point 1650 is based on the changing character of the seismic data. The main fault is interpreted at a change from weak, incoherent reflections on the right to stronger, more coherent reflections on the left (Figure 6.82). The fault is interpreted as post-dolerite (Tertiary), the sense of movement is normal with a throw of about 250 m. No strong evidence for this fault is observed in the topography or in the mapped surface geology. Tertiary Basalt outcrops in this area indicating that faulting preceded the eruption of basalt. The Base Dolerite horizon is interpreted at the base of these weak, incoherent reflections at a zero-crossing between the first strong

(high amplitude) negative and positive reflections (Figure 6.82). Several small offsets in this horizon indicate the presence of several synthetic faults, which display little offset of the Parmeener Supergroup sequences (Figure 6.82).

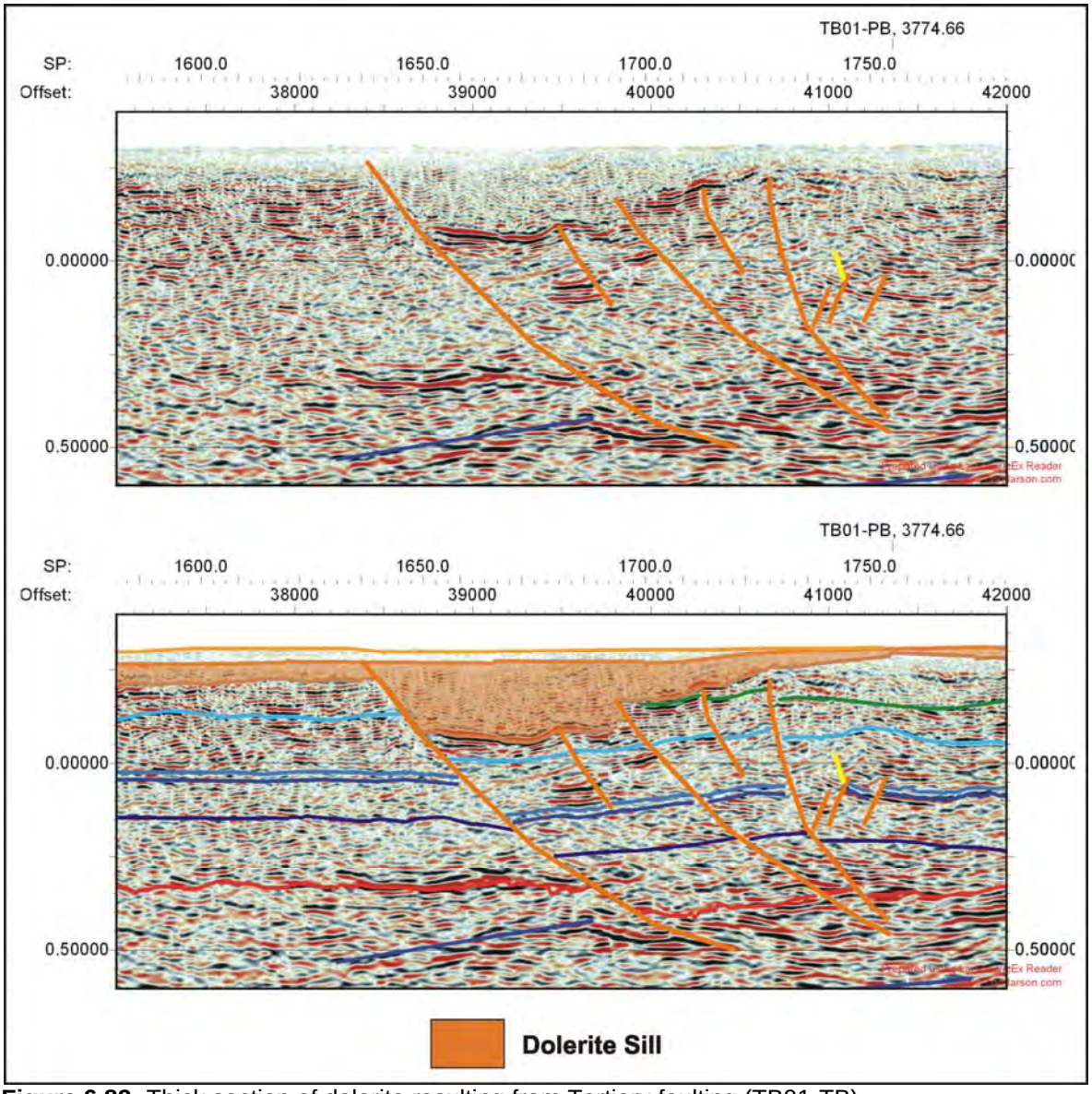

Figure 6.82: Thick section of dolerite resulting from Tertiary faulting (TB01-TB).

The position of the Base Parmeener Unconformity horizon is based partly on the tie with line TB01-PB, and between the intersection with TB01-PB and the main fault at shot-point 1650, the horizon is picked at a change in character at 0.4 seconds TWT (Figure 6.82). Here there is a relative change from incoherent, weak reflections to stronger, and more coherent reflections, which are also thicker (lower frequency) (Figure 6.82). The position of the horizon is defined by similar conditions to the right of the intersection with line TB01-PB, where reflections interpreted to be in the basement are thicker (lower frequency) than reflections in the overlying Parmeener Supergroup sequence.

The positions of the other Parmeener Supergroup horizons are based on the tie with line TB01-PB. The Top Tillite horizon follows a slight change in seismic character to the right of the intersection (Figure 6.82). The interpretation of the other horizons attempts to maintain the unit thicknesses defined at the intersection with line TB01-PB.

There are few definitive basement events in this short section of the line. However, between 0.3 and 2.0 seconds (TWT) reflections are horizontal until they are “pulled up” by the loss of fold towards the edge of the line (Figure 6.79). Below 2.0 seconds (TWT) the seismic data is confused (Figure 6.79).

6.2.7: TB01-TC

Seismic line TB01-TC is located in the southern part of the Central Highlands and is the southernmost line of the survey (Map 5.1, Figure 6.83). The line is 34.58 km long, beginning north of Bothwell on the Lakes Highway (498 251 mE, 5 311 968 mN) where it intersects line TB01-PB (Map 5.1, Figure 6.83). The line follows the Lakes Highway southwest, turning southeast at shot-point 850 and following Hollow Tree Road, then turns back towards the southwest at shot-point 1100 before finishing northeast of Hamilton (489 067 mE, 5 288 268 mN) (Map 5.1, Figure 6.83). The line is acquired in an area of the Central Highlands where the outcrop geology is highly variable. The line passes over Upper Parmeener Supergroup rocks intruded by Jurassic Dolerite, and both are overlain by Tertiary Basalts (Map 5.1, Figure 6.83).

The quality of the seismic data along the line is very poor. Horizons usually interpretable in the other sections by their character or reflection pattern, such as the Top and Base Dolerite and Base Parmeener Unconformity horizons, are largely indistinguishable. The data improves momentarily between shot-points 950 and 1150 where strong, coherent reflections are observed and the Base Parmeener Unconformity horizon can be reliably picked (Figure 6.84). This occurs along the section of the line that runs southeast (Figure 6.83). Why the orientation of the line should affect the quality of flat-lying reflections is not clear. The only constraint on the interpretation is the tie with TB01-PB and the outcrop geology. These coupled with the poor seismic data, has resulted in only a superficial interpretation of this line.

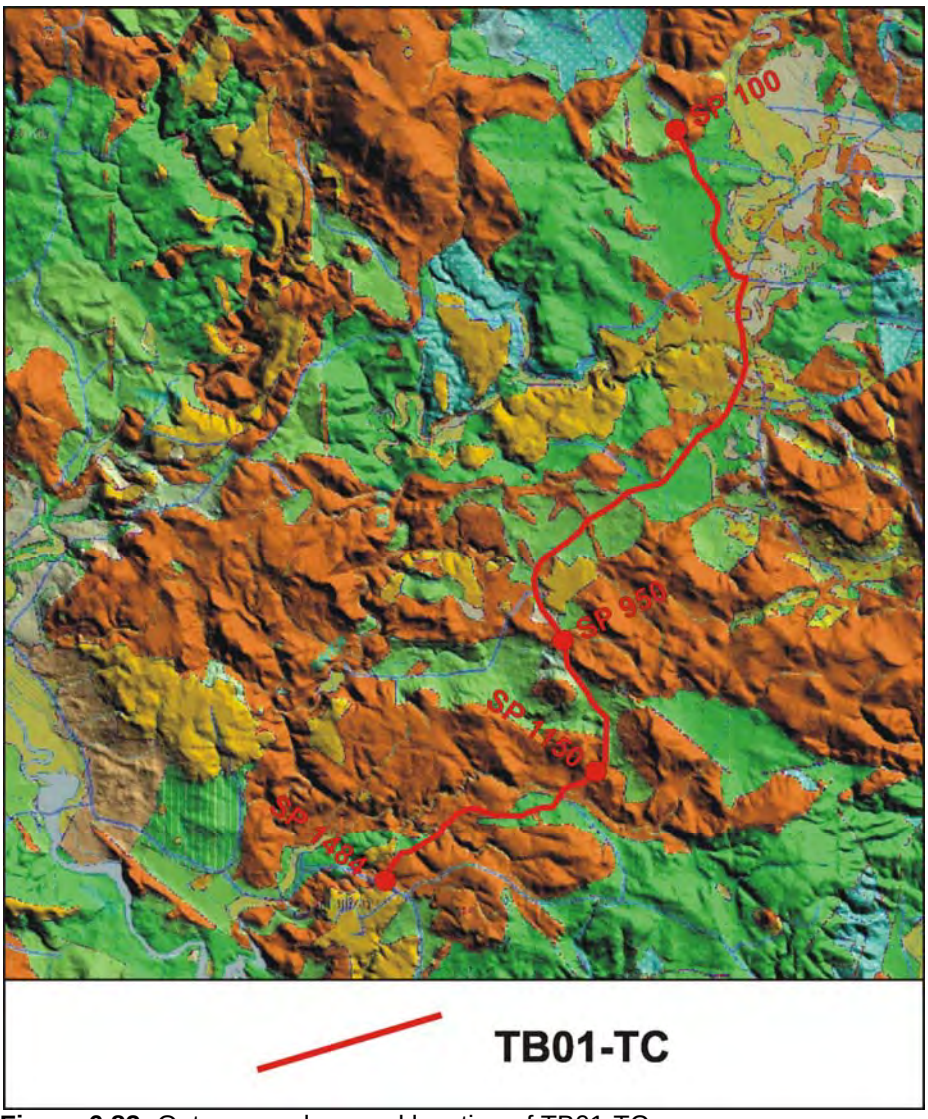

Figure 6.83: Outcrop geology and location of TB01-TC.

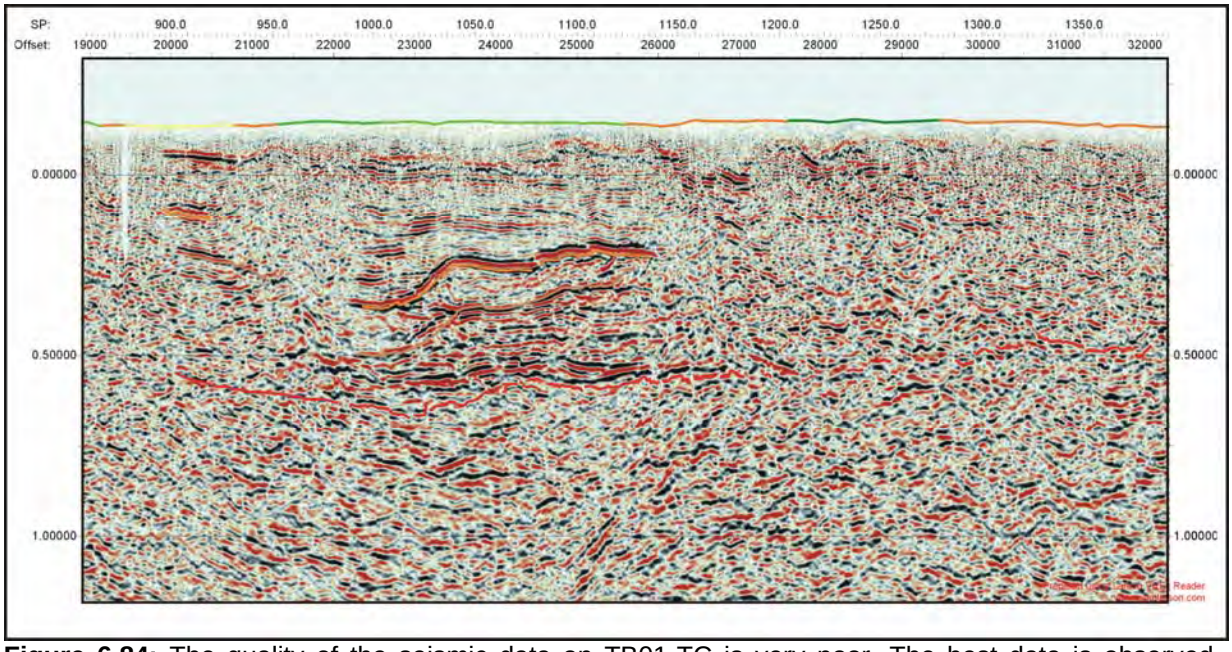

Figure 6.84: The quality of the seismic data on TB01-TC is very poor. The best data is observed between shot-points 950 and 1150, where the Dolerite and Base Parmeener Unconformity horizons can be reliably picked.

Shot-points 100 – 950

(Figure 6.85)

The seismic data in this section of line is for the most part incoherent. The line intersects with TB01-PB between shot-points 100 and 300, helping to constrain the interpretation (Map 5.1). However, the data at this end of line TB01-PB is itself very poor and the interpretation unreliable.

The Base Parmeener Unconformity horizon can be placed with reasonable confidence at the base of incoherent, but strong (high amplitude) reflections between shot-points 100 and 350, below these lie equally incoherent reflections, which are weaker (lower amplitude) and thinner (higher frequency) (Figure 6.86). While in the greyscale image, a distinguishable, strong event is observed in the corresponding position (Figure 6.86). The position of the horizon is ambiguous from shot-point 350 to shot-point 700 where a zone of strong reflections at the same level (0.5 seconds TWT) indicates that the Base Parmeener Unconformity is mostly horizontal across this section of the line (Figure 6.85).

In this section of the line, the seismic character typical of dolerite sills does not readily define the Top and Base Dolerite horizons. Between shot-points 150 and 950 the Top and Base Dolerite horizons are interpreted at the top and base of a zone of strong, highly incoherent reflections that occurs around 0.0 seconds (TWT) (Figure 6.85). This interpretation is based on the strong reflections at 0.1 seconds (TWT) between shot-points 150 and 250, which are similar to reflections picked for the Base Dolerite horizon in other lines of the survey (Figure 6.86).

Events in the basement are interpreted at boundaries where there is either a change in orientation of the reflections or a change in seismic character (Figure 6.85). However, considering the poor nature of the seismic data nearer to the surface, the effective imaging of any structure in the basement seems unlikely and the basement events are interpreted with little confidence.

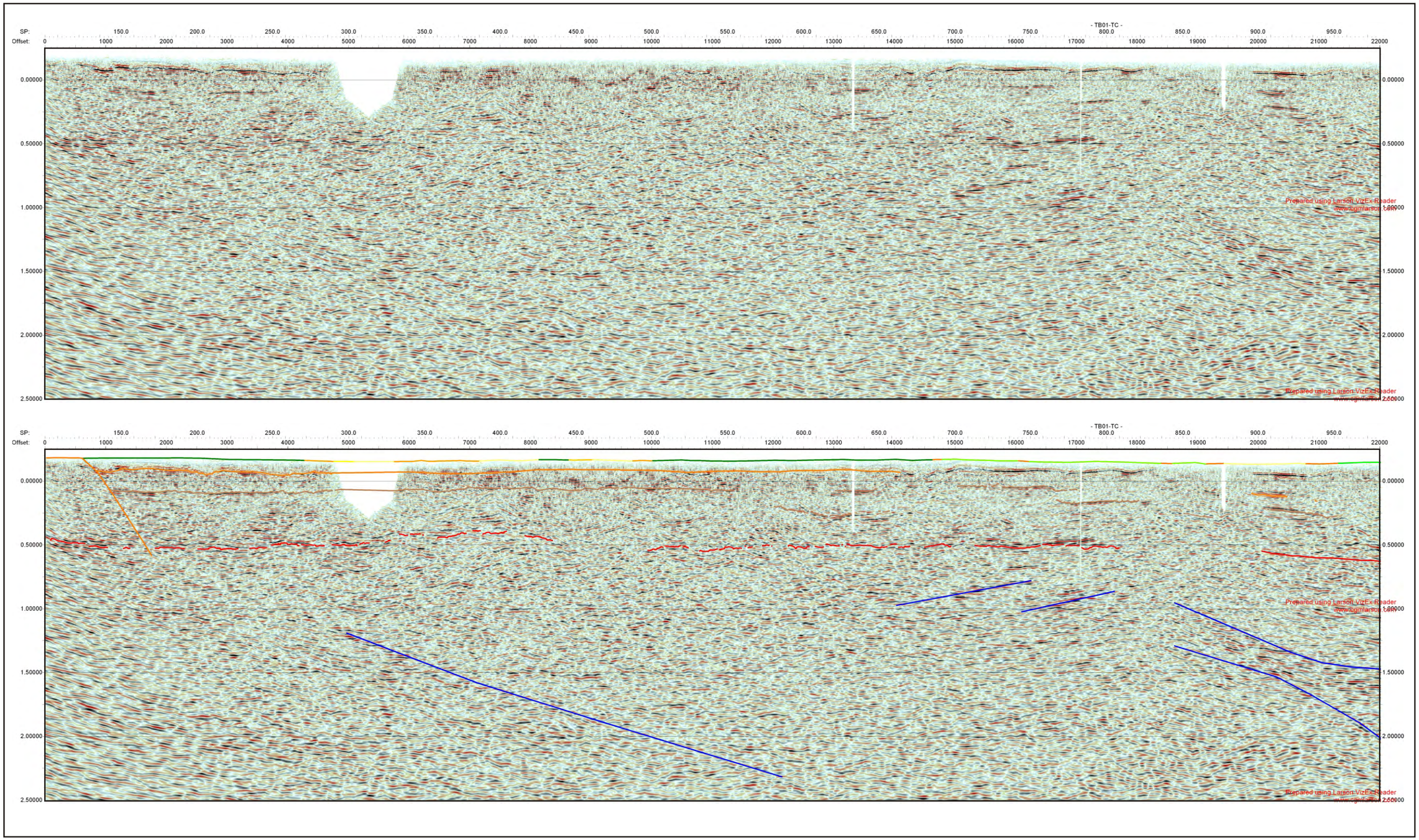

Figure 6.85: Raw and interpreted seismic data from shot-point 100 to 950 (TB01-TC).

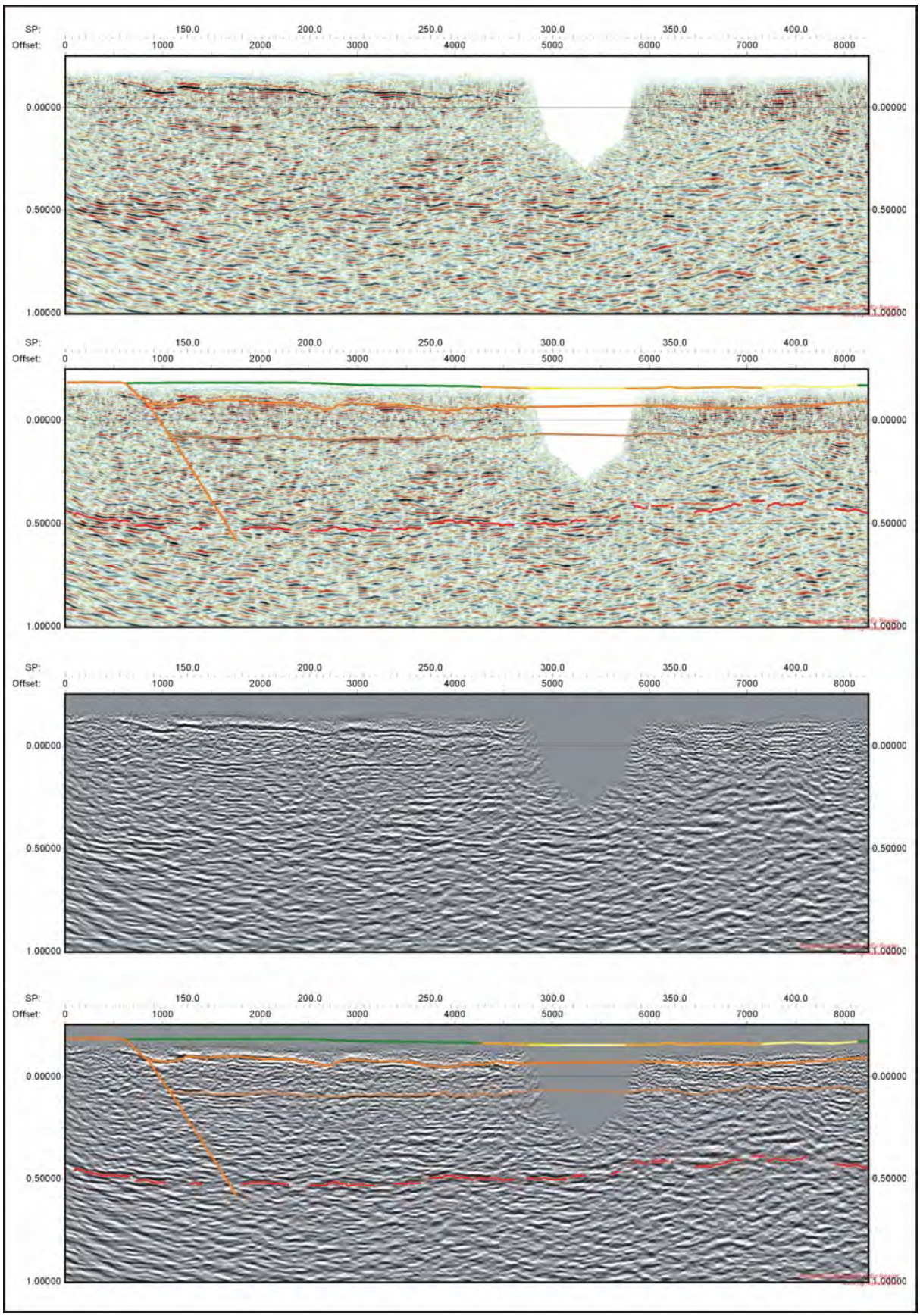

Figure 6.86: The Base Parmeener Unconformity and Top and Base Dolerite horizon picks between shot-points 100 and 350 (TB01-TC).

Shot-points 950 – 1484

(Figure 6.87)

The seismic data quality is again very poor in this section of the line, with the exception of an anomalous zone of coherent data between shot-points 1000 and 1150 (Figure 6.88). The seismic data around this zone is so incoherent that no horizons or structures other than the Base Parmeener Unconformity horizon can be interpreted with any confidence (Figure 6.87). The Base Parmeener Unconformity horizon can be reliably picked between shot-points 1000 and 1150 at the base of a series of strong coherent reflections (Figure 6.88) and is extrapolated to shot-point 1400, guided by some stronger and lower frequency reflections that occur at 0.5 seconds (TWT) (Figure 6.87).

In the zone of coherent reflections between shot-points 1000 and 1150, an event that cuts across horizontal reflections can be seen between 0.25 and 0.5 seconds (TWT) (Figure 6.88). This event has been interpreted as a dolerite sill. Above this, between 0.0 and 0.25 seconds (TWT) is another zone of reflections with similar character has been also interpreted as a dolerite sill (Figure 6.88). This interpretation is inconclusive due to the poor resolution of the data, however, stacked dolerite sills are reported in the Hobart area (Leaman, 1975). The outcrop geology traversed by this line is more complicated than that of the Central Highlands to the north and has a similar complexity to southern Tasmania (Figure 6.89).

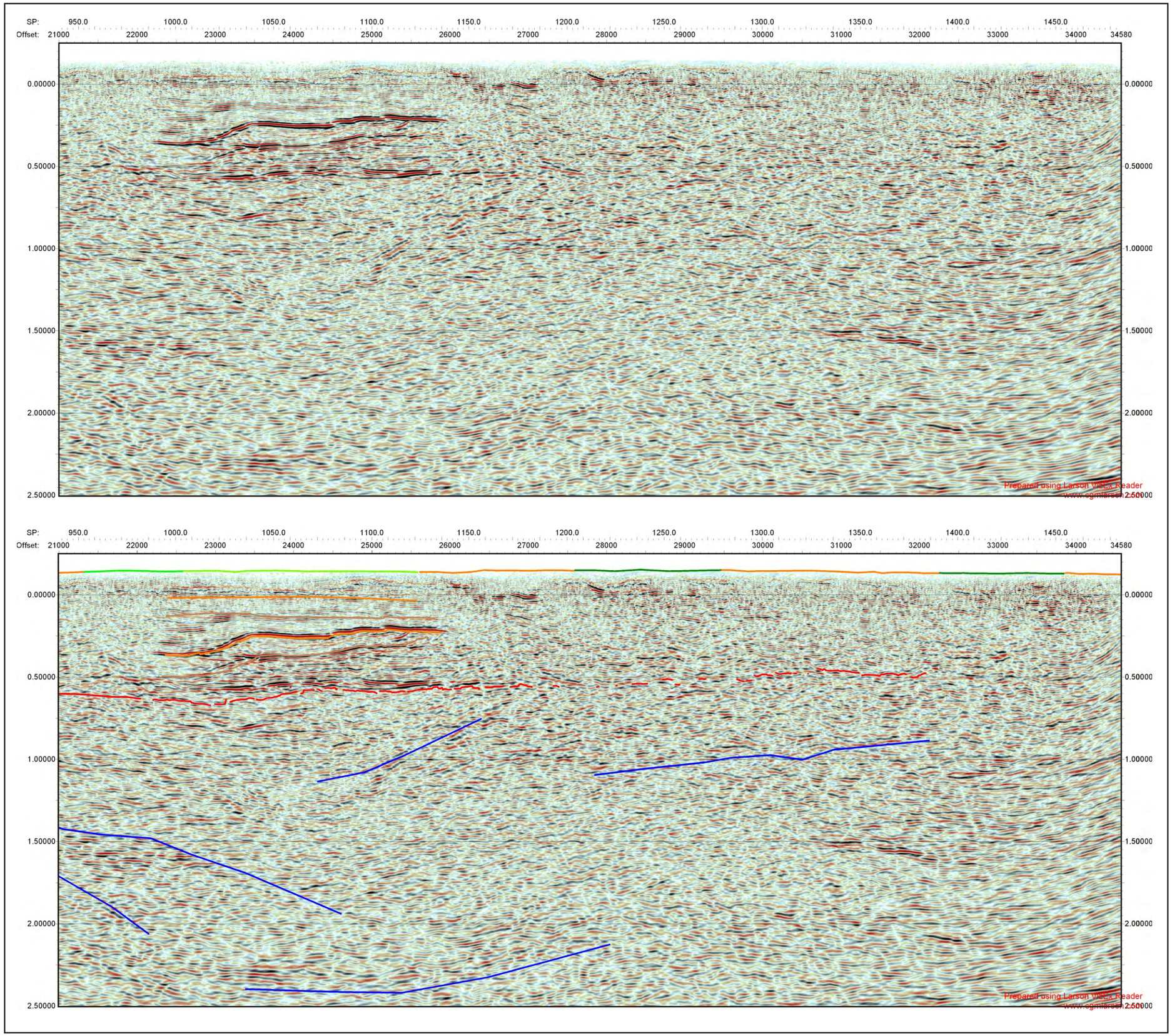

Figure 6.87: Raw and interpreted seismic data from shot-point 950 to 1484 (TB01-TC).

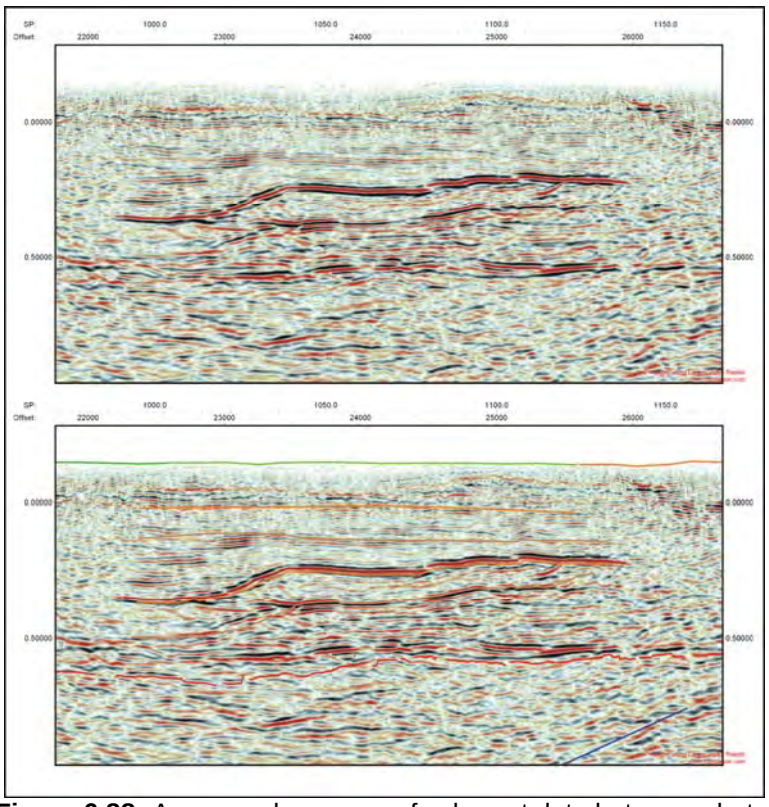

Figure 6.88: An anomalous zone of coherent data between shot-points 1000 and 1150 with horizon picks showing stacked dolerite sills (TB01-TC).

Figure 6.89: The outcrop geology of south-eastern Tasmania traversed by TB01-TC is more complex than that of the Central Highlands.

6.2.8: TB01-TD

Seismic line TB01-TD is located on the western side of the Central Highlands and has been acquired perpendicular to line TB01-PB, which it intersects at the northern end of a window in the outcropping dolerite (Map 5.1, Figure 6.90). The line is 15.29 km long, relatively straight and trends northwest to southeast. The line begins on the escarpment of the Great Pine Tier (465 760 mE, 5 338 713 mN) and finishes on the Bellevue Tier (456 924 mE, 5 349 413 mN) (Map 5.1, Figure 6.90). The line has been mainly acquired over outcropping dolerite, with Upper Marine Sequence rocks outcropping within the "window" (Map 5.1, Figure 6.90).

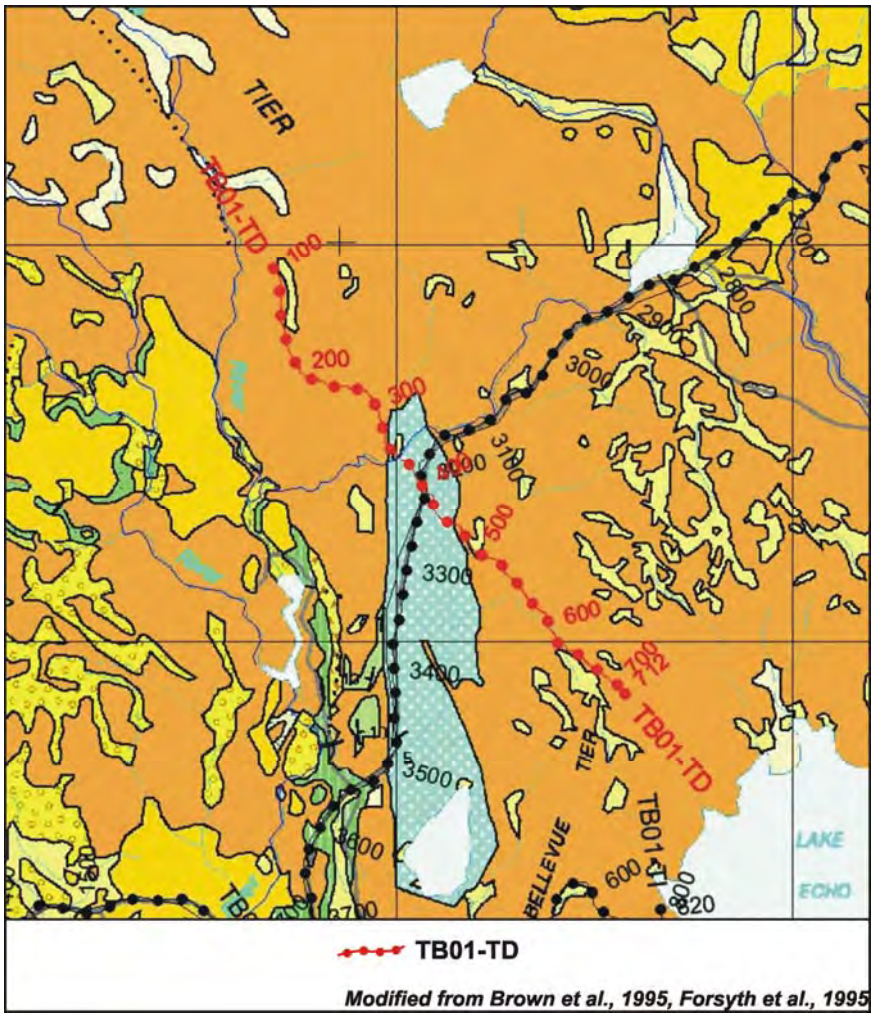

Figure 6.90: Outcrop geology and location of TB01-TD.

The quality of the seismic data along this line is variable. The seismic data in the Parmeener Supergroup part of the section is vague, interspersed with small zones containing more coherent data (Figure 6.91). In the basement section, distinct events can be recognised which correlate well with events interpreted in the basement of line TB01-PB. The interpretation of this line relies heavily on the tie with line TB01-PB.

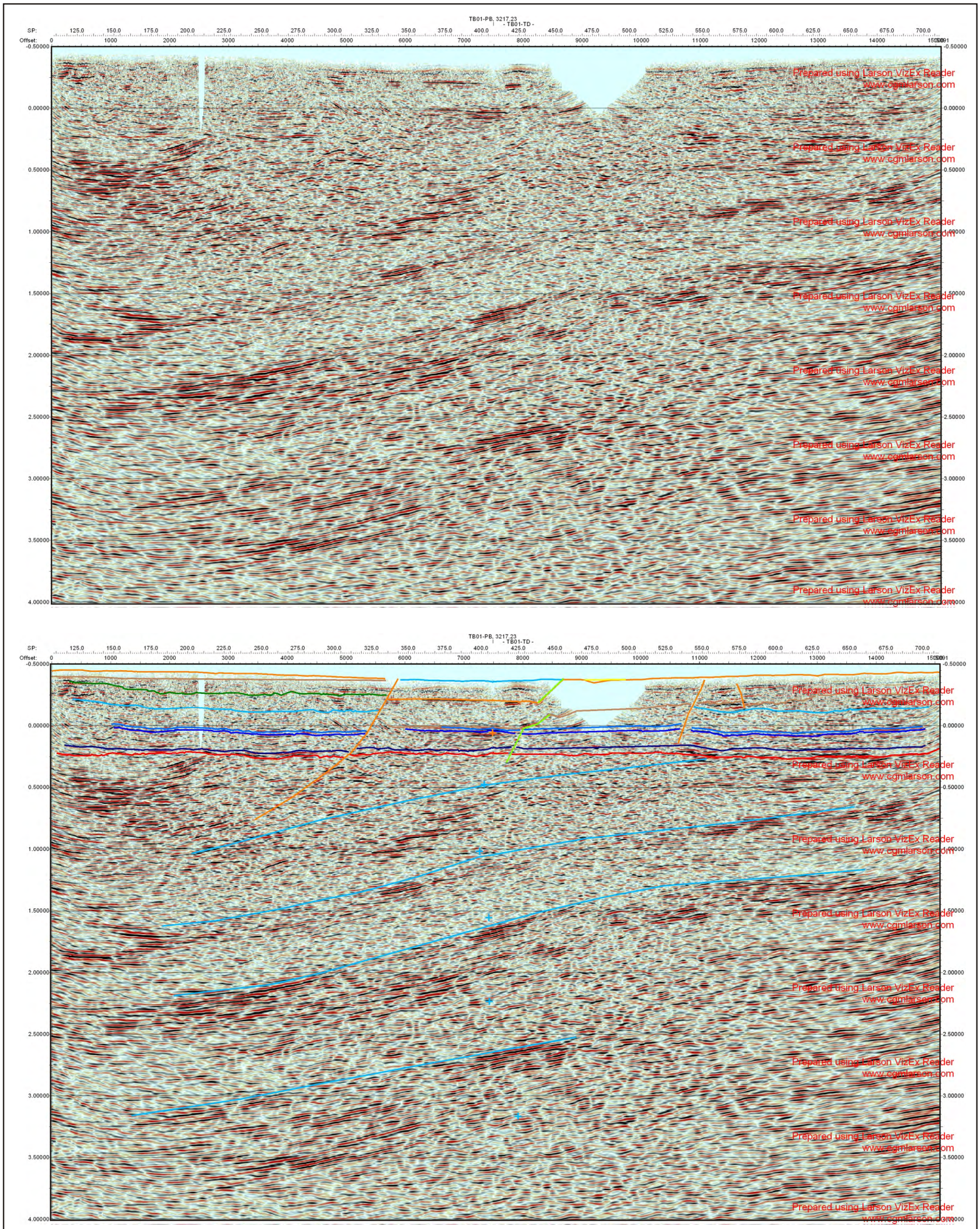

Figure 6.91: Raw and interpreted seismic data for TB01-TD.

Shot-points 100 – 350

(Figure 6.91)

This section of the line runs from the Great Pine Tier to the contact between outcropping dolerite and Upper Marine Sequence rocks that mark the beginning of the "window" (Figure 6.90). The Parmeener Supergroup section is constrained by the interpretation of line TB01-PB between shot-points 3500 and 3800.

The position of the Base Parmeener Unconformity horizon is easily interpreted from the intersection of horizontal and dipping reflections at 0.25 seconds TWT at shot-point 200 (Figure 6.92). The interpretation is strengthened by a distinct change in seismic character from strong, coherent reflections to more incoherent reflections at the same time between shot-points 185 and 250 (Figure 6.92).

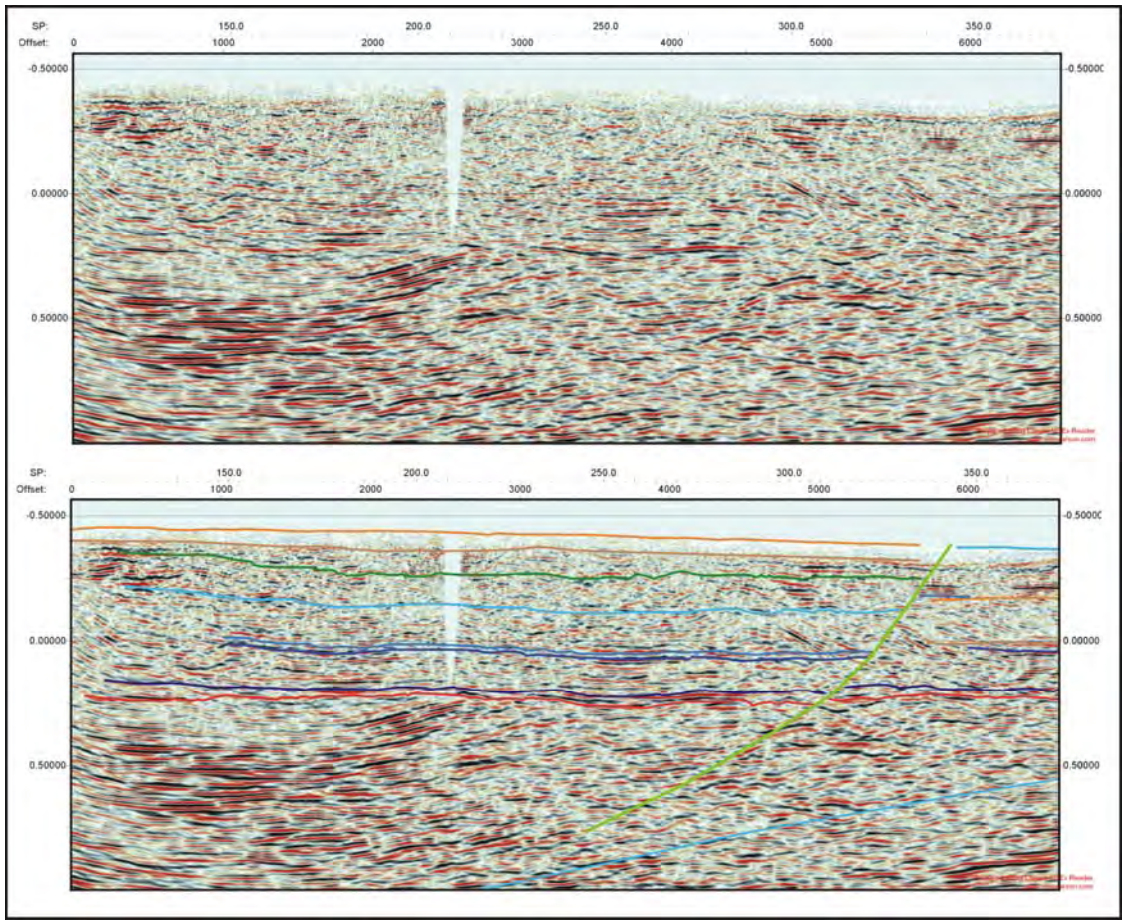

Figure 6.92: Raw and interpreted seismic data showing horizon picks between shot-points 100 and 350 (TB01-TD).

The thickness of the dolerite sill is 250 m, calculated from elevations derived from the DEM. This estimate was made by taking the elevation of shot-point 200 (highest outcropping dolerite in this section of line), and assuming that the contact at the base is flat lying,

subtracting the elevation of the nearest base dolerite – Upper Parmeener Supergroup contact (Figure 6.93). Between the interpreted Base Dolerite and Base Parmeener Supergroup horizons, there is sufficient space to place the entire Lower Parmeener Supergroup section and units of the Upper Parmeener Supergroup, based on the thicknesses interpreted on line TB01-PB between shot-points 3500 and 3800 (Figure 6.92).

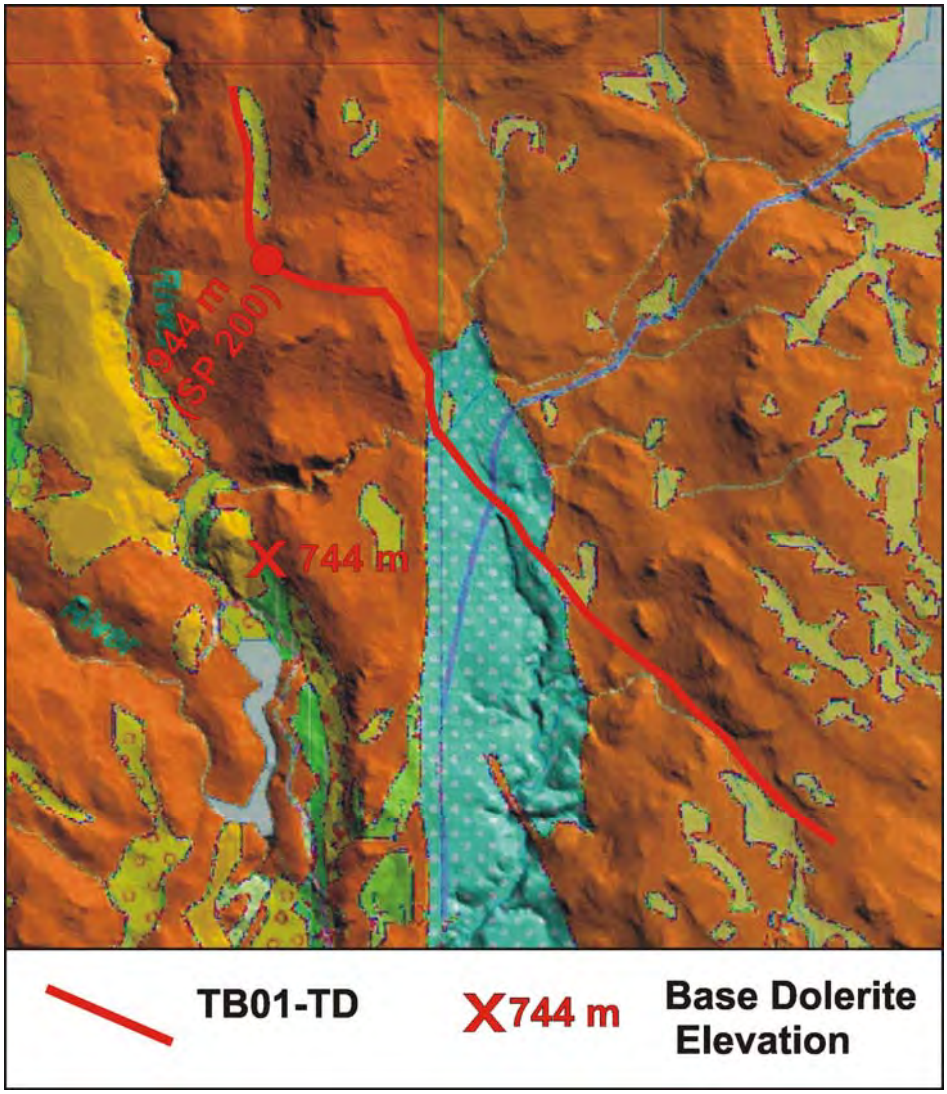

Figure 6.93: Elevations of the top and base of the dolerite sill used to calculate the thickness of the sill.

A fault, down to the west is interpreted at shot-point 350. This fault should have a similar history to the fault interpreted at shot-point 3500 on line TB01-PB. The position of the top of the fault is constrained by the dolerite-Parmeener Supergroup contact, the trace of the fault is not obvious and the interpretation is guided by dipping reflections at 0.5 seconds TWT at shot-point 300 (Figure 6.92). Steeply dipping reflections can be recognised at 0.00 seconds TWT on either side of the fault (Figure 6.92). It is not clear if these are related to the geology, or diffractions or processing artefacts.

Shot-points 350 – 550

(Figure 6.91)

To the southeast of the contact Upper Marine Sequence rocks outcrop (Forsyth et al., 1995, Brown et al., 1995) (Figure 6.90). A series of coherent reflections at -0.2 seconds TWT indicate layered rocks down to this level. Below these a sudden change in character to weak, incoherent reflections indicates the top of the dolerite sill. Coherent reflections at 0.00 seconds (TWT) indicate the position of the base of the dolerite sill (Figure 6.91). Both of these picks correlate with the tie to TB01-PB. The Base Parmeener Unconformity is difficult to pick in this section of line and the tie with TB01-PB guides the interpretation of the horizon.

Southeast of the tie with line TB01-PB, near the contact on south-eastern side of the window, there is a 2 km gap in the seismic data resulting from a river crossing that prevented data acquisition (Figure 6.91). Dolerite is mapped at the surface from shot-point 450 and as no faults can be interpreted from the seismic data or from the DEM it is not clear how the dolerite sill steps up through the section across this boundary. The Parmeener Supergroup horizons are extrapolated across the gap in the seismic data, terminating at a fault at shot-point 550.

Basement

Events interpreted in the basement are similar to events on line TB01-PB and are picked on similar changes in character (Figure 6.94). The events dip towards the northwest at ~10°, indicating the anticline interpreted on line TB01-PB plunges gently towards the northwest.

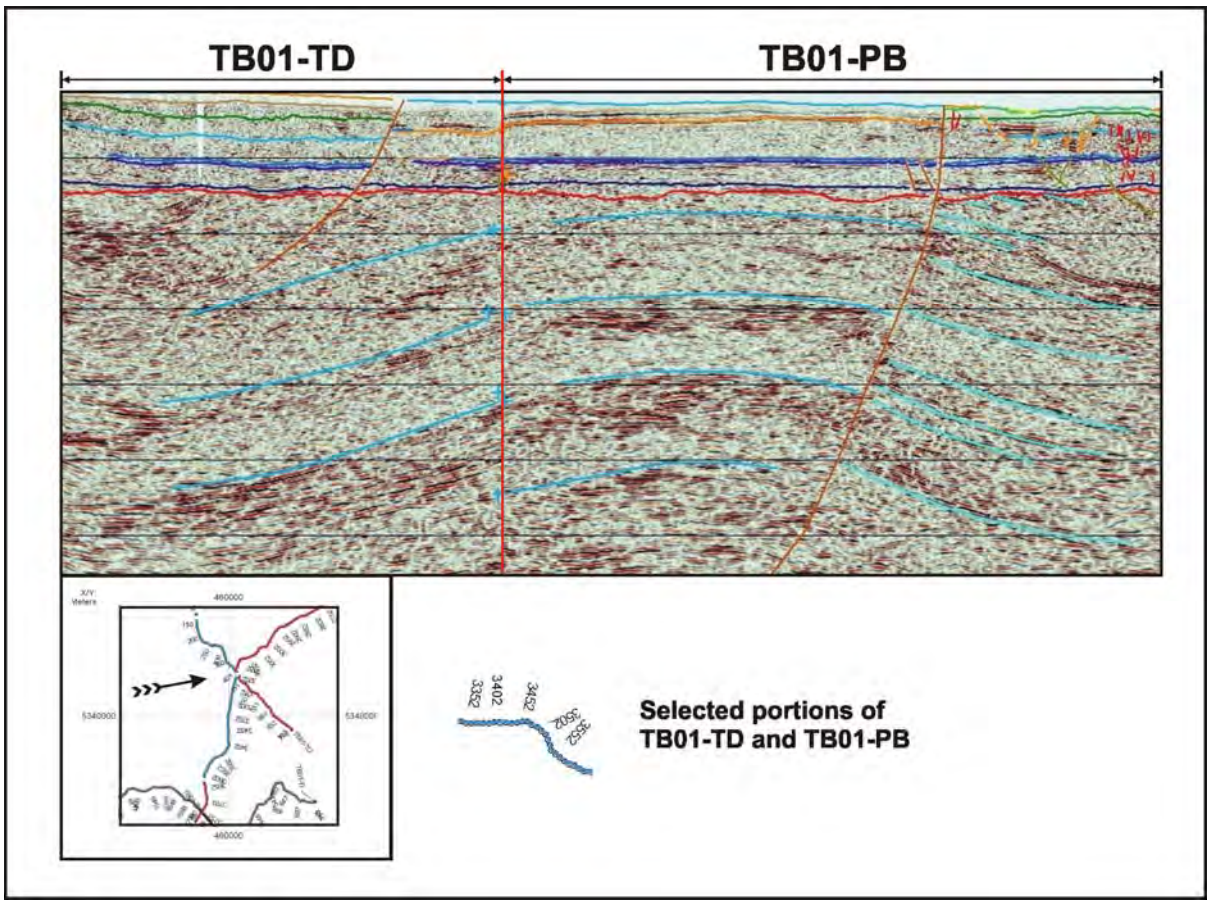

Figure 6.94: Arbitrary line created through TB01-TD and PB showing the continuity of the horizon picks in the basement section.

6.2.9: TB01-TH

Seismic line TB01-TH has been acquired across the Meander Valley, the Great Western Tiers and in the northern part of the Central Highlands (Map 5.1, Figure 6.95). The line is 67.86 km in length and has been recorded along the Lake Highway. The line begins south of the town of Deloraine (470 887 mE, 5 401 993 mN) and heads towards the southwest as far as shot-point 200 (Map 5.1, Figure 6.95). From shot-point 200, the line heads south to shot-point 350, then southeast to shot-point 1000 (Map 5.1, Figure 6.95). From shot-point 1000 the line, although rather windy, heads south to shot-point 2750, where it turns east around the bottom of Great Lake, finishing west of the township of Miena (474 704 mE, 5 351 055 mN) (Map 5.1, Figure 6.95).

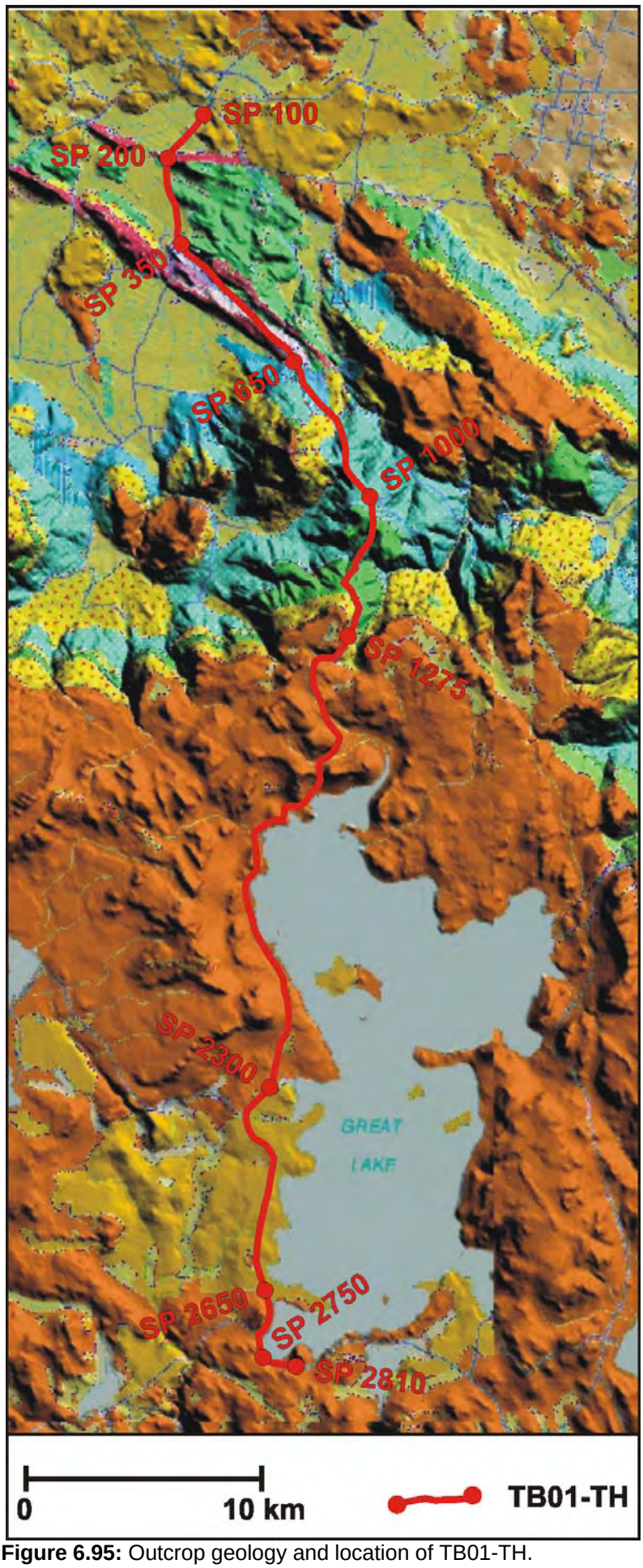

Figure 6.95: Outcrop geology and location of TB01-TH.

From Deloraine to shot-point 650, the line passes over Quaternary sequences and steeply dipping rocks of Late Cambrian to Neoproterozoic age (McClenaghan and Calver, 1994) (Map 5.1, Figure 6.95). From shot-point 650, the line moves up though the Parmeener Supergroup sequence, beginning in rocks of the Lower Marine Sequence of the Lower Parmeener Supergroup and finishing at the top of the Great Western Tiers (shot-point 1275) in rock of Unit 2 of the Upper Parmeener Supergroup (McClenaghan and Calver, 1994) (Map 5.1, Figure 6.95). The remainder of the line is acquired over dolerite, with the exception of a short section near Liawenee (shot-points 2300-2650) where Tertiary Basalt is mapped (Forsyth et al., 1995) (Map 5.1, Figure 6.95). The main constraints on the interpretation of this line are the drill hole at Golden Valley and the Parmeener Supergroup section mapped in the escarpment of the Great Western Tiers, constraint of the basement structure is supplied by mapped outcrop between Deloraine and the Golden Valley drill hole (Map 5.1, Figure 6.95).

Shot-points 100 – 650

(Figure 6.96)

This section of line is important as it is the only data in the entire survey to have been recorded over mapped basement rocks (Barton et al., 1969). The seismic data in this section is typical of seismic data recorded for the basement. The data is incoherent with subtle changes in seismic character. In the top 0.1 seconds (TWT) of the section, there is a zone at where the data is very incoherent, the base of this zone is defined by negative, positive, negative, high amplitude, low frequency event. The interpretation of the events in the basement was conducted similarly to other lines in the survey, where the events are primarily picked at changes in seismic character and often guided by coherent reflections.

The seismic data between shot-points 100 and 650 should show events with similar dips (apparent dips) to those indicated by geological mapping. Figure 6.97 shows the paths of the seismic line across the section of outcropping basement rocks. Using the formula: Tan (apparent dip) = Tan (true dip) x Sin (angle between strike and the cross-section), the apparent dips were calculated for shot-points 200, 350 and 575, where adjacent strike and dip data can be projected onto the line (Table 6.1). These results were then drawn onto the section ($V/H \approx 1$) in their correct locations and projected to 1 km depth (Figure 6.98).

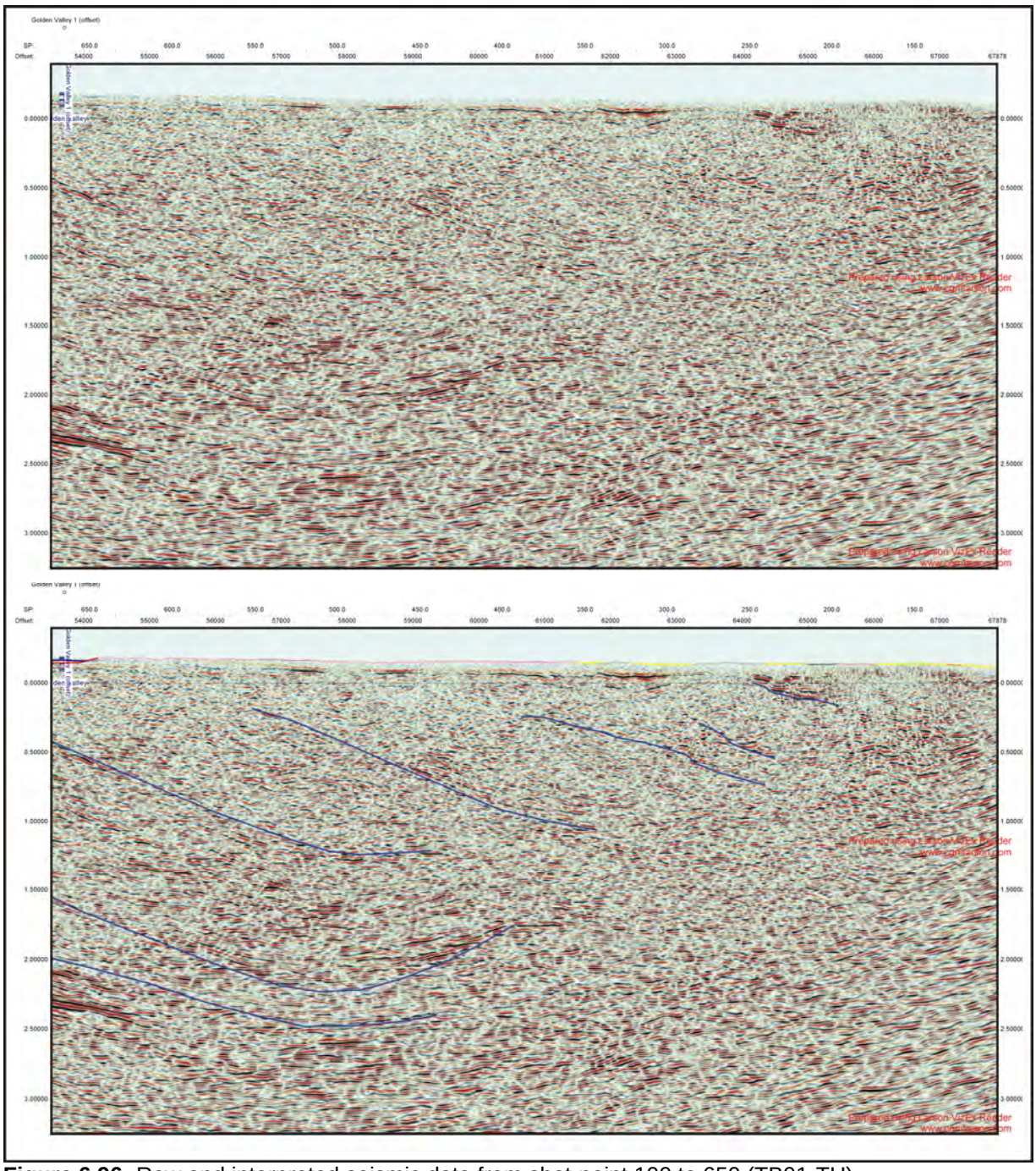

Figure 6.96: Raw and interpreted seismic data from shot-point 100 to 650 (TB01-TH).

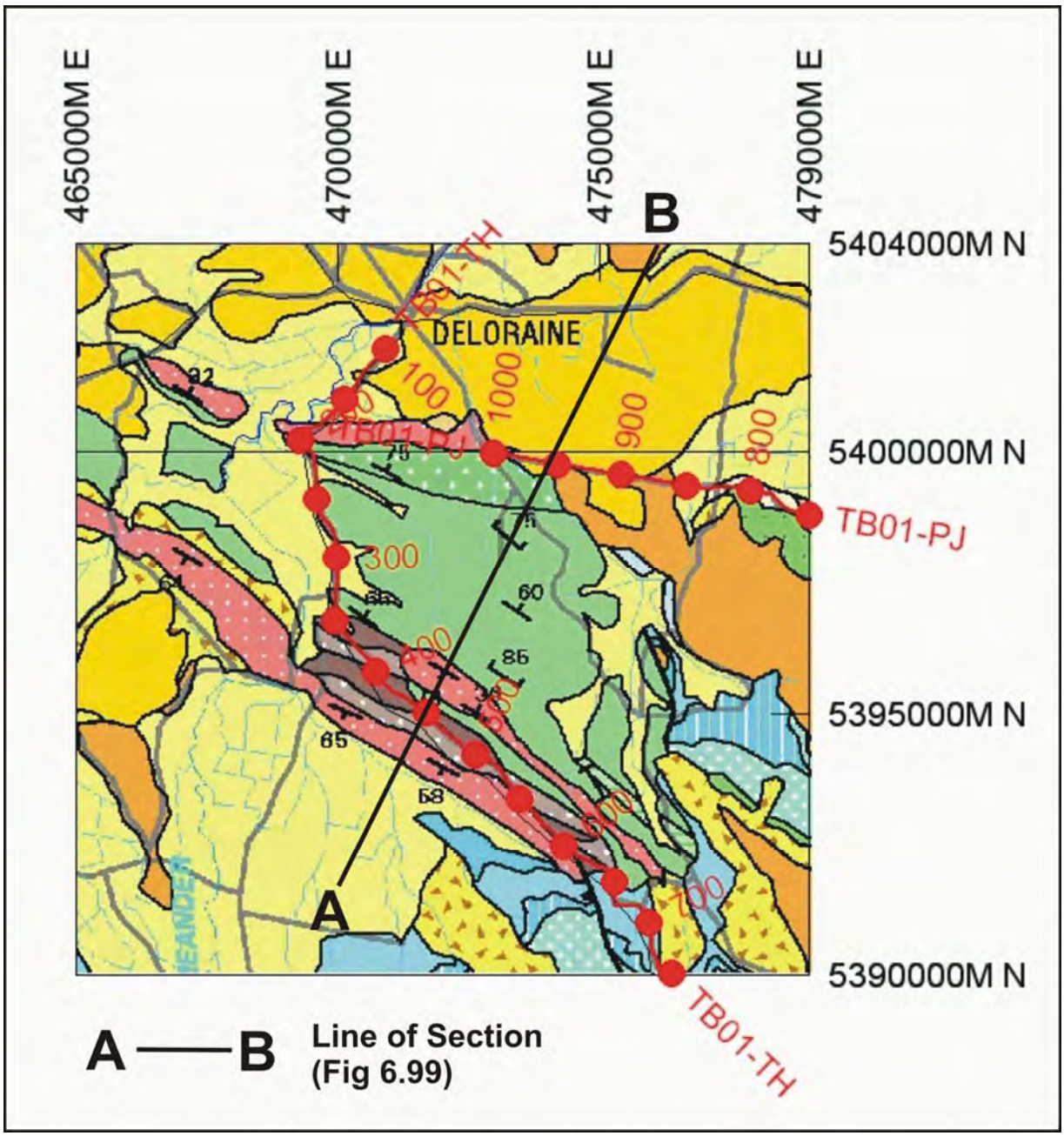

Figure 6.97: Outcrop geology and path of TB01-TH between shot-points 100 and 650. (Modified from McClenaghan and Calver, 1994)

Table 6.1: Apparent dip calculations for shot-points located in outcropping basement rocks.

Shot-point location	True Dip	Angle between strike and the seismic line	Calculated Apparent Dip
200	53°	90°	53°
350	65°	60°	62°
575	87°	14°	78°

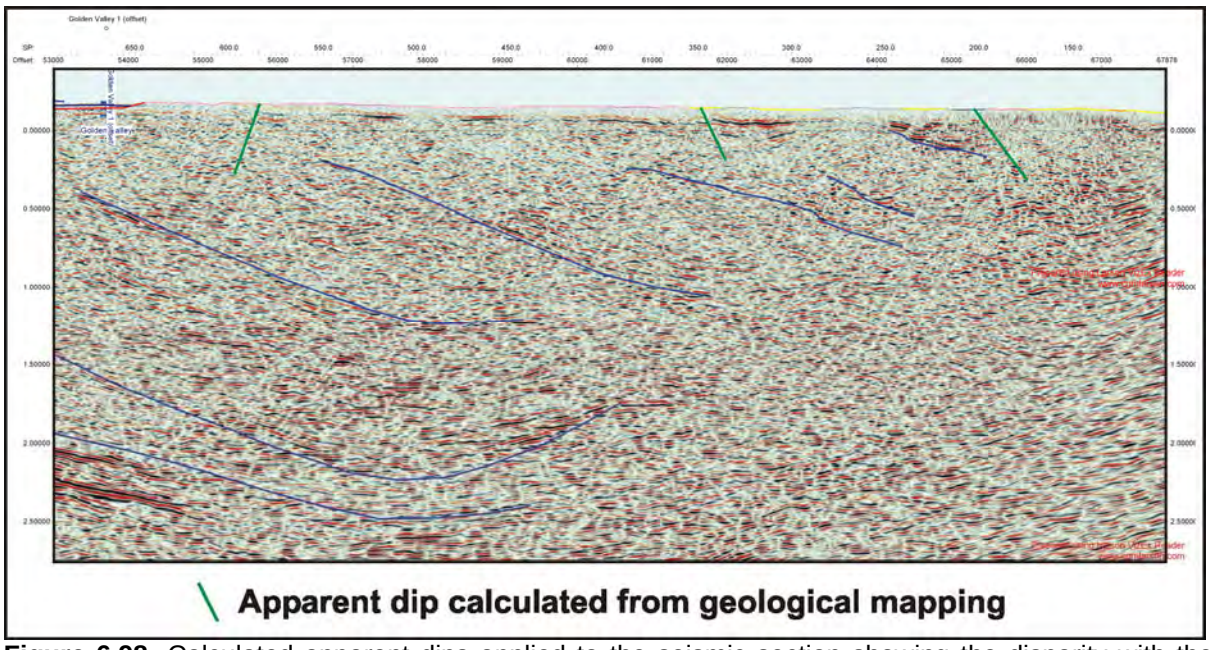

Figure 6.98: Calculated apparent dips applied to the seismic section showing the disparity with the interpreted seismic events in the basement (TB01-TH).

The most readily identifiable events in the basement in this part of the line all dip between 10° and 20° and do not reflect the dips calculated (Figure 6.98). At shot-point 200, the calculated dip does correspond to a change in character (Figure 6.98). However, this change is ambiguous and can be followed for only a short distance. While at shot-points 350 and 575, the calculated dips do not correspond with any distinctive seismic events (Figure 6.98). The seismic data in the first 0.5 seconds TWT of the section cannot be confidently interpreted to correspond to the steep dips calculated. Deeper in the section there are no events that can be confidently correlated with the steeply dipping strata that might be expected. The expected complexity of the section is shown in Figure 6.99. The seismic data in this portion of line does not image this complex geology. Therefore complex events in the basement are probably below the resolution of the seismic data and the interpreted basement events are unlikely to reflect folded bedding. Some other feature is being imaged.

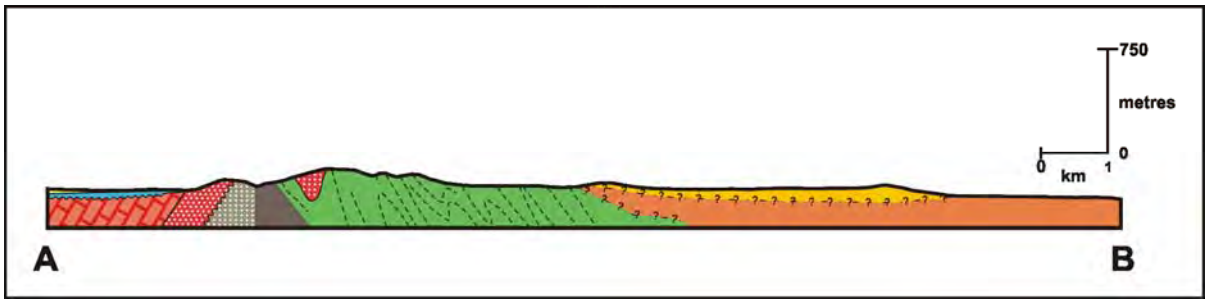

Figure 6.99: Cross-section though outcropping basement units. (Modified from Pike et al., 1973)

Shot-points 650 – 1650

(Figure 6.100)

At shot-point 650, the line moves from outcropping basement rocks to the Parmeener Supergroup. The interpretation of this section of line in extremely well constrained by outcrop in the escarpment of the Great Western Tiers. The seismic data is coherent, allowing the horizons to be confidently picked until shot-point 1650. The Parmeener Supergroup dips between 3°and 5° towards the southwest across in this area (Pike et al., 1973). This matches the data on the geological map of the area, where the geological boundaries closely follow topographic contours (Figure 6.101).

From shot-point 650 to 1275, the interpretation of the Parmeener Supergroup horizons is based on the mapped outcrop in the escarpment, except for the Top Tillite and Base Parmeener Unconformity horizons, which are interpreted based on the unit thicknesses recorded in the Golden Valley drill hole. The Base Parmeener Unconformity horizon is picked on a strong group of reflections (black, red, black). This event often marks the boundary between horizontal, coherent reflections, underlain by less coherent, occasionally dipping reflections (Figure 6.102).

Beyond shot-point 1275, the Parmeener Supergroup is intruded by dolerite (Figure 6.100). The interpreted horizons follow the coherent seismic data from the lithological contacts seen in mapped outcrop (Figure 6.100). Where the seismic data is less coherent the thicknesses of the mapped units calculated from the DEM are used to constrain the interpretation. It is assumed that the base of the dolerite is conformable with the Parmeener Supergroup horizons, therefore the Base Dolerite horizon is picked parallel to the Parmeener Supergroup horizons until shot-point 1450 (Figure 6.100). After this point, an increase in measured gravity field indicates thickening of the dolerite sill (Figure 6.103).

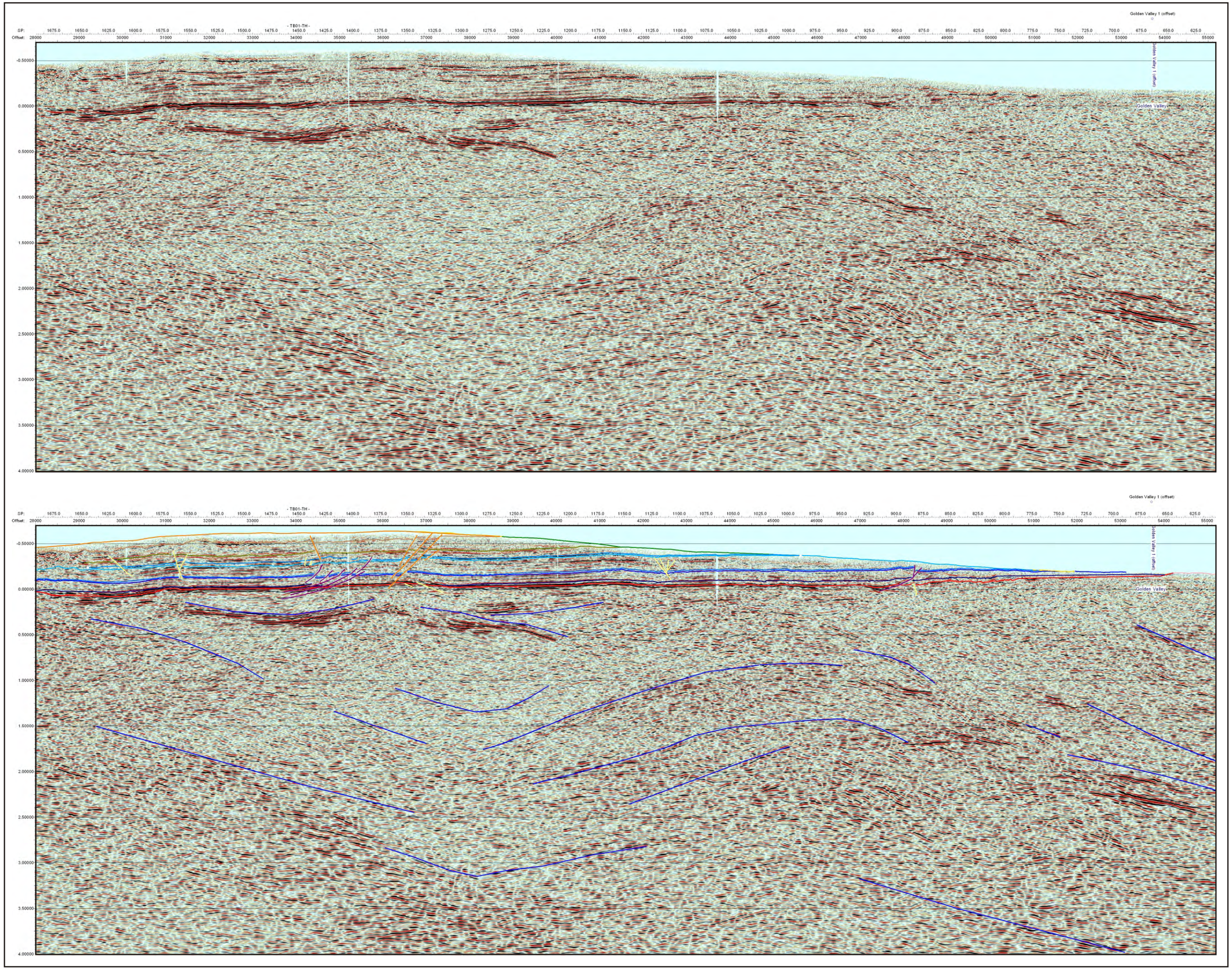

Figure 6.100: Raw and interpreted seismic data from shot-point 650 to1650 (TB01-TH).

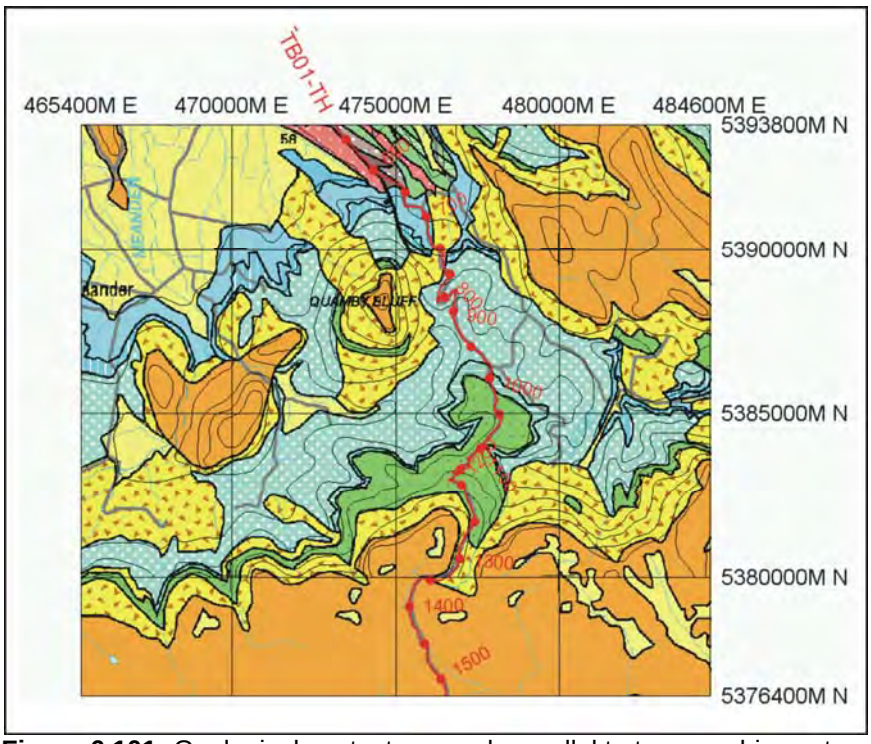

Figure 6.101: Geological contacts are sub-parallel to topographic contours, indicating the Parmeener Supergroup in this region is flat-lying.
(Modified from McClenaghan and Calver, 1994)

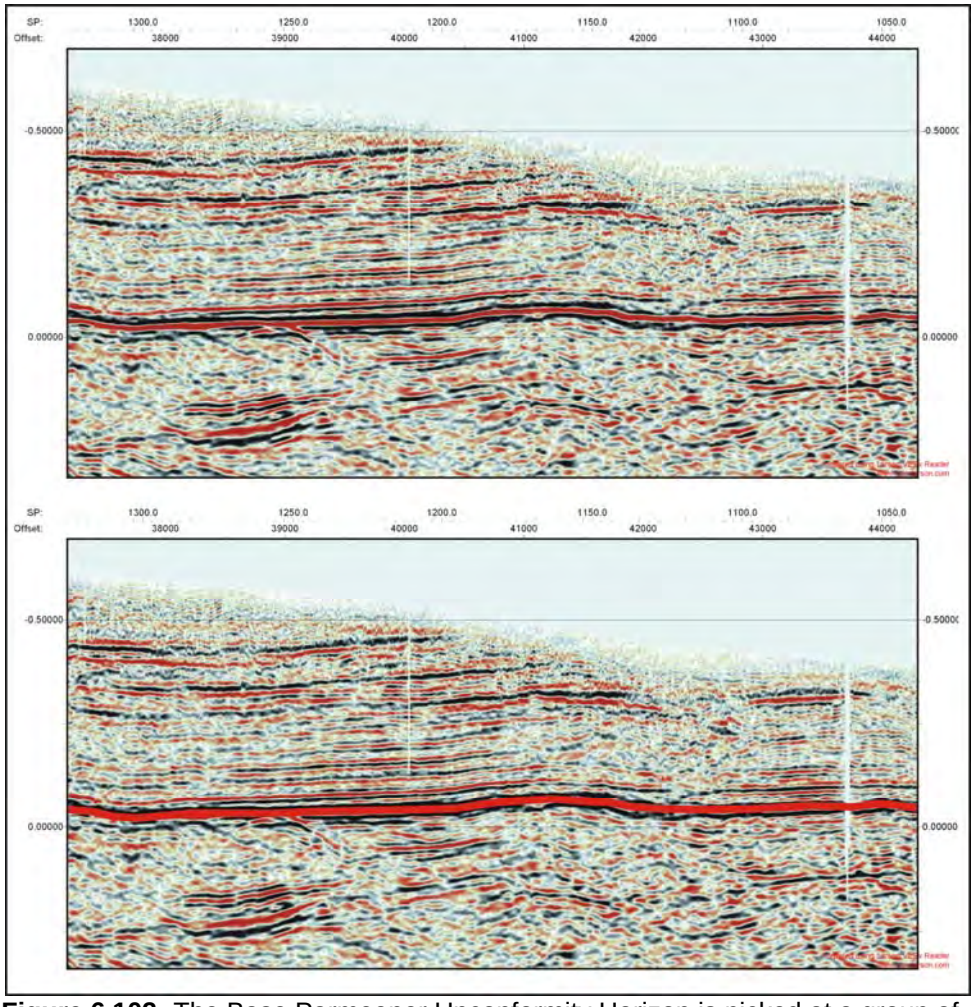

Figure 6.102: The Base Parmeener Unconformity Horizon is picked at a group of strong reflections, which mark a boundary between horizontal, coherent reflections and less coherent, occasionally dipping reflections (TB01-TH).

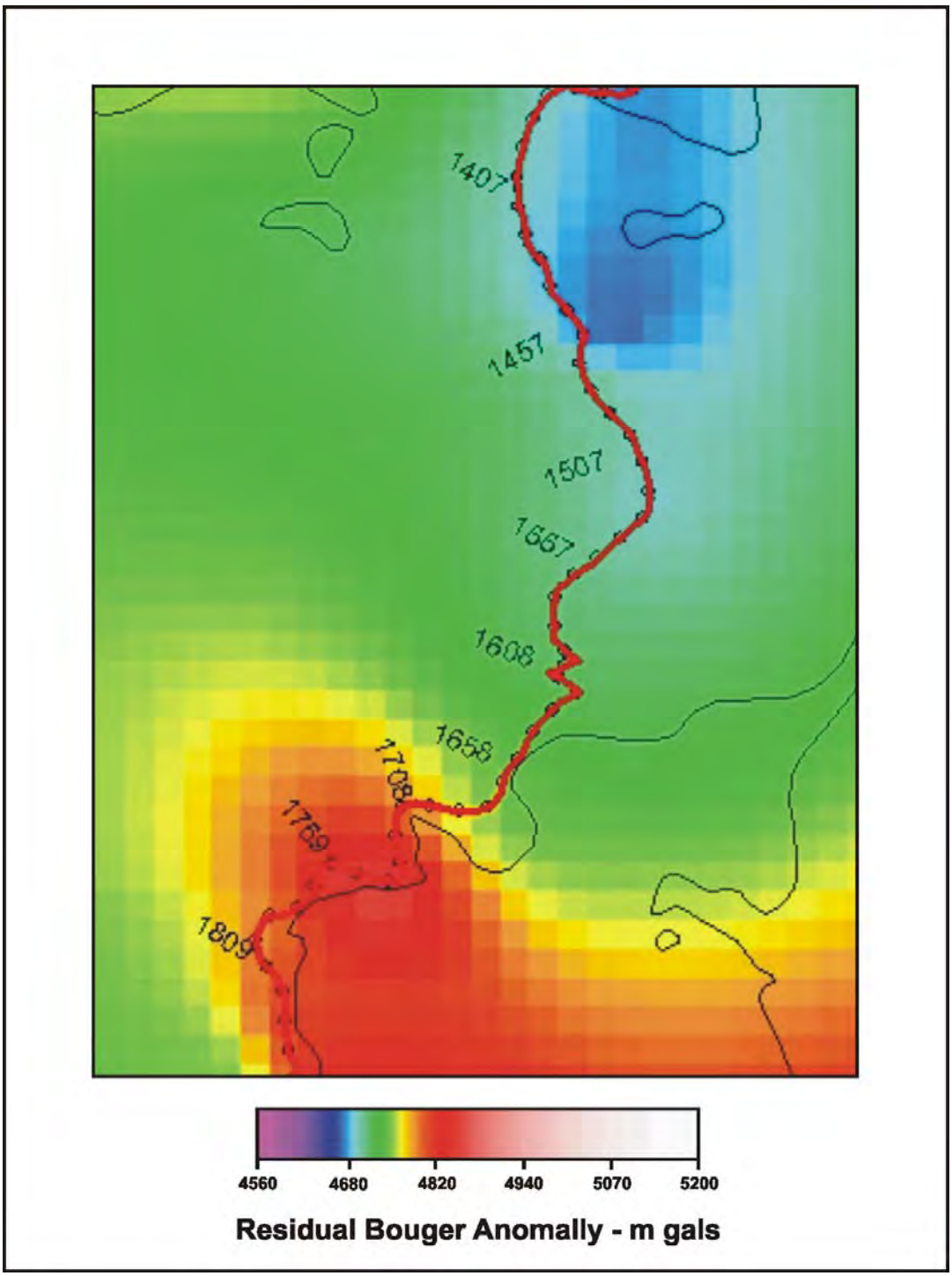

Figure 6.103: A small increase in the measured gravity field at about shot-point 1450 is coincident with a slight increase in thickness of the dolerite sill (TB01-TH).

A strong event (red, black, red) is observed in Unit 2 at -0.4 seconds (TWT) at shot-point 1300 (Figure 6.100). This Intra Unit 2 horizon is interpretable from shot-point 1300 to 1650 and provides a marker horizon across the fault zones (Figure 6.100). The interpretation of the first fault zone between shot-point 1300 and 1350 is based on offsets observed in the Base Parmeener Unconformity and Intra Unit 2 horizons (Figure 6.104). The faults in this zone are normal, down to the south (left of section), with throw of ~50 m. The fault on the north side of the zone (right) is interpreted as Pre-Jurassic as it does not appear to penetrate the dolerite

sill (Figure 6.104). On the south side of the zone, the faults are interpreted as Undifferentiated Tertiary, i.e. they formed post-dolerite coinciding with a linear feature at the surface (Figure 6.105), although it is likely they were also active prior to the intrusion of dolerite. The faults in the second zone between shot-points 1375 and 1450 are interpreted as Pre-Jurassic, "Not Intruded" reverse faults (Figure 6.104). The faults in the basal part of the section are low angle reverse faults that dip towards the south (left of section) and penetrate no further than the Top Upper Marine Sequence horizon (Figure 6.104). Above these, an antithetic Undifferentiated Tertiary, normal fault displaces the Upper Marine Sequence, Intra Unit 2 and Base Dolerite horizons. The basement beneath the entire zone has a small amount of relief (0.25 seconds (TWT), ~50 m), which is onlapped by the tillite sequence (Figure 6.104).

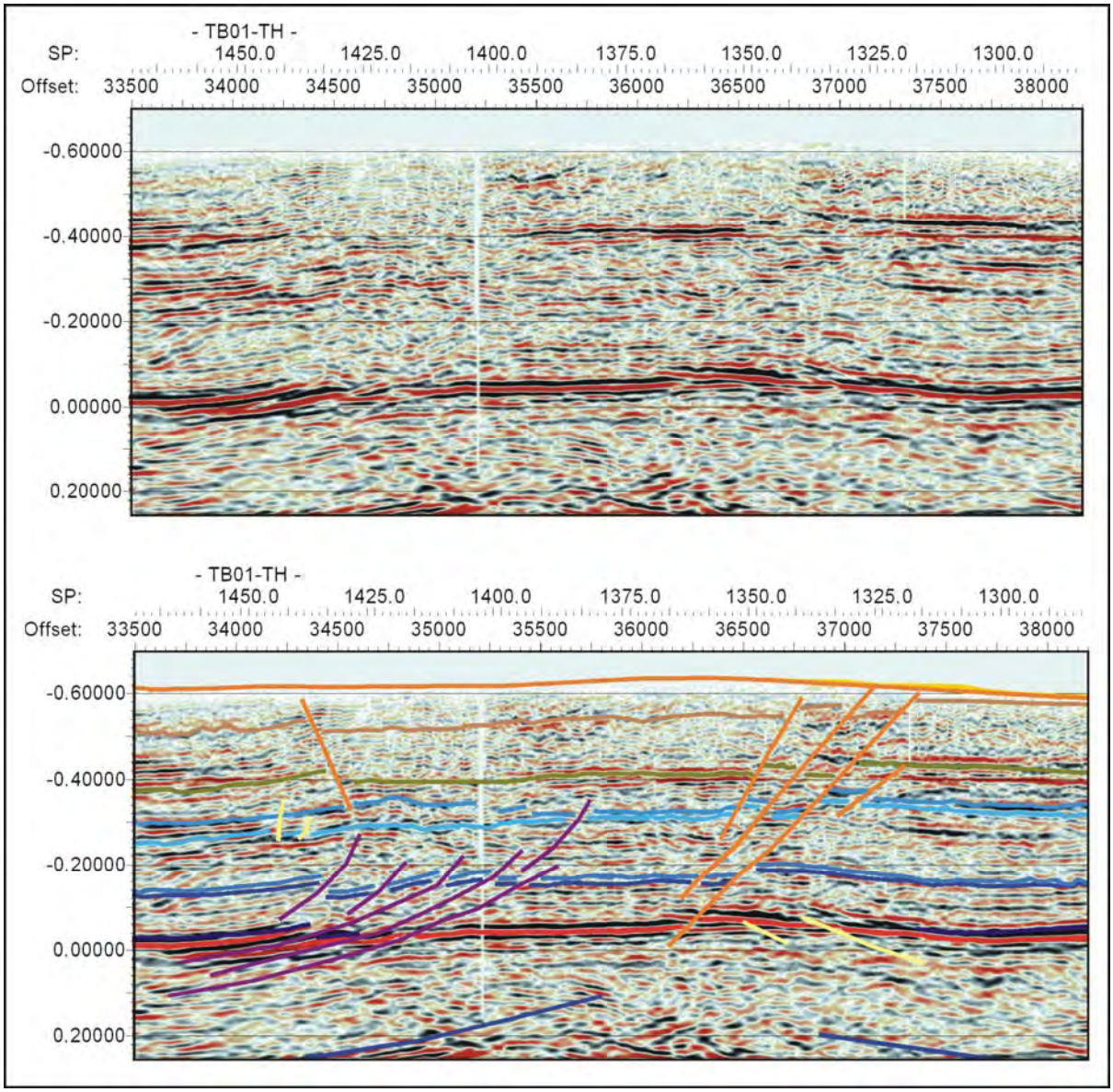

Figure 6.104: Raw and interpreted seismic data showing zones of Undifferentiated Tertiary and Pre-Jurassic faults interpreted between shot-points 1300 and 1450 (TB01-TH).

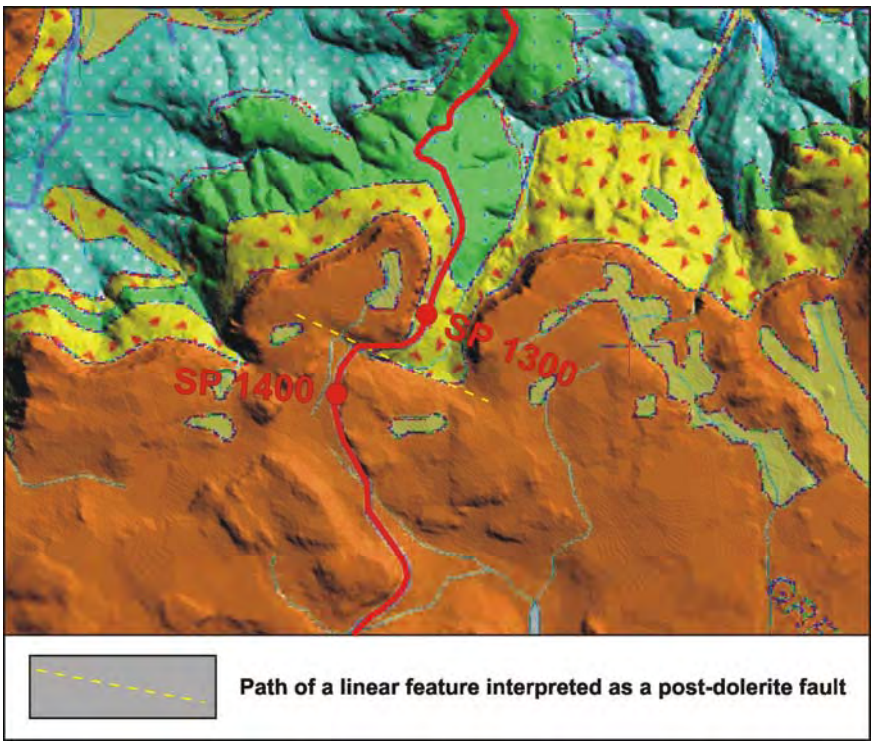

Figure 6.105: Lineaments above the Undifferentiated Tertiary faults Interpreted between shot-points 1300 and 1350 (TB01-TH).

After shot-point 1450, the dolerite sill thickens slightly, indicated by a change in the measured gravity field (Figures 6.100, 6.103). The seismic data in the Parmeener Supergroup section remains coherent between shot-points 1450 and 1650 and the Parmeener Supergroup horizons are confidently picked on the coherent reflections (Figure 6.100) The distance between the Intra Unit 2 and Upper Marine Sequence horizons becomes smaller towards shot-point 1650, indicating thinning of the Unit 2 sequence (Figure 6.100).

In the basement portion of the section, events are interpreted based on changes in the seismic character. Up to shot-point 950, the interpreted events dip towards the north (right of section). Between shot-points 800 and 900 the line rapidly changes direction several times, resulting in a zone of confused reflections (Figure 6.100). After shot-point 950, the interpreted events dip towards the south (left of section), with some rollover towards shot-point 900 (Figure 6.100). This antiform has a wavelength of 9 km. South (left of section) of shot-point 1250 events dip back towards the north and a hinge of a synform is interpreted at shot-point 1275 and 1.40, 1.70 and 3.15 seconds (TWT) (Figure 6.100). Similar sized structures, such as the extension of the Mole Creek Syncline are known 20 km along strike to the northwest (Jennings, 1963, Pike et al., 1973). However, the difficulties in confidently interpreting structures within the basement have been discussed earlier (shot-points 100 and 650). Therefore, the identification of large-scale structures in the basement section must be treated with some care.

Shot-points 1650 – 2810

(Figure 6.106)

The seismic data for the Parmeener Supergroup part of this section of line is highly degraded when compared to the previous section (shot-points 650-1650) (Figure 6.100). This section of line has been acquired over outcropping dolerite and Tertiary Basalts. However, extremely good data was acquired over outcropping dolerite between shot-points 1350 and 1650 (Figure 6.107). Seismic data quality appears to relate to the proximity of Great Lake to the line. The poorest data occurs between shot-points 1650 and 2100 where the line is very close to the western shore of Great Lake (Figure 6.107). The data improves marginally between shot-point 2100 and 2650 where the line moves away from the shore, but is again degraded when the line is close to the shore between shot-points 2650 and 2810 (Figure 6.107).

The interpretations for this section of line is constrained at the ends by the tie with line TB01-PB and the interpretation of the better quality data between shot-points 650 and 1650 (Figure 6.106). The better data between shot-points 2100 and 2650 also aids the positioning the interpreted horizons. In general, the horizons of the Parmeener Supergroup have been simply extrapolated across these zones of poor data, their relative positions based on maintaining the thicknesses interpreted at the ends of this section.

In the section between shot-point 1650 and 2100 the Base Parmeener Supergroup Unconformity horizon remains roughly horizontal and is interpreted along an intermittent strong reflection best viewed on the greyscale image (Figure 6.108). From shot-point 2100 to 2650, the horizon can be picked at the base of zones of coherent reflections (Figure 6.109). After shot-point 2650, the horizon is extrapolated to the tie with line TB01-PB (Figure 6.106).

The Base Dolerite horizon is very difficult to interpret as it occurs mainly in the incoherent zone at the top of the section. The horizon can be picked in only a few places with confidence, such as between shoot-points 2350 and 2450 (Figure 6.109).

Events within the basement section are interpreted at changes in character. Between shot-points 1650 and 2500, the interpreted events dip shallowly towards the north (right of section) (Figure 6.106). At shot-point 2500, the line changes direction by 90° to the east, which probably accounts for the change in orientation of the events seen in the section at that point (Figure 6.106). The poor data quality in the Parmeener Supergroup part of this section probably extends into the basement resulting in the paucity of significant events.

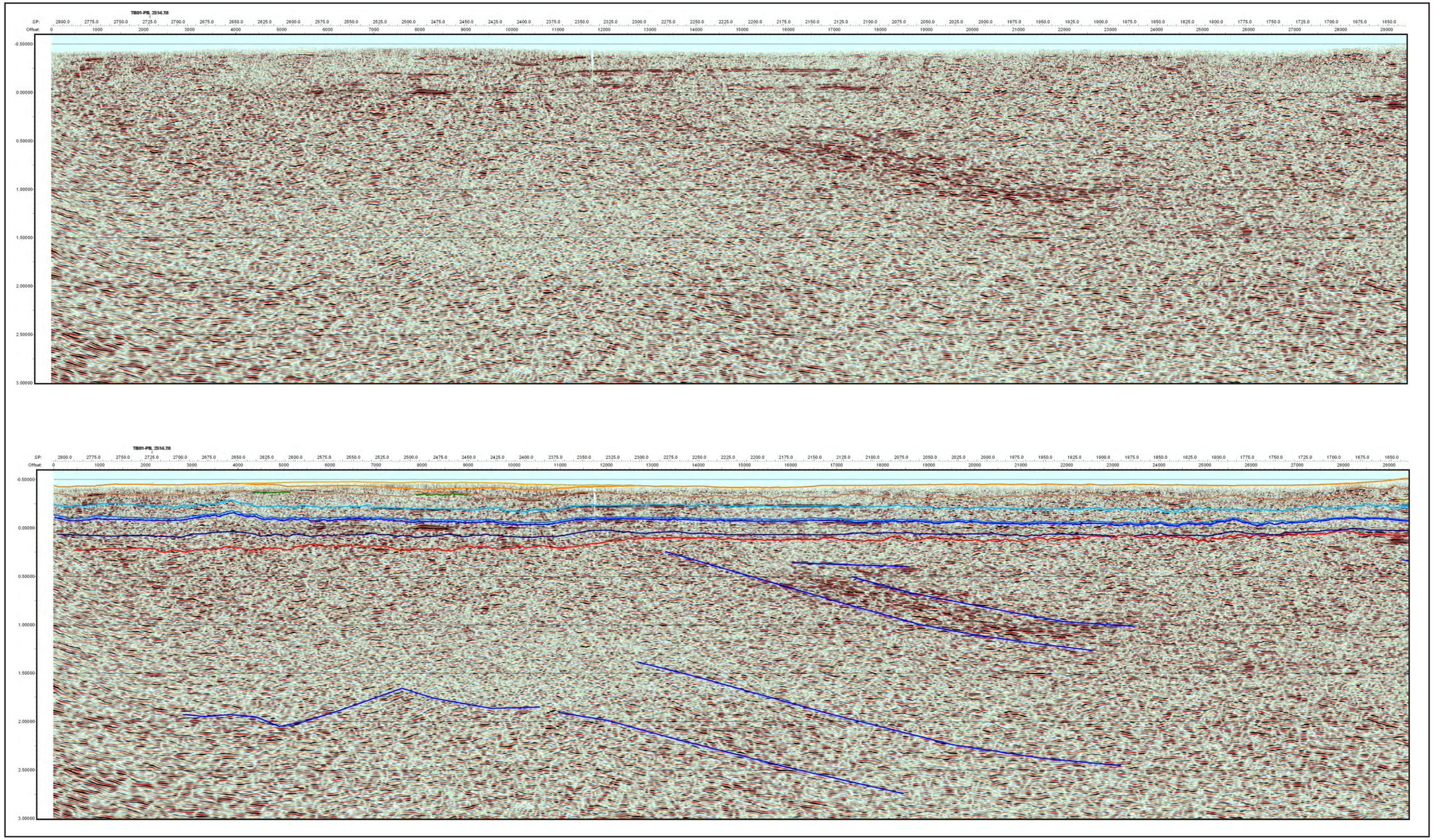

Figure 6.106: Raw and interpreted seismic data from shot-point 1650 and 2810 (TB01-TH).

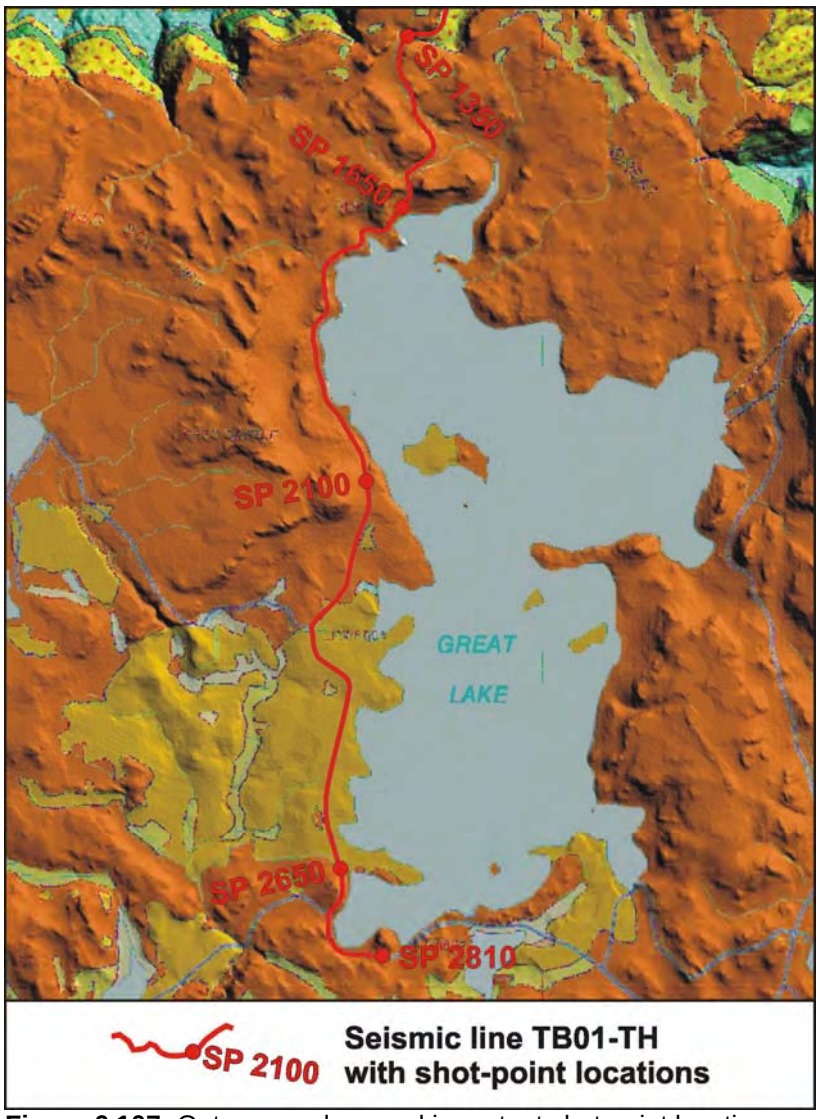

Figure 6.107: Outcrop geology and important shot-point locations.

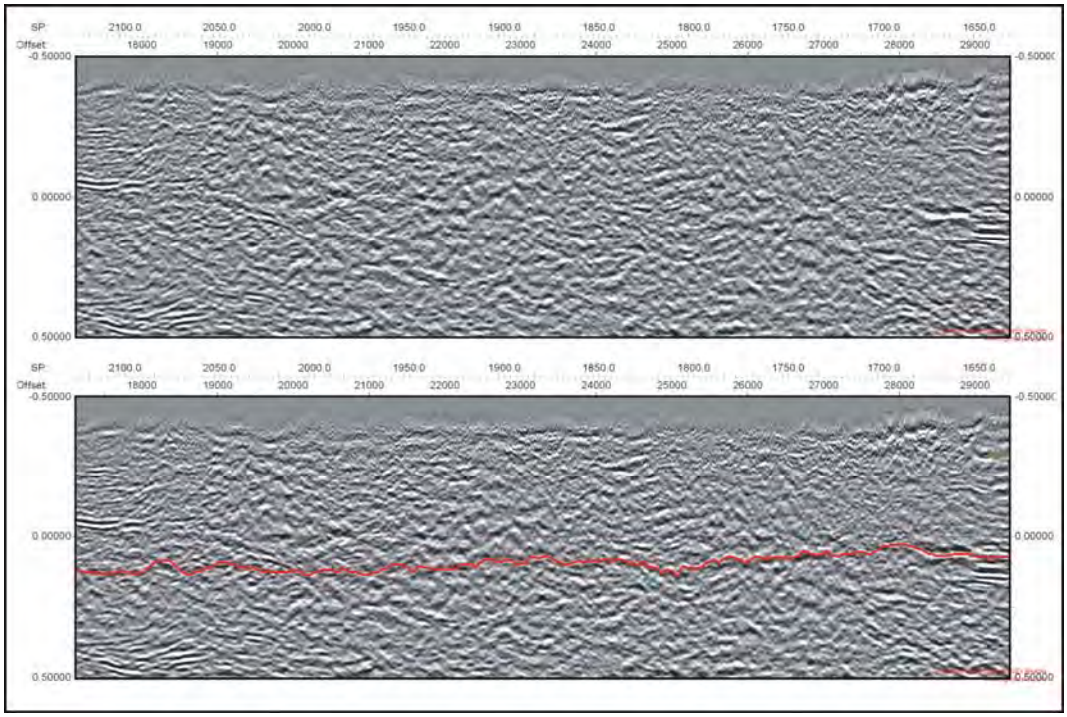

Figure 6.108: Raw and interpreted seismic data from shot-points 1650 to 2100 showing the reflections used to pick the Base Parmeener Unconformity Horizon (TB01-TH).

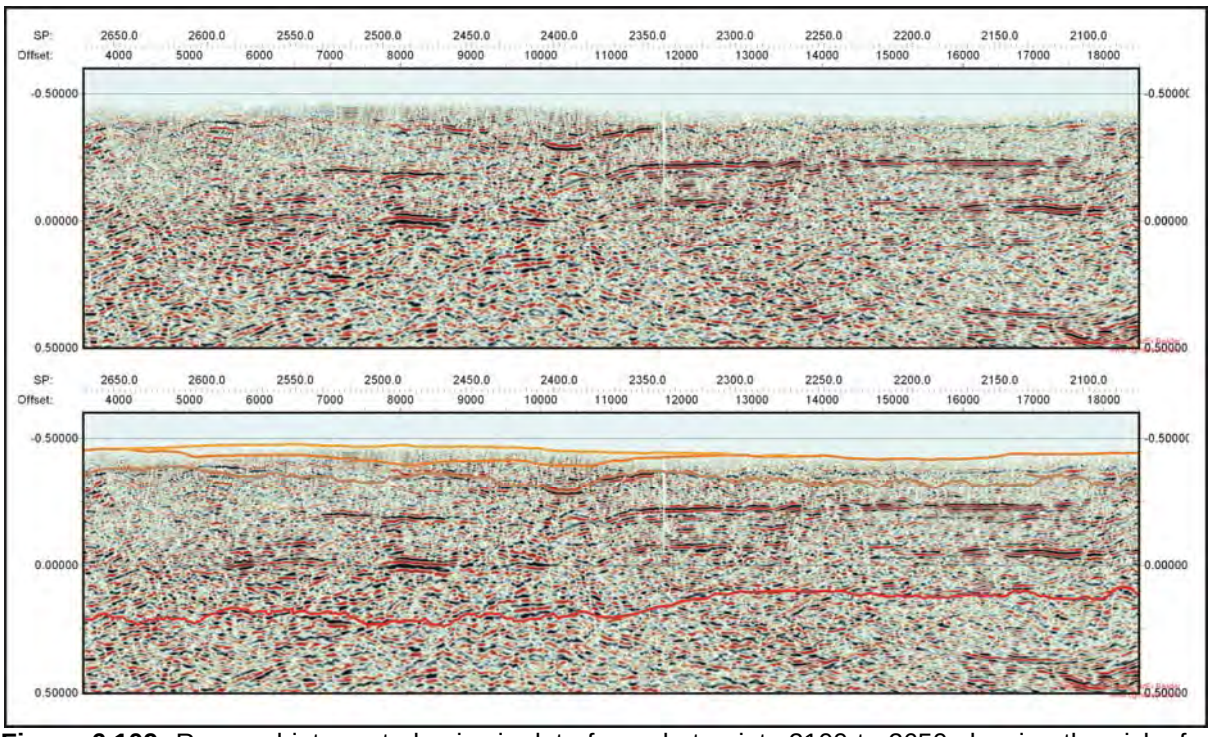

Figure 6.109: Raw and interpreted seismic data from shot-points 2100 to 2650 showing the picks for the Base Dolerite and Base Parmeener Unconformity horizons (TB01-TH).

6.2.10: TB01-TI

Seismic line TB01-TI is located to the west of Lake Echo in the Central Highlands. The line is 18 km long, beginning on the Lyell Highway (shot-point 100) southeast of where it crosses the Nive River (457 423 mE, 5 331 434 mN) and heads in a south-easterly direction. The line then moves onto Victoria Valley Road (shot-point 200) while still heading towards the southeast. At shot-point 325 the line turns north-northeast along Brown Marsh Road, changing direction back towards the southeast at shot-point 575 finishing to the west of Divers Shore on Lake Echo (shot-point 750) (466 667 mE, 5 333 285 mN) (Map 5.1, Figure 6.110). Dolerite is the dominant outcropping lithology (Forsyth et al., 1995) (Figure 6.110).

On the western (left) side of the line, the Base Dolerite horizon is tied to TB01-PB. To the left and right of shot-point 300 and from shot-point 375-475 the Base Dolerite horizon is picked at the first occurrence of strong, coherent reflections at the base of a zone of weak, incoherent data (0.1 seconds TWT) (Figure 6.111). The path of the horizon in between these confident picks follows the base of the incoherent zone.

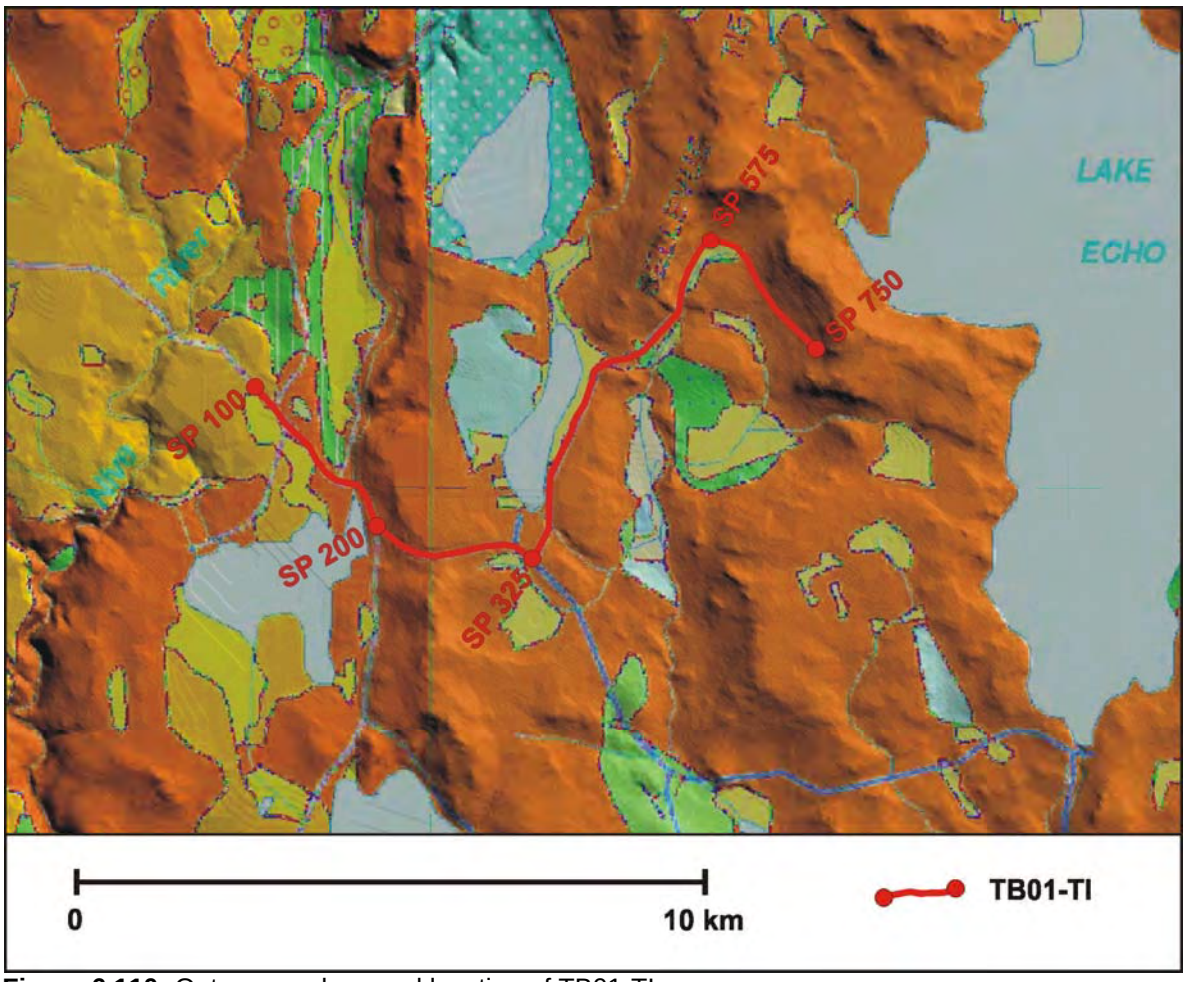

Figure 6.110: Outcrop geology and location of TB01-TI.

The pick for the Base Parmeener Unconformity horizon on the left of the section again ties to TB01-PB. The path of the horizon follows a relative character change between incoherent reflections underlain by reflections with higher amplitudes (stronger) and lower frequencies (thicker) (Figure 6.111).

The picks for the other horizons in the Lower Parmeener Supergroup are based on the tie with TB01-PB (Figure 6.111). With little to constrain the interpretation, the horizons are extrapolated to the right, maintaining the thicknesses established at the tie.

In the basement, simple dipping events have been interpreted mainly from coherent reflections rather than at changes in character. The orientation of the interpreted events is highly dependant on the orientation of the line. In the basement section between shot-points 100 and 325, where the line is orientated northwest to southeast, reflections are roughly horizontal (Figure 6.111). From shot-point 325 to 575 the reflections dip towards the left (south) between 10° and 20° and beyond shot-point 575, where the line is heading towards the southeast again, the reflections dip very gently towards the right (southeast) (Figure 6.111).

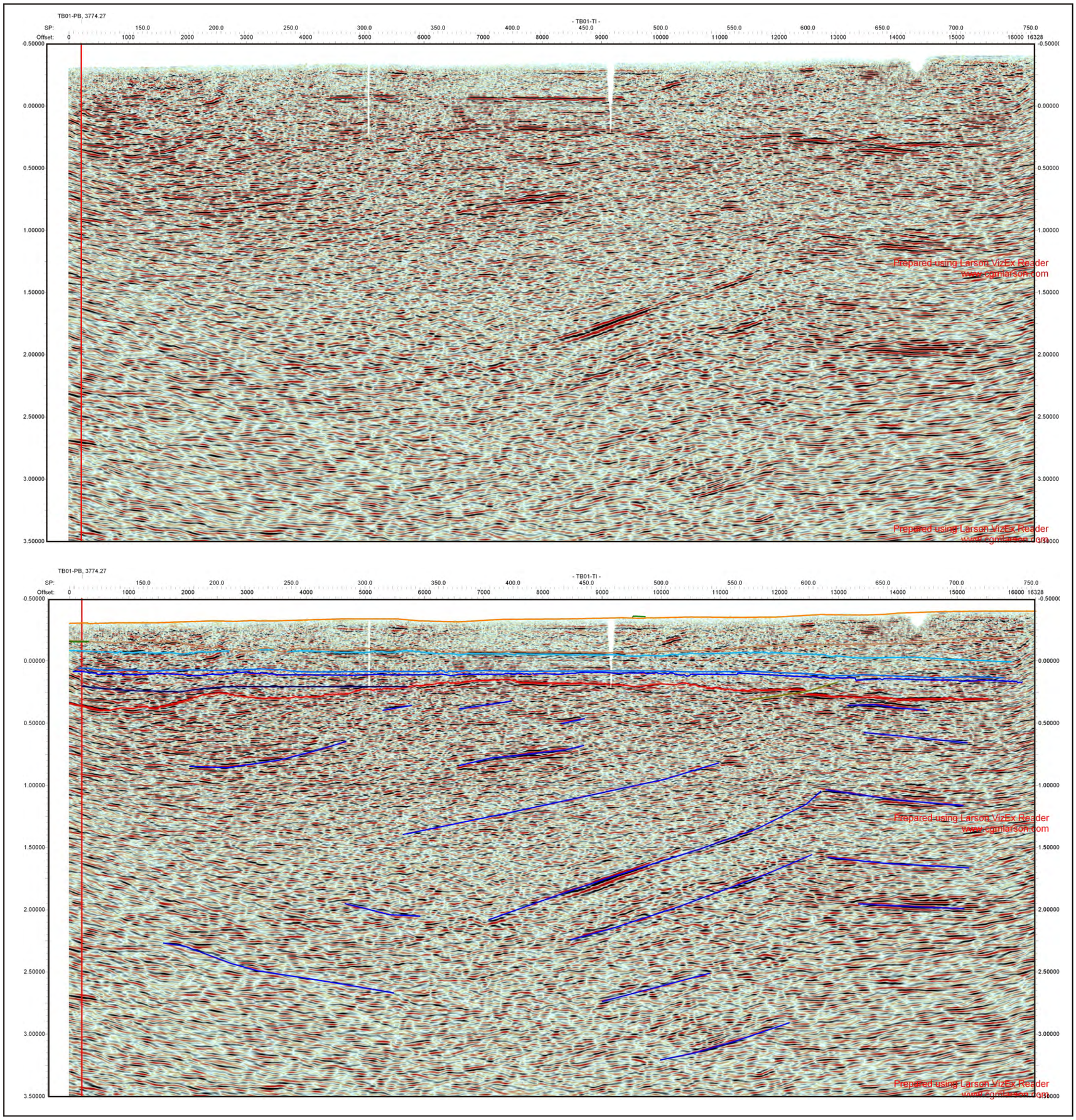

Figure 6.111: Raw and interpreted seismic data for TB01-TI.

6.2.11: 95AGST4

Seismic line 95AGS-T4 was acquired in the Northern Midlands of Tasmania by the Australia Geological Survey Organisation (AGSO, now Geoscience Australia) as part of an industry/research program aimed at defining crustal structure. The line is located west of the towns of Ross and Tunbridge in an area of low relief between the Great Western Tiers and Macquarie Tier (Map 5.1, Figure 6.112). The line is 16.20 km long and strikes south southeast, beginning at 528 735 mE, 5 346 282 mN and finishing on the Midlands Highway south of Tunbridge at 532 166 mE, 5 330 671 mN.

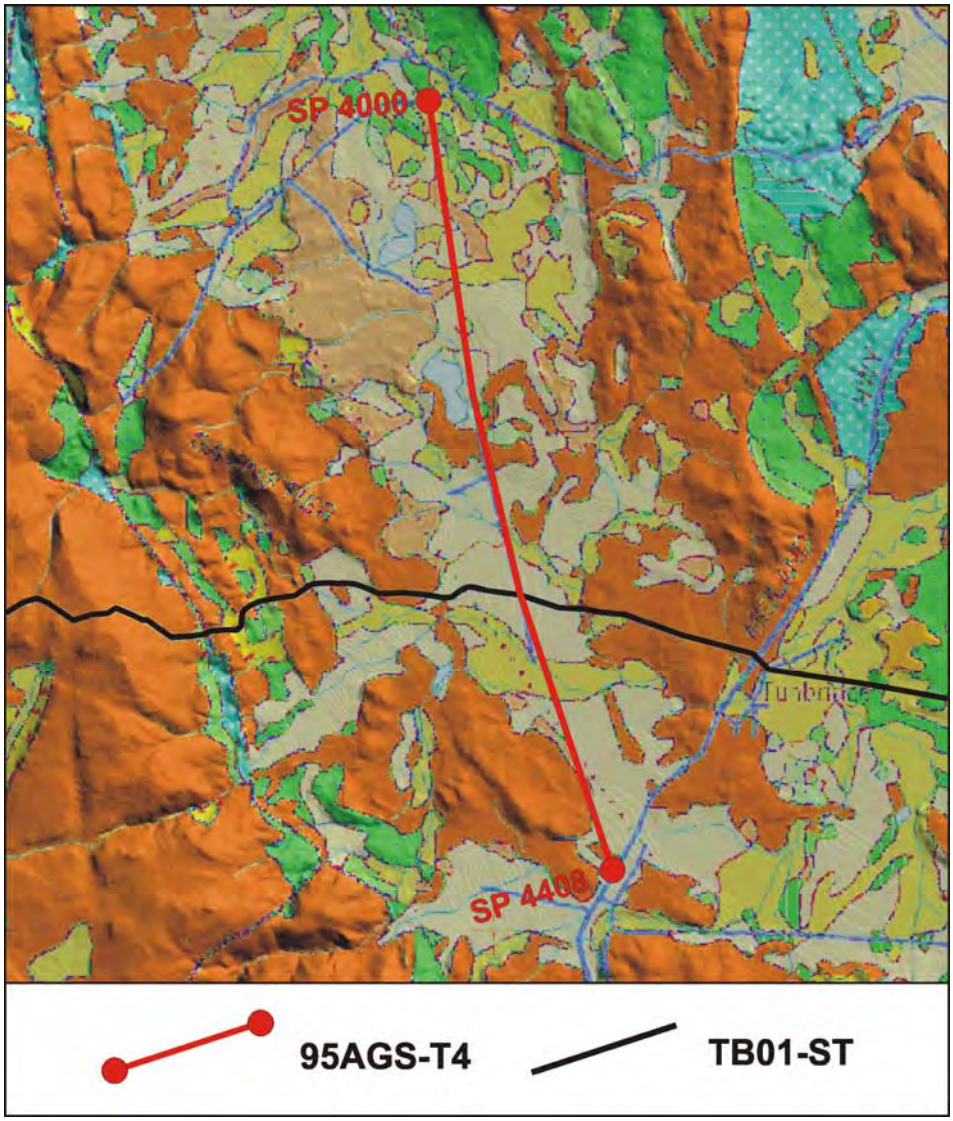

Figure 6.112: Outcrop geology and location of 95AGS-T4.

The line is recorded over Quaternary alluvial material with sporadic outcrops of Jurassic Dolerite and Unit 2 sandstone (Map 5.1, Figure 6.112). The line is parallel to the strike of structures interpreted in the Longford Sub-basin and Tasmania Basin and near to, and parallel with, a major terrane boundary in basement (Figure 6.113).

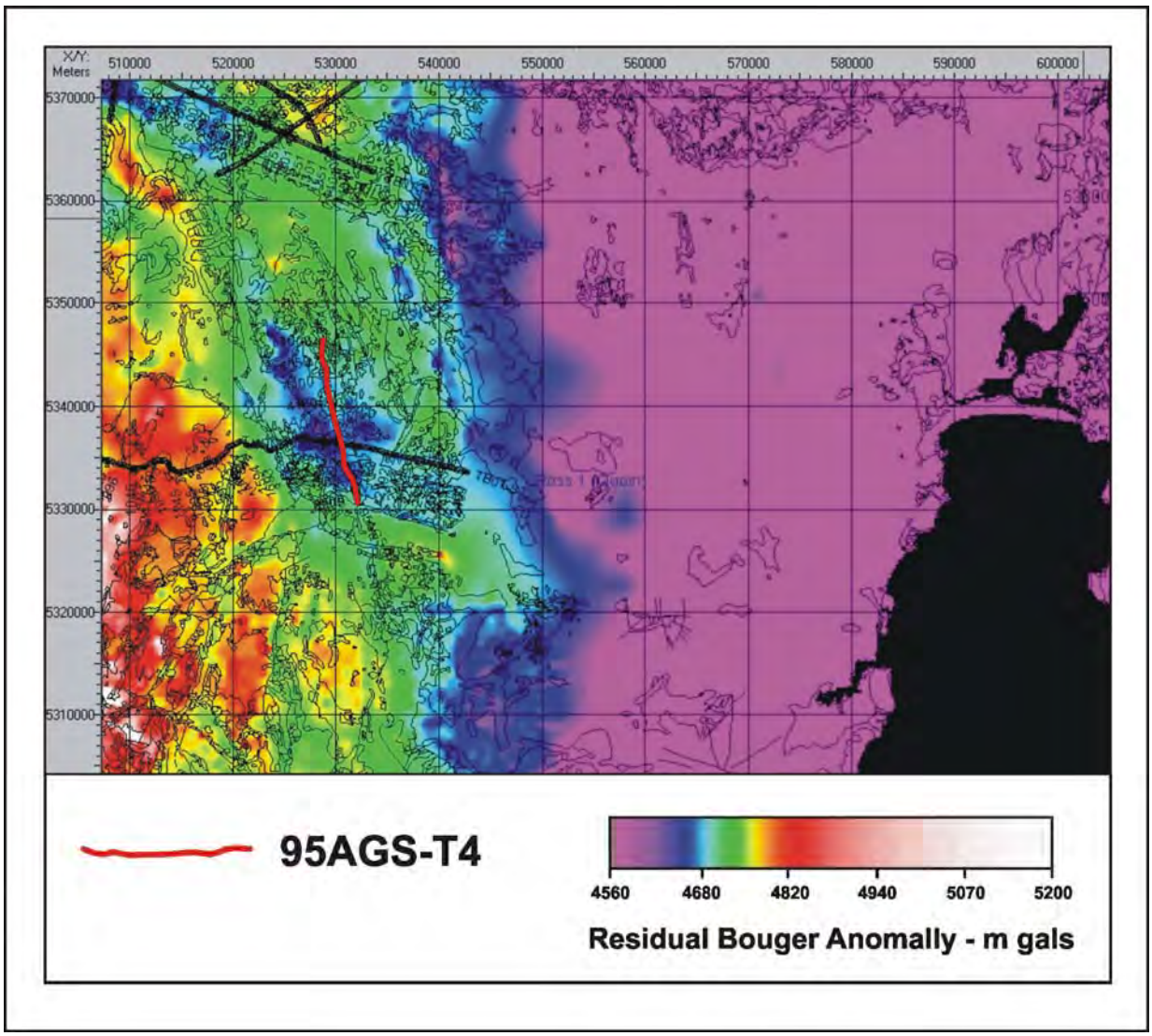

Figure 6.113: 95AGS-T4 lies parallel to a major terrane boundary in the basement, which is well defined by the measured gravity field.

The seismic data in the resulting stacked section is quite poor over the majority of the line (Figure 6.114). At its northern (left) end, the seismic data is considerably better than that of the rest of the line (Figure 6.114). Here, the dolerite sill lies 500 m below the surface resulting in coherent and continuous data in the underlying section (Figure 6.114). In the remainder of the section, coherent reflections occur only in patches. Here the dolerite sill lies at or very near the surface resulting in poor data down to 1.5 to 2 seconds (TWT) (Figure 6.114). The quality of the data is probably further diminished from the peculiar location chosen for the line and from the simple processing stream applied.

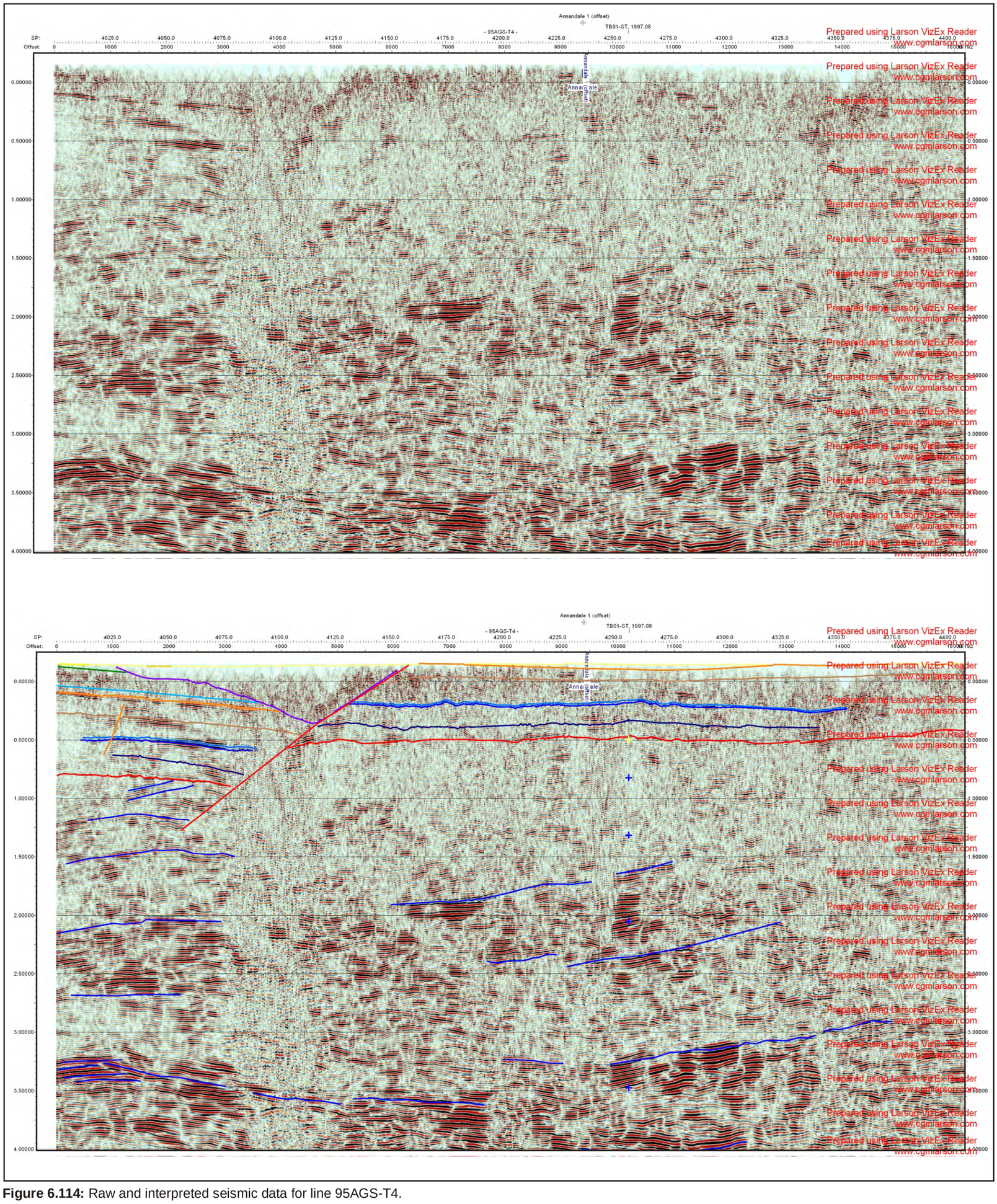

Figure 6.114: Raw and interpreted seismic data for line 95AGS-T4.

Shot-points 4000 – 4150

(Figure 6.114)

Between shot-points 4000 and 4150 the Parmeener Supergroup and an associated dolerite sill dip gently towards the south. The dolerite sill was interpreted first, characterised by strong (high amplitude) reflections at its top between shot-points 4000 and 4100, and at its base between shot-points 4025 and 4075 (Figure 6.114). The Base Parmeener Unconformity horizon is picked at a coherent, negative to positive zero-crossing at the termination of dipping reflections around shot-point 4050 (Figure 6.115). The position of the Base Parmeener Unconformity horizon below the Base Dolerite horizon correlates well with the thickness of the Parmeener Supergroup indicated between these horizons at the intersection with line TB01-ST. The positions of the other Parmeener Supergroup horizons interpreted below the sill are based on their positions at the intersection with line TB01-ST. For the horizons located above the sill, their position is based on thicknesses observed in TB01-ST where they could be interpreted.

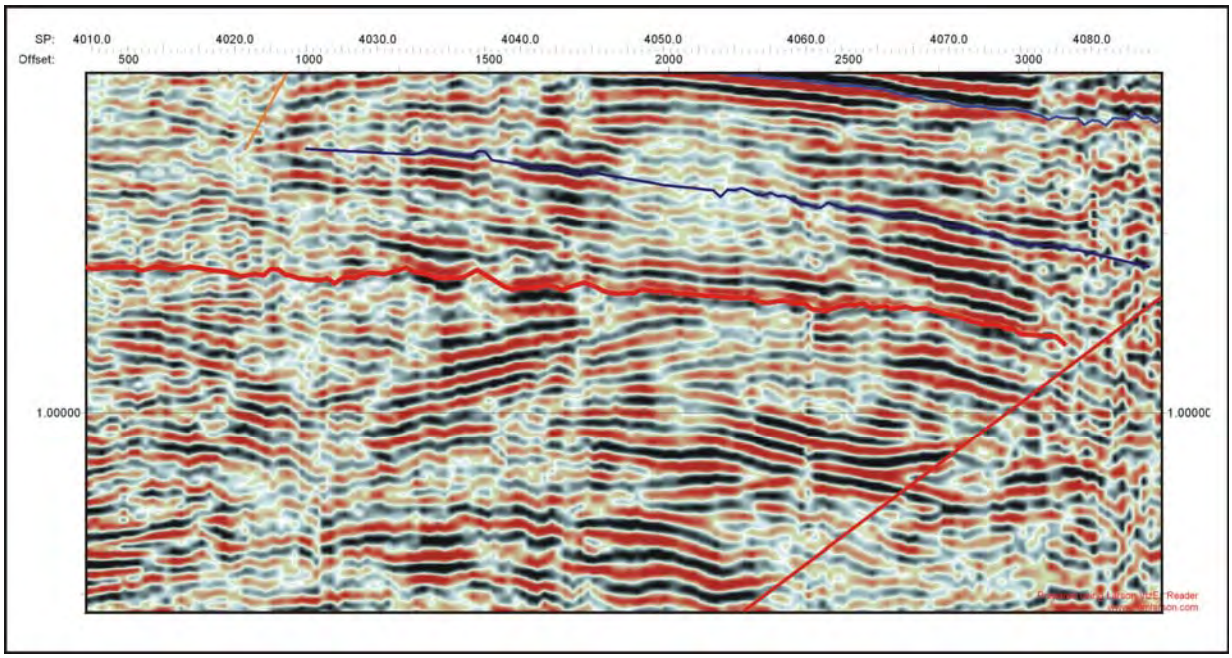

Figure 6.115: Interpreted path of the Base Parmeener Unconformity Horizon from shot-point 4010 to 4100 (95AGS-T4).

At the top of the section, a small Tertiary basin or part of a basin is seen (Figure 6.114). The basin is 500 m thick at its deepest point. The contact with the underlying Parmeener Supergroup is depositional to the north, with the basin bounded by a fault to the south (Figure 6.114). The data in the Tertiary section is too poor to interpret growth, however the general shape of the fault indicates that it was probably active during Tertiary deposition (Figure 6.114).

Shot-points 4150 – 4408

(Figure 6.114)

The seismic data across this section of line is very poor with rare coherent and continuous reflections to aid the interpretation. The positions of the various Parmeener Supergroup and dolerite horizons are based solely on the intersection with line TB01-ST. The horizons are extrapolated horizontally from the intersection, occasionally following continuous reflections while maintaining the relative thicknesses between units established at the tie.

Basement

The basement seismic events interpreted in this section represent the form rather than discrete structures in the basement, due to the poor, discontinuous data. At the northern (left) end of the section, events above 3.0 seconds (TWT) appear to be horizontal (Figure 6.114). Below 3.0 seconds (TWT), horizontal reflections truncate reflections dipping towards the south (Figure 6.114). For the remainder of the line south (right) of shot-point 4100, events interpreted in the basement begin to dip at about 15° towards the north. The horizontal reflections in the basement are easily reconcilable with its orientation, while the dipping reflections in the south (right) of the section are more difficult to understand. However, the southern end of the line is close to where the Launceston Tertiary Basin terminates. In this location the north-northwest striking faults forming the western boundary of the basin bend towards the east (Figure 6.116). The changing orientation of these faults may reflect a change in basement structure, illustrated by these dipping reflections.

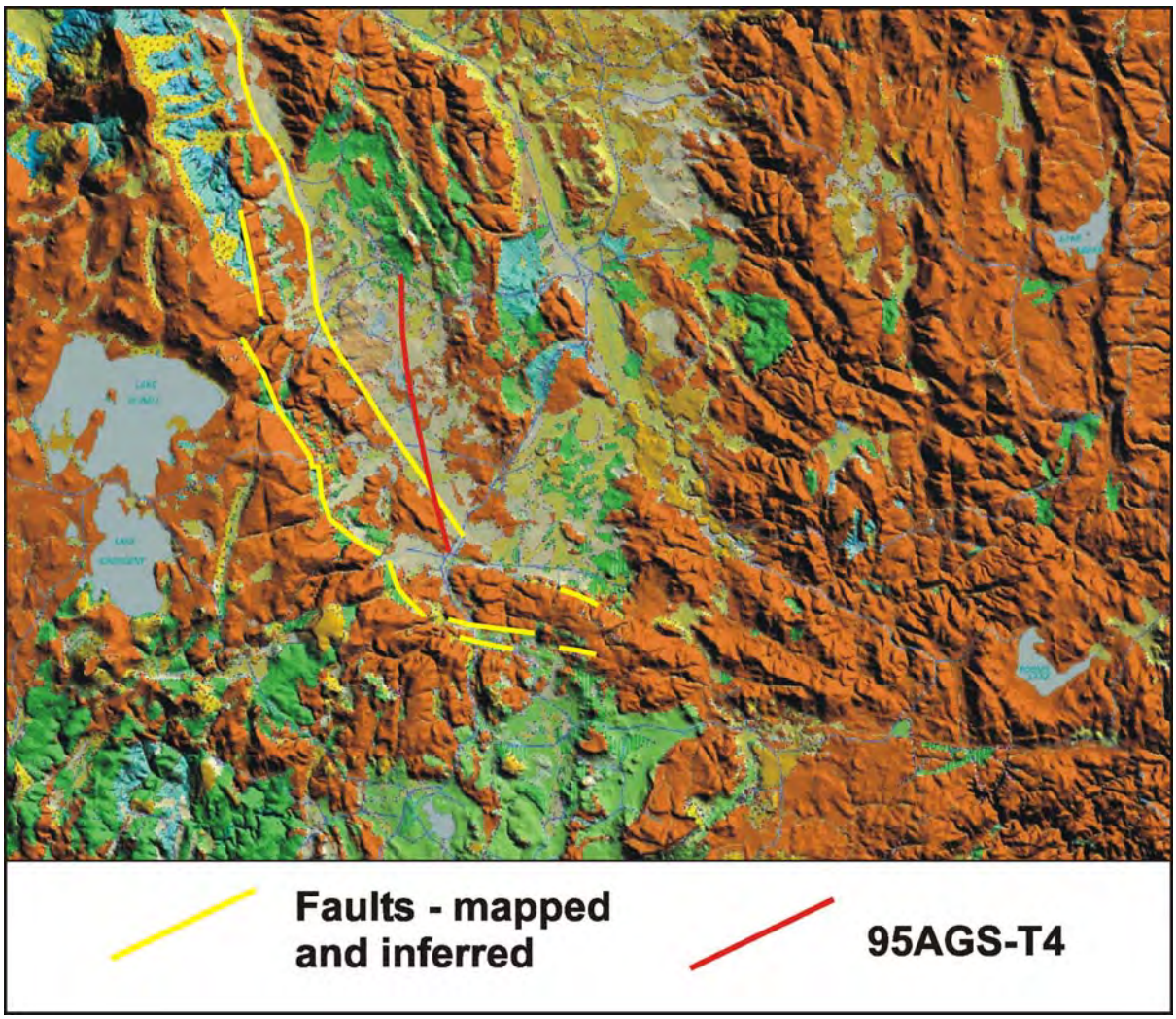

Figure 6.116: Basin boundary faults and the location of 95AGS-T4.

6.3: LONGFORD SUB-BASIN

6.3.1: TB01-PF

Seismic line TB01-PF is a strike line tying TB01-PT in the south to TB01-PG in the central part of the Longford Sub-basin (Figure 6.117). The line is 34.32 km long, beginning at the intersection with line TB01-PG (502 148 mE, 5 376 356 mN), it has been acquired towards the southeast, roughly parallel to the scarps of the Great Western and Macquarie Tiers, finishing about 8 km northwest of Campbell Town (533 633 mE, 5 362 756 mN) (Map 5.1, Figure 6.117).

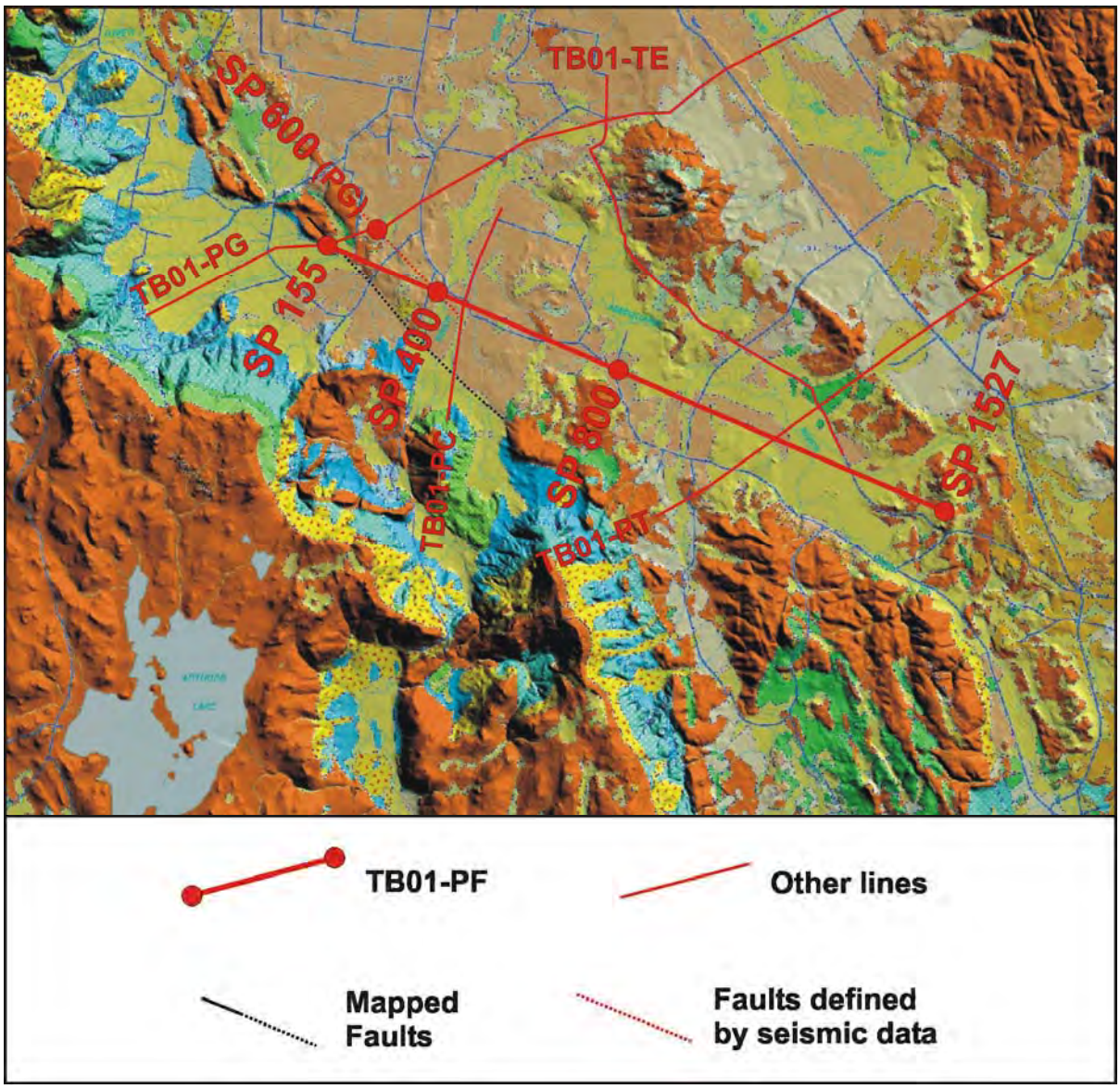

Figure 6.117: Outcrop geology and location of TB01 PF and other lines in the southern Longford Sub-basin.

Shot-points 155 – 400

The two faults between shot-points 155 and 400 correspond to the two faults interpreted between shot-point 500 and 550 on line TB01-PG (Figure 6.118). The fault at shot-point 200 is picked at a change in seismic character from strong, incoherent reflections in the hanging wall to weak, incoherent reflections between shot-points 250 and 300, and 0.3 and 0.6 seconds TWT (Figure 6.118). The second fault at shot-point 400 is picked on the tie with line TB01-PC and from truncated reflections at shot-point 550 and 0.65 seconds TWT (Figure 6.118). The Base Parmeener Unconformity Horizon between shot-point 155 to the fault at shot-point 200 and between shot-points 200 and 450 is picked based on tie with line TB01-PG.

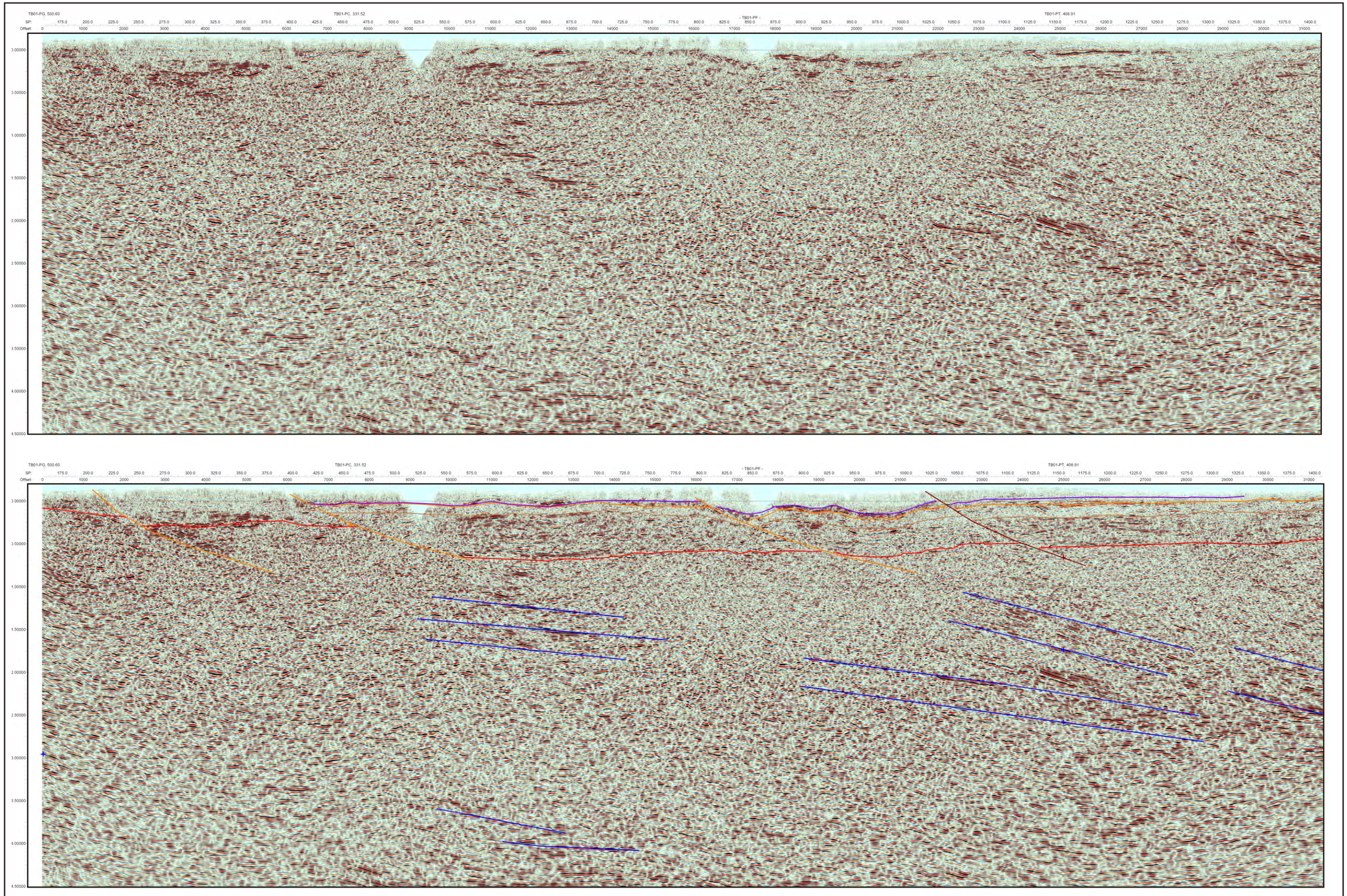

Figure 6.118: Raw and interpreted seismic data from shot-point 155 to 1527 (TB01-PF).

Shot-points 400 – 800

The Base Tertiary Unconformity horizon is interpreted for the first time in this section of the line. The Tertiary sequence on this line is thin (Figure 6.118), unlike the lines in the central part of the sub-basin on which a much thicker Tertiary sequence is observed. The large Early Tertiary Fault interpreted at shot-point 565 on line TB01-PG is not seen on this line, indicating a major change in the geometry of the basin just south line TB01-PG.

This section of line is bounded by major faults interpreted at shot-points 400 and 800 (Figure 6.118). These faults are classified as Undifferentiated Tertiary, because their affect on the Tertiary sequence is ambiguous. The fault at shot-point 400 has a throw of about 900 m and is probably the extension of the fault interpreted at shot-point 565 on line TB01-PG, which has a similar throw (Figures 6.121, 6.117).

The Base Parmeener Unconformity Horizon is confidently picked at a change in seismic character from strong reflections, to reflections that are weaker and less coherent observed at 0.65 seconds TWT (Figure 6.118). The Top and Base Dolerite Horizons are picked between shot-points 550 and 800 at the boundary of a zone of reflections with seismic character typical of dolerite (Figure 6.118). The Base Tertiary Unconformity Horizon is interpreted at the contact with the Jurassic Dolerite in the northwest (left), while it lies about 100 m above the dolerite at the south-eastern (right) end of the section (Figure 6.118). This interpretation ties with the interpretation of the horizon on TB01-PC and PT. The positions of the Base Tertiary Unconformity and Top Dolerite horizons between shot-points 700 and 800 have been identified based on a thickening of the Parmeener Supergroup section as the dolerite sill drops towards the northwest (left) (Figure 6.118).

Shot-points 800 – 1527

Between shot-points 800 and 1527 the dolerite sill is recognised from its distinctive seismic character (Figure 6.118). The Base Parmeener Unconformity Horizon is picked after the fault interpreted at shot-point 1025, at a change is seismic character from relatively strong and coherent reflections to weaker, highly incoherent reflections (Figure 6.118). The Base Tertiary Unconformity Horizon is picked from the tie with TB01 PT and extrapolated to the northwest (left) along a change in seismic character from weak reflections to stronger, more coherent reflections (Figure 6.118).

A fault is interpreted at shot-point 800, based on an offset in the dolerite sill. The interpretation of the fault at shot-point 1025 is based on a change in seismic character from stronger to weaker reflections from the hanging wall to the footwall and steeply dipping reflections adjacent to the fault in the hanging wall (Figure 6.118).

Basement

The interpretation seismic events in the basement section have been made at changes in seismic character. The interpreted events dip between 5° and 15° towards the east-southeast (right).

6.3.2: TB01-PG

Seismic line TB01-PG is the longest line acquired in the Longford Sub-basin region. The line is 57 km long and is a dip line acquired from southwest to northeast across the basin. This is the only line striking orthogonal to and crossing the major basin boundary faults, the Tiers Fault system in the southwest and the Castle Carey Fault in the northeast (Bacon et al., 2000). The line begins at the base of the escarpment of the Great Western Tiers (492 885 mE, 5 372 788 mN) and finishes in the foothills of the North-eastern Highlands (540 736 mE, 5 398 595 mN). The line has been mainly acquired over unconsolidated sediments of Quaternary and Tertiary age (Forsyth et al., 1995, McClenaghan and Calver, 1994) (Map 5.1, Figure 6.119).

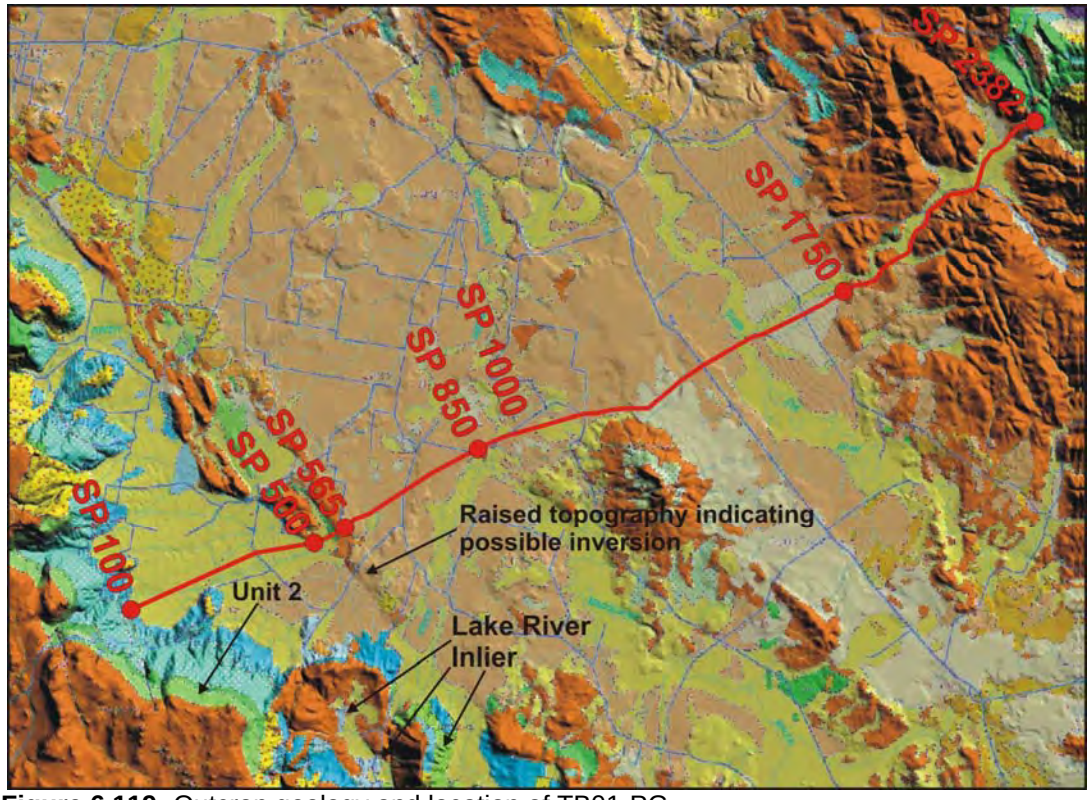

Figure 6.119: Outcrop geology and location of TB01-PG.

The quality of the seismic data in this section is good and the three main elements, the Tertiary, Parmeener Supergroup and basement sequences are recognised. The best quality seismic data is in the Tertiary section where distinct layering and growth faults are recognised. The quality of the data diminishes beneath a dolerite sill in the Parmeener Supergroup section. While in the basement section the data quality is good enough to estimate the general structural form.

Shot-points 100 – 500

(Figure 6.120)

Unconsolidated Quaternary sediments are mapped at the surface over the length of this section of the line (Forsyth et al., 1995) (Figure 6.119). However, basal Parmeener Supergroup rocks are mapped adjacent to shot-point 100 (Lower Marine Sequence) and shot-point 500 (Basal Tillite) (Forsyth et al., 1995) (Figure 6.119), indicating the basal units of the Parmeener Supergroup probably lie close to the surface in this area. The seismic data supports this interpretation. Horizontal reflections between 0.00 to 0.25 seconds (TWT) truncate dipping basement reflections and the Base Parmeener Unconformity horizon is interpreted at this event (Figure 6.120). The path of this horizon can be followed confidently until it is truncated by a major fault at shot-point 500 (Figure 6.120).

Shot-points 500 – 1800

(Figure 6.121)

This section of line contains three distinct Tertiary depocentres, developed in half-graben formed by south-westerly dipping fault blocks. The western most half-graben lies between shot-points 500 and 975 (Figure 6.121). From shot-point 500 to 575, the Parmeener Supergroup is down faulted ~1500 m towards the northeast across several normal faults (Figure 6.121). These faults are coincident with the inferred location of the Tiers Fault (Direen, 1995), the scarp of the Great Western Tiers is its eroded remnant.

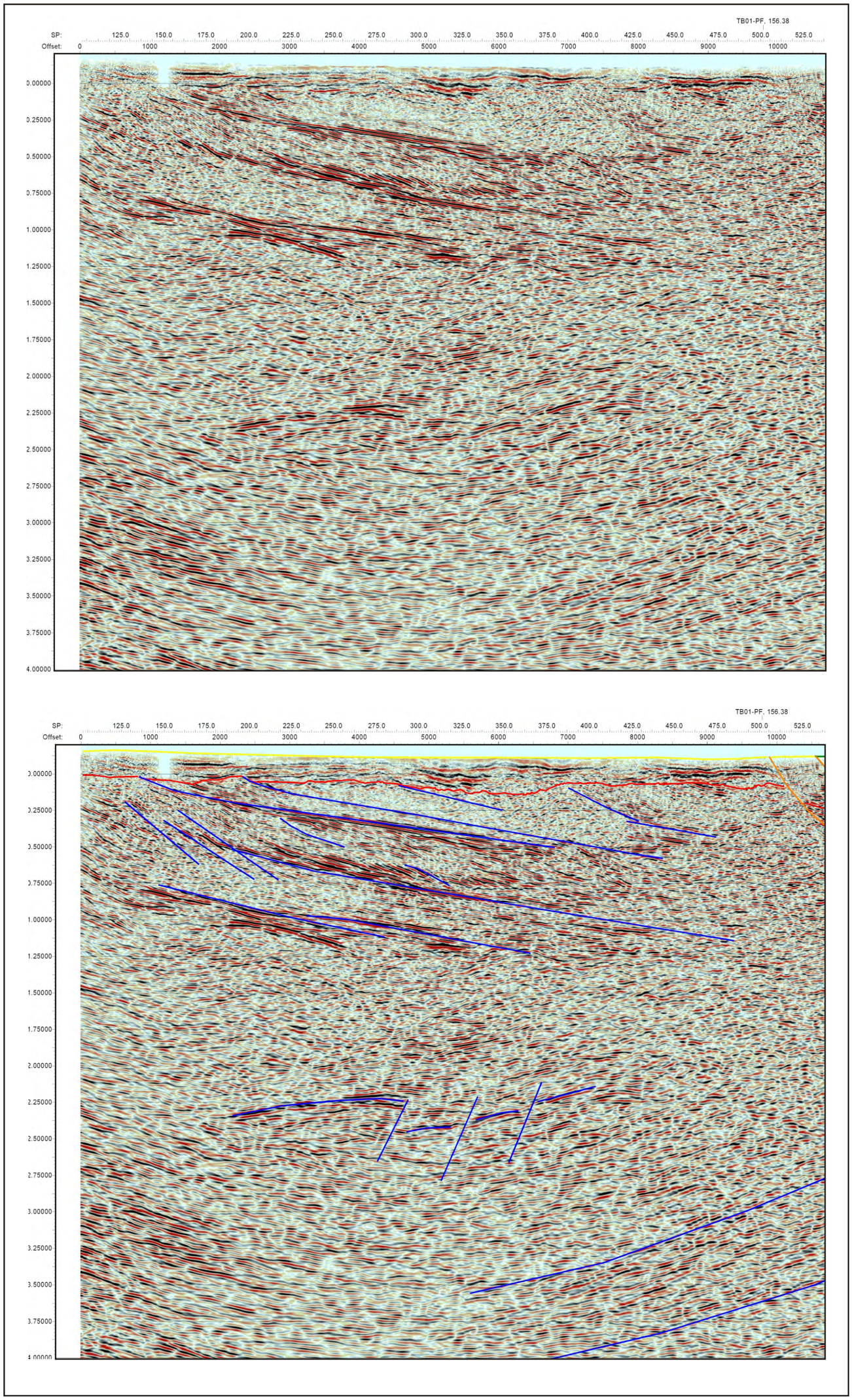

Figure 6.120: Raw and interpreted seismic data from shot-point 100 to 500.

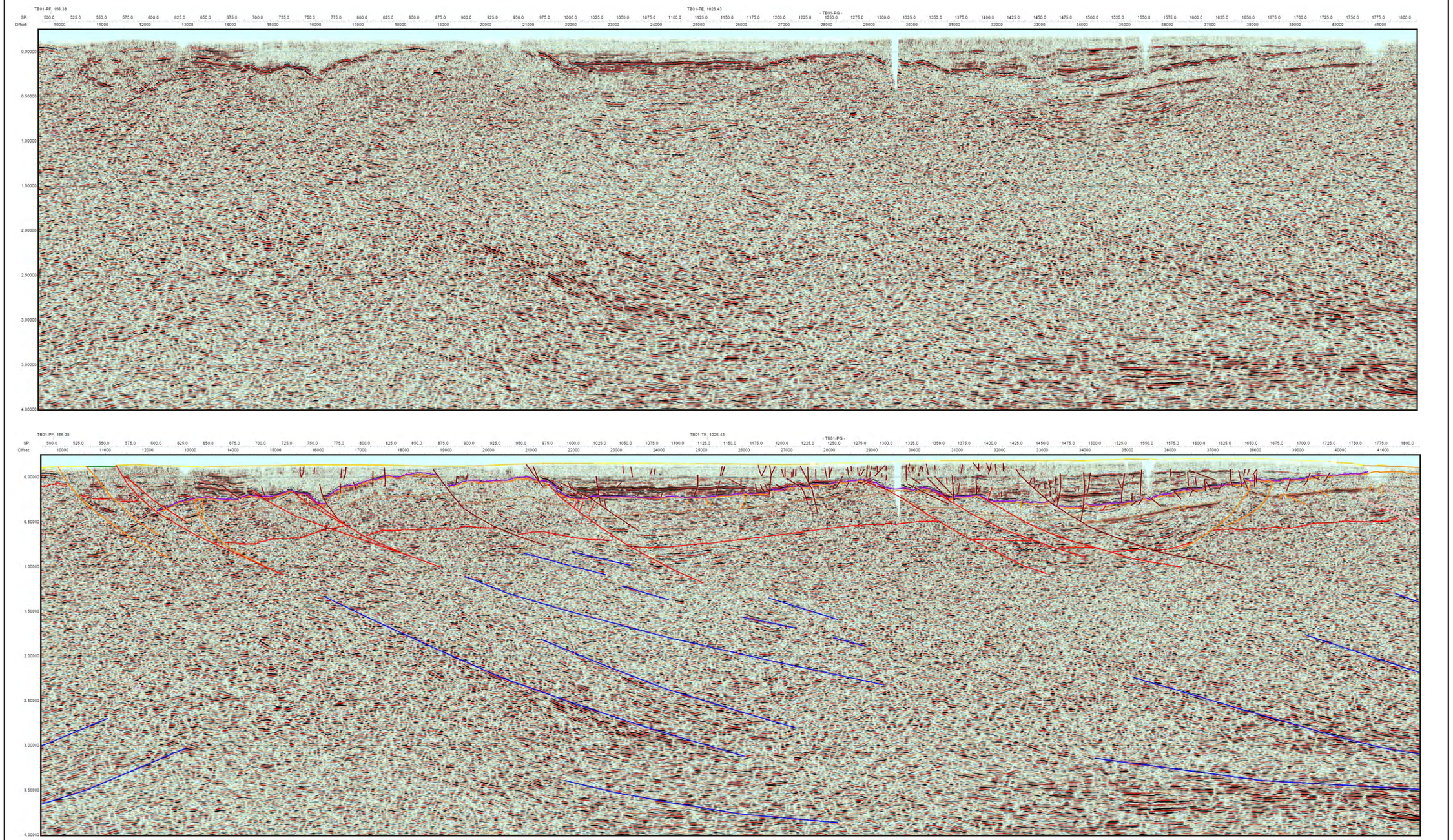

Figure 6.121: Raw and interpreted seismic data from shot-point 500 to 1800 (TB01-PG).

The first two faults displace the Base Parmeener Unconformity horizon by about 300 m (Figure 6.121). These faults have been classified as Undifferentiated Tertiary Faults. It is not clear from the seismic data whether these faults affect the dolerite sill; however movement on these faults has affected Unit 2 of the Upper Parmeener Supergroup, therefore movement was certainly post-Triassic. Based on the histories of adjacent faults, these faults probably result from early Tertiary extension. Unit 2 outcrops between shot-points 530 and 550 and the position of the Base Parmeener Unconformity horizon between the faults is estimated from the thickness of the Parmeener Supergroup below Unit 2, observed in the adjacent scarp of the Great Western Tiers (Figures 6.119, 6.121).

The Parmeener Supergroup is down-faulted by over 1000 m to the northeast across a major fault between shot-points 565 and 725 (Figure 6.121). This fault has a complex history. From the DEM, Tertiary rocks outcropping on the north-eastern side of the fault are topographically higher indicating the fault was probably inverted late in the Tertiary. The Base Tertiary Unconformity Horizon is identified between shot-points 625 and 900 by a strong (high amplitude), negative (red) reflection at the base of coherent horizontal reflections (Figure 6.121). The horizon is less well defined between shot-points 565 and 625 where the data is less coherent (Figure 6.121). Here, the horizon is picked along a strong, dipping reflection at the base of reflections. While lacking the coherency of reflections to the northeast (right of section) of shot-point 625, they have similar character (Figure 6.121). The fault at shot-point 565 marks the edge of the Tertiary basin and is thus classified an Early Tertiary Fault. From close examination of the data, growth is interpreted in the Tertiary section, indicating syn-depositional movement (Figure 6.122).

Between shot-points 600 and 975 the Jurassic Dolerite sill is interpreted to lie directly beneath the Base Tertiary Unconformity horizon. The sill is interpreted in a zone incoherent data, the character of the reflections in this zone make it appear lighter than the equally incoherent data below it (Figure 6.121). The Base Dolerite Horizon is picked along a series of strong (high amplitude) reflections that mark the lower boundary if the lighter reflections (Figure 6.123).

The seismic data corresponding to the Parmeener Supergroup section is incoherent. The position of the Base Parmeener Unconformity Horizon is estimated from the sub-dolerite thickness of the Parmeener Supergroup exposed in the scarp of the Great Western Tiers (Figure 6.119).

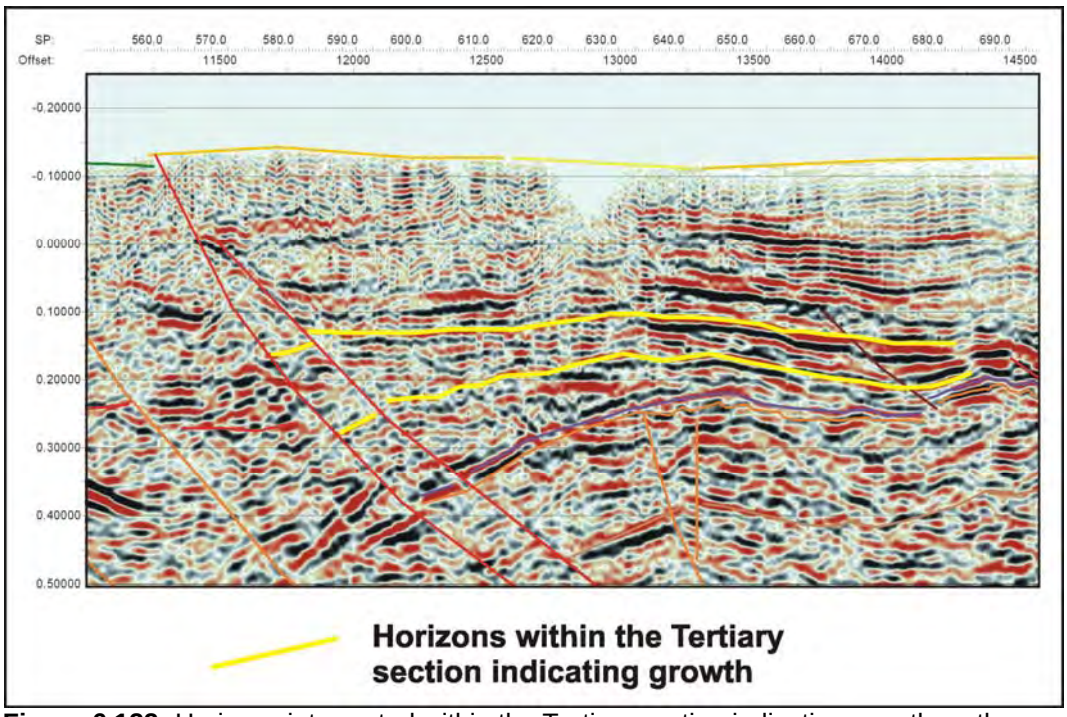

Figure 6.122: Horizons interpreted within the Tertiary section indicating growth on the adjacent fault (TB01-PG).

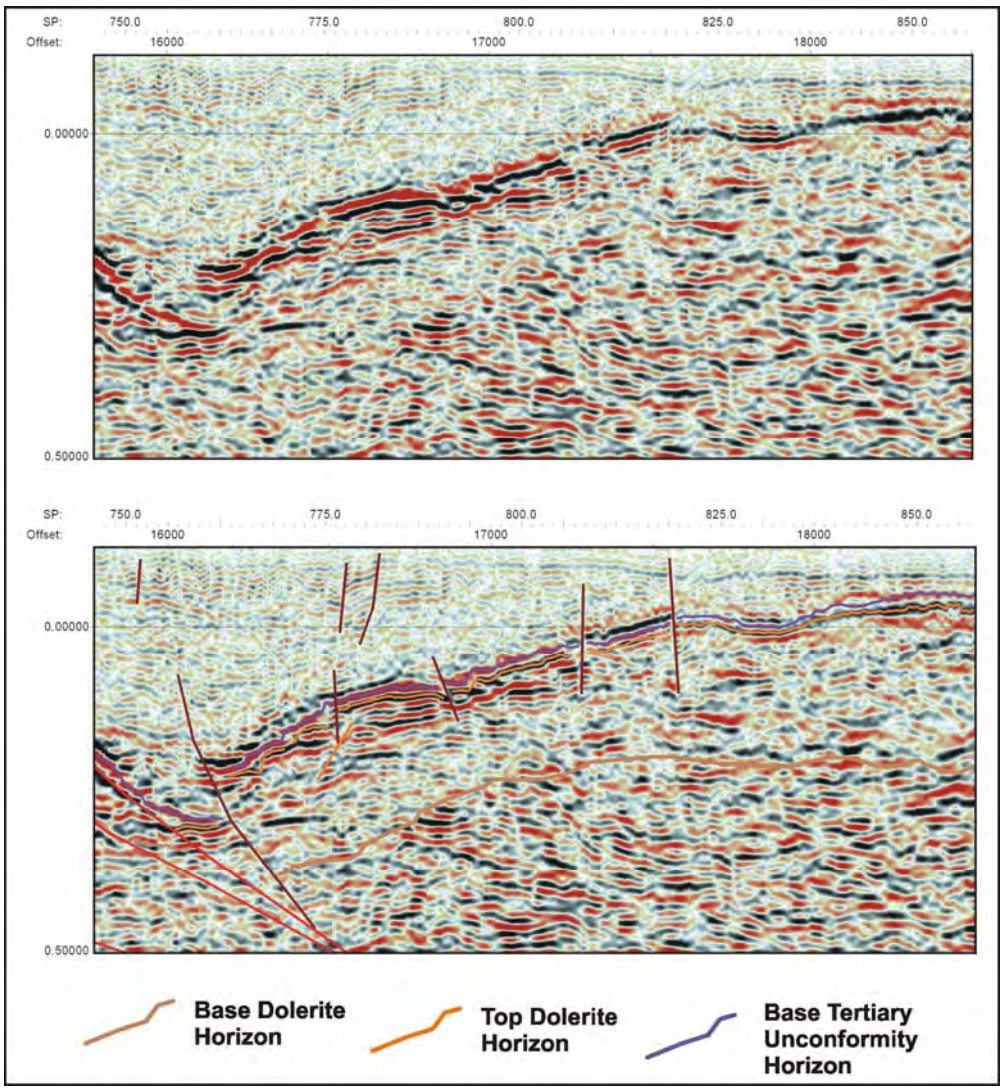

Figure 6.123: Raw and interpreted seismic data from shot-point 750 to 850 showing the picks for the Base Dolerite, Top Dolerite and Base Tertiary Unconformity horizons (TB01-PG).

A zone containing several large, synthetic faults is observed between shot-points 700 and 750 (Figure 6.121). These faults offset the Base Parmeener Unconformity Horizon by about 300 m and either penetrate the Tertiary section or are coincident with growth, indicating a syn-depositional, early Tertiary age (Figure 6.124). The north-eastern most of these faults has, however been classified as Later Tertiary. The last movement on this fault probably occurred post-Tertiary deposition, the fault shows reverse movement offsetting the Base Tertiary Unconformity Horizon by about 150 m (Figure 6.124).

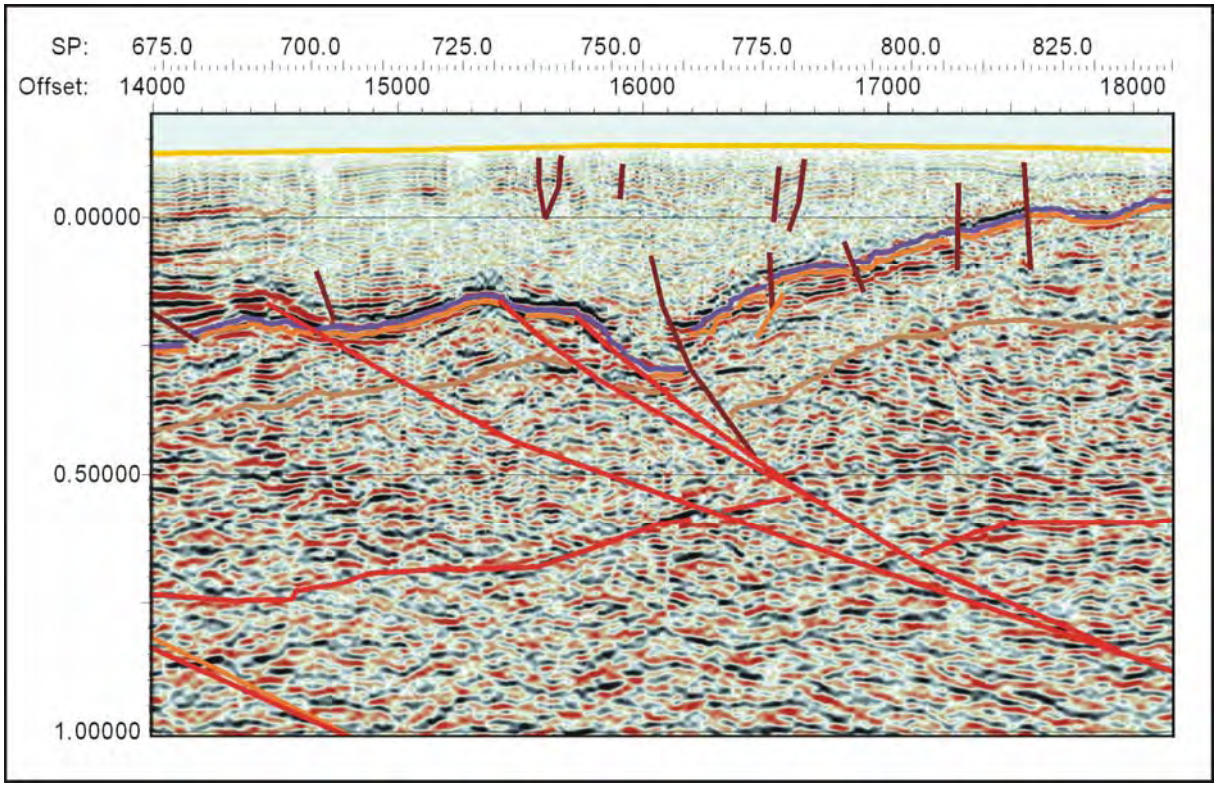

Figure 6.124: Zone of Early Tertiary faults and synthetic Later Tertiary reverse fault (TB01-PG).

Between shot-points 600 and 975, numerous Later Tertiary Faults (normal and reverse) are interpreted within the Tertiary sequence. A large Later Tertiary Fault is interpreted at shot-point 875 (Figure 6.121). The fault is down towards the northeast, displacing the Base Tertiary Horizon by ~200 m. Reflections at 0.05 seconds TWT at the base of the hanging wall are concave up, indicating fault drag and post-depositional movement (Figure 6.125).

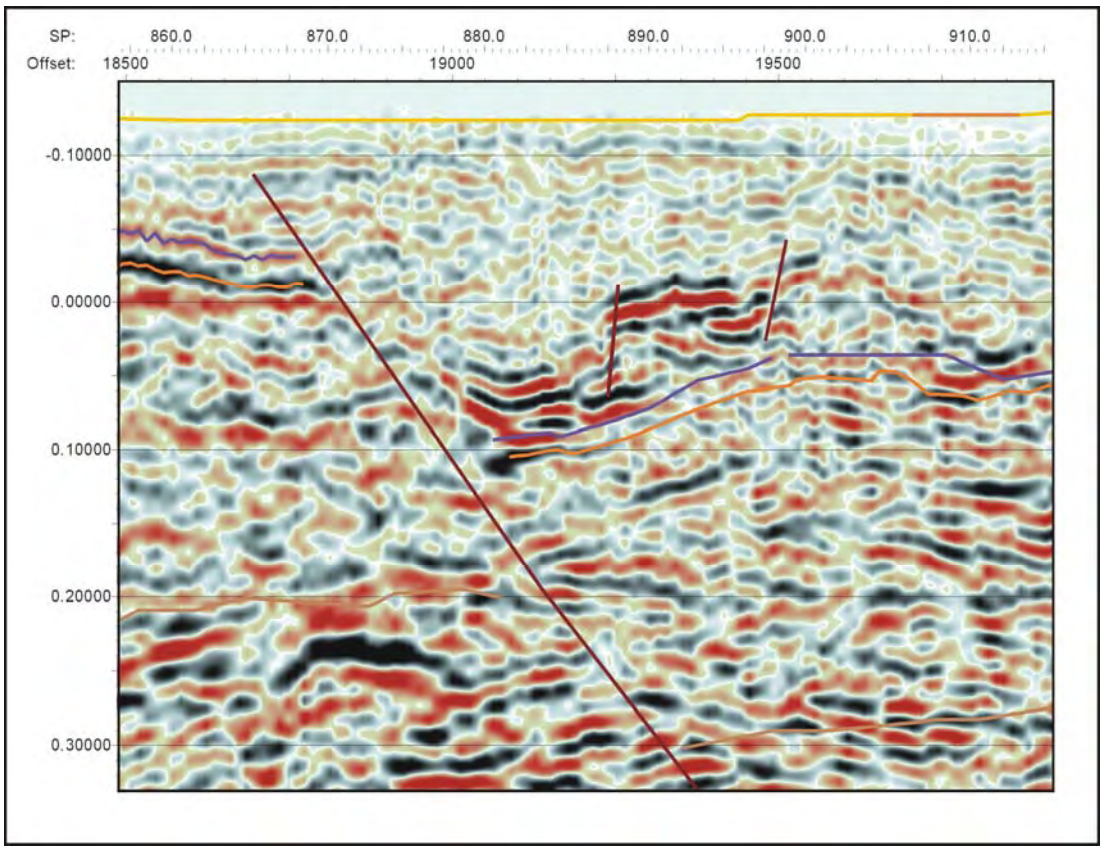

Figure 6.125: Interpreted fault drag on a Later Tertiary Fault at shot-point 875 (TB01-PG).

The second major Tertiary half-graben depocentre lies between shot-points 975 and 1275 (Figure 6.121). The Tertiary section is extremely well defined by strong (high amplitude) reflections. The Base Tertiary Unconformity Horizon is picked at a strong (high amplitude), negative (red) reflection the base of these reflections, where there is a significant change in seismic character to less coherent reflections with lower amplitudes (Figure 6.126). The Parmeener Supergroup section is displaced by about 300 m across boundary fault at shot-point 975 (Figure 6.121). Reflections in the Tertiary section drape this fault (Figure 6.127), indicating movement creased earlier than on the Tiers Fault System to the southwest. This fault does not displace reflections in the Tertiary sequence and is therefore classified as an Early Tertiary Fault.

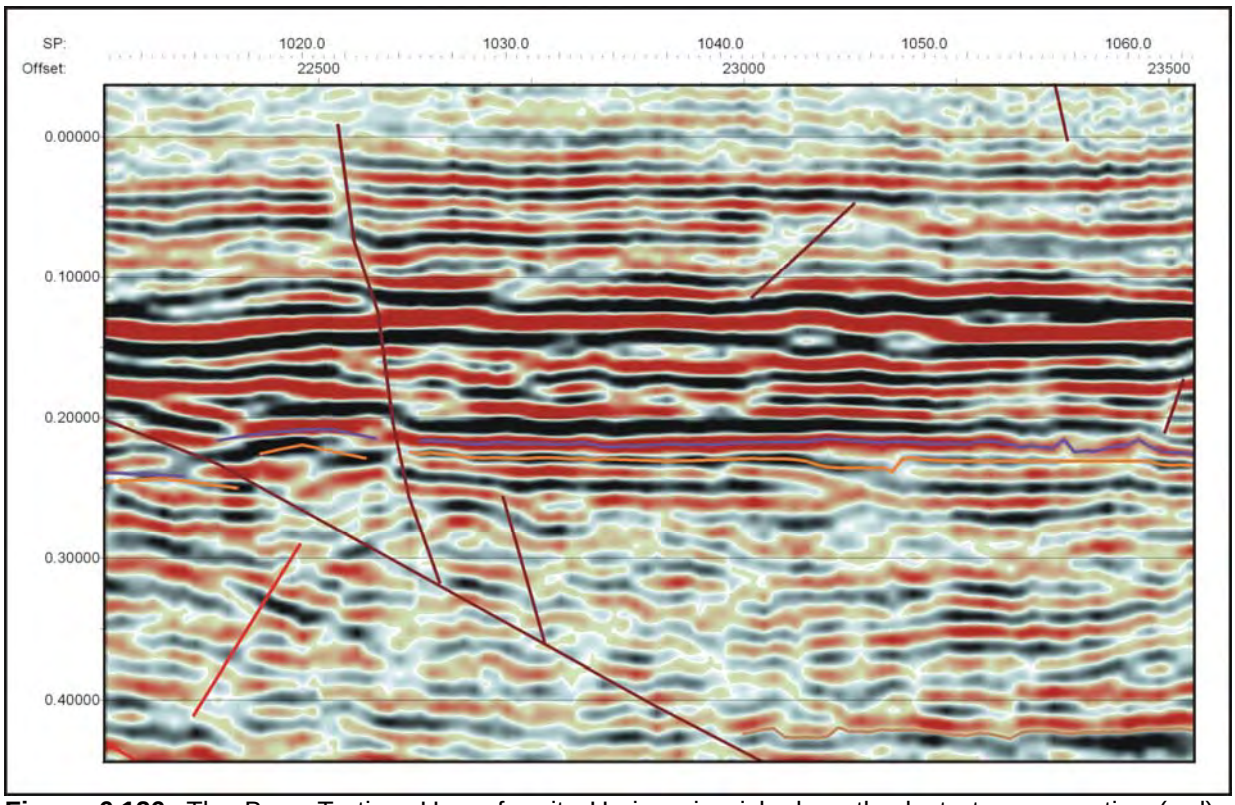

Figure 6.126: The Base Tertiary Unconformity Horizon is picked on the last strong negative (red) reflection before a significant change in seismic (TB01-PG).

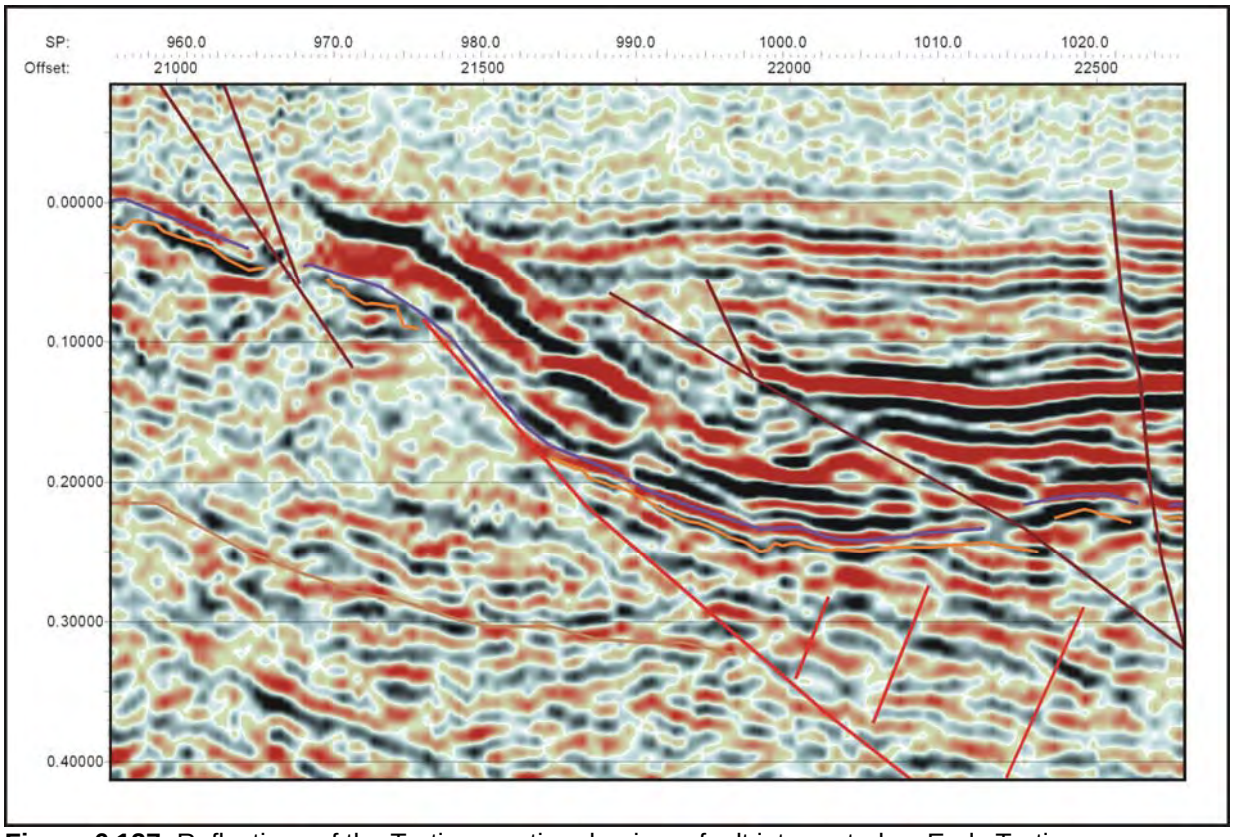

Figure 6.127: Reflections of the Tertiary section draping a fault interpreted as Early Tertiary (TB01-PG).

Between shot-points 975 and 1275 the Jurassic Dolerite sill and the Parmeener Supergroup section comprise a single tilted block (Figure 6.121). The Base Dolerite and Base Parmeener Supergroup horizons are difficult to determine and their positions in this section is extrapolated from reliable data between shot-points 1500 and 1600 (Figure 6.121).

The third half-graben depocentre lies between shot-points 1275 and 1750 (Figure 6.121). The Tertiary sequence is deposited across several faults that step down towards the northeast between shot-points 1275 and 1400 (Figure 6.121). The throw of these faults ranges from 150 – 350 m, they do not affect reflections in the Tertiary section and are therefore all classified as Early Tertiary Faults. Conversely, faults in a zone between shot-point 1425 and 1500 are classified as Later Tertiary as they displace reflections in the Tertiary section (Figure 6.128).

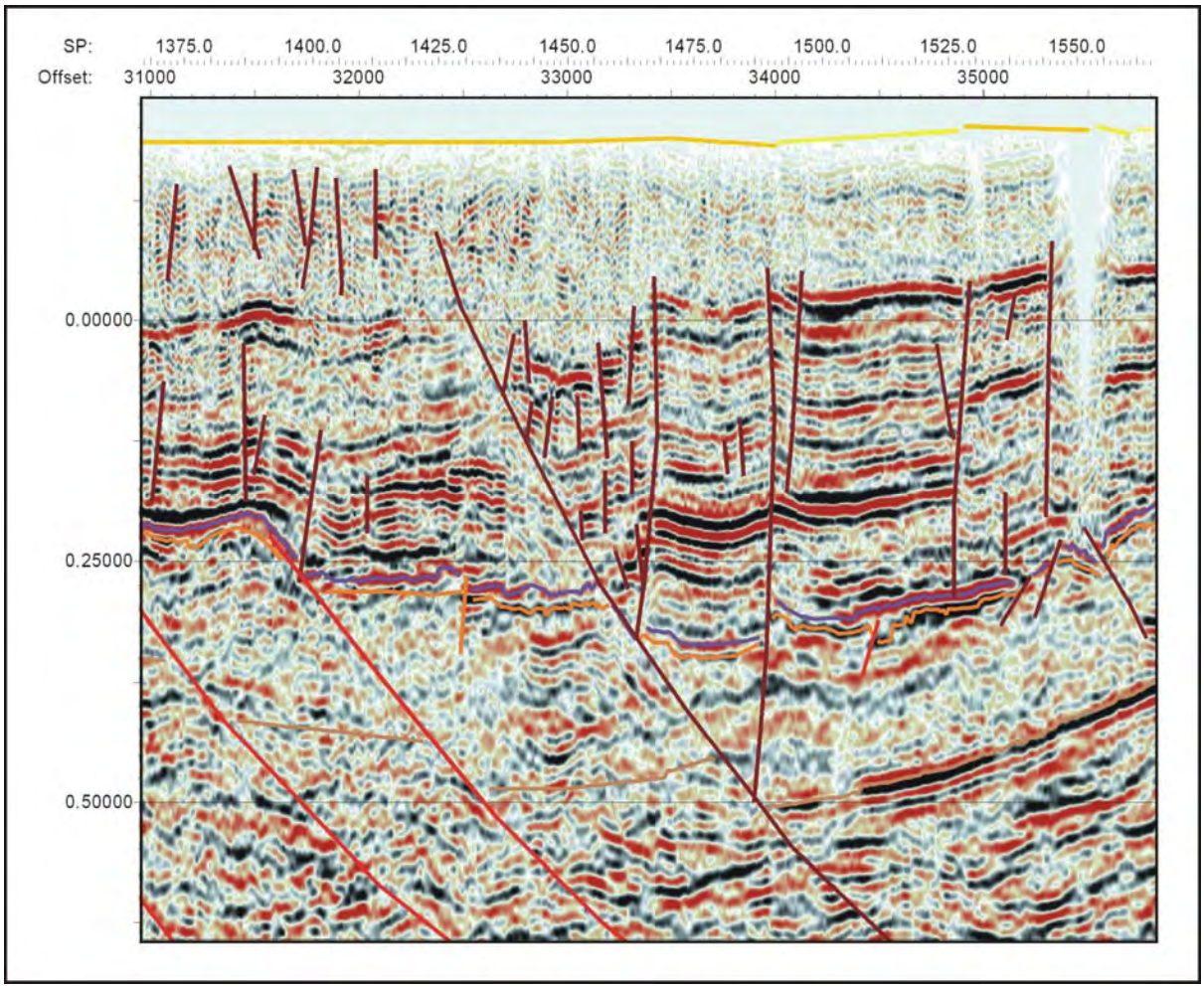

Figure 6.128: A zone of faults displacing reflections in the Tertiary section between shot-points 1425 and 1500 are classified as Later Tertiary (TB01-PG).

Between shot-points 1300 and 1750 the position of the Jurassic Dolerite sill is well defined by a zone of incoherent, low amplitude reflections (Figure 6.121). The Base Dolerite Horizon is interpreted at the first negative to positive (red to black) zero-crossing at the base of this zone

(Figure 6.129). In a wedge between shot-points 1425 and 1650, the Base Parmeener Unconformity Horizon is picked at a change in seismic character between strong (high amplitude), relatively coherent reflections and extremely incoherent data (Figure 6.129). At shot-point 1650, a large fault displaces the Base Parmeener Unconformity horizon by ~200 m

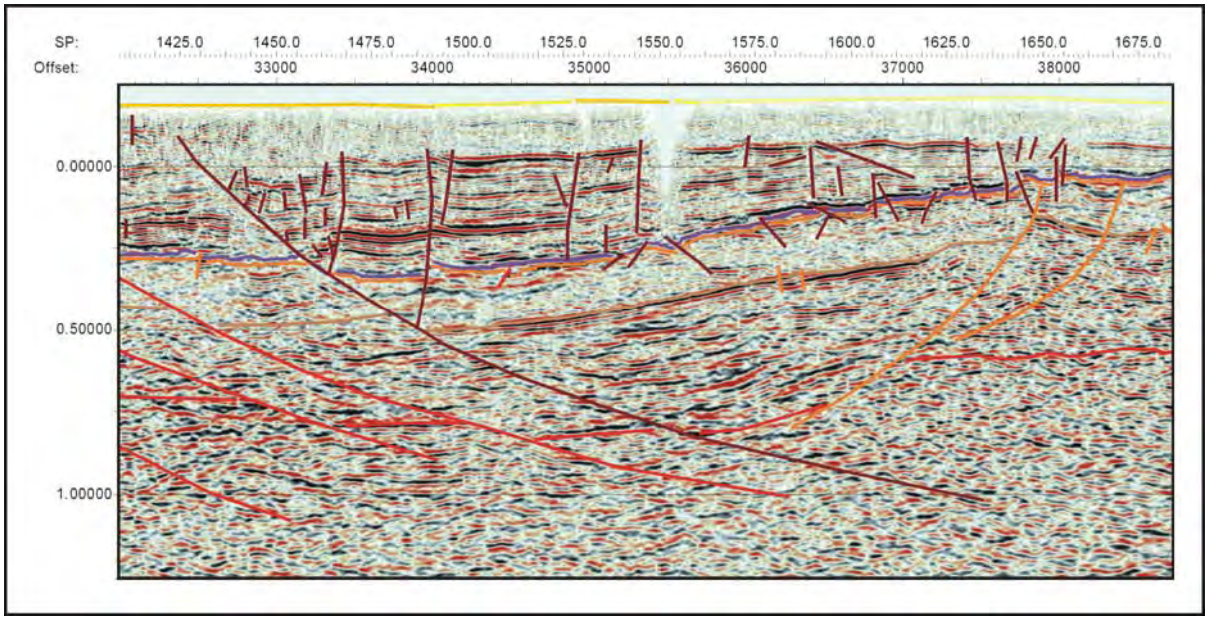

Figure 6.129: The Tertiary section, the Dolerite sill and the Base Parmeener Unconformity are all well defined by changes in seismic character between shot-points1425 and 1650 (TB01-PG).

Shot-points 1800 – 2382

(Figure 6.130)

From shot point 1800 to the end of the line the seismic data is poor. Dolerite is interpreted at the surface between shot-points 1750 and 2100, while a separate, shallow dolerite sill is also visible (Figure 6.130). The interpretation of the shallow sill is based on the occurrence of strong reflections between shot-points 1825 and 1875 and 0.15 and 0.4 seconds TWT (Figure 6.130). These reflections have similar character and the distance between them corresponds to the thickness of the dolerite sill interpreted between shot-points 1500 and 1800 (Figure 6.121). From shot-point 1750, the line follows a valley with up to 300 m of dolerite outcropping in the surrounding hills (Figure 6.119). This observation assists the interpretation, as it is unlikely that the outcropping dolerite is part of the same sill as the cumulative thickness would be over 900 m. Therefore the interpretation indicates two separate, closely spaced sills (Figure 6.130).

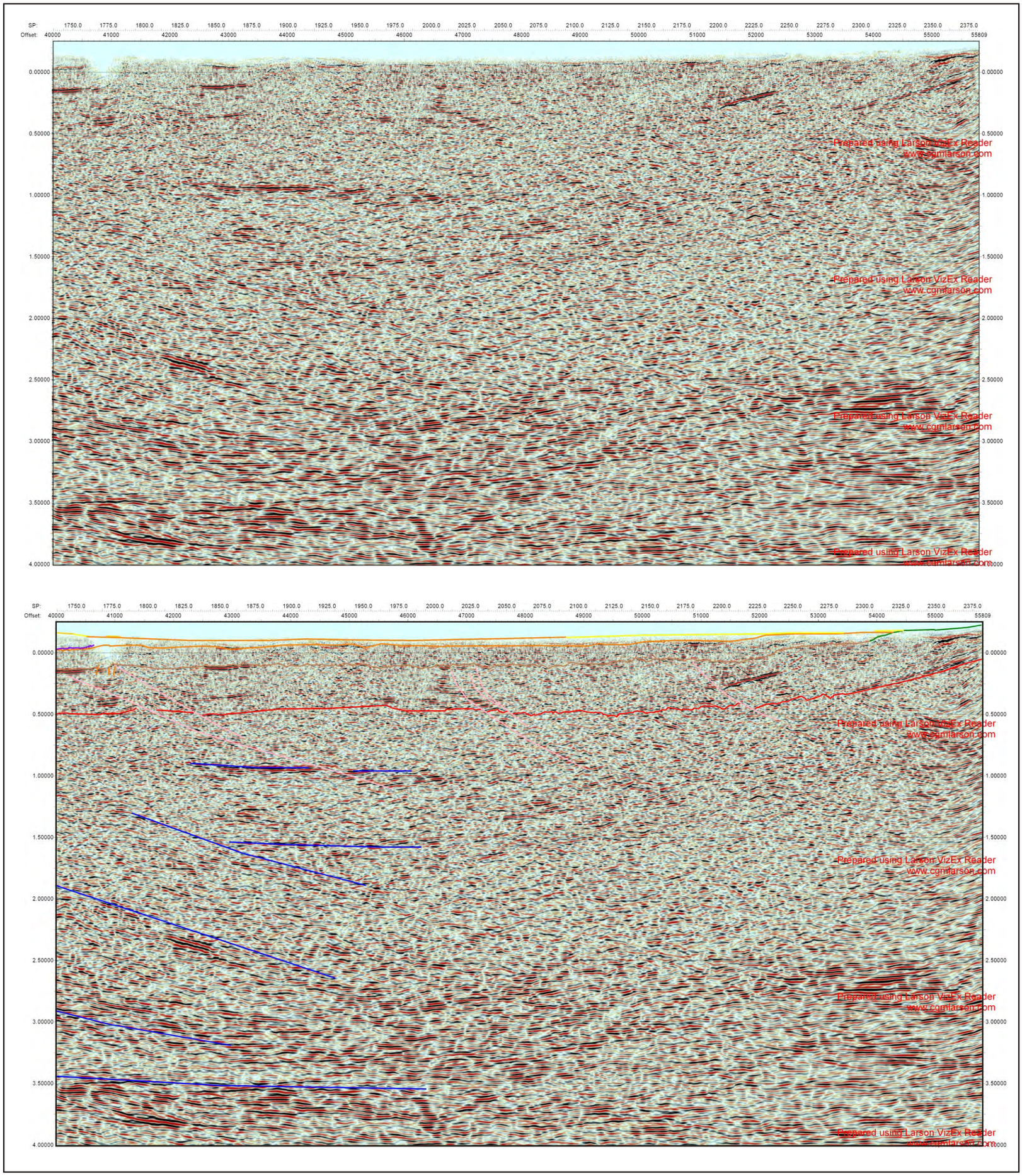

Figure 6.130: Raw and interpreted seismic data from shot-point 1800 to 2382.

The Base Parmeener Supergroup Horizon is difficult to pick from the seismic data and its position is estimated below the Base Dolerite Horizon from the more reliable pick at shot-point 1500. At shot-point 2200 the horizon is interpreted dipping into the basin from the northeast. This interpretation is based on the estimated thickness of the section between Unit 2 (outcropping after shot-point 2300) and the base of the Parmeener Supergroup. This interpretation is reinforced by truncated reflections observed at shot-point 2300 and 0.25 seconds TWT (Figure 6.131). The Parmeener Supergroup section is interrupted in several locations by relatively large faults, interpreted as pre-Jurassic. These faults are long (in the section), but have very small throws and do not affect the Jurassic Dolerite, hence the classification (Figure 6.130). No major basin-bounding fault is encountered at this end of the line.

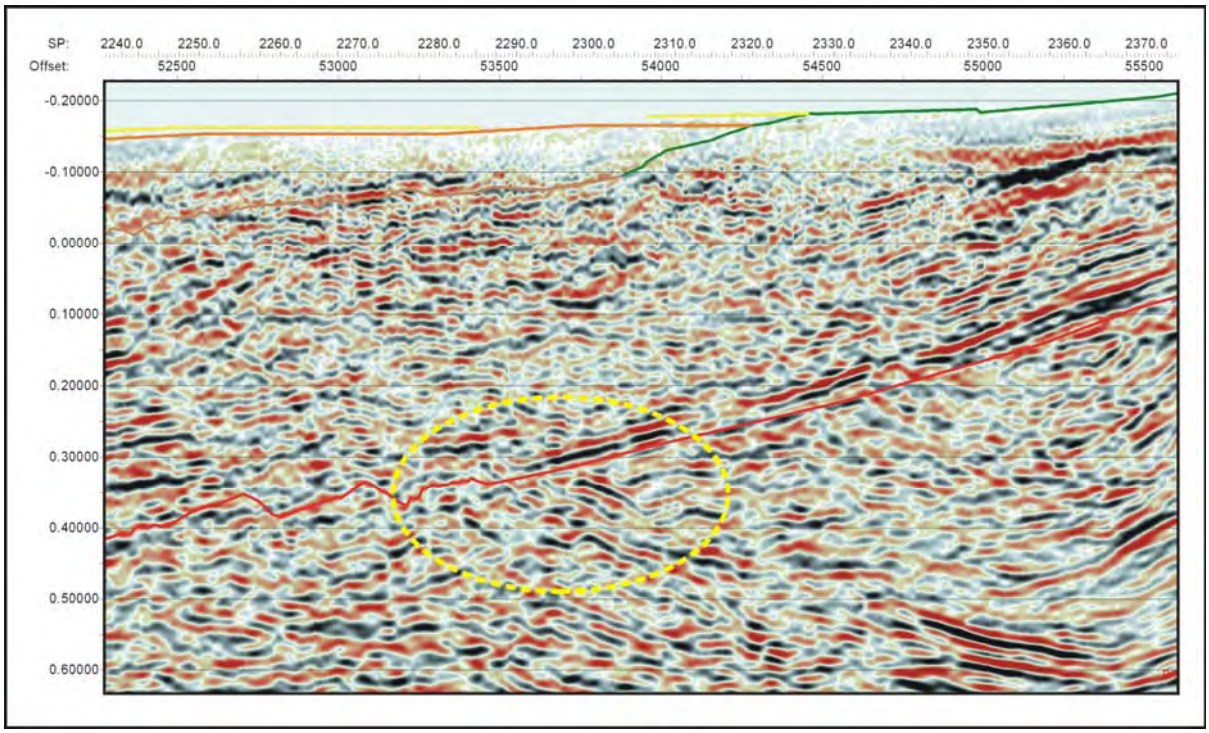

Figure 6.131: Base Parmeener Unconformity Horizon pick is aided by truncated dipping reflections (TB01-PG).

Basement

(Figure 6.120, 6.121)

The structural form of the basement is recognised from the interpretation of boundaries between zones of differing seismic character and by relatively continuous reflections. The basement section comprises two structurally different zones, one lying between shot-points 100 and 500 and another from shot-point 500 to the end of the line. The common boundary of these zones is the Tiers Fault System (Figure 6.120, 6.121).

Between shot-points 100 and 500 the events interpreted between 0.00 and 1.50 seconds (TWT) dip towards the northeast (right of section) at about 10° and are often truncated by horizontal reflections at 0.00 seconds (TWT) (Figure 6.120). The events are interpreted along strong, continuous reflections that form the boundary between zones of differing character.

Basement rocks outcrop 15 km southeast of the western end of the line. The Lake River inlier (Figure 6.119) contains volcaniclastic and metasedimentary rocks, ?Proterozoic to ?Cambrian in age. These outcrops occur along strike from the zone of strong reflections between shot-points 150 and 400 and between 0.25 and 0.75 seconds (TWT). This zone is bounded top and bottom by shallowly dipping, continuous reflections (Figure 6.120). Within this zone reflections curve into the bounding events (Figure 6.120). Between shot-points 150 and 200 and 0.50 seconds (TWT) the central event is cut by several events that dip more steeply towards the northeast (Figure 6.120). These long, continuous, bounding events may reflect the boundaries of thrust slices, while the events within the zone may represent deformed bedding planes. Below the northeast dipping events the interpreted events dip gently towards the southwest (left of section) (Figure 6.120). Events at 2.00 to 3.00 seconds (TWT) are cut by other events steeply dipping toward the southwest (Figure 6.120).

In contrast to the basement section between shot-points 100 and 500, the section after shot-point 500 comprises interpreted events that dip mainly towards the northeast at between 15° and 20° flattening out to a possible décollement between 3.5 and 4.0 seconds TWT (Figure 6.121).

6.3.3: TB01-PM

Seismic line TB01-PM is an 23 km long dip line. The line begins at the base of the Great Western Tiers (492 944 mE, 5 384 782 mN) and has been acquired towards the northeast finishing 2.5 km south of Perth (514 277 mE, 5 393 997 mN) (Map 5.1, Figure 6.132).

The seismic data shows a thick Tertiary sequence deposited in a half-graben, underlain by several tilt-blocks comprising Jurassic Dolerite and the Parmeener Supergroup section (Figure 6.133). The seismic data corresponding to the basement is highly incoherent, and the clearest events dip shallowly towards the northeast (Figure 6.133).

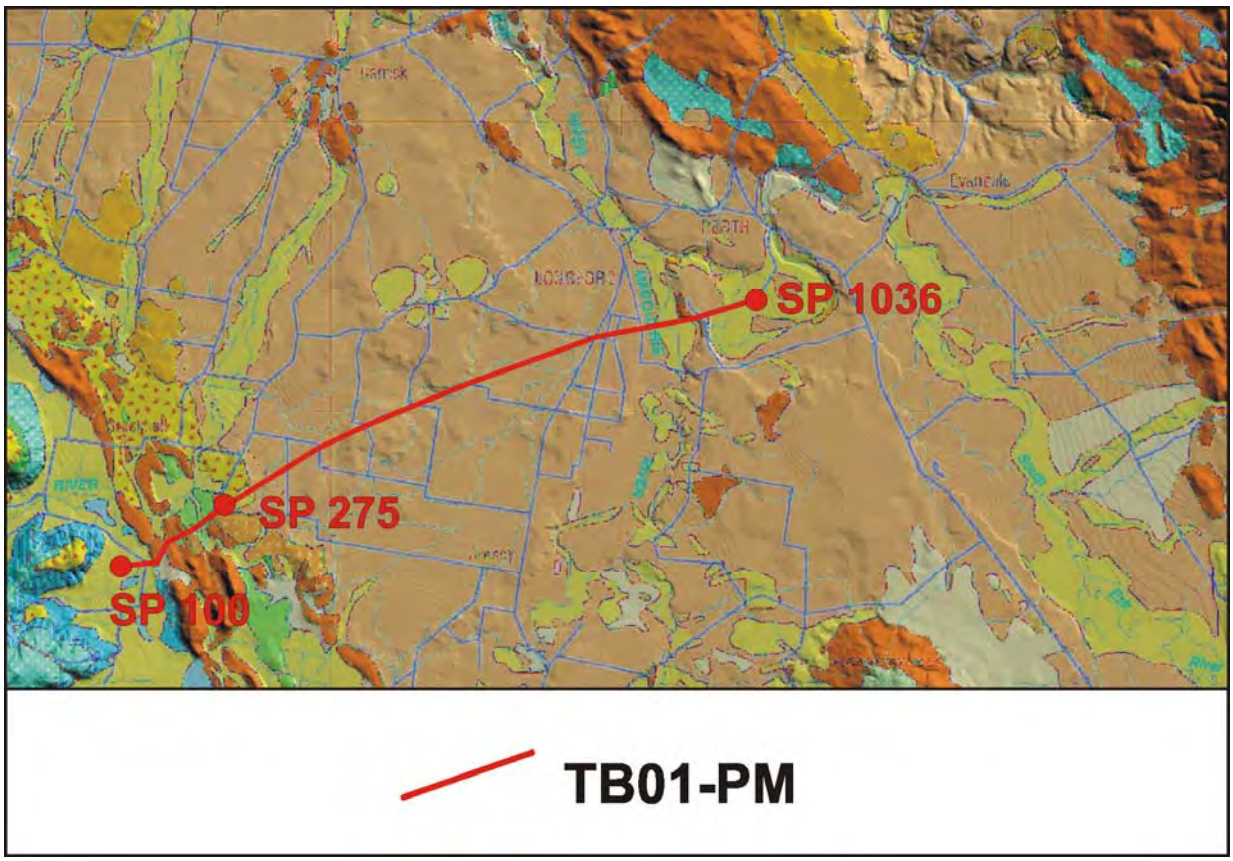

Figure 6.132: Outcrop geology and location of TB01-PM.

Shot-points 100 – 275

Between shot-points 100 and 275, Jurassic Dolerite and Parmeener Supergroup rocks are outcropping (Figure 6.132). From shot-point 100 to 130 the Base Parmeener Unconformity Horizon lies at 0.1 seconds TWT at the base of a series of strong coherent reflections (Figure 6.133). After shot-point 130 the seismic character changes becoming more incoherent. A fault is interpreted at this change in character (Figure 6.133). The fault terminates at the surface on the south-western boundary of outcropping dolerite and displaces the Base Parmeener Unconformity Horizon by ~450 m, where the horizon is picked along a series of strong reflections at 0.4 seconds TWT (Figure 6.133). While no Tertiary section is present, the fault displaces both the Jurassic Dolerite and the Parmeener Supergroup and is therefore classified as Undifferentiated Tertiary.

From shot-point 130 to 275 the Parmeener Supergroup and the Jurassic Dolerite dip towards the northeast (right of section) (Figure 6.133). This interpretation is based on the path of the Base Parmeener Unconformity Horizon, which follows strong reflections and a change in seismic character from incoherent reflections in the Parmeener Supergroup section to slightly stronger and more coherent reflections that correspond to the basement (Figure 6.133).

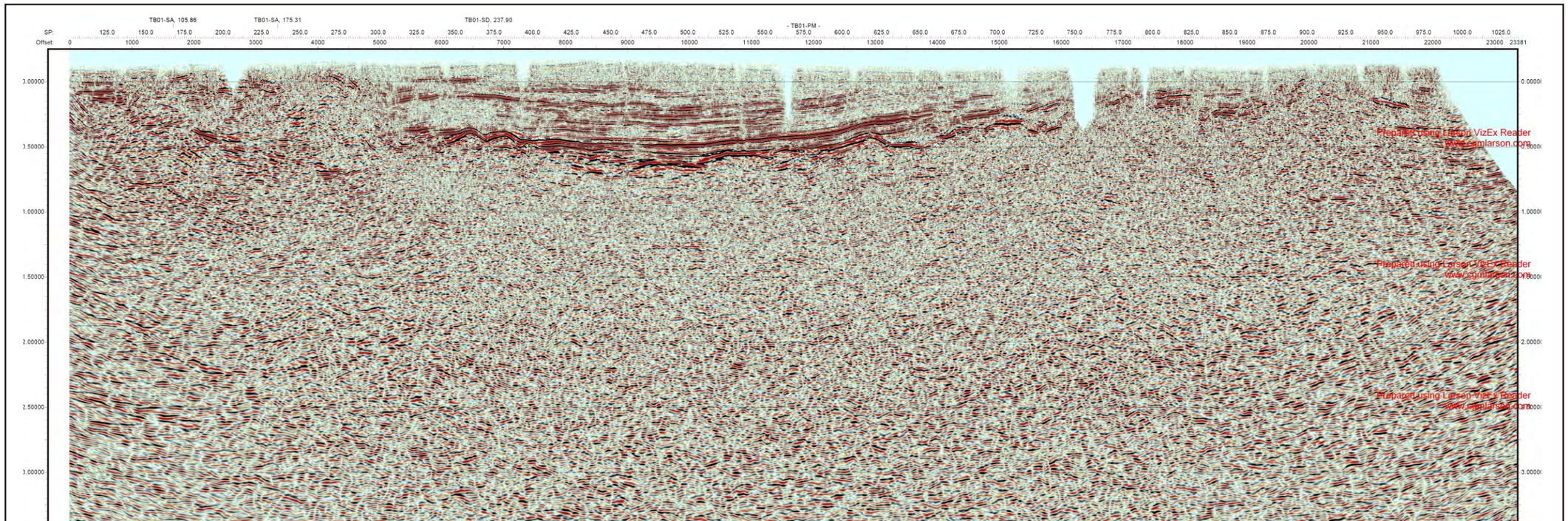

Figure 6.133: Raw and interpreted seismic data from shot-point 100 to 1036 (TB01-PM).

Shot-points 275 – 1036

This section of line contains a half-graben in which Tertiary sediments were deposited (Figure 6.133). The Tertiary sequence contains many strong, laterally coherent reflections (Figure 6.133). A distinctive marker horizon in the lower part of the sequence is interpreted along a strong (high amplitude) negative reflection (Figure 6.133). The Base Tertiary Unconformity Horizon is easily recognised at the base of these reflections and is picked on the last strong (high amplitude) negative (red) reflection (Figure 6.133). Faults are interpreted at dislocations in the Base Tertiary Unconformity Horizon (Figure 6.133).

The master fault of the half-graben is interpreted at shot-point 275 (Figure 6.133). The fault plane is picked at a lateral change in seismic character and dips steeply towards the northeast (right of section) displacing the Parmeener Supergroup section by ~1000 m (Figure 6.133). Growth is observed in the lower part of the Tertiary sequence below the marker horizon between the faults at shot-point 275 and 350, indicating early Tertiary, syn-depositional movement of the master fault (Figure 6.133). The marker horizon drapes two closely spaced faults interpreted around shot-point 375 indicating that while they were active during early Tertiary deposition, movement continued later (Figure 6.133). Reflections in the sequence below the marker horizon are truncated by it between shot-points 425 and 450 forming an angular unconformity indicating erosion of an earlier sequence (Figure 6.133). This earlier sequence thickens towards the deepest part of the depocentre at shot-point 500, thickening even further across faults at shot-points 625, 725 and 825, indicating that the earliest Tertiary deposition probably took place in these zones and that these faults were probably active before the master fault (Figure 6.133). They dip more shallowly than those at the south-western end of the line (Figure 6.133).

The seismic data below the Tertiary sequence is extremely poor and strong reflections or changes in seismic character do not assist in the interpretation of the Base Dolerite and Base Parmeener Unconformity horizons in this section of line. The position of these horizons is based on the thicknesses of the Jurassic Dolerite and Parmeener Supergroup from more reliable interpretation made on the adjacent line TB01-PU.

6.3.4: TB01-PT

Seismic line TB01-PT is the southernmost dip line acquired across the Longford Sub-basin. The line begins in an area between the Great Western Tiers and Macquarie Tier (518 519 mE, 5 362 457 mN) and is acquired towards the northeast finishing about 10 km east of Epping Forest (537 735 mE, 5 375 383 mN) (Map 5.1, Figure 6.134)

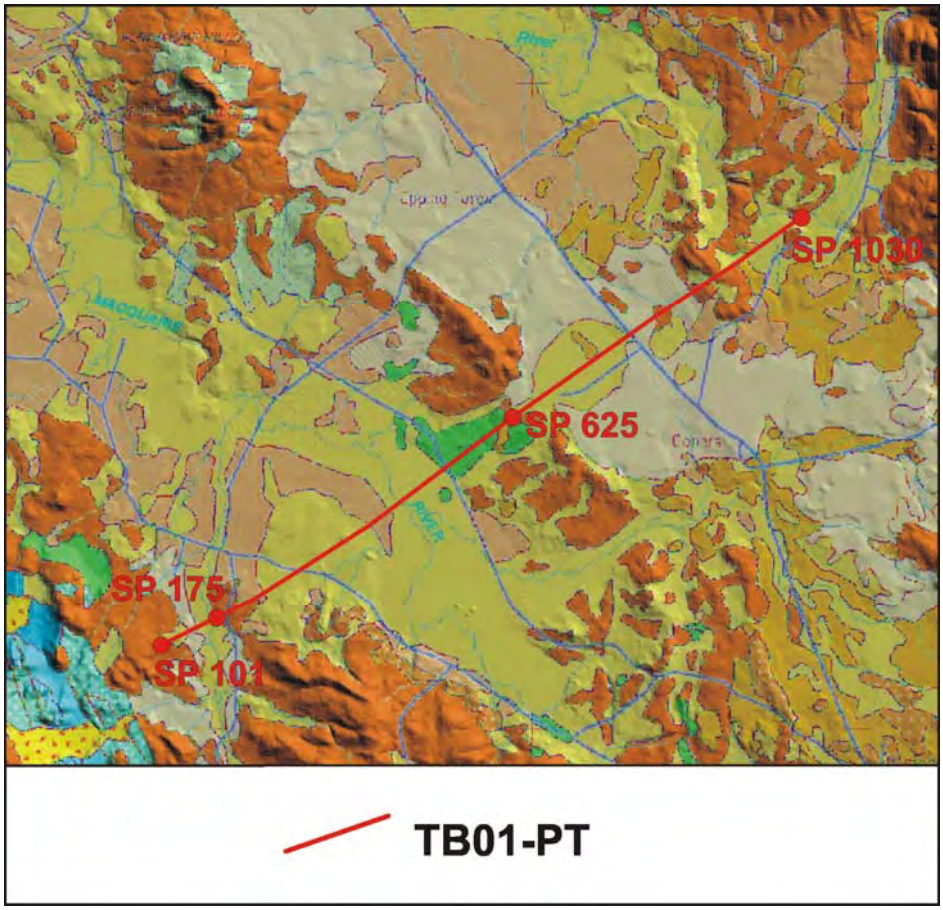

Figure 6.134: Outcrop geology and location of TB01-PT.

The interpretation mainly covers the south-western (left) end of the line where the seismic data and constraints are reasonable. Beyond the fault at shot-point 625 a small part of the Tertiary sequence is discernable below this the seismic data is incoherent (Figure 6.135).

Shot-points 101 – 625

The section from shot-points 101 – 625 is not typical of other lines recorded further north in the Longford Sub-basin. Rather, the section is more similar to the Northern Midlands section at the eastern end of line TB01-ST, where Jurassic Dolerite and Parmeener Supergroup form large fault blocks bounded by normal and reverse faults and the Tertiary sequence, where it occurs, is thin.

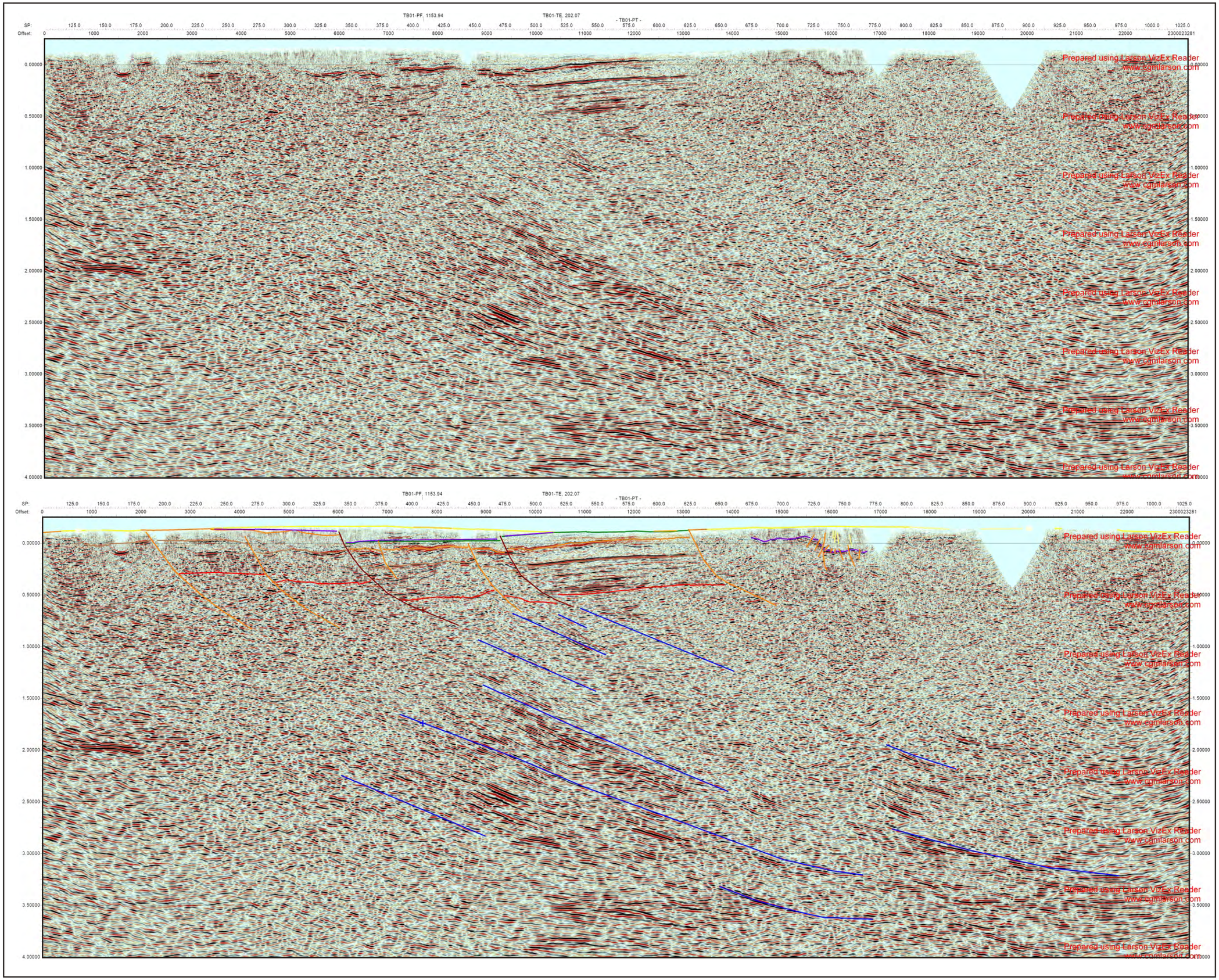

Figure 6.135: Raw and interpreted seismic data from shot-point 101 to 1030 (TB01-PT).

From shot-point 101 to 175, Jurassic Dolerite outcrops and a sill is interpreted close to the surface. The Base Dolerite Horizon is picked at shot – point 175 at the top of a group of strong reflections at 0.0 seconds TWT (Figure 6.135). The fault interpreted at shot-point 175 has no observable displacement and the interpretation is based on steeply dipping reflections between shot-points 200 and 225, and at 0.25 seconds TWT, as well as a change in seismic character from the hanging wall to the footwall (Figure 6.135). Between shot-points 225 and 250 the Base Dolerite Horizon is picked at -0.95 seconds TWT, above a group of strong (high amplitude) reflections at the base of a zone of incoherent data, which is typical for this horizon. A similar set of reflections can be seen below at 0.1 seconds TWT (Figure 6.135), however if the Base Dolerite Horizon was picked at this event the sill would be 850 m thick, which is inconsistent with the thickness in other parts of this section. Between shot-points 175 and 350, the Base Parmeener Unconformity Horizon is picked based on its sub-dolerite thickness, which is confidently picked at shot-point 375 and between shot-points 475 and 625 (Figure 6.135). At shot-point 265 a displacement of about 200 m in the Base Dolerite is observed and a fault interpreted (Figure 6.135).

Between shot-points 350 and 475, the picks corresponding to the Top and Base Dolerite Horizons and the Base Parmeener Unconformity Horizon are constrained by the very confident picks on line TB01-PF (Figure 6.118), and extrapolated from the tie (Figure 6.135). The Base Tertiary Unconformity Horizon is not a confident pick on this or line TB01-PF. Outcropping Unit 2 between shot-points 525 and 625 indicates there should be about 200 m of Parmeener Supergroup sequence above the dolerite sill in this location (Figure 6.135). The interpretation of the position of the horizon is an attempt to accommodate the extra sequence in a zone of poor data. The fault at shot-point 350 is classified as Later Tertiary as it displaces the Base Tertiary Unconformity Horizon, as well as the dolerite sill and the Base Parmeener Unconformity horizons (Figure 6.135). This fault is also observed on line TB01-PF. It strikes 340° (NNW). Smaller faults at shot-point 375 and 450 are classified as Undifferentiated Tertiary, as the youngest strata they displace is Jurassic Dolerite (Figure 6.135).

From shot-point 475 to 625 the Top and Base Dolerite horizons are confidently picked at the top and base of incoherent seismic data that is characteristic of dolerite (Figure 6.135). The Base Parmeener Unconformity Horizon is picked at the base of a series of strong laterally coherent reflections (Figure 6.135). The sub-dolerite thickness of the Parmeener Supergroup in this section of line corresponds to the thickness at the equally confident pick on line TB01-PF (Figure 6.118). The fault interpreted at shot-point 475 is classified as Later Tertiary as it

affects the Tertiary sequence (Figure 6.135). The fault is reverse with about 200 m of displacement. Below the level of the Base Parmeener Unconformity the fault links with a basement structure interpreted at a change in seismic character (Figure 6.135).

Basement

Structures in the basement are particularly well resolved in this section. Events are interpreted at changes in seismic character that mainly corresponding to changes in amplitude. In the central and north-eastern (right) part of the section the reflection are dominantly straight, coherent and dip towards the northeast at about 20° converging on a décollement at 3.5 seconds TWT in the lower, right corner of the section (Figure 6.135).

6.3.5: TB01-PU

Seismic line TB01-PU is a 29.5 km long dip line acquired over mainly Quaternary and Tertiary age sediments (Forsyth et al., 1995, McClenaghan and Calver, 1994). The line is acquired from southwest to northeast, beginning near the base of the Great Western Tiers (498 438 mE, 5 378 187 mN) and finishing at the Nile Road (523 284 mE, 5 393 914 mN) (Map 5.1, Figure, 6.136).

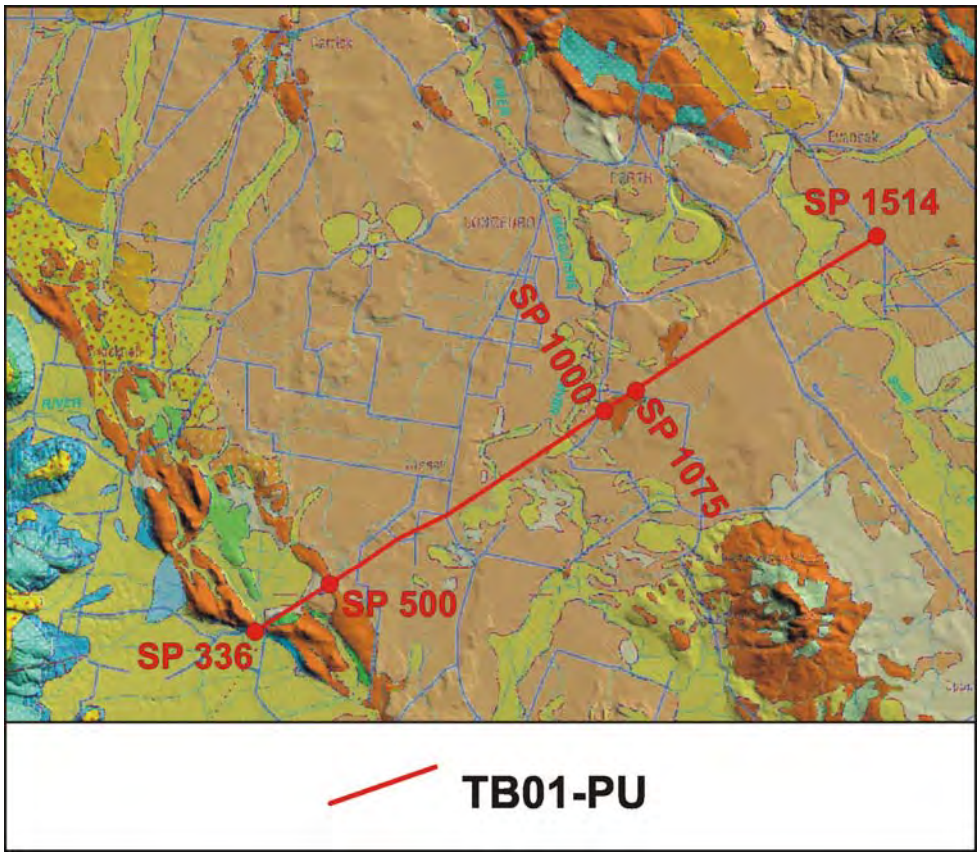

Figure 6.136: Outcrop geology and location of TB01-PU.

The interpretation indicates two Tertiary depocentres separated by a high between shot-points 1000 and 1075, where dolerite outcrops (Figure 6.136). The Tertiary sequence is identified between shot-points 500 and 1000 and shot-point 1075 and the end of the line by a zone of low amplitude reflections at the top of the section (Figure 6.137). The Base Tertiary Unconformity Horizon is picked at the base of this zone along a strong (high amplitude) negative (red) reflection (Figure 6.137).

Shot-points 336 - 500

From shot-point 336 to 500, Upper Parmeener Supergroup, Tertiary and Quaternary sediments outcrop (Figure 6.136). The Base Parmeener Supergroup Horizon is interpreted at a series of strong reflections between 0.0 and 1.0 seconds TWT (Figure 6.137). These reflections a segmented by several Undifferentiated Tertiary Faults, which drop the Base Parmeener Supergroup Horizon down by about 900 m towards the northeast (Figure 6.137).

Shot-points 500 – 1075

At shot-point 500 a large Early Tertiary Fault forms the south-western boundary of the Tertiary half-graben depocentre (Figure 6.137). Reflections adjacent to the fault within the Tertiary sequence show a small amount of growth, indicating the fault was active during early Tertiary deposition (Figure 6.138). From shot-points 500 to 1075 the Jurassic Dolerite and the Parmeener Supergroup section are sub-divided into several fault blocks by Early Tertiary faults (Figure 6.137). The interpretation of the faults at shot-points 665 and 735 is based on dislocation of the Base Tertiary Unconformity Horizon, while the interpretation of the fault at shot-point 700 is based on an offset in the Base Dolerite Horizon (Figure 6.138). The fault at shot-point 915 is also based on an offset in the Base Tertiary Unconformity Horizon as well as offsets in the Base Dolerite and Base Parmeener Unconformity Horizon (Figure 6.137).

Across this zone the Jurassic Dolerite sill is not as prominent. Here the interpretation of the Base Dolerite Horizon follows a series strong reflections occurring between shot-points 550 to 575, 650 to 675, 675 to 700 and 700 to 725 (Figure 6.137). The position of the Base Parmeener Unconformity Horizon is interpreted from the estimated thickness of the sub-dolerite Parmeener Supergroup section in the scarp of the Great Western Tiers.

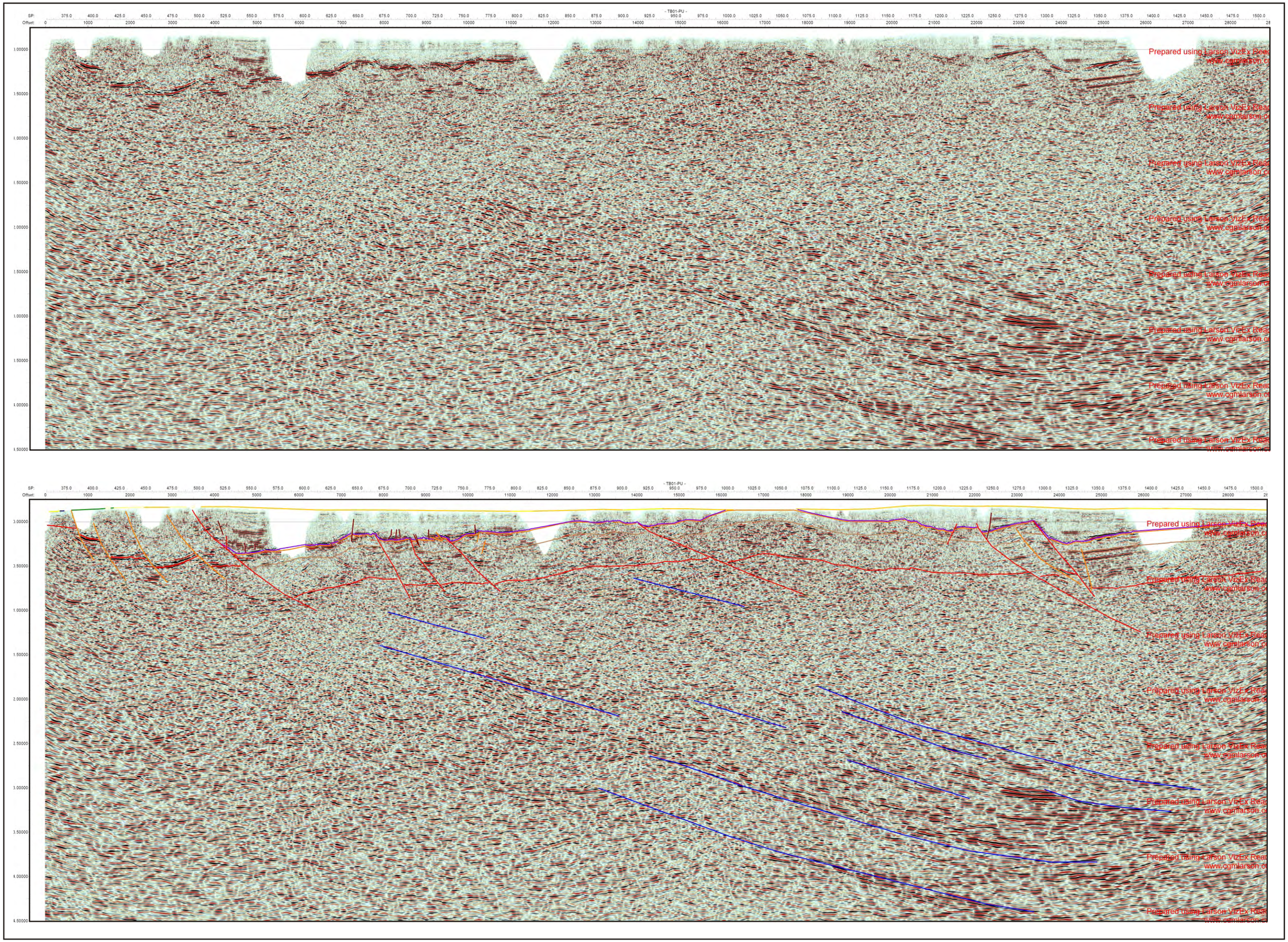

Figure 6.137: Raw and interpreted seismic data from shot-point 336 to 1512 (TB01-PU).

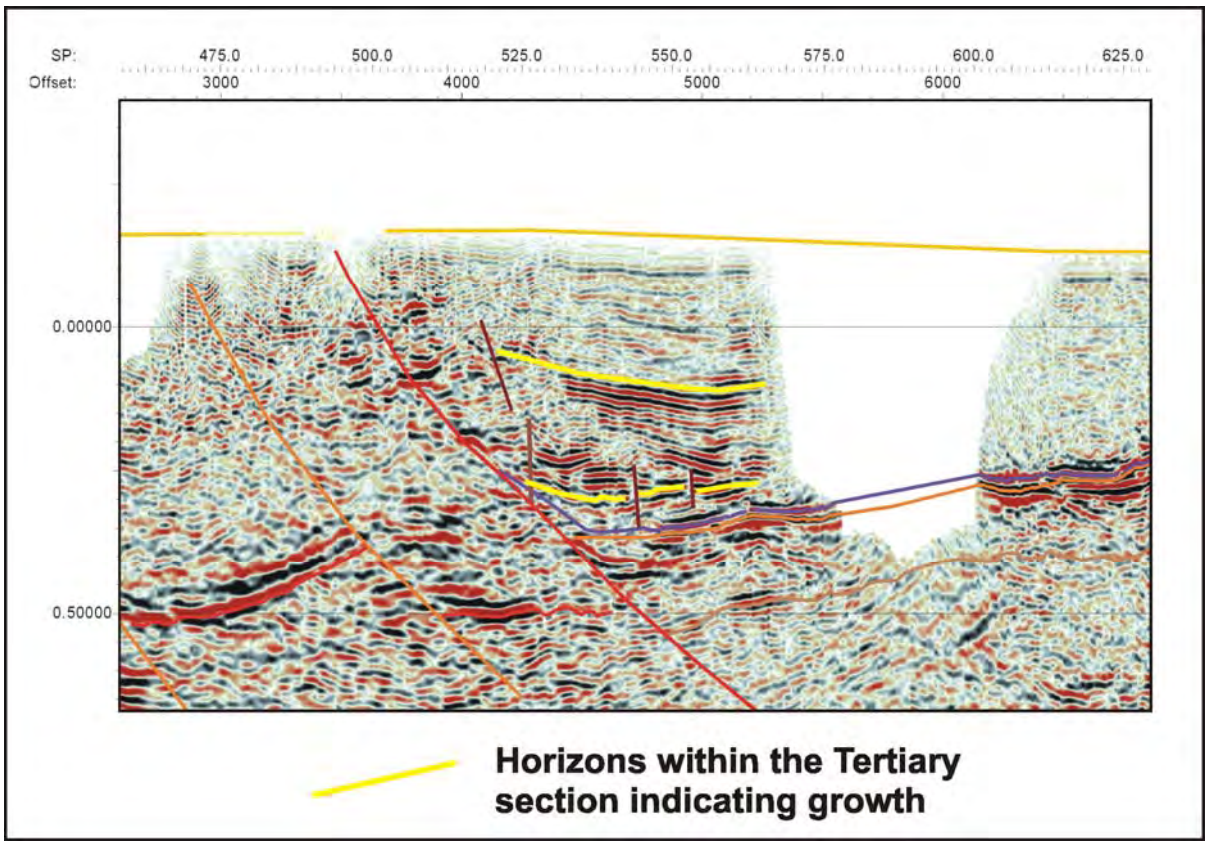

Figure 6.138: Marker horizons indicating growth on the fault at shot-point 500 (TB01-PU).

Between shot-points 1000 and 1075, Jurassic Dolerite is mapped at the surface (Figure 6.136) (McClenaghan and Calver, 1994). No faulting can be observed at the margins of the outcropping dolerite and the Base Tertiary Unconformity Horizon can be interpreted with reasonable confidence shallowing with the dolerite sill between shot-points 925 and 1000 (Figure 6.137). Therefore the outcrop is interpreted to result from the exposed crest of an anticline affecting both the Jurassic Dolerite and Parmeener Supergroup section indicating it was formed post-Jurassic. The Base Dolerite Horizon in this short section of line is picked at a change in seismic character from low amplitude, incoherent reflections to high amplitude reflections occurring at 0.0 seconds TWT (Figure 6.137). The Base Parmeener Unconformity Horizon is picked at a subtle change in seismic character between 0.35 and 0.4 seconds TWT, where strong (high amplitude), moderately coherent reflections change to reflections that are slightly weaker and less coherent (Figure 6.137). This change in seismic character also coincides with where the horizon would be picked based on thickness estimates, adding to the confidence of the interpretation.

Shot-points 1075 – 1514

The Tertiary depocentre in this section of line is symmetrical about a series of faults between shot-points 1225 and 1300 (Figure 6.137). No growth is interpreted on these faults. They do,

however displace the underlying stratigraphy and do not appear to penetrate far into the Tertiary section indicating a probable early Tertiary history (Figure 6.137). Other faults in this zone either penetrate deeply into the Tertiary sequence indicating later movement (Later Tertiary Faults) or only affect the Jurassic Dolerite and Parmeener Supergroup and are classified as Undifferentiated Tertiary Faults (Figure 6.139). The Base Tertiary Unconformity Horizon is picked at a significant change in seismic character from low amplitude incoherent reflections to a series of strong coherent reflections, where the Base Tertiary Unconformity is picked on the first strong, negative (red) reflection and the Top Dolerite Horizon on the first strong positive (black) reflection (Figure 6.139).

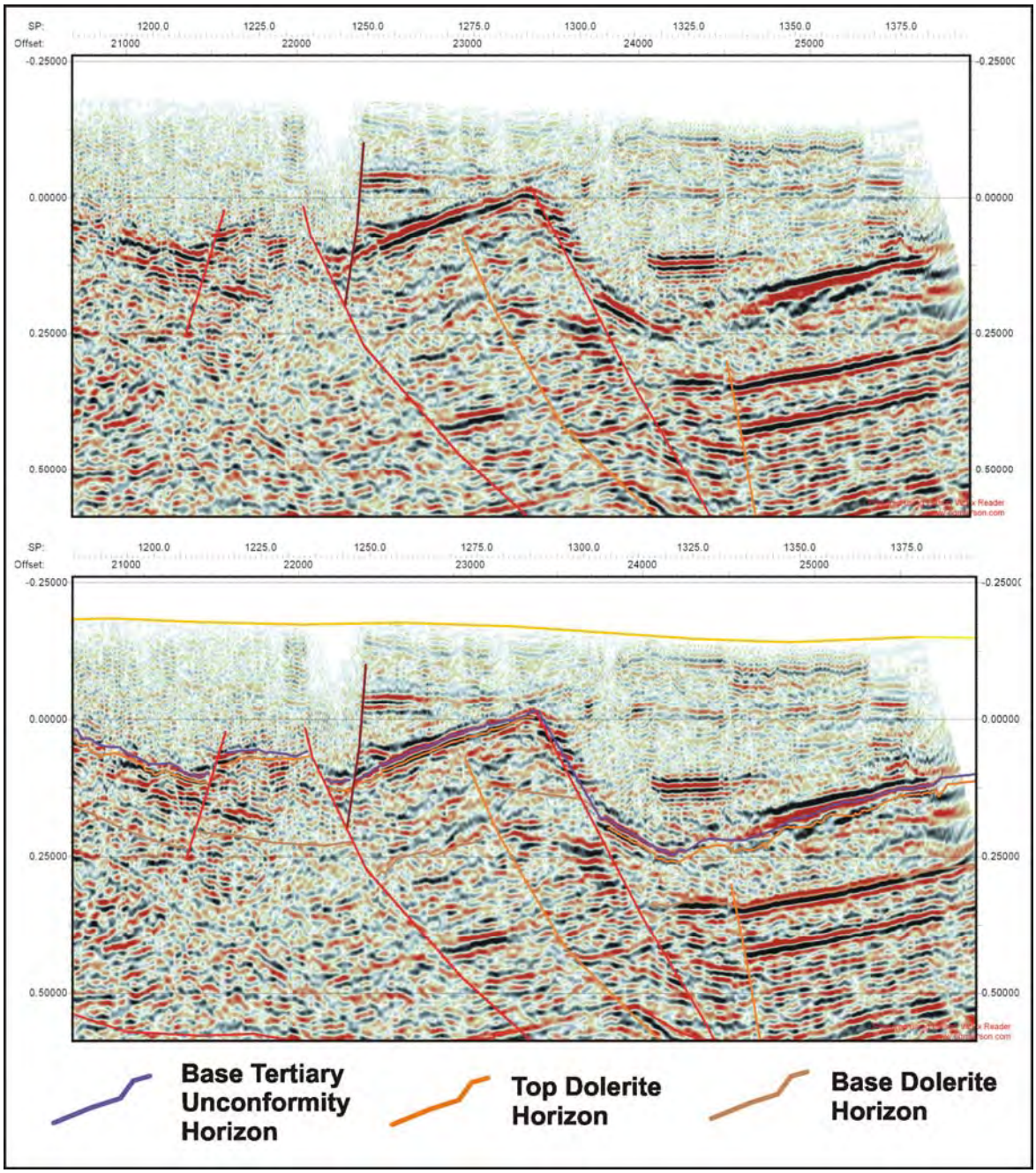

Figure 6.139: Raw and interpreted seismic data between shot-points 1175 and 1375 showing major faults, the Base Tertiary Unconformity, Top and Base Dolerite horizons (TB01-PU).

The typical seismic character of Jurassic Dolerite, is more recognisable in this section of the line, particularly from shot-points 1075 to 1130 and 1300 to 1375. The Base Dolerite Horizon is picked at the first set of high amplitude reflections at the base of the weak data (Figures 6.137, 6.139). The path of the Base Parmeener Unconformity Horizon is not clear from the seismic data. The position of the horizon in most easily picked at the base of coherent reflections at shot-point 1350 (Figure 6.137), this pick is consistent with the estimated thickness of the sub-dolerite Parmeener Supergroup section.

Basement

The seismic data corresponding to the basement is poor, however the general form of the basement can be roughly interpreted based mainly on linear events and seismic character changes. The best data occurs towards the base of the section in the northeast (right) and shows a series of long, straight events dipping at ~20° towards the northeast (Figure 6.137).

6.3.6: TB01-PW

Seismic line TB01-PW is the northernmost dip line recorded across the Longford Sub-basin. The line is 22.6 km long, acquired towards the northwest the line begins inboard of the Tiers Fault System (493 5627 mE, 5 395 825 mN) and finishing about 7 km southwest of Launceston (511 710 mE, 5 407 218 mN) (Map 5.1, Figure 6.140).

The section shows Tertiary rocks deposited in two distinct depocentres (Figure 6.141). The seismic line begins inboard of the boundary of the south-western depocentre. Based on the form of depocentres on adjacent lines it is assumed that this depocentre is a half-graben bounded in the southwest by the Tiers Fault System.

Shot-points 370 – 850

Between shot-points 370 and 850 the location of the Tertiary sequence is interpreted from the characteristic strong laterally coherent reflections (Figure 6.141). The Base Tertiary Unconformity Horizon is picked at the base of these coherent reflections along a strong, coherent, negative (red) reflection that has a slightly lower frequency (thicker) than the overlying reflections (Figure 6.141).

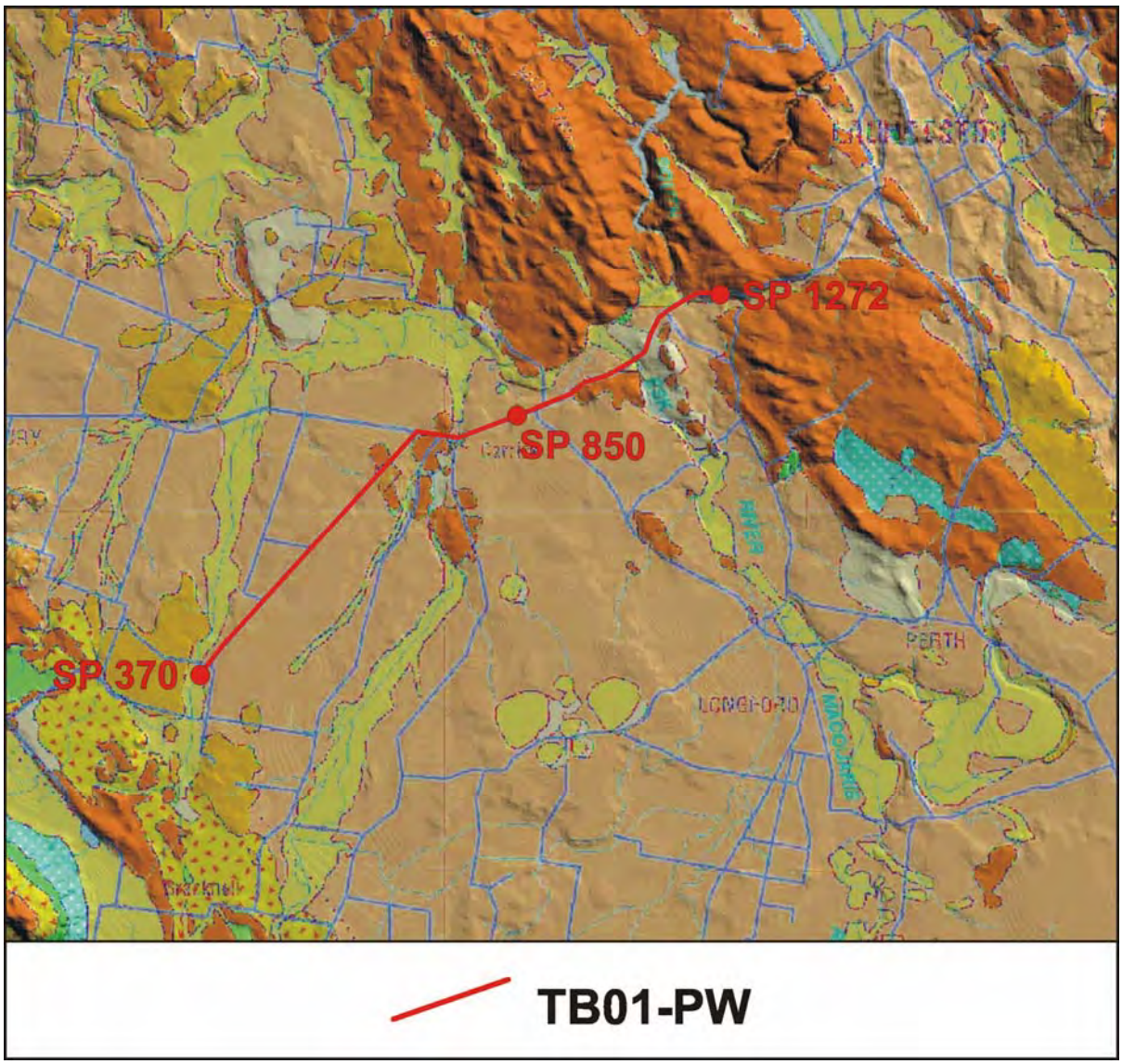

Figure 6.140: Outcrop geology and location of TB01-PW.

The Base Parmeener Unconformity Horizon pick is constrained by an estimate of the thickness of the Parmeener Supergroup section from adjacent lines. The pick is made at a change in character between shot-point 450 and 575 and guided by coherent dipping reflections from shot-point 550 to 675 (Figure 6.141). The Base Dolerite Horizon is placed at the base of a zone of incoherent data (typical of dolerite) between shot-points 450 and 650 and extrapolated left and right across zones of poor data (Figure 6.141).

Shot-points 850 – 1272

The Undifferentiated Tertiary Fault interpreted at shot-point 850 is not mapped and has no surface expression (Figure 6.140). The interpretation is based on the displacement down to the northeast of the Base Tertiary Unconformity Horizon and a change in seismic character at shot-point 950, between 0.5 and 1.0 seconds TWT, and projected through the gap in the seismic data (Figure 6.142).

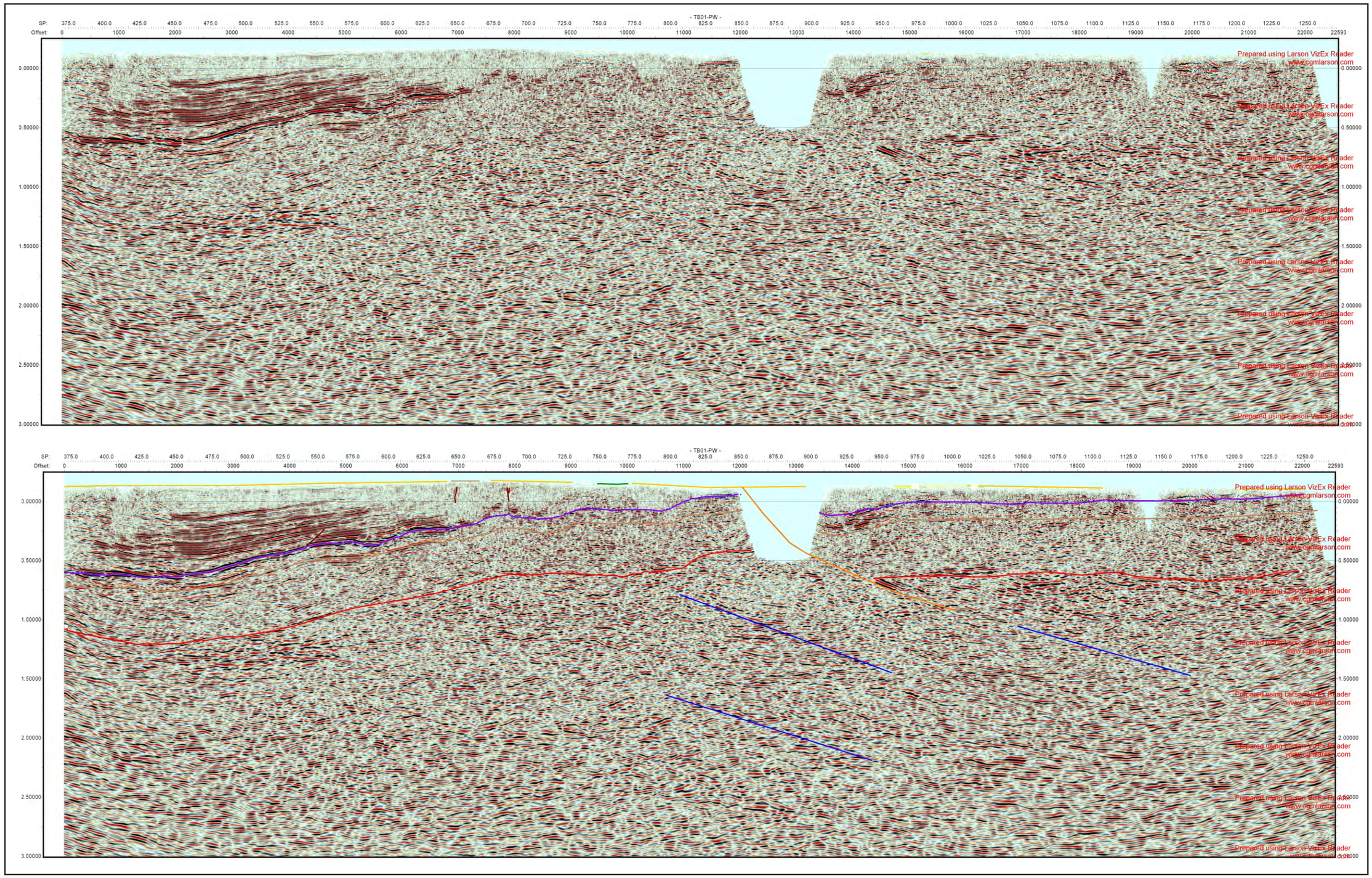

Figure 6.141: Raw and interpreted seismic data from shot-point 370 to 1272 (TB01-PW).

The Base Tertiary Unconformity Horizon is picked at the first strong negative (red) reflection at the base of a zone of incoherent, weak reflections between shot-points 900 and 975 (Figure 6.141). The Base Parmeener Unconformity Horizon is more confidently picked at the truncation of strong coherent dipping reflections by horizontal reflections adjacent to the fault at shot-point 950 and 0.625 seconds TWT (Figure 6.142). The horizon can be followed with confidence along a change in seismic character from incoherent data above to stronger, thicker reflections below (Figure 6.142). The Base Dolerite Horizon pick is based mainly on its thickness below the Base Tertiary Unconformity Horizon extrapolated from other parts of the line.

Basement

Events reflecting the general form of the basement are picked from relatively linear events occurring at changes in seismic character (Figure 6.141). The events picked, dip towards the northwest at about 20° and link to faults affecting the Parmeener Supergroup (Figure 6.141).

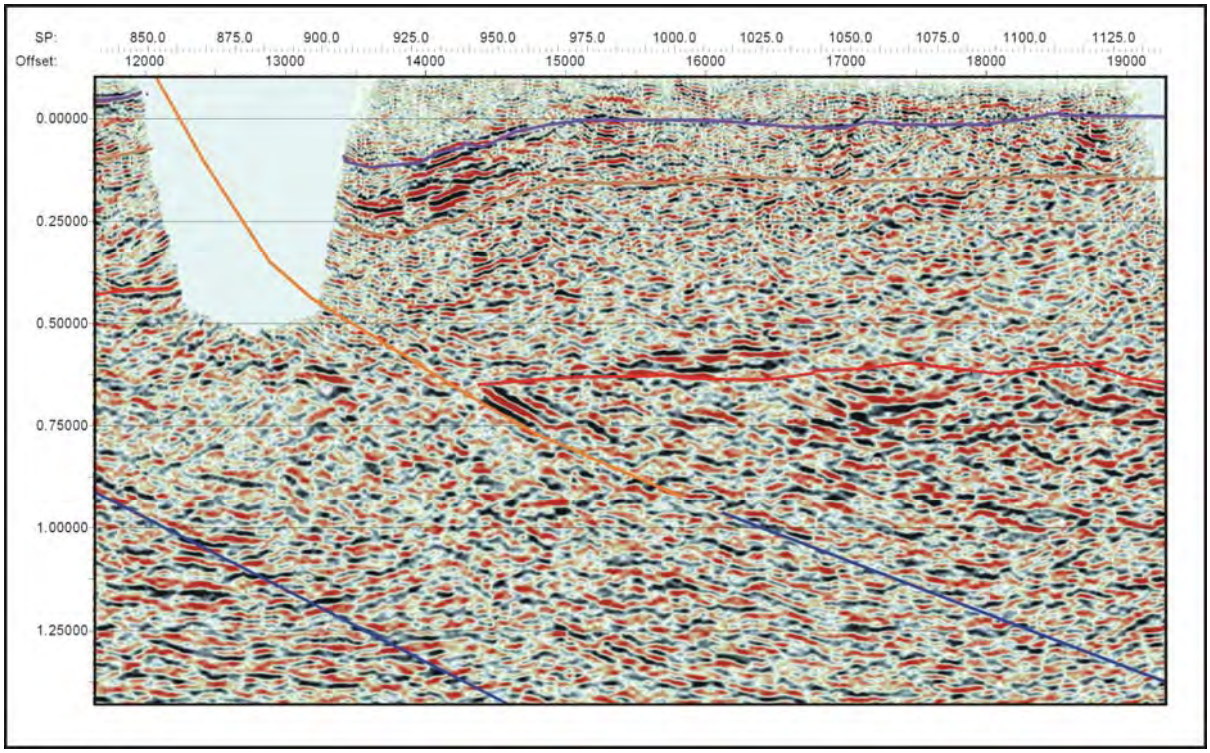

Figure 6.142: The interpretation of the fault at shot-point 850 is based on the displacement of the Base Parmeener Unconformity Horizon (TB01-PW).

6.3.7: TB01-TE

Seismic line TB01-TE is a second tie line between lines TB01-PF and PG. The line is 25.5 km long, beginning 10 km southwest of Conara (528 450 mE, 5 365 762 mN). It follows the Mount Joy Road towards the northwest around the southern side of a distinctive topographical feature know as Hummocky Hills, finishing 5 km to its northwest (516 287 mE, 5 385 182.70 mN) (Map 5.1, Figure 6.143).

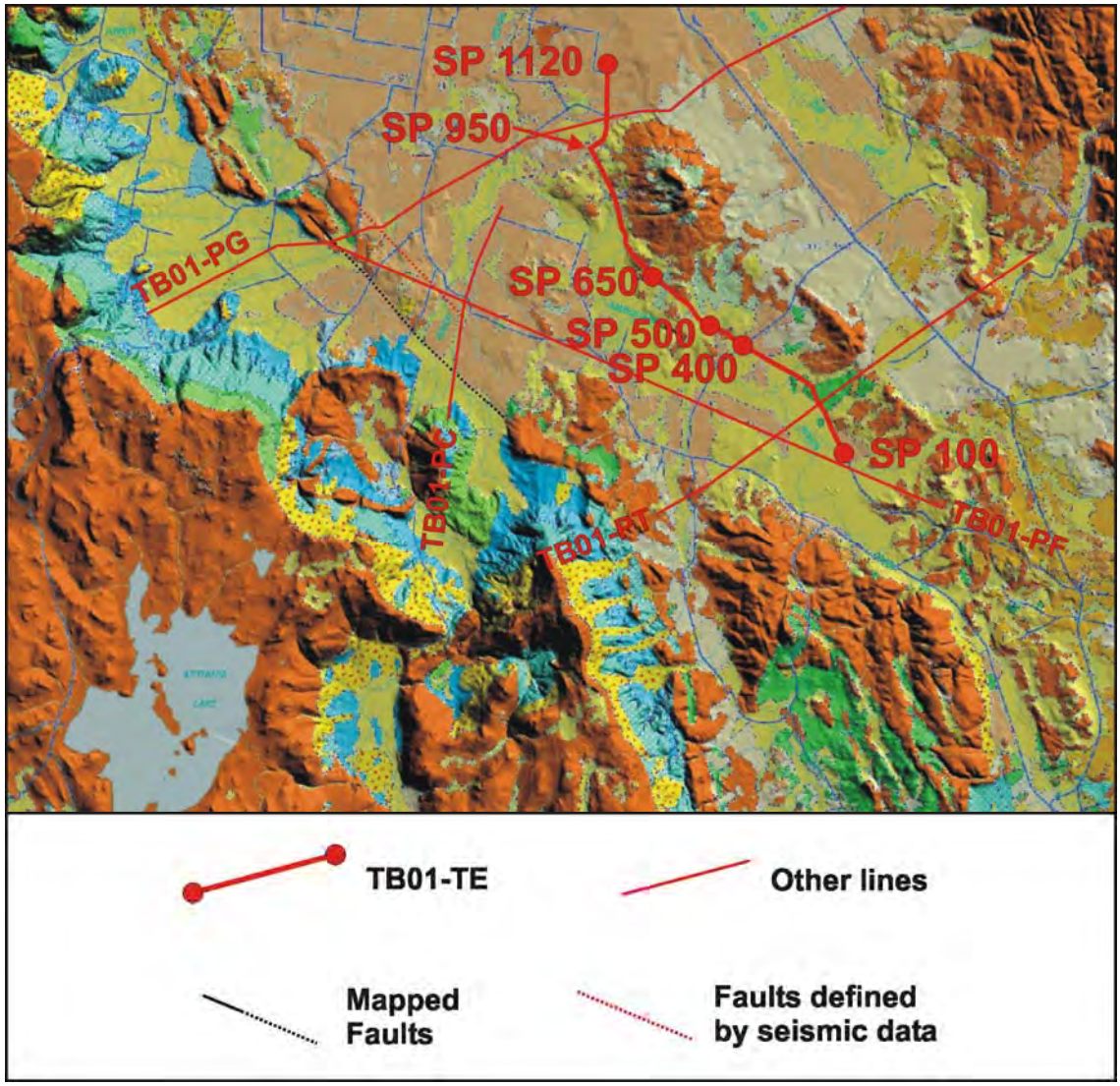

Figure 6.143: Outcrop geology, location of TB01-TE, tie and adjacent lines.

The Parmeener Supergroup section is devoid of faults, and this may be because the line is sub-parallel to regional strike. From shot-point 100 to 400, the Base Parmeener Unconformity Horizon is identified at the base of strong, coherent reflections at 0.5 seconds TWT (Figure 6.144). The Top and Base Dolerite horizons are interpreted at the edges of incoherent data with typical dolerite character (Figure 6.144). After shot-point 400 the dolerite sill is discernable as a zone of weaker, more incoherent data above zone of strong coherent data between shot-points 450 to 650 and 850 to 950 (Figure 6.144).

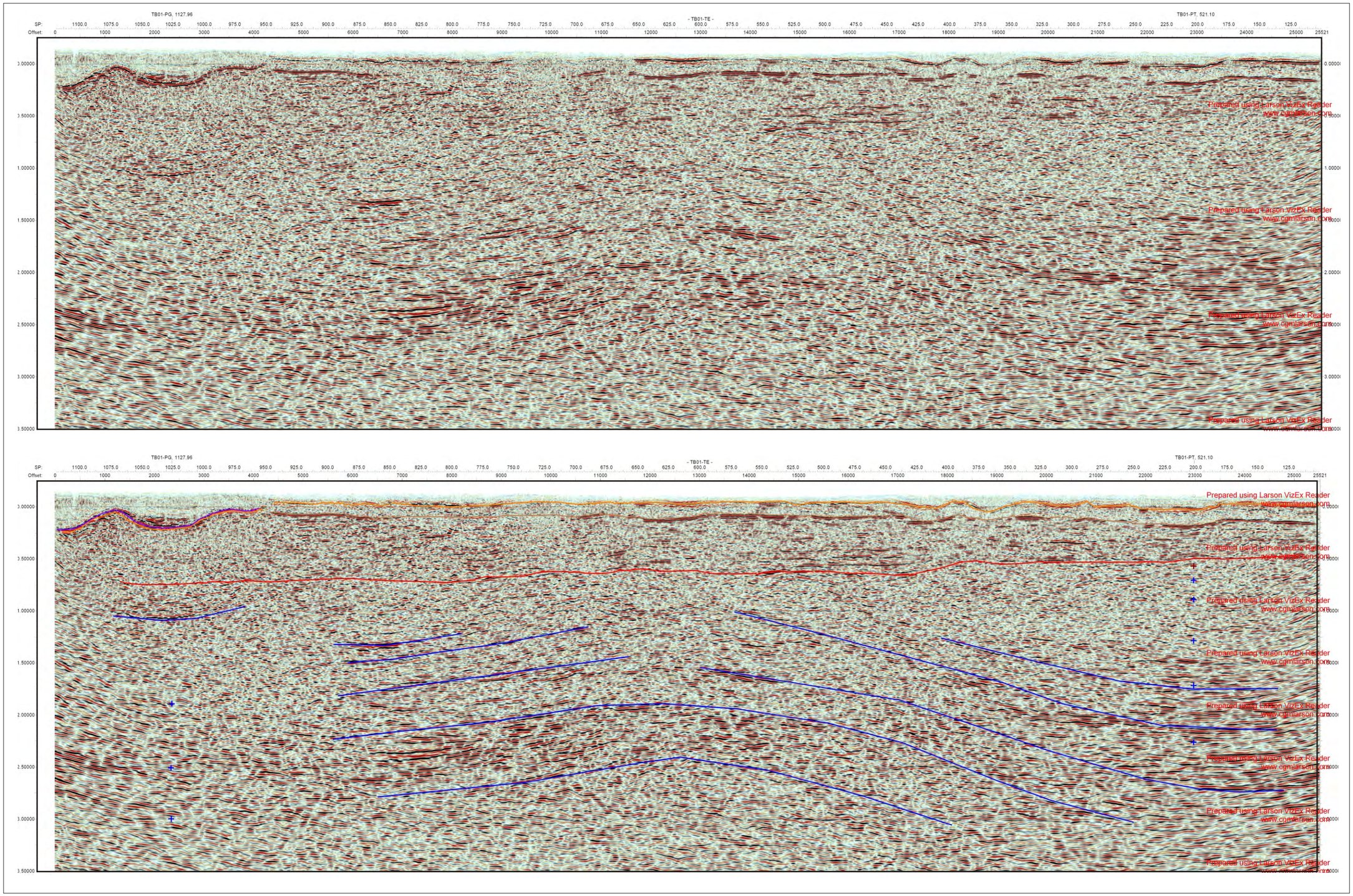

Figure 6.144: Raw and interpreted seismic data from shot-point 1120 to100 (TB01-TE).

The Parmeener Supergroup sequence thickens after shot-point 400 from 1000 to 1200 m thick, and thickens again at shot-point 800 to 1350 m (Figure 6.144). The thickening probably coincides with the dolerite sill cutting up section. Geological mapping indicates quartz sandstone (Unit 2) associated with dolerite at shot-point 200, while between shot-point 500 and 650 volcaniclastic sandstone (Unit 4) from higher in the stratigraphy is associated with dolerite, indicating the a change in the stratigraphic position of the dolerite (Figure 6.143). Between shot-points 400 and 600 the Base Parmeener Unconformity Horizon is picked at the base of strong laterally coherent reflections that truncate underlying dipping reflections (Figure 6.145). The Base Parmeener Unconformity Horizon is picked to the end of the line at the base of the strong laterally coherent reflections, where discernable, and interpolated between the zones where the picks are reliable (Figure 6.144).

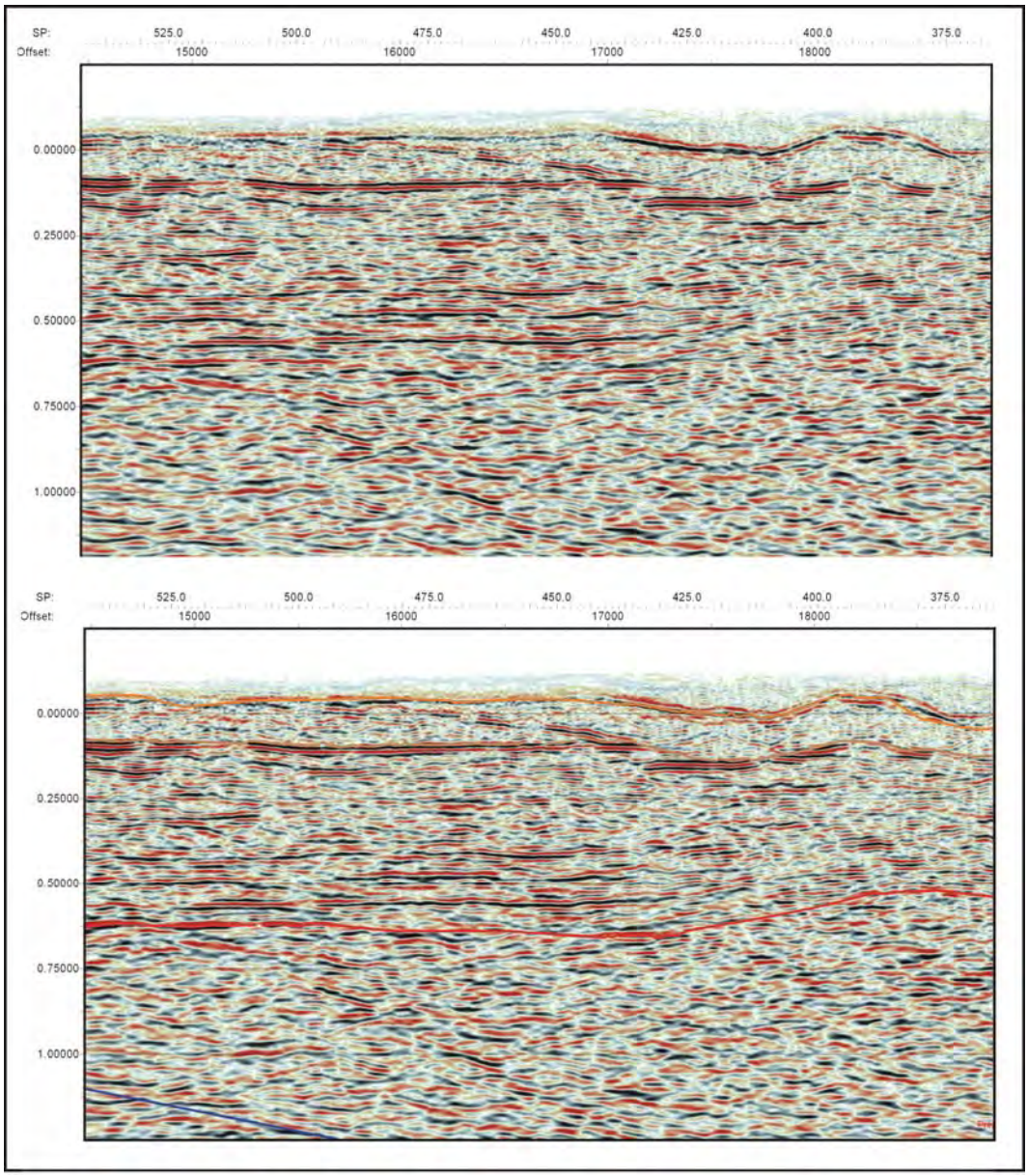

Figure 6.145: Raw and interpreted seismic data between shot-points 550 and 375 showing the Base Parmeener Unconformity Horizon pick (TB01-TE).

At shot-point 950 there is a major change in the interpreted stratigraphy. This occurs at a point where the seismic line changes direction suddenly by 90° (Figure 6.143), no structure is identified associated with this change (Figure 6.144). Beyond shot-point 950, a 500 m thick Tertiary sequence is interpreted overlying the dolerite sill. The interpretation is based on the tie with line TB01-PG, where a thick Tertiary sequence is confidently identified (Figure 6.121). Elsewhere the horizon is picked at the intersection of strong reflections occurring at the base of a zone of very weak incoherent reflections (Figure 6.144).

Basement

The seismic data in the basement section is both coherent and incoherent with varying amplitudes (Figure 6.144). Seismic events in the basement are picked at changes in seismic character. The interpretation shows the basement is folded to form an antiform with a wavelength of 15 km (Figure 6.144). The north-western limb (left) dips shallowly, around 5°, while the south-eastern limb dips at about 10° (Figure 6.144). However, the line is not straight, but rather shallowly concave towards the northeast, with the apex between shot-point 500 and 700 (Figure 6.143), about the same position as the crest of the structure in the section (Figure 6.144). The structure observed here is probably an artefact of the change in direction.

CHAPTER 7
SEISMIC INTERPRETATION – RESULTS

7.1: STRATIGRAPHY

Numerous workers have described the rocks of the Tasmania Basin as "generally flat-lying". The interpretation of the seismic data confirms that the Tasmania Basin strata are flat lying across the survey area. The exception is the part of the survey covering in the Longford Sub-basin, where half-graben formation has resulted in tilting of the Parmeener Supergroup (Figure 7.1). The Tertiary section in the Longford Sub-basin section was not interpreted beyond its top and base. Other interpreters have recognised inversion in this sequence from the seismic data (Blackburn, 2004). Structures resulting from inversion of the Tertiary sequence are recognised from the DEM draped with the 1:250 000 scale geology.

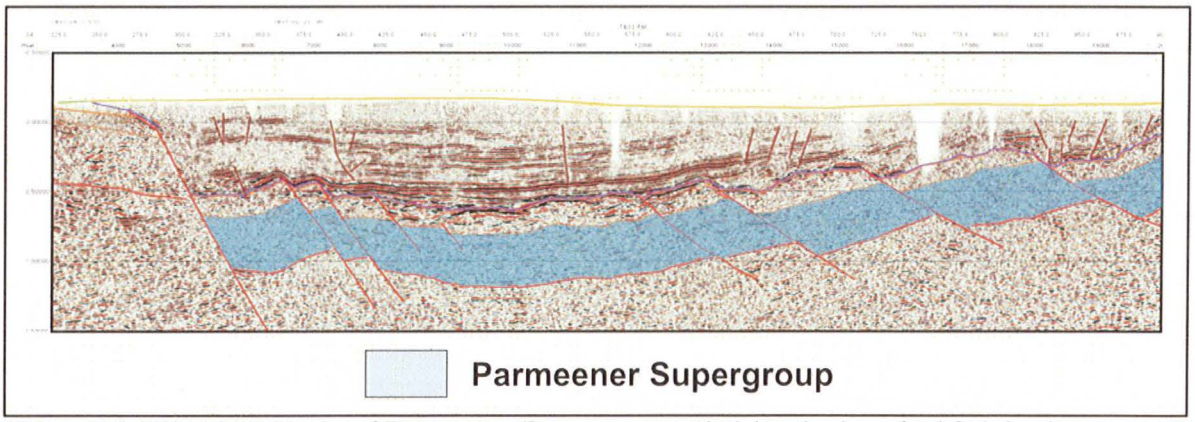

Figure 7.1: Tilted fault blocks of Parmeener Supergroup underlying the Longford Sub-basin (TB01-PM).

7.2: STRUCTURE

7.2.1: Tasmania Basin and Longford Sub-basin

Faults

Distribution

Numerous faults of varying size, timing and importance are interpreted throughout the survey area. Figure 7.2 shows the type, distribution and, where possible, the strike of the major faults that have been recognised.

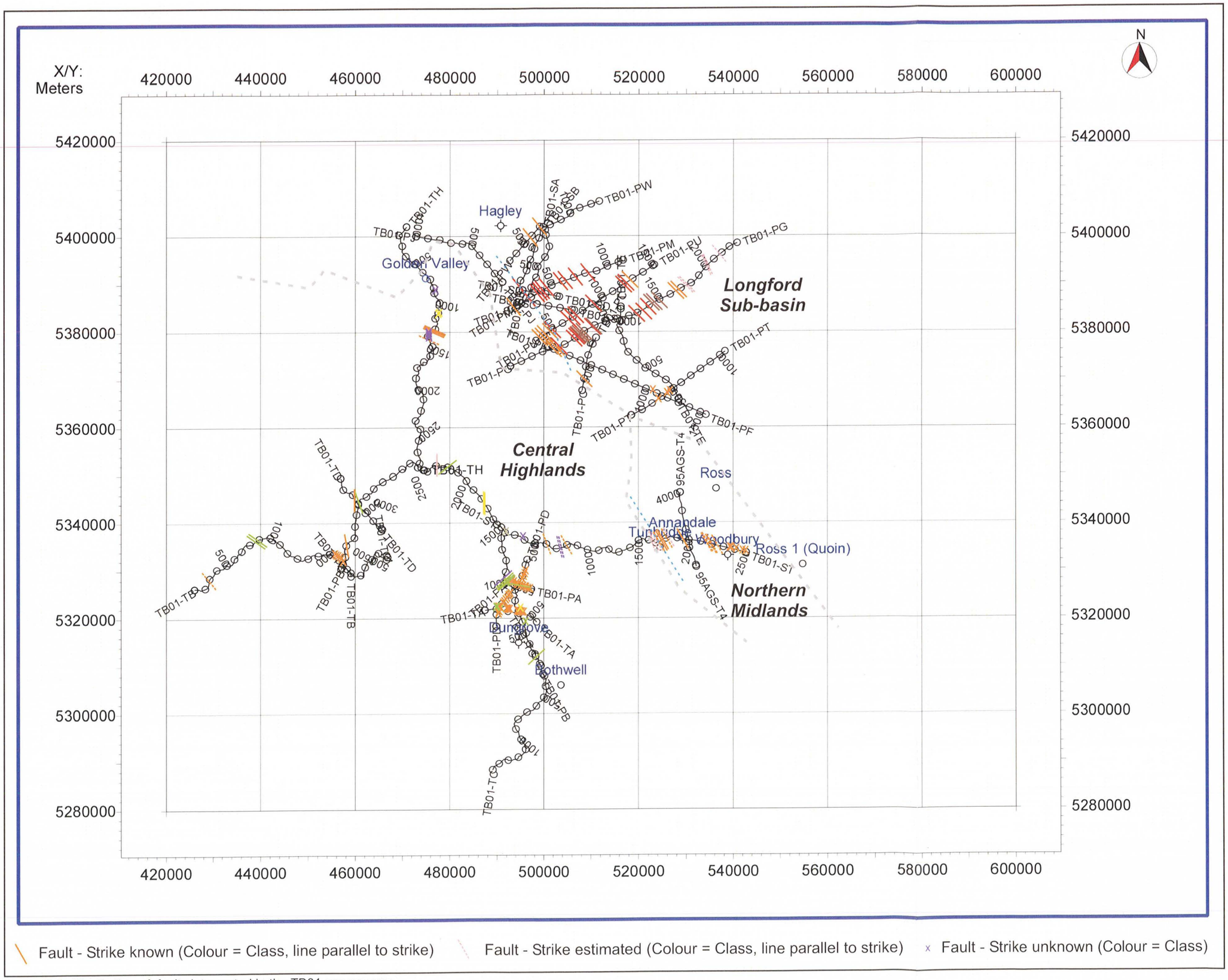

Fault - Strike known (Colour = Class, line parallel to strike) Fault - Strike estimated (Colour = Class, line parallel to strike) x Fault - Strike unknown (Colour = Class)

Figure 7.2: Distribution of faults interpreted in the TB01 survey area.

The strike of faults where mapped, or where indicated with certainty by geologic boundaries or topography are shown on the map by a strike-parallel solid line. Where there is some doubt regarding strike, faults are indicated by dashed lines (Figure 7.2). Many of the faults are blind and lack significant topographic expression or other evidence to indicate their strike. These faults are indicated on the figure with an "x" (Figure 7.2).

The Fault Map clearly indicates a significant difference in the density, distribution and age of faulting in the Longford Sub-basin/Northern Midlands regions compared to the Central Highlands. The major faults in the Longford Sub-basin/Northern Midlands region are overwhelmingly Tertiary in age and all strike towards the northwest (315° to 320° in the Longford Sub-basin, 330° in the Northern Midlands). In the Longford Sub-basin the faults with large throws are all down towards the northeast, forming a series of southwest dipping half-graben. In the Northern Midlands faults are mostly down towards the east, but throws are less and the faults are steeper. There is also a distinctive strike-slip component to several faults in the Northern Midlands. The interpretation indicates extension was less in the Northern Midlands.

All of the defined fault classes (see Chapter 5, Section 5.5.6) are represented in the Central Highlands region. The overall density of faulting is considerably less than that observed in the Longford Sub-basin/Northern Midlands region, with faults concentrated mainly around windows in the outcropping dolerite and to a lesser extent at the margins of the Highlands region (Figure 7.2). While the strike of many faults identified from the seismic interpretation cannot be determined, where it can, faults of all classes mainly strike between west-northwest and north (Figure 7.3). On TB01-TH, faults between shot-points 1000 and 1500 strike northwest. Outcropping basement structures 15 km to the north have a similar strike (see Figure 6.97), suggesting a strong basement control on faulting. A group of north-easterly striking faults are concentrated at the northern boundary of the dolerite "window" near Hunterston. These are interpreted as pre-Jurassic and control the contact between the Parmeener Supergroup and the dolerite in this location.

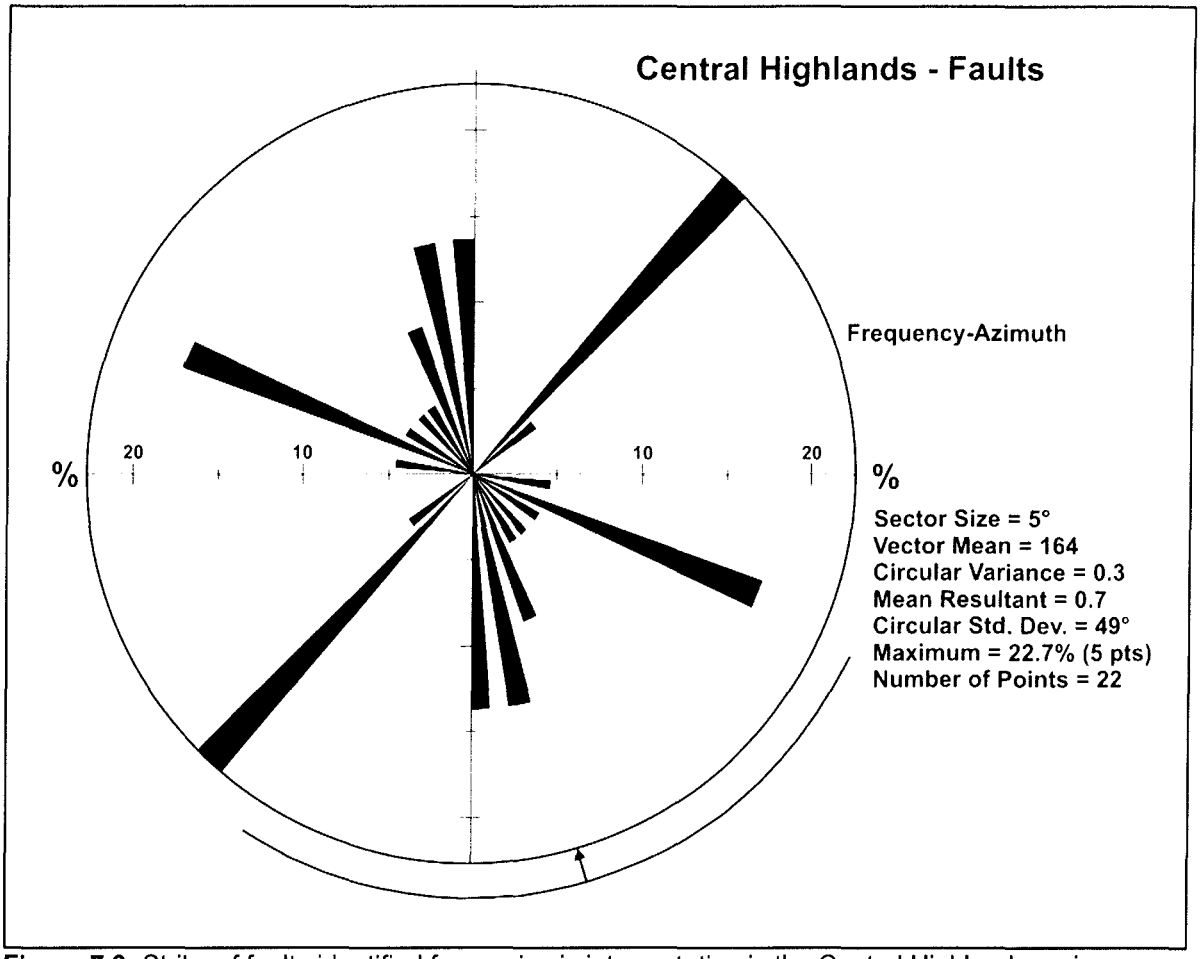

Figure 7.3: Strike of faults identified from seismic interpretation in the Central Highlands region.

History of Generation

Faults are divided into classes based on their latest movement with respect to the Middle Jurassic Dolerite intrusions. Faults that occurred after the intrusion of dolerite (Post-Jurassic Faults) are subdivided into Later Tertiary, Early Tertiary and Undifferentiated Tertiary Faults. These faults are thought to result from latest Cretaceous to early Tertiary uplift and extension and subsequent late Tertiary compression. Four classes of Pre-Jurassic Fault are recorded, based on the offset (normal or reverse) and whether or not they were intruded by dolerite. For a large number of faults there is insufficient evidence to allow a reliable interpretation of their timing with respect to dolerite intrusion, these were classed as indeterminate.

Early Tertiary faults have a clear association with early Tertiary deposition i.e. they usually display growth (Figure 7.4). This association is not observed for the Later Tertiary faults, which generally displace the Tertiary Sequence. Tertiary aged normal faults are likely to have resulted from east-northeast directed extension in the latest Cretaceous and early Tertiary, while subsequent inversion, was probably due to Mio-Pliocene compression.

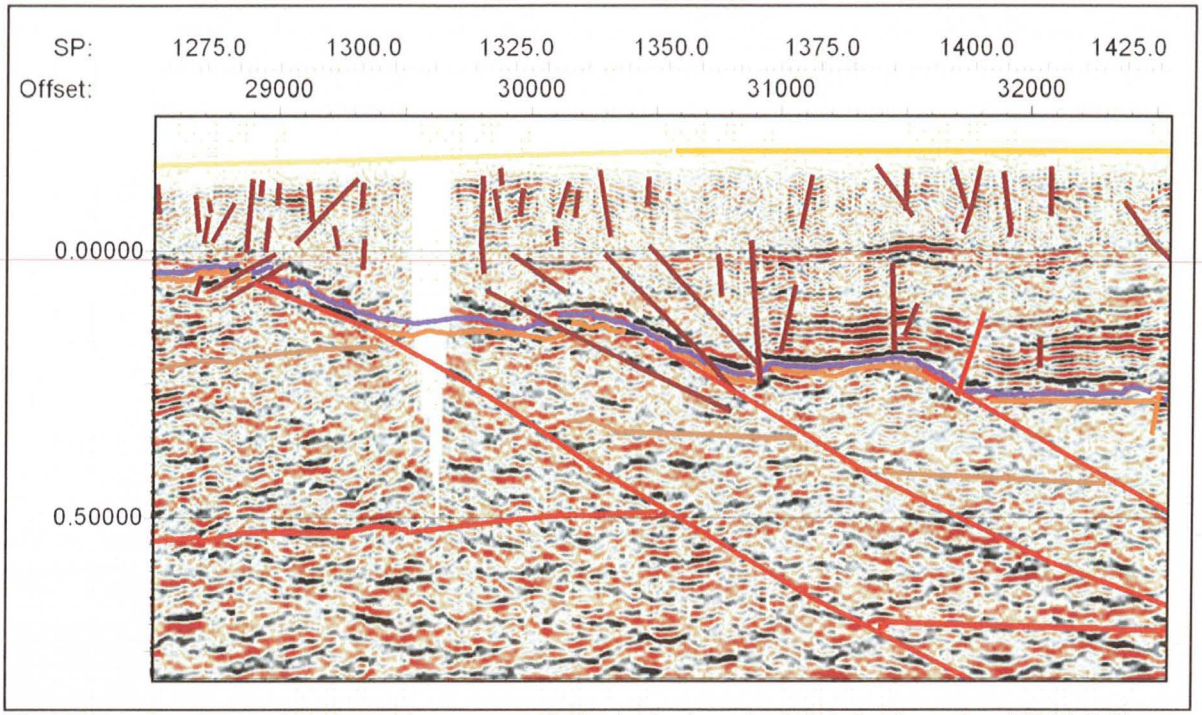

Figure 7.4: Examples of early Tertiary growth faults in the Longford Sub-basin region (TB01-PG).

Many of the Tertiary aged faults may result from the reactivation of existing basement faults, and the most compelling evidence for this interpretation is observed in the Longford Sub-basin/Northern Midlands region. Evidence can be seen in geological maps north of the Longford Sub-basin in the Dazzler Range region (Figure 7.5). Here the strike of northeast dipping normal faults in Permian strata corresponds with that of northeast dipping thrust faults in the basement. This orientation also corresponds to the strike and dip of major faults in the Longford Sub-basin (Figure 7.2). Evidence is not as clear in the seismic sections, due to the generally poor reflections from the basement. However, evidence derived from the DEM indicates extension is concentrated in this area and many Tertiary faults in Longford Sub-basin/Northern Midlands regions are interpreted above strong basement events (Figure 7.6). It is highly likely that the geometry observed in the northwest continues along strike south-eastward and that extension reactivated the Devonian thrusts to form half-graben.

Many faults classed as pre-Jurassic are either truncated by or have been intruded by Jurassic dolerite sills, and were therefore active either pre- or syn-intrusion of dolerite. Pre-Jurassic Faults are more common in the Central Highlands, with normal faults being far more numerous than reverse faults. The throw of the reverse faults is only 10's of metres. Reactivation of these faults by Tertiary extension may disguise their early history.

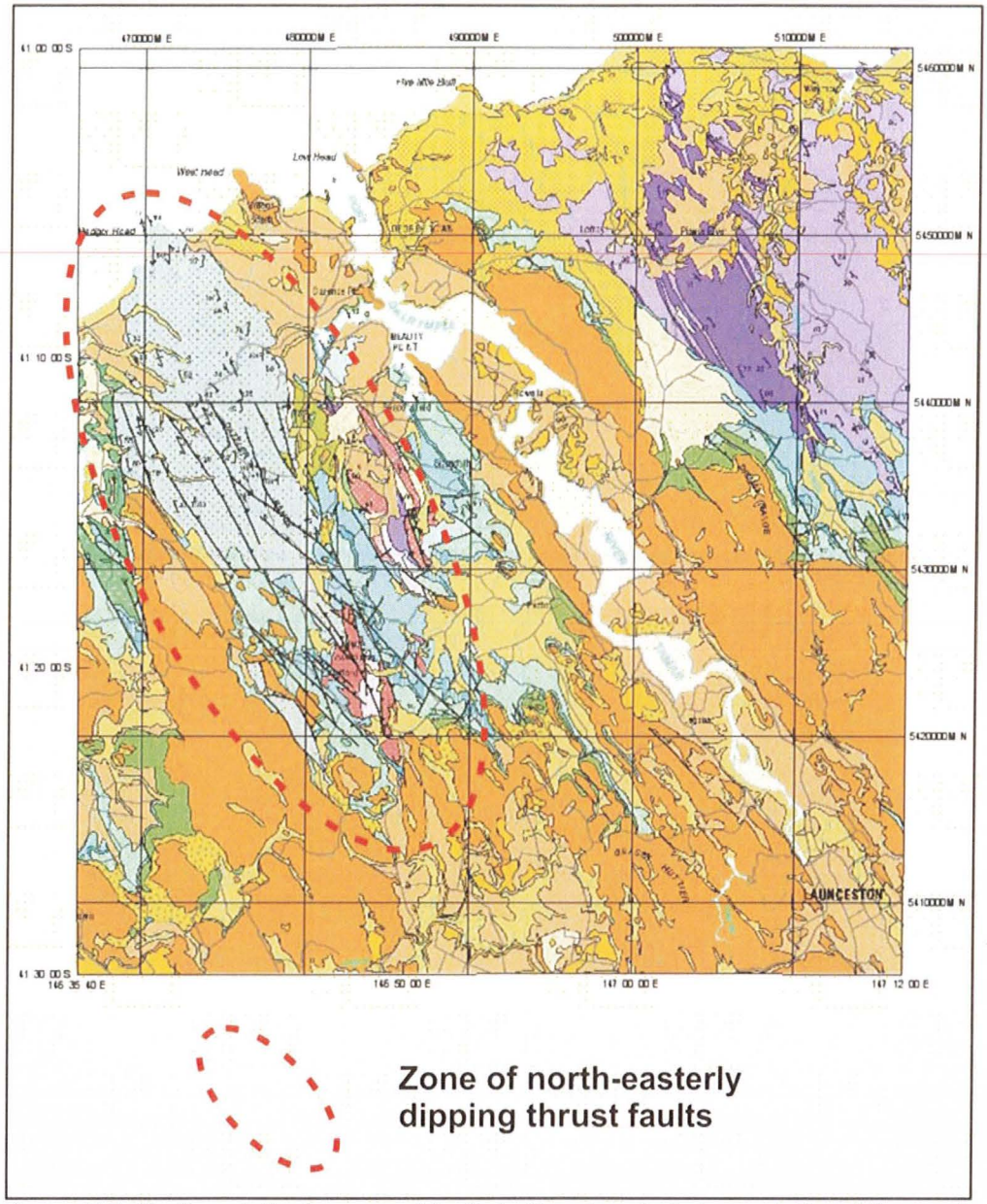

Figure 7.5: Northeast dipping normal faults in Permian strata have similar strikes and often connect to northeast dipping thrust faults in the basement.
(Modified from McClenaghan and Calver, 1994)

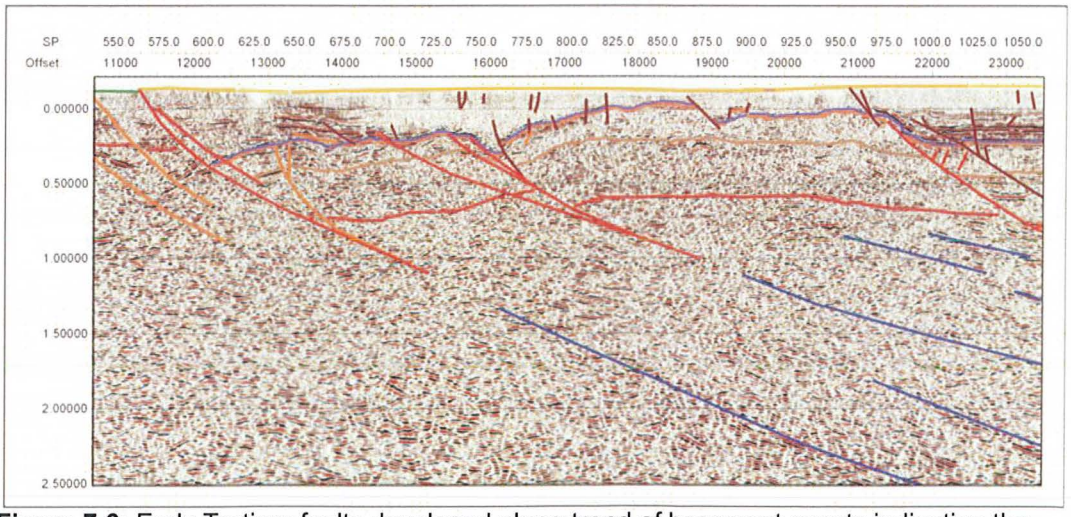

Figure 7.6: Early Tertiary faults developed along trend of basement events indicating the reactivation of basement structures probably resulted in the development of the early Tertiary structures (TB01-PG).

Folds

Type and Distribution

Folding of the Parmeener Supergroup is observed across the survey area, while rare folds are seen in the Tertiary sequences of the Longford Sub-basin. Horizontal, upright, gentle folds are visible across the survey area forming numerous anticlines and synclines (Figure 7.7). The age of these folds was determined by whether they affect the dolerite sills, i.e. folding of the dolerite sill with Parmeener Supergroup strata indicates the fold probably formed post-Jurassic. However, for gentle folds this is not certain as a sill might still follow the bedding. The majority of folds recognised in the Central Highlands region were formed prior to the intrusion of dolerite, while folds in the Longford Sub-basin were formed post-dolerite (Figure 7.7).

Gentle folds are mainly recognised in the Central Highlands region. These are characterised by long wavelengths and low amplitudes with both with symmetrical and asymmetrical folds observed (Figure 7.8). These structures are defined by a single seismic line. In section, these folds are on average 4200 m long, with amplitudes of 180 m. While some of these folds are reliably defined by strong reflectors, several are dubious, occurring in zones of poor data or in areas where processing and/or surface conditions may act to "pull up" or "push down" the seismic reflections.

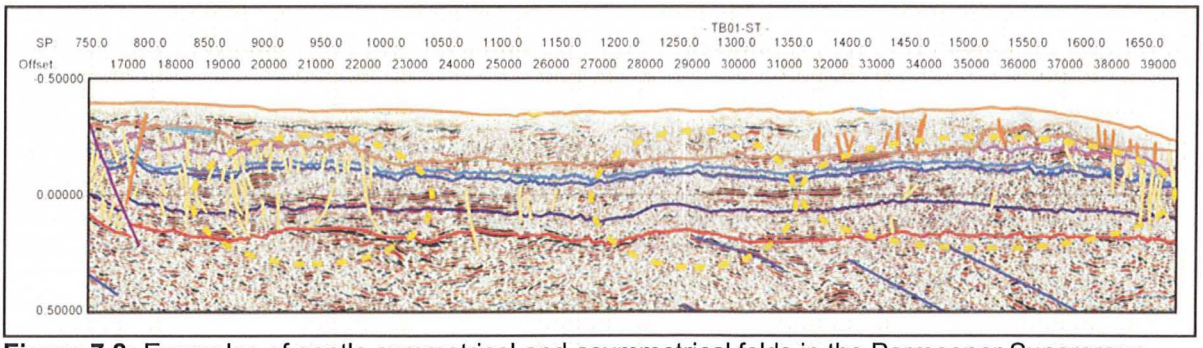

Figure 7.8: Examples of gentle symmetrical and asymmetrical folds in the Parmeener Supergroup (TB01-ST).

Several small, fault related folds are observed widely distributed across the Central Highlands region (Figure 7.7). The folds mainly result from reverse drag in the footwall of steep Pre-Jurassic reverse faults with small throws (Figure 7.9). The reason for this association is not clear. These structures are not the result of Mio-Pliocene inversion as the faults are mostly truncated by, and do not affect dolerite sills. They may result from strike-slip movement. These structures are mainly interpreted in zone where the seismic data is not coherent and may be processing artefacts.

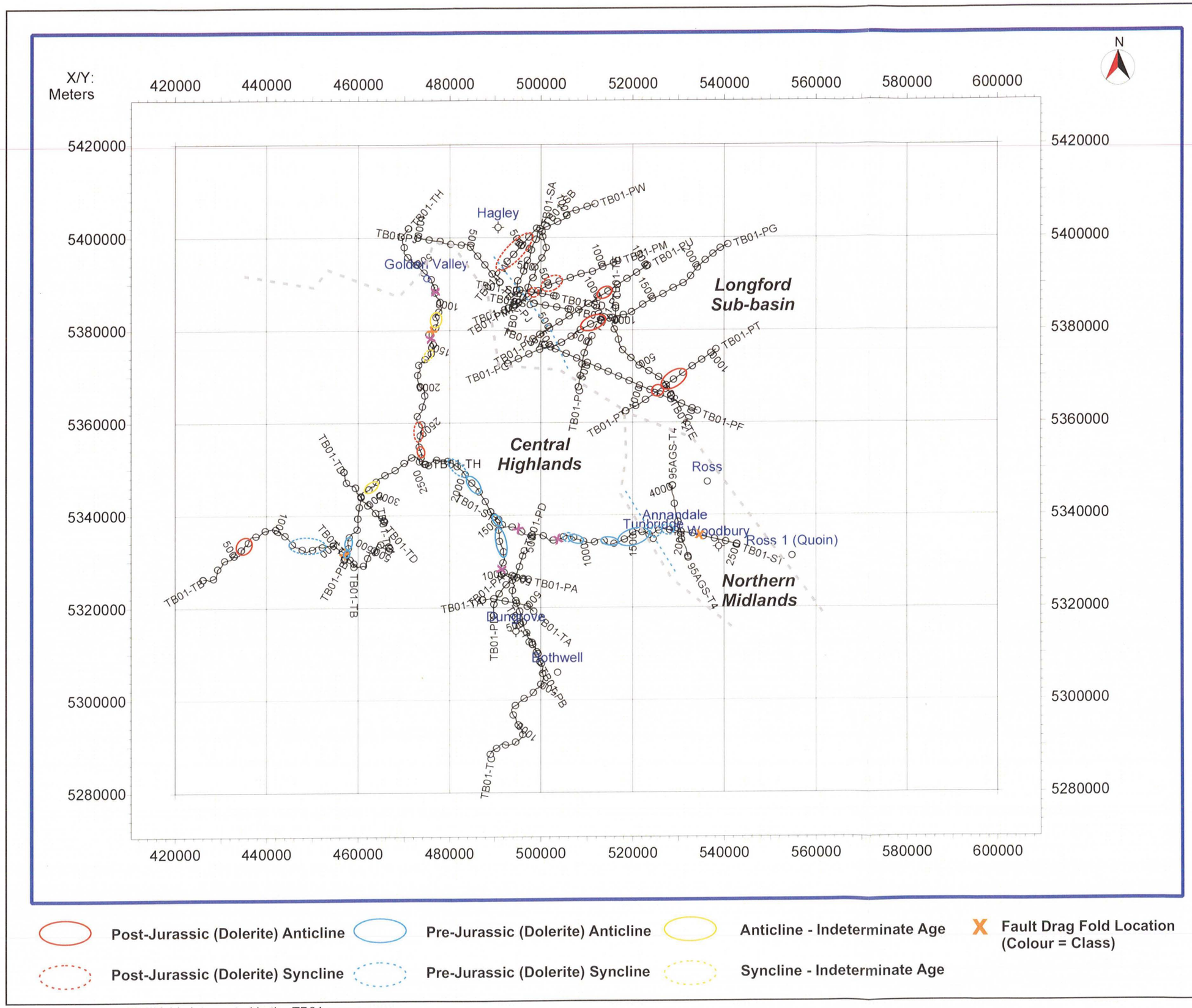

Figure 7.7: Distribution of folds interpreted in the TB01 survey area.

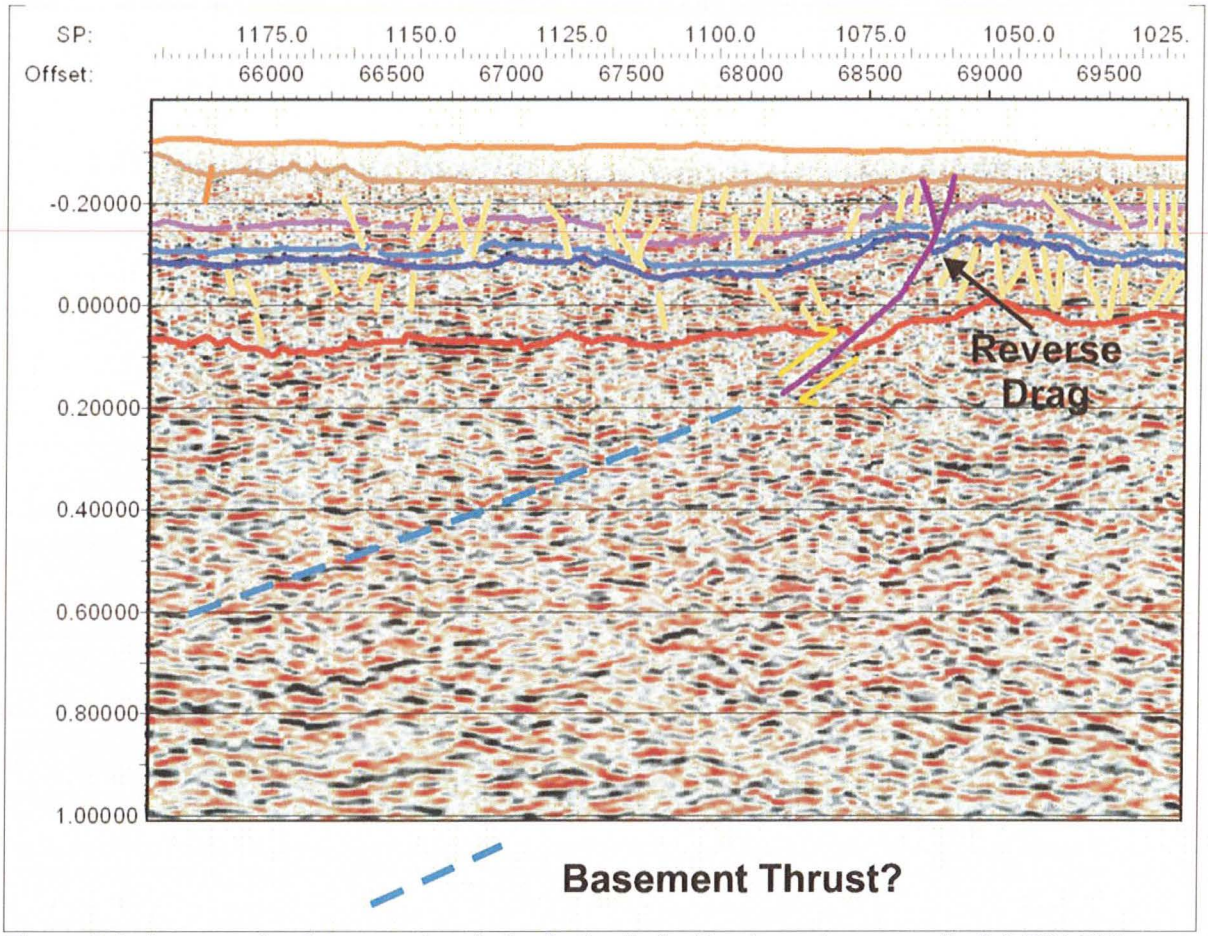

Figure 7.9: An example of reverse drag in the footwall of a Pre-Jurassic reverse fault (TB01-PB).

In the Longford Sub-basin, major folds affecting the Parmeener Supergroup are rare. The major structures recognised are rollover anticlines (reverse drag fold) on TB01-PU and PG, a footwall fold drag fold on TB01-PG, and hanging wall synclines on lines on lines TB01-PW and TB01-PM (Figure 7.7) The rollover anticline on TB01-PU is interpreted from the curvature of the Base Dolerite and Base Parmeener Unconformity horizons (Figure 710). Reflectors in the Tertiary sequence (above the purple line) onlap the dolerite sill indicating folding took place prior to Tertiary deposition. On line TB01-PG the fault drag fold is recognised in the footwall from the Base Dolerite and Base Parmeener Unconformity horizons (Figure 7.11).

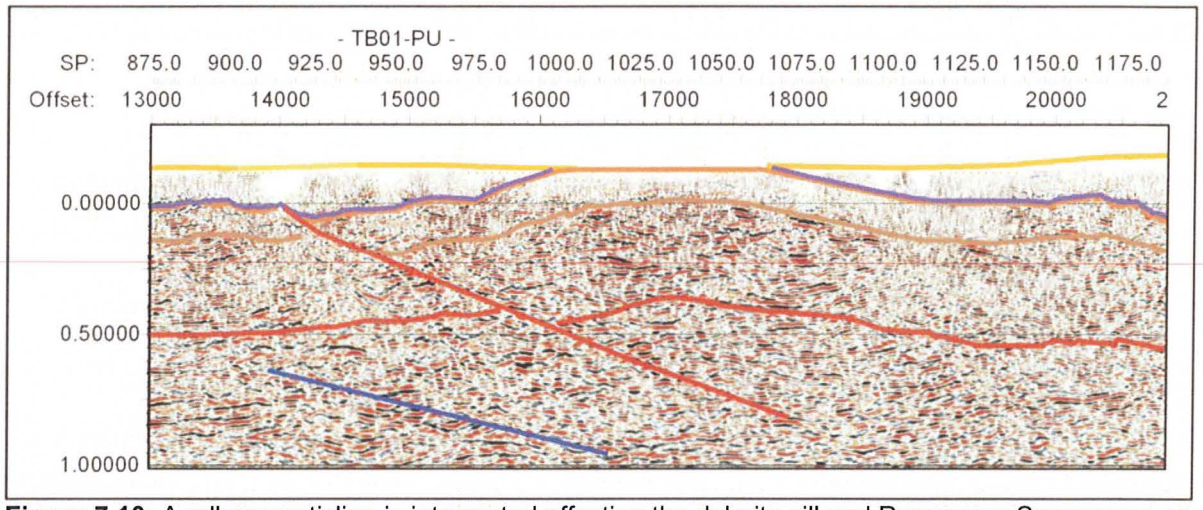

Figure 7.10: A rollover anticline is interpreted affecting the dolerite sill and Parmeener Supergroup on TB01-PU.

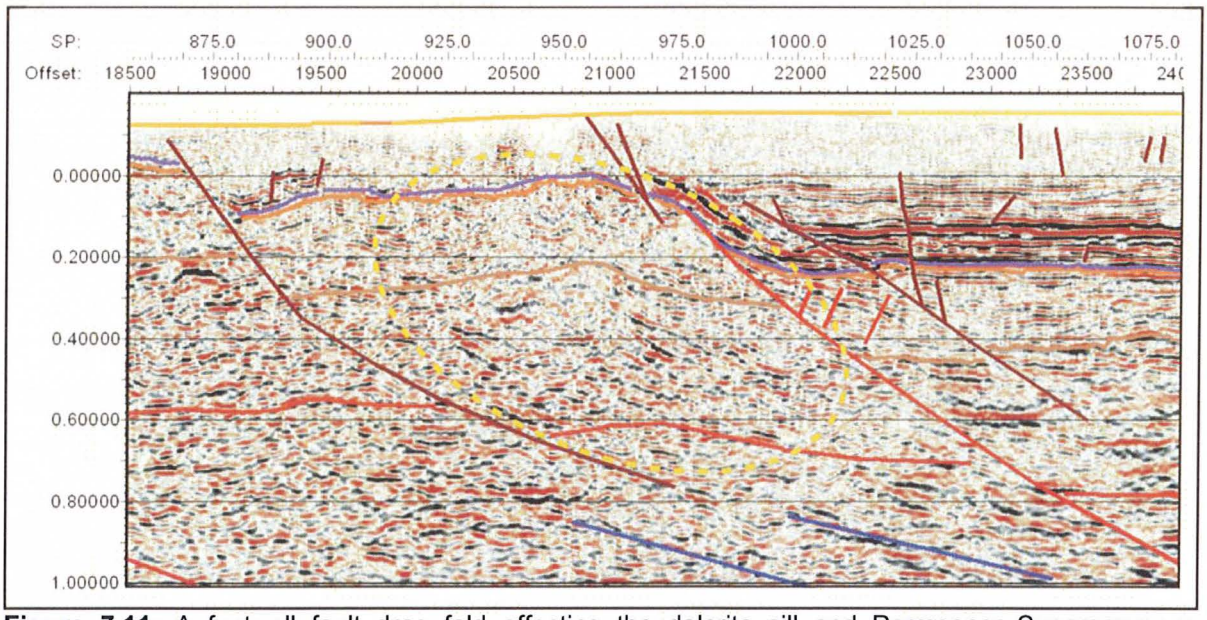

Figure 7.11: A footwall fault drag fold affecting the dolerite sill and Parmeener Supergroup on TB01-PG.

Significant structures in the Tertiary sequence of the Longford Sub-basin are very rare. A gentle anticline, known as the Bracknell Dome is recognised on TB01-PM (Lane, 2002) (Figure 7.12). This structure probably results from inversion of early Tertiary faults during the Mio-Pliocene. Evidence for inversion is shown on Figure 7.12, where small drape folds are easily distinguished by strong reflectors over the two, closely spaced faults between shot-points 350 and 400.

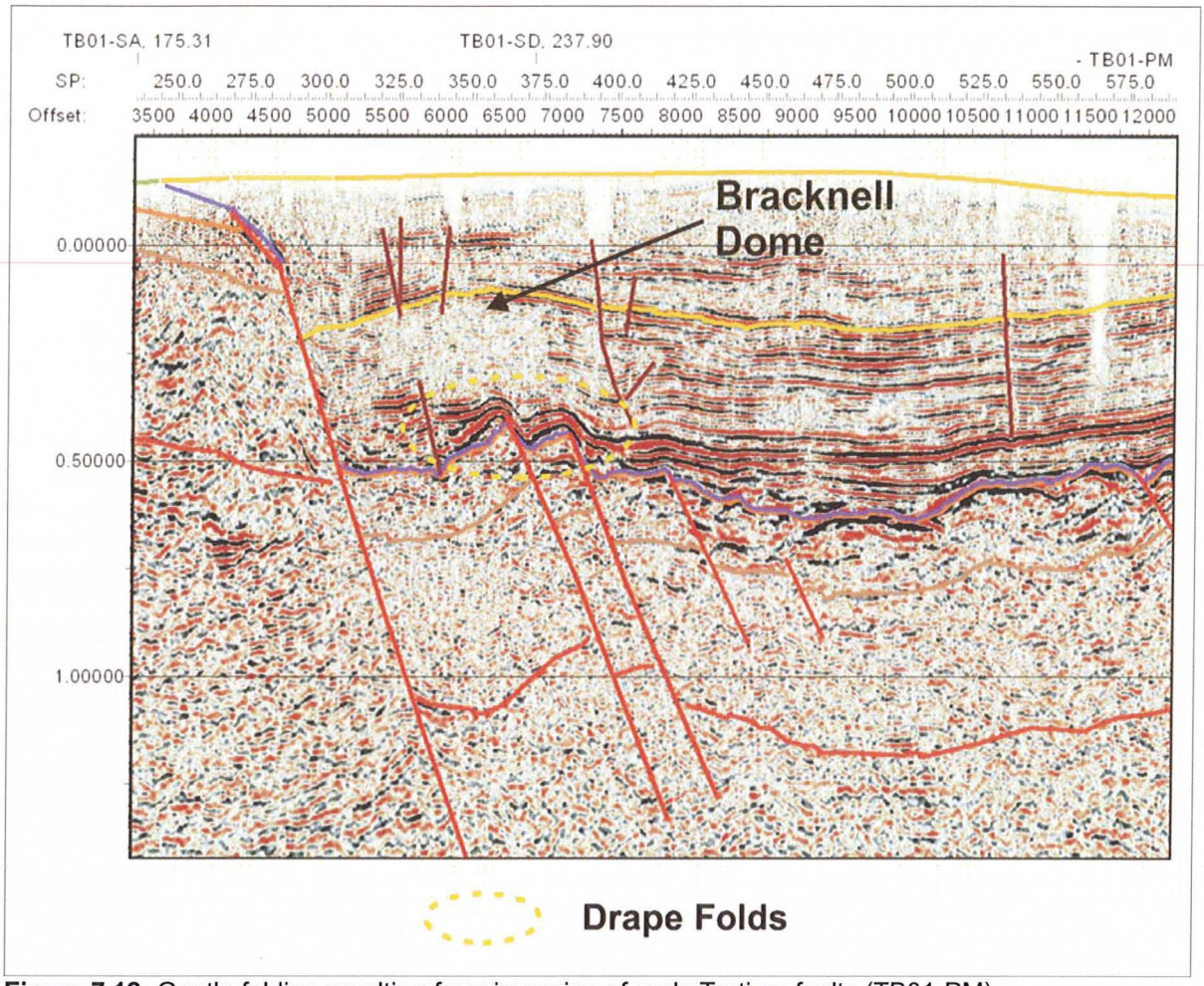

Figure 7.12: Gentle folding resulting from inversion of early Tertiary faults (TB01-PM).

7.2.2: Basement

Structural Domains

Beneath the Longford Sub-Basin/Northern Midlands region reflectors dip towards the northeast soling out at about 3 to 3.5 seconds TWT (Figure 7.10). No folding is interpreted in this region and the stacked reflectors observed in the seismic data are interpreted as thrusts, this structural style is similar to a series of anastomosing north-easterly dipping thrust faults observed in outcropping Neoproterozoic basement to the north in the Dazzler Range (Figure 7.5).

Inboard of the margins of the Central Highlands region, on lines TB01-ST and TH the seismic character differs from that observed in the Longford Sub-basin/Northern Midlands region (Figure 7.13). The data is less coherent and fewer long straight features are distinguishable, folding (reflectors rolling over) becomes more apparent (Figure 7.13). Seismic data at the southern end of line TB01-TH and the central portion of TB01-PB is generally poor and little of the structural form in the basement is distinguishable. Further west, at the end of line TB01-PB and on line TB01-TB (Figure 7.13), a series of anticlines and synclines are

recognised. The Bellevue Anticline on TB01-PB, plunges towards the northwest. This structure is similar in scale and orientation to a north-north-westerly plunging syncline mapped in the Florentine Valley 50 km to the south-southwest (Figure 7.14).

Seismic data indicates the presence of three, relatively distinct structural domains in the basement. These consist of a series of easterly dipping thrust stacks beneath the Longford Sub-basin/Northern Midlands region. The large faults affecting the Parmeener Supergroup and Tertiary sequences were probably produced by reactivation of these thrusts during extension. Beneath the Central Highlands lies a mix of folds and thrusts, while further to the west the basement becomes more fold dominated. Thrusts and minor folding are prevalent about the margins of the region, while large folds are recognised in the southwest of the survey area (Figure 7.13).

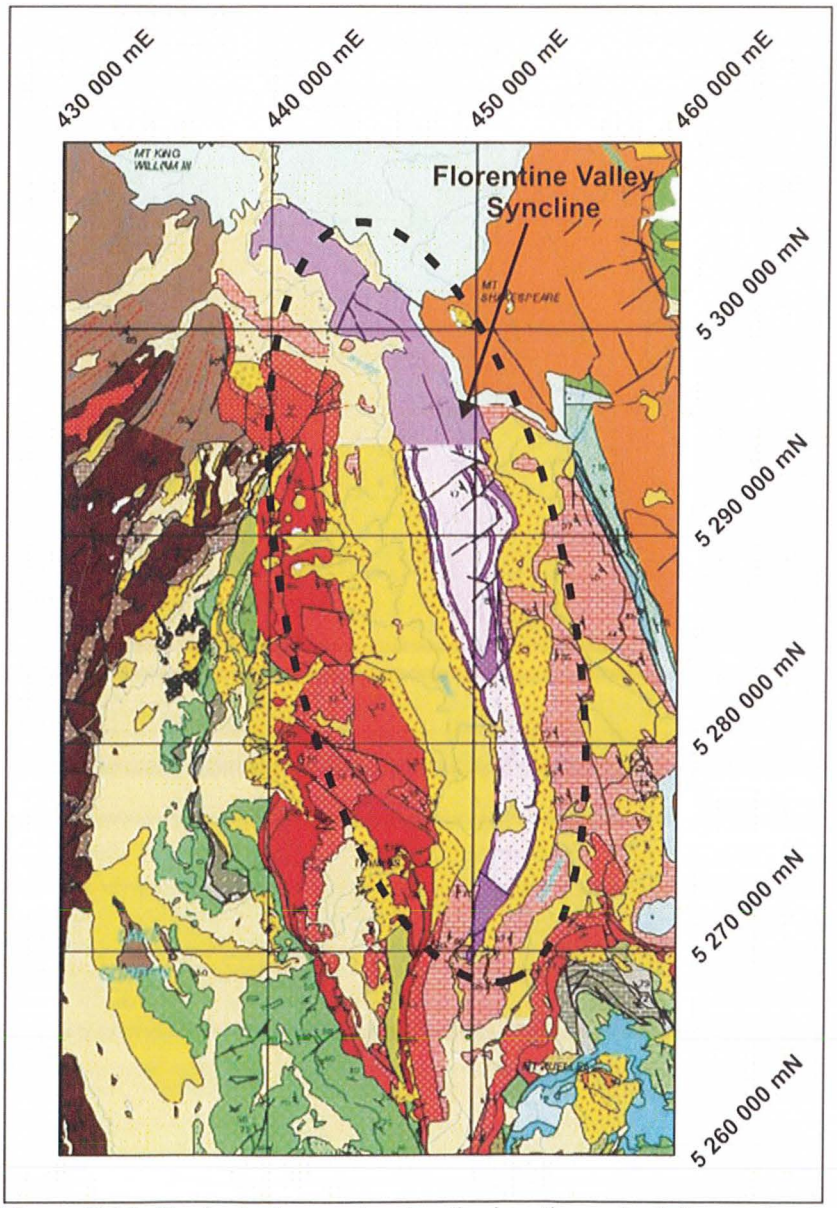

Figure 7.14: Geological map showing the location, orientation and extent of the Florentine Valley Syncline. *(Modified from Brown et al., 1995)*

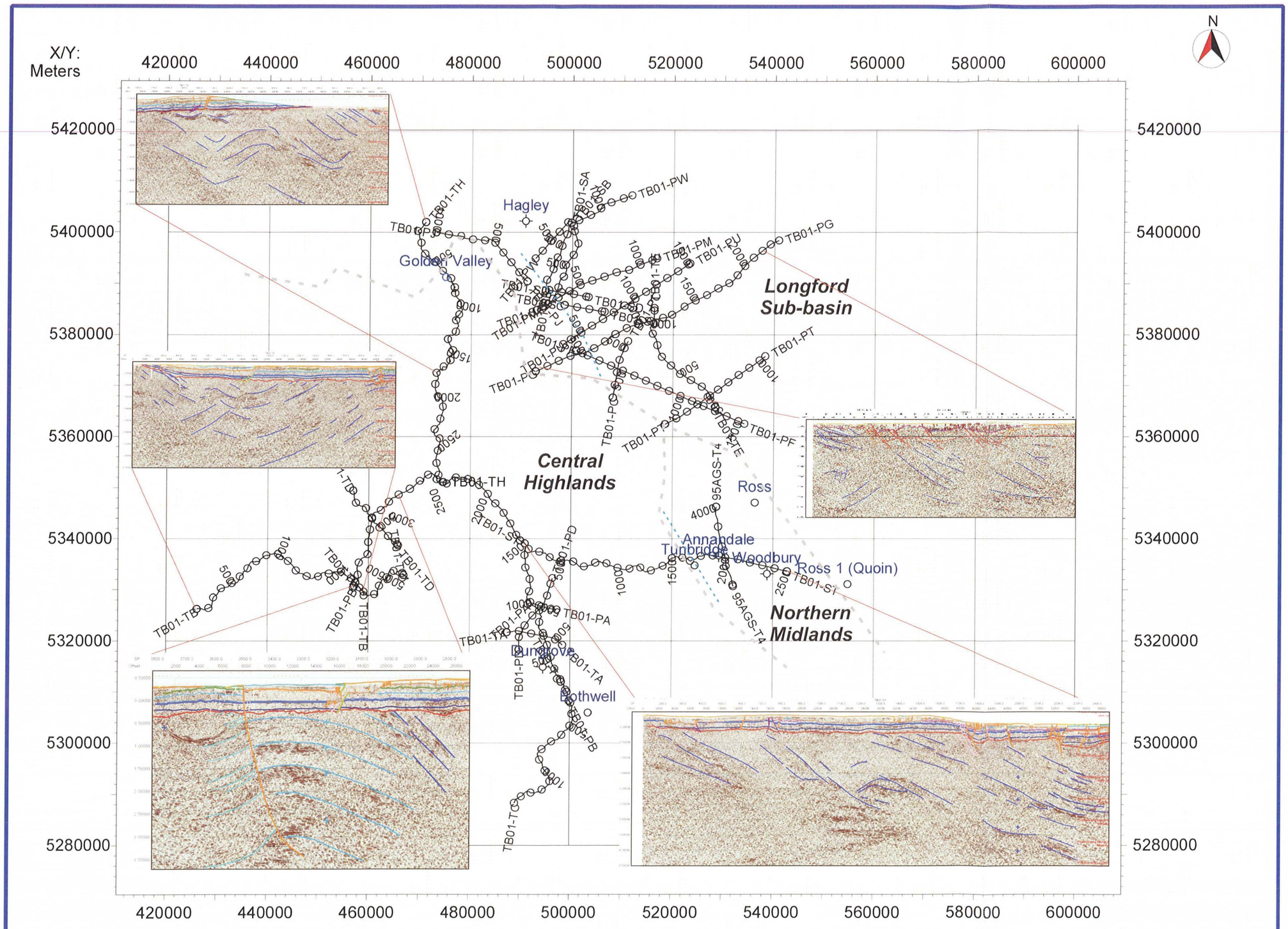

Figure 7.13: Structural style of the basement at several locations across the TB01 survey area.

7.3: BASIN GEOMETRY

7.3.1: Longford Sub-basin

The Longford Sub-basin is a major depocentre within the Launceston Tertiary Basin (Figure 7.15). Previous work on the 100 x 30 km depocentre defined its gross geometry as two half-graben separated by a central horst (Hinch, 1965, Longman, 1966, Longman and Leaman, 1971, Mathews, 1983). Detailed modelling by Direen (1995) interpreted a basin composed of a series of half-graben downthrown to the east, compartmentalised by northeast striking faults and divided by a central horst at Hummocky Hills. This model is supported by Lane (2002), based on interpretation of seismic data.

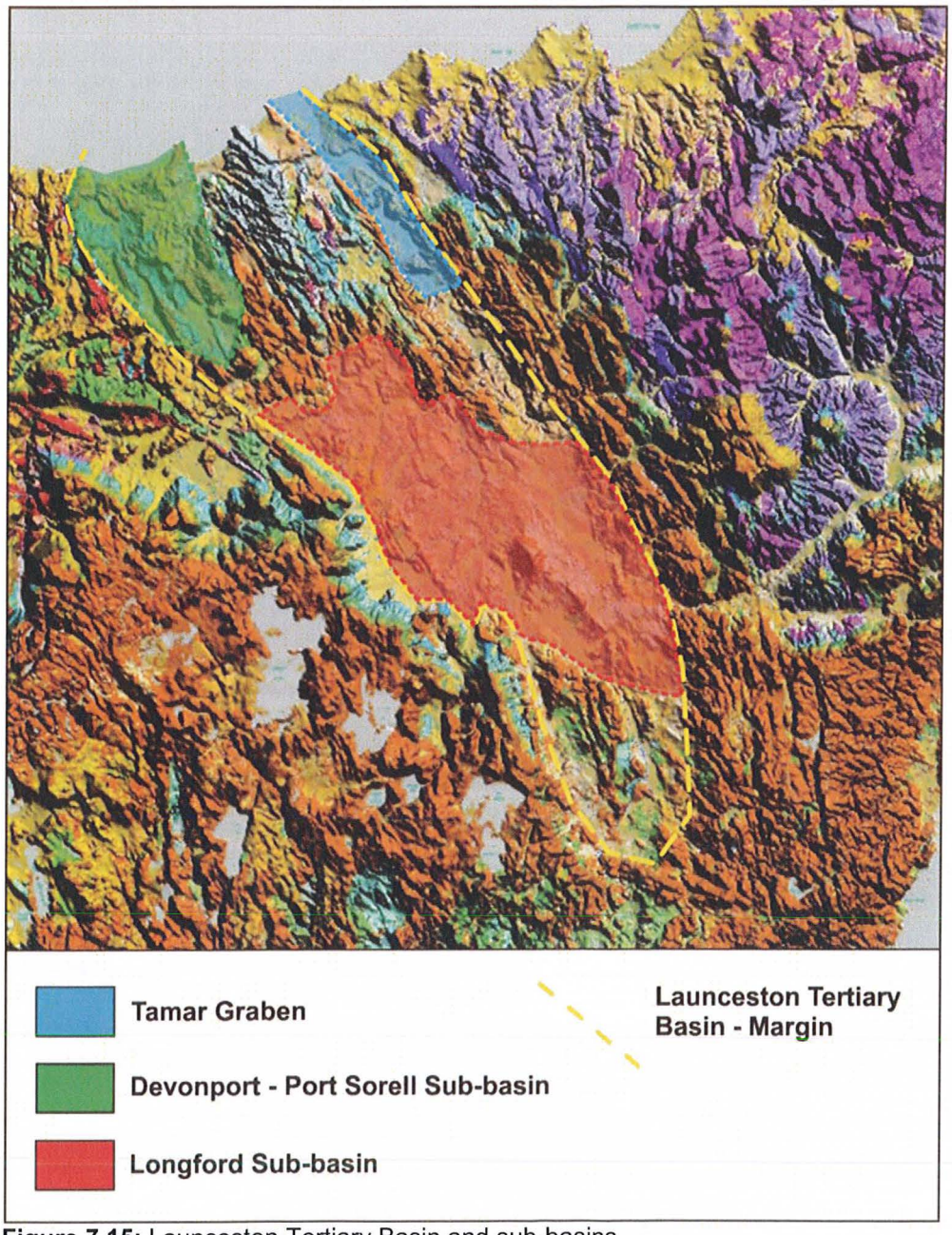

Figure 7.15: Launceston Tertiary Basin and sub-basins.

Gravity data acquired in the survey area compares well with the Base Tertiary TWT Structure map, both images show the thickness of the Tertiary sequence and the general structure of the basin. Both the gravity image and TWT Structure map clearly show the sharp, northwest striking boundary of the Tertiary sequence (Figure 7.16). This boundary is formed by the Tiers Fault System. The deepest part of the basin lies adjacent to this fault system (Figure 7.16). Both datasets indicate the thickness of the Tertiary sequence along this boundary decreases towards the southeast, from 1125 m on TB01-PW to 750 m on TB01-PG, and becoming very thin (225 m) in the southeast of the survey area (Figure 7.16). The thickness of the Tertiary sequence also decreases steadily towards the northeast while in the south there is rapid thinning of the sequence in the vicinity of line TB01-PT (Figure 7.16).

The geometry in the north of the basin appears relatively simple. Illustrated by seismic lines TB01-PW and PM, which contain a single half-graben. The Tertiary sequence is approximately 1000 m thick adjacent to the Tiers Fault System and thins towards the northeast (Figure 7.17). Farther south, lines TB01-PU and PG illustrate a geometry consisting of two half-graben separated by a basement high of folded Parmeener Supergroup (Figure 7.17), not a symmetrical central horst as indicated by previous studies. Furthermore, the high trends towards the southwest rather than north along the basin axis from Hummocky Hills (Figure 7.17). The south-westerly trend is anomalous, when most other structures are parallel to the basin axis and may result from offset by a northeast striking transfer fault. Direen (1995) interpreted a series of northeast striking transfer faults compartmentalising the basin and the fault interpreted here corresponds to his Billop Fault.

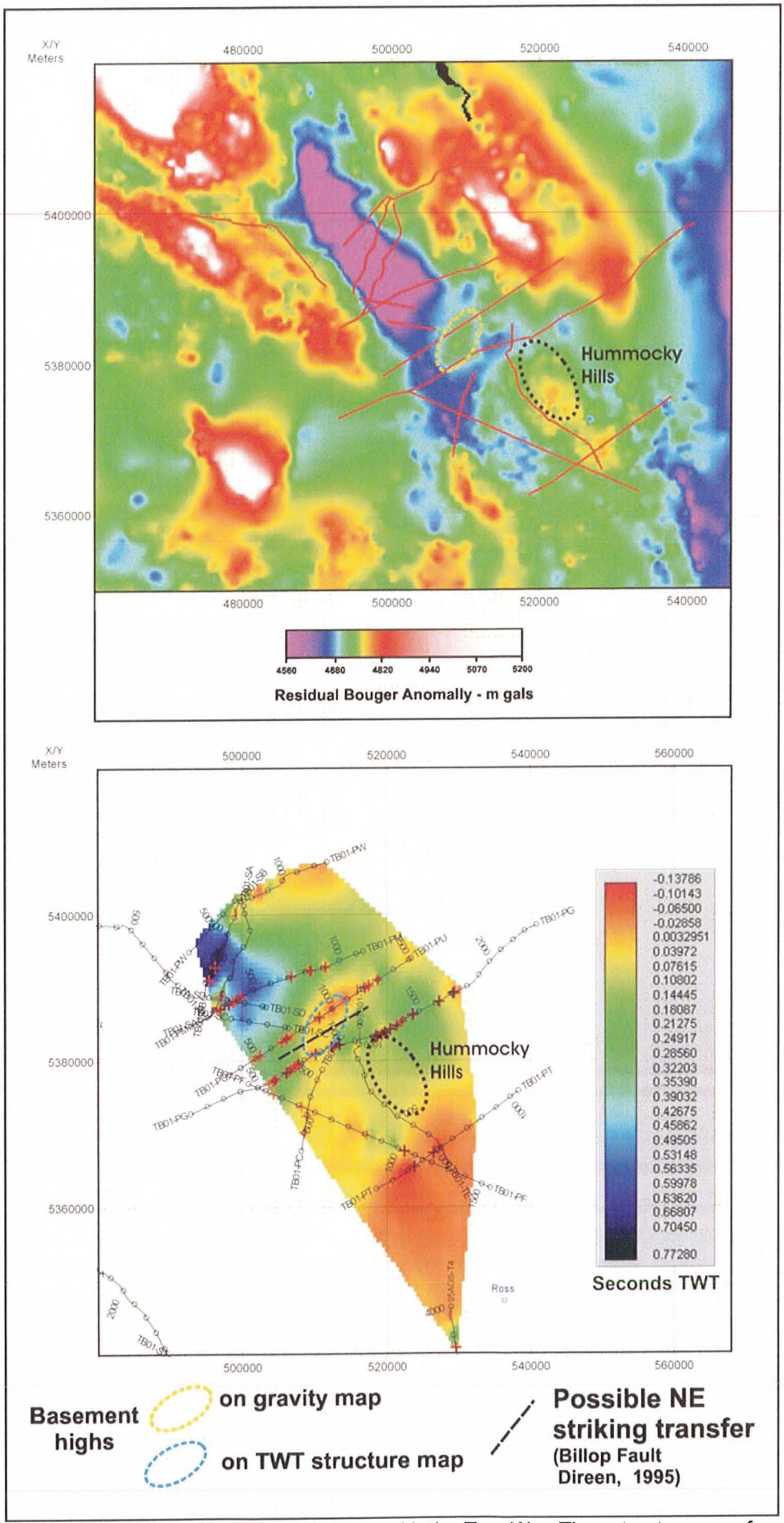

Figure 7.16: Comparison of gravity data with the Two-Way-Time structure map for the Base Tertiary Unconformity Horizon.

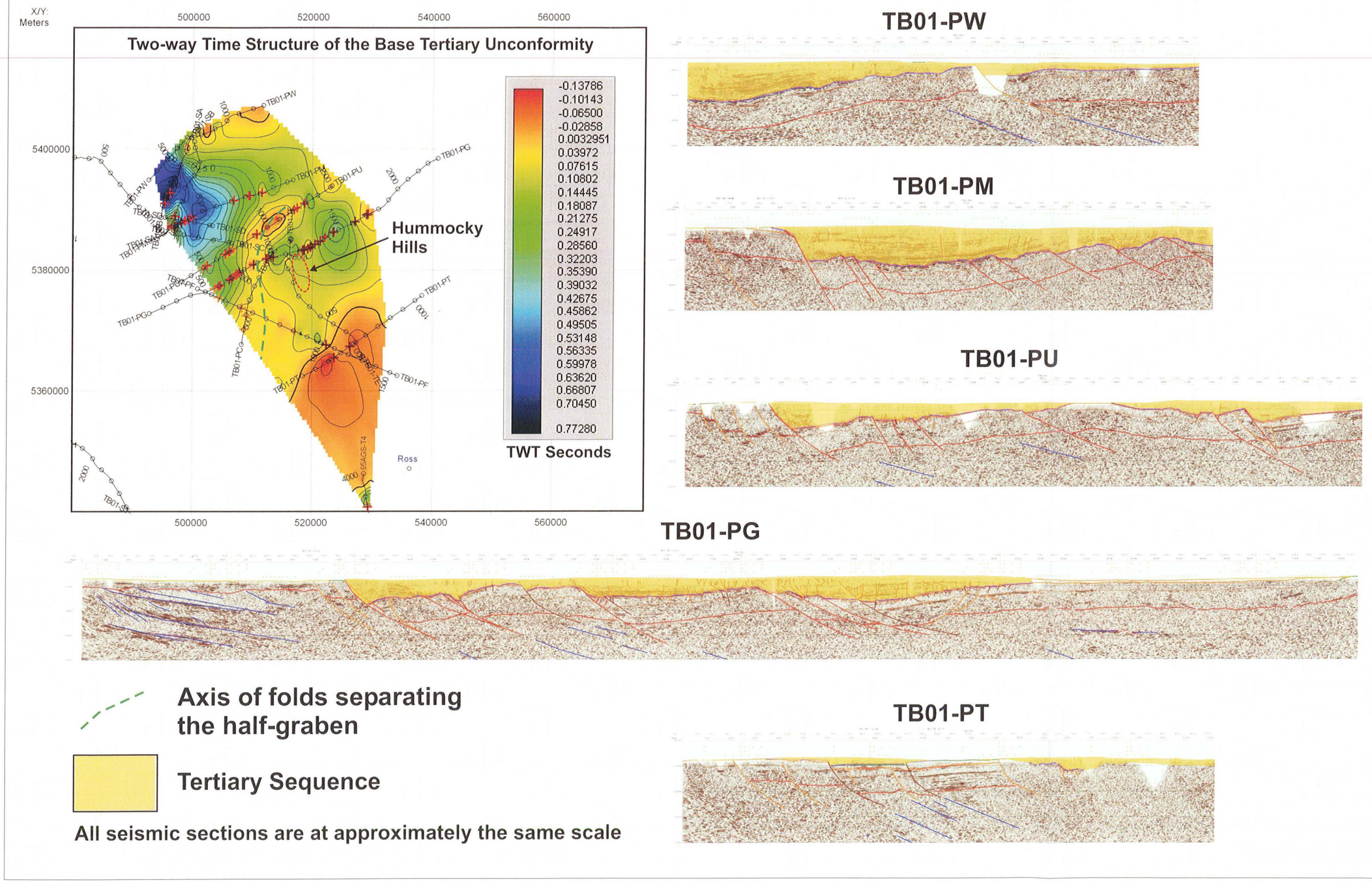

Figure 7.17: Geometry of the Longford Sub-basin

7.3.2: Tasmania Basin

The TB01 Seismic Survey does not cover the full extent of the Tasmania Basin, therefore the discussion here about basin geometry only refers to the area of the survey. Previous work on basin geometry is limited to palaeogeographic reconstructions and isopach maps based on outcrop and limited drill hole data (Banks and Clarke, 1987, Clarke, 1989, Reid et al., in prep) (Figure 7.18). The isopach maps indicate initial deposition was in a topographically varied basin, with high areas occurring north, south and through central Tasmania. The thickest deposits generally occur in a zone coincident with the Tamar Fracture System (Figure 7.18).

Comparison of isopach sections derived from the seismic interpretation and from the existing isopach maps show a marked difference in the proposed geometry of the Base Parmeener Unconformity (Figure 7.19). The section derived from seismic was created by flattening the Lower Marine Sequence horizon on TB01-ST. Flattening low in the section eliminates the effects of the large, Tertiary faults and removes thickness variations due to the dolerite sills. The resultant east to west section contains the Lower Marine Sequence and Basal Tillite and shows the geometry of the early depositional basin. The second section was derived from the addition of the Basal Tillite and Lower Marine Sequence isopach maps of Reid et al. (in prep).

The resolution of the isopach based section is considerably less than that of the seismic based section. The isopach section indicates the thickest deposits are concentrated along the axis of the Tamar Fracture System (Figure 7.18, 7.19). However, the geometry of the Base Parmeener Unconformity derived from the seismic interpretation indicates a reasonably constant (400 - 500 m) thickness of Lower Parmeener Supergroup sediments across the region, with the thickest part of the section east of the Ross RG-146 drill hole (Figure 7.19). This indicates that initial sedimentation was not concentrated along the Tamar Fracture System as previously thought (Banks and Clarke, 1987, Clarke, 1989), but has occurred over a much wider depocentre (Figure 7.19).

Late Carboniferous → *Early Permian* →

Basal Tillite
(Wynyard,Tillite, Stockers Tillite, Truro Tillite)

Lower Marine Sequence
(Woody Island Siltstone, Quamby Mudstone)

(Bundella Mudstone, Golden Valley Group)

Lower Freshwater Sequence
(Liffey Group, Faulkner Group, Mersey Group)

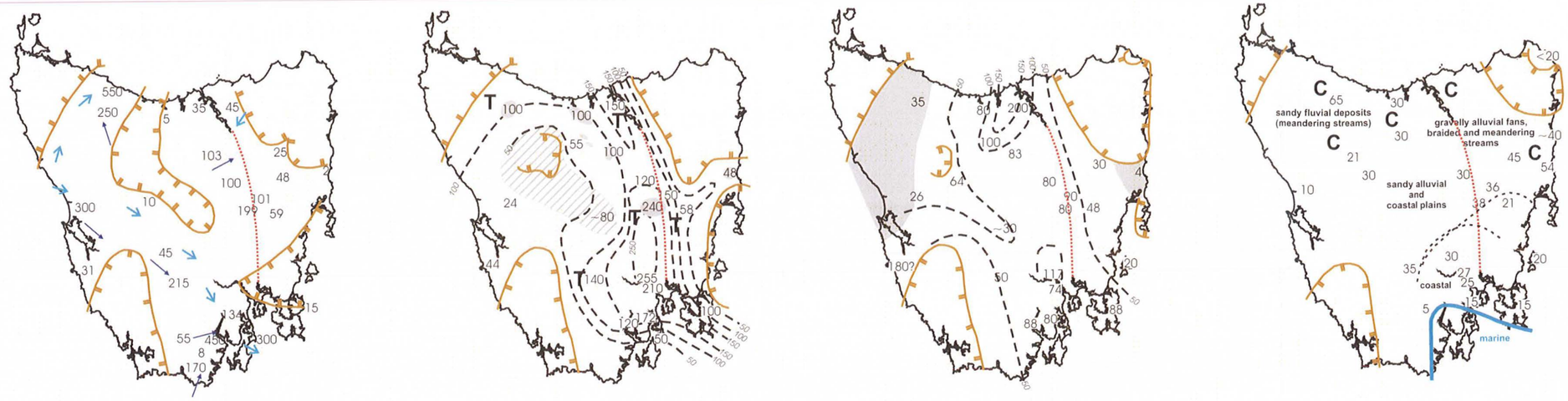

↘ Direction of ice movement (Clarke and Banks, 1987)

↘ Direction of ice movement (Hand, 1993)

Tasmanite Oil Shale

T Dispersed *Tasmanites*

Conglomeratic Facies

Earliest development of freshwater environments

C Coal development

Extent of brief marine incursions

Late Permian →

Upper Marine Sequence
(Cascades Group, Poatina Group)

(Deep Bay & Minnie Point Formations, Malbina Formation; MarraFormation; Garcia Sandstone, Springmount Mudstone & Palmer Sandstone)

(Ferntree Formation, Bogan Gap Formation)

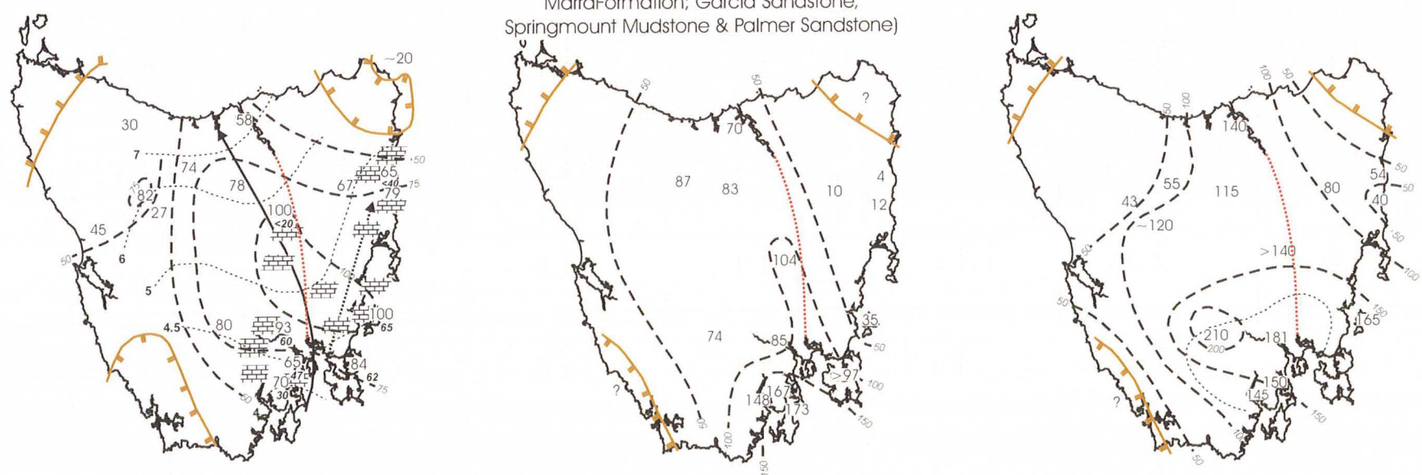

Limestone - approx thickness in metres

Younging direction of calcareous beds

Faunizone age at the base of the calcareous units

Younging direction of limestone

Extent of Risdon Sandstone deposition

156 Thickness (metres)

100 Isopachs (metres)

Topographic highs

Tamar Fracture Zone

Modified from Reid (in prep)

Figure 7.18: Isopach maps of for the major stratigraphic units of the Lower Parmeener Supergroup.

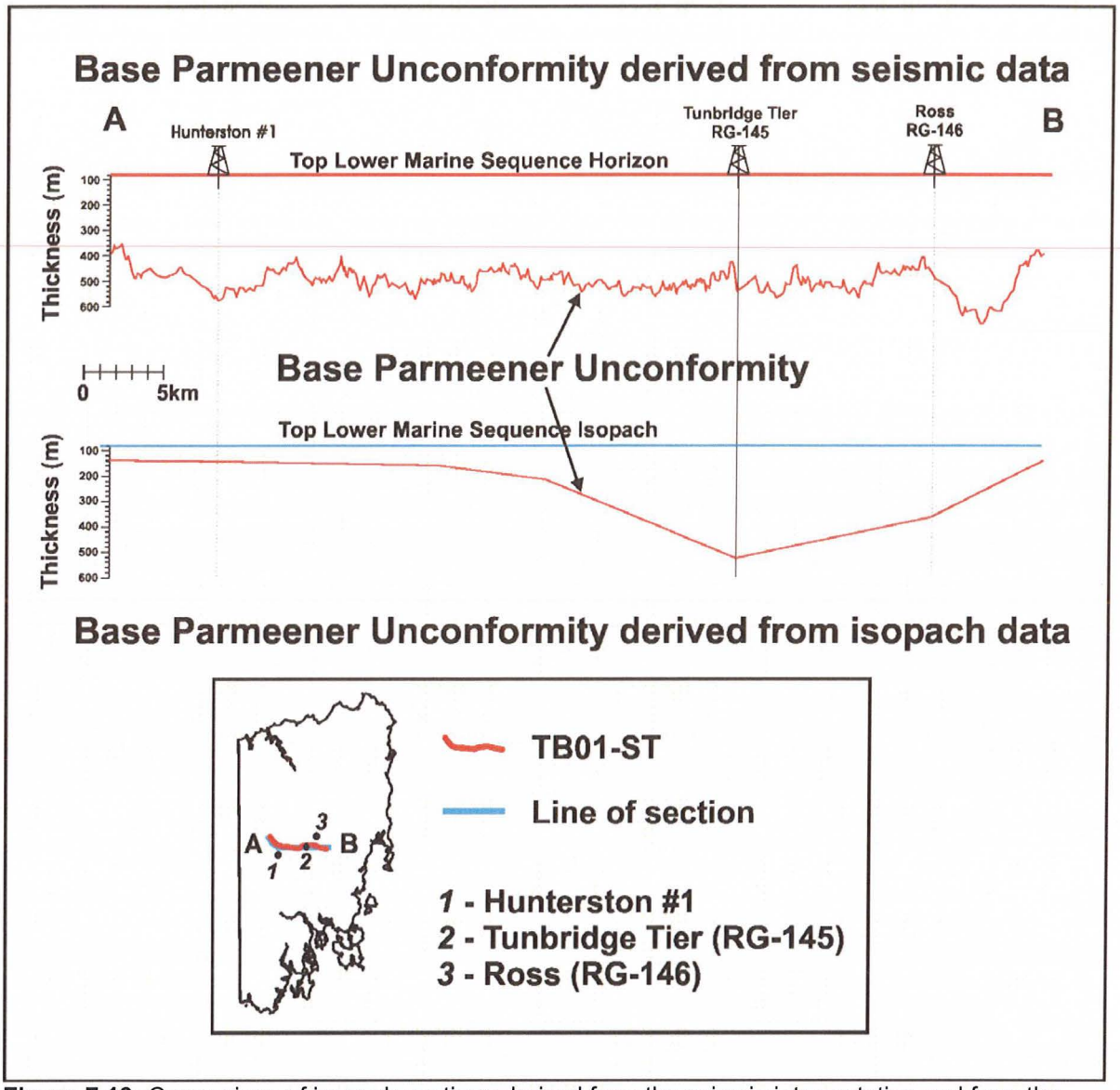

Figure 7.19: Comparison of isopach sections derived from the seismic interpretation and from the current isopach maps.

7.4: GEOMETRY OF DOLERITE INTRUSION

A single, thick sill of Jurassic Dolerite is recognised on all of the survey lines. Mapped outcrop along the margins of the Central Highlands indicate the dolerite generally intrudes in a zone between the top of Unit 2 (Upper Parmeener Supergroup) and the base of the Upper Marine Sequence (Lower Parmeener Supergroup). In the north of the survey area, the dolerite sill is high in the sequence, at or near the top of Unit 2, while it occupies a position towards the base of Unit 2 or the top of the Upper Marine Sequence in the east (Figure 7.20). Dolerite outcropping above subsurface sills and the existence of dykes above the main sill suggest the previous existence of higher sills (Figure 7.21).

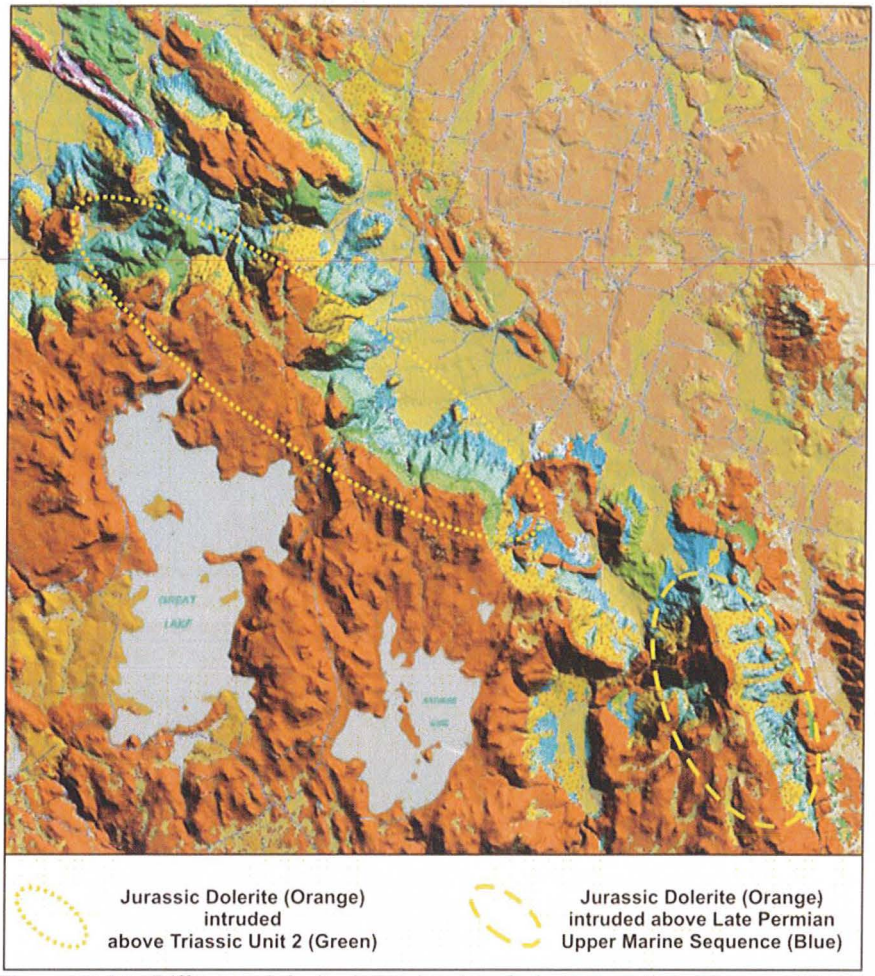

Figure 7.20: Different dolerite intrusion levels in the north and east of the survey area.

The dolerite sill, ranges from 300 m thick on line TB01-TB and in the middle of TB01-PB, up to 500 m thick on lines TB01-TH and ST. Rapid thickening/thinning of the sill is common, especially where they intersect faults (Figure 7.22). Drilling and seismic interpretations indicate that the dolerite sill is thicker in the sub-surface than when it outcrops. The sill beneath the "window" near Hunterston is 650 m thick at the Hunterston 1 DDH, the interpretation of TB01-PB indicates that this thickness is maintained towards the south (Figure 7.23). The sill beneath the "window" east of Bronte Park is 800 m thick (Figure 7.24), while the sill at the western end of TB01-TB is up to 800 m thick until SP 900 where it moves higher in the section and has been partly removed by erosion (Figure 7.25).

The seismic interpretation shows that the dolerite sills are roughly conformable with the Parmeener Supergroup sequence over most of the survey area (Figures 7.24, 7.25). An exception occurs below the "window" at Hunterston, where over 10 km, the dolerite sill (sheet) cuts down through the section towards the south (Figure 7.23). Dolerite sills stepping up through the stratigraphy across faults is common mainly towards the margins of the Central Highlands region.

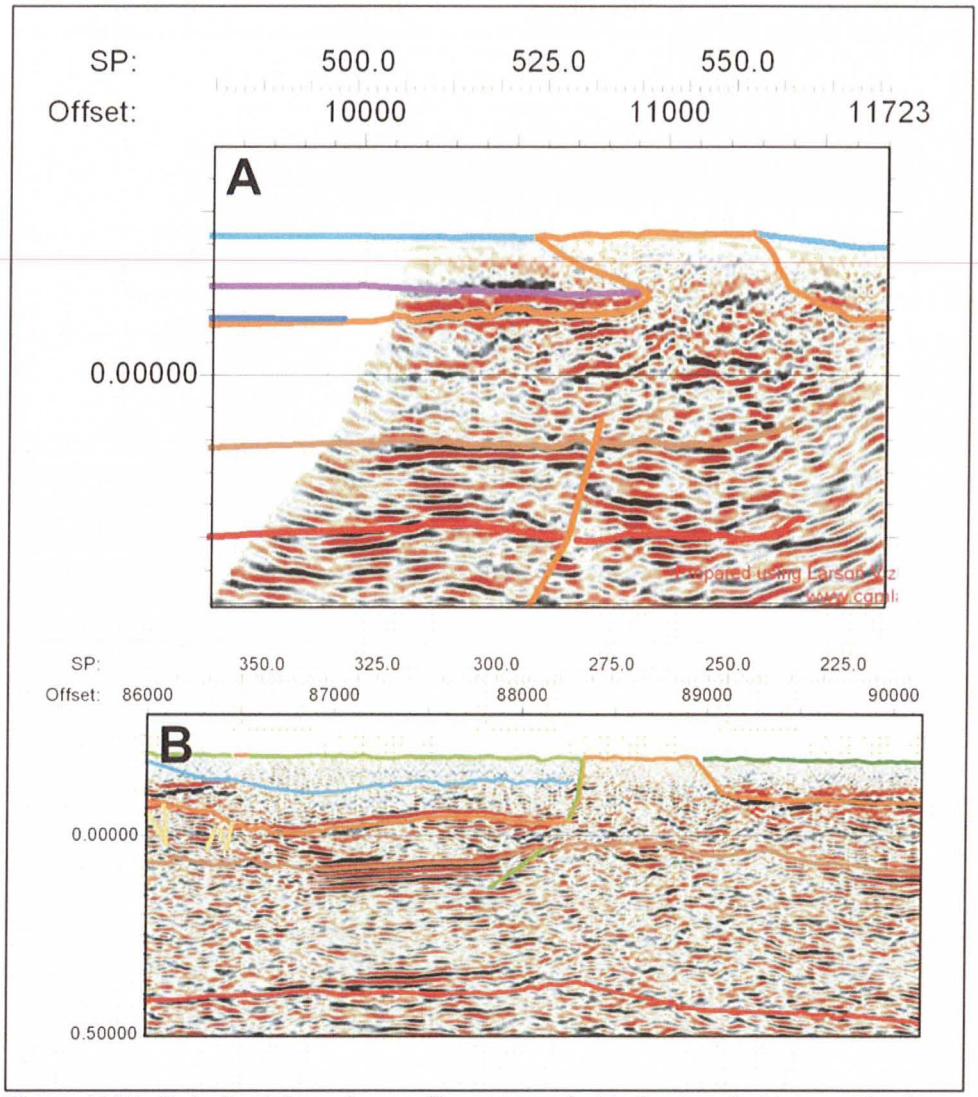

Figure 7.21: Dolerite dykes above sills were probably feeders to higher sills since removed by erosion (TB01-TA & PB).

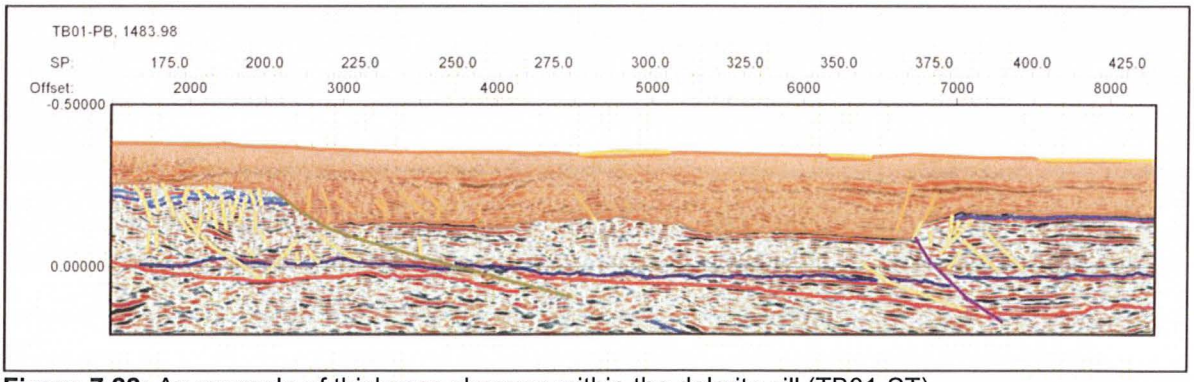

Figure 7.22: An example of thickness changes within the dolerite sill (TB01-ST).

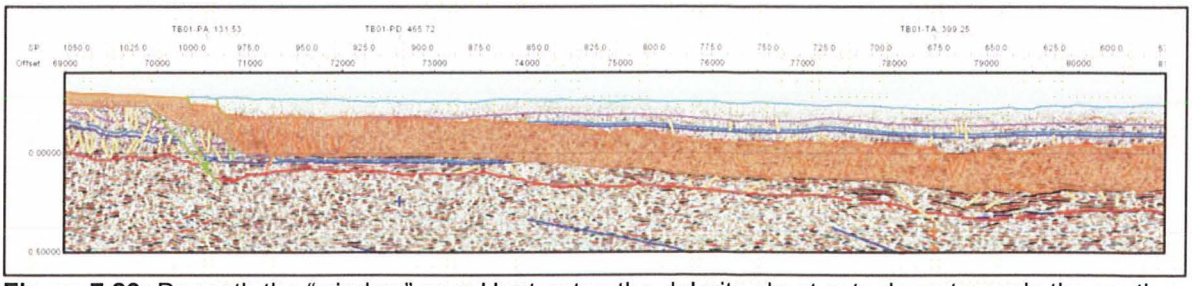

Figure 7.23: Beneath the "window" near Hunterston the dolerite sheet cuts down towards the south with a consistent thickness of ~650 m (TB01-PB).

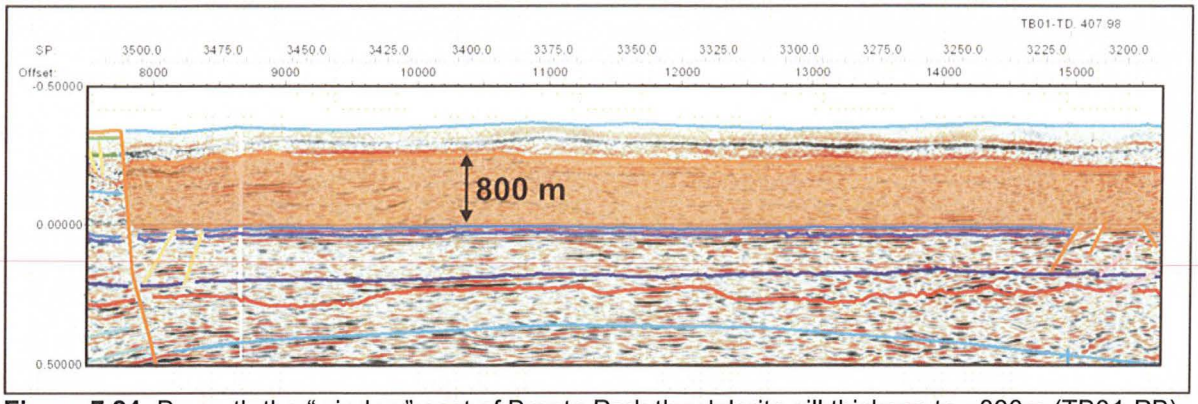

Figure 7.24: Beneath the "window" east of Bronte Park the dolerite sill thickens to ~800m (TB01-PB).

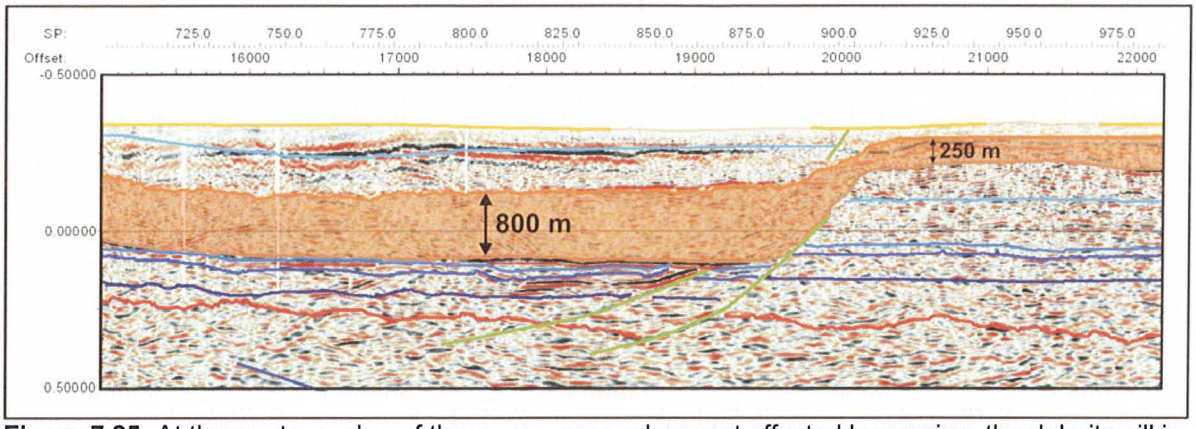

Figure 7.25: At the western edge of the survey area, where not affected by erosion, the dolerite sill is extremely thick (TB01-TB).

7.5: PETROLEUM GEOLOGY

7.5.1: Potential Hydrocarbon Trap Styles

Stratigraphic Traps

Pinch Outs

Potential hydrocarbon traps exist in the Tasmania Basin section where shallowly dipping dolerite intrusions cut across (pinch out) and seal reservoir rocks such as the Lower Freshwater Sequence (Figure 7.26). Pinch out traps are observed on line TB01-ST (SP 512) where the Lower Freshwater Sequence is truncated by a westerly dipping intrusion, and on lines TB01-PB (SP 864) and TB01 PD (SP 424) where the dolerite dips towards the south (Figure 7.27).

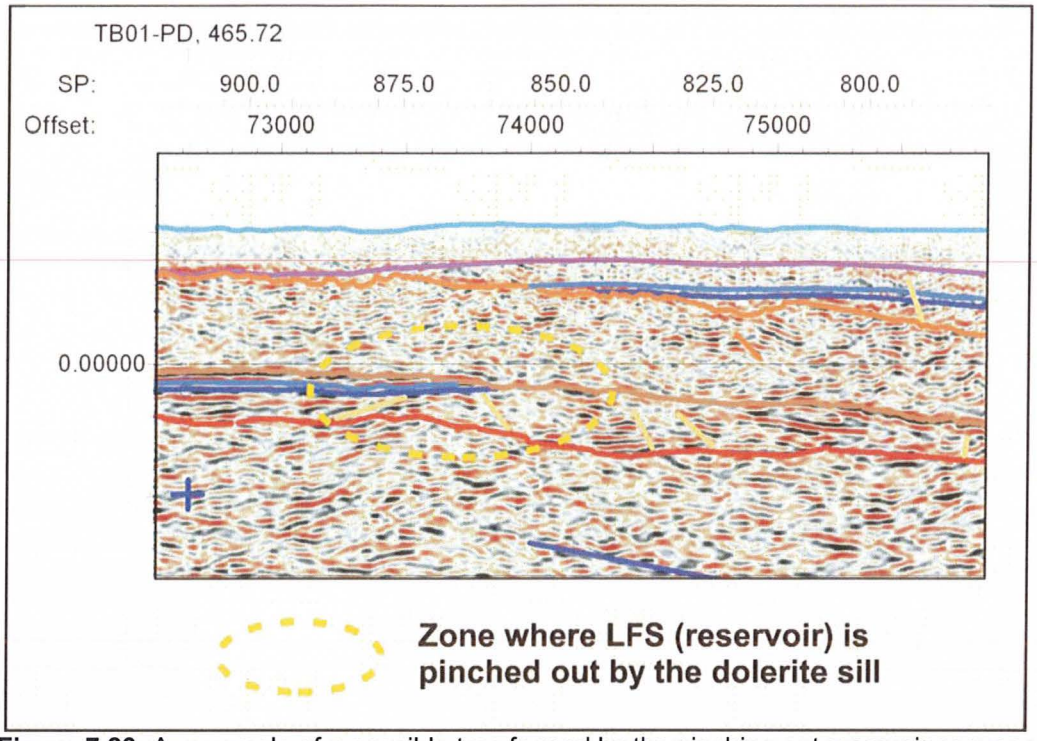

Figure 7.26: An example of a possible trap formed by the pinching out reservoir sequence by a down cutting dolerite sheet (TB01-PB).

Unconformity Traps

Base Parmeener Supergroup Unconformity

There are many locations where the Base Parmeener Supergroup Unconformity truncates dipping basement reflectors, forming possible sub-unconformity traps (Figure 7.28). While these traps are common, the stratigraphy of the basement below the Tasmania Basin is poorly understood and Mesozoic hydrocarbon generation and migration from Ordovician carbonate source rocks, based on current knowledge, appears unlikely.

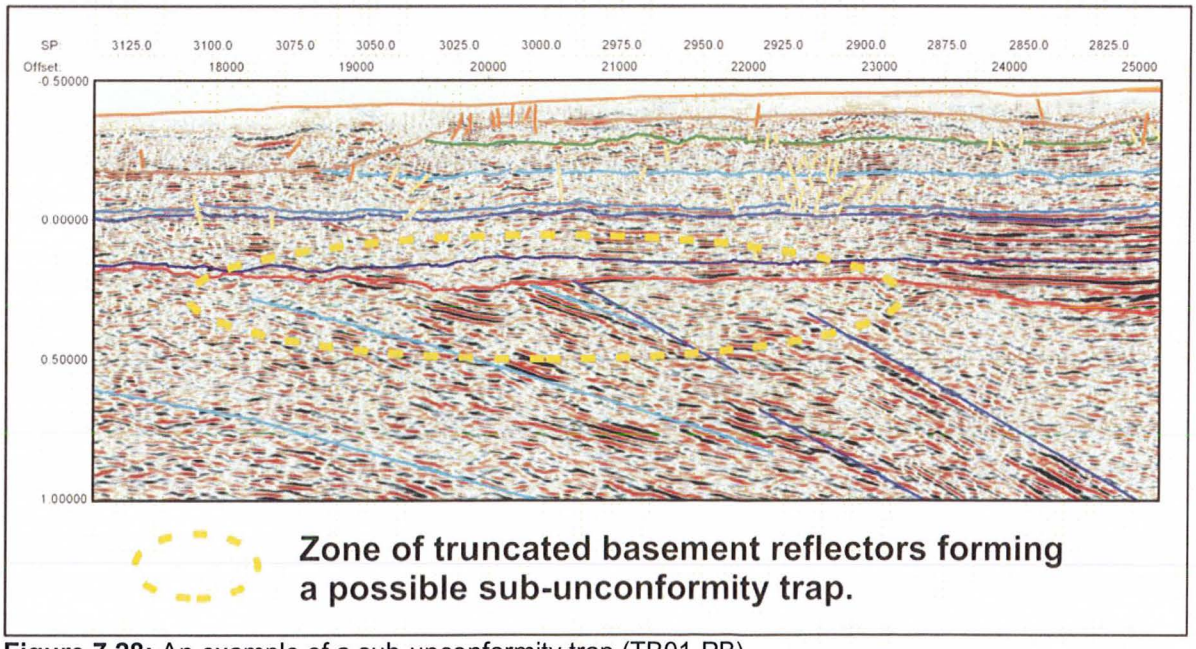

Figure 7.28: An example of a sub-unconformity trap (TB01-PB).

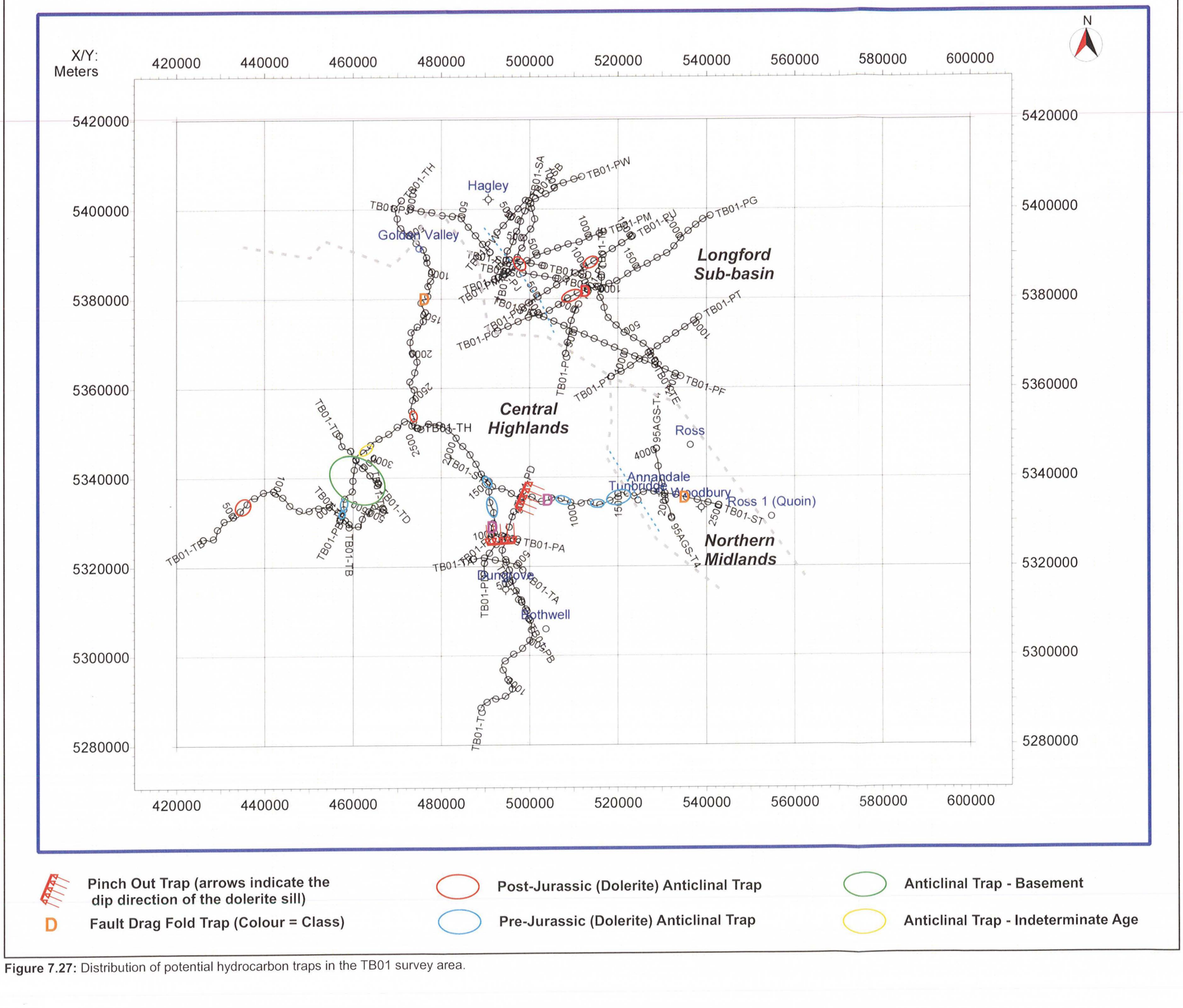

Figure 7.27: Distribution of potential hydrocarbon traps in the TB01 survey area.

Structural Traps

Anticline Traps

Numerous anticlines are recorded in both the Tasmania Basin and the basement. Potential anticline traps in the Tasmania Basin section are distributed across the survey area (Figure 7.27). Potential traps in the Central Highlands are in the gentle folds mostly formed pre- or syn-intrusion of Jurassic dolerite. Rollover anticlines on TB01-PG and PU, formed during early Tertiary extension are potential traps in the Parmeener Supergroup (Tasmania Basin) section of the Longford Sub-basin. The only potential trap seen in the Tertiary sequences of the Longford Sub-basin is the structure known as the Bracknell Dome (Figure 7.12). Potential anticline traps are formed by symmetrical and asymmetrical structures and the nature of the seismic survey means that in most cases only two-way closures can be calculated (Table 7.1).

In the basement section, a large, faulted, north-westerly plunging, anticline is interpreted at the western end of line TB01-PB and on cross-line TB01-TD. The structure is up to 15 km long with at least 3-way dip closure (Figure 6.94, 7.29). A fault disrupts the southern limb of the structure and both hanging and footwall traps are likely to be developed (Figure 7.29). High amplitude, horizontal reflectors (bright spots) at the crests of the structure warrant further investigation (Figure 7.29).

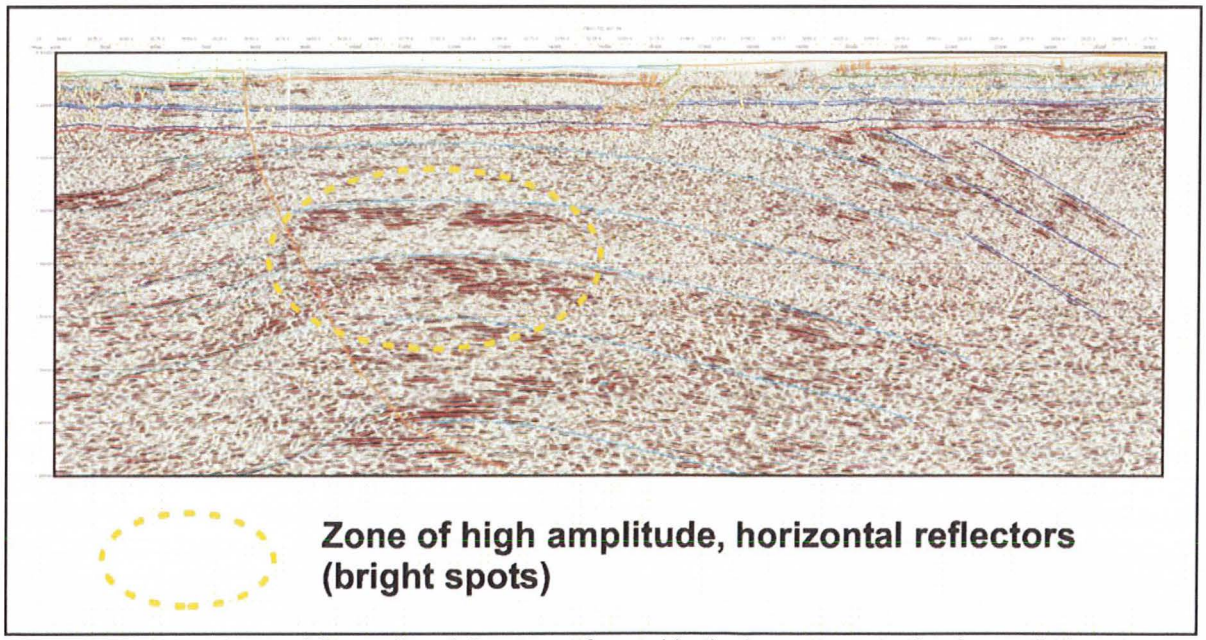

Figure 7.29: Hanging and footwall anticline traps formed in the basement section beneath the Bellevue Tiers (TB01-PB).

Line	Anticline			Trap (@ Reservoir Level)			Timing	Shape	Vergence
	SP Range	Amplitude (m)	Wavelength (m)	SP Range	Closure (m)	Length (m)			
TB	560-735	50	4500	560-735	50	4500	Post-Dolerite	Symmetrical	
PB	1150-1425	340	6850	1150-1360	60	1150	Pre-Dolerite	Asymmetrical	North
PB	1445-1560	120	2750	1445-1560	120	2750	Pre-Dolerite	Symmetrical	
PB	1795-1985	200	4800	Structure cut by large Indeterminate Faults			Pre-Dolerite	Asymmetrical	South
PB	2940-3035	60	2300	2940-3035	60	2300	?	Symmetrical	
PB	3505-3615	100	3800	3575-3615	20	1000	Pre-Dolerite	Asymmetrical	Southwest
PB	3630-3675	70	1000	3630-3775	70	1000	Pre-Dolerite	Symmetrical	
TH	2610-2710	180	2500	2610-2710	180	2500	Pre-Dolerite	Symmetrical	
ST	865-1010	100	3600	865-1010	100	3600	Pre-Dolerite	Symmetrical	
ST	1175-1345	150	4200	1220-1345	90	3000	Pre-Dolerite	Symmetrical	
ST	1345-1700	140	9000	1370-1620	100	6300	Pre-Dolerite	Asymmetrical	East
PT	410-475	130	1600	435-475	50	1000	Post-Dolerite	Asymmetrical	Southwest
PT	475-780	350	6600	475-725	280	6300	Post-Dolerite	Asymmetrical	Northeast
PG	750-875	300	3000	775-825	120	1000	Post-Dolerite	Asymmetrical	Southwest
PU	995-1130	440	3500	995-1095	230	2250	Post-Dolerite	Asymmetrical	Southwest
	Average	182 m	4000 m	**Average**	109 m	2311 m			

Table 7.1: Location and main features of possible anticlinal traps formed in the Tasmania Basin.

Fault Related Traps

Potential traps related to faults are widespread in the survey area. These structures are recognised near the margins of the Central Highlands region, around the "windows" in the dolerite and in the Longford Sub-basin/Northern Midlands regions. Both pre-Jurassic and Tertiary faulting has developed traps, the age of faulting indicates the time of trap formation. The integrity of the fault seal is critical to whether the traps are viable. Many older faults may have been reactivated by Late Cretaceous, early Tertiary tectonics and could have leaked.

Fault Drag Fold Traps

Several potential traps formed in fault drag folds are interpreted in the Central Highlands and Longford Sub-basin/Northern Midlands regions (Figure 7.27). These traps are associated with either Tertiary Faults or reverse drag in Pre-Jurassic reverse faults. The traps formed by pre-Jurassic faults being the most likely to be charged. Fault seal is crucial to the integrity of this style of trap. Folds are asymmetric, formed in the footwall of reverse faults and hanging walls of normal fault. The faults have wavelengths of around 700 – 800 m with closures less than 300 m (Figure 7.27).

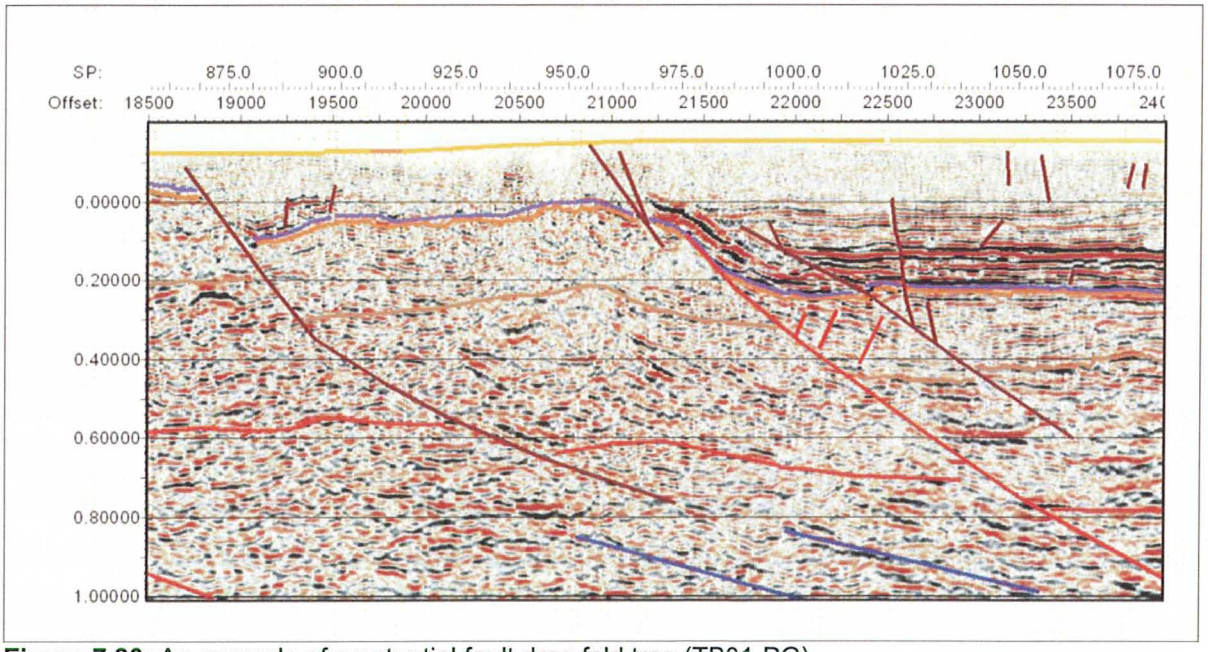

Figure 7.30: An example of a potential fault drag fold trap (TB01-PG).

Fault Block Traps

Potential hydrocarbon traps formed by wedges, horsts, grabens and half-grabens are common, occurring mainly on the margins of the Central Highlands and across the Longford Sub-basin/Northern Midlands region. These structures vary markedly in size, ranging from a few hundred metres to several kilometres across. Multiple small, tilted blocks were recognised in fault zones on lines TB01-TB (SP 1670-1750) and TH (SP 1395-1450) (Figure 7.28). Large horst blocks are interpreted inboard of the margin of the Central Highlands on line TB01-ST (SP 730-760) and PB (SP 1000-1060) (Figure 7.32). Numerous, wedges and small tilted blocks are interpreted on the eastern ends of line TB01-PA and TA and on line TB01- PD affecting the reservoir above and below a thick dolerite sill at the "window" near Hunterston (Figure 7.33). The eastern section of line TB01-ST covering the Northern Midlands region contains an assortment of potential traps formed by fault blocks, wedges, horsts and grabens. The section between shot-points 1700 and 1950 consists mainly of fault blocks and wedges ranging in size from about 800 – 2500 m (Figure 7.34). A three kilometre section between shot-points 2140 and 2240 contains many small wedges formed around a Tertiary aged wrench structure (Figure 7.35), while large horst and graben are interpreted east of shot-point 2240 (Figure 7.35).

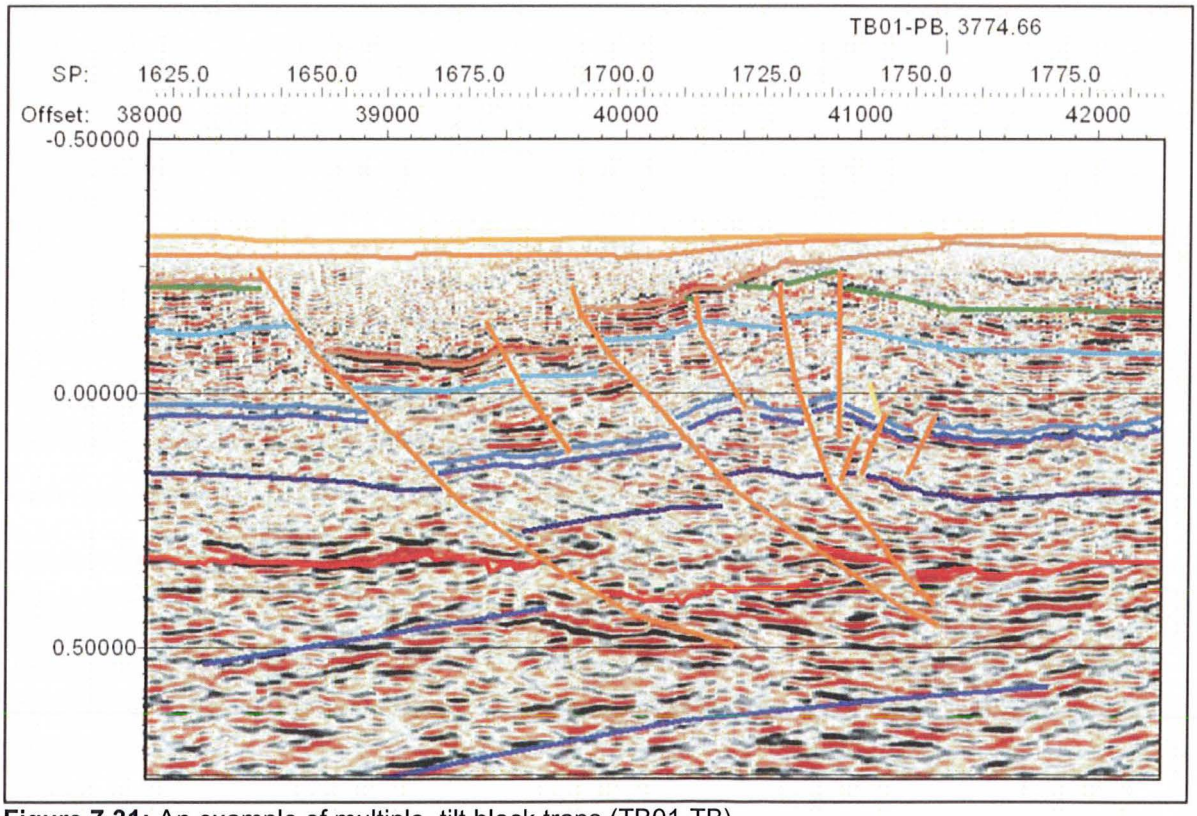

Figure 7.31: An example of multiple, tilt block traps (TB01-TB).

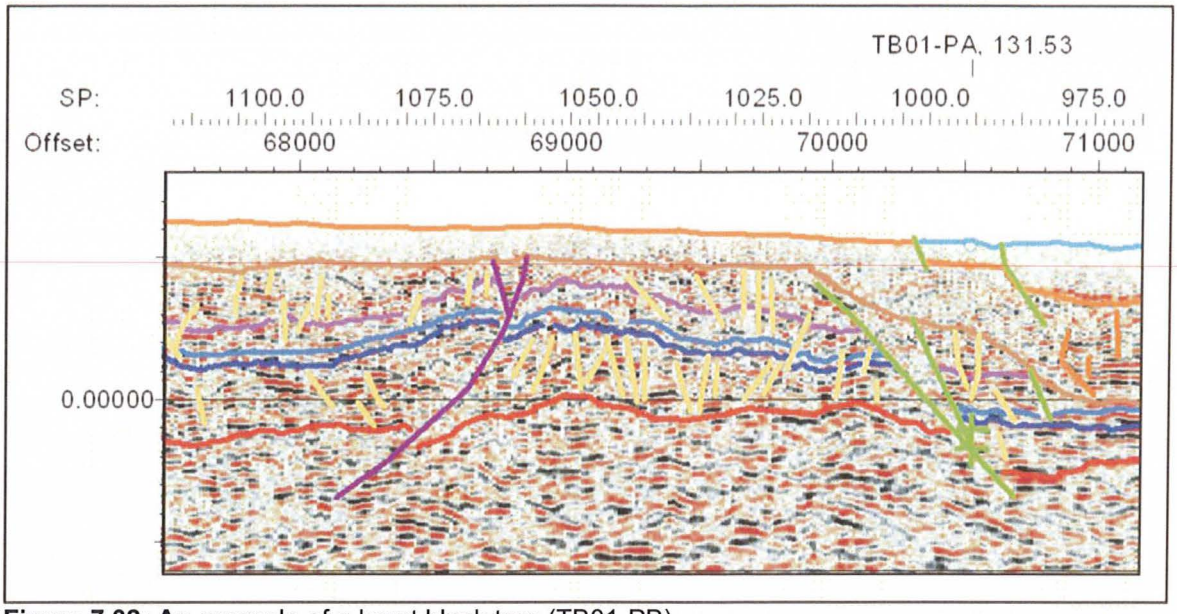

Figure 7.32: An example of a horst block trap (TB01-PB).

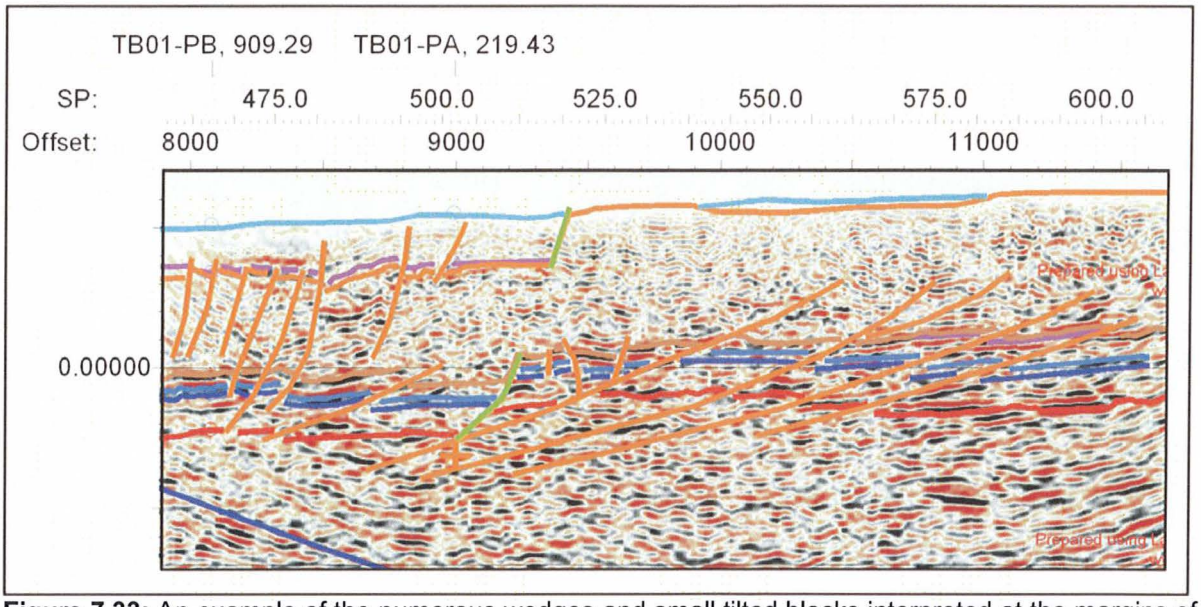

Figure 7.33: An example of the numerous wedges and small tilted blocks interpreted at the margins of the "window" near Hunterston (TB01-TA).

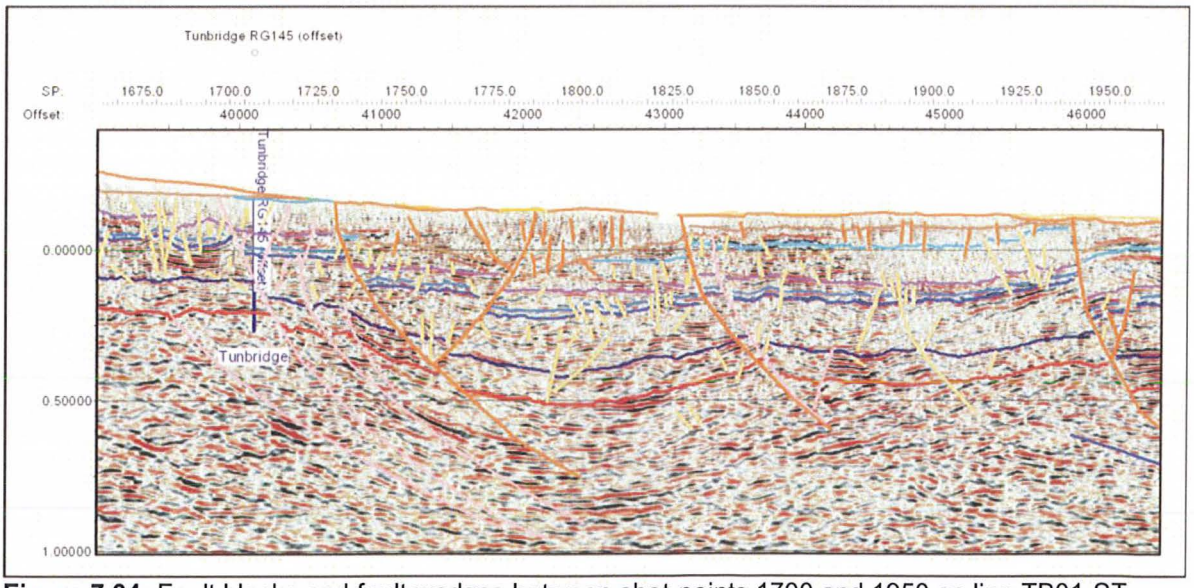

Figure 7.34: Fault blocks and fault wedges between shot-points 1700 and 1950 on line TB01-ST.

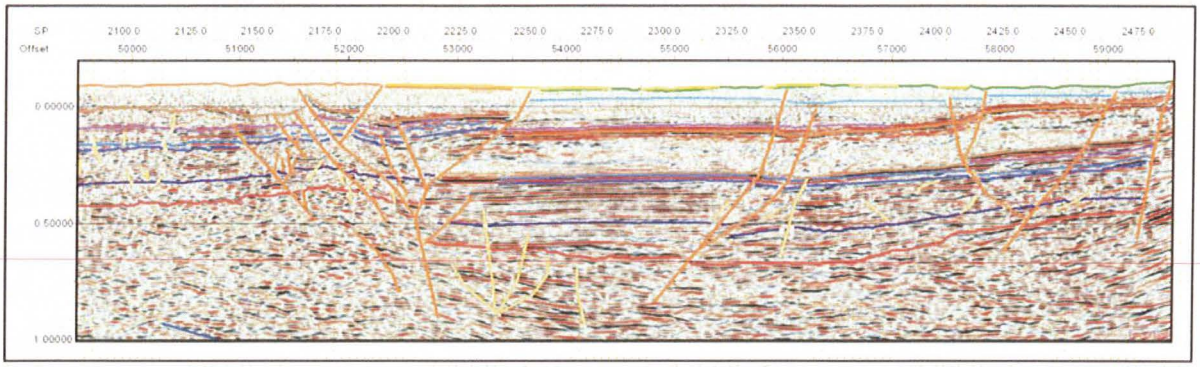

Figure 7.35: Kilometre scale horst and graben interpreted east of shot-point 2240 on line TB01-ST.

Early Tertiary extension in the Longford Sub-basin has resulted in the formation of numerous tilted blocks of Parmeener Supergroup (Figure 7.36). The size and density of these structures makes them an important potential trap style. The tilt blocks are capped by dolerite (Figure 7.36) and the depth to the Base Parmeener Unconformity horizon indicates these blocks are likely to contain up to Unit 2 of the Upper Parmeener Supergroup and a complete Lower Parmeener Supergroup sequence. Therefore these structures probably contain two possible reservoirs, Unit 2 and the Lower Freshwater sequence.

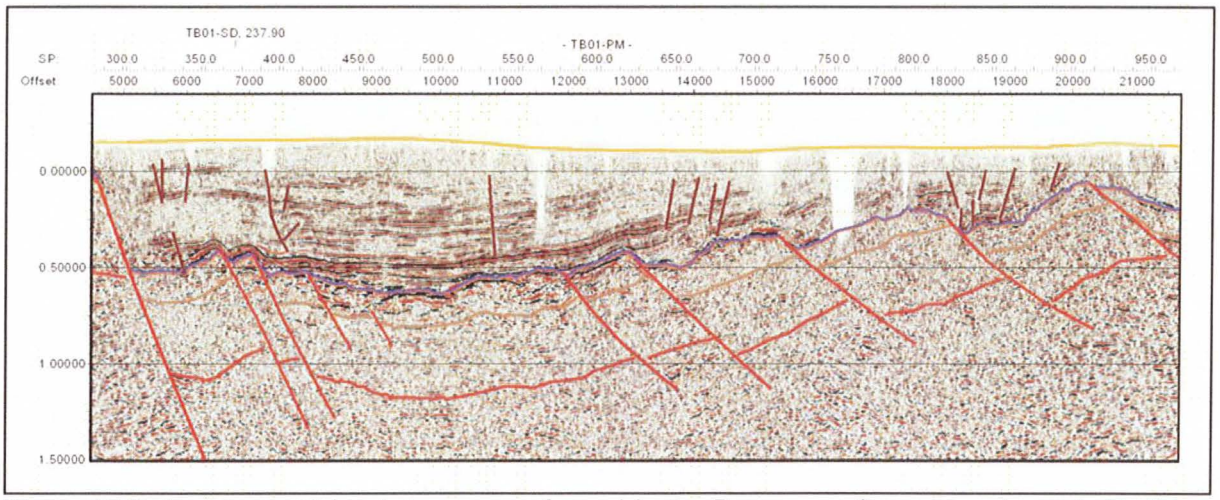

Figure 7.36: Numerous tilt-block traps were formed in the Parmeener Supergroup by early Tertiary extension in the Longford Sub-basin region (TB01-PM).

The dip sections indicate these structures range from 0.5 to 2 km across (Figure 7.36). The along strike dimensions of these structures is unknown. However, Direen (1995) proposed several north-easterly striking faults, approximately 10 km apart compartmentalising the basin.

Conclusions

Many differing potential hydrocarbon trap styles, both structural and stratigraphic are interpreted across the survey area. Timing of formation of these structures is important. For the Tasmania Basin, hydrocarbon generation and migration probably occurred from the Middle Jurassic through to the Cretaceous, therefore traps which formed prior to the Jurassic and that have maintained their integrity during subsequent tectonic events are more likely to have been charged by migrating hydrocarbons. Traps of this age are common in the Central Highlands. Latest Cretaceous – Tertiary deformation is strongest in the Longford Sub-basin/Northern Midlands regions and may have modified or destroyed many of these older traps and migration of remobilised hydrocarbons into traps formed by these events is a possibility, but very difficult to predict.

Although the stratigraphy of the basement is not well understood and the source potential of the Ordovician Carbonates is debatable, at least one major trap structure is recognised. The nature of the seismic reflections associated with the structure, make it a compelling exploration prospect.

CHAPTER 8
CONCLUSIONS

8.1: INTRODUCTION

Onshore Tasmania is a frontier exploration province. This project forms part of a broader investigation into the hydrocarbon prospectivity of onshore Tasmania. The main aim of this research was to define the geometry of structures in the Tasmania Basin, the Tertiary basins in the north and the pre-Late Carboniferous basement and to describe their history – the structural history of Tasmania from the Devonian to the Recent.

The seismic data set acquired in northern Tasmania was analysed to determine the location, type and timing of the structures present. Deep drill holes are sparse in the survey area and extra, important constraint on the seismic interpretation was provided by the Digital Elevation Model and regional gravity data. The DEM was draped with the 1:250 000 geology of Tasmania and used to determine stratigraphic thickness and interpret faults not identified by mapping. The regional gravity data was very useful in determining local thickness variations dolerite sills.

In addition to integrating several different datasets to produce a structural history of Tasmania, this research has also investigated the tectonic setting of the basin, advancing a new basin model that places the Tasmania Basin in a Gondwana context. This chapter aims to summarise the key events in the development of the Tasmania Basin, present the structural history and to discuss the implications of this research with respect to the hydrocarbon potential of onshore Tasmania.

8.2: THE TASMANIA BASIN

The Tasmania Basin contains both marine and non-marine sedimentary rocks deposited from the Late Carboniferous to the Late Triassic. These sedimentary rocks are known as the Parmeener Supergroup (Banks, 1973). The approximately 1 to 1.5 km thick sequence is generally flat-lying and lies with pronounced unconformity on Late Devonian granites and older folded rocks. The unconformity surface was considered to have an original relief of approximately 1000 m (Banks, 1989a). However, the seismic data reported here indicates the

basin floor had a relatively low relief only shallowing by a few hundred metres over a basement high beneath the Central Highlands (Figure 7.16).

As discussed in Chapter 2, the Tasmania Basin was developed in East Gondwana during the Late Carboniferous, Permian and Triassic adjacent to the Victoria Land Basin. Deposition took place in a back-bulge depozone, behind the Ross High Foreswell, inboard of a major foreland basin system and convergent plate boundary (Figure 2.4). Early deposition comprised terrestrial sediments in Victoria Land (Antarctica) and marine sediments in Tasmania (Barrett and Fitzgerald, 1985). Deposition was not always contemporaneous across the basins, which were separated by the Beardmore-Ross Upland from the Late Permian until the Early Triassic. The rocks of the Tasmania and Victoria Land basins share a similar history from the Early Triassic.

8.3: THE STRUCTURAL HISTORY OF TASMANIA

8.3.1: Pre–Late Carboniferous (Tabberabberan Orogeny)

From examination of the seismic dataset, the large structures observed in the basement do not continue into the overlying Tasmania Basin section (Figure 7.13), indicating they were formed by events predating the Late Carboniferous. The scale, orientation, type and degree of deformation correlate well with regional structures known to have formed during the Middle Devonian-Tabberabberan Orogeny.

Evidence from the seismic data indicates the contact between the Western and Eastern Tasmania Terranes consists of a northwest striking zone of northeast dipping thrust sheets, which is at least 40 km wide beneath the Launceston Tertiary Basin. Along strike, to the northwest, similar structures are observed in the Dazzler Range and Beaconsfield area (Gee and Legge, 1979, Elliot et al., 1993). The seismic data shows this zone of continues at least 75 km further south then previously demonstrated.

To the west and southwest of the Launceston Tertiary Basin, the seismic interpretation indicates a progressive change in the structural style in the basement from thrust dominated in the east to fold dominated in the west (Figure 7.13). Large folds are interpreted on the western end of line TB01-PB (Bellevue Anticline - Figure 7.29) and these structures are correlated with folds in the Florentine Valley and Mole Creek areas. The folding in the Mole Creek area affects Late Cambrian to Early Ordovician rocks (Pike et al., 1973), while Florentine Valley

syncline is formed in Silurian to Early Devonian aged rocks (Brown et al., 1989). It is therefore very likely these folds are the product of the Tabberabberan orogeny.

8.3.2: Late Carboniferous–Middle Jurassic

Structures formed in the Tasmania Basin prior to the intrusion of dolerite in the Middle Jurassic are common, but not as numerous as structures resulting from later events. In the 120 Ma period between the inception of the Tasmania Basin in the Late Carboniferous and the intrusion of dolerite in the Middle Jurassic structures typical of both compression and extension were formed. These include long wavelength, low amplitude folds and faults with both normal and reverse movement. Faults are either truncated by or intruded by dolerite. The relationships observed between these structures and the Jurassic Dolerite has been used to constrain their timing.

The seismic interpretation indicates a reasonably even distribution of structures of this age across the Central Highlands area, however very few pre-dolerite structures were recognised in the Longford Sub-basin/Northern Midlands area (Figures 7.2, 7.7). The latter region was strongly affected by later tectonic events, which probably overprinted and disguised most of the earlier structures.

Numerous pre-Middle Jurassic faults have been previously recognised. For example parts of the Tiers Fault System have Jurassic Dolerite occupying the faulted zones (Mathews et al., 1996). Similar pre-dolerite faults are interpreted in the Oatlands area (Forsyth, 1984). A interstratal, normal fault in north-western Tasmania has been interpreted as Late Permian (Banks, 1979). In the south of Tasmania, Jurassic age normal faults were proposed in the Middle Derwent Valley (Anand Alwar, 1960), while a strong transpressional zone along the Maydena – National Park corridor has the appearance of a dextral positive flower structure, truncated at its eastern end by a major dolerite dyke (Dunster, 1981). A phase of pre- to syn-dolerite rifting is recognised in the Hobart region (Leaman, 1976). While from small faults in the Parmeener Supergroup near Hobart, Berry and Banks (1985) conclude the Hobart area was affected by a north-northwest compressional event that was active both before and after the intrusion of dolerite.

A wide variety of structures have been interpreted to have formed in the period between inception of the Tasmania Basin and the intrusion of dolerite. Many of these structures are nominally Jurassic in age and are considered to have formed by events preceding or

concurrent with the intrusion of dolerite. However, even with the addition of this new seismic data, the nature of pre-Middle Jurassic deformation in Tasmania is difficult to decipher and the significance of these events remains uncertain.

8.3.3: Middle Jurassic–Early Tertiary (Gondwana Break-up)

During this period Tasmania was affected by uplift, erosion and extension, all related to the break-up of Gondwana and particularly the opening of the Tasman Sea. Analysis of both the seismic data and the DEM demonstrate basement structure was extremely significant in the structural development of the Tasmania Basin during early Tertiary, east-northeast extension.

The size and orientation of the Launceston Tertiary Basin was controlled by basement structures. From the seismic data covering the Longford Sub-basin it is clear many of the faults recognised in the basement were reactivated during early Tertiary extension, forming a series of tilted blocks in the Parmeener Supergroup and creating accommodation space for the deposition of Tertiary sediments (Figure 7.6).

Apatite Fission Track (AFT) ages from inland Tasmania record a rapid cooling episode in the middle Cretaceous (~100 – 85 Ma), indicating kilometre scale uplift and denudation (O'Sullivan et al., 1998, O'Sullivan et al., 2000a). The remnants of this event are the Northeast and Central Highlands regions. The structural style of the basement beneath the Central Highlands region differs from that beneath the Launceston Tertiary Basin, becoming increasingly fold dominated towards the west (Figure 7.13). The change in structural style is coincident with a decrease in the density of Tertiary faulting (Figure 7.2) indicating the Central Highlands region acted as a competent block, with locus of extension in the Launceston Tertiary Basin tied to the underlying terrane boundary.

The strike of the basement fabric in the Mathinna Supergroup (Eastern Tasmania Terrane) changes from northwest in northern Tasmania to north-south in central eastern Tasmania and to the northeast on Maria Island in south-eastern Tasmania. In northeast Tasmania, east of the terrane boundary the Tertiary fault pattern is simple, consisting of large equidimensional blocks. Towards the south these blocks decrease in size and become increasingly skewed as the basement fabric becomes more oblique to the extension direction.

The orientation of basement structures of the Western Tasmania Terrane underlying the Tasmania Basin in southern Tasmania is not known. However, the fault pattern formed is more diverse and disorganized then that to the north and east. Assuming the extension direction remained constant, this disorganisation implies the basement fabric of the Western Tasmania Terrane is complex and oriented oblique to the extension direction.

8.3.4: Miocene–Pliocene (Inversion)

The effects of Mio-Pliocene compressional tectonics are widely recognized in Victoria and measurements of the modern stress field indicate that Tasmania was also affected by a northwest compressional stress (Hillis and Reynolds, 2000). Evidence of inversion derived from both the DEM and from the seismic data in the Longford Sub-basin indicate that this area and probably the rest of Tasmania was subject to mild compression some time after the early Tertiary extension event. Zones of uplifted Tertiary aged sediments are observed on the DEM along the western edge of the Longford Sub-basin, while in the seismic data, many reverse faults are recognised within the Tertiary sequence (Later Tertiary Faults) of the Longford Sub-basin. In the Central Highlands region, inversion is extensive and associated with the location of Tertiary volcanics (Blackburn, 2004), while several faults interpreted from the DEM have incised watercourses on the eastern, up-thrown side, indicative of recent inversion (Figure 4.3).

8.3.5: Summary

Pre- Tasmania Basin basement rocks were deformed during the Middle Devonian Tabberabberan Orogeny. From seismic data, the basement beneath the Launceston Tertiary Basin consists of a series of stacked thrust sheets, dipping towards the northeast. This zone is about 40 km wide and coincides with the trend of the proposed Tamar Fracture System. To the west and southwest of the Launceston Tertiary Basin, the structural style is progressively modified from thrusts, through thrusts and folds to a region dominated by large folds.

Deposition of the Tasmania Basin began in the Late Carboniferous. Numerous structures formed either prior to or coeval with the intrusion of dolerite in the Middle Jurassic are recognised from the seismic data and other data. Both extensional and compressional structures are observed. Due to the nature of the structures and their poorly constrained timing, the nature of pre-dolerite deformation in the Tasmania Basin remains contentious.

Events associated with the break up of Gondwana are responsible for the modern topography of Tasmania. Uplift in the middle to Late Cretaceous was followed by significant east-northeast directed extension associated with the opening of the Tasman Sea. Faults and folds relating to this series of events are by far the most numerous in the seismic sections. Many of the faults interpreted from seismic reflection data in the Tasmania Basin are probably located over reactivated basement faults. Analysis of the seismic data and the DEM indicate that the orientation and nature of basement structures controlled the development of the structures in overlying strata during early Tertiary extension.

Tasmania was affected by northwest compressional stress in the Miocene and Pliocene. Evidence from both the DEM and the seismic data in the Longford Sub-basin indicate that the Tasmania Basin was subject to mild inversion after the early Tertiary extension event.

8.4: STRUCTURAL HISTORY AND IMPLICATIONS FOR HYDROCARBON PROSPECTIVITY

8.4.1: Introduction

The structural history proposed indicates that structures likely to act as hydrocarbon traps were formed in basement during the Middle Devonian Tabberabberan Orogeny and in the Tasmania Basin prior to, and during dolerite intrusion in the Middle Jurassic and by major tectonic events related to the break up of Gondwana in the middle to Late Cretaceous and early Tertiary. Assuming the conditions for maturation and migration were favourable, these structures may have been charged.

From information presented in Chapter 3 and from the results of this research, Petroleum systems events charts have been prepared for the proposed Larapintine and Gondwana Petroleum Systems in onshore Tasmania (Figures 8.1, 8.2). These diagrams show the timing of the various elements, from which the risks, especially those to the integrity of traps can be defined.

8.4.2: Larapintine Petroleum System

The most promising play in the Wurawina Supergroup (Larapintine Petroleum System) involves the large anticlines that lie near the margins of the Tasmania Basin in the west and southwest of Tasmania. These structures are indicated by geological mapping and in the

seismic sections. The source rock (Gordon Group) is overmature in northern and western Tasmania, while in southern Tasmania they were in the oil window during the Devonian and currently lie in the gas window (Burrett, 1992, Chester 2006).

Figure 8.1 shows the timing of trap formation with respect to hydrocarbon generation. Chester (2006) considered peak generation probably occurred in the Early Devonian. Traps probably weren't formed until the Middle Devonian, therefore a significant charge risk is associated with this initial phase of generation. However, if a second phase of generation occurred from the Middle Jurassic to Cretaceous (Figure 8.1), then these anticlinal plays with the addition of palaeokarst and sub-unconformity traps in southern Tasmania are potential exploration targets. Faulting associated with late Mesozoic and Cenozoic movement is a potential risk to the integrity of these structures. The Bellevue Anticline is affected by Tertiary extension and by later compression (Figures 6.44, 7.29).

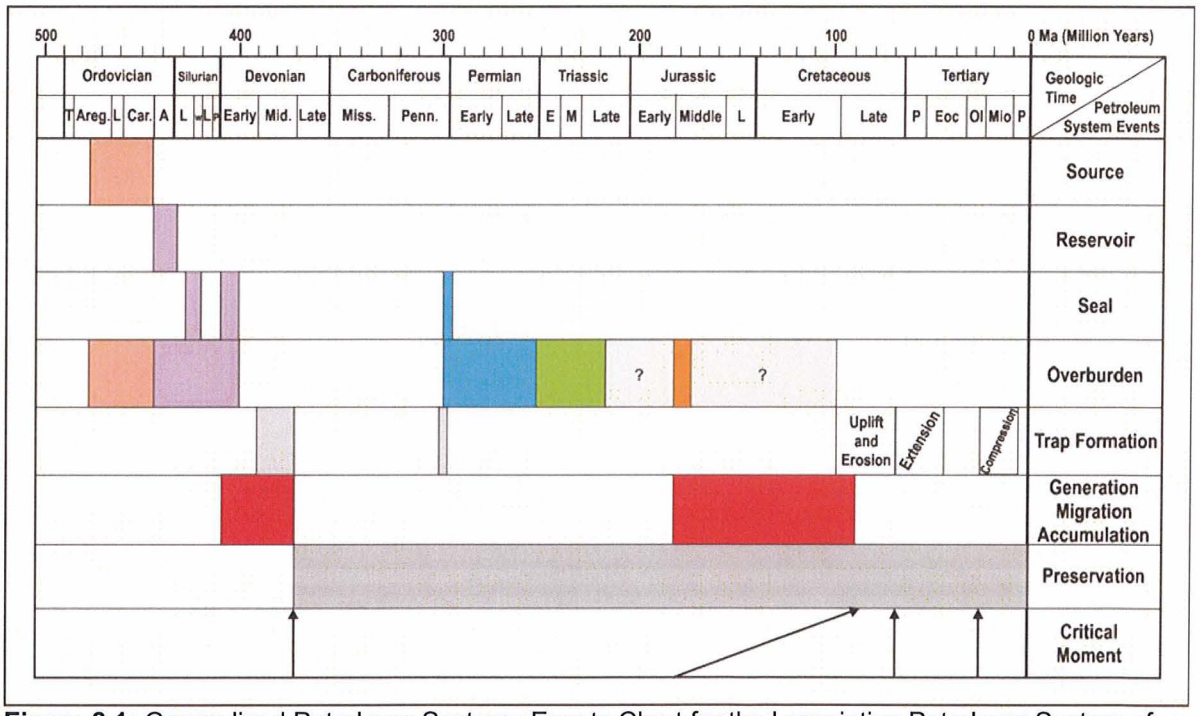

Figure 8.1: Generalised Petroleum Systems Events Chart for the Larapintine Petroleum System of onshore Tasmania.

8.4.3: Gondwana Petroleum System

The structural history suggests that the Tasmania Basin has been affected by three periods of deformation. The first occurring pre- to syn-dolerite intrusion, the second associated with middle to Late Cretaceous uplift and early Tertiary extension, which has probably overprinted/reactivated many structures formed during earlier deformations and finally by mild compression in the Mio-Pliocene (Figure 8.2).

Pre- to syn-dolerite deformation has resulted in the formation of both extensional and compressional structures. Many long wavelength, low amplitude anticlines and fault drag fold traps recognised in the Parmeener Supergroup have been attributed to this period.

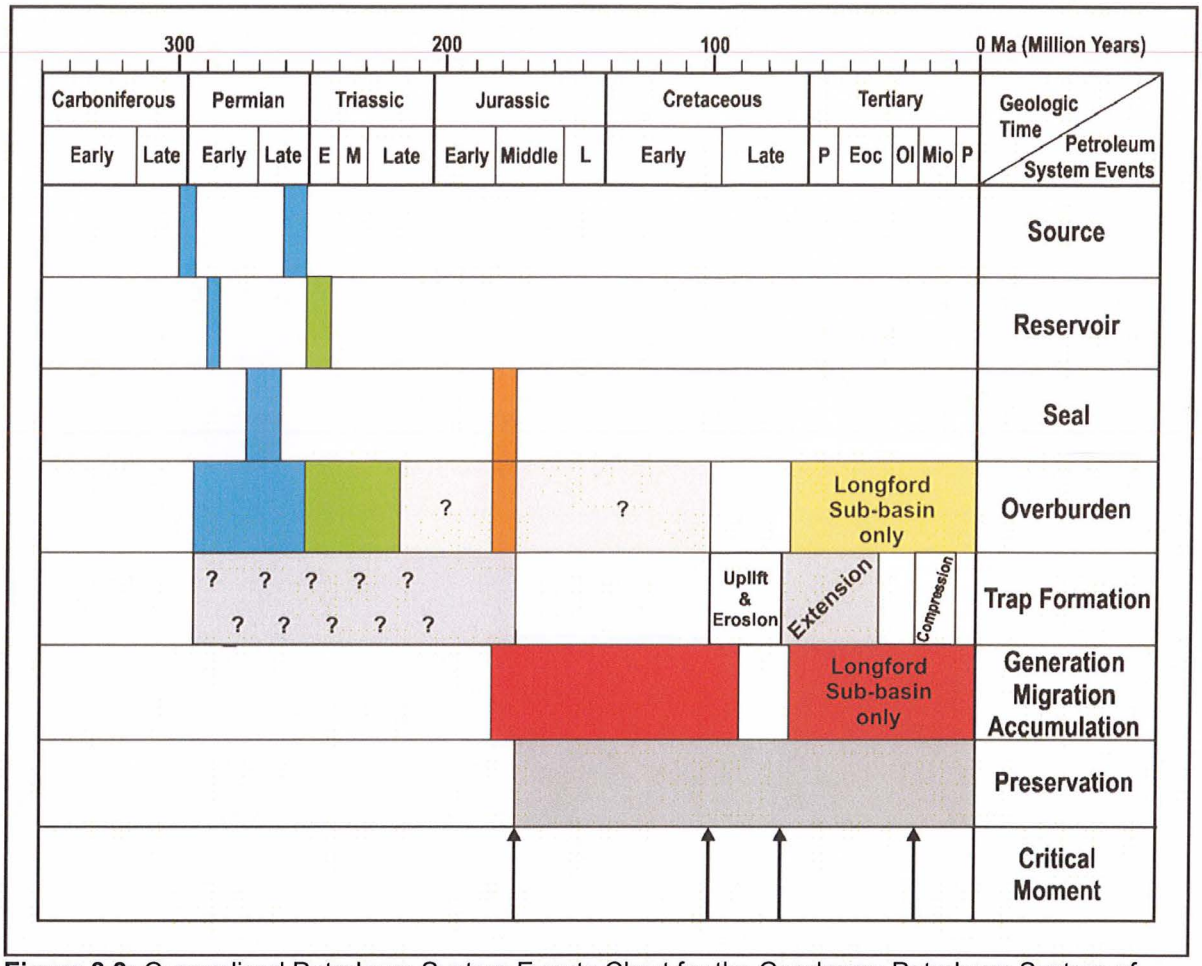

Figure 8.2: Generalised Petroleum System Events Chart for the Gondwana Petroleum System of onshore Tasmania

The most common structures observed in the Tasmania Basin were developed by east-northeast extension in the early Tertiary. In the region covered by the seismic survey they are densest in the Longford Sub-basin and Northern Midlands areas, while concentrated in only a few areas of the Central Highlands (Figures 7.2, 7.7). The number of faults mapped in southern Tasmania where Jurassic Dolerite and Parmeener Supergroup rocks are juxtaposed suggests that Tertiary age structures also dominate the basin in the Derwent and Coal River Grabens.

Assuming generation and migration of hydrocarbons occurred during the Middle Jurassic to Late Cretaceous thermal maximum, traps formed by pre- to syn-dolerite movement are likely to be charged. However, these structures are generally poorly defined, only interpreted on a single seismic line, and many are in zones of poor quality seismic data. Structurally, the best

traps in the Gondwana Petroleum System occur in the Longford Sub-basin and Northern Midlands areas, where several different potential trap styles have been identified (see Chapter 7).

The major risk to traps nominally formed pre- Middle Jurassic is subsequent Cretaceous to Tertiary movement associated with the break-up of Gondwana. Uplift and erosion followed by major extension probably destroyed many traps, remobilising trapped hydrocarbons. In the Central Highlands region, uplift and erosion probably ended hydrocarbon maturation and traps formed by extension probably rely on remobilised hydrocarbons for charge. In the Longford Sub-basin traps formed by early Tertiary extension are also reliant on remobilised hydrocarbons, although the addition of over 800 m of Tertiary sediments may have resulted in the generation of additional hydrocarbons at this time (Figure 8.2).

The effects of Mio-Pliocene compression are poorly understood in Tasmania. However, many of the likely trap structures are fault bounded blocks, therefore fault seal may be important to the integrity of these structures. Mild compression in the Mio-Pliocene may have been advantageous as it kept these faults closed.

8.4.4: Summary

Onshore Tasmania is a challenging petroleum exploration province. Recent work has done much to illustrate its potential; however current understanding of the Larapintine and Gondwana Petroleum Systems in Tasmania is limited. To date there are still many unanswered questions regarding the ability of either system to produce commercial hydrocarbon accumulations.

The major aim of this research was to establish a structural history, an understanding of the type, the timing of formation and distribution of structures formed in and beneath the Tasmania Basin. The interpretation of seismic data reported here indicates structures formed in the basement by the Middle Devonian Tabberabberan Orogeny and in the Tasmania Basin by early Tertiary extension are the most promising exploration targets in terms of their size, extent and the confidence with which they are interpreted. However, the major risk associated with these traps is their timing with respect to predicted maturation and migration of hydrocarbons. Structures in the Tasmania Basin formed prior to the intrusion of dolerite carry less of a charge risk, but many are likely to have been detrimentally affected by later tectonic events. In the basement, trapped Devonian hydrocarbons are unlikely considering the timing

of trap formation. However, anticline, palaeokarst and sub-unconformity plays are valid exploration targets in southern Tasmania, where source rocks are currently in the gas window (Burrett, 1992, Chester 2006).

The continued acquisition of seismic data will be important in constraining the extent of prospective structures revealed by this survey and for finding new prospects. This survey has shown that a major seismic reflection survey can produce workable results for onshore Tasmania. However, the resulting data is patchy. Petroleum explorers in onshore Tasmania are primarily interested in the top one to two seconds (TWT) of survey data and future seismic programs should consider improvements to maximise the quality of data in this region. These should include:

- Sweeping longer at higher frequencies to improve data resolution at the top of the section where it is most important,
- Recent experience has shown that two vibrators rather than three may produce better quality data. Experimentation is required to find the optimal combination of source, vibe-point and geophone spacing for typical geological conditions such as, outcropping dolerite, dolerite at depth and dolerite and Parmeener Supergroup under Tertiary cover,
- Where possible, new lines should be straight and orientated orthogonal to regional strike. This is especially important for delineating dipping basement structures.

With many potential traps in the Central Highlands formed by gentle folds, careful static correction is required to remove any uncertainty regarding their existence. The results of the velocity survey presented here agree with previous estimations and there can now be little doubt regarding the velocity contrast between dolerite and surrounding sediments in the Tasmania Basin section. Careful application of velocity as indicated by rock type during processing to account for this contrast, should do much to improve data quality in the top of the sections.

Onshore Tasmania is not a typical setting for petroleum exploration. The complexities imposed by the major geologic events from Devonian to Recent mean good quality seismic data will be crucial to the discovery of commercial hydrocarbons. Continual refinement of seismic acquisition and processing parameters is necessary to deal with the problems imposed by thick dolerite sills and changing surface conditions, and therefore remove much of the ambiguity seen in the current seismic dataset.

REFERENCES

Golden Software Inc, 2001. Surfer Version 7.04. Help/Contents/Index, type "Blanking File", select blanking file/Faults and Breaklines tab - Faults.

Adams, C. J., Black, L. P. and Green, G. R., 1985. Reconnaissance isotopic studies bearing on the tectonothermal history of Early Palaeozoic & Proterozoic sequences in Western Tasmania. Australian Journal of Earth Sciences. 32, 7-36.

Anand Alwar, M. A., 1960. Geology and Structure of the Middle Derwent Valley. Papers and Proceedings of the Royal Society of Tasmania. 94, 13-24.

Bacon, C. A., 1991. The coal resources of Tasmania. Bulletin of the Geological Survey of Tasmania. 64, 167p.

Bacon, C. A., Calver, C. R., Boreham, C. J., Leaman, D. E., Morrison, K. C., Revill, A. T. and Volkman, J. K., 2000. The petroleum potential of onshore Tasmania: a review. Mineral Resources Tasmania, Geological Survey Bulletin 71. 93p.

Bacon, C. A., Calver, C. R. and Everard, J. L., 1989. Volcanic Rocks. *In:* Burrett, C. F. and Martin, E. L. (Eds), Geology and Mineral Resources of Tasmania. Geological Society of Australia, Special Publication 15, 333-334.

Bacon, C. A. and Everard, J. L., 1981. Pyroclastic in the Upper Parmeener Super-group, near Bicheno, eastern Tasmania. Papers and Proceedings of the Royal Society of Tasmania. 115, 29-36.

Bacon, C. A. and Green, D. C., 1984. A radiometric age for a Triassic tuff from eastern Tasmania. Unpublished Report. Department of Mines, Tasmania. 1984/29.

Baillie, P., 1989. Jurassic-Cainozoic. *In:* Burrett, C. F. and Martin, E. L. (Eds), Geology and mineral resources of Tasmania. Geological Society of Australia, Special Publication 15, 339-409.

Baillie, P. and Pickering, R., 1991. Tectonic Evolution of the Durroon Basin, Tasmania. Exploration Geophysics. 22, 13-17.

Baillie, P. W., 1986. A radiometric age for the Moriarty Basalt, north-western Tasmania, Unpublished Report. Department of Mines, Tasmania, 1986/38.

Baillie, P. W., Bacon, C. A. and Morgan, R., 1986. Geological observations on the Macquarie Harbour beds at Coal Head, western Tasmania. Unpublished Report. Department of Mines Tasmania. UR1986-73.

Baillie, P. W. and Corbett, K. D., 1985. Geological Atlas 1:50000 Series. Sheet 57(7913N). Strahan. Explanatory Report, Geological Survey, Tasmania.

Baillie, P. W. and Hudspeth, J. W., 1989. West Tasmania Region. *In:* Burrett, C. F. and Martin, E. L. (Eds), Geology and mineral resources of Tasmania. Geological Society of Australia, Special Publication 15, 361-365.

Baillie, P. W. and Leaman, D. E., 1989. Southeastern Tasmania. *In:* Burrett, C. F. and Martin, E. L. (Eds), Geology and Mineral Resources of Tasmania. Geological Society of Australia, Special Publication 15, 365-367.

Baillie, P. W., Powell, M. C., Banks, M. R. and Hills, P. B., 1989a. The Eastern Tasmania Terrane. *In:* Burrett, C. F. and Martin, E. L. (Eds), Geology and mineral resources of Tasmania. Geological Society of Australia, Special Publication 15, Hobart, 234-237.

Baillie, P. W., Quilty, P. G. and Richardson, R. G., 1989b. East Tasmania Region. *In:* Burrett, C. F. and Martin, E. L. (Eds), Geology and Mineral Resources of Tasmania. Geological Society of Australia, Special Publication 15, 367-368.

Banks, M. R., 1973. General geology. *In:* Banks, M. R. (Eds), The lake Country of Tasmania: a symposium conducted by the Royal Society of Tasmania at Poatina, Tasmania, November 11-12, 1972, 25-34.

Banks, M. R., 1979. A Permian fault in north-western Tasmania. Papers and Proceedings of the Royal Society of Tasmania. 113, 185-191.

Banks, M. R., 1989a. Late Carboniferous to Triassic, Summary and Structural Development. *In:* Burrett, C. F. and Martin, E. L. (Eds), Geology and mineral resources of Tasmania. Geological Society of Australia, Special Publication 15, Hobart, 293-294.

Banks, M. R., 1989b. Wurawina Supergroup (The Western Tasmania Terrane). *In:* Burrett, C. F. and Martin, E. L. (Eds), Geology and mineral resources of Tasmania. Geological Society of Australia, Special Publication 15, Hobart, 183-234.

Banks, M. R. and Clarke, M. J., 1987. Changes in the geography of the Tasmania Basin in the Late Palaeozoic. *In:* McKenzie, G. D. (Eds), Gondwana Six: Stratigraphy, Sedimentology and Paleontology. American Geophysical Union, Washington, 1-14.

Banks, M. R. and Naqvi, I. H., 1967. Some formations close to the Permo-Triassic boundary in Tasmania. Papers and Proceedings of the Royal Society of Tasmania. 101, 17-30.

Banks, M. R. and Read, D. E., 1962. The Malbina Siltstone and Sandstone. Papers and Proceedings of the Royal Society of Tasmania. 96, 19-31.

Barrett, P. J. and Fitzgerald, P. G., 1985. Deposition of the lower Feather Conglomerate, a Permian braided river deposit in southern Victoria Land, Antarctica, with notes on the regional paleogeography. Sedimentary Geology. 45, 189-208.

Barrett, P. J. and McKelvey, B. C., 1981. Permian tillites of South Victoria Land, Antarctica. *In:* Hambrey, M. J. and Harland, W. B. (Eds), Earth's pre-Pleistocene glacial record. Cambridge University Press, Cambridge, 233-236.

Barton, C. M., Bravo, A. P., Gulline, A. B., Longman, M. J., Marshall, B., Mathews, W. L., Moore, W. R., Naqvi, I. H. and Pike, G. P., 1969. Quamby. Geological Atlas 1 Mile Series. Geological Survey of Tasmania, Department of Mines, Hobart.

Bedi, J. C. S., 2003. Reservoir and source rock potential of the Upper Parmeener Supergroup, Tasmania Basin. B. Sc. Honours Thesis (Unpublished), School of Earth Science, University of Tasmania, 116p.

Bendall, M. R., Burrett, C. F. and Askin, H. J., 2000. Petroleum Systems in Tasmania's Frontier Onshore Basins. APPEA Journal. 26-38.

Berry, R. F., 1989a. The history of movement on the Henty Fault Zone, western Tasmania: an analysis of fault striations. Australian Journal of Earth Sciences. 36, 189-205.

Berry, R. F., 1989b. Microstructural evidence for a westward transport direction during middle Cambrian obduction in Tasmania. Geological Society of Australia Abstracts. 24, 8-9.

Berry, R. F., 1994. Tectonics of western Tasmania: Late Precambrian - Devonian. *In:* Cooke, D. R. and Kitto, P. A. (Eds), Contentious issues in Tasmanian Geology, Geological Society of Australia Abstracts, 39, 6-8.

Berry, R. F. and Banks, M. R., 1985. Striations on minor faults and the structure of the Parmeener Super-group near Hobart, Tasmania. Papers and Proceedings of the Royal Society of Tasmania. 119, 23-29.

Berry, R. F. and Crawford, A. J., 1988. Tectonic significance of Cambrian allochthonous mafic-ultramafic complexes in Tasmania. Australian Journal of Earth Sciences. 35, 523-533.

Berry, R. F., Elliott, C. G. and Gray, D. R. (1990) Excursion guide E3: Structure and tectonics of western and northern Tasmania, 10th Australian Geological Convention, Hobart.

Black, L. P., Calver, C. R. and Seymour, D. B., 2004a. New constraints on age correlation of Tasmanian Proterozoic successions from SHRIMP U-Pb detrital zircon dating. Geological Society of Australia Abstracts. 73, 55.

Black, L. P., McClenagan, M. P., Korsch, R. J., Everard, J. L., Calver, C. R., Seymour, D. B., Reed, A. and Foudoulis, C., 2004b. Using SHRIMP to decipher the history of middle Palaeozoic magmatism in Tasmania. Geological Society of Australia Abstracts. 73, 55.

Blackburn, G., 2004. Summary seismic interpretation onshore Tasmania. Report for Great Southland Minerals, by Terratek Petroleum Consultants Pty Ltd, 46p.

Blevin, J. E., 2003. Petroleum Geology of the Bass Basin - Interpretation report, An output of the Western Tasmanian Regional Minerals Program. Geoscience Australia, Record 2003/19.

Bradshaw, M., 1993. Australian Petroleum Systems. PESA Journal. July, 43-53.

Brauns, C. M., Hergt, J. M., Woodhead, J. D. and Maas, R., 2000. Os isotopes and the origin of the Tasmanian dolerites. Journal of Petrology. 41(7), 905-918.

Bravo, A. P. and Pike, G. P., 1969. Amended and renamed groups of the Upper Permian rocks of the Western Tiers area, Tasmania. Technical Report, Department of Mines, Tasmania. TR13_83_85. 3p.

Brown, A. V., 1989. Eo-Cambrian - Cambrian. *In:* Burrett, C. F. and Martin, E. L. (Eds), Geology and mineral resources of Tasmania. Geological Society of Australia, Special Publication 15, 47-84.

Brown, A. V., Calver, C. R., Corbett, K. D., Forsyth, S. M., Goscombe, B. A., Green, G. R., McClenaghan, M. P., Pemberton, J. and Seymour, D. B., 1995. Geology of Southwest Tasmania. Geological Atlas 1:250,000 digital series. Tasmanian Geological Survey,

Brown, A. V., McClenagan, M. P., Turner, N. J., Baillie, P. W., McClenagan, J. and Calver, C. R., 1989. Geological Atlas 1:50 000 Series. Sheet 73 (8112N) Huntley. Explanatory Report, Department of Mines, Tasmania., 110p.

Burns, K. L., 1964. One Mile Geological Map Series, K'55-6-29 - Devonport. Explanatory Report, Department of Mines, Tasmania. 266p.

Burrett, C. F., 1986. Petroleum prospectivity of central southern Tasmania - a preliminary report, Appendix 5. *In*: Bendall, M. R. Bruny Island Oil, EL 29/84, Annual Report, Conga Oil Pty. Ltd., TCR 87-2570.

Burrett, C. F., 1992. Conodont geothermometry in Palaeozoic carbonate rocks of Tasmania and its economic implications. Australian Journal of Earth Sciences. 39 (1), 61-66.

Burrett, C. F., 1997. Report from the Shittim #1 well, March 1997. Great Southland Minerals Pty Ltd, TCR97-3984CF.

Burrett, C. F. and Martin, E. L., 1989. Geology and Mineral Resources of Tasmania. Geological Society of Australia, Special Publication 15, 574p.

Burrett, C. F. and Tanner, D., 1997. Annual Exploration Report. Great Southland Mineral Pty Ltd, Annual Report. 46p.

Caine, N., 1983. The mountains of northeastern Tasmania: a study of alpine geomorphology. Balkema, 200p.

Calver, C. R., 1998. Isotope stratigraphy of the Neoproterozoic Togari Group, Tasmania. Australian Journal of Earth Sciences. 45, 865-874.

Calver, C. R. and Castleden, R. H., 1981. Triassic basalt from Tasmania. Search. 12, 92-103.

Calver, C. R., Clarke, M. J. and Truswell, E. M., 1984. The stratigraphy of a Late Palaeozoic borehole section at Douglas River, Eastern Tasmania: A synthesis of marine macro-invertebrate and palynological data. Papers and Proceedings of the Royal Society of Tasmania. 118, 137-161.

Calver, C. R., Corbett, K. D., Everard, J. L., Goscombe, B. A., Pemberton, J. and Seymour, D. B., 1995. Geology of Northwest Tasmania. Geological Atlas 1:250,000 digital series. Tasmanian Geological Survey,

Calver, C. R. and Walter, M. R., 2000. The late Neoproterozoic Grassy Group of King Island, Tasmania: correlation and palaeogeographic significance. Precambrian Research. 100, 299-312.

Camp, C. L. and Banks, M. R., 1978. A proterosuchian reptile from the Early Triassic of Tasmania. Alcheringa. 2, 143-158.

Campbell, I. B., 1989. The Port Campbell - Netherby north-northwest structural corridor in southeastern Australia. *In:* LeMaitre, R. W. (Eds), Pathways in geology, essays in honour of Edwin Serbon Hills. Blackwell Scientific, 280-303.

Carey, S. W., 1947. Geology of the Launceston District. Records of the Queen Victoria Museum. 2(1), 31-46.
Carey, S. W., 1958. A new technique for the analysis of the structure of Tasmanian dolerite. Dolerite Symposium. University of Tasmania, Geology Department. 130-169.
Chester, A. D., 2006. Petroleum source rocks, maturation and thermal history onshore Tasmania. Ph.D Thesis (Unpublished), School of Earth Science, University of Tasmania., 180p.
Clark, D., Cupper, M., Sandiford, M. and Kiernan, K., in press. Style and timing of late Quarternary faulting on the Lake Edgar Fault, southwest Tasmania, Australia: implications for hazard assessment in intracratonic areas. Geological Society of America. Special publication: Paleoseismicity, 44p.
Clarke, M. J. (1967) Diamond Drill Core Record - Golden Valley 1, Department of Mines - Tasmania.
Clarke, M. J., 1968. A reappraisal of a Lower Permian type section Golden Valley, Tas. Tasmania, Department of Mines, Geological Survey Record No. 7.
Clarke, M. J., 1989. Lower Parmeener Supergroup. *In:* Burrett, C. F. and Martin, E. L. (Eds), Geology and Mineral Resources of Tasmania. Geological Society of Australia, Special Publication 15, 259-306.
Clarke, M. J., 1990. Late Palaeozoic (Tamarian: Late Carboniferous - Early Permian) cold water brachiopods from Tasmania. Alcheringa. 14, 53-76.
Clarke, M. J. and Baillie, P. W., 1984. Geological Atlas 1:50000 Series. Sheet 77(8512N). Maria. Explanatory Report, Geological Survey, Tasmania. 32p.
Clarke, M. J. and Banks, M. R., 1973. The stratigraphy of the Lower (Permo-Carboniferous) Parts of the Parmeener Super-Group, Tasmania. Third Gondwana Symposium. Canberra. 453-467.
Clarke, M. J. and Farmer, N., 1973. Biostratigraphic nomenclature for Late Palaeozoic rocks in Tasmania. Papers and Proceedings of the Royal Society of Tasmania. 110, 91-109.
Clarke, M. J. and Farmer, N., 1983. A diamond drill hole at The Quoin, south-east of Ross. Mineral Resources Tasmania, Rpt No. UR1983_18.
Colhoun, E. A., 1989. Cainozoic Geomorphology. *In:* Burrett, C. F. and Martin, E. L. (Eds), Geology and mineral resources of Tasmania. Geology Society of Australia, Special Publication 15, 403-409.
Collinson, J. W., Isbell, J. L., Elliot, D. H. and Veevers, J. J., 1994. Permian-Triassic Transantarctic basin. *In:* Veevers, J. J. and Powell, M. C. (Eds), Permian-Triassic Pangean Basins and Foldbelts along the Panthalassan Margin of Gondwanaland. Geological Society of America, Memoir 184, 173-222.
Collinson, J. W., Kemp, N. R. and Eggert, T. J., 1987. Comparison of Triassic Gondwana sequences in the Transantarctic mountains and Tasmania. *In:* McKenzie, G. D. (Eds), Gondwana Six: Stratigraphy, sedimentology and paleontology. Geophysical Monograph, 41, 51-61.
Cook, A. C., 2004. Organic petrology and maturation of three samples from Tasmania. Keiraville Konsultants, Unpublished Report. 13p.
Cox, S. F., 1989. Cape Wickham. *In:* Burrett, C. F. and Martin, E. L. (Eds), Geology and mineral resources of Tasmania. Geological Society of Australia, Special Publication 15, Hobart, 154-181.
Crawford, A. J. and Berry, R. F., 1992. Tectonic implications of Late Proterozoic - Early Palaeozoic igneous rock associations in western Tasmania. Tectonophysics. 214, 37-56.
Cromer, W. C., 1980. Late Eocene basalt date from northern Tasmania. Search. 11, 294-295.
Cromer, W. C., 1989. Devonport-Port Sorell Sub-basin. *In:* Burrett, C. F. and Martin, E. L. (Eds), Geology and mineral resources of Tasmania. Geological Society of Australia, Special Publication 15, 361.

Cromer, W. C., 1993. Geology and groundwater resources of the Devonport - Port Sorell - Sassafras Tertiary Basin. Tasmania Department of Mines, Geological Survey Bulletin 67. 91p.
Crowell, J. C. and Frakes, L. A., 1973. The Late Palaeozoic Glaciation. Third Gondwana Symposium. Canberra. 313-331.
Curran, M., 2003. Processing report for Great Southland Minerals Limited, Tasmania Basin, Tasmania, SEL 13/98, 2001 Seismic Data Processing. Great Southland Minerals, 18p.
De Jersey, N. J., 1973. Microspore zones in the lower Mesozoic of southeastern Queensland. Third Gondwana Symposium. Canberra. 159-172.
DeCelles, P. G. and Giles, K. A., 1996. Foreland Basin Systems. Basin Research. 8, 105-123.
Direen, N. G., 1995. Geophysical modelling of the Longford Basin, northern Tasmania. B. Sc. (Hons), Geology, University of Tasmania, Hobart, 131p.
Direen, N. G. and Crawford, A. J., 2003. The Tasman Line: where is it, what is it, and is it Australia's Rodinian breakup boundary? Australian Journal of Earth Sciences. 50, 491-502.
Direen, N. G. and Leaman, D. E., 1997. Geophysical modelling of structure and tectonostratigraphic history of the Longford Basin, northern Tasmania. Exploration Geophysics. 28(1-2), 29-33.
Domack, E. W., 1991. Miscellaneous Data, Stratigraphic Holes: Parmeener Supergroup. Mineral Resources Tasmania, Rpt No. 91_3280. 16p.
Domack, E. W., Burkley, L. A., Domack, C. R. and Banks, M. R., 1993. Facies analysis of the glacial marine pebbly mudstones on the Tasmania Basin: Implications for regional paleoclimates during the late Paleozoic. Gondwana Eight: Assembly, Evolution and Dispersal. Hobart, Tasmania. 471-484.
DPIWE, 2002. 25m Digital Elevation Model, derived 1:25 000 contours. Department of Primary Industries, Water and Environment, Tasmania,
Duddy, I. R., 1992. Assessment of thermal history data from the Durroon - 1 well, Bass Basin. Geotrack International Pty Ltd, Report #386.
Duncan, R. A. and Richards, M. A., 1991. Hotspots, mantle plumes, flood basalts and true polar wander. Reviews of Geophysics. 29, 31-50.
Dunster, J. N., 1981. Some structural complication of the Parmeener Super-group, Tasmania. B.Sc. Honours Thesis (unpublished), School of Earth Sciences, University of Tasmania, Hobart, 115p.
Eggert, J. T., 1983. Petrology, provenance and diagenesis of quartzose and volcanic lithic Triassic fluvial sandstones, Tasmania, Australia. M. Sc. Thesis, Ohio State University, (unpublished).
Elliot, C. G., Woodward, N. B. and Gray, D. R., 1993. Complex regional fault history of the Badger Head region, northern Tasmania. Australian Journal of Earth Sciences. 40, 155-168.
Etheridge, M. A., Branson, J. C. and Stuart-Smith, P. G., 1985. Extensional basin - forming structures in Bass Strait and their importance for hydrocarbon exploration. APEA Journal. 344-361.
Everard, J. L., Reed, A. R., McClenagan, M. P. and Seymour, D. B., 2000. Field excursion guide notes for the Roger, Sumac and Dempster digital 1:25 000 scale geological map sheets, northwestern Tasmania. Mineral Resources Tasmania, UR 2000/02. 16p.
Evernden, J. F. and Richards, J. R., 1962. Potassium-argon ages in eastern Australia. Journal of the Geological Society of Australia. 9(1), 1-37.
Exon, N. F., Berry, R. F., Crawford, A. J. and Hill, P. J., 1997. Geological evolution of the East Tasman Plateau, a continental fragment southeast of Tasmania. Australian Journal of Earth Sciences. 44, 597-608.
Fairbridge, R. W., 1948. Geology of the Country around Waddamana, Central Tasmania. Papers and Proceedings of the Royal Society, Tasmania, 1948., 111-147.

Farley, W., 1995. ACS Laboratories Pty Ltd. Appendix 8. *In:* Slot, J. 1996. Annual report EL1/88,1995, Bruny Island. Great Southland Minerals, TCR 96-3846CF.
Farmer, N., 1985. Geological Atlas 1:50000 Series. Sheet 88(8311N). Kingborough. Explanatory Report, Geological Survey, Tasmania. 105p.
Findlay, R. H., 1993. Summary of structural and stratigraphic observations on the Proterozoic/Eocambrian/Cambrian units of the Zeehan 1:50 000 quadrangle. Mineral Resources Tasmania Report 1993/29. 27p.
Findlay, R. H. and Brown, A. V., 1992. The 10th Legion Thrust, Zeehan district. Distribution, interpretation, and region economic significance. Mineral Resources Tasmania Unpublished Report 1992/02. 27p.
Fleming, T. H., Elliott, D. H., Foland, K. A., Jones, L. M. and Bowman, J. R., 1993. Disturbance of Rb-Sr and K-Ar isotopic systems in the Kirkpatrick Basalt, North Victoria Land, Antarctica. *In:* Findlay, R. H., Unrug, R., Banks, M. R. and Veevers, J. J. (Eds), Gondwana Eight: Assembly, Evolution and Dispersal. University of Tasmania, Hobart, 411-424.
Forsyth, S. M., 1984. Geological atlas 1:50 000 series. Sheet 68 (8313S). Oatlands. Explanatory Report, Geological Survey, Tasmania. 181p.
Forsyth, S. M., 1987. A review of the Upper Parmeener Supergroup. Tasmania Department of Mines, unpublished report. UR1987_01. 43p.
Forsyth, S. M., 1989a. Tamar Graben. *In:* Burrett, C. F. and Martin, E. L. (Eds), Geology and mineral resources of Tasmania. Geological Society of Australia, Hobart, Special Publication 15, 358-361.
Forsyth, S. M., 1989b. Upper Parmeener Supergroup. *In:* Burrett, C. F. and Martin, E. L. (Eds), Geology and Mineral Resources of Tasmania. Geological Society of Australia, Special Publication 15, 309-333.
Forsyth, S. M., Clarke, M. J., Calver, C. R., McClenaghan, M. P. and Corbett, K. D., 1995. Geology of Southeast Tasmania. Geological Atlas 1:250 000 digital series. Tasmanian Geological Survey, Hobart.
Forsyth, S. M., Farmer, N., Gulline, A. B. and Banks, M. R., 1974. Status and subdivision of the Parmeener Super-group. Papers and Proceedings of the Royal Society of Tasmania. 108, 107-109.
Forsyth, S. M., Sutherland, F. L. and Bacon, C. A., 1989. Geological atlas 1:50 000 series. Sheet 61 (8313N). Interlaken. Explanatory Report, Geological Survey, Tasmania. 90p.
Fournier, P., 2000. The design of a Sonde used to measure Seismic Velocities and Temperature, Tasmania Basin. Honours (unpublished), School of Earth Sciences, University of Tasmania, Hobart, 91p.
Gee, R. D. and Legge, P. J., 1979. One Mile Geological Map Series. Zone 7, Sheet No. 30 (8215N). Beaconsfield. Explanatory Report, Department of Mines, Tasmania. 121p.
Goscombe, B. D., Findlay, M. P., McClenagan, M. P. and Everard, J. L., 1994. Multiscale kinking in NE Tasmania: crustal shortening at shallow crustal levels. Journal of Structural Geology. 16, 1077-1092.
Green, D. H., 1959. Geology of the Beaconsfield District, including the Andersons Creek Ultrabasic Complex. Records of the Queen Victoria Museum, 10.
Gulati, J. S. and Stewart, R. R., 1997. Analysis of mode conversions over high velocity layers. CREWES Research Report - Volume 9, 25-1 - 25-8.
Gulline, A. B., 1963. Explanatory Report, One Mile Geological Map Series, K'55-10-59 - St Clair. Department of Mines, 43p.
Gulline, A. B., Longman, M. J. and Mathews, W. L., 1963. St. Clair. Geological Atlas 1 Mile Series. Geological Survey of Tasmania, Department of Mines, Hobart.
Gurnis, M., 1992. Rapid continental subsidence following the initiation and evolution of subduction. Science. 255, 1556-1558.

Hand, S. J., 1993. Palaeogeography of Tasmania's Permo-Carboniferous glacigenic sediments. Gondwana Eight: Assembly, Evolution and Dispersal. Hobart, Tasmania. 459-468.

Hergt, J. M., McDougall, I., Banks, M. R. and Green, D. H., 1989. Jurassic Dolerite. *In:* Burrett, C. F. and Martin, E. L. (Eds), Geology and mineral resources of Tasmania. Geological Society of Australia, Special Publication 15, 375-381.

Hill, K. C., Hill, K. A., Cooper, G. T., O'Sullivan, A. J., O'Sullivan, P. B. and Richardson, M. J., 1995. Inversion around the Bass Basin, SE Australia. *In:* Buchanan, J. G. and Buchanan, P. G. (Eds), Basin Inversion. Geological Society, Special Publication 88, 88, 525-547.

Hill, P. J., Meixner, A. J., Moore, A. M. G. and Exon, N. F., 1997. Structure and development of the West Tasmanian offshore sedimentary basins; results of recent marine and aeromagnetic surveys. Australian Journal of Earth Sciences. 44(5), 579-596.

Hillis, R. R. and Reynolds, S. D., 2000. The Australian Stress Map. Journal of the Geological Society of London. 157(Part 5), 915-921.

Hills, L., 1921. Search for oil in Tasmania. Unpublished Report, Department of Mines Tasmania, 1920-22, 1-9.

Hills, L., 1922. Tasmania's liquid petroleum possibilities not worth investigating. Unpublished Report, Department of Mines Tasmania, 1920-22, 99-101.

Hinch, A. J., 1965. A gravity survey of the Cressy area, northern Tasmania. B.Sc. (Hons) Thesis, School of Earth Science, University of Tasmania, Hobart,

Holm, O. H. and Berry, R. F., 2002. Structural history of the Arthur Lineament, northwest Tasmania: an analysis of critical outcrops. Australian Journal of Earth Sciences. 49, 167-185.

Holm, O. H., Crawford, A. J. and Berry, R. F., 2003. Geochemistry and tectonic significance of mafic rocks in the Arthur Lineament, western Tasmania. Australian Journal of Earth Sciences. 50, 903-918.

James, C. E., 1950. Report of the Tasmanian Oil Shale Investigation Committee. Tasmanian Department of Mines, GSMR08_2. 210p.

Jennings, D. J. and Sutherland, F. L., 1969. Geology of the Cape Portland area, with special reference to the Mesozoic(?) appinitic rocks. Department of Mines Tasmania, Technical Report 13. 45-81.

Jennings, I. B., 1963. Explanatory Report, One Mile Geological Map Series, K'55-6-45, Middlesex. Department of Mines, Tasmania, 151p.

Jennings, I. B., Macleod, W. N., Burns, K. L., Jack, R. H., Mathews, W. L., Robinson, R. G. and Threader, V. M., 1961. Du Cane. Geolocial Atlas, 1 Mile Series, Zone 7, Sheet N.o. 52. Geological Survey of Tasmania, Department of Mines, Hobart.

Johnston, R. M., 1874. The Launceston Tertiary Basin. Papers and Proceedings of the Royal Society of Tasmania. 53-62.

Johnston, R. M., 1888. A systematic account of the geology of Tasmania. J. Walch and Sons, 408p.

Kiernan, K., 1995. An Atlas of Tasmanian Karst. Tasmanian Forest Research Council Inc, Research report No.10, Vol 1. 351p.

Kohn, B. P., Gleadow, A. J. W., Brown, R. W., Gallagher, K., O'Sullivan, P. B. and Foster, D. A., 2002. Shaping the Australian crust over the last 300 million years: insights from fission track thermotectonic imaging and denudation studies of key terranes. Australian Journal of Earth Sciences. 49(4), 697-717.

Laird, M. G. and Bradshaw, J. D., 1981. Permian tillites of North Victoria Land, Antarctica. *In:* Hambrey, M. J. and Harland, W. B. (Eds), Earth's pre-Pleistocene glacial record. Cambridge University Press, Cambridge, 237-240.

Lane, P., 2002. Seismic Interpretation and Basin Analysis of the Longford Sub-Basin. B.Sc Honours Thesis (unpublished), School of Earth Sciences, University of Tasmania, Hobart, 94p.
Leaman, D. E., 1971. The geology and groundwater resources of the Coal River Basin. Tasmanian Department of Mines, Underground water supply paper, 7. 101p.
Leaman, D. E., 1972. Gravity survey of the Hobart District. Tasmania Department of Mines, Geological Survey Bulletin 52. 52p.
Leaman, D. E., 1975. Form, mechanism, and control of dolerite intrusion near Hobart, Tasmania. Journal of the Geological Society of Australia. 22(2), 175-186.
Leaman, D. E., 1976. Hobart, Tasmania. Geological Atlas 1:50 000 Series. Tasmania Department of Mines, Explanatory Report. Zone 7 Sheet 82(8312S). 116p.
Leaman, D. E., 1990. Inferences concerning the distribution and composition of pre-Carboniferous rocks in southeastern Tasmania. Papers and Proceedings of the Royal Society of Tasmania. 124, 1-12.
Leaman, D. E., 1992. Finding Cambrian Keys: An essay in controversy, prospectivity and tectonic implications. Bulletin of the Geological Survey of Tasmania 70. 124-148.
Leaman, D. E., 1994. The Tamar Fracture System in Tasmania: Does it exist? Australian Journal of Earth Sciences. 41, 73-74.
Leaman, D. E., 1996. Evaluation of AGSO seismic lines T4, T5 Tasmania for Great Southland Minerals. Mineral Resources Tasmania, Rpt. No. 96_3873. 7p.
Leaman, D. E., 2001. Step into history in Tasmanian Reserves. Leaman Geophysics, 416p.
Leaman, D. E., 2002. The Rock which makes Tasmania. Leaman Geophysics,
Leaman, D. E. and Richardson, R. G., 1990. Tasmanian crustal features. Gondwana: Terranes and resources. Tenth Australian Geological Convention, Geological Society of Australia Abstracts - 25. Hobart. 100-101.
Logan, G. A., Calver, C. R., Gorian, P., Summons, R. E., Hayes, J. M. and Walter, M. R., 1999. Terminal Proterozoic mid-shelf benthic microbial mats in the Centralian Basin and their environmental significance. Geochemica et Cosmochimica Acta. 63, 1345-1358.
Longman, M. J., 1966. Launceston, Tasmania. Geological Atlas 1 Mile Series. Tasmanian Department of Mines, Explanatory Report. Sheet 39 (8315S).
Longman, M. J. and Leaman, D. E., 1971. Gravity survey of the Tertiary Basins in northern Tasmania. Tasmania Department of Mines, Bulletin of the Geological Survey of Tasmania 51.
Lucarelli, L. J., 1965. Oil and gas exploration in southeastern Tasmania. Unpublished Report, Mines Department Tasmania. 65-0408, 13p.
Macleod, W. N., Jack, R. H. and Threader, V. M., 1961. One Mile Geological Map Series, K'55-11-52 - Du Cane. Explanatory Report, Department of Mines, Tasmania. 39p.
Martini, I. P. and Banks, M. R., 1989. Sedimentology of the cold-climate, coal-bearing, Lower Permian "Lower Freshwater Sequence" of Tasmania. Sedimentary Geology. 64, 25-41.
Mathews, W. L., 1983. Geology and groundwater resources of the Longford Tertiary Basin. Tasmanian Department of Mines, Geological Survey Bulletin 59. 152p.
Mathews, W. L., 1989. Longford Sub-Basin. *In:* Burrett, C. F. and Martin, E. L. (Eds), Geology and mineral resources of Tasmania. Geological Society of Australia, Special Publication 15, 370-372.
Mathews, W. L., Everard, J. L. and Clarke, M. J., 1996. Geological atlas 1:50 000 series. Sheet 54 (8314S). Lake River. Explanatory Report, Geological Survey, Tasmania. 84p.
Maynard, B. R., 1996. Reservoir characterisation of the Liffey/Faulkner Group. B.Sc. Honours Thesis (Unpublished), School of Earth Science, University of Tasmania, 80p.

McClay, K. R., Dooley, T., Whitehouse, P. and Mills, M., 2002. 4-D evolution of rift systems: Insights from scaled physical models. AAPG Bulletin. 86(6), 935-959.
McClay, K. R. and White, M. J., 1995. Analogue modelling of orthogonal and oblique rifting. Marine and Petroleum Geology. 12, 137-151.
McClenaghan, M. P. and Calver, C. R., 1994. Geology of Northeast Tasmania. Geological Atlas 1:250,000 digital series. Tasmanian Geological Survey,
McDougall, I. and Green, D. C., 1982. Appendix 3. Cretaceous K/Ar ages from northeastern Tasmania. *In:* McClenaghan, M. P., Turner, N. J., Ballie, P. W., Brown, A. V., Williams, P.R., Moore, W. R. (Eds), Geology of the Ringarooma-Boobyalla area. Bulletin Geological Survey Tasmania 61.
McDougall, I. and Leggo, P. J., 1965. Isotopic age determinations on granitic rocks from Tasmania. Journal of the Geological Society of Australia. 12, 295-332.
McKellar, J. B. A., 1957. Geology of the Western Tiers near Great Lake, Tasmania. Records of the Queen Victoria Museum, 7. 1-13.
Meffre, S., Berry, R. F. and Hall, M., 2000. Cambrian metamorphic complexes in Tasmania: tectonic implications. Australian Journal of Earth Sciences. 47, 971-985.
Michon, L. and Sokoutis, D., 2005. Interaction between structural inheritance and extensional direction during graben and depocentre formation: An experimental approach. Tectonophysics. 409, 125-146.
Mitrovica, J. X., Beaumont, C. and Jarvis, G. T., 1989. Tilting of continental interiors by the dynamic effects of subduction. Tectonics. 8, 1079-1094.
Moore, A. M. G., 1991. Western Tasmanian margin + seismic interpretation and mapping. Bureau of Mineral Resources Record, 1991/70 (unpublished),
Moore, A. M. G., Willcox, J. B., Exon, N. F. and O'Brien, G. W., 1992. Continental shelf basins on the west Tasmania margin. APEA Journal.
Moore, W. R., 1972. A re-interpretation of previous drilling and seismic survey in the western section of the northern plains, Gladstone. Mineral Resources Tasmania, Rpt. No. UR1972_52. 11pp., 2 tab.
Moore, W. R., 1989. Scottsdale Sub-basin. *In:* Burrett, C. F. and Martin, E. L. (Eds), Geology and Mineral Resources of Tasmania. Geological Society of Australia, Special Publication 15, 369-370.
Moore, W. R., Baillie, P. W., Forsyth, S. M., Hudspeth, J. W., Richardson, R. G. and Turner, N. J., 1984. Boobyalla Sub-basin: A Cretaceous onshore extension of the southern edge of the Bass Basin. APEA Journal. 24, Part 1, 110-117.
Morley, C. K., 1995. Developments in the structural geology of rifts over the last decade and their impact on hydrocarbon exploration. *In:* Lambiase, J. J. (Eds), Hydrocarbon Habitat in Rift Basins. Geological Society Special Publication No. 80, London, 1-32.
Morley, C. K., 1999a. How successful are analogue models in addressing the influence of pre-existing fabrics on rift structure? Journal of Structural Geology. 21, 1267-1274.
Morley, C. K., 1999b. Influence of Preexisting Fabrics on Rift Structure. *In:* Morley, C. K. (Eds), Geoscience of Rift Systems - Evolution of East Africa. AAPG Studies in Geology No. 44, 151-160.
Muller, R. D., Gaina, C. and Clark, S., 2000. Seafloor spreading around Australia. *In:* Veevers, J. J. (Eds), Billion-year earth history of Australia and neighbours in Gondwanaland. Gemoc Press, Sydney, 18-27.
O'Driscoll, E. S. T., 1990. Lineament tectonics of Australian ore deposits. *In:* Hughes, F. E. (Eds), Geology and mineral deposits of Australia and Papua New Guinea. Aus. IMM, 33-41.
O'Sullivan, A. J. and Kohn, B. P., 1997. Apatite Fission Track Thermochronology of Tasmania. Australian Geodynamics Cooperative Research Centre, School of Earth Sciences, La Trobe University, AGSO Record 1997/35. 61p.

O'Sullivan, A. J., O'Sullivan, P. B. and Hill, K. C., 1996. Late Mesozoic and Cenozoic thermotectonic evolution of Tasmania. *In:* Kennard, J. M. (Eds), Abstracts - Geological Society of Australia, vol.41. Geological Society of Australia, Sydney, 326.

O'Sullivan, P. B., Kohn, B. P. and O'Sullivan, A. J., 1998. Cretaceous and Tertiary Thermotectonic Evolution of Tasmania. Australia Geological Survey Organisation, AGSO Record 1998/2. 144-146.

O'Sullivan, P. B., Kohn, B. P., O'Sullivan, A. J. and Gleadow, A. J. W., 2000a. Mesozoic to Cenozoic thermotectonic evolution of Tasmania: reconciling geological observations with thermochronology data from within a triple rift system. FT 2000, 9th International Conference on Fission Track Dating and Thermochronology. Geological Society of Australia, Abstracts Number 58, 251-253.

O'Sullivan, P. B., Mitchell, M. M., O'Sullivan, A. J., Kohn, B. P. and Gleadow, A. J. W., 2000b. Thermotectonic history of the Bassian Rise, Australia: implications for the breakup of eastern Gondwana along Australia's southeastern margins. Earth and Planetary Science Letters. 182(1), 31-47.

Papworth, T. J., 1985. Seismic exploration over basalt covered areas of the U.K. First Break. 3(4), 20-32.

Parkinson, W. D. and Hermanto, R., 1986. The Tamar conductivity anomoly. Exploration Geophysics. 17, 34-35.

Parkinson, W. D., Hermanto, R., Sayers, J., Bindoff, N. L., Dosso, H. W. and Nienaber, W., 1988. The Tamar conductivity anomaly. Physics of the Earth and Planatary Interiors. 52, 8-22.

Parkinson, W. D. and Richardson, R. G., 1989. The Magnetic Field. *In:* Burrett, C. F. and Martin, E. L. (Eds), Geology and mineral resources of Tasmania. Geological Society of Australia, Special Publication 15, Hobart, 455-458.

Patison, N. L., Berry, R. F., Davidson, G. J., Taylor, B. P., Bottrill, R. S., Manzi, B., Ryba, J. and Shepherd, R. E., 2001. Regional metamorphism of the Mathinna Group, northeast Tasmania. Australian Journal of Earth Sciences. 48 (2), 281-292.

Pike, G. P., Threader, V. M. and Moore, W. R., 1973. One Mile Geological Map Series. Zone 7, Sheet No. 46 (8219N). Quamby. Explanatory Report, Department of Mines, Tasmania. 56p.

Pujol, J., Fuller, B. N. and Smithson, S. B., 1989. Interpretation of vertical seismic profile conduceted in the Columbia Plateau Basalts. Geophysics. 54(10), 1258-1266.

Rao, C. P., 1981. Criteria for recognition of cold-water carbonate sedimentation: Berridale Limestone (Lower Permian), Tasmania, Australia. Journal of Sedimentary Petrology. 51, 491-506.

Rao, C. P., 1988. Oxygen and carbon isotope composition of cold-water Berridale Limestone (Lower Permian), Tasmania, Australia. Sedimentary Geology. 60, 221-231.

Reed, A. R., Calver, C. R. and Bottrill, R. S., 2002. Palaeozoic suturing of eastern and western Tasmania in the west Tamar region: implications for the tectonic evolution of southeast Australia. Australian Journal of Earth Sciences. 49, 809-830.

Reid, C. M., 2003. Permian Bryozoa of Tasmania and New South Wales: systematics and their use in Tasmanian biostratigraphy. Memoirs of the Association of Australasian Palaeontologists. 133p.

Reid, C. M., 2004. The Tasmania Basin - Gondwanan Petroleum System, Final Report. Unpublished Report for Great Southland Minerals Limited. 31p.

Reid, C. M., Chester, A. D., Stacey, A. R. and Burrett, C. F., 2003. Stratigraphic results of diamond drilling of the Hunterston Dome, Tasmania: implications for palaeogeography and hydrocarbon potential. Papers and Proceedings of the Royal Society of Tasmania. 137, 87-94.

Reid, C. M., Forsyth, S. M. and Clarke, M. J., in prep. The Parmeener Supergroup. *In:* Corbett, K. D. and Quilty, P. G. (Eds), The Geological Evolution of Tasmania. Geological Society of Australia, Tasmanian Division, Hobart.

Revill, A. T., 1996. Hydrocarbons isolated from Lanna Vale seep. Swab of bitumen samples. CSIRO Division of Oceanography, TDR-1.

Rice, P. J., 1997. Topographic and Hydrologic Modelling applied to Mineral Exploration. M.Sc Thesis, School of Earth Science, University of Tasmania, Hobart, 226p.

Richardson, R. G., 1987. An experimental seismic reflection survey on Bruny Island. Mineral Resources Tasmania, UR1987-53. 8p.

Richardson, R. G. and Leaman, D. E., 1980. A seismic reflection traverse on the Seymour Coalfield. Mineral Resources Tasmania, UR1980-45. 7p.

Richardson, R. G. and Leaman, D. E., 1981. Fingal Tier Seismic Reflection Traverses 1 and 2. Mineral Resources Tasmania, UR1981-06. 12p.

Riley, T. R. and Knight, K. B., 2001. Review: Age of pre-break-up Gondwana magmatism. Antarctic Science. 13(2), 99-110.

Rosetti, F., Lisker, F., Storti, F. and Laufer, A. L., 2003. Tectonic and denudational history of the Rennick Graben (Northern Victoria Land): Implications for the evolution of rifting between East and West Antarctica. Tectonics. 22 (2)(11), 1-18.

Royer, J. Y. and Rollet, N., 1997. Plate-tectonic setting of the Tasmanian region. Australian Journal of Earth Sciences. 44, 543-560.

Sahagian, D. L. and Collinson, J. W., 1993. Gondwanan Foreland basin along the Panthalassan margin of Antarctica. Gondwana Eight: Assembly, Evolution and Dispersal. Hobart, Tasmania. 497-506.

Schmidt, P. W. and McDougall, I., 1977. Paleomagnetic and potassium-argon dating studies of the Tasmanian dolerites. Journal of the Geological Society of Australia. 21, 91-106.

Schwab, F. L., 1986. Sedimentary 'signitures' of foreland basin assemblages: real or counterfeit? *In:* Allen, P. A. and Homewood, P. (Eds), Foreland Basins. International Association of Sedimentologists, Special Publication 8, 395-410.

Seymour, D. B., in prep. *In:* Corbett, K. D. and Quilty, P. G. (Eds), The Geological Evolution of Tasmania. Geological Society of Australia, Tasmanian Division, Hobart.

Seymour, D. B. and Calver, C. R., 1995. Explanatory notes for the Time-Space Diagram and Stratotectonic Elements Map of Tasmania. Tasmanian Geological Survey Record 1995/01,

Seymour, D. B., Green, G. R. and Calver, C. R., 2006. The geology and mineral deposits of Tasmania: a summary. Mineral Resources Tasmania, Geological Survey Bulletin 72. 32p.

Sharples, C. and Klootwijk, C. T., 1981. Paleomagnetic results from the Gordon Subgroup of Tasmania: further evidence for a Late Cretaceous magnetic overprint in southeastern Australia. Papers and Proceedings of the Royal Society of Tasmania. 115, 85-91.

Sharples, C. E., 1984. Distribution of Clay Types, Halite and Gypsum in Early Triassic Sandstones Drilled near Bothwell. Mineral Resources Tasmania, Rpt. No. UR1984_27. 4p.

Shaw, R. W., 1982. Report on the Oyster Bay seismic survey, Swansea, Tasmania, PEL20/81. Meekatharra Minerals Limited, UR83-1957. 96p.

Shaw, R. W., 1985. Relinquishment report on PEL 20/81 for Meekatharra Minerals. Flower Doery Buchan Pty. Ltd., 85-2369.

Shearman, D. J. and Smith, A. J., 1985. Ikaite, the parent material of jarrowite-type pseudomorphs. Proceedings of the Geological Association. London. 96, 305-314.

Siddoway, C. S., Baldwin, S. L., Fitzgerald, P. G., Fanning, C. M. and Luyendyk, B. P., 2004a. Ross Sea mylonites and the timing of intracontinental extension within the West Antarctic rift system. Geology. 32, 57-60.

Siddoway, C. S., Richard, S. M., Fanning, C. M. and Luyendyk, B. P., 2004b. Origin and emplacement of a middle Cretaceous gneiss dome, Fosdick Mountains, West Antarctica. *In:* Whitney, D. L., Teyssier, C. and Siddoway, C. S. (Eds), Gneiss Domes in Orogeny. Geological Society of America, Special Paper, 380, 267-294.

St. John, B., 1990. Antarctica - Geology and Hydrocarbon Potential. *In:* St. John, B. (Eds), Antarctica as an exploration frontier; hydrocarbon potential, geology and hazards. AAPG, Tulsa, 31, 55-100.

Stacey, A. R. and Berry, R. F., 2004. The structural history of Tasmania, a review for petroleum explorers. Eastern Australasian Basins Symposium 2. Adelaide. 151-162.

Suess, E., Blazer, W., Hess, E. K. S., Muller, P. J., Ungerer, P. J. and Wefer, G., 1982. Calcium carbonate hexahydrate from organic-rich sediments of the Antarctic shelf: precursor of glendonites. Science. 1216, 1128-1131.

Summons, T. G., 1981a. Progress Report to 21/8/81 Exploration Licence 31/80. Rpt No. 81_1587. 367.

Summons, T. G., 1981b. Summary of limestone investigations in the Lune River area. Department of Mines, Tasmania, Unpublished Report 1981/28.

Summons, T. G., 1982. Renewal and Progress Report for Exploration Licence 31/80 for period November 21, 1981 - May 21, 1982. Progress Report. Rpt. No. 82_1767. 115p.

Sutherland, F. L., 1966. Considerations on the emplacement of the Jurassic dolerites of Tasmania. Papers and Proceedings of the Royal Society of Tasmania. 100, 133-145.

Sutherland, F. L., 1989. Tertiary Volcanism. *In:* Burrett, C. F. and Martin, E. L. (Eds), Geology and mineral resources of Tasmania. Geological Society of Australia, Hobart, Special Publication 15.

Sutherland, R., 1999. Basement geology and tectonic development of the Greater New Zealand region: an interpretation from regional magnetic data. Tectonophysics. 308, 341-362.

Tessensohn, F., 1994. The Ross Sea region, Antarctica: structural interpretation in relation to the evolution of the Southern Ocean. Terra Antarctica. 1, 553-558.

Truswell, E. M., 1978. Palynology of the Permo-Carboniferous in Tasmania: an interim report. Tasmanian Department of Mines, Geol. Surv. Bull. 56.

Turner, N. J., 1989. The Precambrian. *In:* Burrett, C. F. and Martin, E. L. (Eds), Geology and mineral resources of Tasmania. Geological Society of Australia, Special Publication 15, Hobart, 5-46.

Turner, N. J., Black, L. P. and Kamperman, M., 1998. Dating the Neoproterozoic and Cambrian orogenies in Tasmania. Australian Journal of Earth Sciences. 45, 789-806.

Turner, N. J. and Calver, C. R., 1987. Geological Atlas 1:50000 Series. Sheet 49(8514N). St Marys. Explanatory Report, Geological Survey, Tasmania. 159p.

Twelvetrees, W. H., 1917. The search for petroleum in Tasmania.

Veevers, J. J., 1984. Phanerozoic earth history of Australia. Clarendon Press,

Veevers, J. J., 2000a. Mid-Cretaceous and Mid-Eocene events in the Indo-Australian and Antarctic Plates. *In:* Veevers, J. J. (Eds), Billion-year earth history of Australia and neighbours in Gondwanaland. GEMOC Press, Sydney, 102-109.

Veevers, J. J., 2000b. Permian - Triassic Pangean basins and foldbelts along the Panthalassan margin of Eastern Australia. *In:* Veevers, J. J. (Eds), Billion-year earth history of Australia and neighbours in Gondwanaland. GEMOC Press, Sydney, 235-252.

Veevers, J. J., 2000c. Permian - Triassic Pangean basins and foldbelts along the Panthalassan margin of Gondwanaland. *In:* Veevers, J. J. (Eds), Billion-year earth history of Australia and neighbours in Gondwanaland. GEMOC Press, Sydney, 292-308.

Veevers, J. J., Collinson, J. W. and Lopez-Gamundi, O. R., 1994a. Synthesis. *In:* Veevers, J. J. and Powell, M. C. (Eds), Permian-Triassic Pangean Basins and Foldbelts along the Panthalassan Margin of Gondwanaland. Geological Society of America, Memoir 184, 331-353.

Veevers, J. J., Conaghan, P. J. and Powell, M. C., 1994b. Eastern Australia. *In:* Veevers, J. J. and Powell, M. C. (Eds), Permian-Triassic Pangean Basins and Foldbelts along the Panthalassan Margin of Gondwanaland. Geological Society of America, Memoir 184, 11-171.

Voisey, A. H., 1948a. The Geology and Country around Great Lake, Tasmania. Papers and Proceedings of the Royal Society of Tasmania. 95-104.

Voisey, A. H., 1948b. The Geology and Country between Arthur's Lakes and the Lake River, Tasmania. Papers and Proceedings of the Royal Society of Tasmania. 105-111.

Webb, J. A., 1981. A radiometric time scale of the Triassic. Journal of the Geological Society of Australia. 28, 107-121.

White, R. and McKenzie, D., 1989. Magmatism at rift zones: the generation of volcanic continental margins and flood basalts. Journal of Geophysical Research. 94, 7685-7729.

Willcox, J. B., Baillie, P. W., Exon, N., Lee, C. S. and Thomas, B., 1989. The geology of western Tasmania and its continental margin - with particular reference to petroleum potential. Record of the Bureau of Mineral Resources Geology and Geophysics of Australia 1989/13,

Williams, A., 1985. Final Report on E.L. 30/80. Rpt No. 84_2116. 165p.

Williams, E., 1979. Tasman fold belt system in Tasmania. Explanatory notes for the 1:500 000 structural map of Pre-Carboniferous rocks of Tasmania. Department of Mines, Tasmania, Revised Edn, 29p.

Williams, E., 1989. Summary and Synthesis, Upper Parmeener Supergroup. *In:* Burrett, C. F. and Martin, E. L. (Eds), Geology and Mineral Resources of Tasmania. Geological Society of Australia, Special Publication 15, 492-493.

Williamson, P. E., Pigram, C. J., Colwell, J. B., Scherl, A. S., Lockwood, K. L. and Branson, J. C., 1987. Review of stratigraphy, structure , and hydrocarbon potential of the Bass Basin, Australia. AAPG Bulletin. 71, 253-280.

Wilstshire, M. J., 1980. Oil shale, coal and petroleum prospects. Appendix 2. *In*: Eshuys, E., Smith, J. O. 1981. Renewal and progress report to May 21 1981. Tasmania Exploration Licence 31/80. Victor Petroleum and Resources, TCR 81-1562.

Withers, R., Eggers, D., Fox, T. and Crebs, T., 1994. A case study of intergrated hydrocarbon exploration through basalt. Geophysics. 59(11), 1666-1679.

Woods, T. J., 1995. Petroleum prospectivity of the Palaeozoic, southeast Tasmania. B.Sc Honours Thesis (Unpublished), School of Earth Science, University of Tasmania.,

Wu, J., 1996. Potential pitfalls of crooked-line seismic reflection surveys. Geophysics. 61(1), 277-281.

Wythe, S. and Watson, M., 1996. Geochemical evaluation of an oil seep from Lonnavale, Tasmania. AMDEL Petroleum Services, Rpt N.o: LQ4496, Unpublished Report for Great Southland Minerals Limited.

Young, I. M., Trupp, M. A. and Gidding, M. J., 1991. Tectonic Evolution of Bass Strait - Origins of Tertiary Inversion. Exploration Geophysics. 22, 465-468.

APPENDIX 1

LOCALITIES MENTIONED IN THE TEXT

Place	Easting	Northing
Beaconsfield	484 675 mE	5 439 499 mN
Bellevue Tier	456 924 mE	5 349 413 mN
Ben Lomond	555 986 mE	5 393 888 mN
Bicheno	608 181 mE	5 362 925 mN
Birches Bay	519 044 mE	5 219 416 mN
Bothwell	499 838 mE	5 308 232 mN
Bridgewater	518 683 mE	5 268 356 mN
Bronte Park	457 893 mE	5 334 822 mN
Bruny Island	527 455 mE	5 207 788 mN
Campbell Town	540 665 mE	5 358 496 mN
Cape Portland	582 659 mE	5 487 572 mN
Conara	536 416 mE	5 368 845 mN
Cressy	506 456 mE	5 429 381 mN
Cygnet	506 235 mE	5 224 498 mN
Dazzler Range	475 722 mE	5 437 834 mE
Deloraine	471 396 mE	5 402 721 mN
Don River	443 140 mE	5 441 320 mN
Douglas River	604 394 mE	5 373 555 mN
Epping Forrest	529 079 mE	5 376 672 mN
Fingal Tier	580 075 mE	5 382 514 mN
Fingal Valley	580 743 mE	5 389 787 mN
Florentine Valley	586 001 mE	5 386 069 mN
Frankford	481 473 mE	5 422 711 mN
Freycinet Peninsula	605 846 mE	5 331 607 mN
Georgetown	485 736 mE	5 449 886 mN
Glenorchy	522 568 mE	5 257 439 mN
Golden Valley	475 815 mE	5 391 321 mN
Granton	518 238 mE	5 266 694 mN
Great Pine Tier	465 760 mE	5 338 723 mN
Great Lake	477 909 mE	5 359 950 mN
Hagley	491 387 mE	5 402 651 mN
Hamilton	487 743 mE	5 287 476 mN
Hellyer Gorge	379 054 mE	5 343 734 mN
Hobart	526 609 mE	5 251 549 mN
Howells Sugarloaf	489 779 mE	5 319 321 mN
Hummocky Hills	519 496 mE	5 380 066 mN
Hunterston	495 089 mE	5 326 509 mN
Huon River	503 712 mE	5 235 295 mN
Huonville	505 038 mE	5 237 499 mN
Ida Bay	492 142 mE	5 189 447 mN
Interlaken	514 161 mE	5 333 918 mN
Jordan River	506 511 mE	5 282 927 mN

Lake Echo	470 718 mE	5 334 227 mN
Lake King William	437 551 mE	5 325 240 mN
Lake Leake	567 977 mE	5 348 269 mN
Lake River	509 208 mE	5 357 916 mN
Lake River Inlier	509 018 mE	5 362 720 mN
Lake St. Clair	431 196 mE	5 342 969 mN
Latrobe	451 270 mE	5 434 753 mN
Launceston	513 263 mE	5 410 493 mN
Liawenee	472 735 mE	5 361 203 mN
Little Pine Lagoon	466 924 mE	5 349 797 mN
Longford	509 949 mE	5 394 627 mN
Lonnavale	485 380 mE	5 243 309 mN
Lune River	492 128 mE	5 191 228 mN
Macquarie Tiers	533 071 mE	5 354 596 mN
Mangalore	519 950 mE	5 276 990 mN
Maria Island	590 922 mE	5 280 483 mN
Maydena	468 902 mE	5 265 921 mN
Meehan Ranges	525 695 mE	5 268 681 mN
Melton Mobray	514 690 mE	5 297 775 mN
Miena	475 800 mE	5 351 124 mN
Mole Creek	450 461 mE	5 399 007 mN
Mt Field East	470 104 mE	5 276 521 mN
Mt King William 1	428 508 mE	5 323 281 mN
Mt Lloyd	497 248 mE	5 255 509 mN
Mt Pelion	491 852 mE	5 447 310 mN
Mt Rufus	426 388 mE	5 336 413 mN
Mt Wellington	519 333 mE	5 250 576 mN
National Park	476 686 mE	5 272 919 mN
North Bruny Island	530 506 mE	5 220 865 mN
Oatlands	530 126 mE	5 316 308 mN
Oonah	384 150 mE	5 434 920 mN
Oyster Bay	596 552 mE	5 328 387 mN
Oyster Cove	521 246 mE	5 227 036 mN
Perth	514 572 mE	5 396 386 mN
Picton River	476 040 mE	5 222 205 mN
Poatina	496 550 mE	5 372 668 mN
Port Dalrymple	485 229 mE	5 445 729 mN
Port Sorell	464 172 mE	5 440 514 mN
Quamby Bluff	474 469 mE	5 388 368 mN
River Tamar	501 551 mE	5 425 378 mN
Ross	540 665 mE	5 346 757 mN
Salmon River	317 486 mE	5 454 065 mN
Sassafras	457 663 mE	5 384 476 mN
Savage River	351 030 mE	5 404 508 mN
Scamander	605 268 mE	5 409 231 mN
Shannon Lagoon	478 264 mE	5 350 922 mN
Shannon Tier	495 465 mE	5 329 313 mN

Shoemaker Bay	473 845 mE	5 172 322 mN
St Marys	598 710 mE	5 395 886 mN
St Pauls River	568 617 mE	5 370 004 mN
Strahn	360 999 mE	5 331 874 mN
Styx Valley	472 508 mE	5 259 914 mN
Surprise Bay	471 742 mE	5 173 885 mN
Swansea	588 965 mE	5 335 550 mN
Synnots Creek	487 400 mE	5 321 659 mN
Tullah	385 443 mE	5 379 346 mN
Tunbridge	535 177 mE	5 335 410 mN
Tunbridge Tier	524 611 mE	5 335 483 mN
Waddamanna	479 005 mE	5 336 054 mN
Weasel Plains	489 490 mE	5 319 163 mN
Woodbridge	519 207 mE	5 221 426 mN
Wylds Craig	449 795 mE	5 297 236 mN
Wynyard	393 495 mE	5 461 526 mN
York Plains	536 408 mE	5 319 690 mN
Zeehan	361 705 mE	5 361 822 mN

APPENDIX 2

SEISMIC SECTION RANGES AND FILENAMES

Seismic Line	Range and Shot-point Range	File Name
TB01-PA	Range: 0 - 5 912 m, SP Range: 106 - 334	TB01-PA_SP 106-334.pdf
TB01-PB	Range: 73 000 - 92 848 m, SP Range: 894 - 100	TB01-PB_SP 894-100.pdf
TB01-PB	Range: 54 500 - 74 000 m, SP Range: 1635 - 854	TB01-PB_SP 1635-854.pdf
TB01-PB	Range: 36 000 - 55 500 m, SP Range: 2376 - 1595	TB01-PB_SP 2376-1595.pdf
TB01-PB	Range: 17 500 - 37000 m , SP Range: 3115 - 2335	TB01-PB_SP 3115-2335.pdf
TB01-PB	Range: 0 - 18 500 m, SP Range: 3816 - 3076	TB01-PB_SP 3816-3076.pdf
TB01-PD	Range: 0 - 11 933 m, SP Range: 142 - 620	TB01-PD_SP 142-620.pdf
TB01-ST	Range: 0 - 21 000 m, SP Range: 100 - 941	TB01-ST_SP 100-941.pdf
TB01-ST	Range: 20 000 - 41 500 m, SP Range: 900 - 1762	TB01-ST_SP 900-1762.pdf
TB01-ST	Range: 39 000 - 59 875 m, SP Range: 1663 - 2499	TB01-ST_SP 1663-2499.pdf
TB01-TA	Range: 0 - 11 725 m, SP Range: 101 - 570	TB01-TA_SP 101-570.pdf
TB01-TB	Range: 0 -22 000 m, SP Range: 100 - 989	TB01-TB_SP 100-989.pdf
TB01-TB	Range: 22 150 - 44 364 m, SP Range: 907 - 1876	TB01-TB_SP 907-1876.pdf
TB01-TC	Range: 0 - 17 340 m, SP Range: 100 - 794	TB01-TC_ SP 100-794.pdf
TB01-TC	Range: 17 240 - 34 580 m, Sp Range: 790 - 1484	TB01-TC_ SP790-1484.pdf
TB01-TD	Range: 0 - 15 091 m, SP Range: 108 - 712	TB01-TD_SP 108-712.pdf
TB01-TH	Range: 51 000 - 67 878 m, SP Range: 774 - 100	TB01-TH_SP 774-100.pdf
TB01-TH	Range: 34 000 - 52 000 m, SP Range: 1453 - 734	TB01-TH_SP 1453-734.pdf
TB01-TH	Range: 17 000 - 35 000 m, SP Range: 2132 - 1414	TB01-TH_SP 2132-1414.pdf
TB01-TH	Range: 0 - 18 000 m, SP Range: 2810 - 2092	TB01-TH_SP 2810-2092.pdf
TB01-TI	Range: 0 - 16 328 m, SP Range: 100 - 753	TB01-TI_SP 100-753.pdf
95AGS-T4	Range: 0 - 16 192 m, SP Range: 4000 - 4408	95AGS-T4.pdf
TB01-PF	Range: 0 - 21 000 m, SP Range: 155 - 1006	TB01-PF_SP 155-1006.pdf
TB01-PF	Range: 15 800 - 34 317 m, SP Range: 770 - 1527	TB01-PF_SP 770-1527.pdf
TB01-PG	Range: 0 - 19 000 m, SP Range: 101 - 878	TB01-PG_SP 101-878.pdf
TB01-PG	Range: 18 500 - 37 500 m, SP Range: 857 - 1634	TB01-PG_SP 857-1634.pdf
TB01-PG	Range: 37 000 - 55 809 m, SP Range: 1613 - 2382	TB01-PG_SP 1613-2382.pdf
TB01-PM	Range: 0 - 17 500 m, SP Range: 101 - 800	TB01-PM_SP 101-800.pdf
TB01-PM	Range: 15 000 - 23 381 m, SP Range: 701 - 1036	TB01-PM_SP 701-1036.pdf
TB01-PT	Range: 0 - 15 000 m, SP Range: 101 - 700	TB01-PT_SP 101-700.pdf
TB01-PT	Range: 12 000 - 23 281 m, SP Range: 580 - 1030	TB01-PT_SP 580-1030.pdf
TB01-PU	Range: 0 - 19 000 m, SP Range: 355 - 1113	TB01-PU_SP 355-1113.pdf
TB01-PU	Range: 14 000 - 28 978 m, SP Range: 914 - 1512	TB01-PU_SP 914-1512.pdf
TB01-PW	Range: 0 - 21 500 m, SP Range: 370 - 1228	TB01-PW_SP 370-1228.pdf
TB01-TE	Range: 12 300 - 25 521 m, SP Range: 628 - 100	TB01-TE_SP 628-100.pdf
TB01-TE	Range: 0 - 12 700 m, SP Range: 1120 - 613	TB01-TE_SP 1120-613.pdf
TB01-PC	Range: 0 - 11 526 m, Sp Range: 101 - 562	TB01-PC_SP 101-562.pdf

APPENDIX 3 – REGIONAL CROSS-SECTIONS

NORTH-SOUTH CROSS- SECTION

1. The north-south cross-section is a composite of seismic lines TB01-PB and TB01-TH,

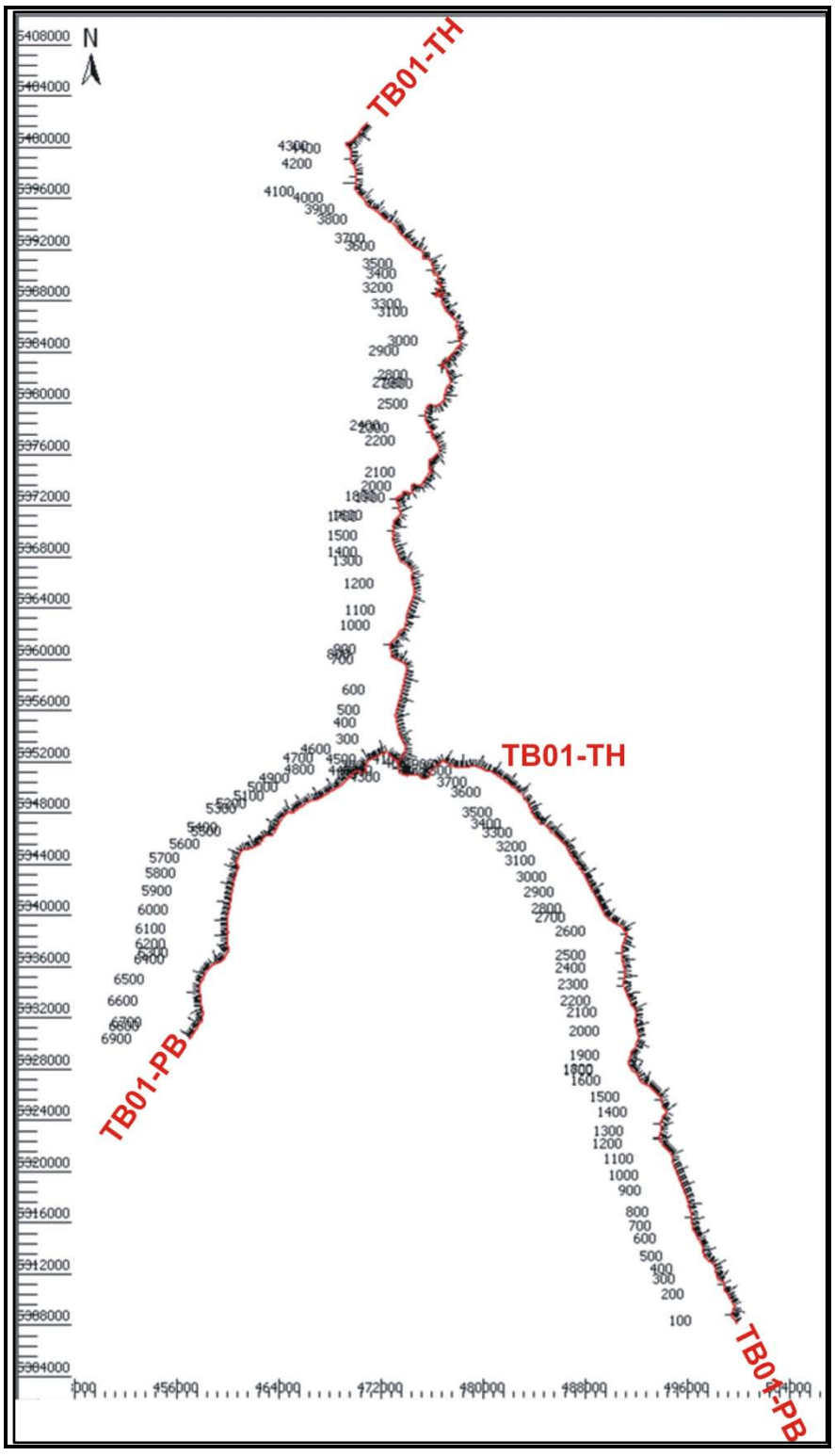

2. An arbitrary north-south seismic line was created, removing the east-west part of seismic line TB01-PB,

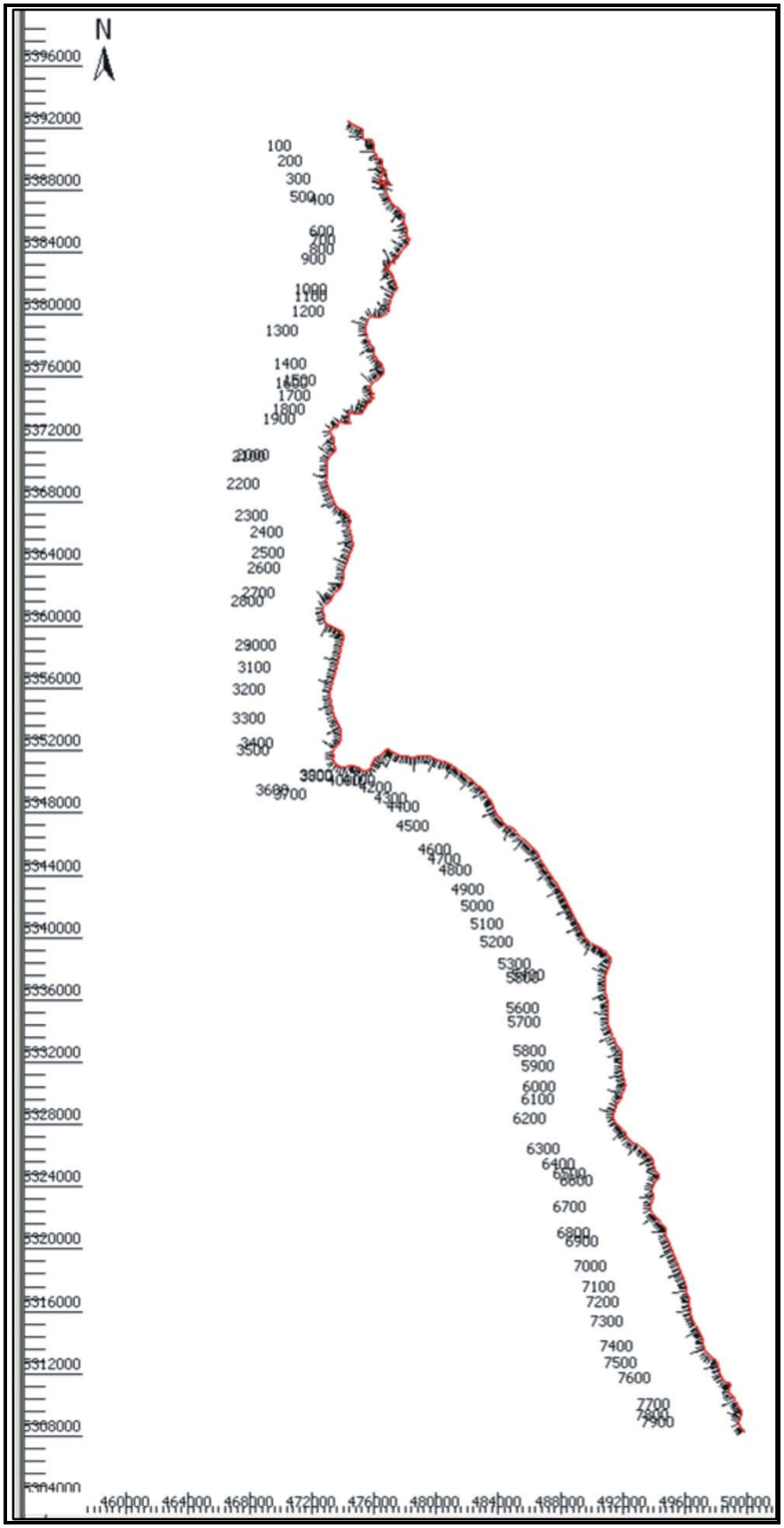

3. The interpreted seismic data was projected onto three new “straight” section lines using 2DMove™ software,

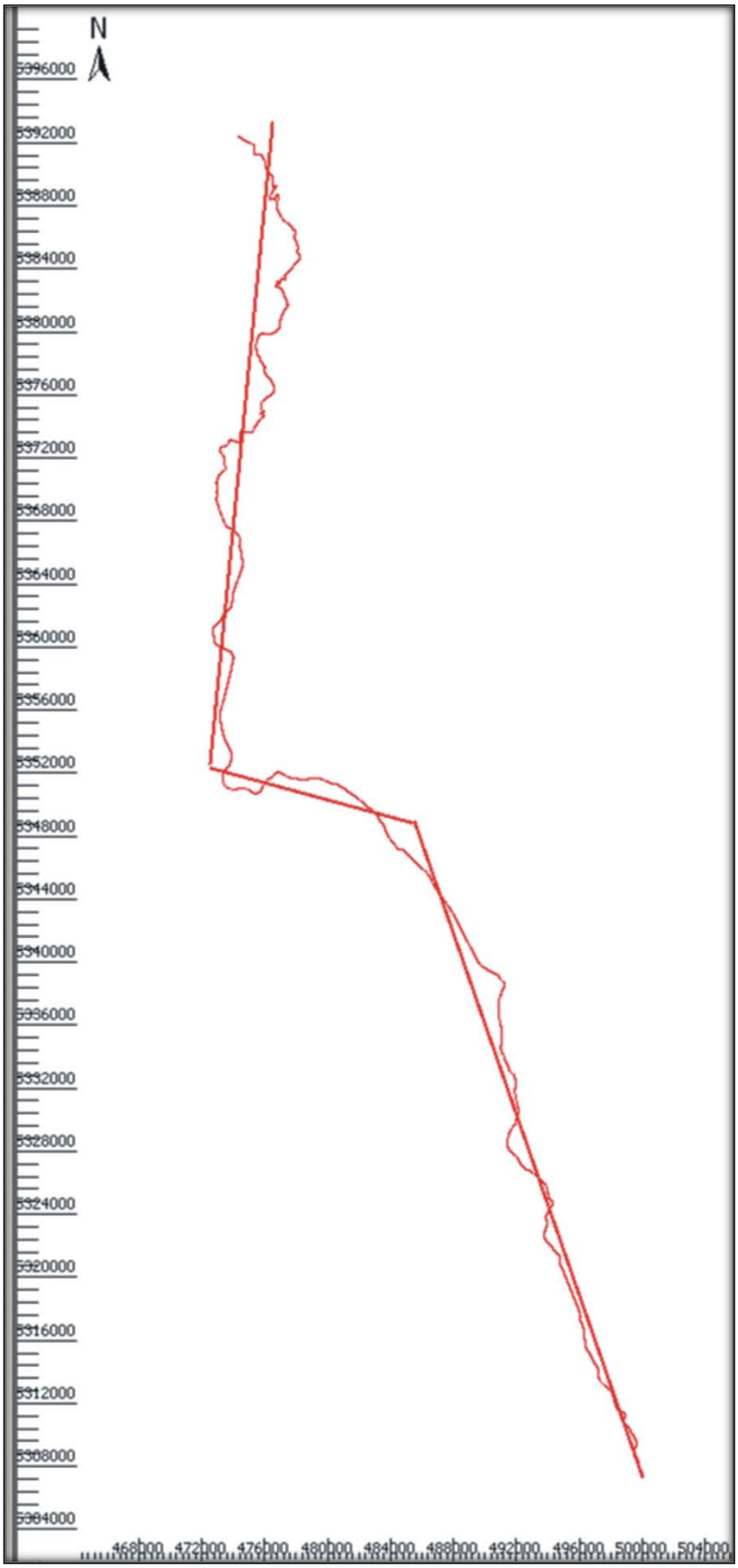

4. Finally, the interpreted seismic data was project from the three intermediate sections onto a single line of section.

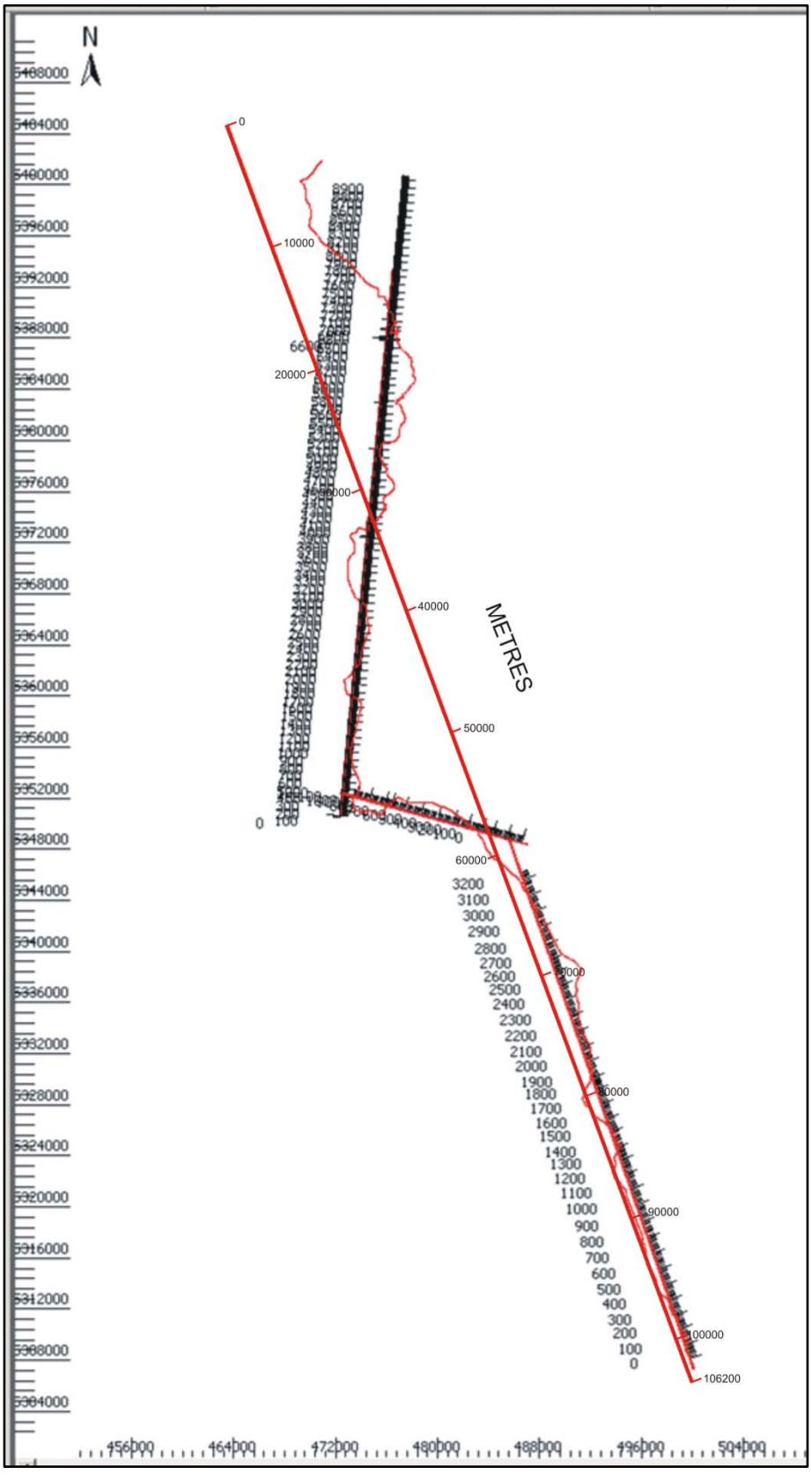

CENTRAL TASMANIA BASIN: NORTH-SOUTH CROSS-SECTION

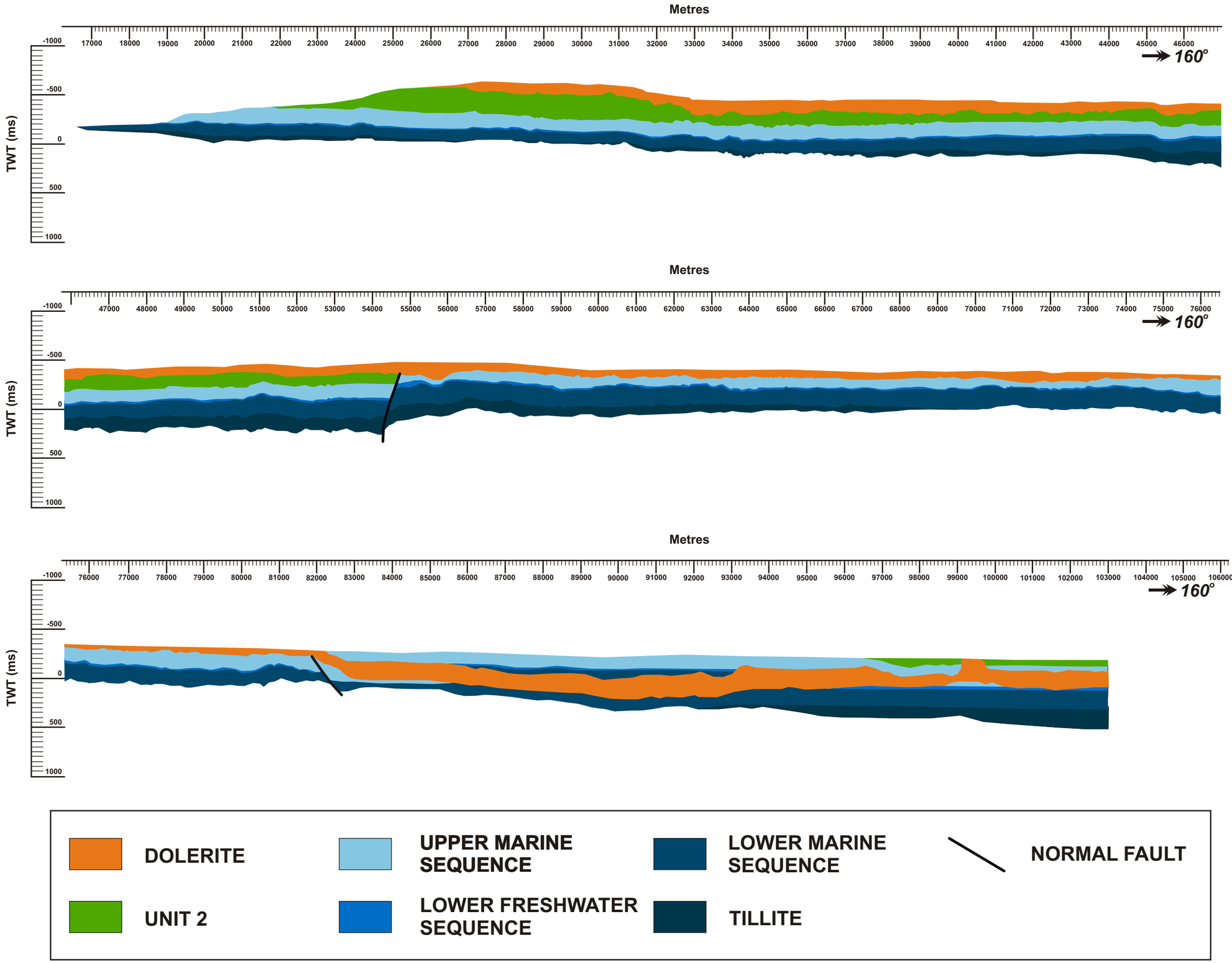

WEST-EAST CROSS- SECTION

1. The west-east cross-section is a composite of seismic lines TB01-TB, TB01-PB and TB01-ST,

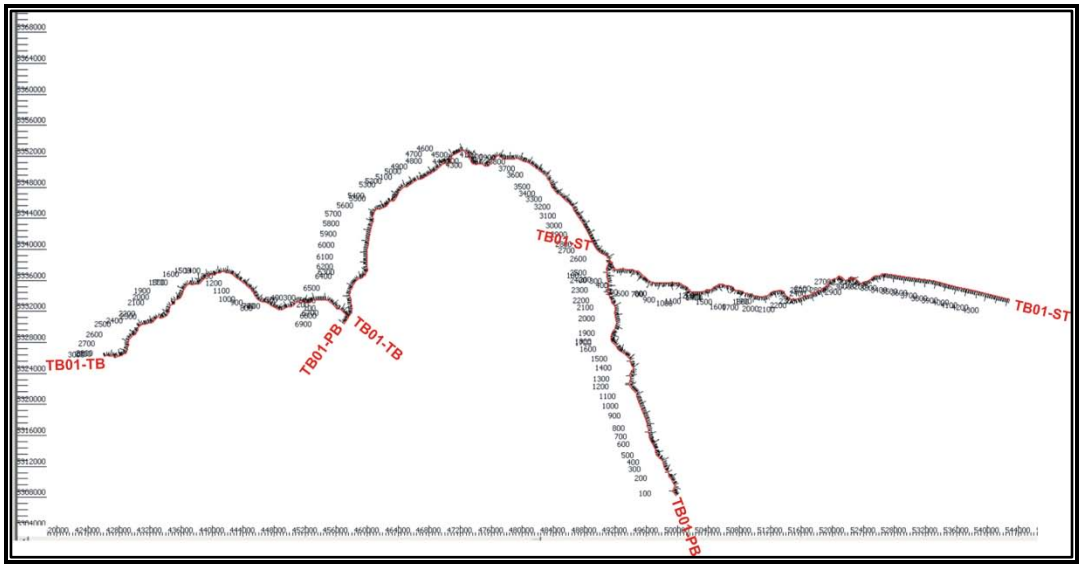

2. An arbitrary west-east seismic line was created, removing the north-south part of seismic line TB01-PB,

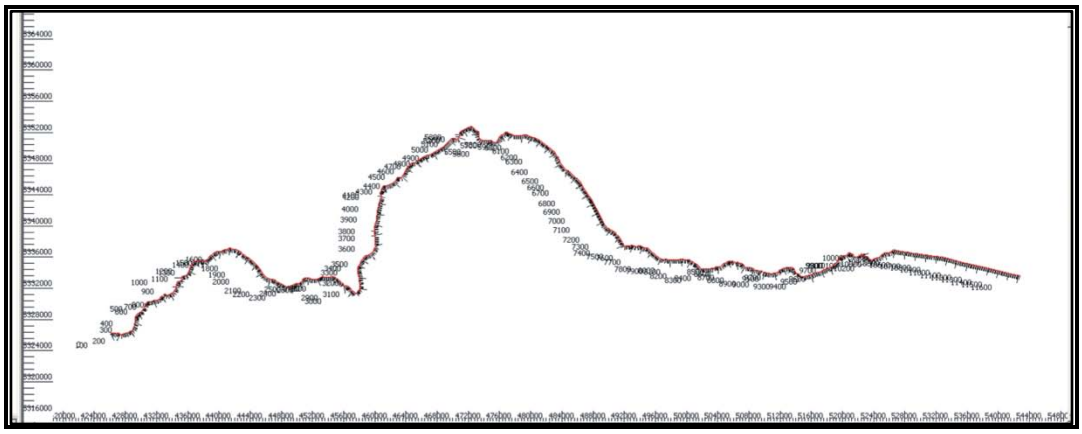

3. The interpreted seismic data was projected onto a new "straight" section lines using 2DMove™ software,

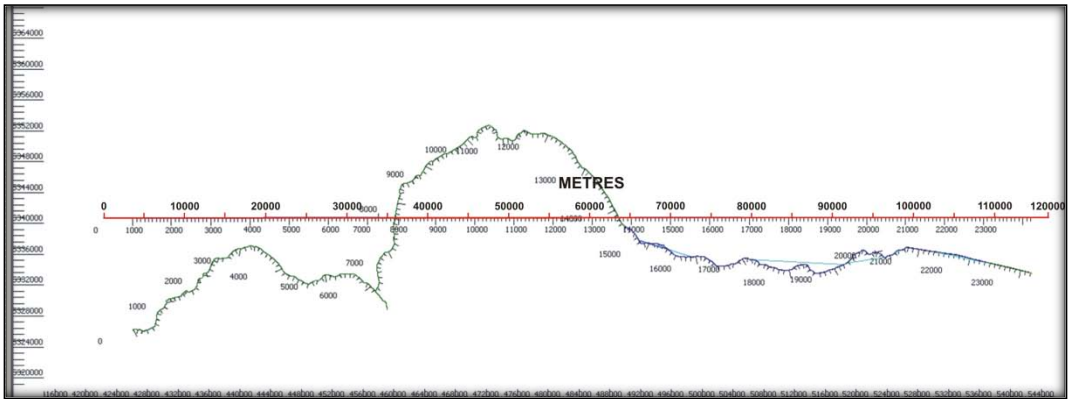

CENTRAL TASMANIA BASIN: WEST-EAST CROSS-SECTION

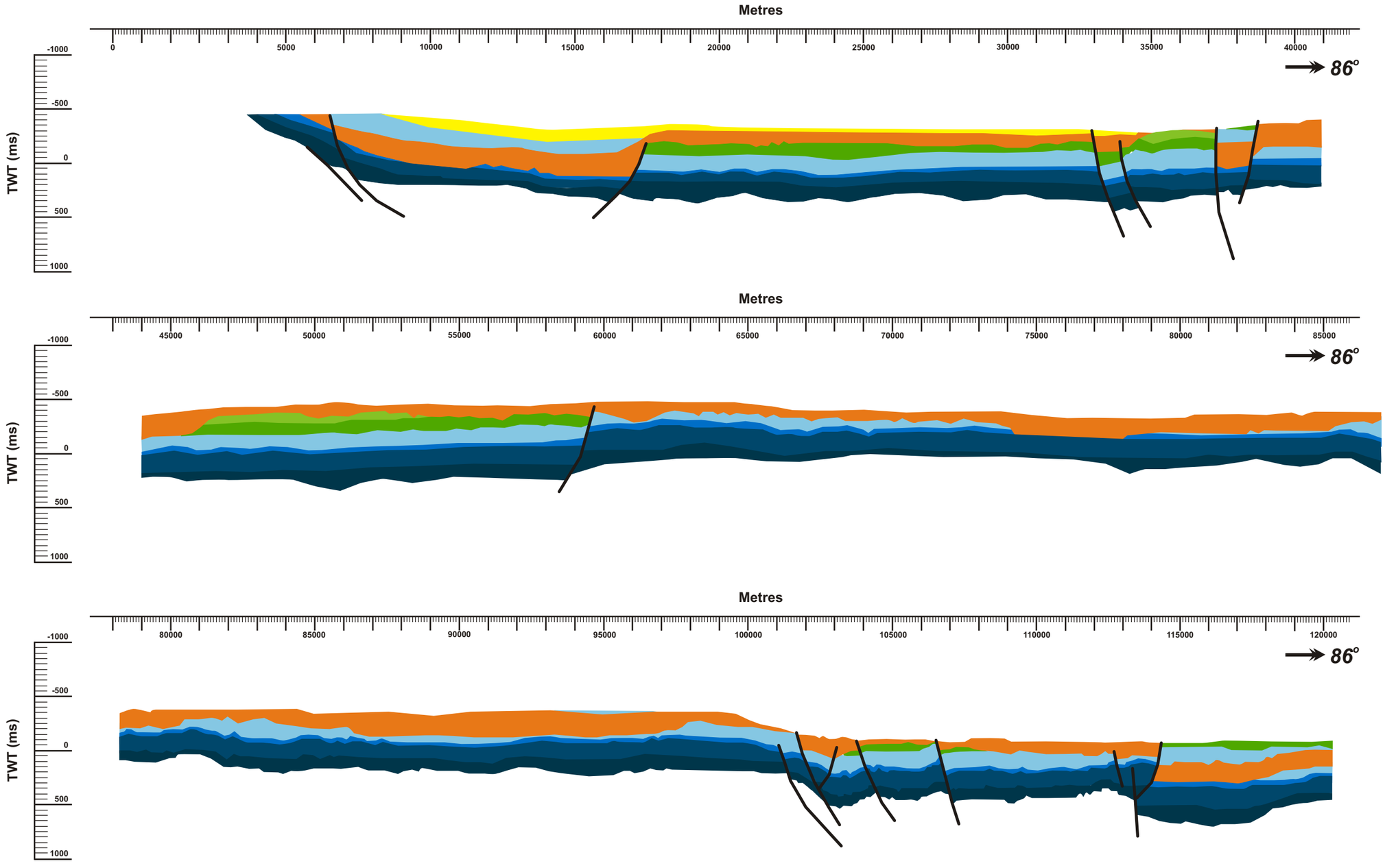

QUATERNARY DEPOSOITS

DOLERITE

UNIT 3

UNIT 2

UPPER MARINE SEQUENCE

LOWER FRESHWATER SEQUENCE

LOWER MARINE SEQUENCE

TILLITE

FAULT